Title
Total Synthesis of Welwitindolinones and Nickel-Catalyzed Reactions of Amide Derivatives

Author
Weires, Nicholas Anthony

Publication Date
2017

Peer reviewed|Thesis/dissertation

UNIVERSITY OF CALIFORNIA

Los Angeles

Total Synthesis of Welwitindolinones and Nickel-Catalyzed Reactions of Amide Derivatives

A dissertation submitted in partial satisfaction of the

requirements for the degree Doctor of Philosophy

in Chemistry

by

Nicholas Anthony Weires

2017

ABSTRACT OF THE DISSERTATION

Total Synthesis of Welwitindolinones and

Nickel-Catalyzed Reactions of Amide Derivatives

by

Nicholas Anthony Weires

Doctor of Philosophy in Chemistry

University of California, Los Angeles, 2017

Professor Neil Kamal Garg, Chair

This dissertation describes our efforts toward the total synthesis of welwitindolinone natural products, as well as the development of reactions involving the nickel-catalyzed activation of amide C–N bonds. The welwitindolinones have been long-standing targets in total synthesis for over two decades, and this dissertation describes two completed total syntheses of these alkaloids. In addition, several nickel-catalyzed transformations of amides are outlined, each of which demonstrate the powerful reactivity of nickel and highlight the utility of amides as synthetic building blocks.

Chapters one and two present our enantiospecific total syntheses of the welwitindolinone alkaloids *N*-methylwelwitindolinone D isonitrile and *N*-methylwelwitindolinone B

isothiocyanate. Our approach to these natural products features an aryne cyclization to construct the bicyclo[4.3.1]decane core of the molecules, as well as a C–H nitrene insertion reaction to introduce the bridgehead nitrogen substituent. In chapter one, a dual C–H functionalization event installs the challenging ether linkage and allows for completion of (–)-*N*-methylwelwitindolinone D isonitrile. In chapter two, a regio- and diastereoselective chlorinative oxabicyclic opening is detailed, which enables the first total synthesis of *N*-methylwelwitindolinone B isothiocyanate.

Chapters three, four, and five describe the development of nickel-catalyzed carbon–carbon bond-forming reactions of amides. More specifically, chapters three and four outline the Suzuki–Miyaura couplings of aromatic and aliphatic amides, respectively, whereas chapter five details the alkylation of amide derivatives. These methodologies represent mild and complementary tools to the Weinreb ketone synthesis, proceeding through the nickel-catalyzed activation of the amide C–N bond. It is shown that amides, which were traditionally thought of as inert functionalities, can be utilized as synthons in C–C bond-forming reactions.

Chapter six describes a method for the benchtop delivery of $Ni(cod)_2$ involving the encapsulation of $Ni(cod)_2$ in paraffin wax. Due to air- and moisture-sensitivity, $Ni(cod)_2$ is normally handled under an inert atmosphere. Using our method of wax encapsulation, several nickel-catalyzed transformations are performed without the use of a glove box, including various amide C–N bond cleavage reactions. These studies are aimed at promoting the widespread use of nickel in transition metal catalysis.

Chapter seven illustrates the kinetic modeling of the nickel-catalyzed esterification of amides. By developing a kinetic model, an optimization is undertaken that allows for the employment of catalyst loadings as low as 0.4 mol% nickel. This demonstration is intended to foster the advancement of kinetic modeling as a powerful tool in methodology development.

The dissertation of Nicholas Anthony Weires is approved.

Jennifer M. Murphy

Yi Tang

Neil Kamal Garg, Committee Chair

University of California, Los Angeles

2017

For Michael, Rebecca, Taylor, Riker, and Emily

"A new world hangs outside the window, beautiful and strange." – Alabama Shakes

TABLE OF CONTENTS

LIST OF FIGURES

CHAPTER ONE

CHAPTER TWO

CHAPTER THREE

CHAPTER FOUR

CHAPTER FIVE

CHAPTER SIX

LIST OF SCHEMES

CHAPTER ONE

CHAPTER TWO

CHAPTER FIVE

LIST OF TABLES

CHAPTER ONE

CHAPTER THREE

CHAPTER FOUR

CHAPTER FIVE

CHAPTER SIX

CHAPTER SEVEN

LIST OF ABBREVIATIONS

$[a]_D$	specific rotation at wavelength of sodium D line
Ac	acetyl, acetate
AcOH	acetic acid
APCI	atmospheric pressure chemical ionization
app.	apparent
aq.	Aqueous
Ar	aryl
B3LYP	Becke, 3-parameter, Lee–Yang–Parr (functional)
Benz-ICy	1,3-bis(cyclohexyl)benzimidazolium
Bn	benzyl
Boc	*tert*-butyloxy carbonyl
br	broad
Bu	butyl
t-Bu	*tert*-butyl
c	concentration for specific rotation measurements
°C	degrees Celsius
calc'd	calculated
CCDC	Cambridge Crystallographic Data Centre
cod	1,5-cyclooctadiene
Cp	cyclopentadienyl
d	doublet
DFT	density functional theorem
DMAP	4-dimethylaminopyridine
DMF	*N*,*N*-dimethylformamide
DMSO	dimethyl sulfoxide
E_a	activation energy
EDC	1-ethyl-3-(3-dimethylaminopropyl)carbodiimide
ee	enantiomeric excess
equiv	equivalent
ESI	electrospray ionization
Et	ethyl

g	gram(s)
h	hour(s)
Het	heterocycle
HOBt	1-hydroxybenzotriazole
HPLC	high performance liquid chromatography
HRMS	high resolution mass spectroscopy
Hz	hertz
IBX	2-iodoxybenzoic acid
ICy	1,3-bis(cyclohexyl)imidazolium
IR	infrared (spectroscopy)
J	coupling constant
kcal/mol	kilocalories to mole ratio
L	liter or ligand
lit	literature
m	multiplet or milli
m	meta
M	molar or metal
m/*z*	mass to charge ratio
μ	micro
Me	methyl
MHz	megahertz
min	minute(s)
mol	mole(s)
mp	melting point
Ms	methanesulfonyl (mesyl)
NaHMDS	sodium hexamethyldisilazide
NBS	*N*-bromosuccinimide
NMO	*N*-methylmorpholine *N*-oxide
NMR	nuclear magnetic resonance
NOESY	Nuclear Overhauser Enhancement Spectroscopy
p	para
Ph	phenyl
PhH	benzene
pin	pinacolato

Piv	pivaloyl
PPh_3	triphenylphosphine
ppm	parts per million
Pr	propyl
i-Pr	isopropyl
pyr	pyridine
q	quartet
rt	room temperature
R_f	retention factor
s	singlet or strong
SFC	supercritical fluid chromatography
SIPr	1,3-bis(2,6-diisopropylphenyl)imidazolin-2-ylidene
t	triplet
TBAF	tetrabutylammonium fluoride
TBS	*tert*-butyldimethylsilyl
TBSCl	*tert*-butyldimethylsilyl chloride
TES	triethylsilyl
TESCl	triethylsilyl chloride
Tf	trifluoromethanesulfonyl (trifyl)
TFA	trifluoroacetic acid
THF	tetrahydrofuran
TLC	thin layer chromatography
TMSCl	trimethylsilyl chloride
Ts	*p*-toluenesulfonyl (tosyl)
UV	ultraviolet
w	weak

ACKNOWLEDGEMENTS

Firstly, I would like to thank my dissertation advisor, Professor Neil Garg, for his constant support and guidance during my graduate studies. I can honestly say that I have always felt like Neil was fighting for me. Whether its getting a manuscript accepted or submitting an award nomination, Neil is truly there for his students. In addition, his creativity and perfectionist approach to fine-tuning all professional documents and presentations is unparalleled, and I really believe that I could not have learned what I learned from Neil anywhere else. He also somehow has an ability to turn up everywhere I go. For example, even if I'm attending a football game 25 miles from campus in Pasadena, seemingly lost among a crowd of 80,000 people, I've learned that Neil will appear out of nowhere.

I've also had the great fortune of interacting with several other outstanding teachers and mentors over the past decade both in Idaho and at UCLA. Eagle High's Bruce Cornell is one of the most talented teachers I have ever known, and without his enthusiasm and dedication I perhaps never would have pursued science. Additionally, my first research advisor at UI, Professor Thomas Bitterwolf, not only taught me the basics of laboratory research during my first two years, but also led an incredible series of courses throughout my undergraduate studies that challenged me from the beginning. I am also very grateful to Professor Patrick Hrdlicka, who was an outstanding lecturer and was the first person to make me consider teaching at the university level. Patrick also introduced me to a new faculty member at that time, Professor Jakob Magolan. I owe so much to Jakob, who was my research advisor for my last two years at UI. Jakob's passion for teaching organic chemistry has been inspirational to me, and I am so lucky that I had the opportunity to work with him. Having been one of Jakob's first students, he

treated me like a graduate researcher, allowing me to run my own projects and train other students. Jakob, I admire you so much and have learned so much from you, and it was because of you that I chose to pursue organic chemistry in graduate school. I would also like to thank Professor Richard Williams, whose rigorous courses in physical organic chemistry and spectroscopy prepared me for my graduate studies. Moreover, many of the faculty members at UCLA have been instrumental in my professional development. I am grateful to Professors Ken Houk, Yi Tang, and Jennifer Murphy for serving on my dissertation committee and for all of their support during my graduate career. Lastly, I would like to acknowledge Professor Patrick Harran for his incredible aptitude for teaching, as his synthesis course was truly outstanding.

Having entered UCLA during Neil's sixth year there as a faculty member, I have had the pleasure of getting to know every single PhD graduate from his group to date. As such, I have many people to thank. I would like to start with those members of the Garg group with whom I have worked directly over the years. Evan Styduhar was my first mentor in the group, and he has become like a brother to me. Evan has excellent taste in music, an unbelievable work ethic, and a hilarious sense of humor, and I have to thank him for all of his incredible contributions to our syntheses of the welwitindolinones, as well as his friendship. Additionally, I would like to thank Alex Huters for being a great coworker and a talented researcher. Emma Baker-Tripp has been my longest-standing colleague, and we have worked in the same room and on many of the same projects for four years. I was Emma's mentor during her first summer in the group, and it has been so awesome to watch her develop into a leader in the laboratory. I would like to thank Emma for being a great person to talk to, for being so hard working, and for the hilarious fits of laughter in which we so often found ourselves. Bryan Simmons has also become a close friend during my time here, and I admire him most for his true love of science. Bryan is certainly the

most likely member of the laboratory to show up at my fume hood on a daily basis to show me some unusual crystals that he grew or a wildly fluorescent compound, and I thank him for keeping the spirit of our work alive. He is also a great friend to talk to and a kind person, despite his rough demeanor. I would also like to thank Jacob Dander, who I learned alongside during our forays into organozinc preparation and paraffin wax fiascos. Jacob is a kind soul with a maturity that is beyond his years, and I am so appreciative of his friendship and teamwork. Most recently, I have worked with a bright colleague named Tim Boit, whom I thank for his tenacity and intellectual curiosity. I'm proud that the lab has such critical thinking and creative first year students as Tim, and I am excited for the future of the Garg group. I would also like to thank Junyong Kim for his hard work on our current project, and also for having a name that can conveniently replace the lyrics to nearly any song. Lastly, I would like to thank Dan Caspi for being an outstanding collaborator. I had a tremendous amount of fun working with Dan during our conference calls, and I appreciate all of his efforts and advice.

I couldn't have asked for a better cohort in the Garg group, and I would be remiss if I didn't acknowledge the camaraderie of Mike Corsello, Jose Medina, and Jesus Moreno. Mike, living with you was one of the most ridiculous times of my life. We laughed until we cried, and the number of inside jokes that were created during those years is simply staggering. I will always be grateful for your friendship. I know that you would agree that we kept each other motivated throughout these years, and I am so thankful that we were there for each other. Jose, our conversations over beers in Weyburn were some of my favorite times in graduate school, and although we had to escape a theater together once, the good times we spent together far outweigh the scary ones. Jesus, I have enjoyed laughing with you over the goofiest little things, and I thank

you for encouraging the ridiculous humor that we shared. For all three of you, our trip to Philadelphia was hilarious, and I look forward to more good times with you in the future.

I have had so many other great colleagues over the years about whom I could write unendingly, but I will try to be concise. Two coworkers that have continually inspired great scientific discussions as well as hilarious conversations are Michael Yamano and Evan Darzi. I have worked directly next to Michael for nearly two years, and I have to say that he may be one of the most unique people I've ever met based on his love of Las Vegas, downhill longboarding, and minivan driving. Although I've only gotten to work with Evan for six month or so, it has become clear that we have a tremendous overlap in both music taste and personality. Thanks for the good laughs, Evan, as well as the good talks. The O.G. bud, Stephen Ramgren is of course, up next. Stephen, you fostered such an intellectual atmosphere for us when we first joined the group, and you really made us feel welcome there. I can't thank you enough for that, and I think it's fair to say that you've had a tremendous impact on Mike, Jose, Jesus, and me. I would also like to thank Joyann Barber for fun conversations and for her friendship, Elias Picazo for being one of the sincerest people I've ever met, Sarah Anthony for her infectious and seemingly permanent smile, Lucas Morill for embracing the lunacy within both of us and not holding back while singing in the lab, Robert Susick for his exquisite taste in metal, Joel Smith for awesome and stimulating scientific discussions, Noah Fine Nathel for being an incredible friend and confidant, as well as for his bone dry sense of humor, Margeux Miller for the good laughs and music discussions, Sophie Racine and Marie Hoffmann for greetings in the French language, Travis McMahon for the beer brewing adventures, Alex Schammel for his kindness and hospitality during many Thanksgivings, Adam Goetz for keeping me in line my first year, Amanda Silberstein for her level-headedness, Grace Chiou for helping me to get settled in Los

Angeles, Tejas Shah for the R&B music and for being a great guy, Liana Hie for her legacy of nickel catalysis, and Melissa Ramirez for the late evening discussions while writing my thesis.

There are so many other people that I have met while living in Los Angeles that I must thank. Joe, I always promised you that I would acknowledge you in my thesis. Thank you for all of your hard work in rebuilding the glove box vacuum pump, and for the good conversations. I would also like to thank my good friends Greg Klein and Greenman, the latter of whom got me through some hard times. Most importantly, Karen and Kenny Tejeda, your hospitality is completely unrivaled and you are such wonderful people. Thank you so much for all of the amazing weekend adventures, for having me as a guest at your home so frequently, and for all of the thoughtful things that you have done for me since I met you. I am so grateful to both of you, and I cannot thank you enough.

Finally, my thesis dedication is reserved for those that inspired me to pursue graduate studies, as well as those without whose support I absolutely never could have succeeded. The unwavering love and support of my parents, Michael and Rebecca Weires, was instrumental in every chapter of my graduate career, as well as for all of my life prior to this, and I could not be more appreciative. I truly mean it when I say that I could not have asked for a better childhood or better parents. You are both amazing and I am so lucky to be your son. My older brother, Taylor, has always been my role model, and I mean it when I say that I would never have pursued science without you. Your guidance and friendship have made me who I am today. My younger brother, Riker, has also had a profound impact on my personality and my life, as we are essentially twins. From the earliest times that we used to work together on homework, you have inspired me to be a teacher, and I am forever grateful to you. Lastly, Emily, you have been there for me every step of the way throughout graduate school, and I am forever indebted to you for all

that you have done for me. From attending my second year talk, to celebrating every little achievement, you have been so incredibly supportive, and I am certain that I would not have survived graduate school without you. You have kept me grounded, and I have become a better person because of you. I love you, and I am so excited to see where life takes us.

Chapter 1 is a version of Styduhar, E. D.; Huters, A. D.; Weires, N. A.; Garg, N. K. *Angew. Chem. Int. Ed.* **2013***, 52,* 12422–12425. Styduhar, Huters, and Weires were responsible for experimental work.

Chapter 2 is a version of Weires, N. A.; Styduhar, E. D.; Baker, E. L.; Garg, N. K. *J. Am. Chem. Soc.* **2014**, *136*, 14710–14713. Weires, Styduhar, and Baker were responsible for experimental work.

Chapter 3 is a version of Weires, N. A.; Baker, E. L.; Garg, N. K. *Nat. Chem.* **2016**, *8*, 75–79. Weires and Baker were responsible for experimental work.

Chapter 4 is a version of Weires, N. A.; Boit, T. B.; Kim, J.; Garg, N. K. *Manuscript in preparation*. Weires, Boit, and Kim were responsible for experimental work.

Chapter 5 is a version of Simmons, B. J.; Weires, N. A.; Dander, J. E.; Garg, N. K. *ACS Catal.* **2016**, *8*, 3176–3179. Simmons, Weires, and Dander were responsible for experimental work.

Chapter 6 is a version of Dander, J. E.; Weires, N. A.; Garg, N. K. *Org. Lett.* **2016**, *18*, 3934–3936. Dander and Weires were responsible for experimental work.

Chapter 7 is a version of Weires, N. A.; Caspi, D. D.; Garg, N. K. *ACS Catal.* [Just accepted manuscript] DOI: 10.1021/acscatal.7b01444. Weires was responsible for experimental work.

BIOGRAPHICAL SKETCH

Education:

University of California, Los Angeles, CA

- Ph.D. Candidate in Chemistry, anticipated graduation Spring 2017
- NSF Graduate Research Fellow
- Current GPA: 3.99/4.00

University of Idaho, Moscow, ID

- B.S. in Chemistry - Professional Option, May 2012
- *Cum Laude*; Cumulative GPA: 3.90/4.00
- Certificate, University Honors Program

Professional and Academic Experience:

Graduate Research Assistant: University of California, Los Angeles, CA

- July 2012 – present; Advisor: Prof. Neil K. Garg.
- Synthesized multigram quantities of late-stage [4.3.1]-bicyclic intermediates and optimized a dual C–H functionalization reaction to facilitate the first enantiospecific total synthesis of the polycyclic natural product *N*-methylwelwitindolinone D isonitrile.
- Established a regio- and diastereoselective chlorinative opening of a [2.2.1]-oxabicycle to complete the first total synthesis of (–)-*N*-methylwelwitindolinone B isothiocyanate.
- Developed the nickel-catalyzed Suzuki–Miyaura coupling of aromatic and aliphatic amides, the first carbon–carbon bond forming reaction of amides utilizing non-precious metal catalysis.
- Optimized the nickel-catalyzed Negishi coupling of amides, the first catalytic alkylation of amides.
- Developed a method for benchtop delivery of $Ni(cod)_2$ using paraffin capsules, allowing for use of this air-sensitive reagent without the need for a glove box.
- Optimized the nickel-catalyzed esterification of amides through kinetic modeling in collaboration with AbbVie, Inc.

Graduate Teaching Assistant: University of California, Los Angeles, CA

- Undergraduate organic chemistry discussion sections (Fall 2012, Spring 2013)
  - Taught students spectroscopy, VSEPR theory, organic reaction mechanisms, and retrosynthetic analysis to access small molecules.
- Undergraduate organic chemistry laboratory (Winter 2013)
  - Supervised a synthetic laboratory course where students performed oxidation, reduction, aldol, and Grignard reactions.

Undergraduate Research Assistant: University of Idaho, Moscow, ID

- Synthesized air-sensitive inorganic and organometallic compounds to be used in photochemistry experiments with Harmen Zijlstra under the direction of Prof. Thomas E. Bitterwolf (Spring 2009 – Spring 2010).
- Developed a one-pot, three step synthesis of benzimidazoles using heterogeneous clay catalysis under the direction of Prof. Jakob Magolan (Fall 2010 – Spring 2012).

Summer Research Assistant: Boise State University, Boise, ID

- Developed green chemistry laboratory exercises to be used in undergraduate curricula (Summer 2010).

Undergraduate Teaching Assistant: University of Idaho, Moscow, ID

- Undergraduate general chemistry laboratory (Spring 2012)
  - Supervised a general chemistry laboratory course where students performed titrations and conducted spectrophotometric analyses.

Honors and Awards:

- Renfrew–Long Scholarship, College of Science, University of Idaho, 2009–2012
- INBRE Fellowship, University of Idaho, 2011
- Brian & Gayle Hill Fellowship, College of Science, University of Idaho, 2011–2012
- William H. Cone Award, Department of Chemistry, University of Idaho, 2012
- John B. George Award, College of Science, University of Idaho, 2012
- Graduate Dean's Scholar Award, UCLA, 2012–2013
- National Science Foundation Graduate Research Fellowship, 2013–2016
- Hanson–Dow Award for Excellence in Teaching, UCLA, 2013
- Christopher S. Foote Fellowship in Organic Chemistry, UCLA, 2015–present
- UCLA ACS Travel Award, ACS National Meeting, San Diego, 2016
- Dissertation Year Fellowship, UCLA, 2016–present

Publications:

1. **Biomass Briquettes: Turning Waste into Energy.** Owen M. McDougal, Seth Eidemiller, Nicholas A. Weires, Mark Swartz, and Michael M. McCormick. *Biomass Power & Thermal* **2010**, *4*, 46–49.

2. **Recycling of Waste Acetone by Fractional Distillation.** Nicholas A. Weires, Aubrey Johnston, Don L. Warner, Michael M. McCormick, Karen Hammond, and Owen M. McDougal. *J. Chem. Educ.* **2011**, *88*, 1724–1726.

3. **Combined Pd/C and Montmorillonite Catalysis for One-Pot Synthesis of Benzimidazoles.** Nicholas A. Weires, Jared Boster, and Jakob Magolan. *Eur. J. Org. Chem.* **2012**, 6508–6512. *Highlighted in*: *Synfacts* **2013**, *9*, 254.

4. **Enantiospecific Total Synthesis of *N*-Methylwelwitindolinone D Isonitrile.** Evan D. Styduhar, Alexander D. Huters, Nicholas A. Weires, and Neil K. Garg. *Angew. Chem. Int. Ed.* **2013**, *52*, 12422–12425. *Highlighted in*: *Synfacts* **2014**, *10*, 11.

5. **Total Synthesis of (–)-*N*-Methylwelwitindolinone B Isothiocyanate via a Chlorinative Oxabicycle Ring-Opening Strategy.** Nicholas A. Weires,[†] Evan D. Styduhar,[†] Emma L. Baker, and Neil K. Garg. *J. Am. Chem. Soc.* **2014**, *136*, 14710–14713. *Highlighted in*: *Synfacts* **2015**, *11*, 11.

6. **Nickel-Catalysed Suzuki–Miyaura Coupling of Amides.** Nicholas A. Weires, Emma L. Baker, and Neil K. Garg. *Nat. Chem.* **2016**, *8*, 75–79. *Highlighted in: C&EN* **2015**, *93* (*45*), 31 and *C&EN* **2015**, *93* (*49*), 23.

7. **Nickel-Catalyzed Alkylation of Amide Derivatives.** Bryan J. Simmons,[†] Nicholas A. Weires,[†] Jacob E. Dander, and Neil K. Garg. *ACS Catal.* **2016**, *6*, 3176–3179. *Highlighted in*: *Synfacts* **2016**, *12*, 735.

8. **Benchtop Delivery of Ni(cod)$_2$ using Paraffin Capsules.** Jacob E. Dander,[†] Nicholas A. Weires,[†] and Neil K. Garg. *Org. Lett.* **2016**, *18*, 3934–3936.

9. **Kinetic Modeling of the Nickel-Catalyzed Esterification of Amides.** Nicholas A. Weires,[†] Daniel D. Caspi,[†] and Neil K. Garg. *ACS Catal.* [Just accepted manuscript] DOI: 10.1021/acscatal.7b01444. *Highlighted in*: *ACS Editors' Choice*.

10. **Aliphatic Amides as Acyl Donors for the Union of Heterocycles.** Nicholas A. Weires,[†] Timothy B. Boit,[†] Junyong Kim, and Neil K. Garg. *Manuscript in preparation*.

11. **The Indolyne Approach to [4.3.1]-Bicyclic Welwitindolinones: Total Synthesis of the B, C, and D Classes of the Welwitindolinone Alkaloids.** Alexander D. Huters,[†] Evan D. Styduhar,[†] Nicholas A. Weires, Kyle W. Quasdorf, Emma L. Baker, Xia Tian, and Neil K. Garg. *Manuscript in preparation.*

CHAPTER ONE

Enantiospecific Total Synthesis of *N*-Methylwelwitindolinone D Isonitrile

Evan D. Styduhar, Alexander D. Huters, Nicholas A. Weires, and Neil K. Garg.

Angew. Chem. Int. Ed. **2013**, *52*, 12422–12425.

1.1 Abstract

The total synthesis of *N*-methylwelwitindolinone D isonitrile has been achieved in 17 steps from a readily available carvone derivative. The route features a double C–H functionalization event involving a keto oxindole substrate to introduce the tetrahydrofuran ring of the natural product.

1.2 Introduction

The welwitindolinone family of natural products (e.g., **1.1**–**1.2**, Figure 1.1) has attracted tremendous attention from the synthetic community over the past two decades.[1,2,3,4,5] Interest in these compounds stems from their promising biological profiles, in addition to their compact, yet daunting structures. Synthetic efforts toward the welwitindolinones have led to at least ten methods for building the bicyclo[4.3.1] core that is common to most of these natural products.[1,4] However, the sheer difficulty associated with late-stage manipulations has plagued most synthetic routes and only a few completed syntheses have been reported in recent years.[5]

One exceptionally challenging synthetic target is *N*-methylwelwitindolinone D isonitrile (**1.2**).[6,7] The compound possesses five stereocenters, two quaternary carbons, and a heavily substituted cyclohexyl ring. Compared to other related family members, **1.2** also possesses an ether linkage between C3 and C14. Thus, a successful synthesis of **1.2** would not only have to

assemble the congested oxindole-fused bicyclo[4.3.1] framework, but would also have to allow for introduction of the ethereal linkage on the sterically congested face of the bicycle. Highlights of synthetic efforts toward **1.2** include the Wood group's assembly of the spirocyclic oxindole[8] and Rawal's elegant total synthesis of (±)-**1.2** in 2011.[5a] Herein, we report our synthetic forays toward **1.2**, which culminate in an enantiospecific synthesis.

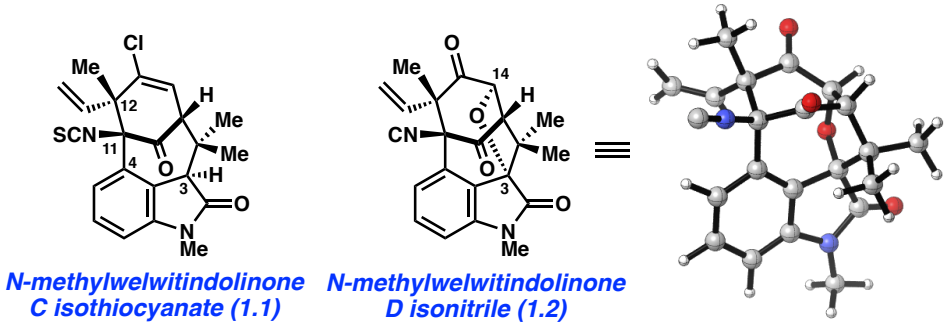

N-methylwelwitindolinone C isothiocyanate (1.1)

N-methylwelwitindolinone D isonitrile (1.2)

Figure 1.1. Welwitindolinones **1.1** and **1.2**.

1.3 Retrosynthetic Analysis of *N*-Methylwelwitindolinone D Isonitrile

Our retrosynthetic plan for the synthesis of **1.2** is presented in Scheme 1.1. The natural product would be accessed from **1.3** via late-stage manipulations. In a key disconnection, the tetrahydrofuran ring would be installed from keto-oxindole derivative **1.4**. Of note, the ability to elaborate **1.4** to **1.3** would hinge on our ability to perform chemoselective and diastereoselective manipulations adjacent to the two carbonyls. The cyclic carbamate was thought to be accessible using an intramolecular nitrene insertion reaction[9] involving oxindole substrate **1.5**. Substrate **1.5** would be derived from ketone **1.6**, which in turn can be readily prepared from known carvone derivative **1.7**[10] in just four steps using our previously established procedure involving an indolyne cyclization.[5b,11]

Scheme 1.1

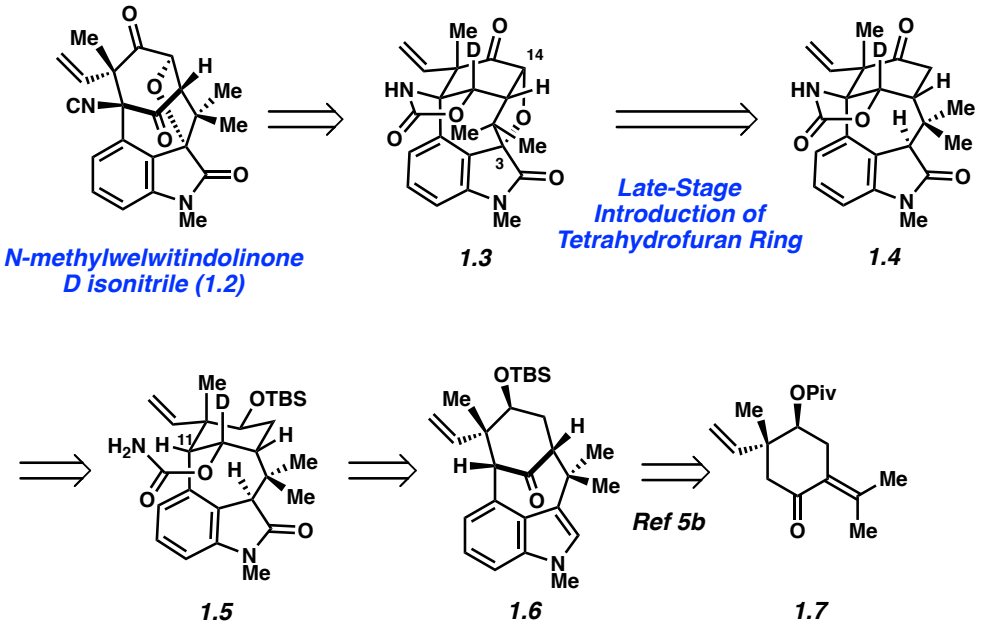

1.4 Elaboration of Bicycle to Keto Oxindole

Our approach toward implementing the retrosynthetic plan is highlighted in Scheme 1.2. Indole **1.6** was converted to oxindole **1.8** using a one-pot oxidation/hydrolysis sequence. As the acidic conditions led to desilylation, reprotection of the alcohol was necessary to provide **1.9**. Deuteride reduction and carbamoylation proceeded without event to furnish **1.5** in quantitative yield. Exposure of **1.5** to Ag-promoted nitrene insertion conditions[12,5e] furnished **1.10** in 70% yield. Note that attempts to use the proteo analog of **1.5** gave only 44% yield of the corresponding insertion product, along with 19% of recovered ketone **1.9**. Consistent with our previous findings on an alternate substrate,[5e] the strategic use of deuterium minimizes an undesirable competitive reaction, thus giving synthetically useful yields of the desired insertion product **1.10**. From **1.10**, a standard deprotection/oxidation sequence delivered key intermediate **1.4**.

Scheme 1.2

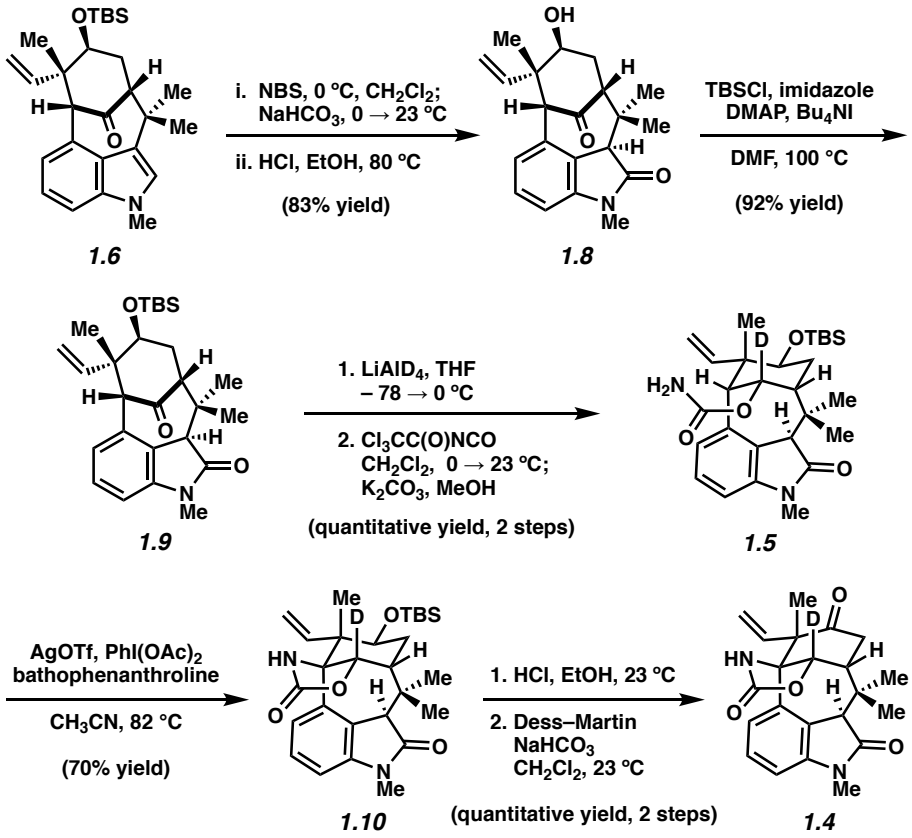

1.5 Unexpected Formation of Spirocyclobutane

Many attempts to introduce the tetrahydrofuran ring from **1.4** were put forth. Unfortunately, efforts toward site-selective functionalization of one carbonyl over the other via enol ethers were unsuccessful. After considerable experimentation, it was found that the keto carbonyl could be α-functionalized first upon treatment of **1.4** with $CuBr_2$ in THF at ambient temperature to yield **1.11** as a single diastereomer (Scheme 1.3). It was hoped that C3 oxidation would provide an alcohol intermediate that would cyclize to give the necessary tetrahydrofuran ring. However, upon treatment of **1.11** with C3 oxidation conditions,[5b] the desired oxidation and cyclization did not occur. Instead, we unexpectedly obtained cyclobutane **1.13** in high yield,

presumably through direct cyclization of the oxindole enolate (see transition structure **1.12**).[13] X-ray analysis of a single crystal of **1.13** validated our structural assignment.[14,7]

Scheme 1.3

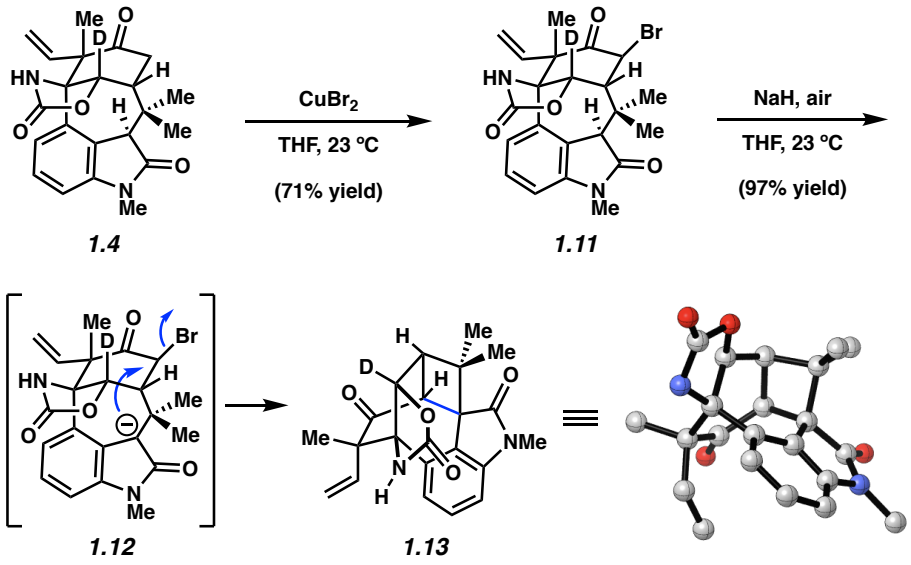

1.6 Conversion of Bromoketone to Acetate and Cyclized Product

As a workaround, we opted to introduce a protected hydroxyl group directly onto C3 of substrate **1.11**. $Mn(OAc)_3$ was deemed a potential reagent for selective C3 acetoxylation, based on its use in benzylic acetoxylation reactions.[15] Treatment of oxindole **1.11** with $Mn(OAc)_3$ in AcOH at 80 °C provided acetoxylated product **1.14** (Table 1.1, entry 1). Interestingly, when the corresponding reaction was conducted at 150 °C, we obtained a 53% yield of **1.3**, which possesses the desired tetrahydrofuran ring. Alternatively, **1.3** could also be prepared in one-pot by performing the acetoxylation at 80 °C, removing the volatiles, and exposing the crude intermediate to K_2CO_3 in MeOH and H_2O at 70 °C.

Table 1.1

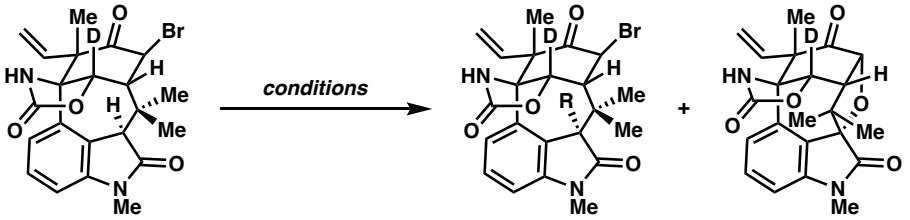

1.11 *1.14 (R = OAc)* *1.3*

Entry	*Conditions*	*Conversion to products* 1.14 (%)	1.3 (%)
1	$Mn(OAc)_3$ (4.0 equiv), AcOH, 80 °C	74	0
2	$Mn(OAc)_3$ (4.0 equiv), AcOH, 150 °C	2	53
3	$Mn(OAc)_3$ (4.0 equiv), AcOH, 80 °C; K_2CO_3, MeOH, H_2O, 70 °C	0	56

1.7 Double C–H Functionalization of Keto Oxindole to Install the Tetrahydrofuran Ring

We also explored the feasibility of directly converting keto oxindole **1.4** to **1.3** (Figure 1.2). Of note, the Wood research group was able to elegantly install a tetrahydrofuran ring from a keto oxindole substrate using basic conditions and O_2.[8] Despite the modest yield, this key precedent laid the groundwork for additional experimentation. To our delight, we found that simple exposure of **1.4** to tetrabutylammonium fluoride (TBAF) in acetonitrile in the presence of air efficiently delivered **1.3**.[16] In previous studies, we[17] and others[18] have found that TBAF/air can facilitate C3 oxidation of oxindoles containing the welwitindolinone scaffold, but the use of TBAF/air to build an ethereal linkage via double C-H functionalization was unknown. Notably, the use of other bases in place of TBAF, such as K_2CO_3 and Cs_2CO_3, also promoted the formation of **1.3**, albeit in lower yields. It is likely that this efficient method for introducing the tetrahydrofuran ring proceeds by initial diastereoselective C3 oxidation, followed by cyclization.[19] Related C3-peroxy compounds have been observed in our studies[20] and in those of the Wood research group.[8]

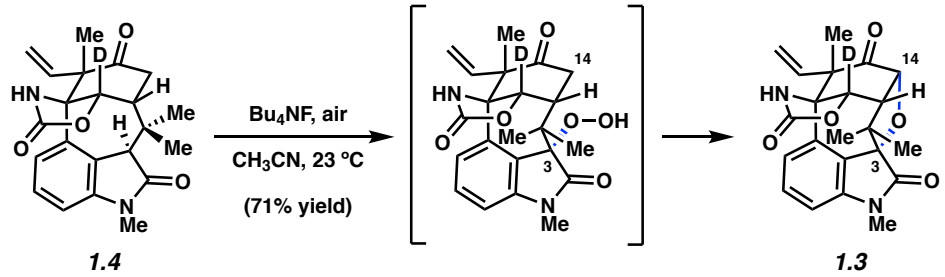

Figure 1.2. Double C–H functionalization of substrate **1.4**.

1.8 Completion of (+)-*N*-Methylwelwitindolinone D Isonitrile

To complete the total synthesis, it remained to elaborate the cyclic carbamate to the ketone and isonitrile functional groups present in **1.2** (Scheme 1.4). Unexpectedly, attempted hydrolysis of **1.3** led to cyclohexyl ring fragmentation, a process that was attributed to the reactivity of the ketone. To circumvent this, ketone **1.3** was reduced to alcohol **1.15** with $LiAlH_4$. Fortunately, upon exposure of **1.15** to hydrolysis conditions, cyclohexyl ring fragmentation was not observed. Hydrolysis gave the desired diol intermediate, which was oxidized with IBX to provide diketone **1.16**. Finally, formylation provided **1.17**, which was directly exposed to standard dehydration conditions to deliver (+)-**1.2**.

Scheme 1.4

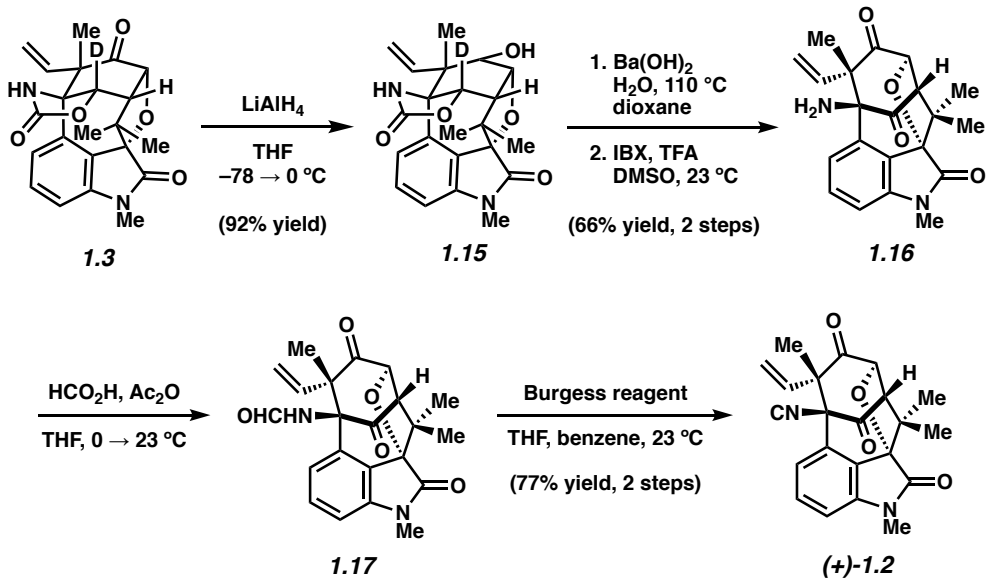

1.9 Conclusion

In summary, we have completed the enantiospecific total synthesis of *N*-methylwelwitindolinone D isonitrile. Several unexpected hurdles, including the formation of the unusual cyclobutane-containing compound **1.13**, were overcome en route to the natural product. Our total synthesis features a double C-H functionalization event of keto oxindole **1.4** to introduce the tetrahydrofuran ring of **1.2** and is achieved in 17 steps from readily available carvone derivative **1.7**.

1.10 Experimental Section

1.10.1 Materials and Methods

Unless stated otherwise, reactions were conducted in flame-dried glassware under an atmosphere of nitrogen using anhydrous solvents (either freshly distilled or passed through activated alumina columns). All commercially available reagents were used as received unless otherwise specified. $Mn(OAc)_3$ (dried *in vacuo* over P_2O_5) and $LiAlD_4$ were obtained from Acros. AgOTf and $CuBr_2$ were obtained from Strem. Bathophenanthroline was obtained from Alfa Aesar. 2-Iodoxybenzoic acid (IBX)[21] and Dess–Martin periodinane[22] were prepared from known literature procedures. 1,4-dioxane was distilled from Na/benzophenone and stored in a Schlenk tube prior to use. Unless stated otherwise, reactions were performed at room temperature (RT, approximately 23 °C). Thin-layer chromatography (TLC) was conducted with EMD gel 60 F254 pre-coated plates (0.25 mm) and visualized using a combination of UV, anisaldehyde, iodine, and potassium permanganate staining. Silicycle silica gel 60 (particle size 0.040–0.063 mm) was used for flash column chromatography. ^{1}H NMR spectra were recorded on Bruker spectrometers (500 MHz). Data for ^{1}H spectra are reported as follows: chemical shift (δ ppm), multiplicity, coupling constant (Hz), integration and are referenced to the residual solvent peak 7.26 ppm for $CDCl_3$, 5.32 ppm for CD_2Cl_2, 4.79 ppm for D_2O, and 1.94 ppm for CD_3CN. Data for ^{2}H NMR spectra are reported as follows: chemical shift (δ ppm, at 77 MHz), multiplicity, coupling constant, integration and are referenced to the residual solvent peak 7.26 ppm for $CDCl_3$. ^{13}C NMR spectra are reported in terms of chemical shift (at 125 MHz) and are referenced to the residual solvent peak 118.26 ppm for CD_3CN, 77.16 ppm for $CDCl_3$, and 53.84 for CD_2Cl_2. IR spectra were recorded on a Perkin-Elmer 100 spectrometer and are reported in terms of frequency absorption (cm^{-1}). Optical rotations were measured with a Rudolph Autopol III

Automatic Polarimeter. Uncorrected melting points were measured using a Mel-Temp II melting point apparatus with a Fluke 50S thermocouple and a Digimelt MPA160 melting point apparatus. High resolution mass spectra were obtained from the UC Irvine Mass Spectrometry Facility.

1.10.2 Experimental Procedures

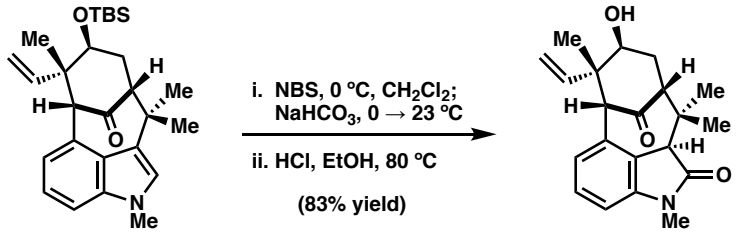

1.6 *1.8*

Oxindole 1.8. To a solution of indole **1.6**[5b] (200 mg, 0.457 mmol, 1.0 equiv) in CH_2Cl_2 (9.2 mL) at 0 ºC was added NBS (82.0 mg, 0.462 mmol, 1.01 equiv) in one portion. The reaction vial was flushed with N_2, and allowed to stir at 0 ºC. After 15 min, solid $NaHCO_3$ (200 mg, 100 wt %) was added in one portion. The reaction was removed from the 0 ºC bath and allowed to stir at room temperature for 5 min. The resulting suspension was evaporated under reduced pressure. Absolute ethanol (9.2 mL) and concentrated aqueous HCl (9.2 mL) were added. After heating to 80 ºC for 17 h, the reaction was cooled to room temperature and transferred to a separatory funnel with H_2O (15 mL) and EtOAc (15 mL). To the funnel was added solid $NaHCO_3$ until gas evolution was no longer observed. The resulting biphasic mixture was extracted with EtOAc (3 x 15 mL) and the organic layers were combined, dried over $MgSO_4$, and evaporated under reduced pressure. The resulting residue was purified by flash chromatography (1:1:1 hexanes:CH_2Cl_2:Et_2O) to afford oxindole **1.8** (130 mg, 83% yield) as a brown solid. Oxindole **1.8**: mp: 203.2 ºC; R_f 0.23 (1:1 hexanes:EtOAc); ^{1}H NMR (500 MHz, $CDCl_3$): δ 7.22 (dd, *J* =

7.8, 7.7, 1H), 6.73 (d, *J* = 7.7, 1H), 6.67 (d, *J* = 7.8, 1H), 5.56 (dd, *J* = 17.5, 10.9, 1H), 5.22 (d, *J* = 10.9, 1H), 5.19 (d, *J* = 17.5, 1H), 4.22 (ddd, *J* = 12.2, 5.6, 2.8, 1H), 3.73 (s, 1H), 3.32 (d, *J* = 1.4, 1H), 3.19 (s, 3H), 2.59 (dd, *J* = 14.9, 5.6, 1H) 2.53 (d, *J* = 8.2, 1H), 2.07 (ddd, *J* = 14.9, 12.2, 8.2, 1H), 1.65 (s, 3H), 1.58 (d, *J* = 2.8, 1H), 1.17 (s, 3H), 0.68 (s, 3H); ^{13}C NMR (125 MHz, $CDCl_3$, 20 of 21 observed): δ 208.3, 174.9, 144.8, 142.0, 130.7, 128.5, 127.2, 125.2, 116.6, 107.2, 68.4, 68.2, 62.2, 53.5, 50.1, 40.2, 30.0, 26.4, 26.3, 22.6; IR (film): 1703, 1687, 1611, 1588, 1461 cm^{-1}; HRMS-ESI (*m/z*) [M + Na]$^+$ calcd for $C_{21}H_{25}NO_3Na$, 362.1732; found 362.1737; $[\alpha]^{25.2}_D$ +6.60° (*c* = 1.000, $CHCl_3$).

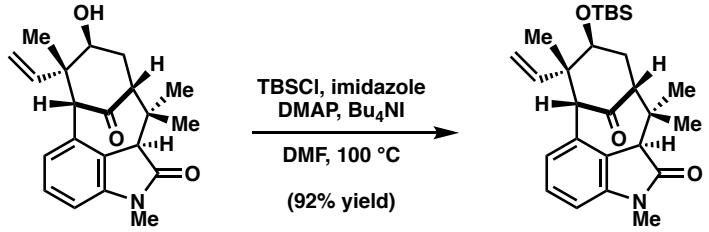

1.8 ***1.9***

Silyl ether 1.9. To a solution of oxindole **1.8** (609 mg, 1.80 mmol, 1.0 equiv) in DMF (18.0 mL) was added imidazole (611 mg, 8.97 mmol, 5.0 equiv), DMAP (219 mg, 1.79 mmol, 1.0 equiv), and tetrabutylammonium iodide (663 mg, 1.79 mmol, 1.0 equiv). The resulting solution was stirred at room temperature for 5 min, and then TBSCl (809 mg, 5.37 mmol, 3.0 equiv) was added in one portion. The flask was fitted with a reflux condenser, flushed with N_2, and then heated to 100 °C. After 25 h, the reaction mixture was cooled to room temperature and transferred to a separatory funnel with EtOAc (50 mL), H_2O (20 mL), and a solution of saturated aqueous NH_4Cl (20 mL). The resulting biphasic mixture was extracted with EtOAc (3 x 50 mL). The organic layers were combined, washed with H_2O (3 x 50 mL), dried over $MgSO_4$, and evaporated under reduced pressure. The resulting residue was purified by flash chromatography

(9:1 hexanes:EtOAc) to afford silyl ether **1.9** (746 mg, 92% yield) as a white solid. Silyl ether **1.9**: mp: 184.5 ºC; R_f 0.64 (2:1 hexanes:EtOAc); ^{1}H NMR (500 MHz, $CDCl_3$): δ 7.21 (dd, *J* = 7.9, 7.7, 1H), 6.73 (d, *J* = 7.7, 1H), 6.66 (d, *J* = 7.9, 1H), 5.40 (dd, *J* = 17.5, 10.8, 1H), 5.15–5.00 (m, 2H), 4.17 (dd, *J* = 11.6, 5.5, 1H), 3.62 (s, 1H), 3.26 (s, 1H), 3.21 (s, 3H), 2.47 (d, *J* = 8.2, 1H), 2.40 (dd, *J* = 15.1, 5.5, 1H), 2.10 (ddd, *J* = 15.1, 11.6, 8.2, 1H), 1.62 (s, 3H), 1.17 (s, 3H), 0.82 (s, 9H), 0.67 (s, 3H), 0.04 (s, 3H), -0.09 (s, 3H); ^{13}C NMR (125 MHz, $CDCl_3$, 24 of 25 observed): δ 208.6, 175.0, 144.6, 143.6, 131.2, 128.4, 127.4, 124.9, 114.6, 107.1, 70.0, 69.2, 62.5, 53.7, 50.3, 40.1, 32.0, 26.4, 25.8, 22.4, 18.1, 16.1, -3.8, -4.4; IR (film): 1707, 1689, 1609, 1590, 1465 cm^{-1}; HRMS-ESI (*m/z*) [M + Na]$^+$ calcd for $C_{27}H_{39}NO_3SiNa$, 476.2597; found 476.2600; $[\alpha]^{26.1}_D$ +12.60° (*c* = 1.000, $CHCl_3$).

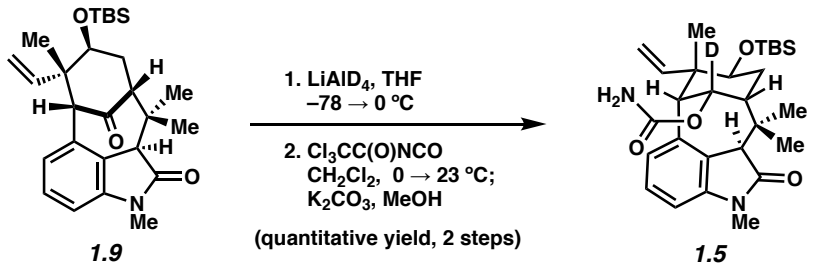

Carbamate 1.5. To a solution of silyl ether **1.9** (178 mg, 0.393 mmol, 1.0 equiv) in THF (13.0 mL) at –78 °C was added a solution of $LiAlD_4$ (1.0 M in THF, 1.18 mL, 1.18 mmol, 3.0 equiv) in a dropwise manner. After stirring at –78 °C for 20 min, the solution was then allowed to warm to 0 ºC. After 20 min, the reaction was quenched at 0 °C with slow addition of a saturated aqueous solution of Rochelle's salt (10 mL), and then allowed to warm to 23 ºC. The resulting biphasic mixture was stirred at room temperature for 1 h, transferred to a separatory funnel with EtOAc (25 mL) and H_2O (20 mL), and extracted with EtOAc (3 x 25 mL). The organic layers

were combined, dried over $MgSO_4$, and evaporated under reduced pressure. The resulting residue was used in the subsequent step without further purification.

To a flask containing the crude residue from the previous step was added CH_2Cl_2 (7.85 mL), cooled to 0 ºC, followed by addition of trichloroacetyl isocyanate (58 μL, 0.490 mmol, 1.25 equiv) in a dropwise manner. The resulting mixture was allowed to stir at 0 °C for 5 min, and then at room temperature for 20 min. The solvent was evaporated under reduced pressure. To the resulting residue was added MeOH (7.85 mL) followed by solid K_2CO_3 (298 mg, 2.16 mmol, 5.5 equiv) in one portion. The reaction was flushed with N_2 and left to stir at room temperature for 80 min. The reaction was quenched with saturated aqueous NH_4Cl (7 mL), and the resulting biphasic mixture was transferred to a separatory funnel with EtOAc (25 mL) and H_2O (20 mL). After extracting with EtOAc (3 x 25 mL), the organic layers were combined, dried over $MgSO_4$, and evaporated under reduced pressure. The resulting residue was purified by flash chromatography (2:1 hexanes:EtOAc) to afford carbamate **1.5** (203 mg, quant. yield, over two steps) as a white solid. Carbamate **1.5**: mp: 106.1 ºC; R_f 0.47 (1:1 hexanes:EtOAc); ^{1}H NMR (500 MHz, $CDCl_3$): δ 7.15 (ddd, *J* = 7.8, 7.7, 0.7, 1H), 6.70 (dd, *J* = 7.7, 0.7, 1H), 6.63 (d, *J* = 7.8, 1H), 5.23 (dd, *J* = 17.4, 10.7, 1H), 5.03 (dd, *J* = 17.4, 1.3, 1H), 4.93 (dd, *J* = 10.7, 1.3, 1H), 4.34 (s, 2H), 4.03 (dd, *J* = 12.5, 5.1, 1H), 3.60 (s, 1H), 3.20 (s, 3H), 2.83 (s, 1H) 2.30 (ddd, *J* = 15.0, 5.1, 1.9, 1H), 2.25 (d, *J* = 6.1, 1H), 1.98 (ddd, *J* = 15.0, 12.5, 6.1, 1H), 1.58 (s, 3H), 1.36 (s, 3H), 0.88 (s, 3H), 0.82 (s, 9H), 0.03 (s, 3H), -0.12 (s, 3H); ^{2}H NMR (77 MHz, $CDCl_3$) δ 5.51 (br. s, 1D); ^{13}C NMR (125 MHz, $CDCl_3$): δ 175.8, 156.1, 146.3, 144.6, 138.1, 128.6, 127.4, 125.3, 113.7, 106.3, 74.5 (t, J_{C-D} = 22.1), 70.9, 56.8, 55.9, 49.0, 48.9, 37.3, 32.4, 29.2, 26.3, 25.9, 24.3, 18.1, 17.1, -3.8, -4.3; IR (film): 2956, 2923, 2857, 1728, 1701, 1607, 1596, 1463 cm^{-1}; HRMS-

ESI (*m/z*) $[M + Na]^+$ calcd for $C_{28}H_{41}N_2O_4SiDNa$, 522.2874; found 522.2872; $[\alpha]^{26.5}_D$ +11.40° (*c* = 1.000, $CHCl_3$).

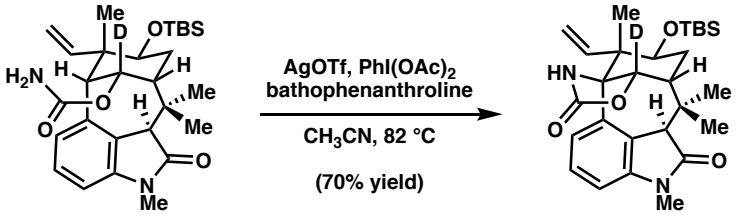

1.5 ***1.10***

Oxazolidinone 1.10. A 1-dram vial containing CH_3CN, a second 1-dram vial charged with bathophenanthroline (10.6 mg, 0.0319 mmol, 0.5 equiv), and a third 1-dram vial containing carbamate **1.5** (33.0 mg, 0.0660 mmol, 1.0 equiv) and $PhI(OAc)_2$ (42.5 mg, 0.132 mmol, 2.0 equiv) were transferred into the glovebox. AgOTf (8.5 mg, 0.033 mmol, 0.5 equiv) and CH_3CN (950 μL) were added to the vial containing the bathophenanthroline, and the resulting suspension was allowed to stir at room temperature for 20 min. Next, CH_3CN (950 μL) was added to the vial containing the carbamate, and the AgOTf/bathophenanthroline suspension was also added to this vial. The vial was then sealed, removed from the glovebox, and the resulting mixture was heated to 82 °C. After 24 h, the reaction was cooled to room temperature and filtered by passage over a plug of silica gel (EtOAc eluent, 10 mL). The filtrate was evaporated under reduced pressure, and the resulting residue was purified by preparative thin layer chromatography (2:1 hexanes:EtOAc) to afford oxazolidinone **1.10** (23 mg, 70% yield) as a yellow solid and recovered silyl ether **1.9** (2 mg, 7% yield) as a white solid. Oxazolidinone **1.10**: mp: 288.0 ºC (decomp.); R_f 0.50 (1:1 hexanes:EtOAc); ^{1}H NMR (500 MHz, $CDCl_3$): δ 7.21 (app t, *J* = 8.0, 1H), 6.77–6.73 (m, 2H), 6.54 (s, 1H), 5.19–5.09 (m, 3H), 3.87 (dd, *J* = 11.7, 5.2, 1H), 3.47 (s, 1H), 3.22 (s, 3H), 2.44 (d, *J* = 6.7, 1H), 2.31 (dd, *J* = 15.2, 5.2, 1H), 2.01 (ddd, *J* = 15.2, 11.7,

6.7, 1H), 1.60 (s, 3H), 1.33 (s, 3H), 0.96 (s, 3H), 0.80 (s, 9H), 0.00 (s, 3H), -0.16 (s, 3H); ^{2}H NMR (77 MHz, $CDCl_3$) δ 4.97 (br. s, 1D); ^{13}C NMR (125 MHz, $CDCl_3$, 25 of 26 observed): δ 174.8, 159.1, 144.1, 144.0, 137.6, 128.0, 125.9, 124.7, 116.3, 107.4, 72.2, 69.9, 55.2, 49.9, 46.8, 37.7, 32.3, 28.0, 26.4, 25.8, 22.8, 18.1, 12.9, -3.8, -4.4; IR (film): 1758, 1708, 1691, 1607, 1590, 1461 cm^{-1}; HRMS-ESI (*m*/*z*) $[M + Na]^+$ calcd for $C_{28}H_{39}N_2O_4SiDNa$, 520.2718; found 520.2719; $[\alpha]^{27.0}_D$ +1.40° (*c* = 1.000, $CHCl_3$).

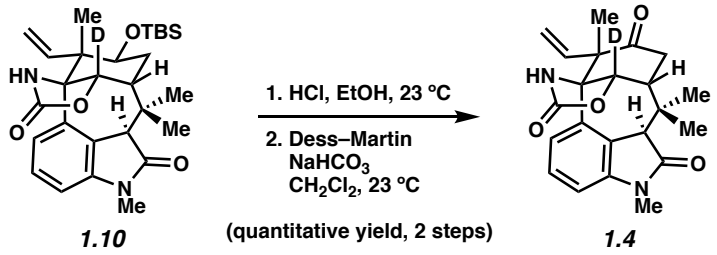

Ketone 1.4. A flask was charged with oxazolidinone **1.10** (576 mg, 1.16 mmol, 1.0 equiv), absolute ethanol (23.0 mL), and concentrated aqueous HCl (23.0 mL). After stirring at 23 ºC for 1 h, the reaction mixture was transferred to a separatory funnel with H_2O (50 mL) and EtOAc (50 mL). To the funnel was added solid $NaHCO_3$ until no more gas evolution was observed. The resulting biphasic mixture was extracted with EtOAc (3 x 50 mL) and the organic layers were combined, dried over $MgSO_4$, and evaporated under reduced pressure. The resulting residue was used in the subsequent step without further purification.

To a flask containing the crude product from the previous step was added solid $NaHCO_3$ (487 mg, 5.80 mmol, 5.0 equiv) in one portion. The reaction vessel was flushed with N_2, and then CH_2Cl_2 (11.6 mL) was added. To the resulting suspension was added the Dess–Martin periodinane reagent (645 mg, 1.52 mmol, 1.3 equiv) in one portion. The flask was flushed with N_2, and the reaction mixture was allowed to stir at room temperature. After 1 h, the reaction

mixture was diluted with a 1:1 mixture of saturated aqueous $NaHCO_3$ and saturated aqueous $Na_2S_2O_3$ (10.0 mL). The resulting biphasic mixture was vigorously stirred until both layers appeared clear. The mixture was then transferred to a separatory funnel with EtOAc (30 mL) and H_2O (30 mL), and then extracted with EtOAc (3 x 30 mL). The organic layers were combined, dried over $MgSO_4$, and evaporated under reduced pressure. The resulting residue was purified by flash chromatography (1:1 hexanes:EtOAc) to afford ketone **1.4** (454 mg, quant. yield, over two steps) as a yellow solid. Ketone **1.4**: mp: 293.5 ºC; R_f 0.42 (1:3 hexanes:EtOAc); ^{1}H NMR (500 MHz, $CDCl_3$): δ 7.20 (app t, *J* = 8.0, 1H), 7.10 (s, 1H), 6.77–6.73 (m, 2H), 5.34 (dd, *J* = 17.6, 10.9, 1H), 5.22–5.16 (m, 2H), 3.34 (s, 1H), 3.18 (s, 3H), 3.17–3.06 (m, 2H), 2.86–2.82 (m, 1H), 1.62 (s, 3H), 1.56 (s, 3H), 0.92 (s, 3H); ^{2}H NMR (77 MHz, $CDCl_3$) δ 5.45 (br. s, 1D); ^{13}C NMR (125 MHz, $CDCl_3$, 21 of 22 observed): δ 209.8, 174.3, 159.3, 144.5, 137.9, 136.0, 128.5, 124.3, 123.4, 116.8, 108.0, 70.8, 57.4, 51.9, 48.2, 40.2, 38.4, 27.3, 26.5, 22.5, 19.8; IR (film): 1760, 1752, 1689, 1611, 1590 cm^{-1}; HRMS-ESI (*m/z*) $[M + Na]^+$ calcd for $C_{22}H_{23}N_2O_4DNa$, 404.1696; found 404.1700; $[\alpha]^{27.3}_D$ –26.67° (*c* = 0.870, $CHCl_3$).

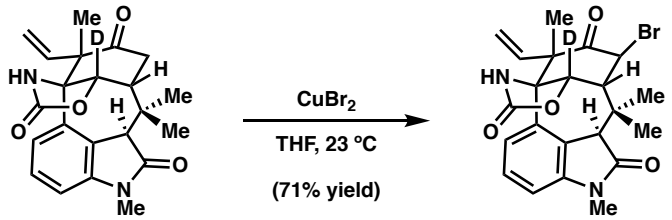

1.4 *1.11*

Bromoketone 1.11. A 1-dram vial was charged with ketone **1.4** (50.0 mg, 0.131 mmol, 1.0 equiv) and transferred into the glovebox. $CuBr_2$ (59.0 mg, 0.264 mmol, 2.0 equiv) was then added and the vial was removed from the glovebox. THF (2.1 mL) was added and the reaction vial was sealed and left to stir at room temperature. After 19 h, the reaction mixture was filtered

by passage over a plug of celite (THF eluent, 10 mL). The filtrate was collected in a test tube, diluted with H_2O (5 mL), and then extracted with $CHCl_3$ (3 x 5 mL). The organic layers were combined, dried over $MgSO_4$, and evaporated under reduced pressure. The resulting residue was adsorbed onto silica gel (2 mL) and purified by flash chromatography (4:1 hexanes:acetone) to afford bromoketone **1.11** (42.5 mg, 71% yield) as a white solid. Bromoketone **1.11**: mp: 273.0 ºC (decomp.); R_f 0.62 (1:3 hexanes:EtOAc); ^{1}H NMR (500 MHz, CD_3CN): δ 7.32 (ddd, J = 8.2, 7.6, 0.8, 1H), 7.21 (s, 1H), 6.89–6.84 (m, 2H), 5.27–5.19 (m, 1H), 5.12–5.03 (m, 2H), 3.10 (s, 3H), 3.05 (s, 2H), 1.87 (s, 3H), 1.59 (s, 3H), 0.81 (s, 3H); ^{2}H NMR (77 MHz, $CDCl_3$) δ 5.87 (br. s, 1D); ^{13}C NMR (21 of 22 observed, 125 MHz, CD_3CN): δ 204.9, 173.3, 157.4, 144.7, 138.3, 136.2, 128.4, 123.7, 122.8, 115.8, 108.0, 70.5, 58.2, 56.0, 50.4, 46.8, 38.7, 25.84, 25.75, 23.3, 21.5; IR (film): 1762, 1702, 1607, 1464 cm^{-1}; HRMS-ESI (m/z) [M + Na]$^+$ calcd for $C_{22}H_{22}O_4DN_2BrNa$, 484.0784; found 484.0809; $[\alpha]^{25.8}_D$ +179.20° (c = 1.000, $CHCl_3$).

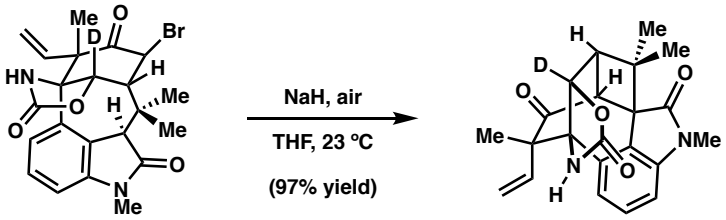

1.11 *1.13*

Cyclobutane 1.13. To a solution of bromoketone **1.11** (4.0 mg, 0.0087 mmol, 1.0 equiv) in THF (870 μL) was added NaH (60% dispersion in mineral oil, 1.7 mg, 0.043 mmol, 5.0 equiv) in one portion. The reaction vial was then opened to air for 10 seconds, sealed and left to stir at room temperature. After 2 h, the reaction mixture was filtered by passage over a plug of silica gel (EtOAc eluent, 6 mL). The filtrate was evaporated under reduced pressure, and the resulting residue was purified by flash chromatography (2:1 hexanes:EtOAc) to afford cyclobutane **1.13**

(3.3 mg, 97% yield) as a white solid. Crystals suitable for X-ray diffraction studies (CCDC 960226) were obtained by concentration of **1.13** from a mixture of $CHCl_3$ and pentane. Cyclobutane **1.13**: mp: 284.0 ºC; R_f 0.51 (1:3 hexanes:EtOAc); ^{1}H NMR (500 MHz, $CDCl_3$): δ 7.27 (app t, *J* = 8.0, 7.8, 1H), 6.88 (d, *J* = 8.0, 1H), 6.79 (d, *J* = 7.8, 1H), 6.42 (s, 1H), 5.09–5.02 (m, 2H), 4.90 (dd, *J* = 17.7, 10.8, 1H), 4.00 (d, *J* = 7.4, 1H), 3.17 (s, 3H), 3.09 (d, *J* = 7.4, 1H), 1.49 (s, 3H), 1.41 (s, 3H), 0.68 (s, 3H); ^{2}H NMR (77 MHz, $CDCl_3$) δ 5.33 (br. s, 1D); ^{13}C NMR (125 MHz, $CDCl_3$): δ 206.7, 172.3, 159.2, 142.9, 137.2, 135.5, 128.9, 124.6, 120.3, 117.4, 108.5, 80.4 (t, J_{C-D} = 21.6), 69.3, 61.1, 57.4, 46.0, 45.3, 41.6, 26.7, 26.1, 21.1, 18.7; IR (film): 1758, 1710, 1607, 1469 cm^{-1}; HRMS-ESI (*m/z*) $[M + Na]^+$ calcd for $C_{22}H_{21}O_4DN_2Na$, 402.1540; found 402.1540; $[\alpha]^{27.3}_D$ –94.00° (*c* = 0.500, $CHCl_3$).

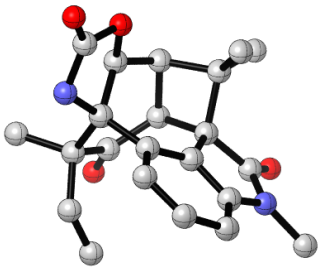

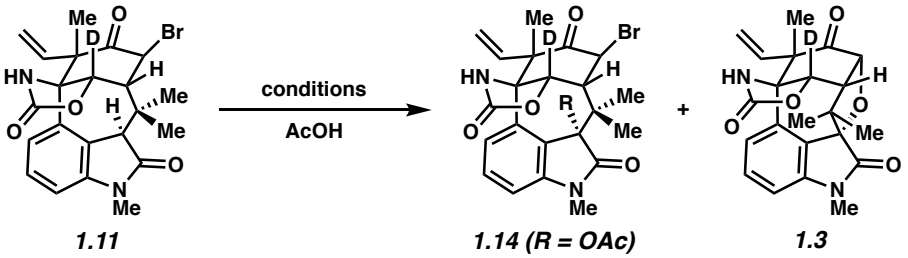

1.11 *1.14 (R = OAc)* *1.3*

General Procedure for Acetoxyoxindole 1.14 + Ether 1.3 From Table 1.1. A 1-dram vial charged with bromoketone **1.11** (5.0 mg, 0.011 mmol, 1.0 equiv) was transferred into the glovebox. $Mn(OAc)_3$ was added and the vial was removed from the glovebox. AcOH (1.1 mL) was then added and the reaction vial was sealed and left to stir at the indicated temperature. For

entries 1–2, after stirring for 24 h the reaction mixture was cooled to room temperature, transferred to a test tube with $CHCl_3$ (2 mL) and aqueous 2M HCl (1 mL), and then extracted with $CHCl_3$ (3 x 2 mL). The organic layers were combined, washed with saturated aqueous $NaHCO_3$ (2 x 2 mL), H_2O (2 x 2 mL), and then dried over $MgSO_4$ and evaporated under reduced pressure. The resulting residue was purified by preparative thin layer chromatography (1:1 $CHCl_3$:EtOAc) to afford acetoxyoxindole **1.14** and/or ether **1.3** as white solids. For entry 3, after stirring for 24 h the reaction mixture was cooled to room temperature and concentrated under reduced pressure. To the resulting residue was added a 1:1 mixture of MeOH:H_2O (1.1 mL) and solid K_2CO_3 (3.8 mg, 0.272 mmol, 25.0 equiv) in one portion. The reaction vial was flushed with N_2, sealed and allowed to stir at 70 ºC. After 19 h, the reaction mixture was cooled to room temperature, diluted with H_2O (2 mL) and transferred to a test tube with $CHCl_3$ (2 mL). The resulting biphasic mixture was extracted with $CHCl_3$ (3 x 2 mL). The organic layers were combined, dried over $MgSO_4$, and evaporated under reduced pressure. The resulting residue was purified by preparative thin layer chromatography (1:1 $CHCl_3$:EtOAc) to afford ether **1.3** (2.4 mg, 56% yield) as a white solid. Acetoxyoxindole **1.14**: mp: 283.0 ºC (decomp.); R_f 0.65 (1:3 hexanes:EtOAc); ^{1}H NMR (500 MHz, $CDCl_3$): δ 7.31 (app t, J = 8.0, 1H), 6.94 (s, 1H), 6.80–6.76 (m, 2H), 5.37 (s, 1H), 5.31 (d, J = 17.0, 1H), 5.21 (d, J = 10.7, 1H), 5.01 (dd, J = 17.0, 10.7, 1 H), 3.20 (s, 3H), 3.04 (s, 1H), 1.91 (s, 3H), 1.88 (s, 3H), 1.64 (s, 3H), 1.02 (s, 3H); ^{2}H NMR (77 MHz, $CDCl_3$) δ 5.87 (br. s, 1D); ^{13}C NMR (23 of 24 observed, 125 MHz, $CDCl_3$): δ 203.1, 171.4, 168.9, 158.4, 145.9, 137.3, 136.5, 131.0, 124.7, 122.6, 118.0, 108.2, 84.3, 70.4, 58.2, 56.3, 48.9, 41.2, 27.1, 25.3, 22.7, 22.6, 21.4; IR (film): 1762, 1732, 1712, 1611, 1597, 1463 cm^{-1}; HRMS-ESI (m/z) $[M + Na]^+$ calcd for $C_{24}H_{24}O_6DN_2BrNa$, 540.0856; found 540.0858; $[\alpha]^{26.9}_D$ – 18.40° (c = 1.000, $CHCl_3$). Ether **1.3**: mp: 317.0 ºC (decomp.); R_f 0.53 (1:3 hexanes:EtOAc); ^{1}H

NMR (500 MHz, $CDCl_3$): δ 7.67 (s, 1H), 7.25 (app t, J = 7.9, 1H), 6.93 (dd, J = 7.9, 0.64, 1H), 6.81 (dd, J = 7.9, 0.64, 1H), 5.22 (dd, J = 17.2, 10.7, 1H), 4.96–4.89 (m, 2H), 4.78 (d, J = 10.7, 1H), 3.30 (d, J = 7.5, 1H), 3.23 (s, 3H), 1.45 (s, 3H), 1.42 (s, 3H), 1.02 (s, 3H); ^{2}H NMR (77 MHz, $CDCl_3$) δ 4.69 (br. s, 1D); ^{13}C NMR (125 MHz, $CDCl_3$): δ 205.2, 171.9, 158.7, 142.8, 137.6, 136.3, 130.4, 126.6, 122.3, 116.4, 108.6, 88.8, 83.3, 81.4 (t, $J_{C–D}$ = 22.6), 70.2, 59.4, 51.4, 48.9, 26.9, 25.4, 21.2, 19.6; IR (film): 1774, 1724, 1710, 1605 cm^{-1}; HRMS-ESI (m/z) $[M + Na]^+$ calcd for $C_{22}H_{21}O_5DN_2Na$, 418.1489; found 418.1476; $[\alpha]^{21.3}_D$ –157.20° (c = 1.000, $CHCl_3$).

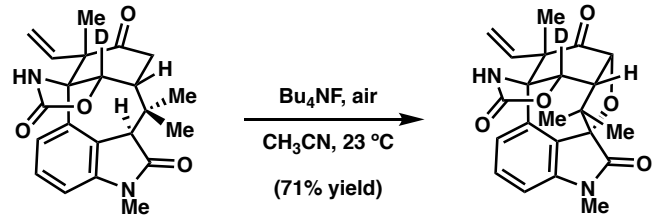

1.4 *1.3*

Ether 1.3. To a solution of ketone **1.4** (30 mg, 0.079 mmol, 1.0 equiv) in CH_3CN (7.9 mL) was added Bu_4NF (1.0 M in THF, 236 μL, 0.236 mmol, 3.0 equiv) in a dropwise manner. The reaction mixture was stirred for 1 min, then opened to air for 30 seconds. The reaction vessel was sealed and left to stir at room temperature. After 2 h, the reaction was quenched with a solution of saturated aqueous NH_4Cl (5 mL). The resulting mixture was transferred to a separatory funnel with EtOAc (10 mL) and H_2O (10 mL). The resulting biphasic mixture was extracted with EtOAc (3 x 10 mL). The organic layers were combined, dried over $MgSO_4$, and evaporated under reduced pressure. The crude residue was purified by flash chromatography (1:1 hexanes:EtOAc) to afford ether **1.3** (22 mg, 71% yield) as a white solid.

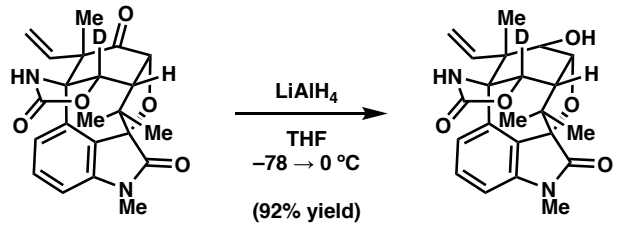

1.3 *1.15*

Alcohol 1.15. To a solution of ether **1.3** (9.4 mg, 0.024 mmol, 1.0 equiv) in THF (2.3 mL) at –78 ºC was added $LiAlH_4$ (1.0 M in THF, 24 μL, 0.024 mmol, 1.0 equiv) in a dropwise manner. After 5 min, the reaction mixture was warmed to 0 ºC. After 20 min, the reaction was quenched at 0 °C with slow addition of a saturated aqueous solution of Rochelle's salt (3.0 mL) and then allowed to warm to 23 ºC. The mixture was stirred at room temperature for 30 min, and then transferred to a separatory funnel with EtOAc (10 mL) and H_2O (10 mL). The resulting biphasic mixture was extracted with EtOAc (3 x 10 mL). The organic layers were combined, dried over $MgSO_4$, and evaporated under reduced pressure. The resulting residue was purified by preparative thin layer chromatography (1:2 $CHCl_3$:EtOAc) to afford alcohol **1.15** (8.7 mg, 92% yield) as a white solid. Alcohol **1.15**: mp: 263.0 ºC; R_f 0.15 (1:3 hexanes:EtOAc); ^{1}H NMR (500 MHz, $CDCl_3$): δ 7.60 (s, 1H), 7.19 (app t, *J* = 7.9, 1H), 6.82 (d, *J* = 7.9, 1H), 6.77 (d, *J* = 7.9, 1H), 5.21 (dd, *J* = 17.4, 10.8, 1 H), 5.09–5.03 (m, 2H), 4.94 (d, *J* = 10.8, 1H), 3.72 (dd, *J* = 11.1, 2.0, 1H), 3.22 (s, 3H), 3.02 (d, J = 7.5, 1H), 2.02 (d, J = 11.1, 1 H), 1.43 (s, 3H), 1.41 (s, 3H), 0.94 (s, 3H); ^{2}H NMR (77 MHz, $CDCl_3$) δ 4.79 (br. s, 1D); ^{13}C NMR (21 of 22 observed, 125 MHz, $CDCl_3$): δ 173.0, 159.4, 142.4, 139.0, 136.4, 130.2, 126.9, 122.4, 117.9, 108.2, 87.3, 82.0, 76.1, 70.9, 49.2, 48.7, 48.3, 26.8, 25.6, 21.3, 19.6; IR (film): 1752, 1722, 1603, 1462 cm^{-1}; HRMS-ESI (*m/z*) $[M + Na]^+$ calcd for $C_{22}H_{23}O_5DN_2Na$, 420.1646; found 420.1631; $[\alpha]^{24.1}_D$ – 49.20° (*c* = 1.000, $CHCl_3$).

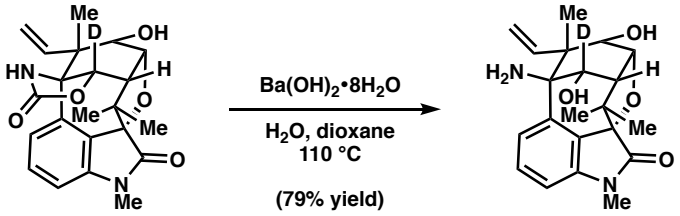

1.15 *1.18*

Aminodiol 1.18. A Schlenk tube was charged with alcohol **1.15** (7.30 mg, 0.0184 mmol, 1.0 equiv) and $Ba(OH)_2 \cdot 8H_2O$ (46.3 mg, 0.147 mmol, 8.0 equiv). The reaction vessel was then evacuated and backfilled with N_2 three times. A 2:1 mixture of 1,4-dioxane:H_2O (634 μL) that had been taken through six freeze-pump-thaw cycles prior to use was then added to the Schlenk tube. The vessel was then sealed and allowed to stir at 110 °C. After 21 h, the contents of the Schlenk tube were transferred to a separatory funnel with EtOAc (5 mL) and H_2O (5 mL). The resulting biphasic mixture was extracted with EtOAc (3 x 5 mL). The organic layers were combined, dried over Na_2SO_4, and evaporated under reduced pressure. The resulting residue was purified by preparative thin layer chromatography (3:1 $CHCl_3$:MeOH) to afford **1.18** (5.4 mg, 79% yield) as a white solid. Aminodiol **1.18**: R_f 0.12 (9:1 $CHCl_3$:MeOH); ^{1}H NMR (500 MHz, D_2O, 22 of 25 observed): δ 7.37 (app t, J = 8.3, 1H), 7.18 (d, J = 8.3, 1H), 7.02 (d, J = 8.2, 1H), 5.50 (dd, J = 17.6, 11.0, 1H), 4.96 (dd, J = 7.3, 1.8, 1 H), 4.92 (d, J = 17.6, 1H), 3.88 (d, J = 1.8, 1H), 3.23 (s, 3H), 2.83 (d, J = 7.3, 1H), 1.91 (s, 2H), 1.37 (s, 3H), 1.28 (s, 3H), 0.85 (s, 3H).

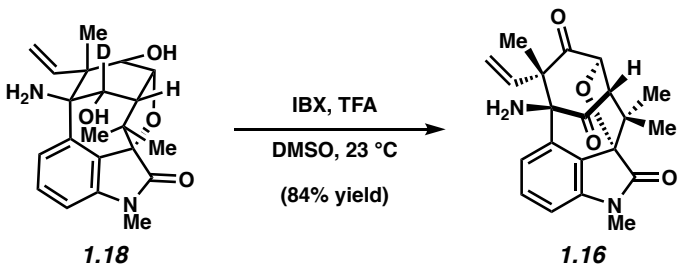

1.18 *1.16*

Aminodiketone 1.16. To a solution of **1.18** (5.4 mg, 0.014 mmol, 1.0 equiv) in DMSO (500 μL) was added TFA (1.2 μL, 0.016 mmol, 1.10 equiv). The mixture was stirred at room temperature. After 5 min, IBX (20.4 mg, 0.0728 mmol, 5.0 equiv) was added in one portion and the vial was flushed with N_2. After stirring at room temperature for 20 h, the reaction mixture transferred to a separatory funnel with a solution of aqueous K_2CO_3 (5 mL, concentration of 50 mg/mL) and EtOAc (5 mL). The resulting biphasic mixture was extracted with EtOAc (3 x 5 mL) and the organic layers were combined, dried over Na_2SO_4, and evaporated under reduced pressure. The resulting residue was purified by preparative thin layer chromatography (9:1 $CHCl_3$:MeOH) to afford aminodiketone **1.16** (4.5 mg, 84% yield) as a white solid. Aminodiketone **1.16**: mp: 190–191 ºC; R_f 0.73 (9:1 CH_3Cl:MeOH); ^{1}H NMR (500 MHz, $CDCl_3$): δ 7.35 (dd, *J* = 8.2, 7.6, 1H), 7.29 (dd, *J* = 8.2, 1.0, 1H), 6.80 (dd, *J* = 7.6, 1.0, 1H), 5.64 (dd, *J* = 17.4, 10.7, 1H), 5.40 (d, *J* = 10.7, 1 H), 5.21 (d, *J* = 17.4, 1H), 4.93 (d, *J* = 7.6, 1H), 3.49 (d, *J* = 7.6, 1H), 3.20 (s, 3H), 2.04 (br. s, 2H), 1.59 (s, 3H), 1.19 (s, 3H), 0.78 (s, 3H); ^{13}C NMR (21 of 22 observed, 125 MHz, $CDCl_3$): δ 204.9, 204.4, 170.2, 143.6, 134.8, 134.8, 130.3, 125.8, 124.2, 118.9, 108.9, 86.5, 79.4, 69.4, 62.5, 62.1, 52.4, 26.9, 25.3, 20.0, 17.6; IR (film): 1718, 1609, 1582, 1459, 1366 cm^{-1}; HRMS-ESI (*m/z*) [M + Na]$^+$ calcd for $C_{21}H_{22}O_4DN_2Na$, 389.1477; found 389.1469; $[\alpha]^{22.9}_D$ +29.20° (*c* = 1.000, $CHCl_3$).

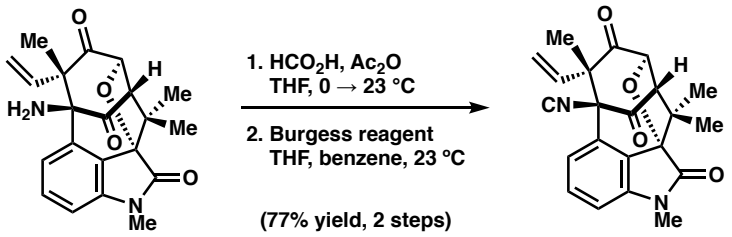

1.16 *(+)-1.2*

(+)-*N*-Methylwelwitindolinone D Isonitrile (1.2). A 1-dram vial was charged with 96% formic acid (0.100 mL) and acetic anhydride (0.100 mL). The resulting mixture was stirred at 60 °C for 1 h. The reaction vessel was cooled to room temperature and 39 μL of the 96% formic acid/acetic anhydride mixture was added to a solution of aminodiketone **1.16** (4.2 mg, 0.010 mmol, 1.0 equiv) in THF (765 μL) at 0 °C. The reaction was then warmed to room temperature. After 2 h, the reaction mixture was transferred to a test tube with EtOAc (2 mL) and a solution of saturated aqueous $NaHCO_3$ (1 mL). The resulting biphasic mixture was extracted with EtOAc (4 x 2 mL). The organic layers were combined, dried over $MgSO_4$, and evaporated under reduced pressure to afford the crude product, which was used directly in the subsequent reaction.

To a vial containing the crude product from the previous step was added THF (600 μL) and benzene (600 μL), followed by Burgess reagent (3.5 mg, 0.011 mmol, 1.0 equiv). The vial was flushed with N_2 and allowed to stir at room temperature for 40 min. An additional amount of Burgess reagent (3.5 mg, 0.015 mol, 1.0 equiv) was then added, and the reaction was allowed to stir at room temperature for 10 min. The reaction was then filtered by passage over a plug of silica gel (EtOAc eluent, 10 mL). The filtrate was evaporated under reduced pressure, and the resulting residue was purified by preparative thin layer chromatography (1:1 hexanes:EtOAc) to afford (+)-**1.2** (3.3 mg, 77% yield, 2 steps) as a white solid. Spectral data for ^{1}H NMR, ^{13}C NMR, and IR for synthetic **1.2** was consistent with literature reports.[2b] (+)-*N*-Methylwelwitindolinone D isonitrile (**1.2**): mp: 156 ºC; R_f 0.50 (1:1 hexanes:EtOAc); ^{1}H NMR (500 MHz, CD_2Cl_2): δ 7.45

(dd, J = 8.3, 7.9, 1H), 7.29 (dd, J = 8.3, 0.7, 1H), 6.93 (dd, J = 7.9, 0.7, 1H), 5.48 (dd, J = 16.3, 10.6, 1H), 5.43 (dd, J = 10.6, 1.5, 1H), 5.35 (dd, J = 16.3, 1.5, 1H), 4.92 (d, J = 7.5, 1H), 3.57 (d, J = 7.5, 1H), 3.19 (s, 3H), 1.55 (s, 3H), 1.39 (s, 3H), 0.80 (s, 3H); ^{13}C NMR (125 MHz, CD_2Cl_2): δ 201.3, 192.8, 169.9, 165.5, 144.4, 133.0, 131.4, 126.8, 125.8, 124.0, 120.6, 110.5, 86.7, 81.1, 79.7, 62.0, 61.7, 53.6, 27.1, 25.0, 20.1, 19.8; IR (film): 2980, 2940, 2139, 1730, 1609, 1592, 1463, 1366, 1344 cm^{-1}; HRMS-ESI (m/z) [M + Na]$^+$ calcd for $C_{22}H_{20}N_2O_4Na$, 399.1321; found 399.1322; $[\alpha]^{22.3}_D$ +4.30° (c = 0.37, CH_2Cl_2). Note: This specific rotation differs from that reported for the natural product ($[\alpha]_D$ –30°, c = 0.37, CH_2Cl_2). This is most likely due to a tabulation error in the isolation report as: (a) the synthesis begins with (S)-carvone >96%+ ee, (b) the specific rotation of bicycle **1.6** in this synthesis is consistent with that of material used in previous syntheses of welwitindolinones,[5b,e] and (c) our specific rotation data has given consistent results across a range of samples and concentrations. Although the sign of rotation differs, the compound we have prepared is assumed to be the natural occurring enantiomer due to its biosynthetic relationship to the *N*-methylweltindolinone C series of natural products, whose absolute configuration have previously been established.[5]

1.11 Spectra Relevant to Chapter One:

Enantiospecific Total Synthesis of *N*-Methylwelwitindolinone D Isonitrile

Evan D. Styduhar, Alexander D. Huters, Nicholas A. Weires, and Neil K. Garg.

Angew. Chem. Int. Ed. **2013**, *52*, 12422–12425.

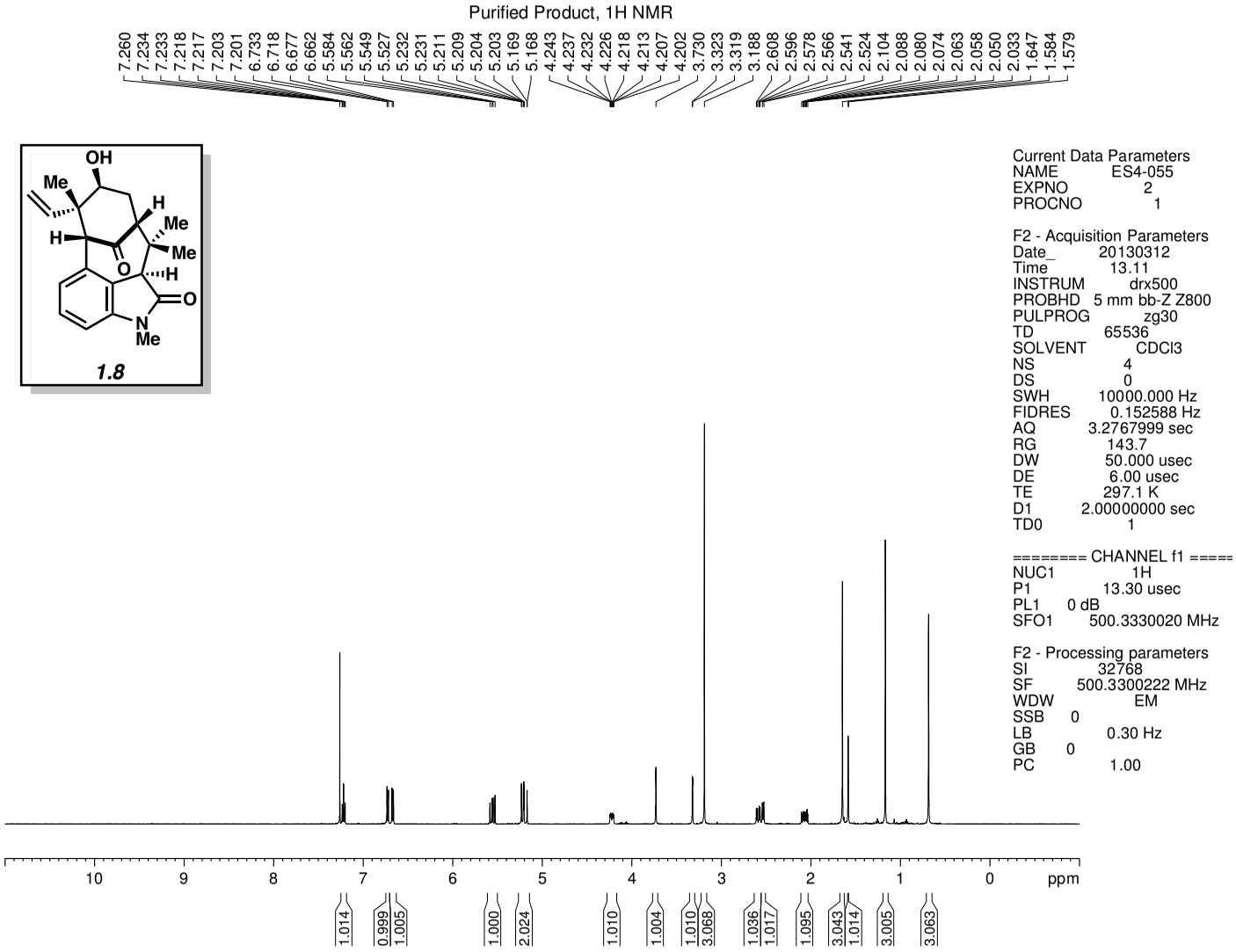

Figure 1.3 ^{1}H NMR (500 MHz, $CDCl_3$) of compound **1.8**.

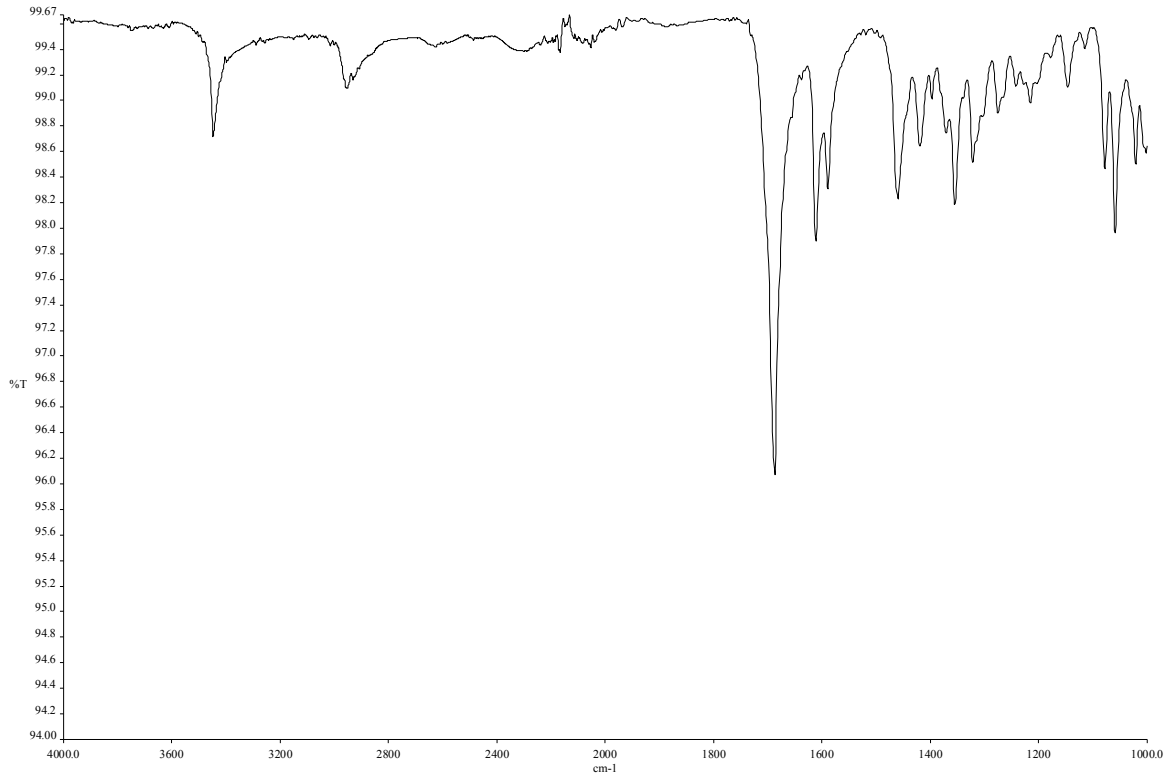

Figure 1.4 Infrared spectrum of compound **1.8**.

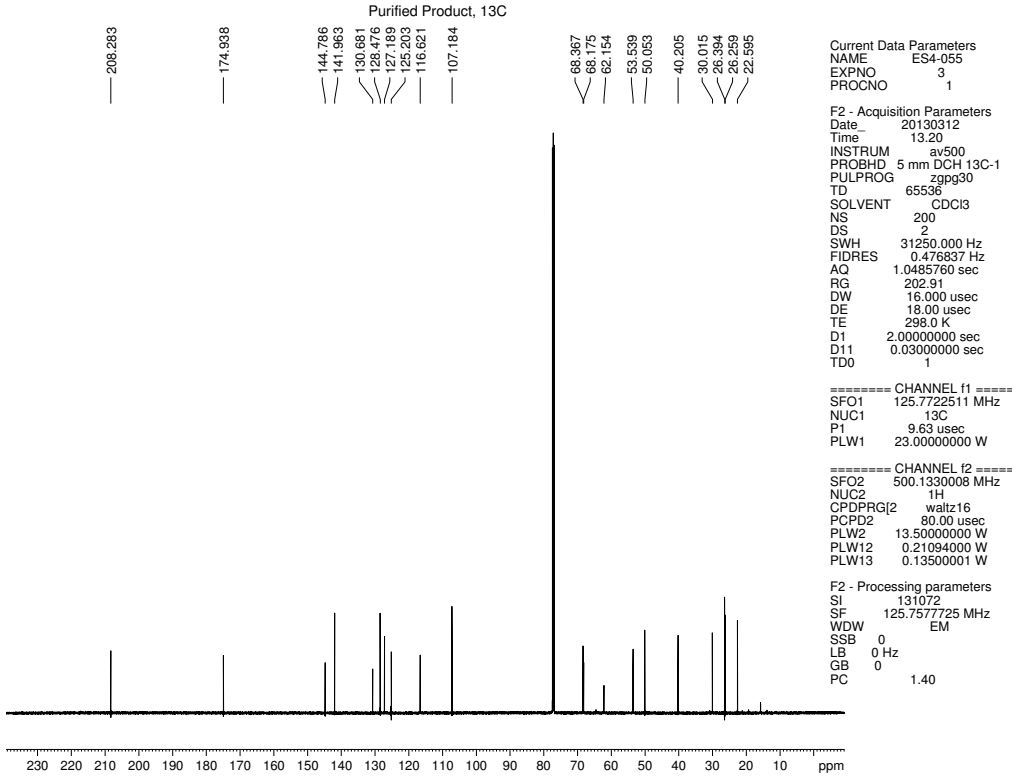

Figure 1.5 ^{13}C NMR (125 MHz, $CDCl_3$) of compound **1.8**.

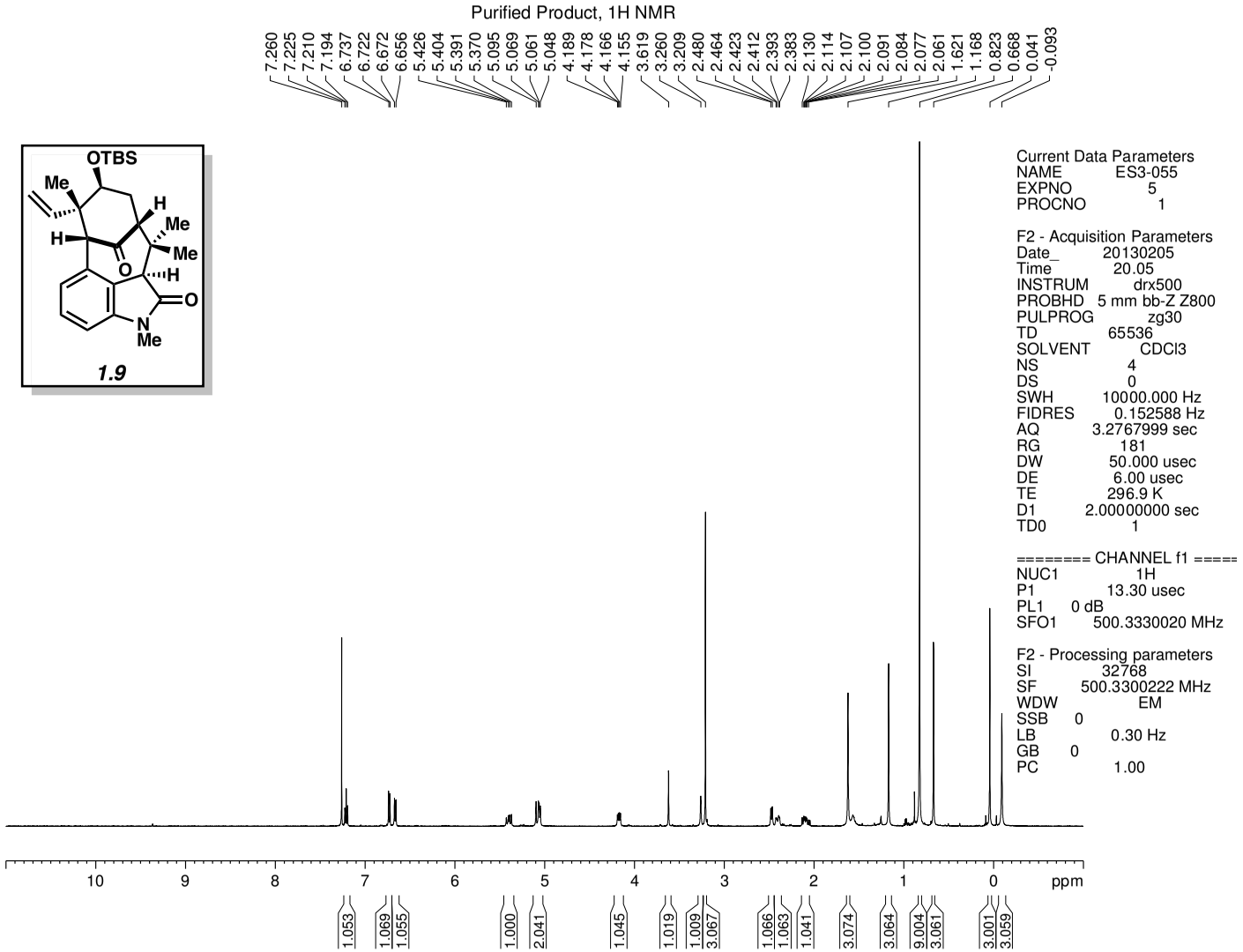

Figure 1.6 ^{1}H NMR (500 MHz, $CDCl_3$) of compound **1.9**.

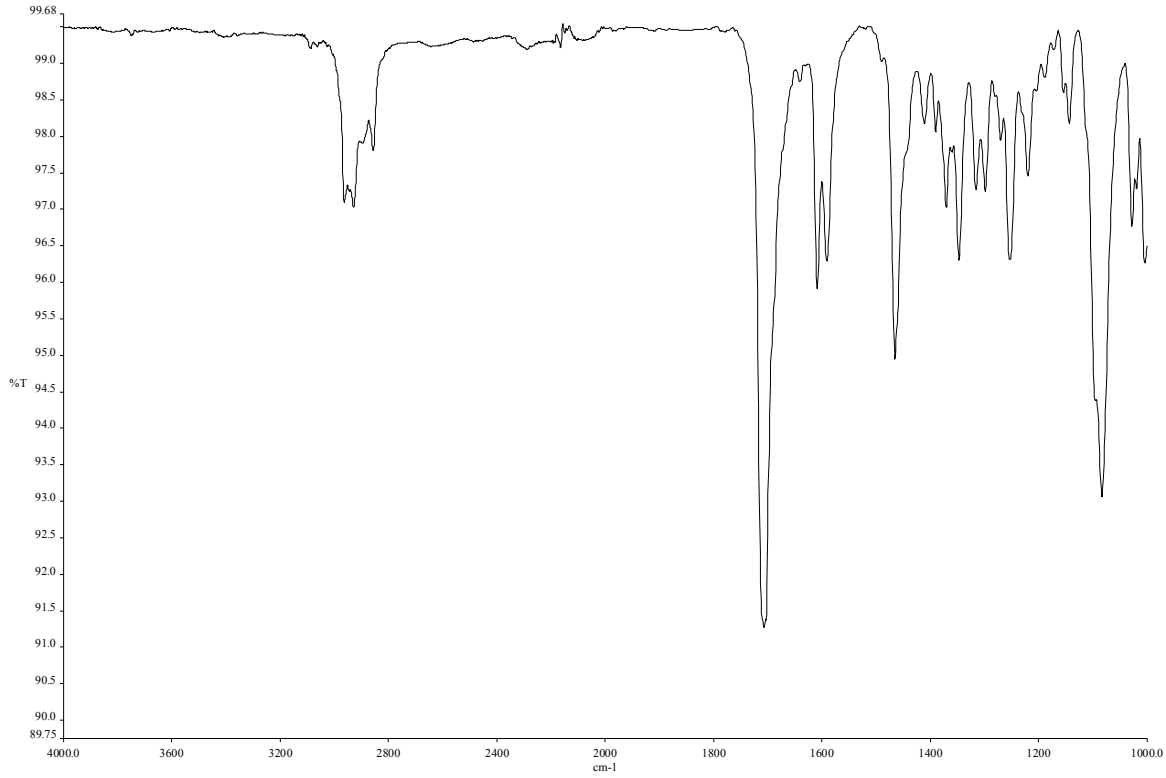

Figure 1.7 Infrared spectrum of compound **1.9**.

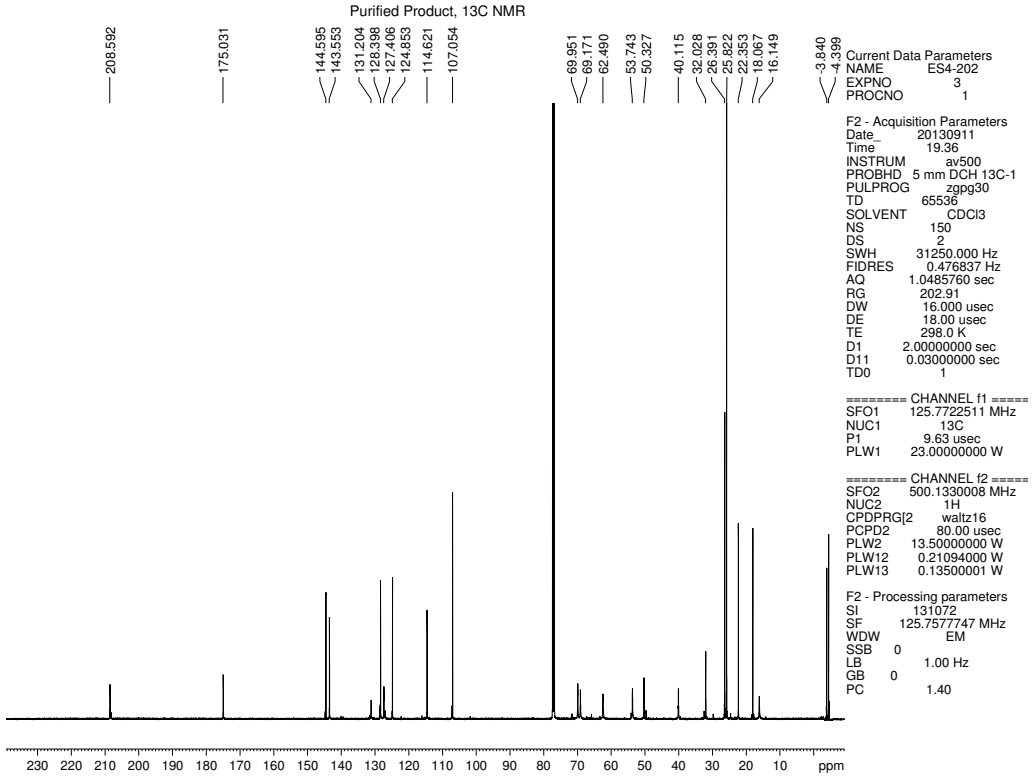

Figure 1.8 ^{13}C NMR (125 MHz, $CDCl_3$) of compound **1.9**.

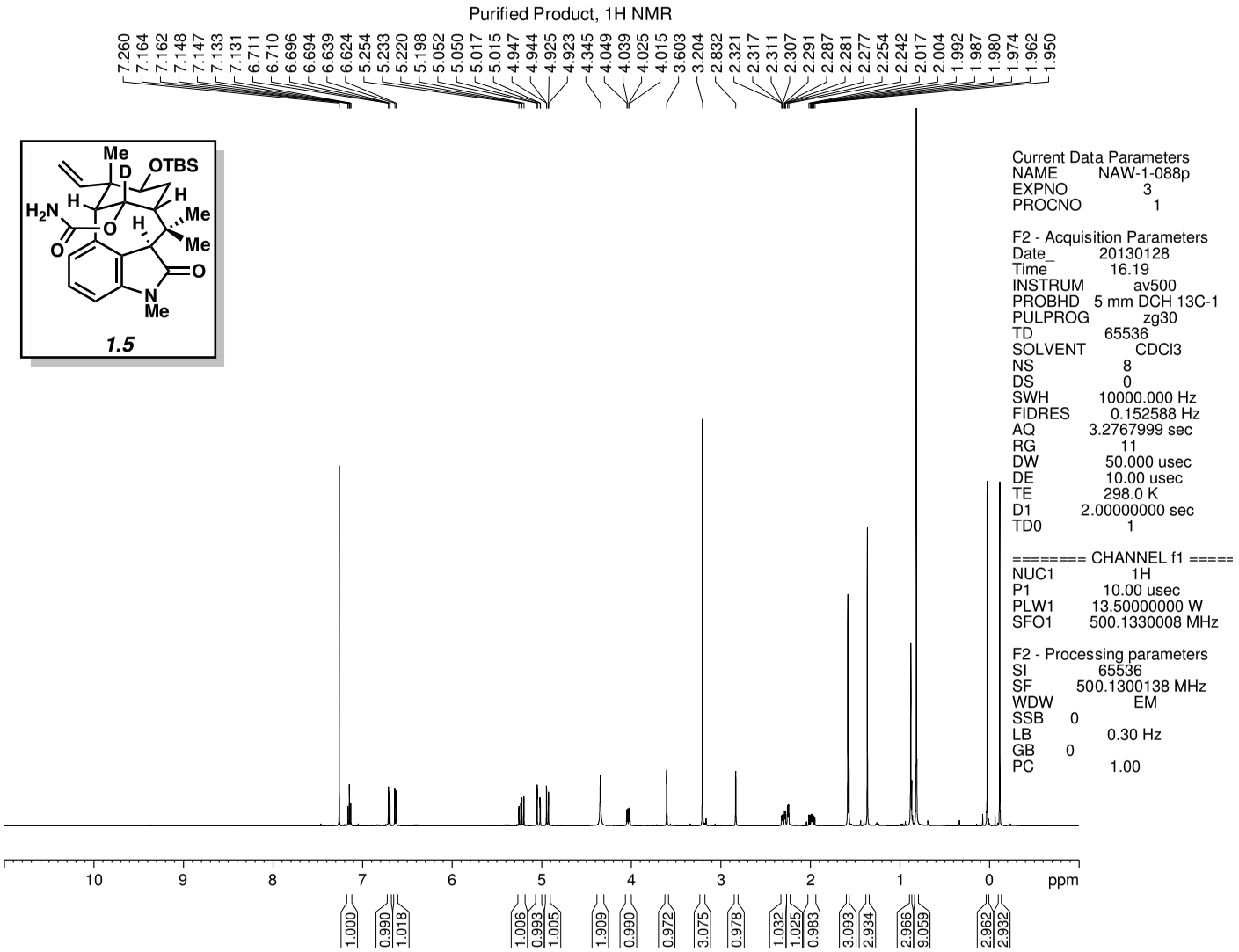

Figure 1.9 ^{1}H NMR (500 MHz, $CDCl_3$) of compound **1.5**.

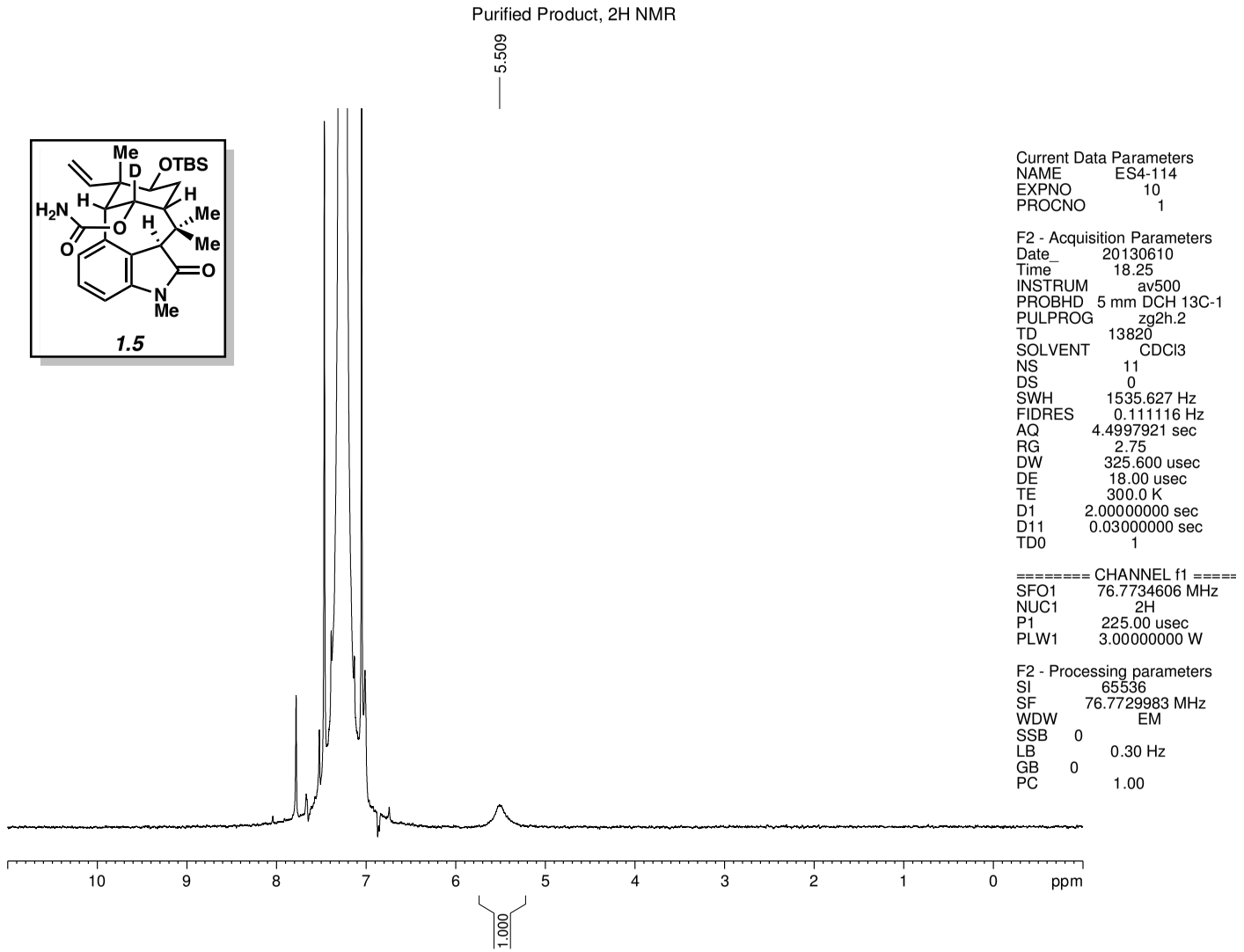

Figure 1.10 ^{2}H NMR (77 MHz, $CDCl_3$) of compound **1.5**.

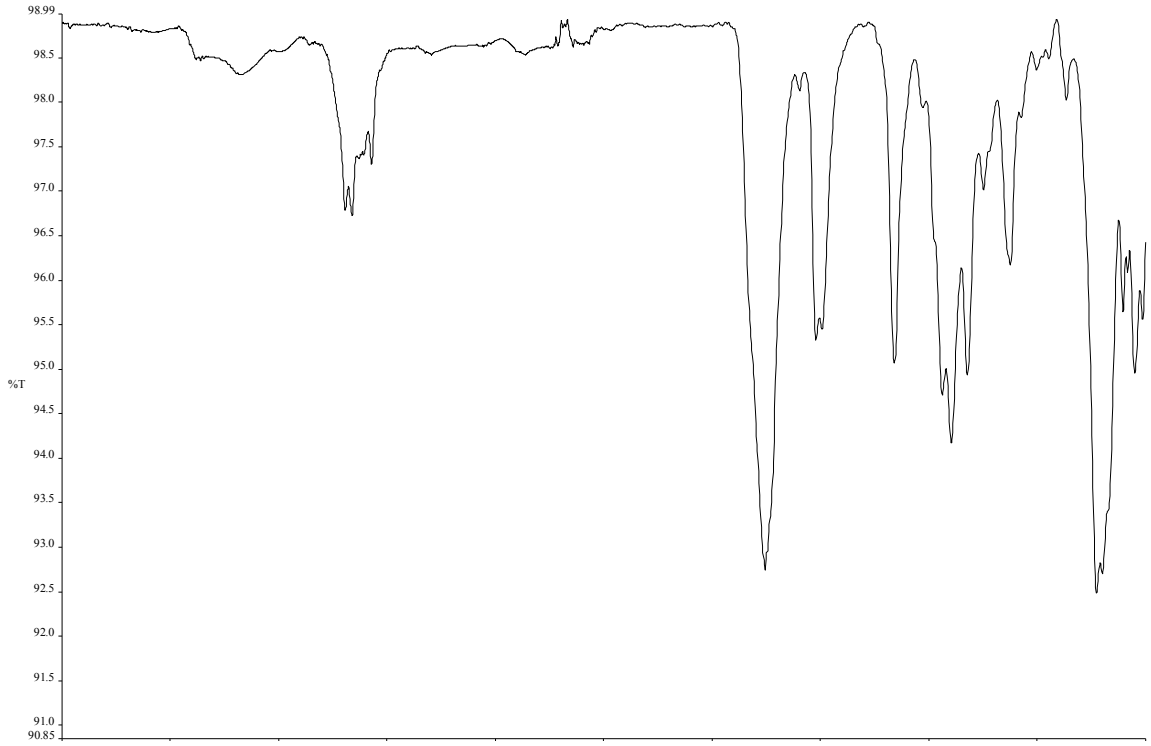

Figure 1.11 Infrared spectrum of compound **1.5**.

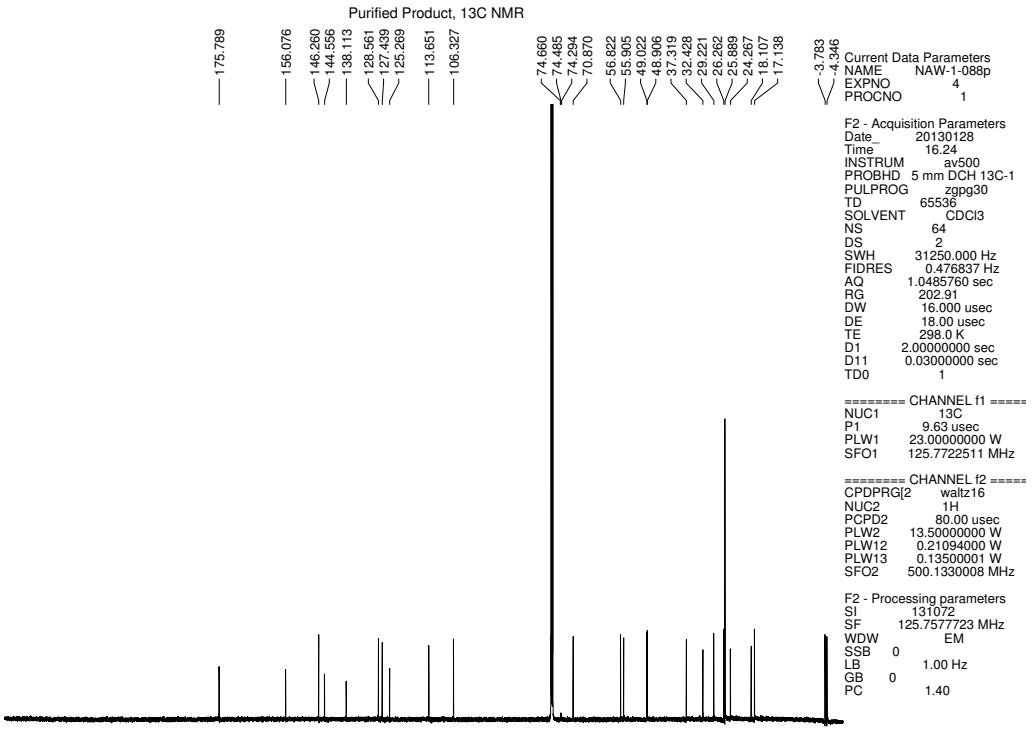

Figure 1.12 ^{13}C NMR (125 MHz, $CDCl_3$) of compound **1.5**.

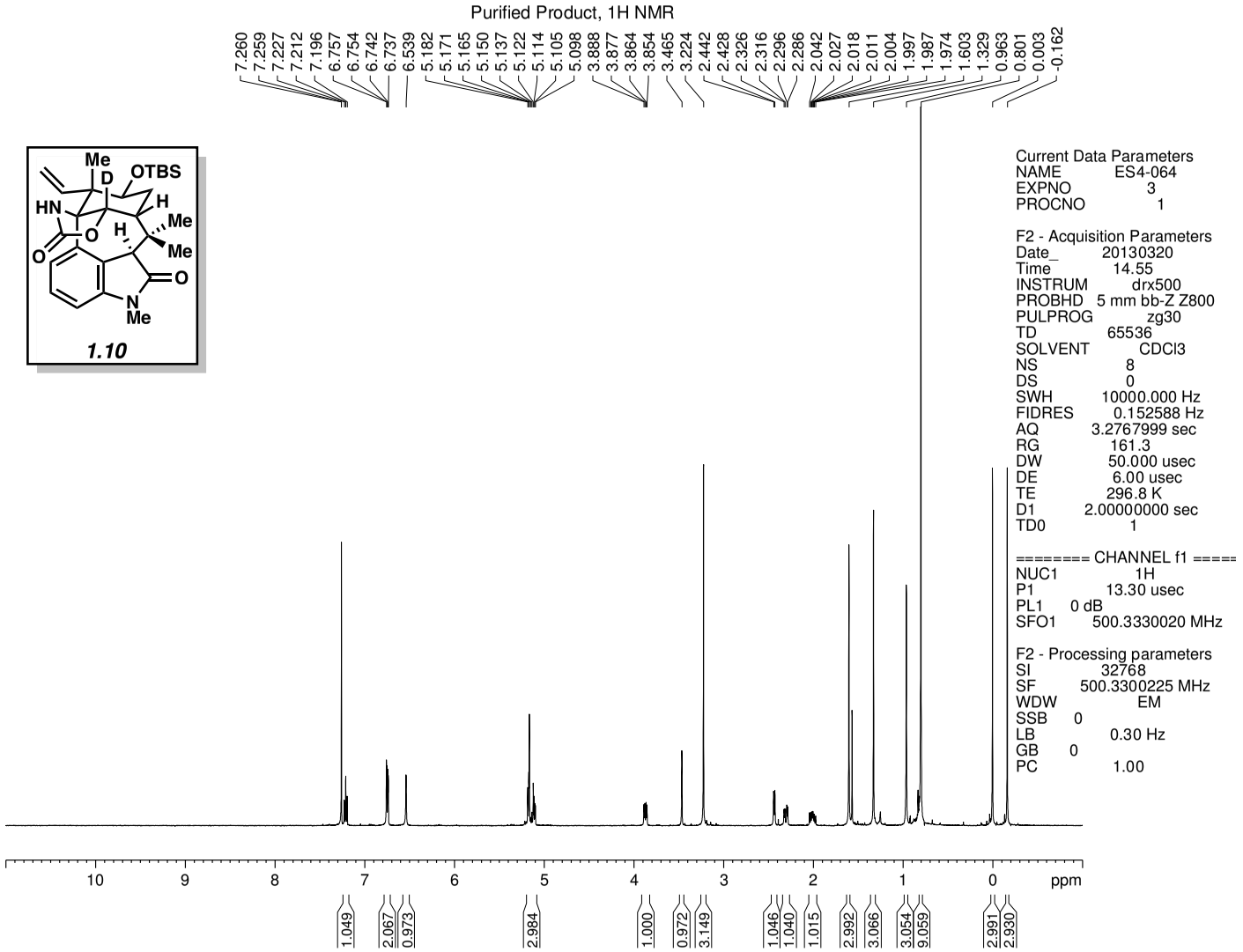

Figure 1.13 ^{1}H NMR (500 MHz, $CDCl_3$) of compound **1.10**.

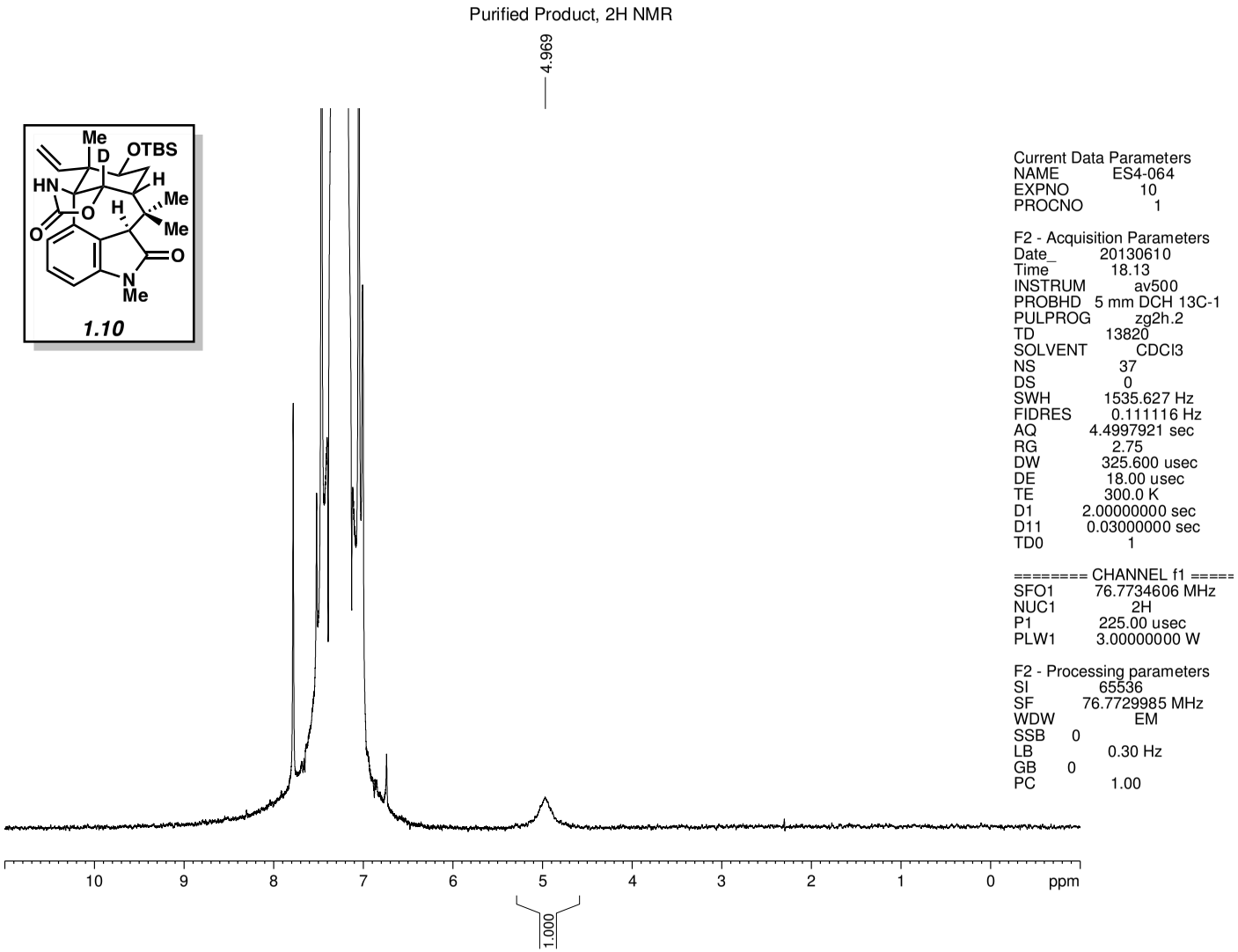

Figure 1.14 ^{2}H NMR (77 MHz, $CDCl_3$) of compound **1.10**.

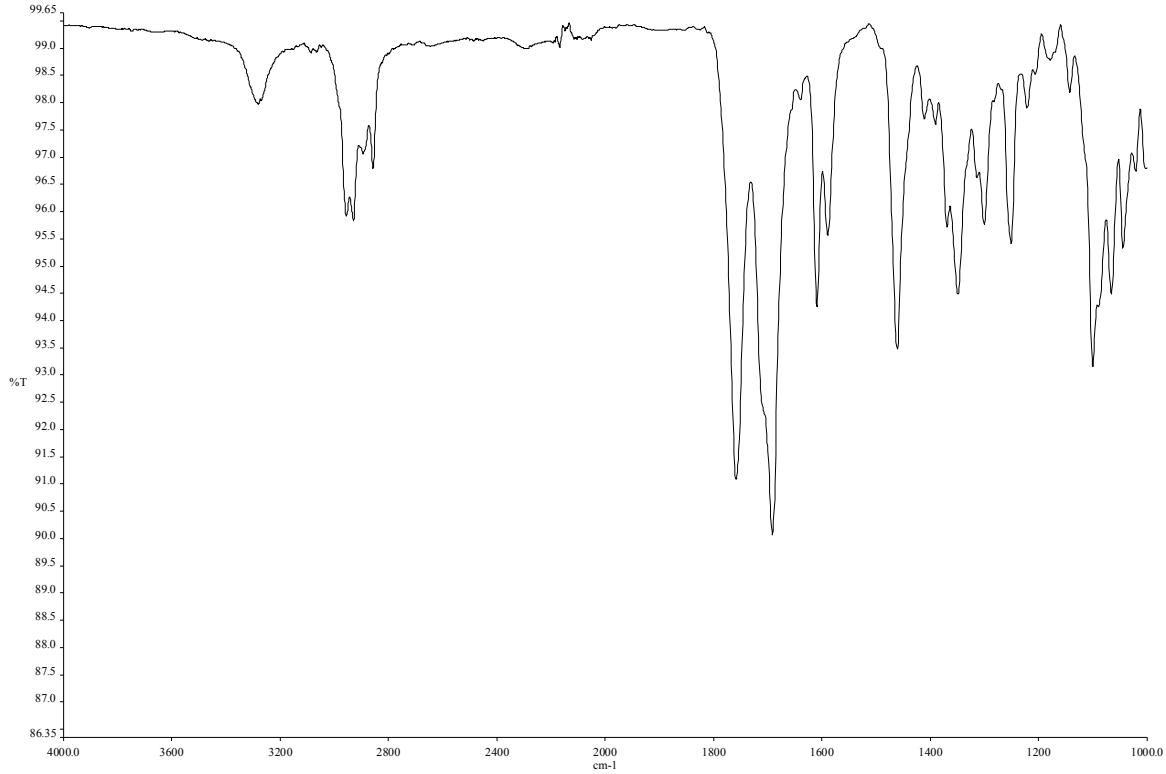

Figure 1.15 Infrared spectrum of compound **1.10**.

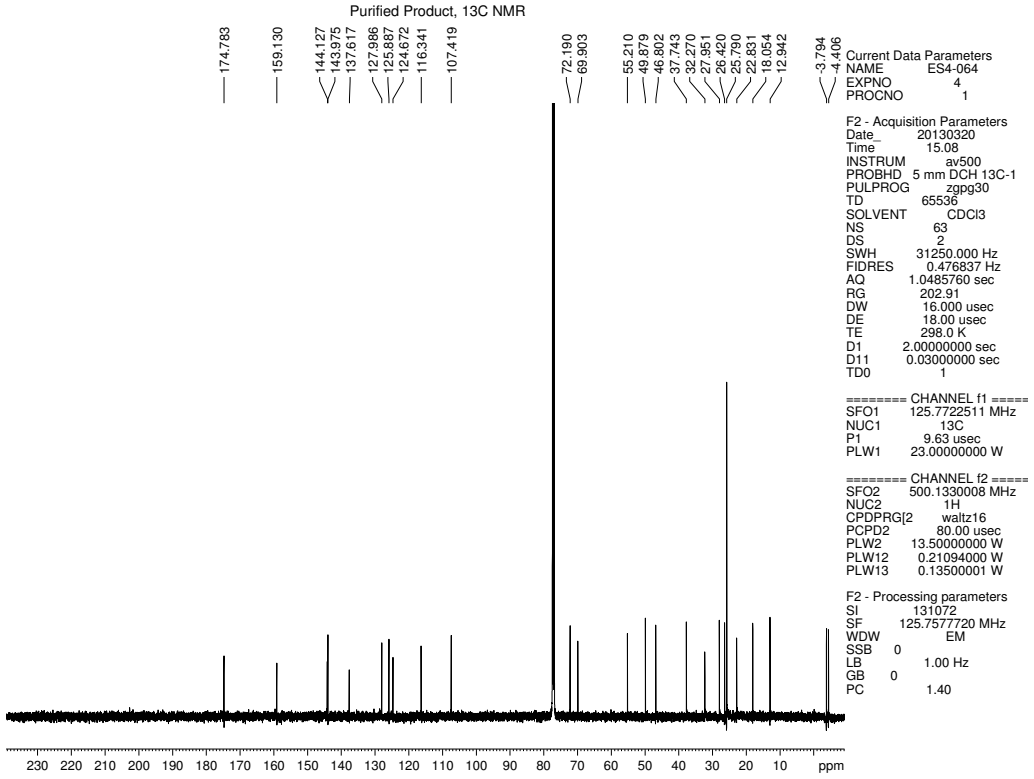

Figure 1.16 ^{13}C NMR (125 MHz, $CDCl_3$) of compound **1.10**.

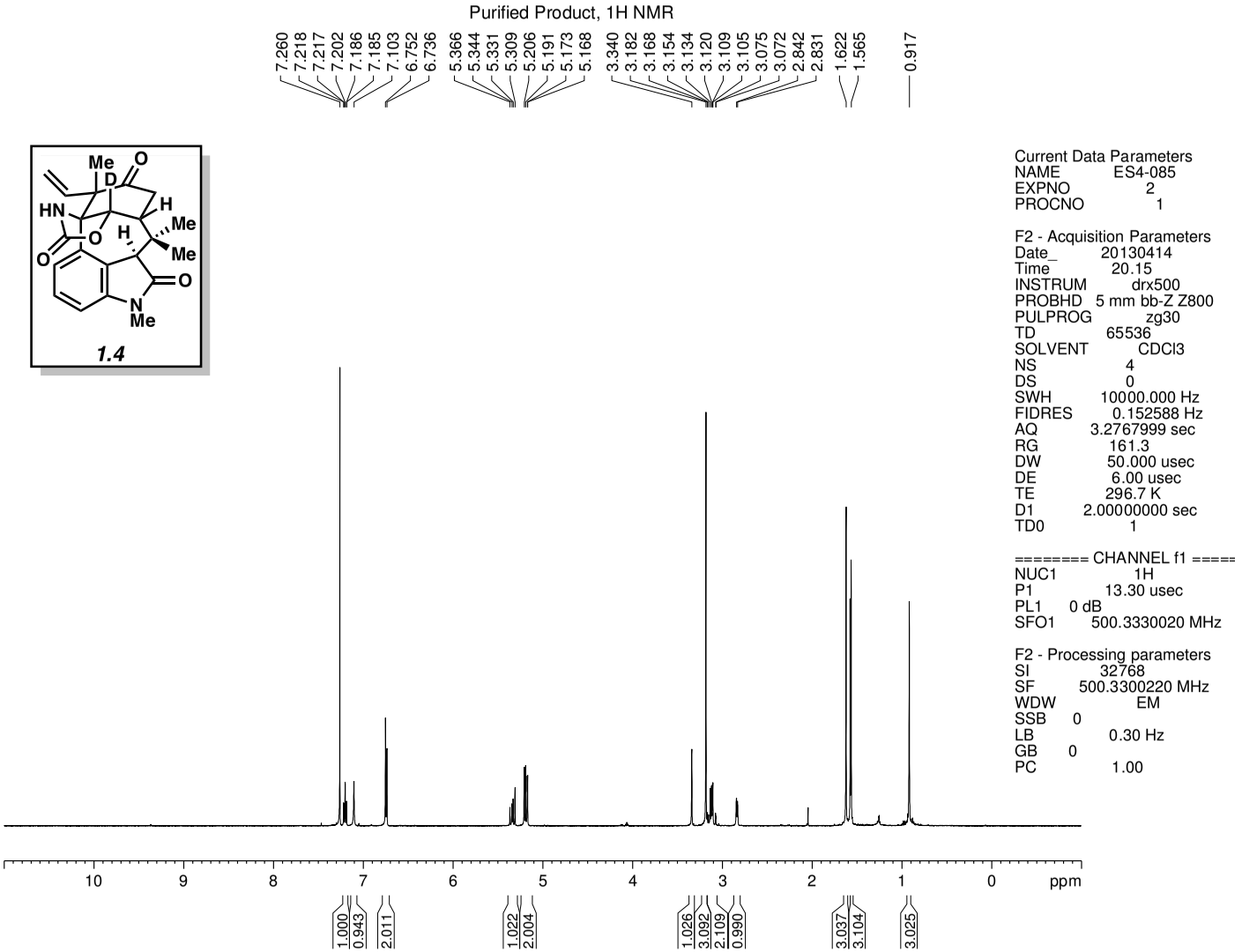

Figure 1.17 ^{1}H NMR (500 MHz, $CDCl_3$) of compound **1.4**.

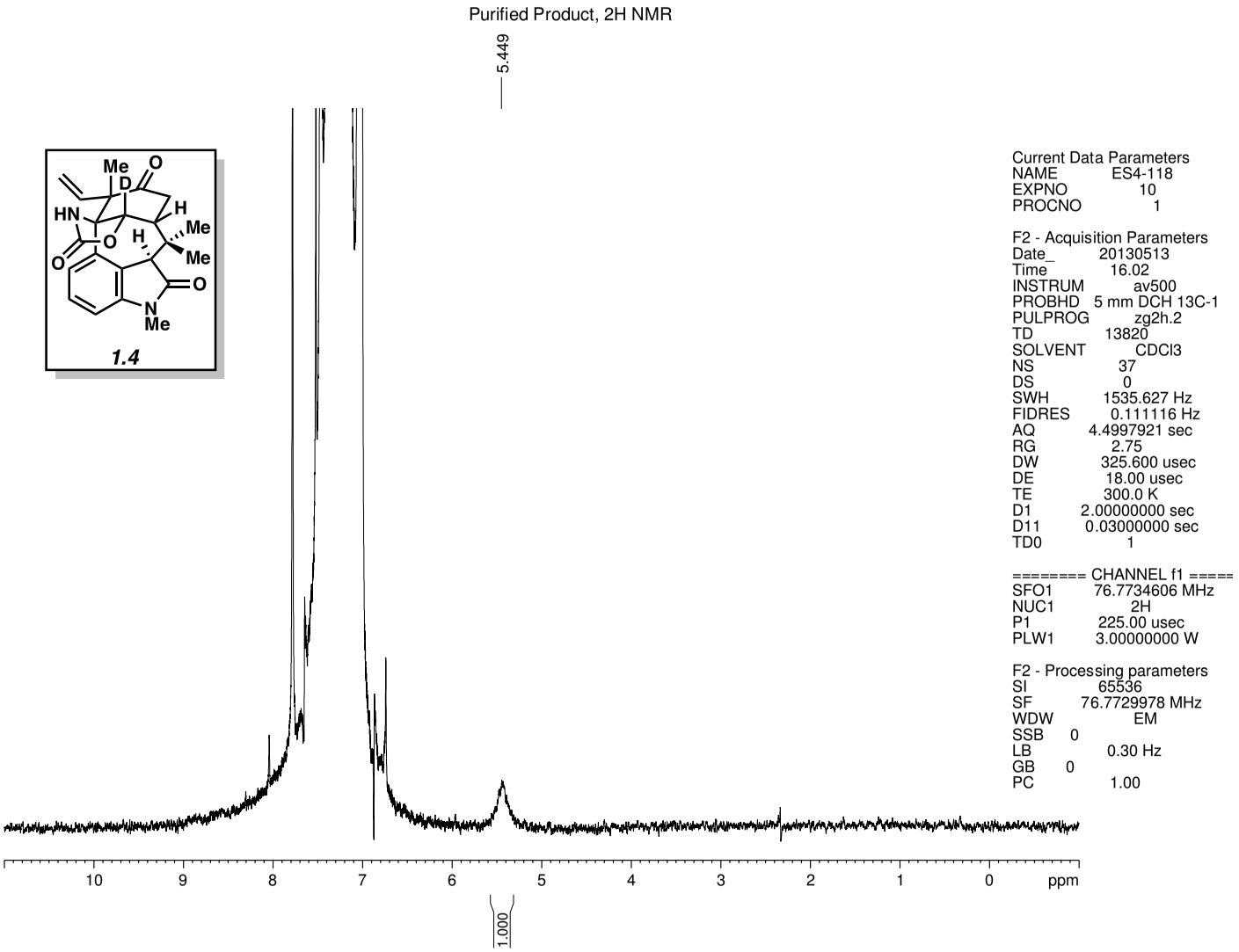

Figure 1.18 ^{2}H NMR (77 MHz, $CDCl_3$) of compound **1.4**.

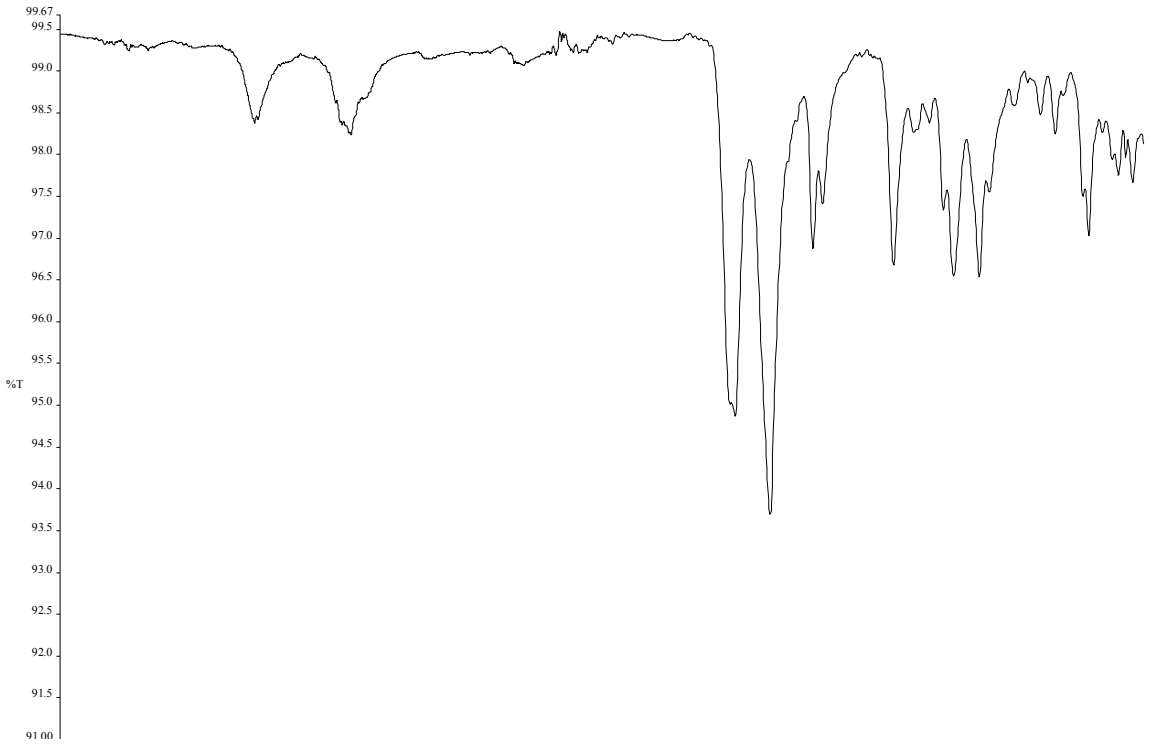

Figure 1.19 Infrared spectrum of compound **1.4**.

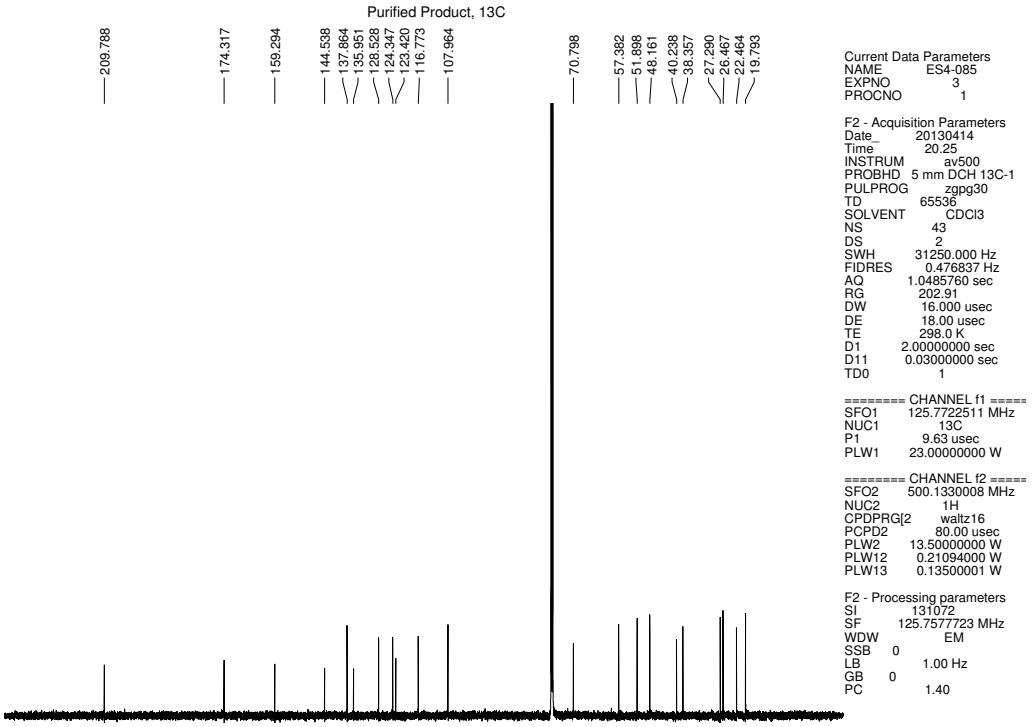

Figure 1.20 ^{13}C NMR (125 MHz, $CDCl_3$) of compound **1.4**.

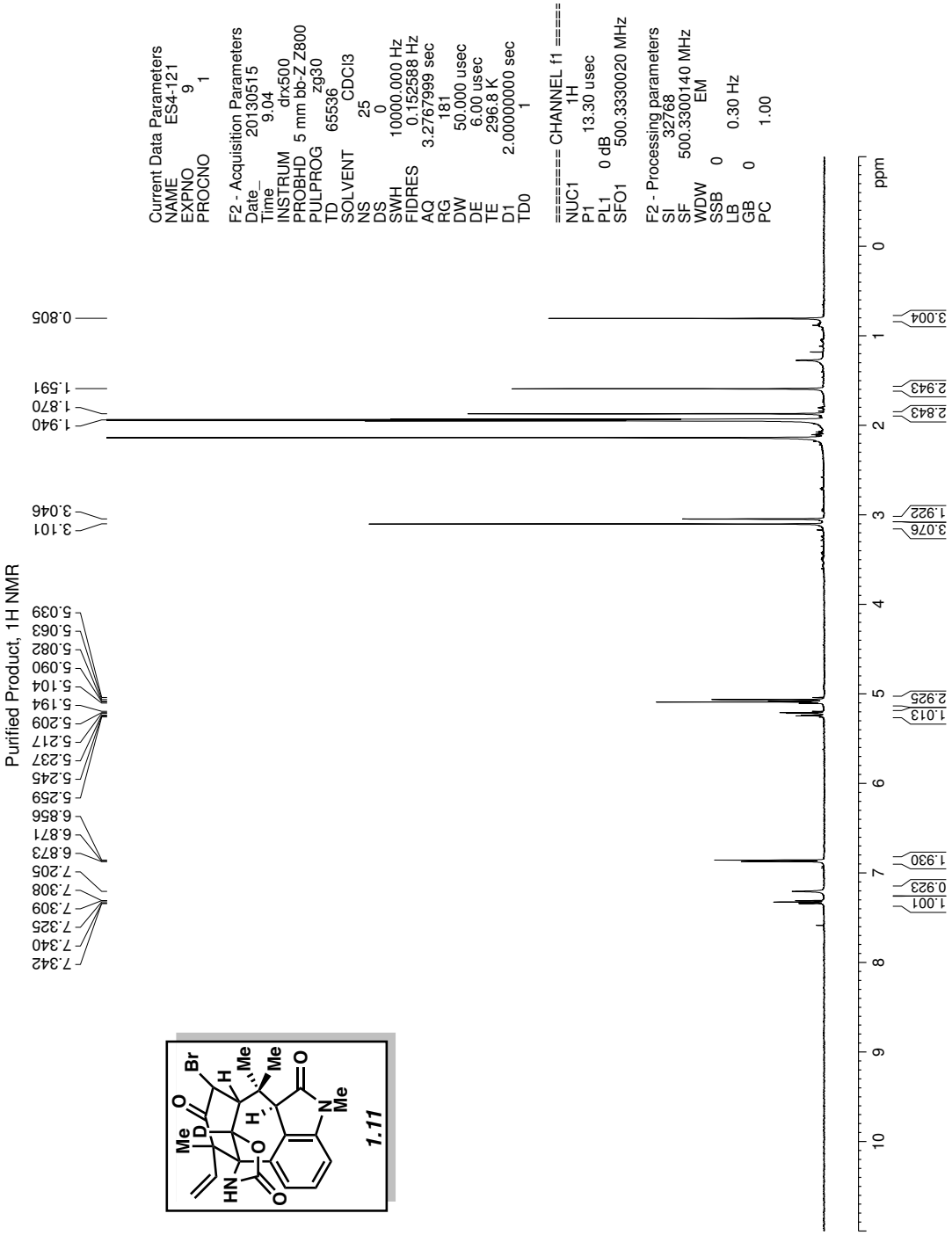

Figure 1.21 ^{1}H NMR (500 MHz, CD_3CN) of compound **1.11**.

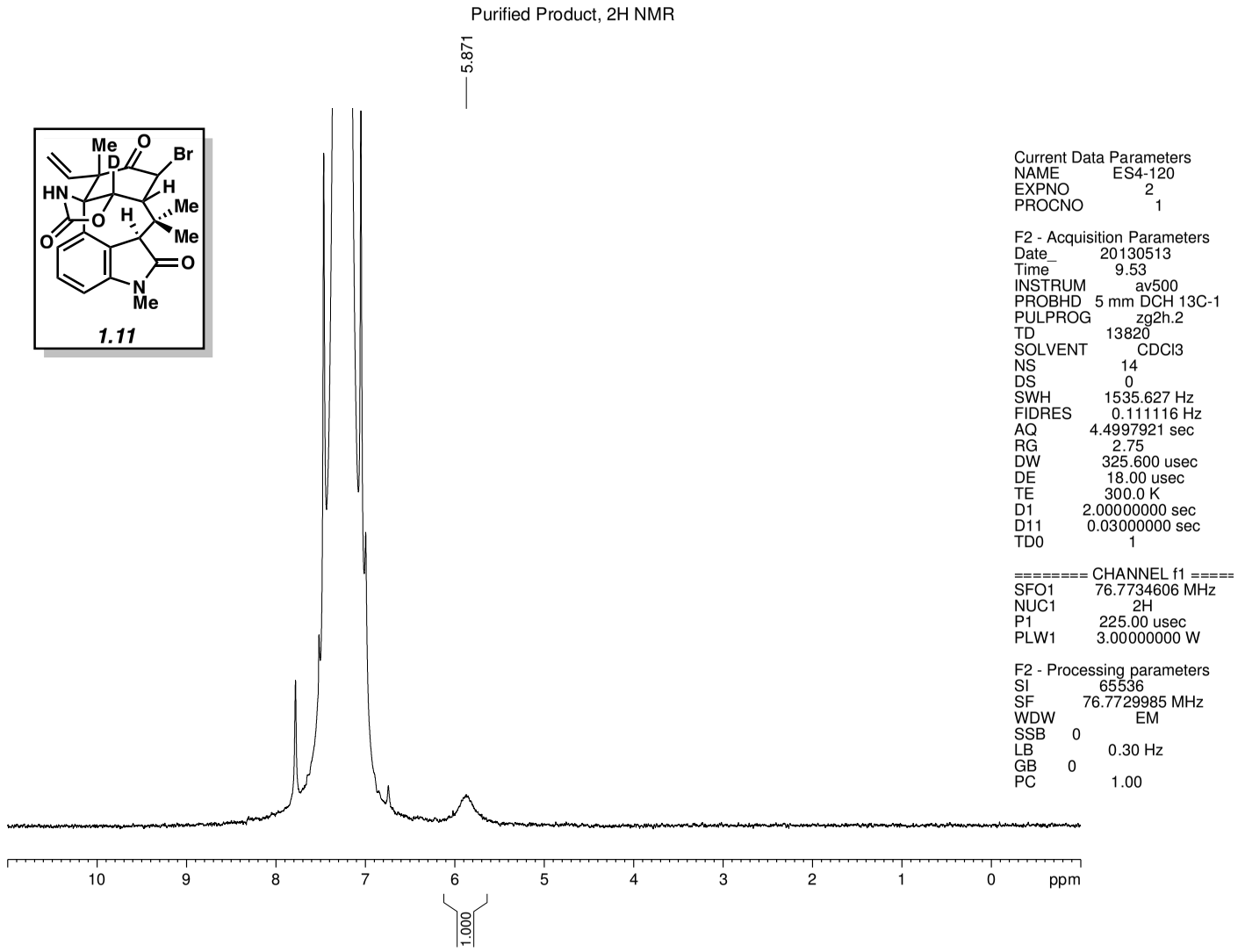

Figure 1.22 ^{2}H NMR (77 MHz, $CDCl_3$) of compound **1.11**.

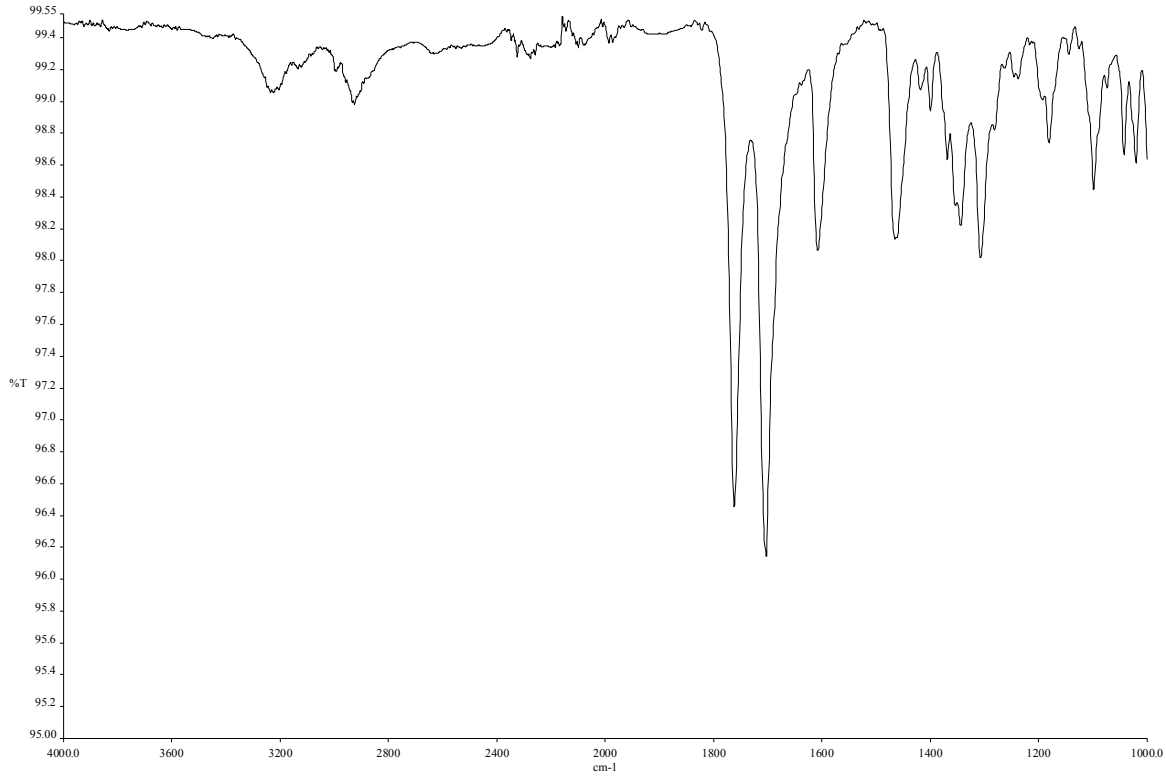

Figure 1.23 Infrared spectrum of compound **1.11**.

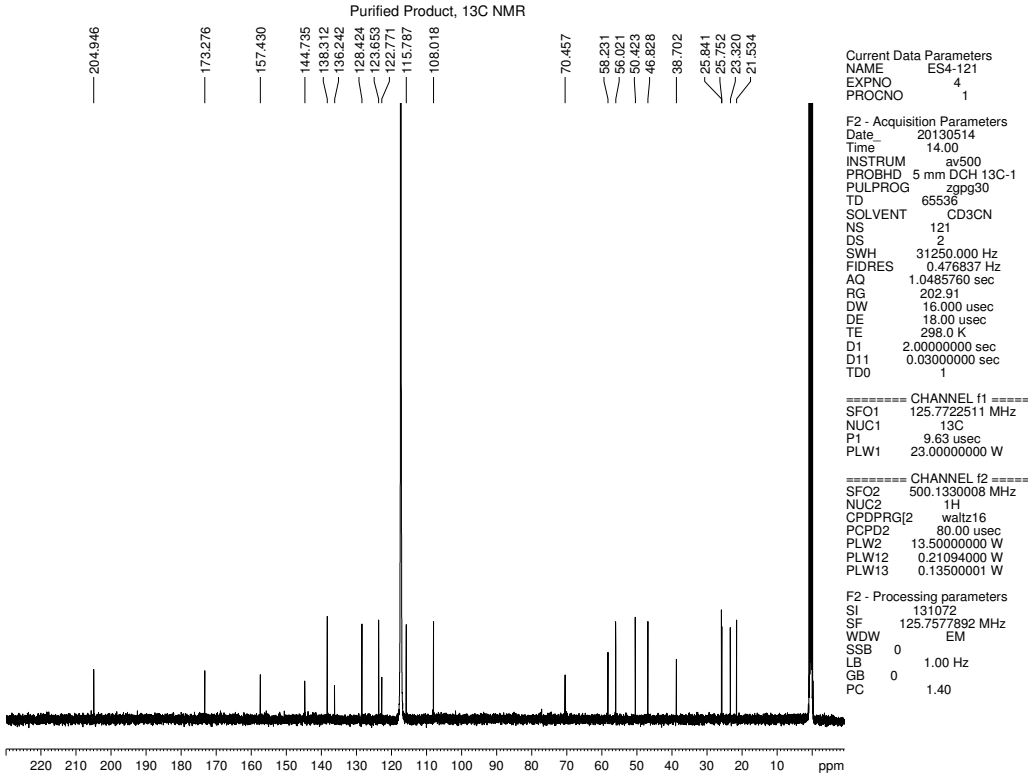

Figure 1.24 ^{13}C NMR (125 MHz, CD_3CN) of compound **1.11**.

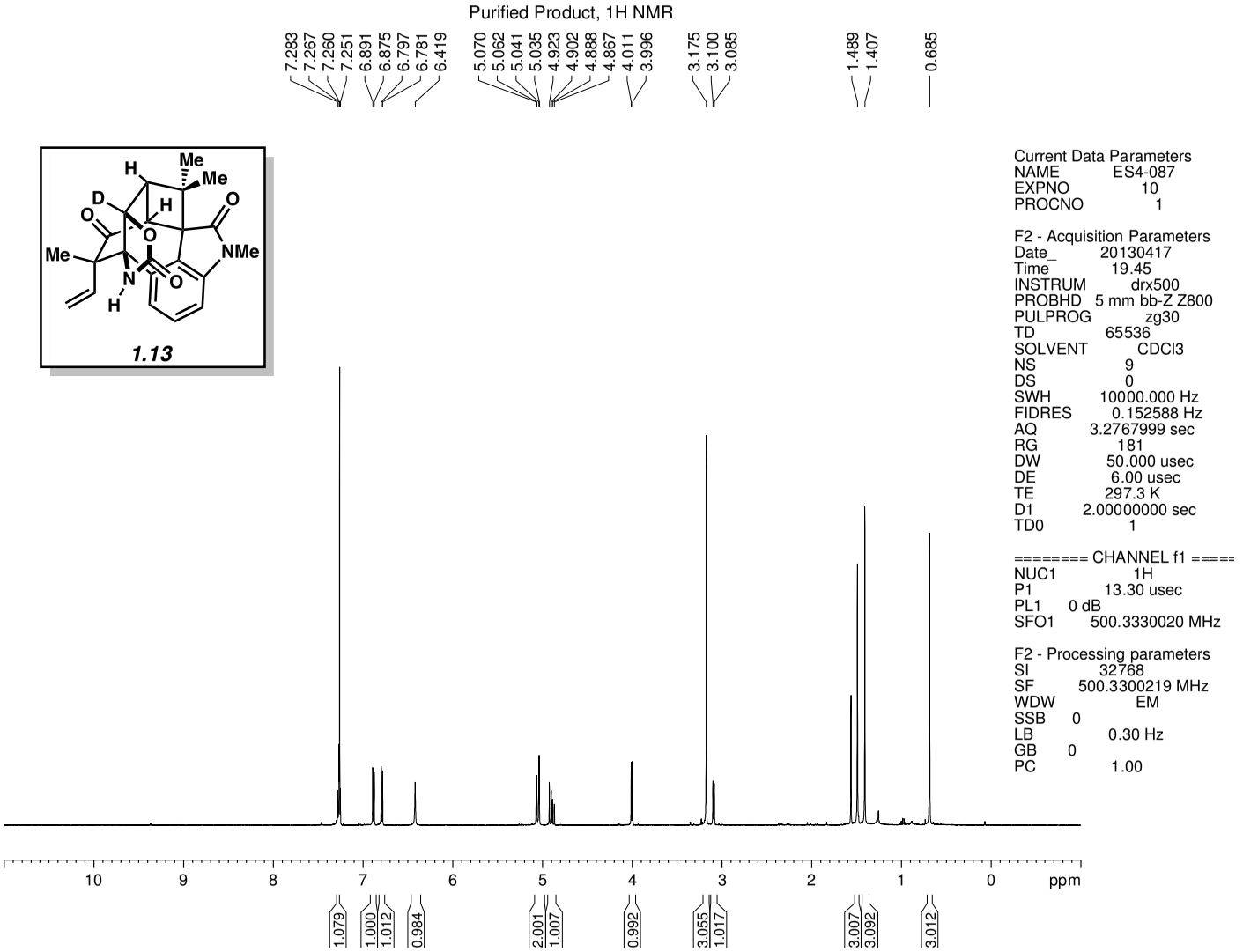

Figure 1.25 ^{1}H NMR (500 MHz, $CDCl_3$) of compound **1.13**.

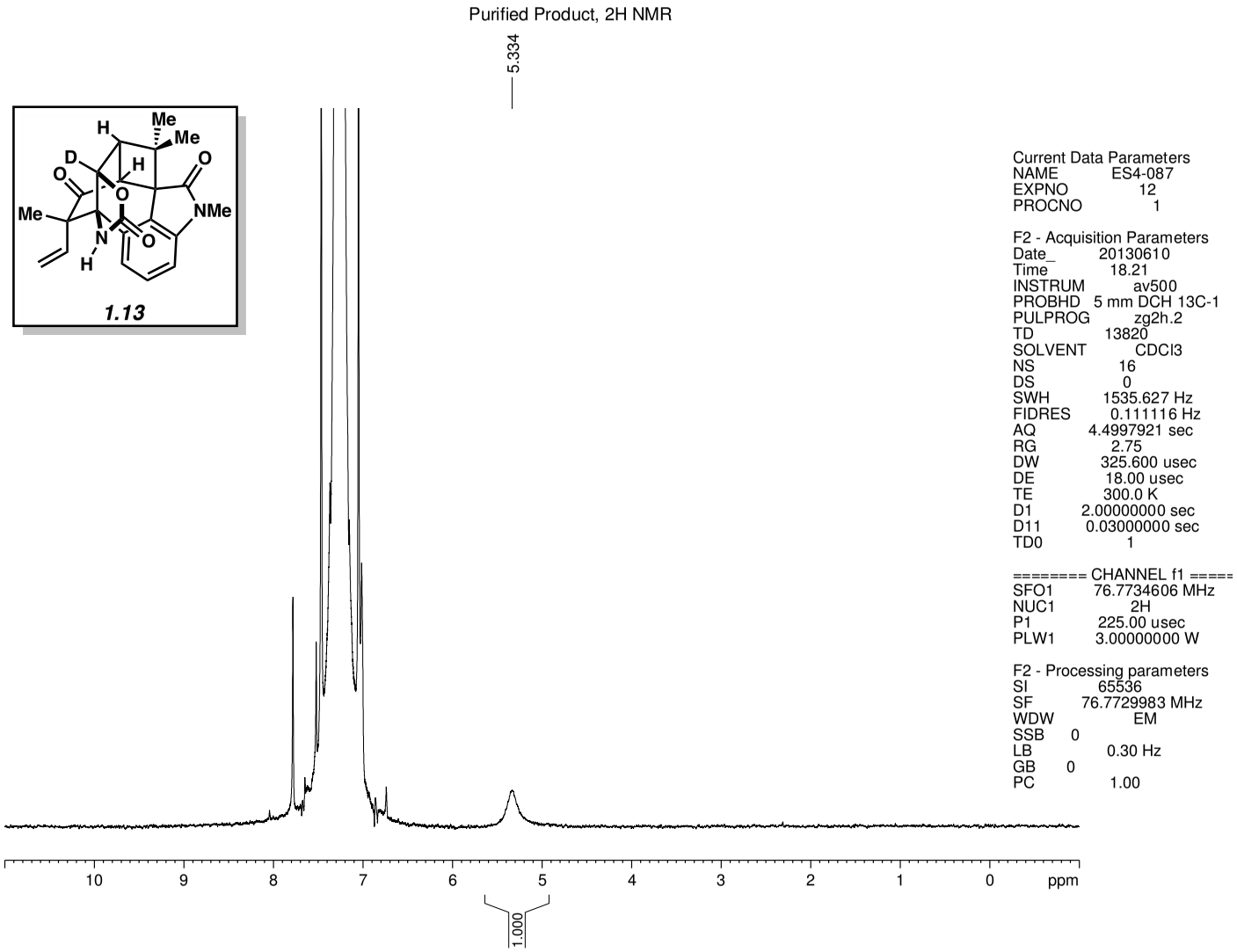

Figure 1.26 ^{2}H NMR (77 MHz, $CDCl_3$) of compound **1.13**.

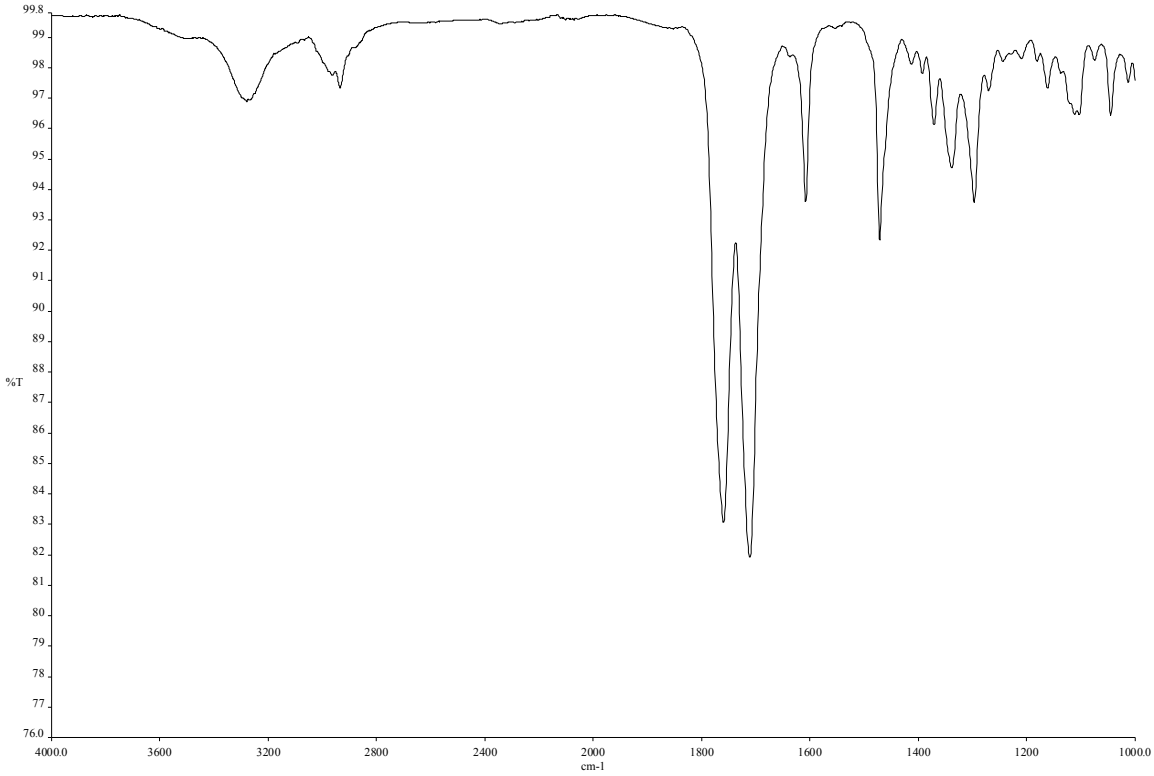

Figure 1.27 Infrared spectrum of compound **1.13**.

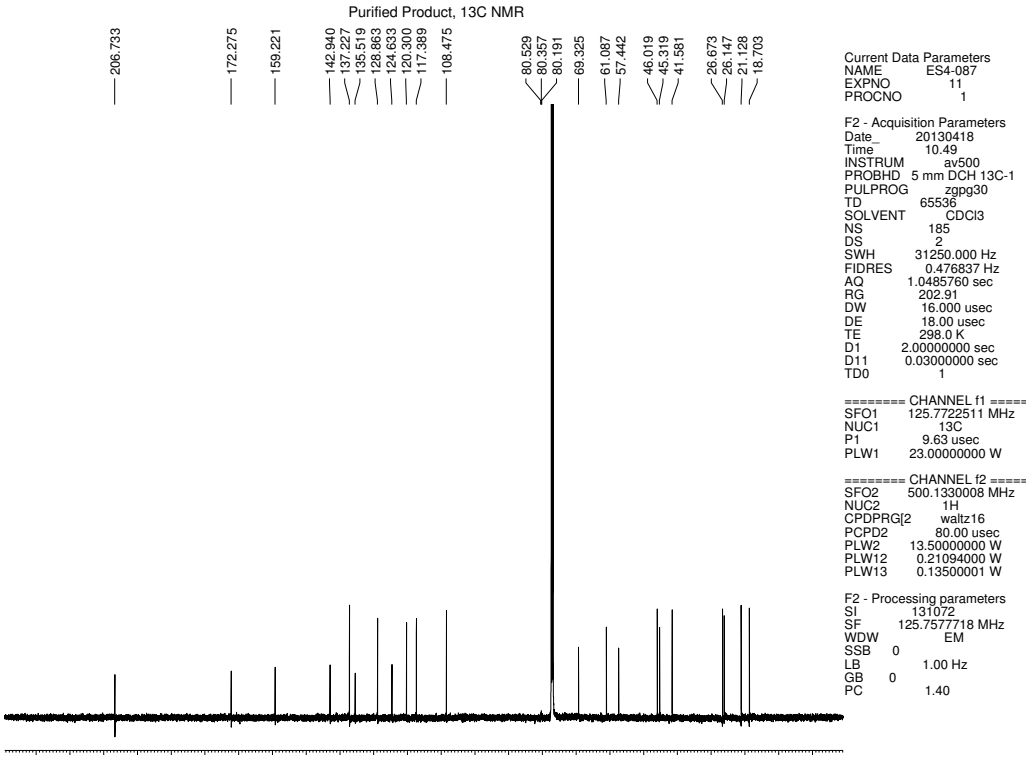

Figure 1.28 ^{13}C NMR (125 MHz, $CDCl_3$) of compound **1.13**.

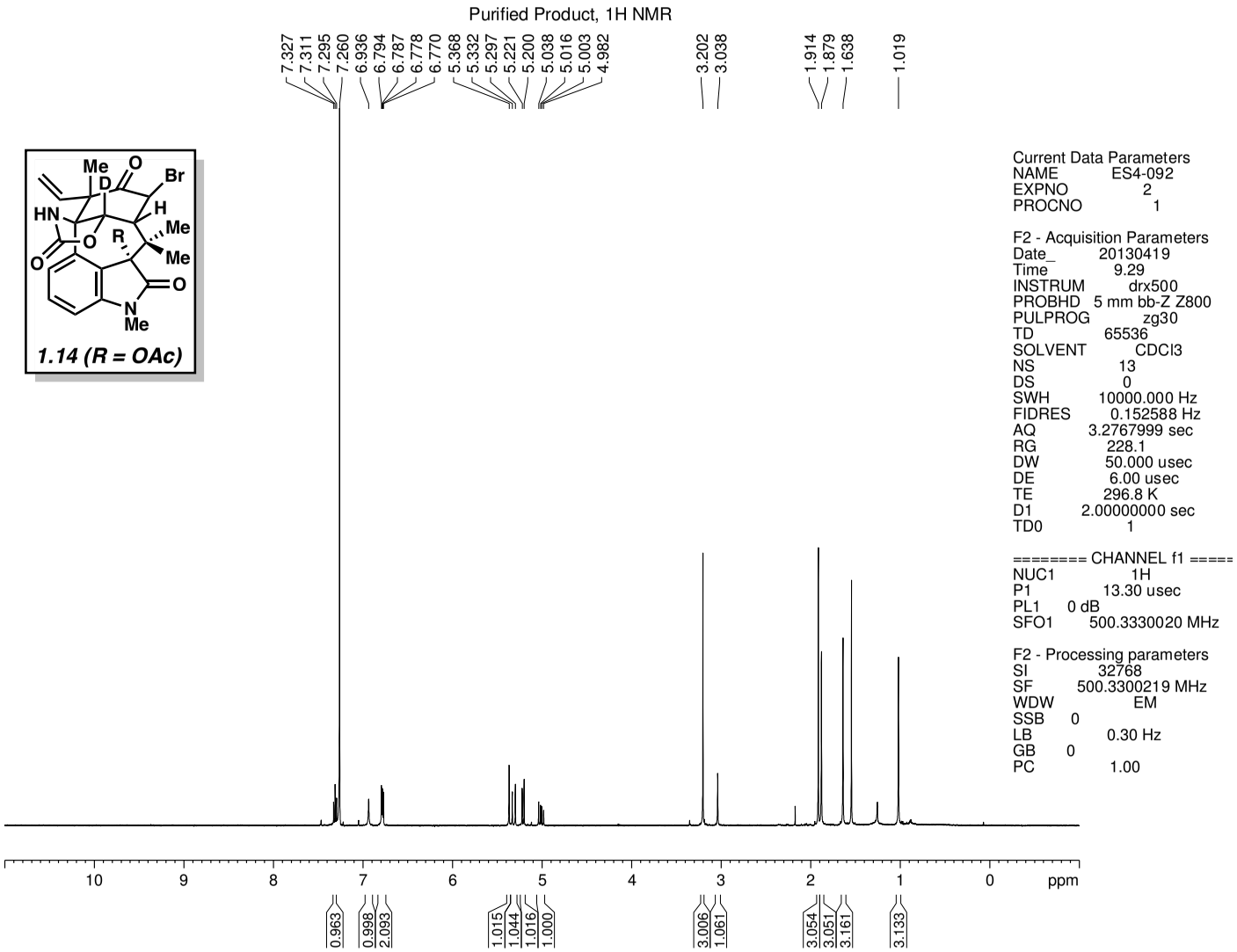

Figure 1.29 ^{1}H NMR (500 MHz, $CDCl_3$) of compound **1.14**.

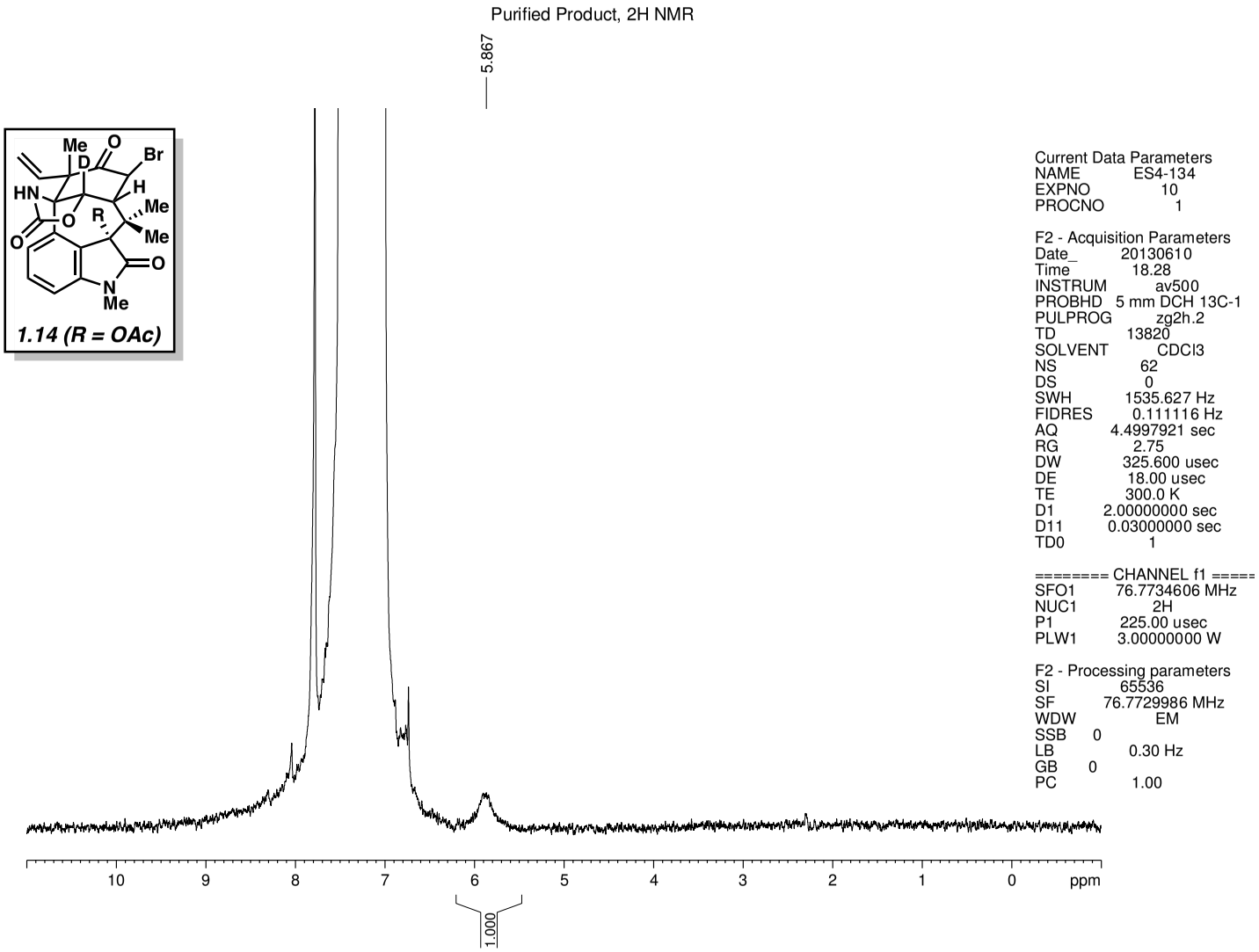

Figure 1.30 ^{2}H NMR (77 MHz, $CDCl_3$) of compound **1.14**.

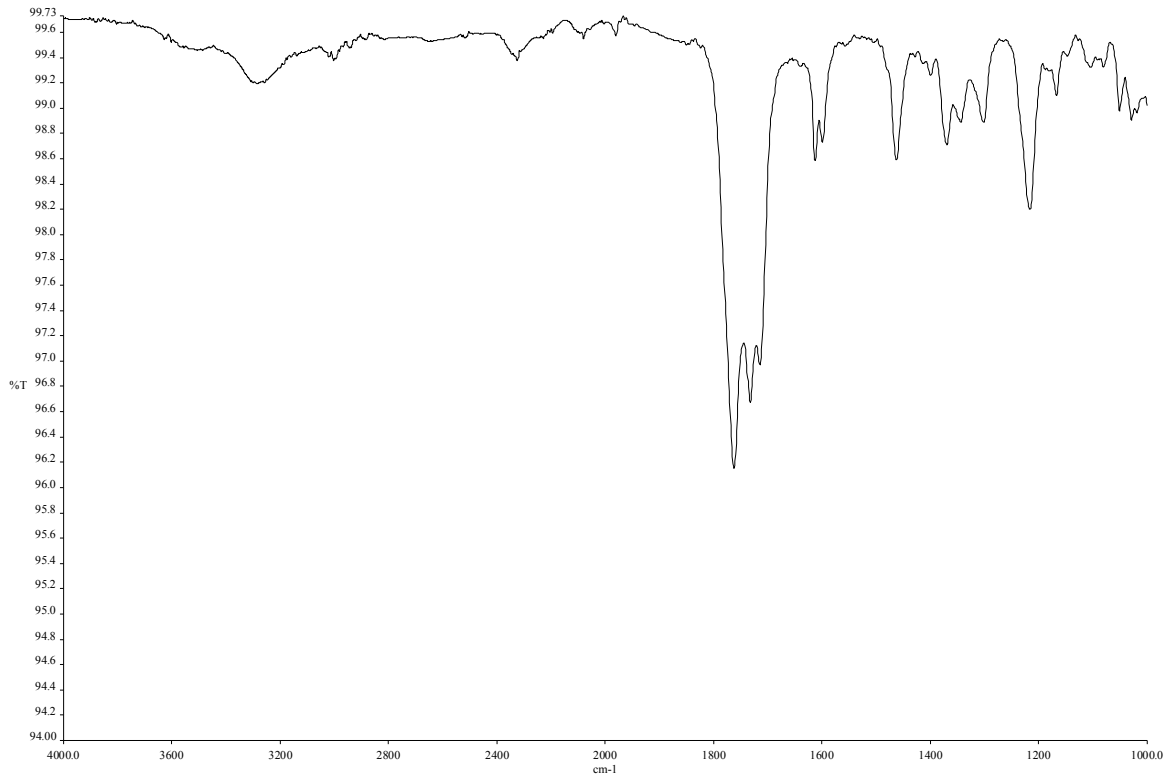

Figure 1.31 Infrared spectrum of compound **1.14**.

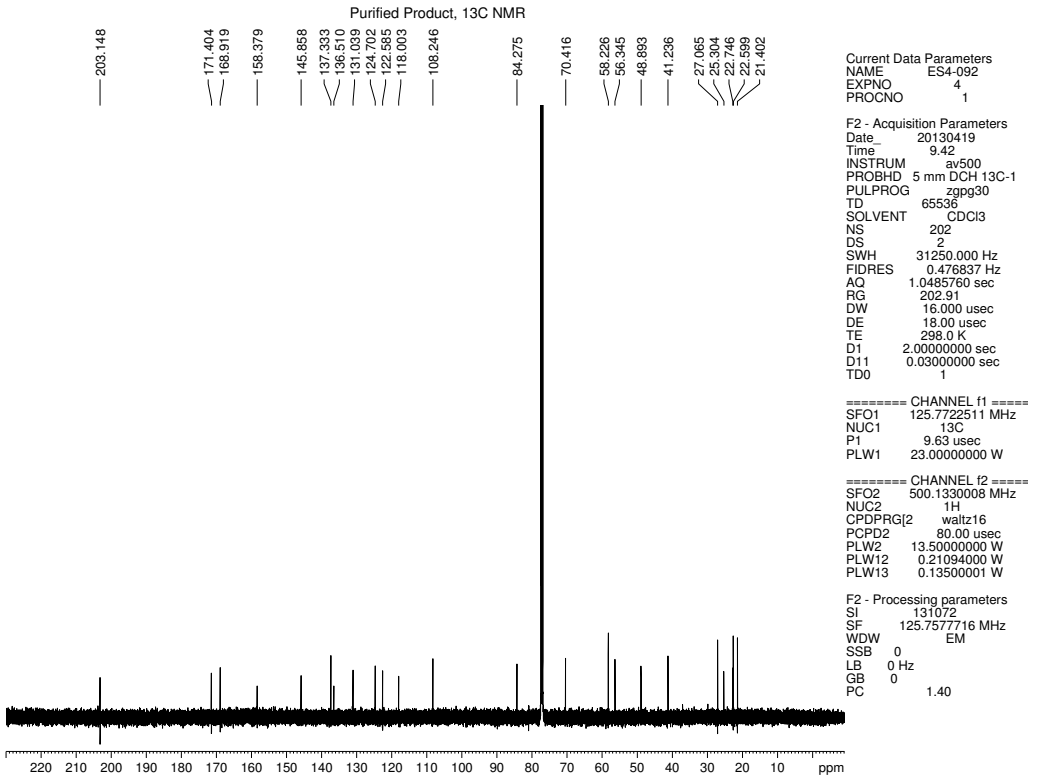

Figure 1.32 ^{13}C NMR (125 MHz, $CDCl_3$) of compound **1.14**.

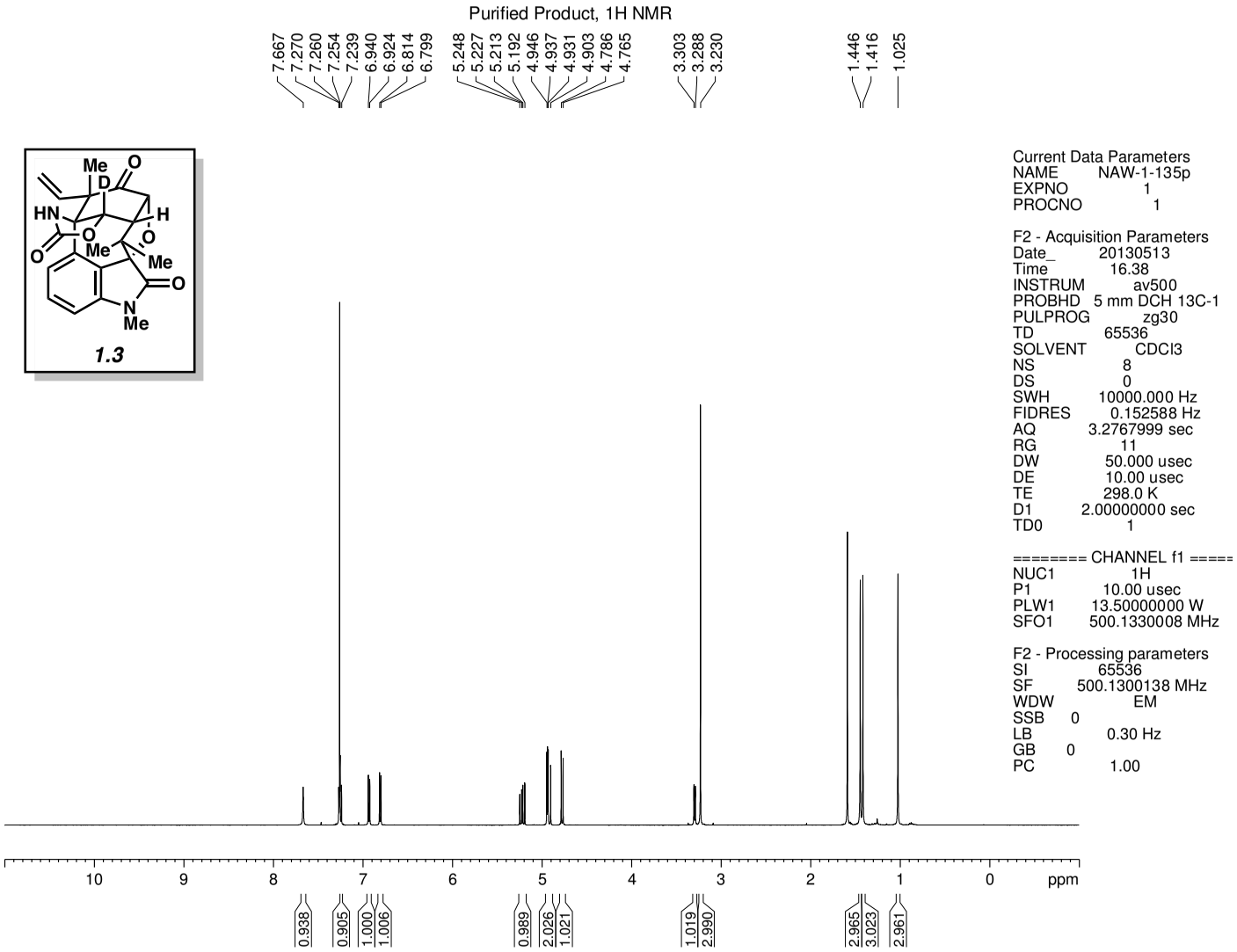

Figure 1.33 ^{1}H NMR (500 MHz, $CDCl_3$) of compound **1.3**.

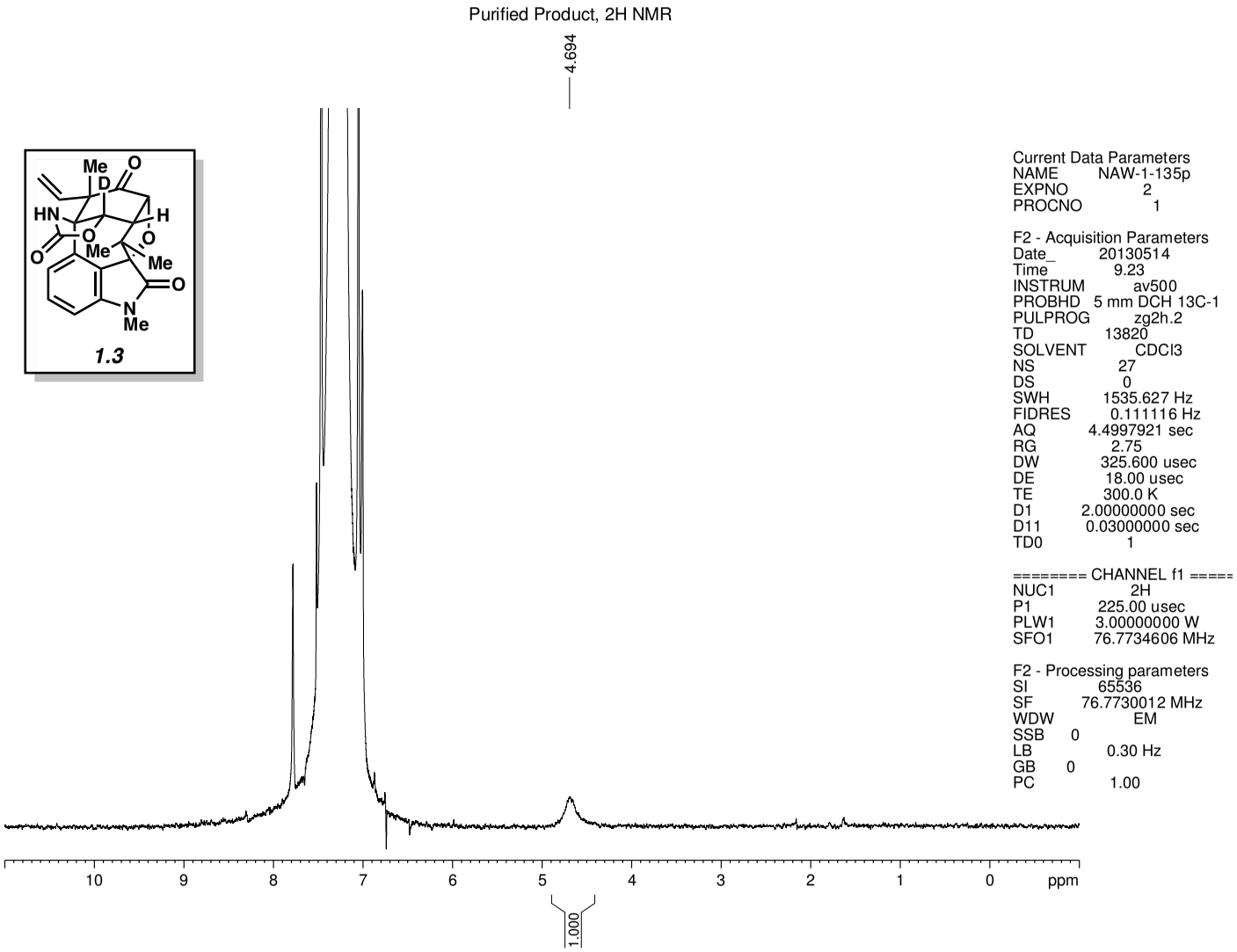

Figure 1.34 ^{2}H NMR (77 MHz, $CDCl_3$) of compound **1.3**.

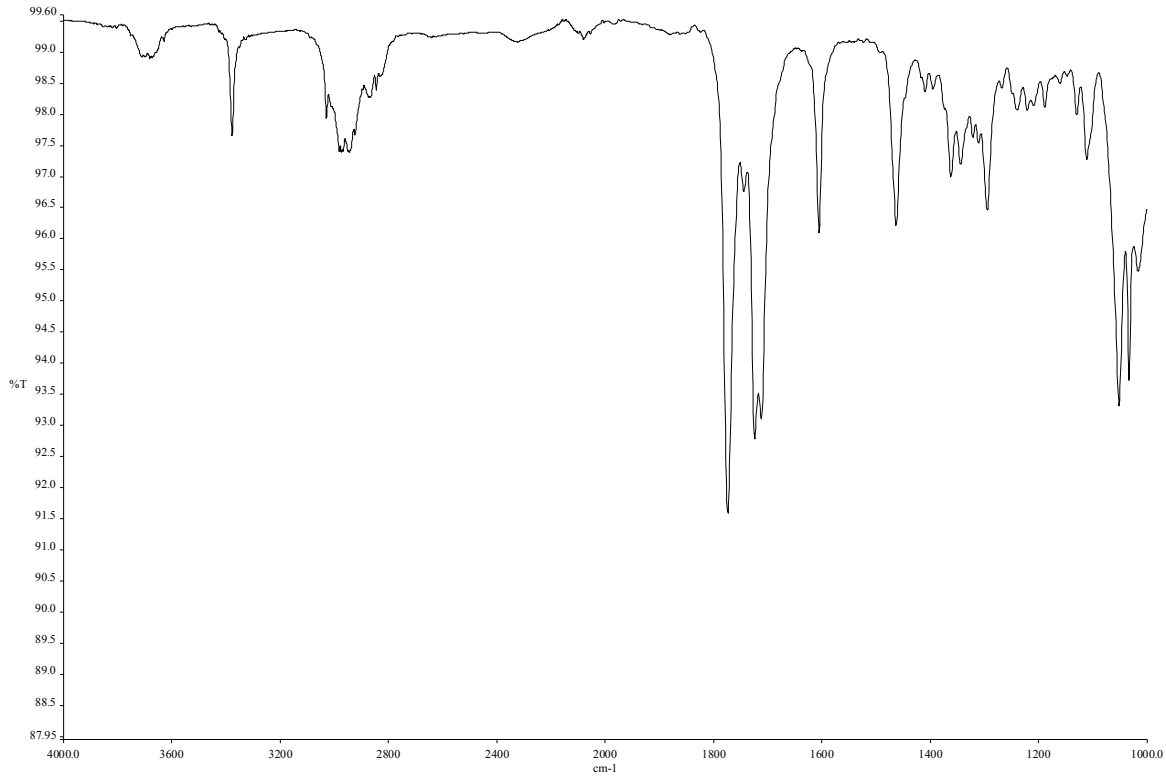

Figure 1.35 Infrared spectrum of compound **1.3**.

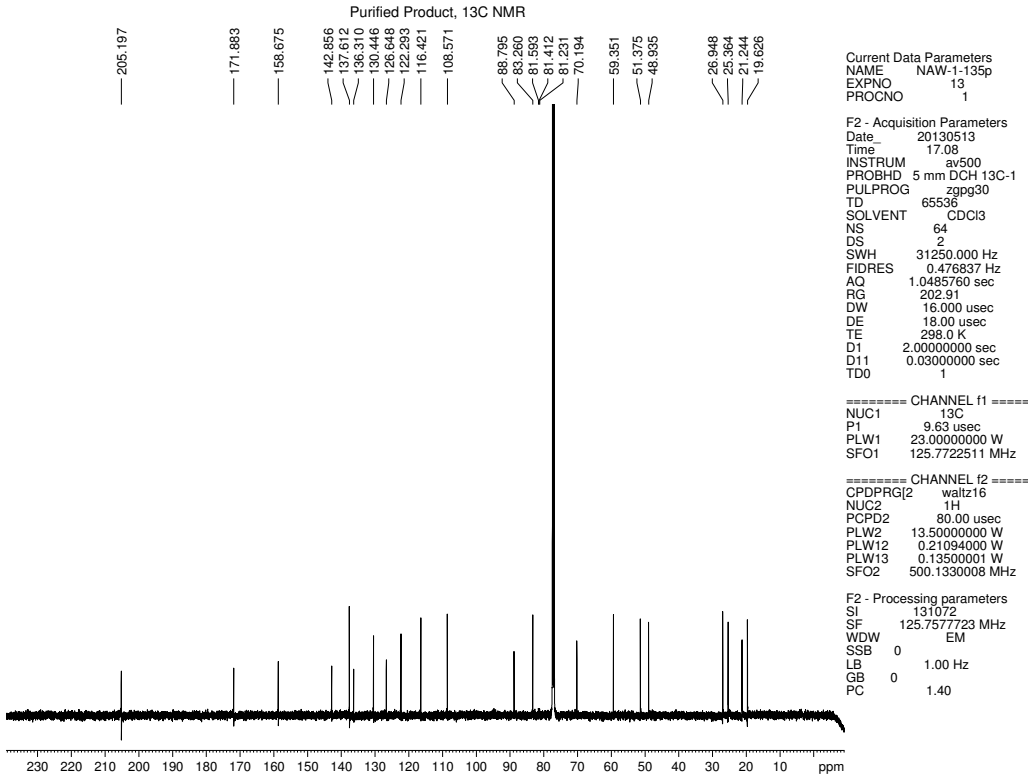

Figure 1.36 ^{13}C NMR (125 MHz, $CDCl_3$) of compound **1.3**.

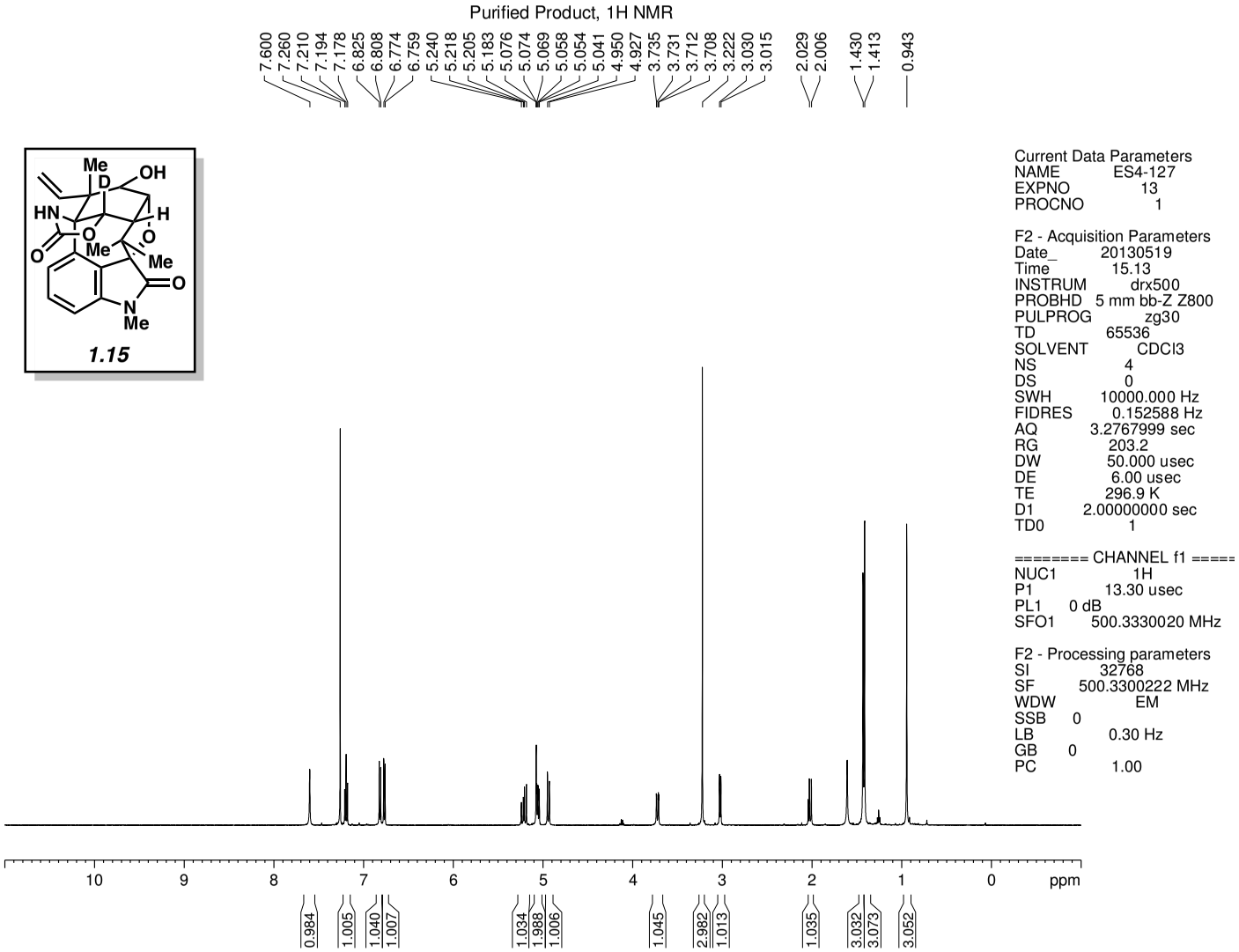

Figure 1.37 ^{1}H NMR (500 MHz, $CDCl_3$) of compound **1.15**.

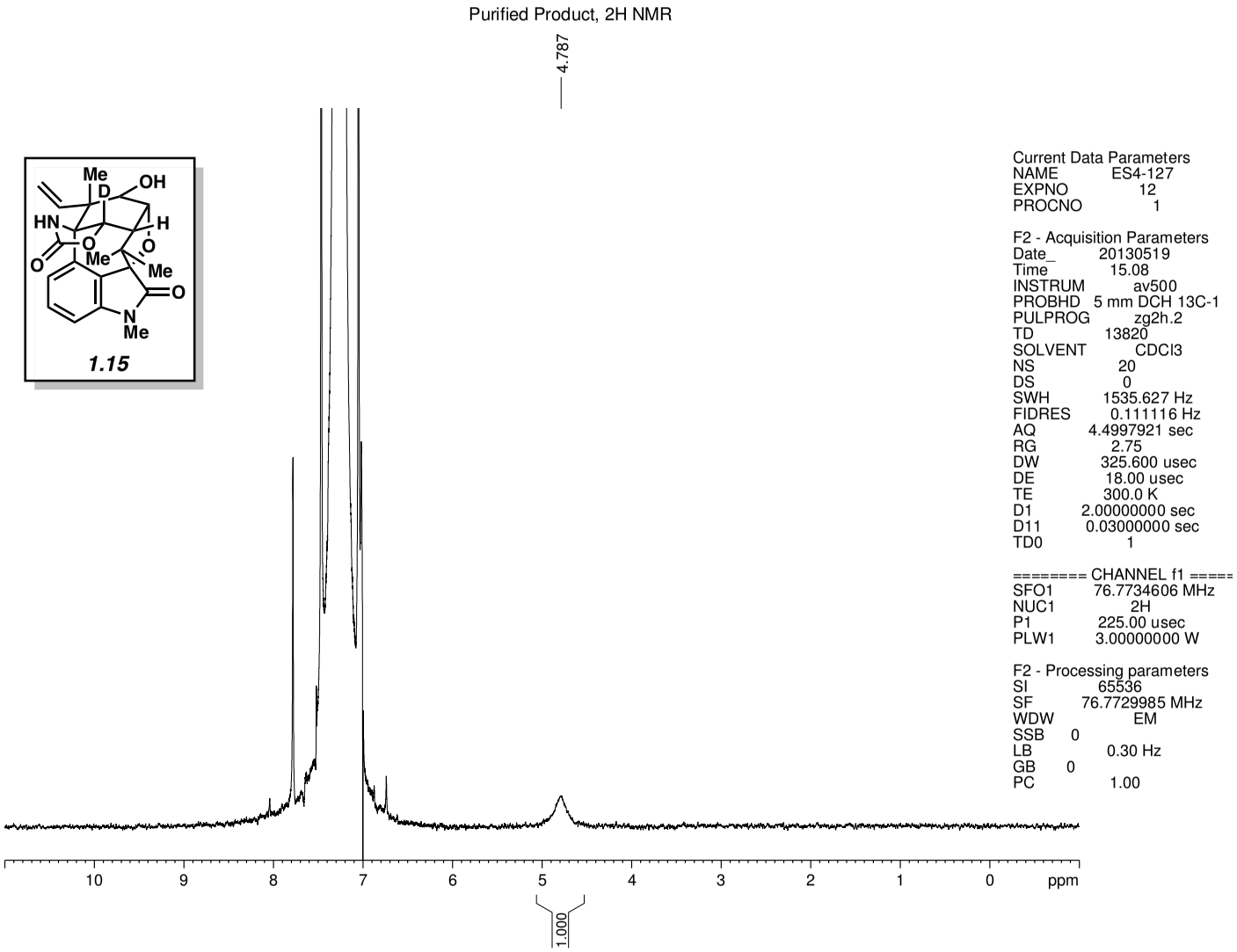

Figure 1.38 ^{2}H NMR (77 MHz, $CDCl_3$) of compound **1.15**.

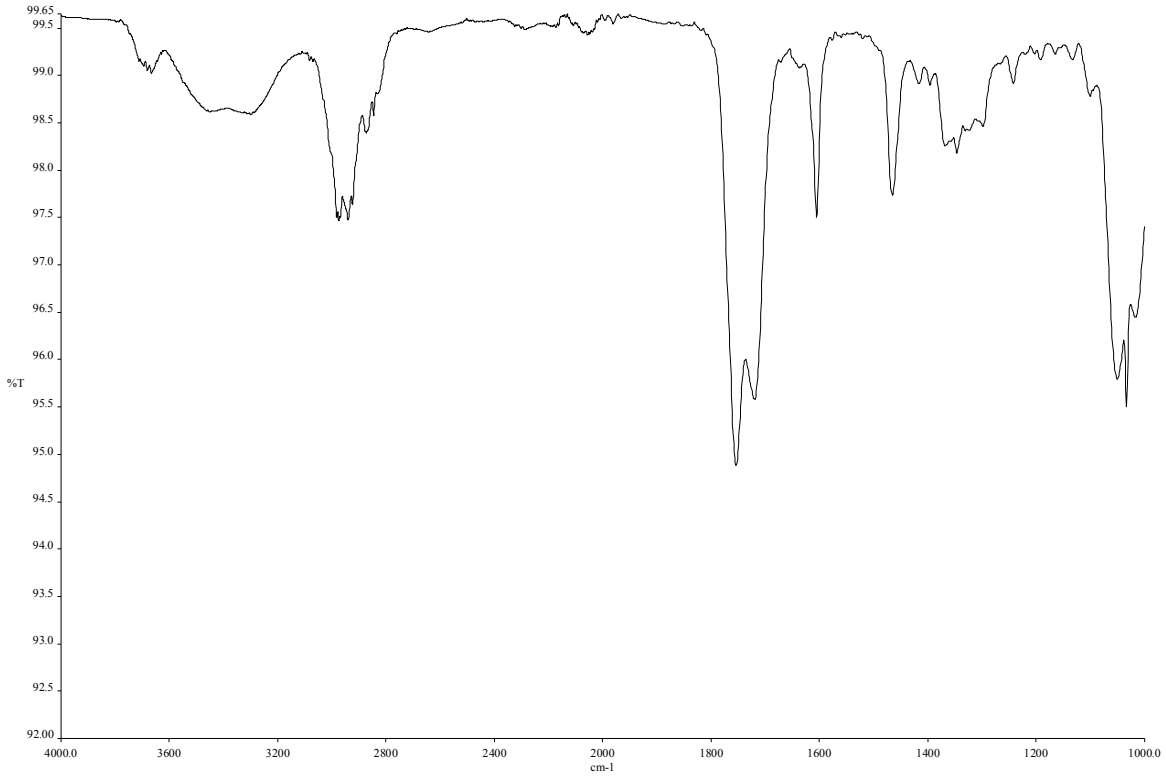

Figure 1.39 Infrared spectrum of compound **1.15**.

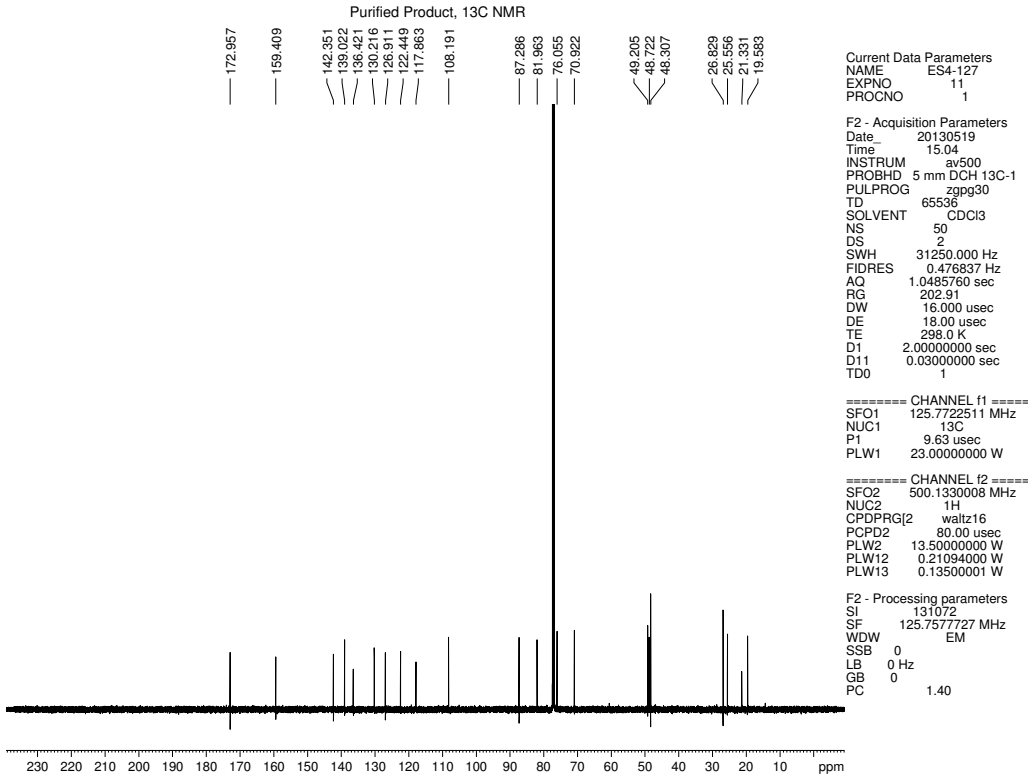

Figure 1.40 ^{13}C NMR (125 MHz, $CDCl_3$) of compound **1.15**.

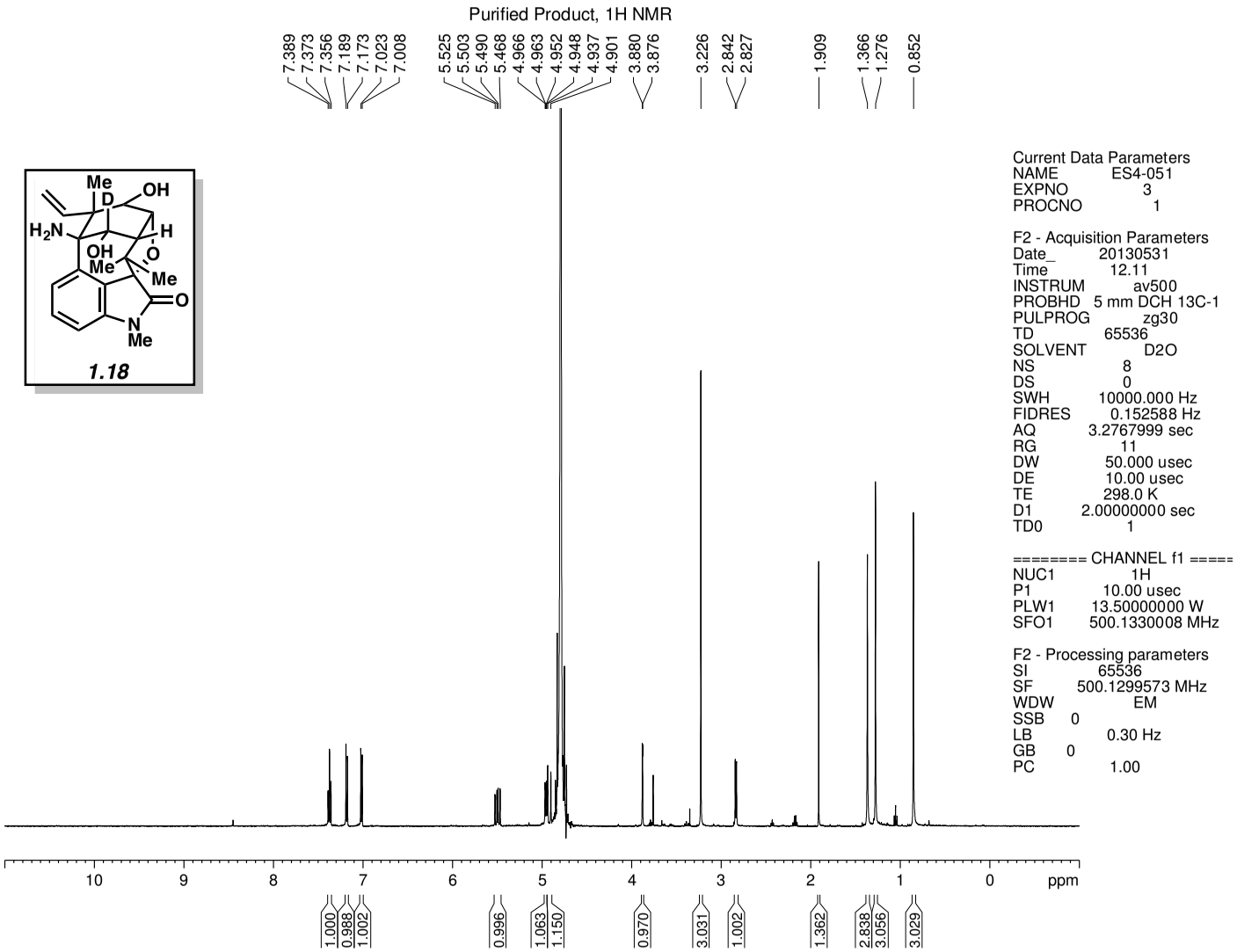

Figure 1.41 ^{1}H NMR (500 MHz, D_2O) of compound **1.18**.

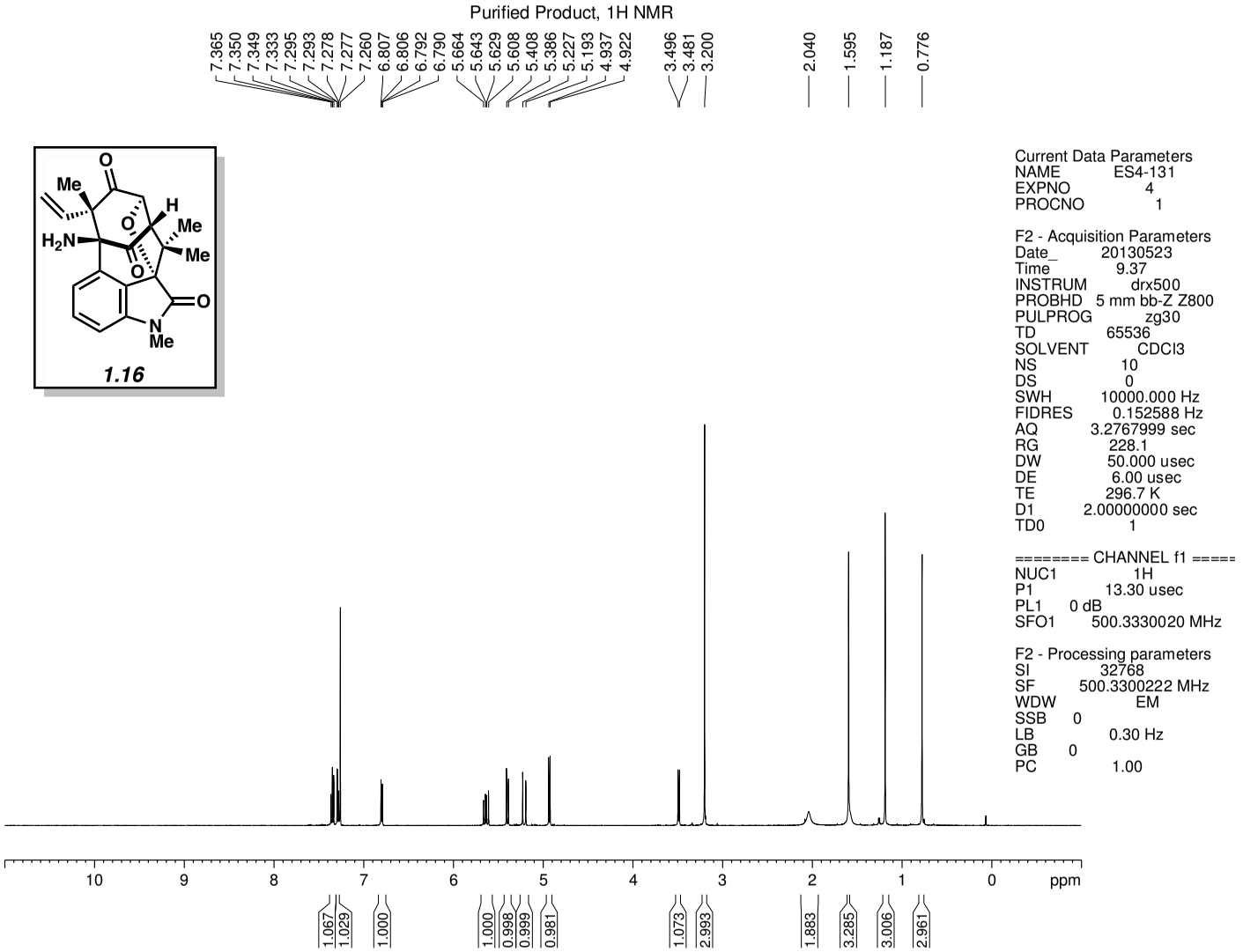

Figure 1.42 ^{1}H NMR (500 MHz, $CDCl_3$) of compound **1.16**.

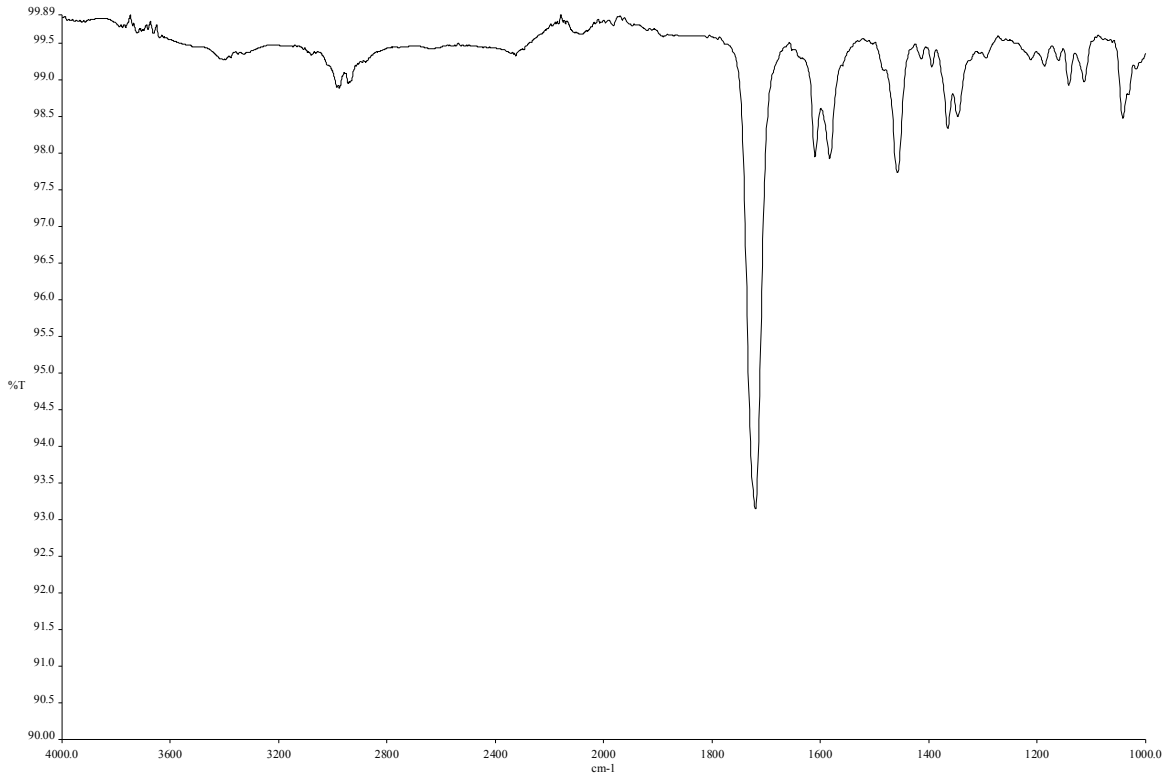

Figure 1.43 Infrared spectrum of compound **1.16**.

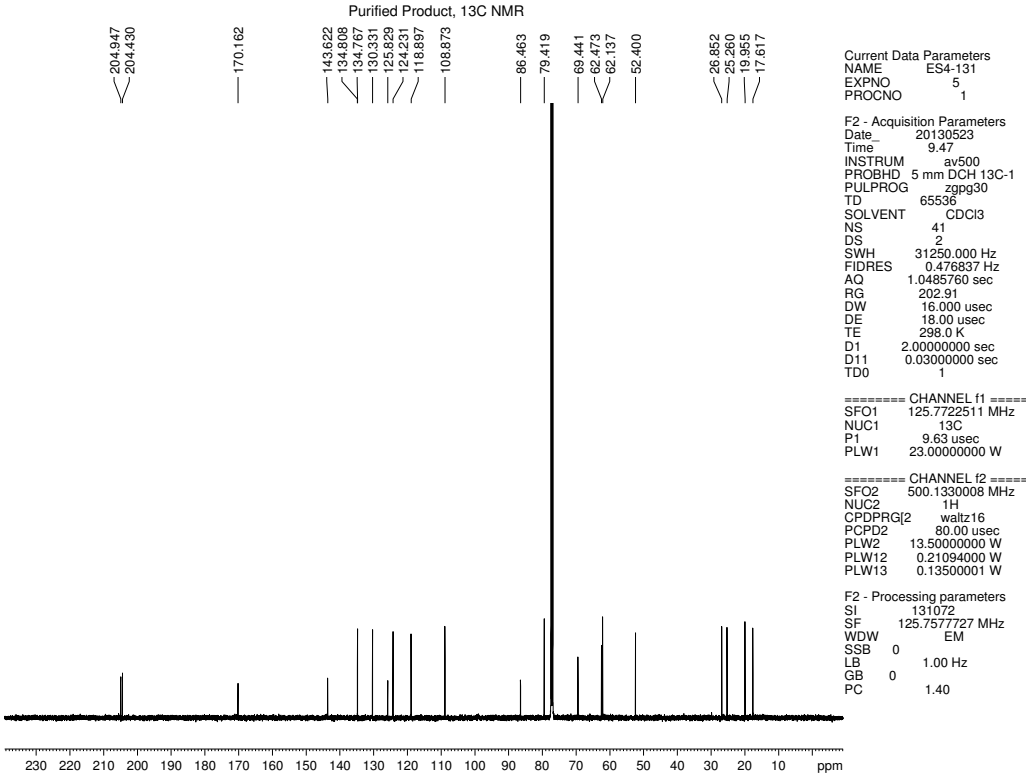

Figure 1.44 ^{13}C NMR (125 MHz, $CDCl_3$) of compound **1.16**.

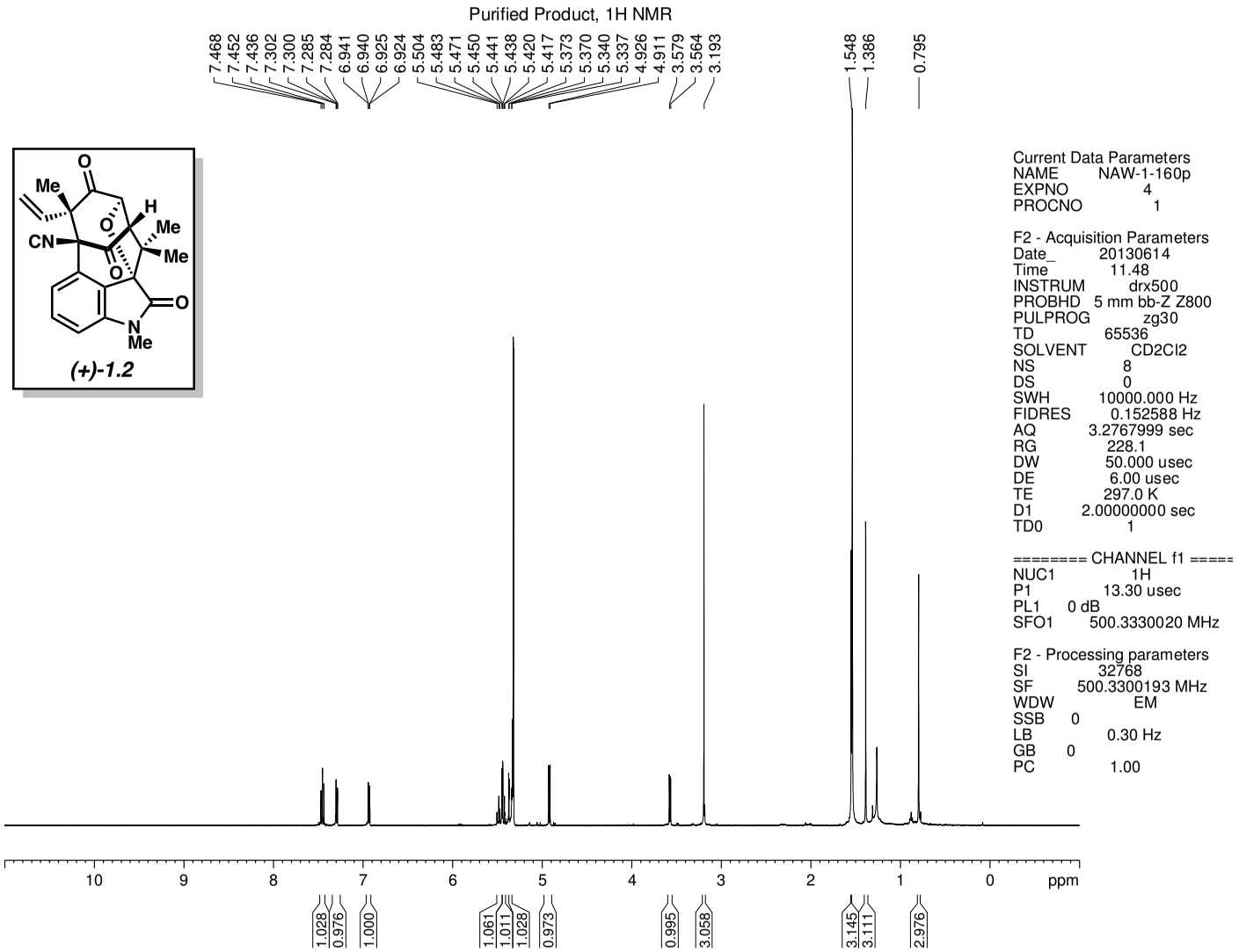

Figure 1.45 ^{1}H NMR (500 MHz, CD_2Cl_2) of compound **1.2**.

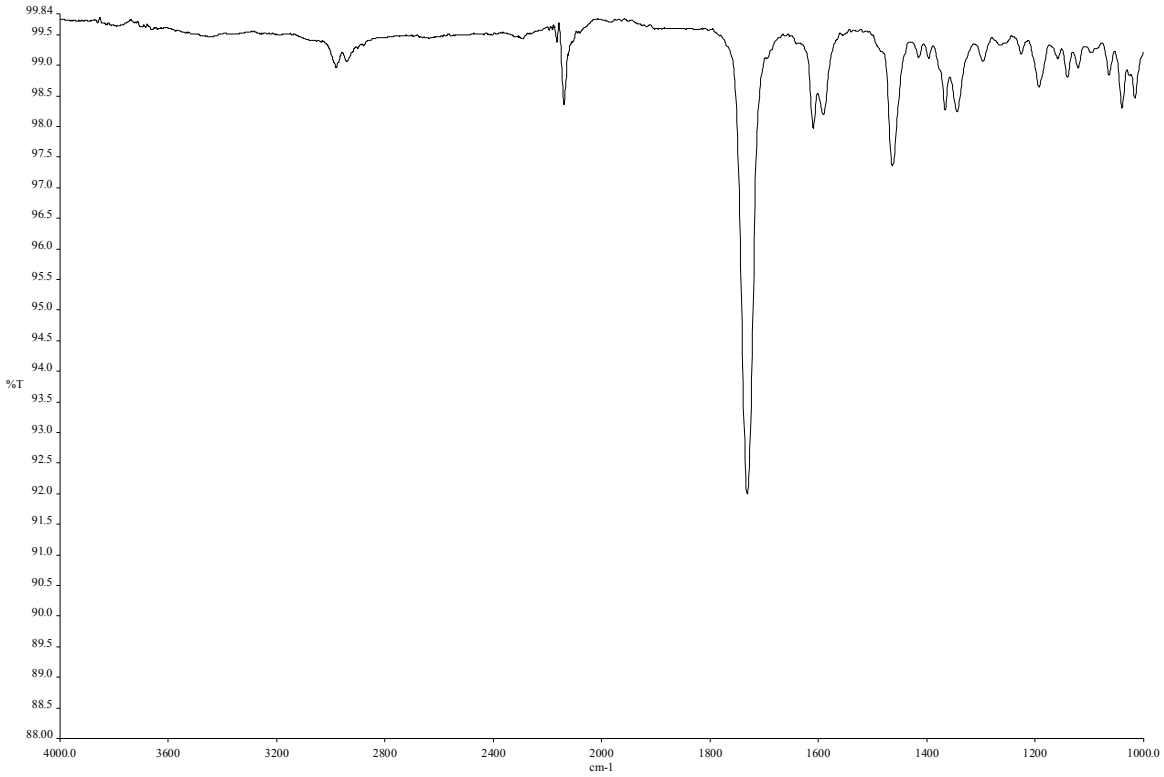

Figure 1.46 Infrared spectrum of compound **1.2**.

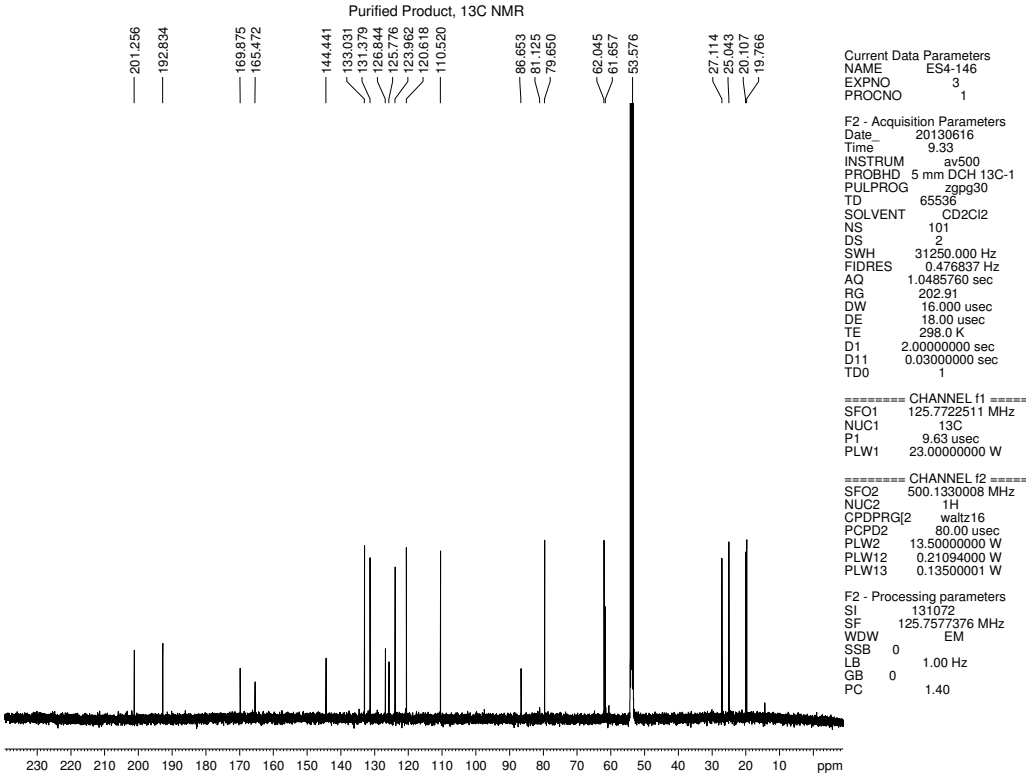

Figure 1.47 ^{13}C NMR (125 MHz, CD_2Cl_2) of compound **1.2**.

1.12 Notes and References

(1) For pertinent reviews, see: (a) Wood J. L. *Nat. Chem.* **2012**, *4*, 341. (b) Huters, A. D.; Styduhar, E. D.; Garg, N. K. *Angew. Chem., Int. Ed.* **2012**, *51*, 3758. (c) Brown, L. E.; Konopelski, J. P. *Org. Prep. Proced. Int.* **2008**, *40*, 411. (d) Avendaño, C.; Menéndez, J. C. *Curr. Org. Synth.* **2004**, *1*, 65.

(2) (a) Stratmann, K.; Moore, R. E.; Bonjouklian, R.; Deeter, J. B.; Patterson, G. M. L.; Shaffer, S.; Smith, C. D.; Smitka, T. A. *J. Am. Chem. Soc.* **1994**, *116*, 9935. (b) Jimenez, J. I.; Huber, U.; Moore, R. E.; Patterson, G. M. L. *J. Nat. Prod.* **1999**, *62*, 569.

(3) For total syntheses of welwitindolinone A isonitrile, see: (a) Baran, P. S.; Richter, J. M. *J. Am. Chem. Soc.* **2005**, *127*, 15394. (b) Reisman, S. E.; Ready, J. M.; Hasuoka, A.; Smith, C. J.; Wood, J. L. *J. Am. Chem. Soc.* **2006**, *128*, 1448.

(4) For progress toward the synthesis of bicyclo[4.3.1]-welwitindolinones, see: (a) Konopelski, J. P.; Deng, H.; Schiemann, K.; Keane, J. M.; Olmstead, M. M. *Synlett* **1998**, 1105. (b) Wood, J. L.; Holubec, A. A.; Stoltz, B. M.; Weiss, M. M.; Dixon, J. A.; Doan, B. D.; Shamji, M. F.; Chen, J. M.; Heffron, T. P. *J. Am. Chem. Soc.* **1999**, *121*, 6326. (c) Kaoudi, T.; Quiclet-Sire, B.; Seguin, S.; Zard, S. Z. *Angew. Chem., Int. Ed.* **2000**, *39*, 731. d) Deng, H.; Konopelski, J. P. *Org. Lett.* **2001**, *3*, 3001. (e) Jung, M. E.; Slowinski, F. *Tetrahedron Lett.* **2001**, *42*, 6835. (f) López-Alvarado, P.; García-Granda, S.; Álvarez-Rúa, C.; Avendaño, C. *Eur. J. Org. Chem.* **2002**, 1702. (g) MacKay, J. A.; Bishop, R. L.; Rawal, V. H. *Org. Lett.* **2005**, *7*, 3421. (h) Baudoux, J.; Blake, A. J.; Simpkins, N. S. *Org. Lett.* **2005**, *7*, 4087. (i) Greshock, T. J.; Funk, R. L. *Org. Lett.* **2006**, *8*, 2643. (j) Lauchli, R.; Shea, K. J. *Org. Lett.* **2006**, *8*, 5287. (k) Guthikonda, K.; Caliando, B. J.; Du Bois, J. Abstracts of Papers, 232nd

ACS National Meeting, September, **2006**, abstr ORGN-002. (l) Xia, J.; Brown, L. E.; Konopelski, J. P. *J. Org. Chem.* **2007**, *72*, 6885. (m) Boissel, V.; Simpkins, N. S.; Bhalay, G.; Blake, A. J.; Lewis, W. *Chem. Commun.* **2009**, 1398. (n) Boissel, V.; Simpkins, N. S.; Bhalay, G. *Tetrahedron Lett.* **2009**, *50*, 3283. (o) Tian, X.; Huters, A. D.; Douglas, C. J.; Garg, N. K. *Org. Lett.* **2009**, *11*, 2349. (p) Trost, B. M.; McDougall, P. J. *Org. Lett.* **2009**, *11*, 3782. (q) Brailsford, J. A.; Lauchli, R.; Shea, K. J. *Org. Lett.* **2009**, *11*, 5330. (r) Freeman, D. B.; Holubec, A. A.; Weiss, M. W.; Dixon, J. A.; Kafefuda, A.; Ohtsuka, M.; Inoue, M.; Vaswani, R. G.; Ohki, B. D.; Doan, S. E.; Reisman, S. E.; Stoltz, B. M.; Day, J. J.; Tao, R. N.; Dieterich, N. A.; Wood, J. L. *Tetrahedron* **2010**, *66*, 6647. (s) Heidebrecht, R. W., Jr.; Gulledge, B.; Martin, S. F. *Org. Lett.* **2010**, *12*, 2492. (t) Ruiz, M.; López-Alvarado, P.; Menéndez, J. C. *Org. Biomol. Chem.* **2010**, *8*, 4521. (u) Bhat, V.; Rawal, V. H. *Chem. Commun.* **2011**, *47*, 9705. (v) Bhat, V.; MacKay, J. A.; Rawal, V. H. *Org. Lett.* **2011**, *13*, 3214. (w) Bhat, V.; MacKay, J. A.; Rawal, V. H. *Tetrahedron* **2011**, *67*, 10097. (x) Zhang, M.; Tang, W. *Org. Lett.* **2012**, *14*, 3756. (y) Cleary, L.; Brailsford, J. A.; Lauchli, R.; Shea, K. J. Abstracts of Papers, 245th ACS National Meeting, April, **2013**, abstr ORGN-391.

(5) For complete and formal total syntheses of bicyclo[4.3.1]-welwitindolinones, see: (a) Bhat, V.; Allan, K. M.; Rawal, V. H. *J. Am. Chem. Soc.* **2011**, *133*, 5798. (b) Huters, A. D.; Quasdorf, K. W.; Styduhar, E. D.; Garg, N. K. *J. Am. Chem. Soc.* **2011**, *133*, 15797. (c) Fu, T.-h.; McElroy, W. T.; Shamszad, M.; Martin, S. F. *Org. Lett.* **2012**, *14*, 3834. (d) Allan, K. W.; Kobayashi, K.; Rawal, V. H. *J. Am. Chem. Soc.* **2012**, *134*, 1392. (e) Quasdorf, K. W.; Huters, A. D.; Lodewyk, M. W.; Tantillo, D. J.; Garg, N. K. *J. Am. Chem. Soc.* **2012**, *134*,

1396. (f) Fu, T.-h.; McElroy, W. T.; Shamszad, M.; Heidebrecht, R. W., Jr.; Gulledge, B.; Martin, S. F. *Tetrahedron* **2013**, *69*, 5588.

(6) 3D representation of **1.2** was obtained using B3LYP/6-31G* calculations (geometry optimization), using MacSpartan software.

(7) Image prepared using CYLview: C. Y. Legault, CYLview, 1.0b; Université de Sherbrooke: Québec, Montreal, Canada, 2009; http://www.cylview.org.

(8) A. A. Holubec, Progress Toward the Total Synthesis of the Welwitindolinone Alkaloids: Efficient Construction of the Carbocyclic Skeleton. Ph.D. Dissertation, Yale University, New Haven, CT, **2000**.

(9) For a recent review on C–N bond forming reactions involving C(sp^3)–H bonds, see: Jeffrey, J. L.; Sarpong, R. *Chem. Sci.* **2013**, *4*, 4092.

(10) Sakagami, M.; Muratake, H.; Natsume, M. *Chem*. *Pharm*. *Bull*. **1994**, *42*, 1393.

(11) For our laboratory's recent studies involving indolynes and other heterocyclic arynes, see: (a) Bronner, S. M.; Bahnck, K. B.; Garg, N. K. *Org. Lett.* **2009**, *11*, 1007. (b) Cheong, P. H.-Y.; Paton, R. S.; Bronner, S. M.; Im, G.-Y. J.; Garg, N. K.; Houk, K. N. *J. Am. Chem. Soc.* **2010**, *132*, 1267. (c) Im, G.-Y. J.; Bronner, S. M.; Goetz, A. E.; Paton, R. S.; Cheong, P. H.-Y.; Houk, K. N.; Garg, N. K. *J. Am. Chem. Soc.* **2010**, *132*, 17933. (d) Bronner, S. M.; Goetz, A. E.; Garg, N. K. *J. Am. Chem. Soc.* **2011**, *133*, 3832. (e) Goetz, A. E.; Bronner, S. M.; Cisneros, J. D.; Melamed, J. M.; Paton, R. S.; Houk, K. N.; Garg, N. K. *Angew. Chem., Int. Ed.* **2012**, *51*, 2758. (f) Goetz, A. E.; Garg, N. K. *Nat. Chem.* **2013**, *5*, 54. (g) Bronner, S. M.; Goetz, A. E.; Garg, N. K. *Synlett* **2011**, 2599.

(12) (a) Li, Z.; Capretto, D. A.; Rahaman, R.; He, C. *Angew. Chem., Int. Ed.* **2007**, *46*, 5184. (b) Cui, Y.; He, C. *Angew. Chem., Int. Ed.* **2004**, *43*, 4210.

(13) Variations in reaction conditions (e.g., employing a variety of bases, saturating with O_2) did not overcome the formation of **1.13**.

(14) CCDC 960226 contains the supplementary crystallographic data for this paper. These data can be obtained free of charge from the Cambridge Crystallographic Data Centre via www.ccdc.cam.ac.uk/data_request/cif.

(15) Citterio, A.; Finzi, C.; Santi, R.; Strology, S. *J. Chem. Res., Synop.* **1988**, 156.

(16) For recent alkaloid syntheses that feature the strategic use of indole oxidation chemistry, see: (a) Han, S.; Movassaghi, M. *J. Am. Chem. Soc.* **2011**, *133*, 10768. (b) Qi, X.; Bao, H.; Tambar, U. K. *J. Am. Chem. Soc.* **2011**, *133*, 10050.

(17) Huters, A. D.; Quasdorf, K. W.; Garg, N. K. University of California, Los Angeles, CA. Unpublished work, **2010**.

(18) Buckley, B. R.; Fernández D.-R., B. *Tetrahedron Lett.* **2013**, *54*, 843.

(19) Treatment of **1.4** with 3.0 equiv TBAF and 50.0 equiv MeOD in CH_3CN under an atmosphere of N_2 at ambient temperature gave 40% deuterium incorporation at C3 after 10 min, whereas treatment under the same conditions for 1 h gave 50% deuterium incorporation at C3 and 25% deuterium incorporation at C14.

(20) Efforts to isolate the putative peroxy species (Figure 1.2) have been unsuccessful; however, we have isolated several related compounds, such as **1.19** and **1.20**, by oxidation of the corresponding oxindoles.

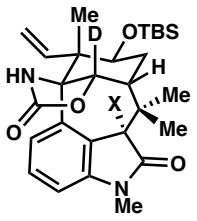

1.19, X = OOH

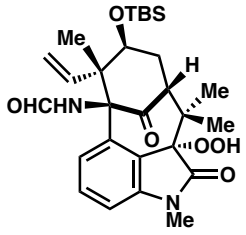

1.20

(21) Frigerio, M.; Santagostino, M.; Sputore, S. *J. Org. Chem.* **1999**, *64*, 4537.

(22) Niu, C.; Pettersson, T.; Miller, M. J. *J. Org. Chem.* **1996**, *61*, 1014.

CHAPTER TWO

Total Synthesis of (–)-*N*-Methylwelwitindolinone B Isothiocyanate via a Chlorinative Oxabicyclic Ring-Opening Strategy

Nicholas A. Weires, Evan D. Styduhar, Emma L. Baker, and Neil K. Garg.

J. Am. Chem. Soc. **2014**, *136*, 14710–14713.

2.1 Abstract

The first total synthesis of *N*-methylwelwitindolinone B isothiocyanate is reported. The route features several key steps, including a regio- and diastereoselective chlorinative oxabicycle ring-opening reaction to introduce the challenging alkyl chloride motif.

2.2 Introduction

The total synthesis of indole alkaloids continues to be a fruitful area of scientific pursuit. One particular class of molecules that has provided an exciting arena of chemical discovery is the welwitindolinone natural products, wherein the majority of congeners contain a [4.3.1]-bicyclic core (e.g., **2.2**–**2.4**, Figure 2.1).[1,2] Since Moore's first isolation report in 1994,[3] roughly 25 manuscripts describing efforts toward these complex structures have appeared from many research groups worldwide.[2b,4] The majority of initially reported studies established a variety of methods for assembling the [4.3.1]-bicyclic core and subsequent efforts have focused on completing the total syntheses. Towards this latter end, the most recent publications describe formal,[5] as well as total syntheses of **2.3**, **2.4**, and C3-oxidized variants of **2.3**.[6,7]

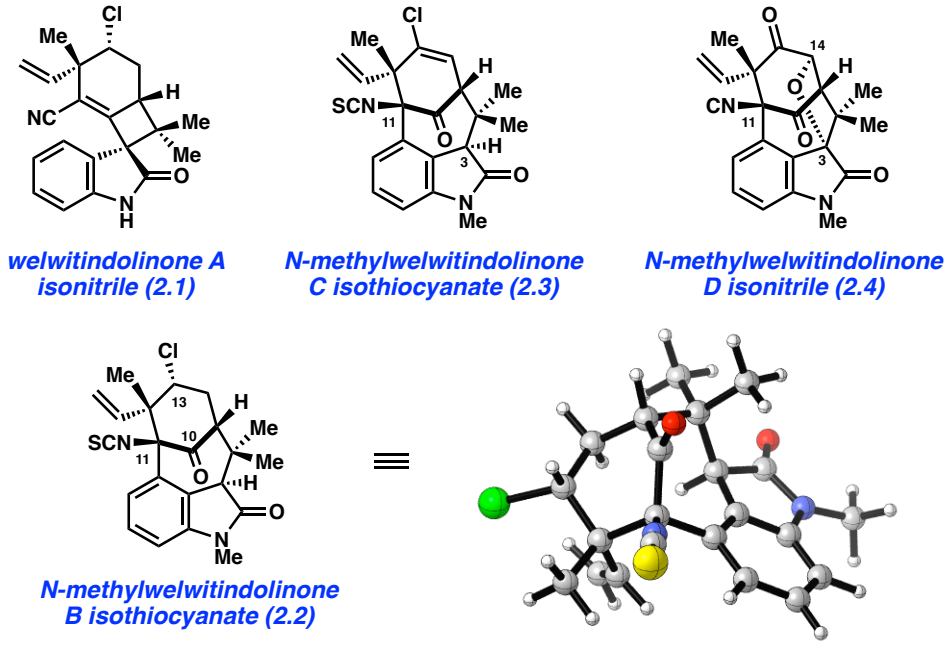

Figure 2.1. Welwitindolinones **2.1–2.4**.

Although [4.3.1]-bicyclic welwitindolinones in the C- and D- 'series' have been synthesized (e.g., **2.3** and **2.4**), compounds in the B- 'series' (e.g., **2.2**) have yet to be prepared by total synthesis.[4u,y] Structurally, **2.2** is quite similar to **2.3** with the key difference being a variation in the oxidation state at C13.[8,9] However, this seemingly simple change is deceptive, as the alkyl chloride resides on the more congested face of the [4.3.1]-bicycle, adjacent to a quaternary center,[10] and thus presents a formidable challenge with regard to synthesis. In addition to this subtle feature, the alkyl chloride in these systems is prone to undergo a variety of undesirable side-reactions under basic reaction conditions.[4y,11] Herein, we describe our efforts toward (–)-**2.2** and the first total synthesis of this elusive natural product.

2.3 Initial Approaches Toward Installation of the Alkyl Chloride

In our initial efforts, we considered several approaches to **2.2** that ultimately proved unsuccessful (Scheme 2.1). In what can be considered the most direct assault, we envisioned **2.2** as arising from C13–14-reduction of **2.5** or a related derivative. However, attempts to realize this strategy were thwarted by the facile reduction of the terminal olefin.[12] We also pursued a strategy wherein the alkyl chloride would derive from alcohol **2.6** by activation and chlorination with stereochemical inversion. Similar to the observations made by Rawal,[4u] we found that the proximal vinyl group underwent formal migration to C13 upon activation of the alcohol.[13] Even in the absence of the vinyl group, the chlorination is known to be difficult and only proceeds under specialized conditions,[4u] as the necessary approach of a chloride nucleophile is somewhat hampered by the steric congestion of the bicyclic scaffold.[14]

Scheme 2.1

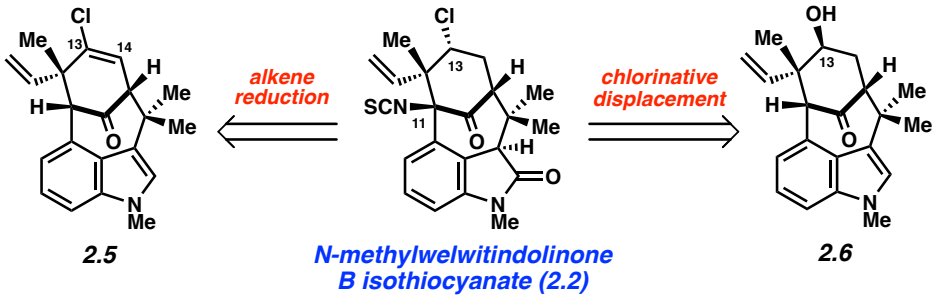

2.5 ***N*-methylwelwitindolinone B isothiocyanate (2.2)*** ***2.6***

2.4 Modified Retrosynthetic Plan for the Total Synthesis of (–)-*N*-Methylwelwitindolinone B Isothiocyanate

After numerous failed attempts to advance late-stage intermediates from our previous synthesis, we devised the alternative retrosynthetic plan highlighted in Scheme 2.2. In this revised approach, it was envisioned that **2.2** would arise from oxazolidinone **2.7** by late-stage

cleavage of the carbamate and further manipulation, all in the presence of the sensitive alkyl chloride. In turn, oxazolidinone **2.7** would derive from nitrene insertion of carbamate **2.8**.[15] We have previously studied related insertion reactions for C11 functionalization of welwitindolinone scaffolds, but in all prior cases the substrates possessed the opposite stereochemical configuration at C10.[7] Thus, the attempted nitrene insertion of **2.8** would serve as an opportunity to probe the generality of this method for C11 functionalization. In a critical transformation, we sought to introduce the alkyl chloride of **2.8** by performing a regio- and diastereoselective chlorinative ring-opening of an oxabicycle-containing intermediate (see transition structure **2.9**). This transformation, largely inspired by Shea's seminal studies,[4y] could provide a solution to the challenge faced earlier. Namely, the necessary approach of the chloride appeared favorable, owing to the restricted conformation of the oxabicycle unit.[16] Importantly, the oxabicycle was envisioned to be readily available from indole **2.10**, which would be accessed from enantioenriched carvone derivative **2.11** and indole **2.12** in three steps using our previously established procedure involving an indolyne cyclization.[7a,17]

Scheme 2.2

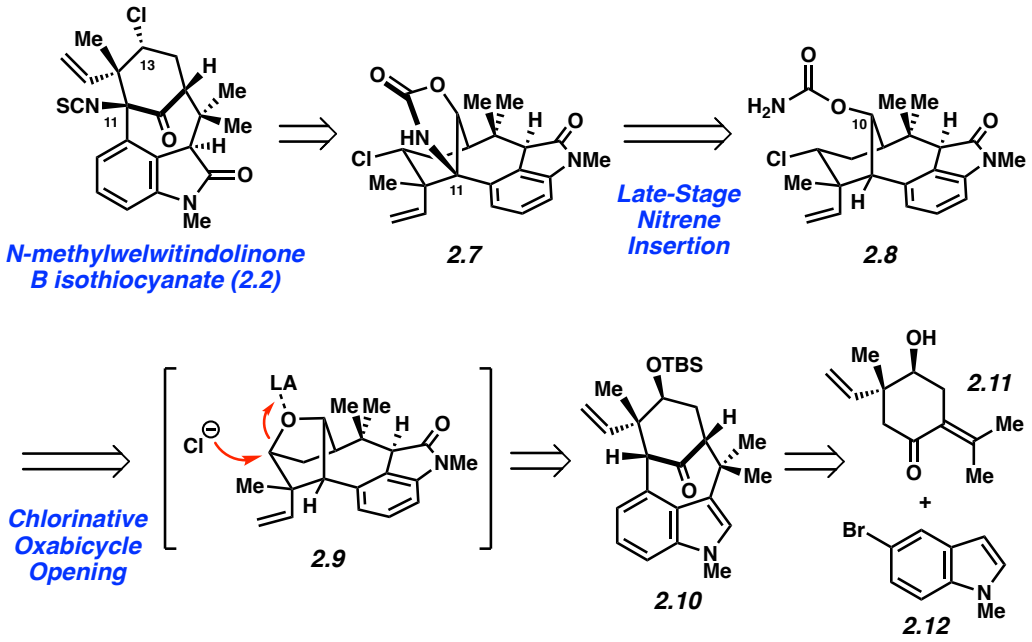

2.5 Construction of Oxabicycle and Chlorination Studies

To implement the plan illustrated in Scheme 2.2, we first targeted construction of oxabicycle **2.15** (Scheme 2.3). To this end, ketone **2.10** was elaborated to mesylate **2.13** in two steps involving reduction with $LiAlH_4$ followed by sulfonylation. Upon treatment of **2.13** with Bu_4NF in THF at 80 °C, desilylation readily occurred with concomitant cyclization to afford oxabicycle **2.14** in 84% yield. Subsequently, a one-pot oxidation / hydrolysis protocol was used to elaborate **2.14** to the corresponding oxindole **2.15**, which was formed as a single diastereomer.

Scheme 2.3

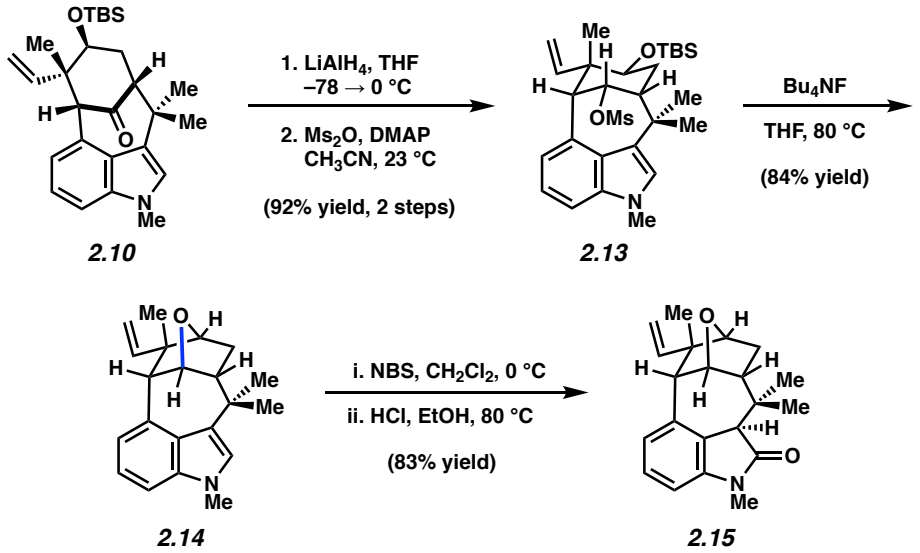

2.10 *2.13* *2.14* *2.15*

With rapid access to oxabicycle **2.15**, we were poised to attempt the key chlorinative ring-opening reaction (Scheme 2.4).[18] We surveyed several conditions that have previously been used for related transformations such as $ZnCl_2$ and acetyl chloride,[19] ethanolic HCl,[20] and $TiCl_4$.[21] Although the use of most reaction conditions led to the recovery of starting material or decomposition, treatment of **2.15** with BCl_3[22] led to consumption of the substrate with opening of the oxabicycle. Unfortunately, the two products obtained were **2.16**, which had undergone formal vinyl migration, and **2.17**, an unproductive constitutional isomer of the desired product, which forms as a result of undesired chloride attack at C10 (rather than C13). In hope of avoiding the vinyl migration, and to perturb the electronic environment at C13,[4u] alkene **2.15** was exposed to modified oxidative cleavage conditions,[23] which furnished aldehyde **2.18**. To our delight, treatment of **2.18** with BCl_3 in CH_2Cl_2 at 50 °C delivered the desired chlorinated product **2.19** in 64% yield. Of note, **2.19** was obtained as a single diastereomer and the analogous undesired regioisomer was not observed.[24]

Scheme 2.4

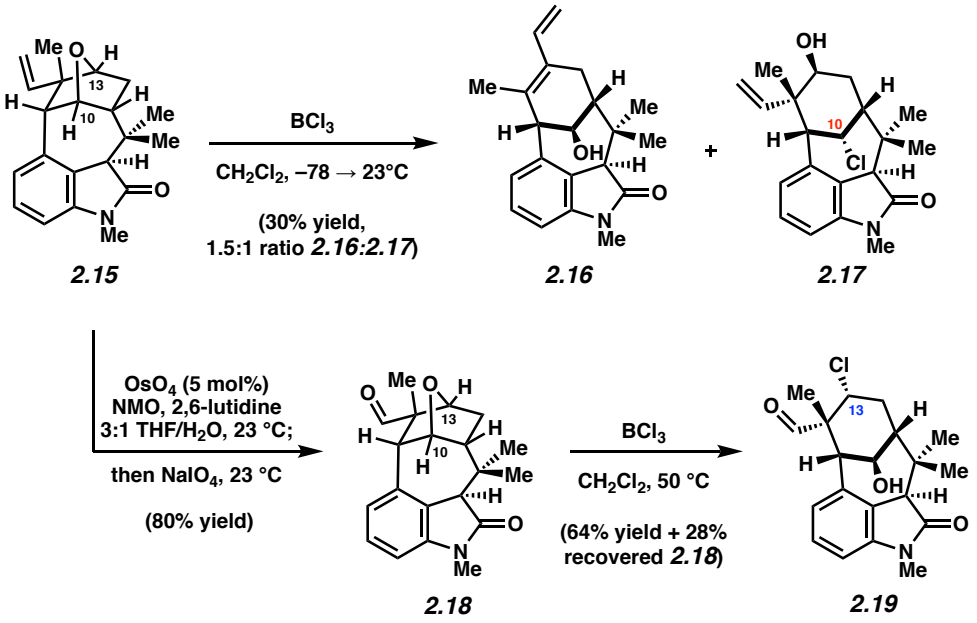

2.6 Attempted Introduction of the C11 Bridgehead Nitrogen Substituent

Having introduced the alkyl chloride, we turned our attention to installing the C11 nitrogen substituent via the key nitrene insertion reaction (Scheme 2.5). The requisite substrate for this transformation (**2.8**), was accessed from **2.19** in four steps that began with conversion to silyl ether **2.20** using a protection / olefination sequence.[25] Deprotection of **2.20** followed by carbamoylation delivered the nitrene insertion substrate **2.8** in quantitative yield over two steps. As mentioned above, our previous studies of related nitrene insertion reactions were performed on substrates epimeric at C10.[7] Although these prior attempts routinely delivered the desired C11-functionalized products, Ag-[26] or Rh-promoted[27] nitrene insertion reactions of **2.8** were regrettably found to predominantly furnish **2.21**, the product of nitrene insertion into the C9–H bond.[28]

Scheme 2.5

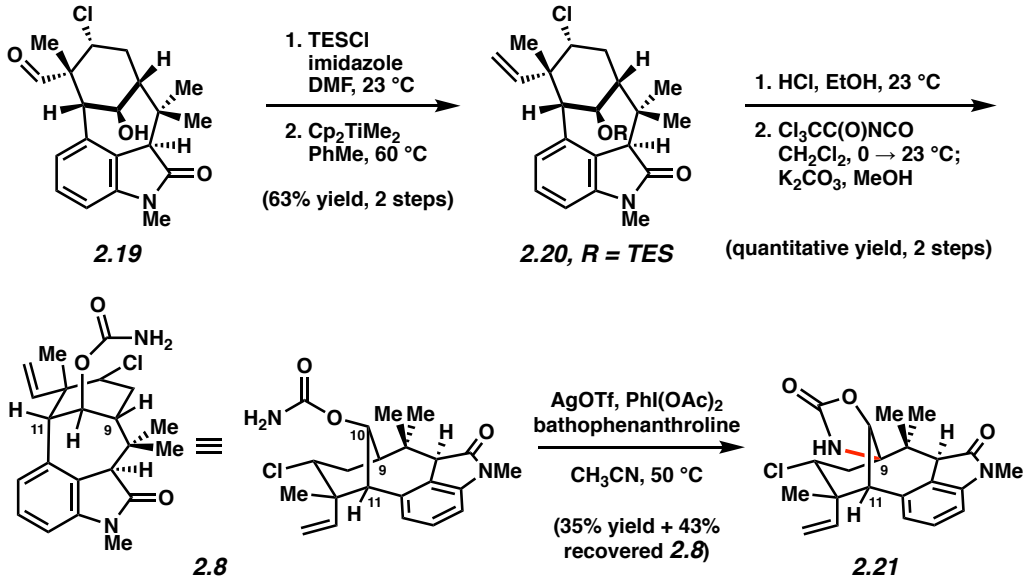

2.7 Nitrene Insertion, Oxazolidinone Cleavage, and Completion of (–)-*N*-Methylwelwitindolinone B Isothiocyanate

To test if the formation of **2.21** was strictly an artifact of the stereochemical configuration, we prepared the corresponding C10 epimer of nitrene insertion substrate **2.8** (Scheme 2.6). To that end, oxidation of alcohol **2.19**, followed by Wittig olefination, afforded ketone **2.22**. Subsequent reduction of **2.22** with $LiAlD_4$[29] occurred with complete diastereoselectivity to furnish an alcohol intermediate, which was carbamoylated to provide **2.23**. Fortunately, carbamate **2.23** proved to be a viable substrate for the desired nitrene insertion reaction; upon treatment of **2.23** with AgOTf, $PhI(OAc)_2$, and bathophenanthroline in CH_3CN at 50 °C, we obtained the C11 functionalized product **2.24** in 55% yield with 10% recovered **2.22**. The dichotomy regarding the nitrene products derived from substrates **2.8** and **2.23** underscores the subtleties often seen in late-stage manipulations in total synthesis. Moreover, the successful

formation of **2.24** is noteworthy in that He's Ag-based nitrene insertion conditions[26] tolerate the sensitive alkyl chloride unit.

Scheme 2.6

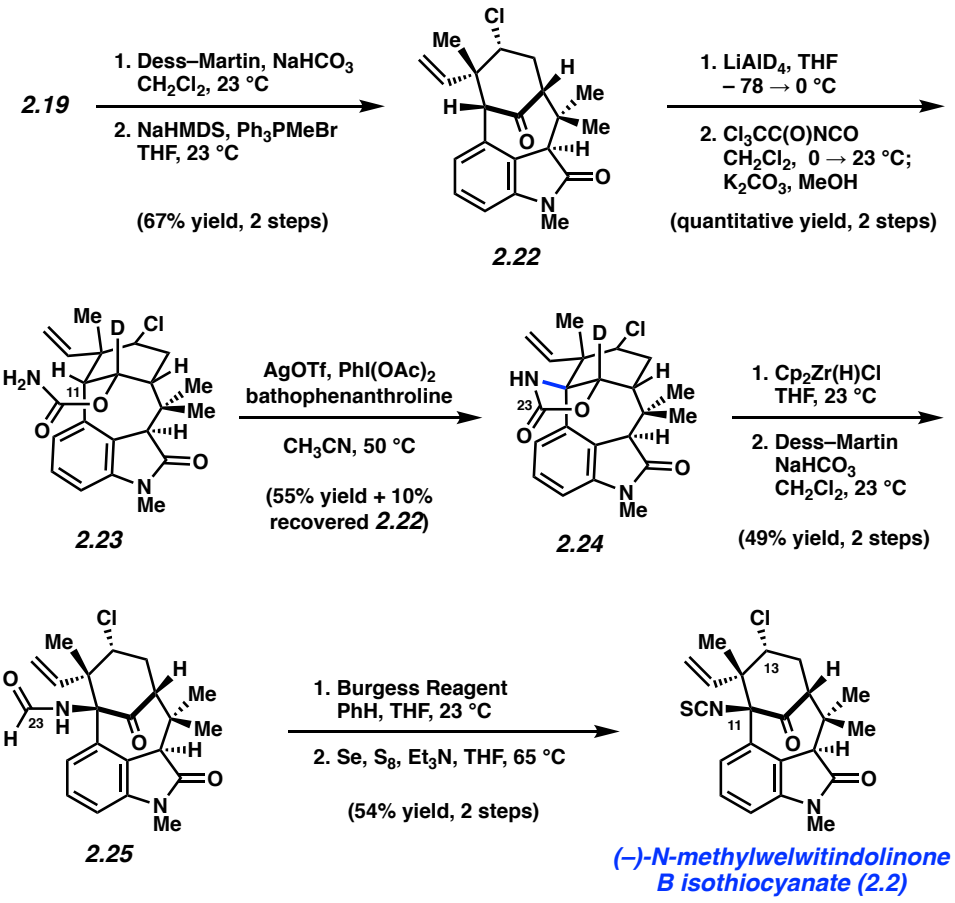

From insertion product **2.24**, all that remained to complete the total synthesis of **2.2** was cleavage of the carbamate, followed by oxidation and *N*-functionalization. Despite previously having success with carbamate hydrolysis on related compounds, we found that treatment of **2.24** with $Ba(OH)_2$ led to decomposition of the alkyl chloride. This led us to develop a milder means for cleaving the carbamate. Prompted by Snieckus' recent report of cleaving *N*,*N*-dialkylcarbamate derivatives of phenols,[30] cyclic carbamate **2.24** was exposed to Schwartz'

reagent in THF (Scheme 2.6). Gratifyingly, the carbamate was cleaved selectively to give an amidoalcohol intermediate, where C23 of **2.24** had conveniently been retained as a formyl group on the bridgehead nitrogen. Oxidation of the alcohol intermediate delivered **2.25**. With the chloride still intact, dehydration with Burgess reagent and sulfurization[31] afforded (–)-*N*-methylwelwitindolinone B isothiocyanate (**2.2**). Analytical data for (–)-**2.2** were found to be identical to that of the natural material in all respects.

2.8 Conclusion

In summary, we have completed the first total synthesis of (–)-*N*-methylwelwitindolinone B isothiocyanate (**2.2**) in 15 steps from indolyne cyclization product **2.10**. Critical to the success of our enantiospecific route is the use of a regio- and diastereoselective chlorinative oxabicycle ring-opening reaction to introduce the challenging alkyl chloride. To complete the synthesis, a number of steps were taken, including substrate-specific installation of the C11 nitrogen substituent and oxazolidinone cleavage, all of which proceeded in the presence of the alkyl chloride motif. With our completed synthesis of (–)-**2.2**, all structural classes of the welwitindolinones are now accessible by synthetic chemistry.

2.9 Experimental Section

2.9.1 Materials and Methods

Unless stated otherwise, reactions were conducted in flame-dried glassware under an atmosphere of nitrogen using anhydrous solvents (either freshly distilled or passed through activated alumina columns). All commercially available reagents were used as received unless otherwise specified. $LiAlD_4$ was obtained from Acros. AgOTf and Schwartz' reagent were obtained from Strem. Bathophenanthroline and selenium metal were obtained from Alfa Aesar. Ms_2O and BCl_3 were obtained from Aldrich. Petasis reagent[32] and Dess–Martin periodinane[33] were prepared from known literature procedures. Unless stated otherwise, reactions were performed at room temperature (RT, approximately 23 °C). Thin-layer chromatography (TLC) was conducted with EMD gel 60 F254 pre-coated plates (0.25 mm) and visualized using a combination of UV, anisaldehyde, iodine, and potassium permanganate staining. Silicycle silica gel 60 (particle size 0.040–0.063 mm) was used for flash column chromatography. ^1H and 2D NMR spectra were recorded on Bruker spectrometers (500 MHz). Data for ^1H spectra are reported as follows: chemical shift (δ ppm), multiplicity, coupling constant (Hz), integration and are referenced to the residual solvent peak 7.26 ppm for $CDCl_3$ and 7.16 for C_6D_6. Data for ^2H NMR spectra are reported as follows: chemical shift (δ ppm, at 77 MHz), multiplicity, coupling constant, integration and are referenced to the residual solvent peak 7.26 ppm for $CDCl_3$. ^{13}C NMR spectra are reported in terms of chemical shift (at 125 MHz) and are referenced to the residual solvent peak 77.16 ppm for $CDCl_3$.[34] IR spectra were recorded on a Perkin-Elmer 100 spectrometer and a JASCO 4100 spectrometer and are reported in terms of frequency absorption (cm^{-1}). Optical rotations were measured with a Rudolph Autopol III Automatic Polarimeter. Uncorrected melting points were measured using a Mel-Temp II melting point apparatus with a

Fluke 50S thermocouple and a Digimelt MPA160 melting point apparatus. High resolution mass spectra were obtained from the UC Irvine Mass Spectrometry Facility and the UCLA Molecular Instrumentation Center.

2.9.2 Experimental Procedures

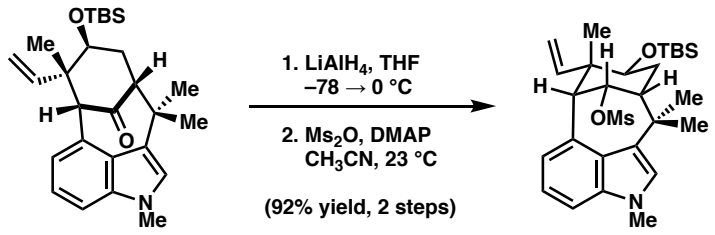

2.10 *2.13*

Mesylate 2.13. To a solution of indole **2.10**[7a] (500 mg, 1.14 mmol, 1.0 equiv) in THF (38.0 mL) at –78 °C was added a solution of $LiAlH_4$ (1.0 M in THF, 3.44 mL, 3.44 mmol, 3.0 equiv) in a dropwise manner. After stirring at –78 °C for 5 min, the solution was then allowed to warm to 0 ºC. After 20 min, the reaction was quenched at 0 °C with slow addition of a saturated solution of aqueous Rochelle's salt (30 mL), and then allowed to warm to 23 ºC. The resulting biphasic mixture was stirred at room temperature for 30 min, transferred to a separatory funnel with EtOAc (30 mL) and H_2O (30 mL), and extracted with EtOAc (3 x 20 mL). The organic layers were combined, dried over Na_2SO_4, and evaporated under reduced pressure. The resulting residue was used in the subsequent step without further purification.

To a flask containing the crude product (382 mg, 0.87 mmol, 1.0 equiv) from the previous step was added DMAP (637 mg, 5.22 mmol, 6.0 equiv) and Ms_2O (409 mg, 2.35 mmol, 2.7 equiv) as solids. The flask was flushed with N_2, to which CH_3CN (7.77 mL) was then added and the reaction mixture was allowed to stir at room temperature. After 2 h the reaction was filtered by passage through a plug of silica gel (5:1 hexanes:EtOAc eluent) to afford mesylate

2.13 (413 mg, 92% yield, over two steps) as a white foam. Mesylate **2.13**: mp: 71.5 ºC; R_f 0.53 (5:1 hexanes:EtOAc); ^{1}H NMR (500 MHz, $CDCl_3$): δ 7.17 (dd, *J* = 8.1, 0.6, 1H), 7.06 (dd, *J* = 8.1, 7.2, 1H), 6.95 (s, 1H), 6.66 (d, *J* = 7.1, 1H), 5.79 (app t, *J* = 5.8, 1H), 4.92 (dd, *J* = 17.5, 1.1, 1H), 4.78 (dd, *J* = 11.0, 1.1, 1H), 4.44 (dd, *J* = 17.4, 10.9, 1H), 4.77 (s, 3H), 3.64 (dd, *J* = 12.3, 4.2, 1H), 3.33 (d, *J* = 5.4, 1H), 2.85 (s, 3H), 2.55–2.48 (m, 1H), 2.18 (ddd, *J* = 14.7, 4.0, 2.7, 1H), 1.95 (ddd, *J* = 14.7, 12.4, 5.6, 1H), 1.57 (s, 3H), 1.42 (s, 3H), 1.36 (s, 3H), 0.73 (s, 9H), –0.16 (s, 3H), –0.38 (s, 3H); ^{13}C NMR (125 MHz, $CDCl_3$): δ 146.8, 136.7, 130.5, 126.4, 125.7, 124.4, 124.2, 120.5, 112.5, 107.8, 82.4, 68.2, 57.7, 49.2, 48.7, 40.5, 39.1, 37.4, 33.0, 32.8, 32.0, 25.9, 18.0, 16.1, -4.0, -4.6; IR (film): 2952, 2895, 1607, 1533, 1472 cm^{-1}; HRMS-ESI (*m/z*) [M + H]$^+$ calcd for $C_{28}H_{44}NO_4SSi$, 518.27603; found 518.27472; $[\alpha]^{21.6}_D$ +59.60° (*c* = 1.000, $CHCl_3$).

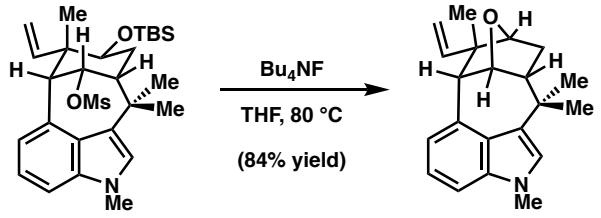

2.13 *2.14*

Oxabicycle 2.14. To a Schlenk tube containing a solution of mesylate **2.13** (118 mg, 0.23 mmol, 1.0 equiv) in THF (5.8 mL) was added TBAF (1.0 M in THF, 681 μL, 0.68 mmol, 3.0 equiv) in a dropwise manner. The Schlenk tube was then sealed and heated to 80 °C. After 21 h, the solution was then allowed to cool to 23 ºC and then filtered by passage over a plug of silica gel (EtOAc eluent, 30 mL). The filtrate was concentrated and the resulting residue was purified by flash chromatography (9:1 hexanes:EtOAc) to afford oxabicycle **2.14** (56 mg, 84% yield) as a white solid. Oxabicycle **2.14**: mp: 108.8 ºC; R_f 0.66 (3:1 hexanes:EtOAc); ^{1}H NMR (500 MHz, $CDCl_3$): δ 7.16–7.08 (m, 2H), 6.91 (s, 1H), 6.72 (d, *J* = 6.4, 1H), 4.93 (app t, *J* = 4.4, 1H), 4.75–

4.71 (m, 1H), 4.65–4.59 (m, 1H), 4.55–4.52 (m, 1H), 4.16 (d, *J* = 6.1, 1H), 3.75 (s, 3H), 3.46 (d, *J* = 5.3, 1H), 2.44–2.34 (m, 1H), 1.89–1.83 (ddd, *J* = 23.8, 11.8, 6.3, 1H), 1.64–1.60 (dd, *J* = 12.4, 8.5, 1H), 1.43 (s, 3H), 1.37 (s, 3H), 1.23 (s, 3H); ^{13}C NMR (500 MHz, $CDCl_3$) δ 140.7, 137.4, 131.3, 126.2, 124.6, 122.0, 121.5, 120.5, 114.3, 107.3, 87.2, 82.2, 59.8, 55.7, 53.0, 35.9, 34.9, 32.9, 28.7, 28.4, 27.5; IR (film): 2962, 2904, 2864, 1632, 1541, 1456 cm^{-1}; HRMS-ESI (*m/z*) $[M + H]^+$ calcd for $C_{21}H_{26}NO$, 308.20144; found 308.20022; $[\alpha]^{21.4}_D$ +115.40° (*c* = 1.000, $CHCl_3$).

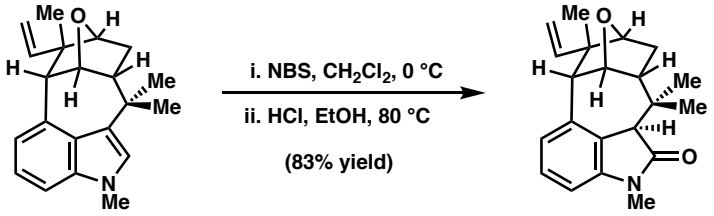

2.14 ***2.15***

Oxindole 2.15. To a solution of indole **2.14** (137 mg, 0.44 mmol, 1.0 equiv) in CH_2Cl_2 (8.2 mL) at 0 ºC was added NBS (80.0 mg, 0.45 mmol, 1.01 equiv) in one portion. The reaction vial was flushed with N_2, and allowed to stir at 0 ºC. After 15 min, solid $NaHCO_3$ (137 mg, 100 wt %) was added in one portion. The reaction was removed from the 0 ºC bath and allowed to stir at room temperature for 5 min. The resulting suspension was then evaporated under reduced pressure. Absolute ethanol (7.0 mL) and concentrated aqueous HCl (7.0 mL) were added. After heating to 80 ºC for 2 h, the reaction mixture was cooled to room temperature and transferred to a separatory funnel with H_2O (14 mL) and EtOAc (14 mL). To the separatory funnel was slowly added solid $NaHCO_3$ until gas evolution was no longer observed. The resulting biphasic mixture was extracted with EtOAc (3 x 14 mL) and the organic layers were combined, dried over Na_2SO_4, and evaporated under reduced pressure. The resulting residue was purified by flash

chromatography (9:1 hexanes:EtOAc) to afford oxindole **2.15** (120 mg, 83% yield) as a white solid. Oxindole **2.15**: mp: 138.4 ºC; R_f 0.59 (1:1 hexanes:EtOAc); ^{1}H NMR (500 MHz, $CDCl_3$): δ 7.19 (ddd, *J* = 7.8, 7.8, 0.6, 1H), 6.76 (d, *J* = 7.5, 1H), 6.70 (d, *J* = 7.7, 1H), 5.53 (dd, *J* = 17.9, 11.2, 1H), 4.96 (dd, *J* = 11.2, 1.2, 1H), 4.84 (dd, *J* = 17.9, 1.2, 1H), 4.47 (app t, *J* = 5.0, 1H), 4.38 (d, *J* = 5.8, 1H), 3.46 (s, 1H), 3.19 (s, 3H), 3.02 (d, *J* = 4.5, 1H), 2.31–2.22 (m, 1H), 2.11 (dd, *J* = 12.9, 6.6, 1H), 1.98 (ddd, *J* = 12.2, 12.2, 5.8, 1H), 1.43 (s, 3H), 1.35 (s, 3H), 0.73 (s, 3H); ^{13}C NMR (125 MHz, $CDCl_3$: δ 176.6, 144.2, 140.6, 134.3, 128.1, 126.5, 126.2, 116.4, 106.6, 87.0, 80.8, 60.3, 56.5, 51.2, 49.9, 37.0, 31.9, 27.8, 27.6, 26.3, 23.2; IR (film): 2962, 1703, 1605, 1469, 1324 cm^{-1}; HRMS-ESI (*m/z*) [M + H]$^+$ calcd for $C_{21}H_{26}NO_2$, 324.19635; found 324.19514; $[\alpha]^{21.4}_D$ +28.20° (*c* = 1.000, $CHCl_3$).

The structure of **2.15** was confirmed by a 2D-NOESY experiment, as the following interactions were observed:

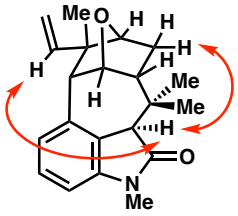

2.15

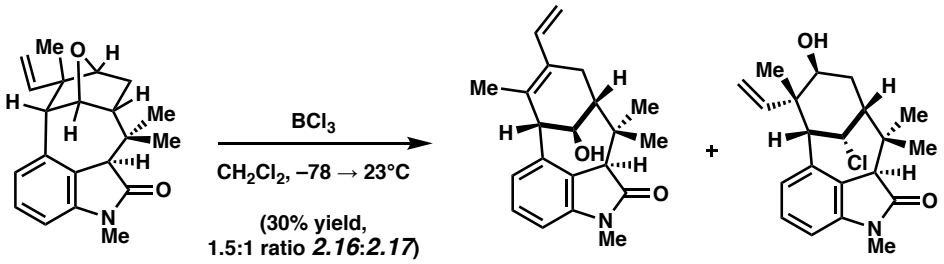

2.15 ***2.16*** ***2.17***

Diene 2.16 and Alkyl Chloride 2.17. A solution of oxindole **2.15** (6.1 mg, 0.019 mmol, 1.0 equiv) in CH_2Cl_2 (1.89 mL) was cooled to –78 °C. A solution of BCl_3 (1.0 M in CH_2Cl_2, 145.4

μL, 0.14 mmol, 7.7 equiv) was added in a dropwise manner. The resulting solution was allowed to stir at –78 °C. After 30 min, the solution was then allowed to warm to 0 ºC. After 2 h the solution was then warmed to room temperature. After 4 h the reaction was quenched with addition of a saturated aqueous solution of $NaHCO_3$ (1 mL) and transferred to a separatory funnel with EtOAc (6 mL) and H_2O (4 mL), and extracted with EtOAc (3 x 3 mL). The organic layers were combined, dried over Na_2SO_4, and evaporated under reduced pressure. The resulting residue was purified by preparative thin layer chromatography (1:1 hexanes:EtOAc) to afford diene **2.16** (1.1 mg, 18% yield) and alkyl chloride **2.17** (0.8 mg, 12% yield) as amorphous solids. Diene **2.16**: R_f 0.60 (1:1 hexanes:EtOAc); ^{1}H NMR (500 MHz, $CDCl_3$): δ 7.21 (ddd, *J* = 7.8, 7.8, 0.6, 1H), 6.91 (d, *J* = 7.3, 1H), 6.76 (dd, *J* = 17.2, 11.0, 1H), 6.67 (d, *J* = 7.8, 1H), 5.32 (d, *J* = 17.2, 1H), 5.09 (d, *J* = 11.1, 1H), 4.24 (br. s, 1H), 3.32 (s, 1H), 3.25 (s, 1H), 3.14 (s, 3H), 2.73 (d, *J* = 18.7, 1H), 2.56 (dd, *J* = 18.7, 7.9, 1H), 2.02 (d, *J* = 7.9, 1H), 1.79 (d, *J* = 6.7, 1H), 1.68 (s, 3H), 1.54 (s, 3H), 0.73 (s, 3H); ^{13}C NMR (125 MHz, $CDCl_3$): δ 176.4, 144.4, 135. 8, 134.0, 128.9, 128.1, 126.6, 126.4, 123.5, 112.9, 106.4, 67.5, 54.4, 50.9, 49.1, 39.0, 28.0, 26.1, 22.5, 21.2, 17.8; IR (film): 3412, 2969, 1690, 1608, 1470 cm^{-1}; HRMS-ESI (*m/z*) $[M + H]^+$ calcd for $C_{21}H_{26}NO_2$, 324.19635; found 324.19417; $[\alpha]^{21.4}_D$ –264.00° (*c* = 0.150, $CHCl_3$). Alkyl chloride **2.17**: R_f 0.52 (1:1 hexanes:EtOAc); ^{1}H NMR (500 MHz, $CDCl_3$, 25 of 26 observed): δ 7.16 (ddd, *J* = 7.8, 7.8, 0.7, 1H), 6.68 (dd, *J* = 7.8, 0.7, 1H), 6.65 (d, *J* = 7.7, 1H), 5.31 (dd, *J* = 17.4, 10.7, 1H), 5.12 (dd, *J* = 17.4, 1.0, 1H), 5.03 (dd, *J* = 10.7, 1.0, 1H), 4.69 (br. s, 1H), 4.12 (dd, *J* = 10.3, 7.1, 1H), 3.57 (s, 1H), 3.20–3.18 (m, 1H), 3.17 (s, 3H), 2.37–2.32 (m, 2H), 2.28–2.25 (m, 1H), 1.67 (s, 3H), 1.57 (s, 3H), 0.89 (s, 3H); ^{13}C NMR (125 MHz, $CDCl_3$): δ 175.2, 146.3, 145.0, 138.7, 128.0, 126.8, 124.1, 114.8, 106.8, 69.7, 59.3, 58.2, 56.8, 54.8, 46.5, 39.4, 27.3, 26.3, 25.3,

23.3, 19.0; IR (film): 3451, 2962, 2872, 1699, 1609 cm^{-1}; HRMS-ESI (*m/z*) $[M + H]^+$ calcd for $C_{21}H_{27}ClNO_2$, 360.17303; found 360.17087; $[\alpha]^{21.2}_D$ –9.00° (*c* = 0.400, $CHCl_3$).

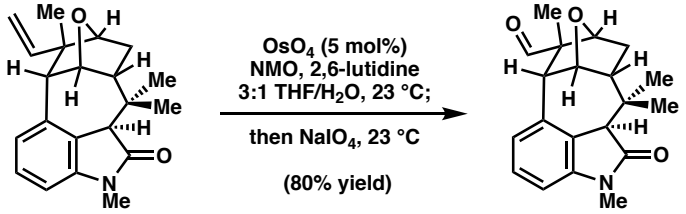

2.15 *2.18*

Aldehyde 2.18. To a solution of oxindole **2.15** (45 mg, 0.14 mmol, 1.0 equiv) in a 3:1 mixture of THF/H_2O (1.4 mL) was added 2,6-lutidine (32 μL, 0.28 mmol, 2.0 equiv), OsO_4 (20 mg/mL in H_2O, 84 μL, 0.007 mmol, 0.05 equiv), and NMO (65 mg, 0.56 mmol, 4.0 equiv). The resulting solution was flushed with N_2 and stirred at room temperature. After 19 h, solid $NaIO_4$ (89 mg, 0.42 mmol, 3.0 equiv) was added in one portion and the reaction mixture was stirred at room temperature. After 13 min, the reaction mixture was quenched with a saturated aqueous solution of $Na_2S_2O_3$ (1 mL) and stirred vigorously at room temperature. After 30 min the resulting mixture was transferred to a test tube with EtOAc (5 mL) and H_2O (5 mL). The resulting biphasic mixture was extracted with EtOAc (3 x 3 mL). The organic layers were combined, dried over Na_2SO_4, and evaporated under reduced pressure. The resulting residue was purified by preparative thin layer chromatography (3:1 hexanes:EtOAc) to afford aldehyde **2.18** (36 mg, 80% yield) as a white solid. Aldehyde **2.18**: mp: 181.1 ºC; R_f 0.53 (1:1 hexanes:EtOAc); ^{1}H NMR (500 MHz, $CDCl_3$): δ 9.17 (s, 1H), 7.24 (dd, *J* = 7.7, 7.7, 1H), 6.89 (d, *J* = 7.7, 1H), 6.74 (d, *J* = 7.8, 1H), 4.55 (t, *J* = 4.9, 1H), 4.47 (d, *J* = 5.0, 1H), 3.26 (s, 1H), 3.18–3.16 (m, 4H), 2.37–2.29 (m, 1H), 2.16–2.07 (m, 2H), 1.43 (s, 3H), 1.37 (s, 3H), 0.74 (s, 3H); ^{13}C NMR (125 MHz, $CDCl_3$): δ 204.6, 175.9, 144.7, 131.8, 128.8, 125.65, 125.60, 107.4, 84.6, 81.0, 59.1, 58.9,

56.0, 49.3, 36.9, 282, 27.5, 26.4, 25.4, 23.2; IR (film): 2959, 2928, 1708, 1606, 1470 cm^{-1}; HRMS-ESI (*m/z*) $[M + H]^+$ calcd for $C_{20}H_{24}NO_3$, 326.17562; found 326.17443; $[\alpha]^{21.6}_D$ +23.80° (*c* = 1.000, $CHCl_3$).

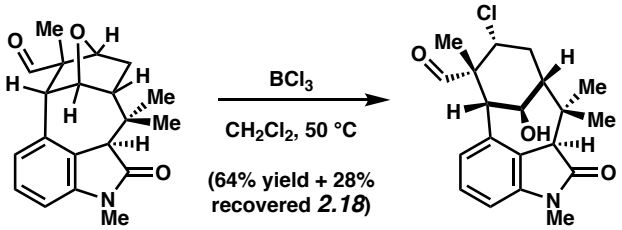

2.18 ***2.19***

Alkyl Chloride 2.19. To a scintillation vial containing oxindole **2.18** (19.3 mg, 0.059 mmol, 1.0 equiv) was added a solution of BCl_3 (1.0 M in CH_2Cl_2, 178.2 μL, 0.178 mmol, 3.0 equiv) in a dropwise manner. The reaction vial was then sealed and heated to 50 °C. After 2 h, the solution was then allowed to cool to 23 ºC and quenched with addition of a saturated aqueous solution of $NaHCO_3$ (1 mL) and transferred to a separatory funnel with EtOAc (6 mL) and H_2O (6 mL), and extracted with EtOAc (3 x 3 mL). The organic layers were combined, dried over Na_2SO_4, and evaporated under reduced pressure. The resulting residue was purified by preparative thin layer chromatography (1:1 hexanes:EtOAc) to afford alkyl chloride **2.19** (13.7 mg, 64% yield) as a white solid and recovered oxindole **2.18** (5.4 mg, 28% yield). Alkyl chloride **2.19**: mp: 176.4 ºC; R_f 0.42 (1:1 hexanes:EtOAc); ^{1}H NMR (500 MHz, $CDCl_3$): δ 9.29 (s, 1H), 7.18 (dd, *J* = 7.7, 7.7, 1H), 6.75 (d, *J* = 7.7, 1H), 6.70 (d, *J* = 7.8, 1H), 5.13–5.04 (m, 1H), 4.18 (s, 1H), 3.47 (s, 1H), 3.24–3.21 (m, 1H), 3.16 (s, 3H), 2.61–2.56 (m, 2H), 2.20–2.16 (m, 1H) 1.90 (s, 1H), 1.58 (s, 3H), 1.56 (s, 3H), 0.88 (s, 3H); ^{13}C NMR (125 MHz, $CDCl_3$): δ 200.3, 175.8, 144.9, 133.8, 128.9, 125.1, 124.8, 107.5, 69.6, 61.8, 57.4, 53.8, 51.6, 50.5, 39.5, 31.3, 26.4, 26.1, 25.9, 22.8;

IR (film): 3443, 2967, 1689, 1609, 1594 cm^{-1}; HRMS-ESI (*m/z*) $[M + H]^+$ calcd for $C_{20}H_{25}ClNO_3$, 362.15230; found 362.15085; $[\alpha]^{23.0}_D$ +59.60° (*c* = 1.000, $CHCl_3$).

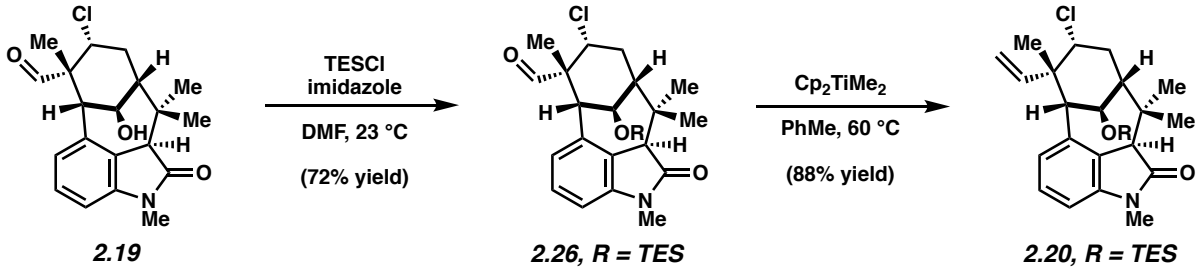

Silyl Ether 2.20. To a solution of **2.19** (18.8 mg, 0.052 mmol, 1.0 equiv) in DMF (944 μL) was added imidazole (35.3 mg, 0.52 mmol, 3.0 equiv). The reaction vial was then purged with N_2 and TESCl (26.2 μL, 0.156 mmol, 3.0 equiv) was added in a dropwise manner. The resulting solution was stirred at room temperature. After 1 h the reaction was quenched by addition of a saturated aqueous solution of $NaHCO_3$ (2 mL) and transferred to a separatory funnel with EtOAc (6 mL) and H_2O (4 mL). After extracting with EtOAc (3 x 3 mL), the organic layers were combined, dried over Na_2SO_4, and evaporated under reduced pressure. The resulting residue was purified by preparative thin layer chromatography (1:1 hexanes:EtOAc) to afford **2.26** (18 mg, 72% yield) as an amorphous solid. **2.26**: R_f 0.69 (1:1 hexanes:EtOAc); ^{1}H NMR (500 MHz, $CDCl_3$): δ 9.30 (s, 1H), 7.18 (ddd, *J* = 7.8, 7.7, 0.65, 1H), 6.72 (d, *J* = 7.6, 1H), 6.70 (d, *J* = 7.8, 1H), 5.12–5.03 (m, 1H), 4.10–4.04 (m, 1H), 3.46 (s, 1H), 3.16 (s, 3H), 3.14–3.10 (m, 1H), 2.61–2.51 (m, 2H), 2.19–2.11 (m, 1H), 1.55 (s, 3H), 1.54 (s, 3H), 0.96 (t, *J* = 7.9, 9H), 0.86 (s, 3H), 0.59 (q, *J* = 7.9, 6H).

To a vial containing **2.26** (17.9 mg, 0.038 mmol, 1.0 equiv) was added the Petasis reagent (1.0 M in PhMe, 444 μL, 0.444 mmol, 11.8 equiv) in the absence of light. The reaction vessel was then sealed and heated to 60 °C. After 4.5 h the reaction was cooled to room temperature and filtered by passage over a plug of silica gel (3:1 hexanes:EtOAc eluent, 15 mL). The filtrate

was evaporated under reduced pressure and the resulting residue was purified by preparative thin layer chromatography (3:1 hexanes:EtOAc) to afford silyl ether **2.20** (15.6 mg, 88% yield) as an amorphous solid. Silyl Ether **2.20**: R_f 0.57 (3:1 hexanes:EtOAc); ^{1}H NMR (500 MHz, $CDCl_3$): δ 7.14 (dd, *J* = 7.7, 7.7, 1H), 6.65 (d, *J* = 7.6, 1H), 6.62 (d, *J* = 7.6, 1H), 5.65 (dd, *J* = 17.2, 10.9, 1H), 5.15 (dd, *J* = 12.7, 4.5, 1H), 4.85 (dd, *J* = 17.3, 0.9, 1H), 4.80 (d, *J* = 11.1, 1H), 4.04 (br. s, 1H), 3.46 (s, 1H), 3.17 (s, 3H), 3.12–3.08 (m, 1H), 2.43–2.34 (m, 1H), 2.19–2.03 (m, 2H), 1.51 (s, 3H), 1.50 (s, 3H), 0.96 (t, *J* = 7.9, 9H), 0.85 (s, 3H), 0.58 (q, *J* = 7.8, 6H); ^{13}C NMR (125 MHz, $CDCl_3$): δ 176.2, 144.5, 138.6, 138.3, 128.0, 125.5, 124.4, 115.0, 106.3, 70.0, 65.3, 60.7, 54.8, 50.6, 44.4, 39.7, 31.5, 29.7, 26.3, 25.9, 22.6, 7.1, 4.9; IR (film): 2956, 2912, 1708, 1610, 1597 cm^{-1}; HRMS-ESI (*m/z*) $[M + H]^+$ calcd for $C_{27}H_{41}ClNO_2Si$, 474.25951; found 474.25746; $[\alpha]^{21.0}_D$ –1.40° (*c* = 1.000, $CHCl_3$).

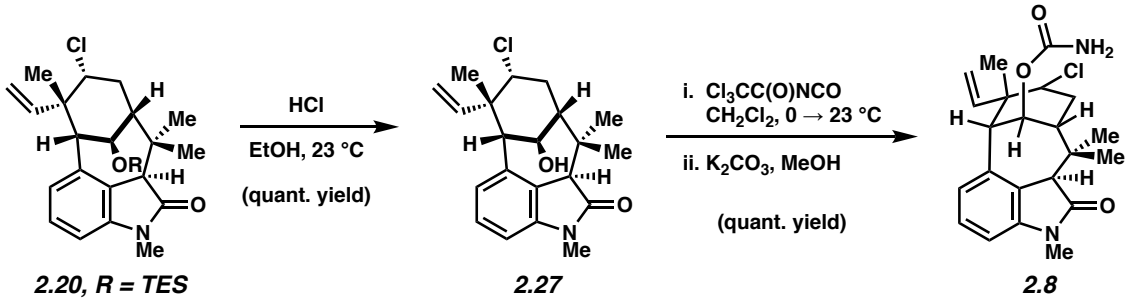

Carbamate 2.8. A flask was charged with silyl ether **2.20** (5.4 mg, 0.011 mmol, 1.0 equiv), followed by the addition of absolute ethanol (542 μL) and concentrated aqueous HCl (542 μL). The solution was then allowed to stir at room temperature. After 20 min, the reaction mixture was transferred to a separatory funnel with EtOAc (6 mL). To the funnel was added a saturated aqueous solution of $NaHCO_3$ (5 mL) slowly until gas evolution was no longer observed. The resulting biphasic mixture was extracted with EtOAc (3 x 3 mL) and the organic layers were combined, dried over Na_2SO_4, and evaporated under reduced pressure. The resulting residue was

purified by preparative thin layer chromatography (1:1 hexanes:EtOAc) to afford **2.27** (4.1 mg, quant. yield) as an amorphous solid. Alcohol **2.27**: R_f 0.18 (3:1 hexanes:EtOAc); ^{1}H NMR (500 MHz, $CDCl_3$): δ 7.14 (dd, *J* = 7.7, 7.7, 1H), 6.67–6.63 (m, 2H), 5.64 (dd, *J* = 17.3, 11.0, 1H), 5.14 (dd, *J* = 12.8, 4.5, 1H), 4.87 (dd, *J* = 17.2, 0.8, 1H), 4.81 (d, *J* = 11.1, 1H), 4.15 (s, 1H), 3.47 (s, 1H), 3.17 (s, 3H), 2.42 (ddd, *J* = 14.7, 10.8, 5.3,1H), 2.21–2.07 (m, 2H), 1.54 (s, 3H), 1.52 (s, 3H), 0.85 (s, 3H).

To a solution of **2.27** (4.1 mg, 0.011 mmol, 1.0 equiv) in CH_2Cl_2 (228 μL) at 0 °C was added trichloroacetyl isocyanate (1.7 μL, 0.0142 mmol, 1.25 equiv) in a dropwise manner. The resulting mixture was allowed to stir at 0 °C for 5 min, and then at room temperature for 30 min. The solvent was evaporated under reduced pressure. To the resulting residue was added MeOH (228 μL) followed by addition of solid K_2CO_3 (8.6 mg, 0.0626 mmol, 5.5 equiv) in one portion. The reaction was flushed with N_2 and left to stir at room temperature. After 1 h, the reaction was quenched with a saturated aqueous solution of NH_4Cl (1 mL), and the resulting biphasic mixture was transferred to a separatory funnel with EtOAc (6 mL) and H_2O (4 mL). After extracting with EtOAc (3 x 3 mL), the organic layers were combined, dried over Na_2SO_4, and evaporated under reduced pressure. The resulting residue was purified by preparative thin layer chromatography (1:1 hexanes:EtOAc) to afford carbamate **2.8** (4.6 mg, quant. yield) as an amorphous solid. Carbamate **2.8**: R_f 0.44 (1:1 hexanes:EtOAc); ^{1}H NMR (500 MHz, $CDCl_3$): δ 7.15 (dd, *J* = 7.8, 7.8, 1H), 6.70–6.63 (m, 2H), 5.62 (dd, *J* = 17.2, 10.8, 1H), 5.14–5.09 (m, 1H), 4.88 (dd, *J* = 17.2, 0.7, 1H), 4.84 (d, *J* = 11.0, 1H), 4.77 (dd, *J* = 12.7, 4.7, 1H), 4.66 (s, 2H), 3.47 (s, 1H), 3.28–3.25 (m, 1H), 3.18 (s, 3H), 2.44–2.34 (m, 1H), 2.23–2.13 (m, 2H), 1.53, (s, 3H), 1.50 (s, 3H), 0.93 (s, 3H); ^{13}C NMR (125 MHz, $CDCl_3$): δ 175.9, 155.3, 144.5, 137.9, 137.0, 128.2, 125.7, 124.4, 115.6, 106.7, 73.2, 64.6, 57.0, 51.1, 50.7, 44.1, 39.7, 31.0, 29.4, 26.4, 25.7, 22.3; IR (film): 3489,

3348, 2966, 1694, 1610 cm^{-1}; HRMS-ESI (*m/z*) $[M + H]^+$ calcd for $C_{22}H_{28}ClN_2O_3$, 403.17885; found 403.17618; $[\alpha]^{23.4}_D$ –89.33° (*c* = 1.000, $CHCl_3$).

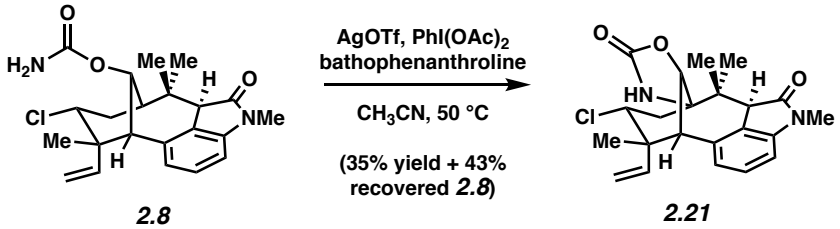

Oxazolidinone 2.21. A 1-dram vial containing CH_3CN, a second 1-dram vial charged with bathophenanthroline (3.8 mg, 0.011 mmol, 1.0 equiv), and a third 1-dram vial containing carbamate **2.8** (4.6 mg, 0.011 mmol, 1.0 equiv) and $PhI(OAc)_2$ (14.7 mg, 0.046 mmol, 4.0 equiv) were transferred into the glovebox. AgOTf (2.9 mg, 0.011 mmol, 1.0 equiv) and CH_3CN (200 μL) were added to the vial containing the bathophenanthroline, and the resulting suspension was allowed to stir at room temperature for 20 min. Next, CH_3CN (126 μL) was added to the vial containing the carbamate, and the AgOTf/bathophenanthroline suspension was also added to this vial. The vial was then sealed, removed from the glovebox, and the resulting mixture was heated to 50 °C. After 20.5 h, the reaction was cooled to room temperature and filtered by passage over a plug of celite (EtOAc eluent, 10 mL). The filtrate was evaporated under reduced pressure, and the resulting residue was purified by preparative thin layer chromatography (1:2:2 PhH:CH_2Cl_2:Et_2O) to afford oxazolidinone **2.21** (1.6 mg, 35% yield) as an amorphous solid and recovered carbamate **2.8** (2.0 mg, 43% yield). Oxazolidinone **2.21**: R_f 0.43 (1:2:2 PhH:Et_2O:CH_2Cl_2); ^{1}H NMR (500 MHz, $CDCl_3$): δ 7.21 (dd, *J* = 7.8, 7.8, 1H), 6.75–6.68 (m, 2H), 5.77 (s, 1H), 5.39 (dd, *J* = 17.1, 10.8, 1H), 5.02 (d, *J* = 17.2, 1H), 4.94 (d, *J* = 10.8, 1H) 4.71 (d, *J* = 2.0, 1H), 4.62 (dd, *J* = 13.7, 3.6, 1H), 3.59 (s, 1H), 3.46 (s, 1H), 3.20 (s, 3H), 2.67 (app t, *J* = 14.3, 1H), 2.19 (dd, *J* = 14.7, 3.6, 1H), 1.61 (s, 3H), 1.58 (s, 3H), 0.95 (s, 3H); ^{13}C

NMR (125 MHz, $CDCl_3$): δ 174.2, 158.0, 144.7, 137.9, 136.4, 128.7, 126.7, 123.0, 116.0, 107.3, 78.7, 67.5, 61.7, 53.6, 52.7, 44.4, 41.3, 40.2, 28.3, 26.5, 21.1, 17.8; IR (film): 3268, 2975, 1754, 1702, 1610 cm^{-1}; HRMS-ESI (*m/z*) $[M + H]^+$ calcd for $C_{22}H_{26}ClN_2O_3$, 401.16320; found 401.16188; $[\alpha]^{20.5}_D$ +68.60° (*c* = 1.000, $CHCl_3$).

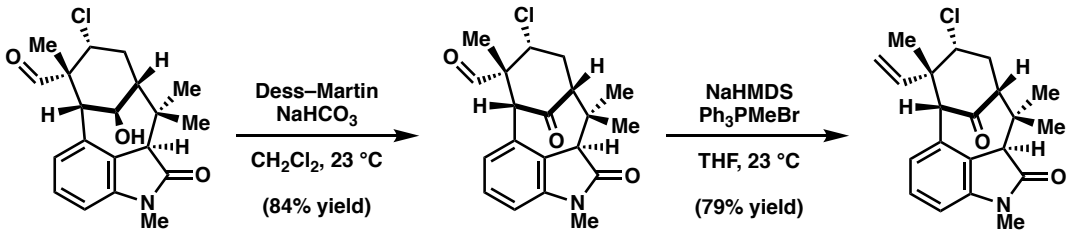

2.19 *2.28* *2.22*

Ketone 2.22. A flask containing alkyl chloride **2.19** (15.1 mg, 0.042 mmol, 1.0 equiv) was added solid $NaHCO_3$ (17.5 mg, 0.054 mmol, 5.0 equiv) in one portion. The reaction vessel was flushed with N_2, and then CH_2Cl_2 (834 μL) was added. To the resulting suspension was added the Dess–Martin periodinane reagent (23.0 mg, 0.21 mmol, 1.3 equiv) in one portion. The flask was flushed with N_2, and the reaction mixture was allowed to stir at room temperature. After 1 h, the reaction mixture was diluted with a 1:1 mixture of saturated aqueous $NaHCO_3$ and saturated aqueous $Na_2S_2O_3$ (1.0 mL). The resulting biphasic mixture was vigorously stirred until both layers appeared clear. The mixture was then transferred to a separatory funnel with EtOAc (6 mL) and H_2O (4 mL), and then extracted with EtOAc (3 x 3 mL). The organic layers were combined, dried over Na_2SO_4, and evaporated under reduced pressure. The resulting residue was purified by preparative thin layer chromatography (1:1 hexanes:EtOAc) to afford **2.28** (12.6 mg, 84% yield) as a white foam. Keto aldehyde **2.28**: R_f 0.88 (1:3 hexanes:EtOAc); ^1H NMR (500 MHz, C_6D_6): δ 9.06 (d, *J* = 1.2, 1H), 6.76 (ddd, *J* = 7.8, 7.8, 0.8, 1H), 6.33 (d, *J* = 7.6, 1H), 6.00 (d, *J* = 7.5, 1H), 3.41 (d, *J* = 2.2, 1H), 3.40 (s, 1H), 3.35 (ddd, *J* = 13.5, 4.5, 0.9, 1H), 2.84 (m,

1H), 2.52 (s, 3H), 2.28–2.21 (m, 1H), 1.93 (ddd, *J* = 14.6, 10.7, 4.6, 1H), 1.40 (s, 3H), 1.13 (s, 3H), 0.70 (s, 3H).

To a vial containing methyltriphenylphosphonium bromide (373 mg, 1.04 mmol, 15.0 equiv) was added THF (1.7 mL). The reaction vessel was cooled to 0 °C and NaHMDS (1.0 M in THF, 836 μL, 0.84 mmol, 12.0 equiv) was added in a dropwise manner. The vial was allowed to warm to room temperature and left to stir for 20 min. A solution of **2.28** (25.0 mg, 0.070 mmol, 1.0 equiv) in THF (2.4 mL) was added dropwise in three portions and the reaction was left to stir at room temperature. After 30 min the reaction was quenched with the addition of a saturated aqueous solution of NH_4Cl (5 mL). The resulting biphasic mixture was transferred to a separatory funnel with EtOAc (15 mL) and H_2O (10 mL). After extracting with EtOAc (3 x 15 mL), the organic layers were combined, dried over $MgSO_4$, and evaporated under reduced pressure. The resulting crude mixture was filtered by passage over a plug of silica gel (1:1 hexanes:EtOAc, 40 mL). The filtrate was evaporated under reduced pressure and resulting residue was purified by flash chromatography (7:1 hexanes:EtOAc) to afford ketone **2.22** (77.4 mg, 79% yield) as a white solid. Ketone **2.22**: mp: 110.4 ºC; R_f 0.67 (1:1 hexanes:EtOAc); ^{1}H NMR (500 MHz, $CDCl_3$): δ 7.21 (dd, *J* = 7.7, 7.7, 1H), 6.70 (d, *J* = 7.6, 1H), 6.68 (d, *J* = 7.7, 1H), 5.82 (dd, *J* = 17.4, 11.1, 1H), 5.00–4.95 (m, 2H), 3.99 (dd, *J* = 12.1, 3.6, 1H), 3.72 (s, 1H), 3.61 (d, *J* = 2.0, 1H), 3.19 (s, 3H), 2.75–2.64 (m, 2H), 2.54–2.47 (m, 1H), 1.55 (s, 3H), 1.48 (s, 3H), 0.71 (s, 3H); ^{13}C NMR (125 MHz, $CDCl_3$): δ 207.6, 175.3, 144.6, 136.2, 132.1, 129.0, 125.2, 124.4, 117.9, 107.3, 68.9, 64.5, 62.5, 50.9, 48.6, 41.8, 32.6, 29.7, 26.5, 25.0, 22.2; IR (film): 1702, 1607, 1591, 1465 cm^{-1}; HRMS-ESI (*m/z*) $[M + H]^+$ calcd for $C_{21}H_{25}ClNO_2$, 358.15738; found 358.15590; $[\alpha]^{23.4}_D$ +12.0° (*c* = 1.000, $CHCl_3$).

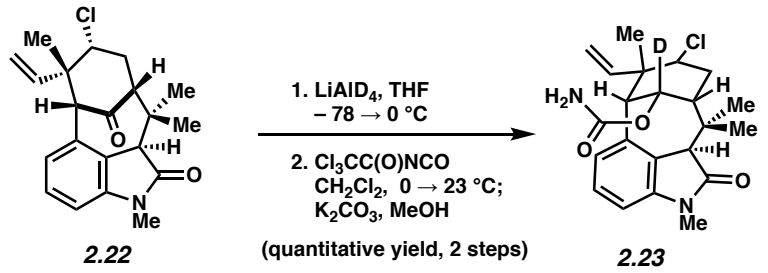

2.22 *2.23*

Carbamate 2.23. To a solution of ketone **2.22** (87 mg, 0.244 mmol, 1.0 equiv) in THF (24.4 mL) at –78 °C was added a solution of $LiAlD_4$ (1.0 M in THF, 731 μL, 0.731 mmol, 3.0 equiv) in a dropwise manner. After stirring at –78 °C for 10 min, the solution was then allowed to warm to 0 ºC. After 12 min, the reaction was quenched at 0 °C with slow addition of a saturated solution of aqueous Rochelle's salt (10 mL), and then allowed to warm to 23 ºC. The resulting biphasic mixture was stirred at room temperature for 1 h, transferred to a separatory funnel with EtOAc (10 mL) and H_2O (10 mL), and extracted with EtOAc (3 x 10 mL). The organic layers were combined, dried over $MgSO_4$, and evaporated under reduced pressure. The resulting residue was used in the subsequent step without further purification.

To a flask containing the crude residue from the previous step was added CH_2Cl_2 (4.9 mL). The reaction vessel was cooled to 0 ºC and trichloroacetyl isocyanate (36.3 μL, 0.305 mmol, 1.25 equiv) was added in a dropwise manner. The resulting mixture was allowed to stir at 0 °C for 5 min, and then at room temperature for 20 min. The solvent was evaporated under reduced pressure. To the resulting residue was added MeOH (4.9 mL) and solid K_2CO_3 (185 mg, 1.34 mmol, 5.5 equiv) in one portion. The reaction was flushed with N_2 and left to stir at room temperature for 1 h. The reaction was quenched by the addition of a solution of saturated aqueous NH_4Cl (5.0 mL), and the resulting biphasic mixture was transferred to a separatory funnel with EtOAc (10 mL) and H_2O (10 mL). After extracting with EtOAc (3 x 10 mL), the organic layers were combined, dried over $MgSO_4$, and evaporated under reduced pressure. The

resulting residue was purified by flash chromatography (2:1 → 1:1 hexanes:EtOAc) to afford carbamate **2.23** (98 mg, quantitative yield, over two steps) as a white solid. Carbamate **2.23**: mp: 102.8 ºC; R_f 0.56 (2:1 EtOAc:hexanes); ^{1}H NMR (500 MHz, $CDCl_3$): δ 7.14 (dd, *J* = 7.7, 7.7, 1H), 6.68 (d, *J* = 7.6, 1H), 6.61 (d, *J* = 7.7, 1H), 5.72 (dd, *J* = 17.1, 10.9, 1H), 4.87–4.84 (m, 2H), 4.47–4.4 (m, 3H), 3.69 (s, 1H), 3.19 (s, 3H), 3.14 (s, 1H), 2.54–2.46 (m, 2H), 2.39–2.29 (m, 1H), 1.51 (s, 3H), 1.45 (s, 3H), 0.90 (s, 3H); ^{2}H NMR (77 MHz, $CDCl_3$) δ 5.43 (br. s, 1D); ^{13}C NMR (125 MHz, $CDCl_3$): δ 176.3, 155.8, 144.3, 137.9, 137.5, 127.8, 126.5, 125.3, 116.1, 106.6, 64.1, 56.1, 51.5, 46.6, 46.3, 39.1, 33.0, 29.0, 26.7, 26.4, 24.0; IR (film): 1724, 1701, 1607, 1467, 1376, cm^{-1}; HRMS-ESI (*m*/*z*) $[M + H]^+$ calcd for $C_{22}H_{27}DClN_2O_3$, 404.18512; found 404.18342; $[\alpha]^{24.3}_D$ –3.20° (*c* = 1.000, $CHCl_3$).

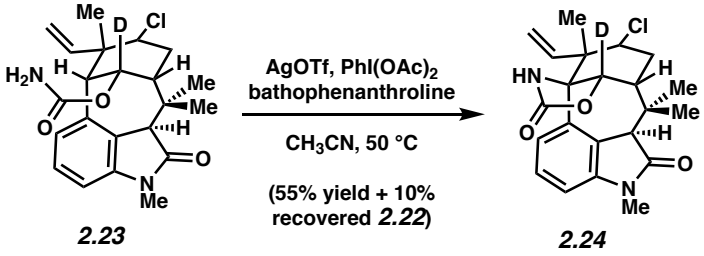

Oxazolidinone 2.24. A 1-dram vial containing CH_3CN, a second 1-dram vial charged with bathophenanthroline (13 mg, 0.039 mmol, 1.0 equiv), and a third 1-dram vial containing carbamate **2.23** (15.8 mg, 0.039 mmol, 1.0 equiv) and $PhI(OAc)_2$ (50 mg, 0.157 mmol, 4.0 equiv) were transferred into the glovebox. AgOTf (10 mg, 0.039 mmol, 1.0 equiv) and CH_3CN (550 μL) were added to the vial containing the bathophenanthroline, and the resulting suspension was allowed to stir at room temperature for 20 min. Next, CH_3CN (550 μL) was added to the vial containing the carbamate, and the AgOTf/bathophenanthroline suspension was also added to this vial. The vial was then sealed, removed from the glovebox, and the resulting mixture was heated

to 50 °C. After 24 h, the reaction was cooled to room temperature and filtered by passage over a plug of silica gel (EtOAc eluent, 10 mL). The filtrate was evaporated under reduced pressure, and the resulting residue was purified by preparative thin layer chromatography (2:1:1 benzene:Et_2O:CH_2Cl_2) to afford oxazolidinone **2.24** (8.7 mg, 55% yield) as a white solid and recovered ketone **2.22** (1 mg, 10% yield). Oxazolidinone **2.24**: mp: 183.2 ºC; R_f 0.32 (1:2:2 benzene:Et_2O:CH_2Cl_2); ^{1}H NMR (500 MHz, $CDCl_3$): δ 7.76 (s, 1H), 7.09 (dd, *J* = 7.9, 7.9, 1H), 6.69 (d, *J* = 7.8, 1H), 6.66 (d, *J* = 8.2, 1H), 5.54 (dd, *J* = 17.3, 10.7, 1H), 5.06 (d, *J* = 17.3, 1H), 5.00 (d, *J* = 10.9, 1H), 4.38–4.32 (m, 1H), 3.97 (s, 1H), 3.21 (s, 3H), 2.71–2.60 (m, 2H), 2.55–2.45 (m, 1H), 1.57 (s, 3H), 1.52 (s, 3H), 1.11 (s, 3H); ^{2}H NMR (77 MHz, $CDCl_3$) δ 4.91 (br. s, 1D); ^{13}C NMR (125 MHz, $CDCl_3$): δ 175.1, 159.5, 143.6, 138.7, 137.5, 128.2, 125.3, 124.1, 115.9, 107.0, 70.3, 63.1, 53.3, 47.9, 45.5, 38.2, 32.3, 27.1, 26.4, 23.3, 21.0; IR (film): 1748, 1703, 1683, 1610, 1591 cm^{-1}; HRMS-ESI (*m/z*) $[M + H]^+$ calcd for $C_{22}H_{25}DClN_2O_3$, 402.16947; found 402.16849; $[\alpha]^{23.1}_D$ +8.20° (*c* = 1.000, $CHCl_3$).

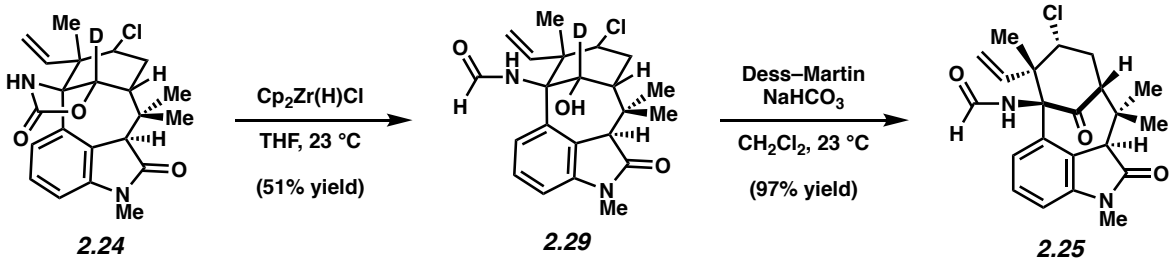

2.24 *2.29* *2.25*

Formamide 2.25. Two 1-dram vials were charged with **2.24** (7.0 mg, 0.017 mmol, 1.0 equiv each) and taken into the glovebox. Each reaction vessel was charged with Schwartz' reagent (5.9 mg, 0.023 mmol, 1.3 equiv each) and THF (1.74 mL each), which had previously been taken through six freeze-pump-thaw cycles, was added. The reaction vessels were sealed and left to stir at room temperature. After 14 h, the reaction vials were removed from the glovebox and

quenched with saturated aqueous solution of NH_4Cl (1 mL) for each vial. The resulting biphasic mixtures were transferred to a test tube with EtOAc (2 mL) and brine (1 mL). After extracting with EtOAc (3 x 2 mL). The organic layers were combined, dried over $MgSO_4$, and evaporated under reduced pressure. The resulting residue was purified by preparative thin layer chromatography (1:1 hexanes:acetone) to afford **2.29**[35] (7.2 mg, 51% yield) as a white solid and recovered oxazolidinone **2.24** (3.1 mg, 22% yield). **2.29**: R_f 0.09 (1:1 hexanes:EtOAc); ^{1}H NMR (500 MHz, $CDCl_3$):[36] 8.3–8.25 (m, 1.36H), 7.95 (s, 0.47H), 7.31–7.27 (m, 1.25H), 6.96 (d, *J* = 8.2, 0.41H), 6.87 (d, *J* = 8.1, 1H), 6.78-6.73 (m, *J* = 8.3, 2.0H), 6.22 (s, 1H), 6.10 (d, *J* = 11.2, 0.41H), 5.92 (dd, *J* = 17.8, 11.4, 1H), 5.88-5.80 (m, 0.87H), 5.05–4.97 (m, 0.8H), 4.94–4.85 (m, 3H), 4.79 (dd, *J* = 9.9, 5.5, 1H), 4.48 (dd, *J* = 9.2, 5.2, 0.5H), 4.33 (d, *J* = 8.2, 5.7, 0.38H), 4.20 (s, 0.36H), 4.10 (s, 0.38H), 4.06 (s, 1H), 3.23–3.19 (m, 5.7H), 2.73–2.49 (m, 4.5H), 2.44–2.36 (m, 1.5H), 1.57 (s, 3H), 1.56 (s, 3.5H), 1.52 (s, 4.4H), 1.50 (s, 1.71H), 1.23 (s, 1.34H), 1.18 (s, 3H), 0.95 (s, 1.4H).

A 1-dram vial was charged with **2.29** (5.2 mg, 0.013 mmol, 1.0 equiv) and solid $NaHCO_3$ (5.4 mg, 0.065 mmol, 5.0 equiv) in one portion. The reaction vessel was flushed with N_2, and then CH_2Cl_2 (260 μL) was added. To the resulting suspension was added the Dess–Martin periodinane reagent (7.1 mg, 0.017 mmol, 1.3 equiv) in one portion. The flask was flushed with N_2, and the reaction mixture was allowed to stir at room temperature. After 1 h, the reaction mixture was diluted with a 1:1 mixture of saturated aqueous $NaHCO_3$ and saturated aqueous $Na_2S_2O_3$ (1.0 mL). The resulting biphasic mixture was vigorously stirred until both layers appeared clear. The mixture was then transferred to a test tube with EtOAc (2 mL) and brine (2 mL), and then extracted with EtOAc (3 x 2 mL). The organic layers were combined, dried over $MgSO_4$, and evaporated under reduced pressure. The resulting residue was purified by flash

chromatography (5:1 → 3:1 hexanes:acetone) to afford formamide **2.25** (5.0 mg, 97% yield) as a white solid. formamide **2.25**: mp: 213.3 ºC; R_f 0.41 (3:1 EtOAc:hexanes); ^{1}H NMR (500 MHz, $CDCl_3$ at –44 °C):[37] δ 8.21 (d, *J* = 1.1, 0.25H), 7.53 (d, *J* = 12.0, 1H), 7.32 (dd, *J* = 8.1, 7.9, 1.25H), 7.02 (d, *J* = 8.1, 1H), 7.00 (d, *J* = 8.3, 0.25H), 6.82 (d, *J* = 7.5, 1H), 6.79 (d, *J* = 7.5, 0.25H), 6.38 (dd, *J* = 17.3, 11.0, 0.25H), 6.28 (dd, *J* = 17.3, 10.7, 1H), 5.78 (s, 0.25H), 5.73 (d, *J* = 11.5, 1H), 5.51 (d, *J* = 11.2, 0.25H), 5.48 (d, *J* = 11.0, 1H), 5.42–5.30 (m, 1.25H), 4.40 (s, 1H), 4.32 (s, 0.25H), 4.24 (d, *J* = 7.4, 1H), 4.19 (d, *J* = 7.1, 0.25H), 3.22 (s, 3H), 3.21 (s, 0.75H), 3.20–3.14 (m, 1H), 3.08–2.90 (m, 2.6H), 2.81 (d, *J* = 17.4, 1H), 2.75 (d, *J* = 16.4, 0.25H), 1.68 (s, 3H), 1.63 (s, 0.75H), 1.28 (s, 3.75H), 0.98 (s, 0.75H), 0.87 (s, 3H); ^{13}C NMR (125 MHz, $CDCl_3$): δ 202.8, 174.3, 167.3, 144.0, 137.2, 133.7, 128.4, 126.7, 124.8, 118.2, 108.1, 71.5, 62.2, 60.2, 55.0, 49.8, 38.2, 31.8, 26.3, 26.1, 22.9, 20.9; IR (film): 2967, 2932, 1696, 1609, 1585 cm^{-1}; HRMS-ESI (*m/z*) $[M + H]^+$ calcd for $C_2H_{26}ClN_2O_3$, 401.16320; found 401.16143; $[\alpha]^{22.4}_D$ +9.60° (*c* = 1.000, $CHCl_3$).

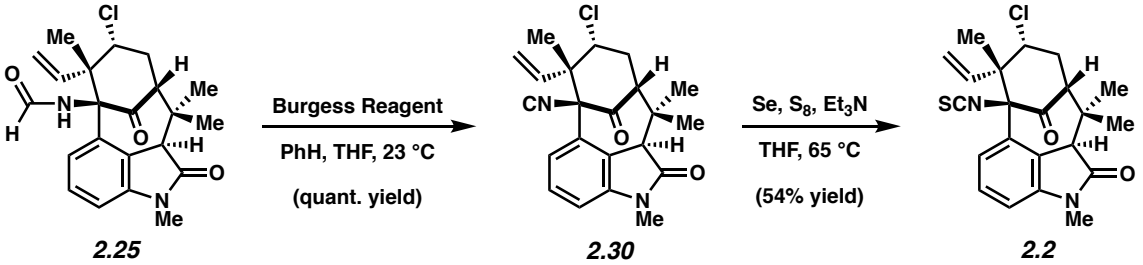

2.25 *2.30* *2.2*

(–)-*N*-Methylwelwitindolinone B Isothiocyanate (2.2). To a solution of formamide **2.25** (3.3 mg, 0.008 mmol, 1.0 equiv) in 1:1 THF/PhH (660 μL) was added Burgess reagent (2.0 mg, 0.008 mmol, 1.0 equiv). The reaction vessel was purged with N_2, sealed and left to stir at room temperature. After stirring for 1 h, an additional portion of Burgess reagent (0.5 mg, 0.002 mmol, 0.25 equiv) was added. After stirring at room temperature for 30 min, a final portion of Burgess

reagent (0.5 mg, 0.002 mmol, 0.25 equiv) was added and the resulting solution was stirred at room temperature. After 25 min the reaction was filtered by passage over a plug of silica gel (EtOAc eluent, 6 mL). The filtrate was evaporated under reduced pressure and the resulting residue was purified by flash chromatography (5:1:1 hexanes:Et_2O:CH_2Cl_2) to afford **2.30** (3.2 mg, quant. yield) as a white solid. **2.30**: R_f 0.55 (1:1:1 hexanes:Et_2O:CH_2Cl_2); ^{1}H NMR (500 MHz, C_6D_6): δ 7.41 (d, *J* = 8.3, 1H), 6.86 (dd, *J* = 8.0, 8.0, 1H), 6.04 (d, *J* = 7.7, 1H), 5.82 (dd, *J* = 17.2, 11.0, 1H), 4.95–4.81 (m, 2H), 3.83 (s, 1H), 3.43 (dd, *J* = 6.4, 6.2, 1H), 2.55 (s, 3H), 2.36 (dd, *J* = 9.9, 3.6, 1H), 2.19–2.11 (m, 1H), 1.91–1.81 (m, 1H), 1.46 (s 3H), 1.26 (s, 3H), 0.75 (s, 3H).

To two 1-dram vials containing **2.30** (2.9 mg, 0.008 mmol, 1.0 equiv each) was added powdered Se (1.8 mg, 0.023 mmol, 3.0 equiv each) and S_8 (1.9 mg, 0.590 mmol, 76.4 equiv each). The reaction vessels were purged with N_2 and to each vessel was added THF (584 μL, previously sparged with N_2 for 20 min) and NEt_3 (81 μL, 0.590 mmol, 26.4 equiv), which were then sealed and heated to 65 °C. After 17 h the reaction vials were cooled to room temperature and filtered by passage over a plug of silica gel (EtOAc eluent, 6 mL). The filtrate was evaporated under reduced pressure and the resulting residue was purified by preparative thin layer chromatography (1:1:1 hexanes:Et_2O:CH_2Cl_2) to afford (–)-**2.2** (3.4 mg, 54% yield) as a white solid. (–)-*N*-Methylwelwitindolinone B isothiocyanate (**2.2**): mp: 186.4 ºC; R_f 0.61 (1:1 hexanes:EtOAc); ^{1}H NMR (500 MHz, $CDCl_3$): δ 7.34 (ddd, *J* = 8.3, 0.8, 1H), 7.25 (dd, *J* = 8.3, 0.9, 1H), 6.80 (d, *J* = 7.7, 1H), 5.99 (dd, *J* = 17.5, 11.1, 1H), 5.22–5.15 (m, 2H), 4.17 (app t, *J* = 6.3, 1H), 4.13 (s, 1H), 3.20 (s, 3H), 2.95 (app t, *J* = 7.2, 1H), 2.78 (app t, *J* = 6.5, 1H), 1.62 (s 3H), 1.48 (s, 3H), 0.83 (s, 3H); ^{13}C NMR (125 MHz, $CDCl_3$): δ 198.6, 174.3, 144.1, 139.6, 136.4, 131.2, 128.8, 123.9, 122.6, 118.1, 108.3, 83.5, 62.5, 60.2, 53.3, 52.9, 39.8, 31.5, 26.4,

25.4, 24.1, 22.5; IR (film): 2969, 2933, 2049, 1710, 1607, 1587, 1460 cm^{-1}; HRMS-ESI (*m/z*) [M + H]$^+$ calcd for $C_{22}H_{24}ClN_2O_2S$, 415.12470; found 415.12245; $[\alpha]^{20.9}_D$ –133.71° (*c* = 0.071, CH_2Cl_2).[38]

2.10 Spectra Relevant to Chapter Two:

Total Synthesis of (–)-*N*-Methylwelwitindolinone B Isothiocyanate via a Chlorinative Oxabicyclic Ring-Opening Strategy

Nicholas A. Weires, Evan D. Styduhar, Emma L. Baker, and Neil K. Garg.

J. Am. Chem. Soc. **2014**, *136*, 14710–14713.

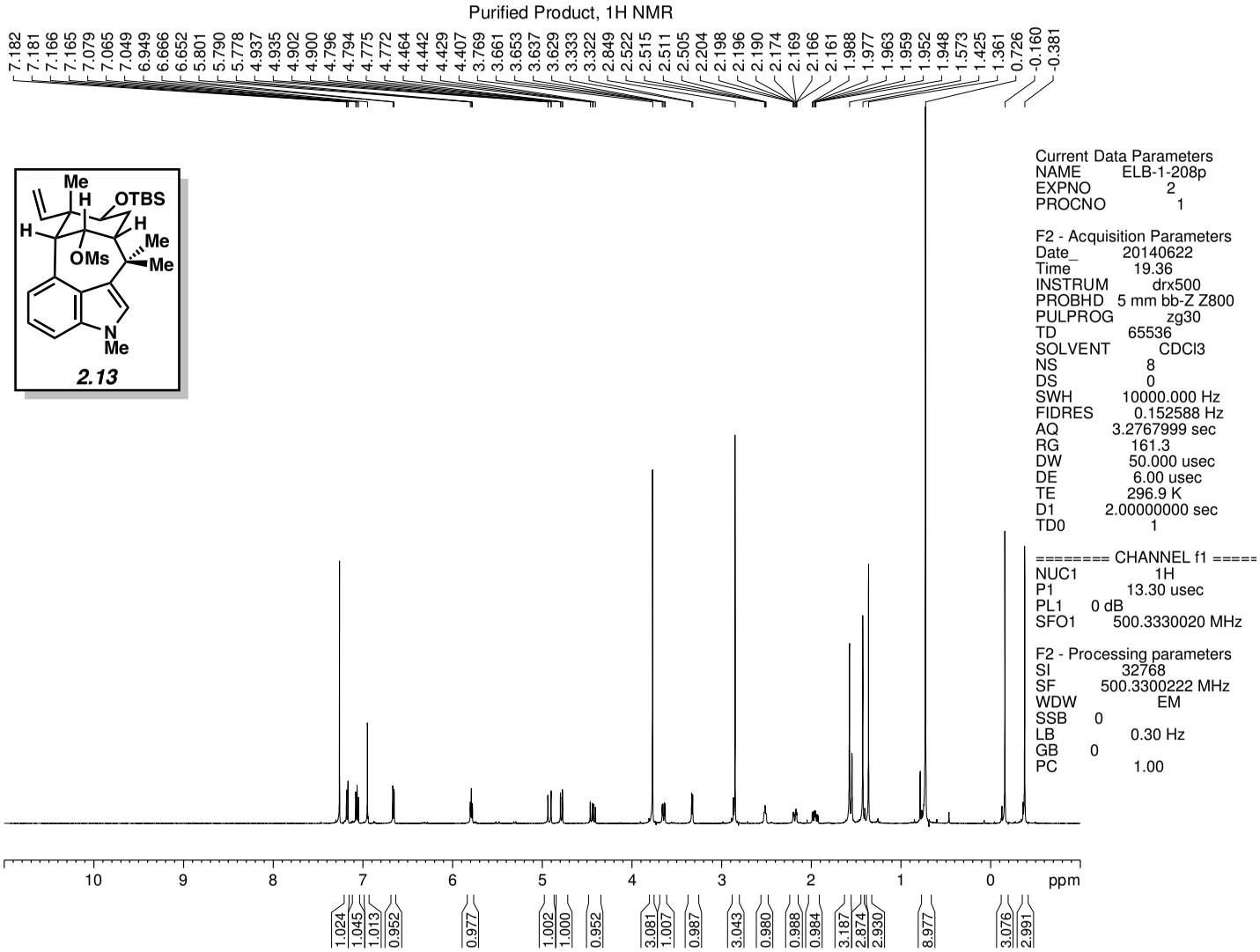

Figure 2.2 ^{1}H NMR (500 MHz, $CDCl_3$) of compound **2.13**.

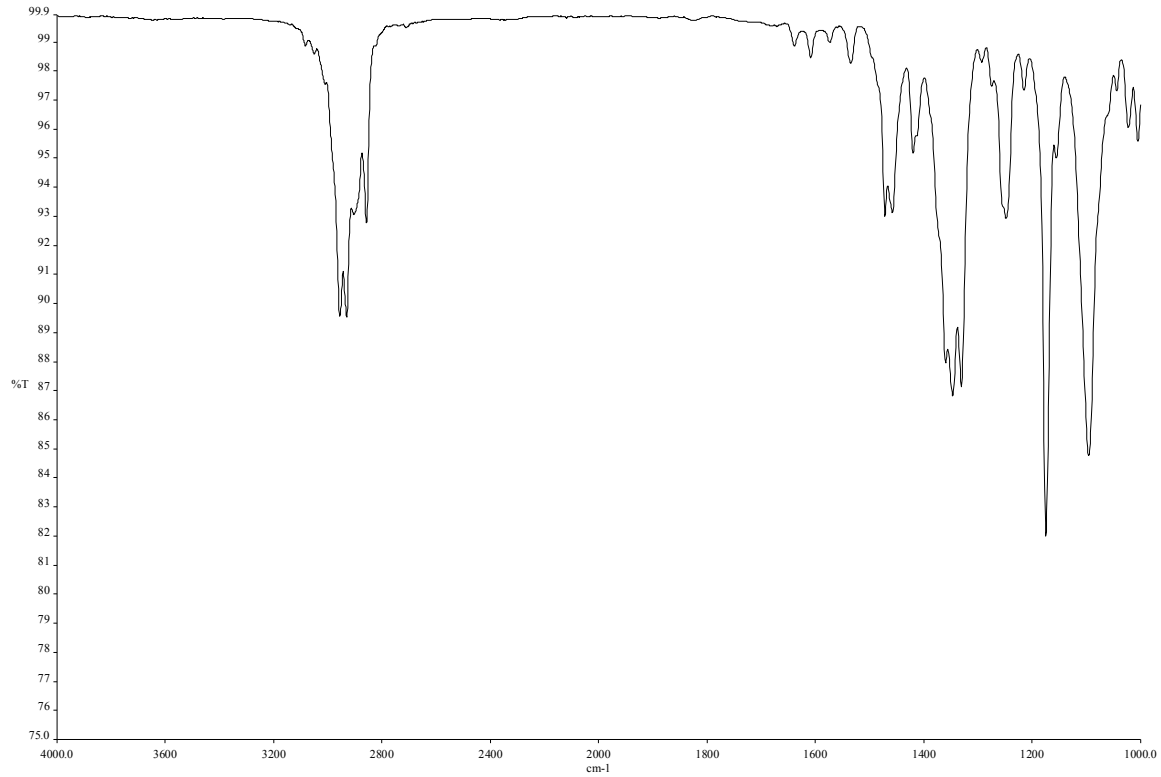

Figure 2.3 Infrared spectrum of compound **2.13**.

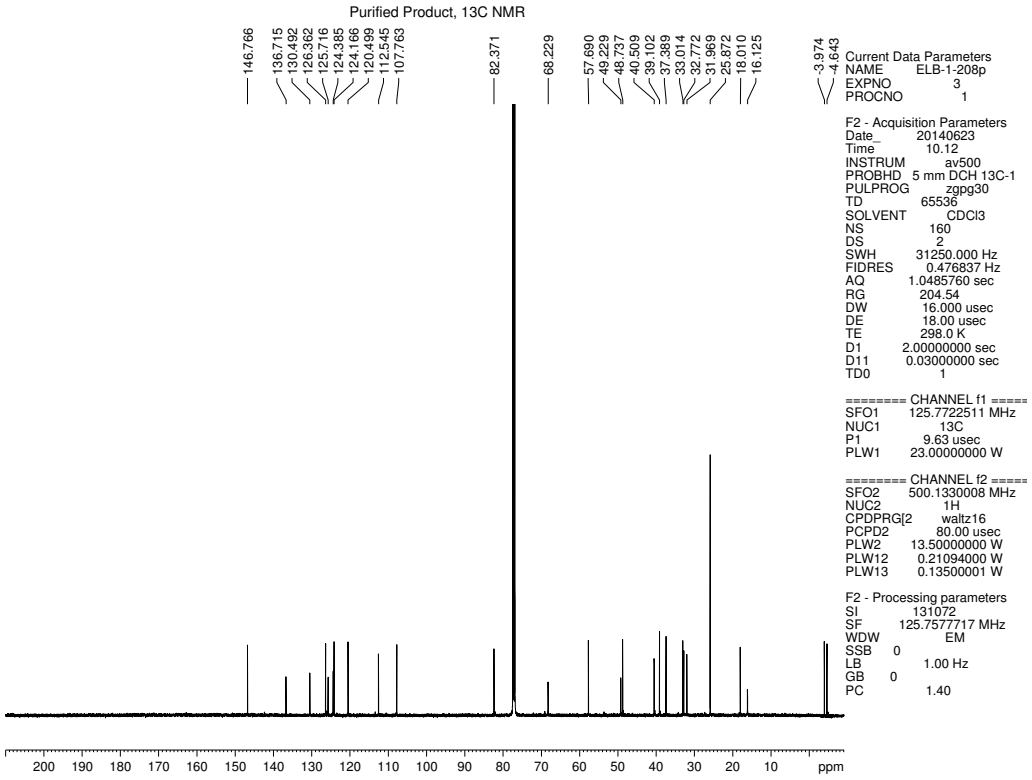

Figure 2.4 ^{13}C NMR (125 MHz, $CDCl_3$) of compound **2.13**.

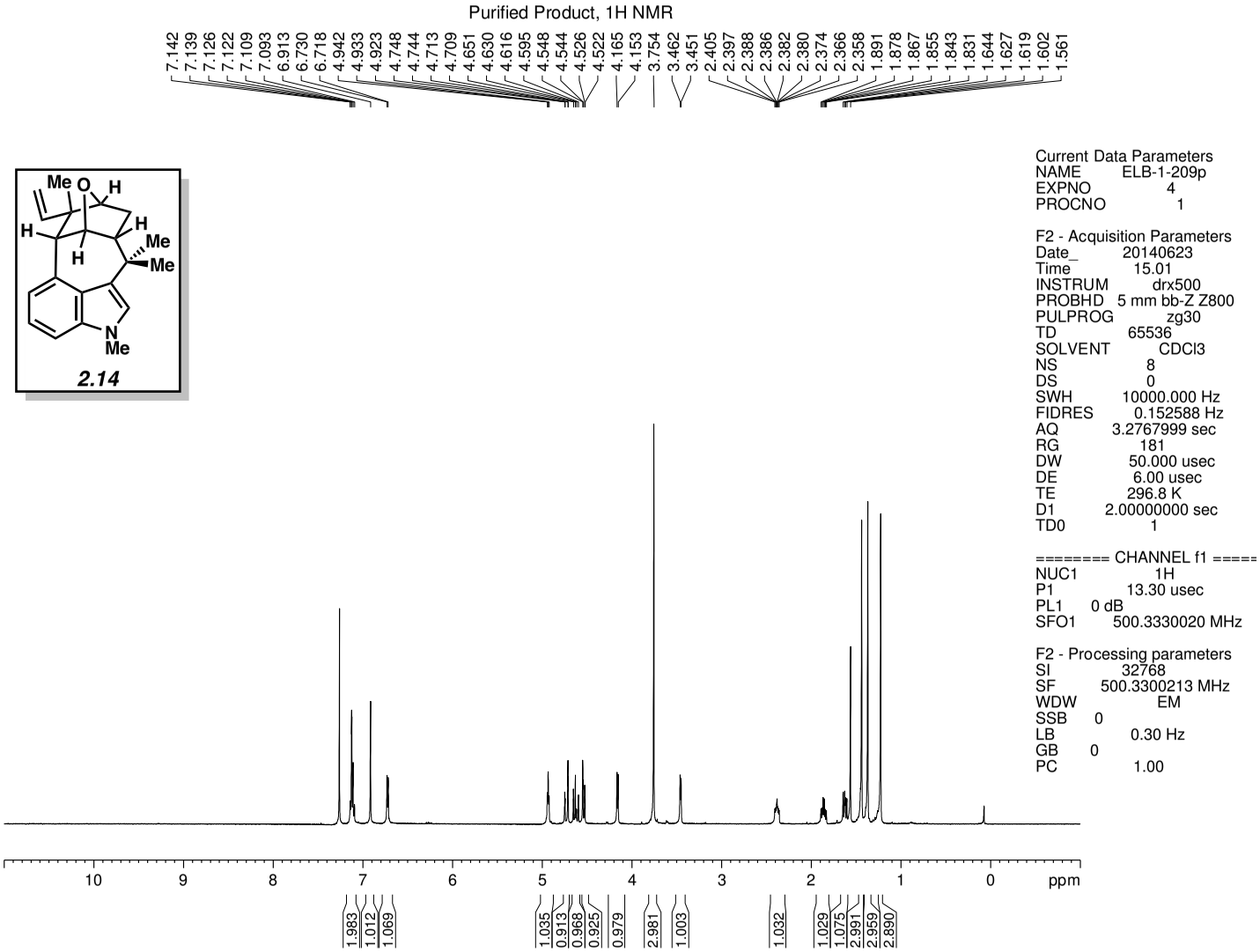

Figure 2.5 ^{1}H NMR (500 MHz, $CDCl_3$) of compound **2.14**.

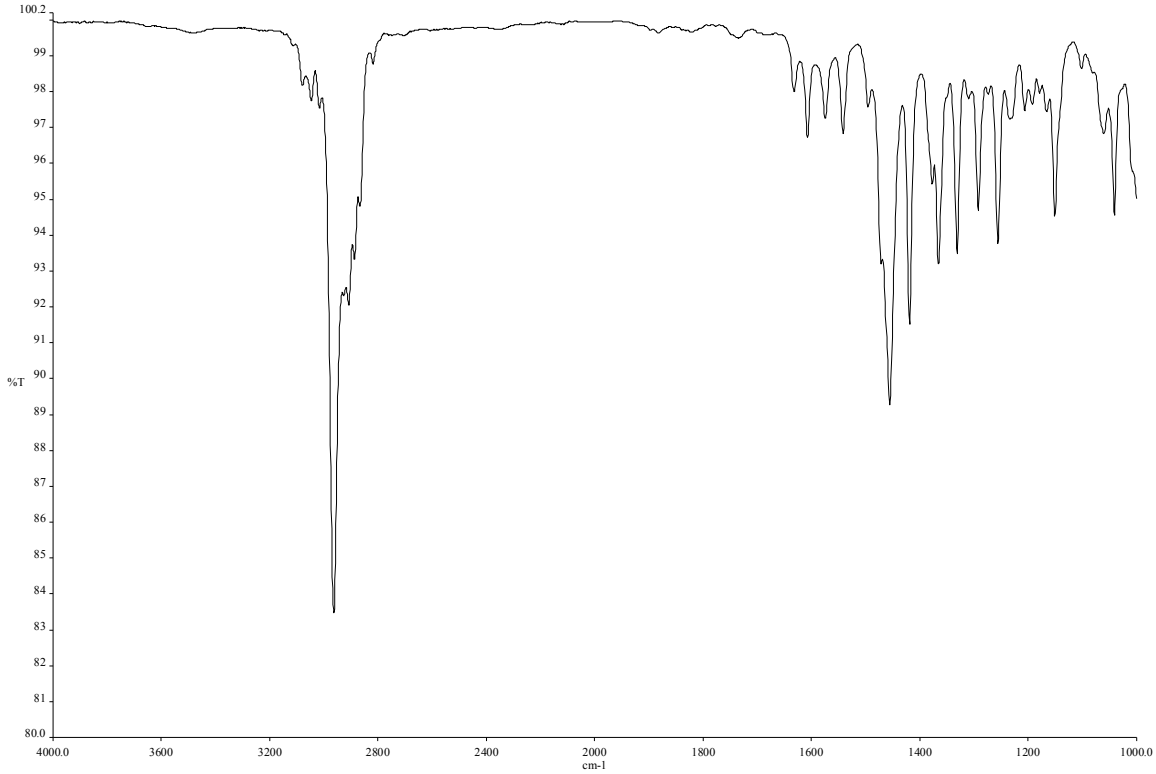

Figure 2.6 Infrared spectrum of compound **2.14**.

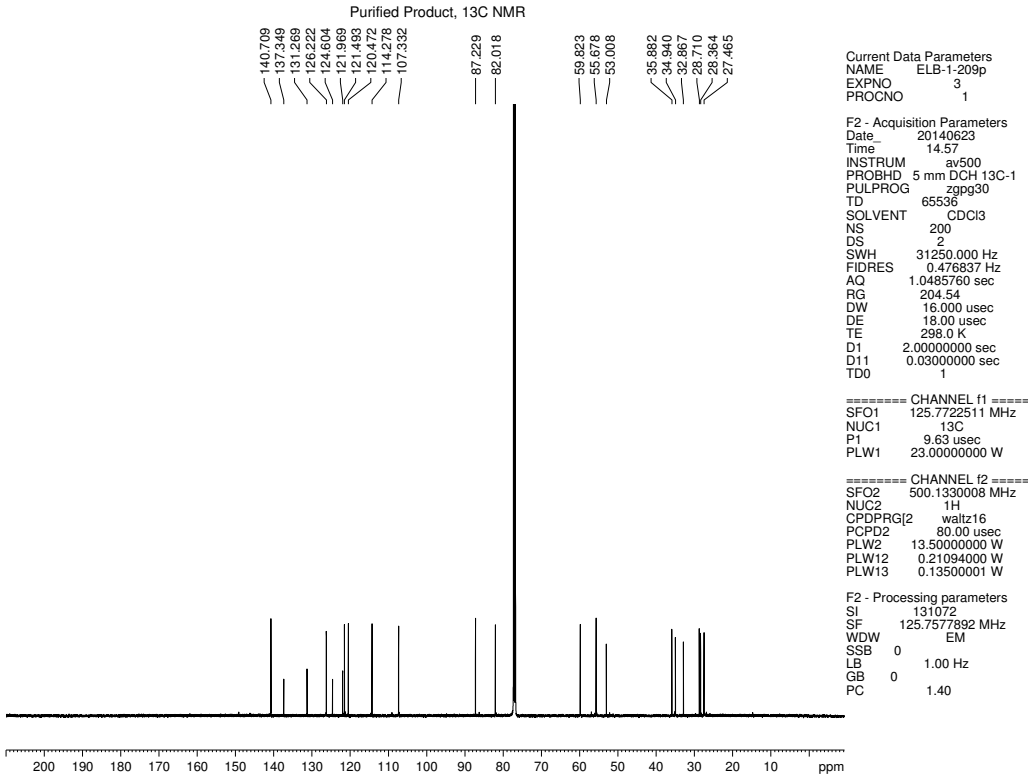

Figure 2.7 ^{13}C NMR (125 MHz, $CDCl_3$) of compound **2.14**.

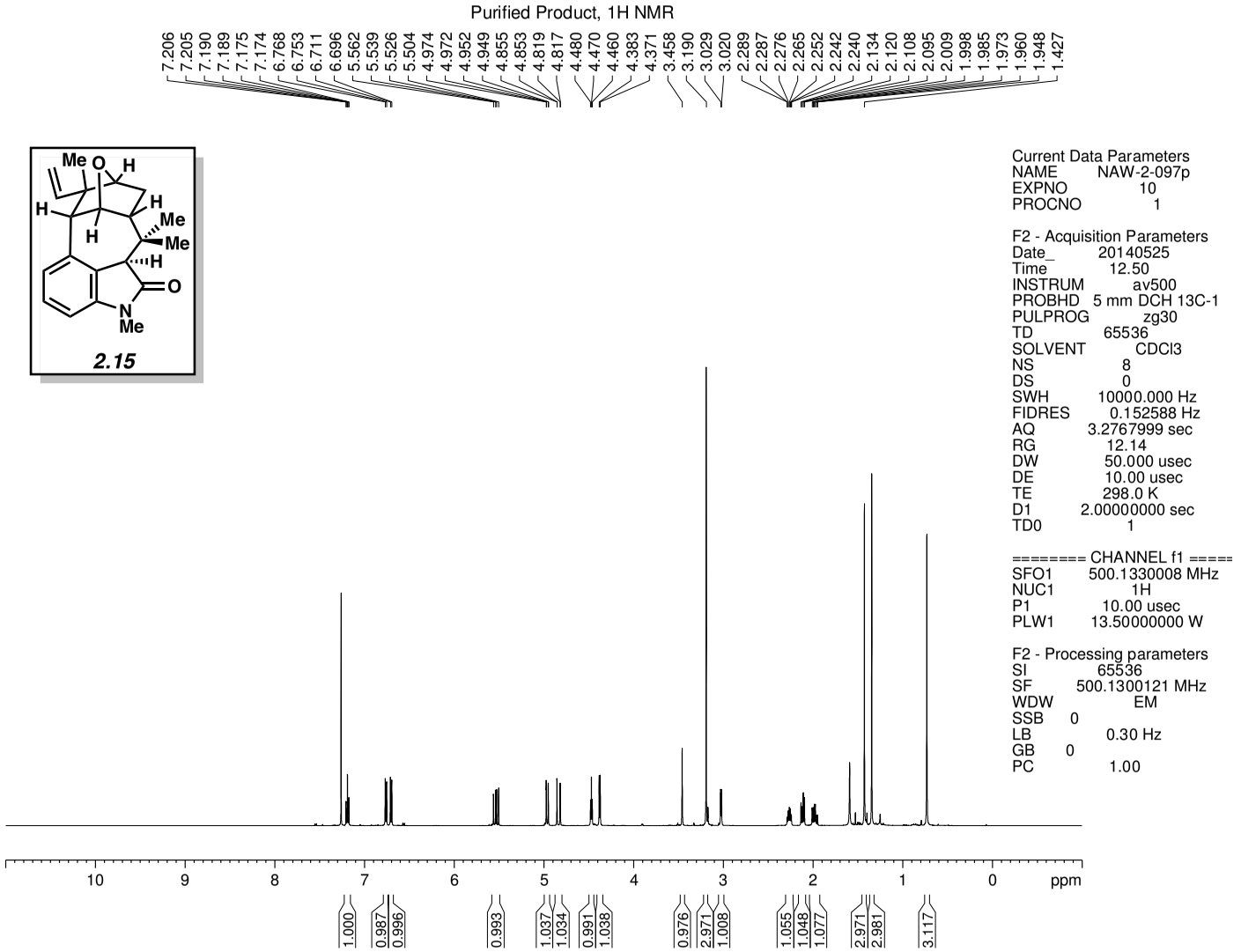

Figure 2.8 ^{1}H NMR (500 MHz, $CDCl_3$) of compound **2.15**.

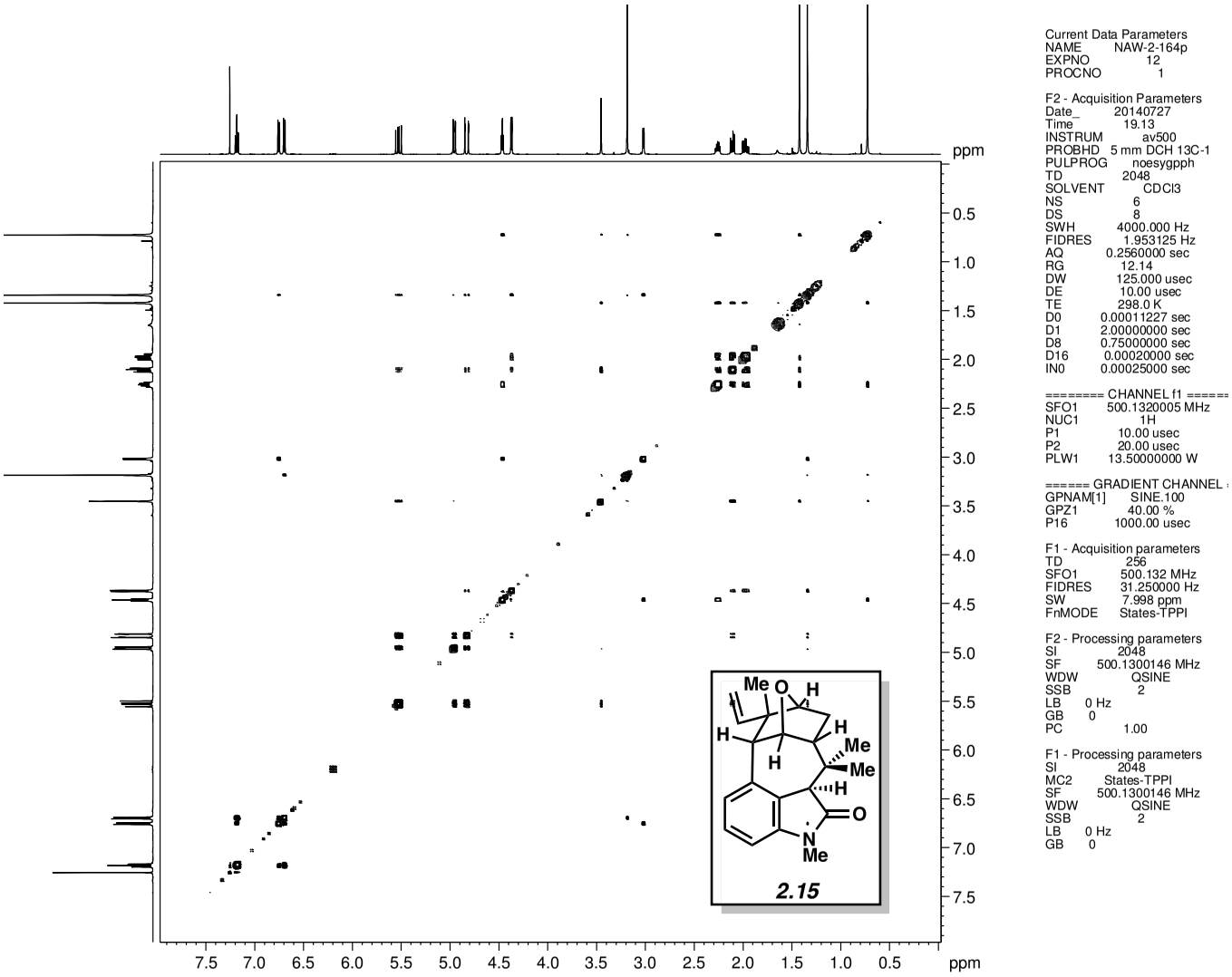

Figure 2.9 2D-NOESY NMR (500 MHz, $CDCl_3$) of compound **2.15**.

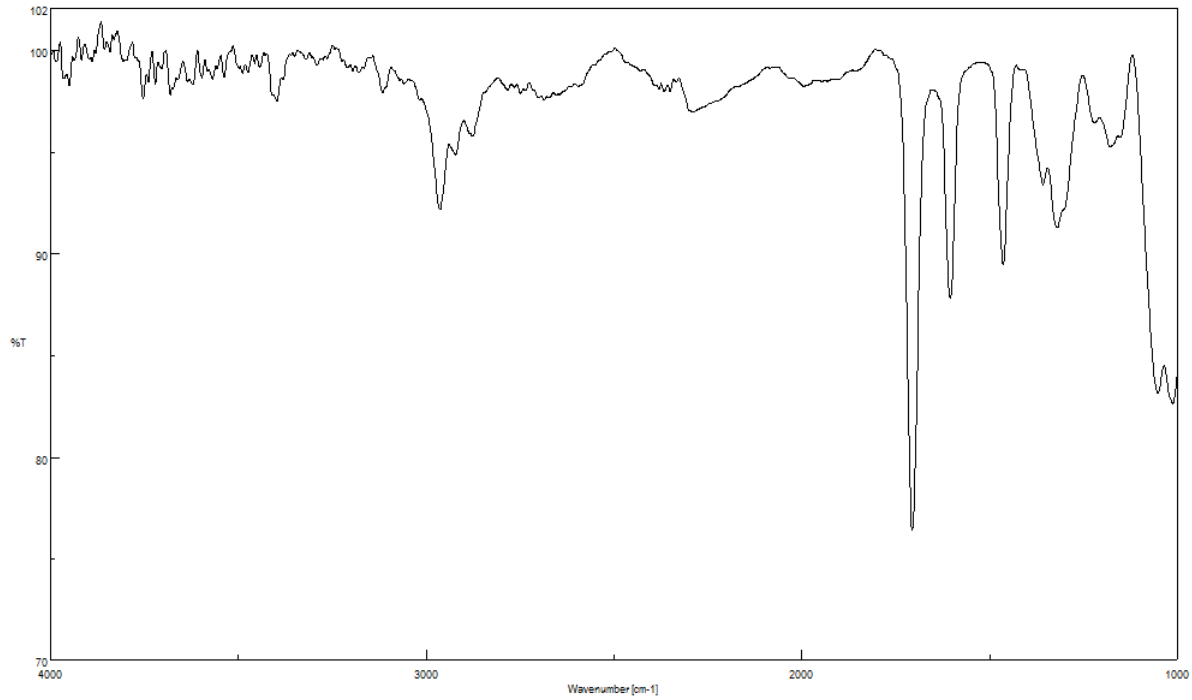

Figure 2.10 Infrared spectrum of compound **2.15**.

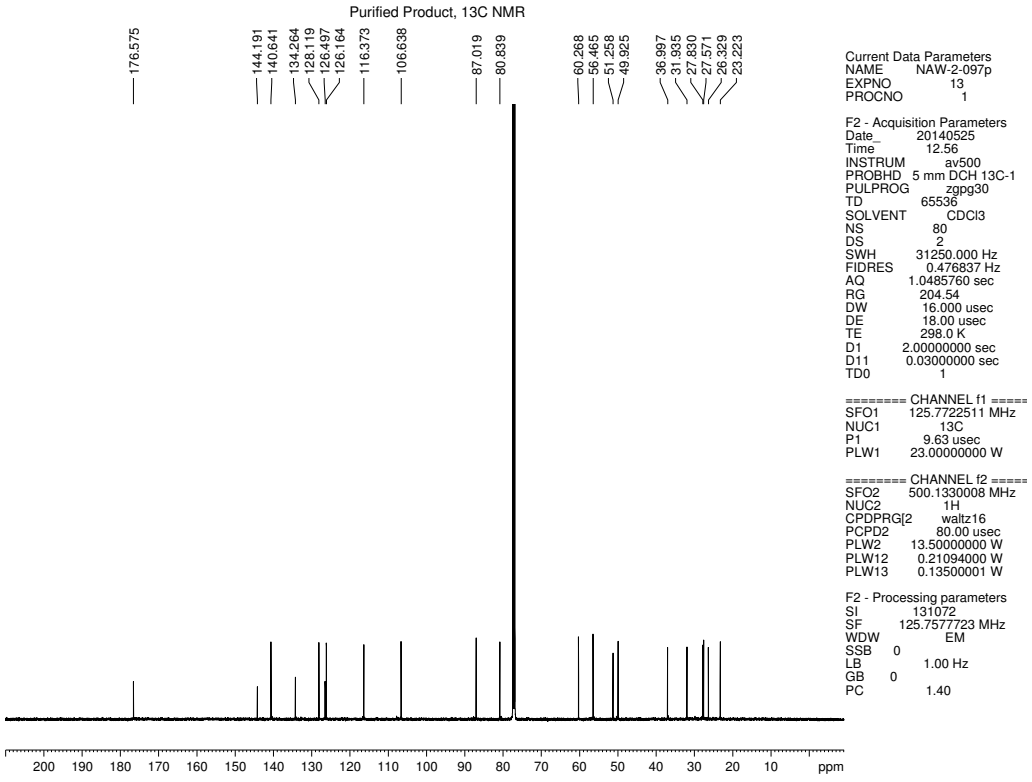

Figure 2.11 ^{13}C NMR (125 MHz, $CDCl_3$) of compound **2.15**.

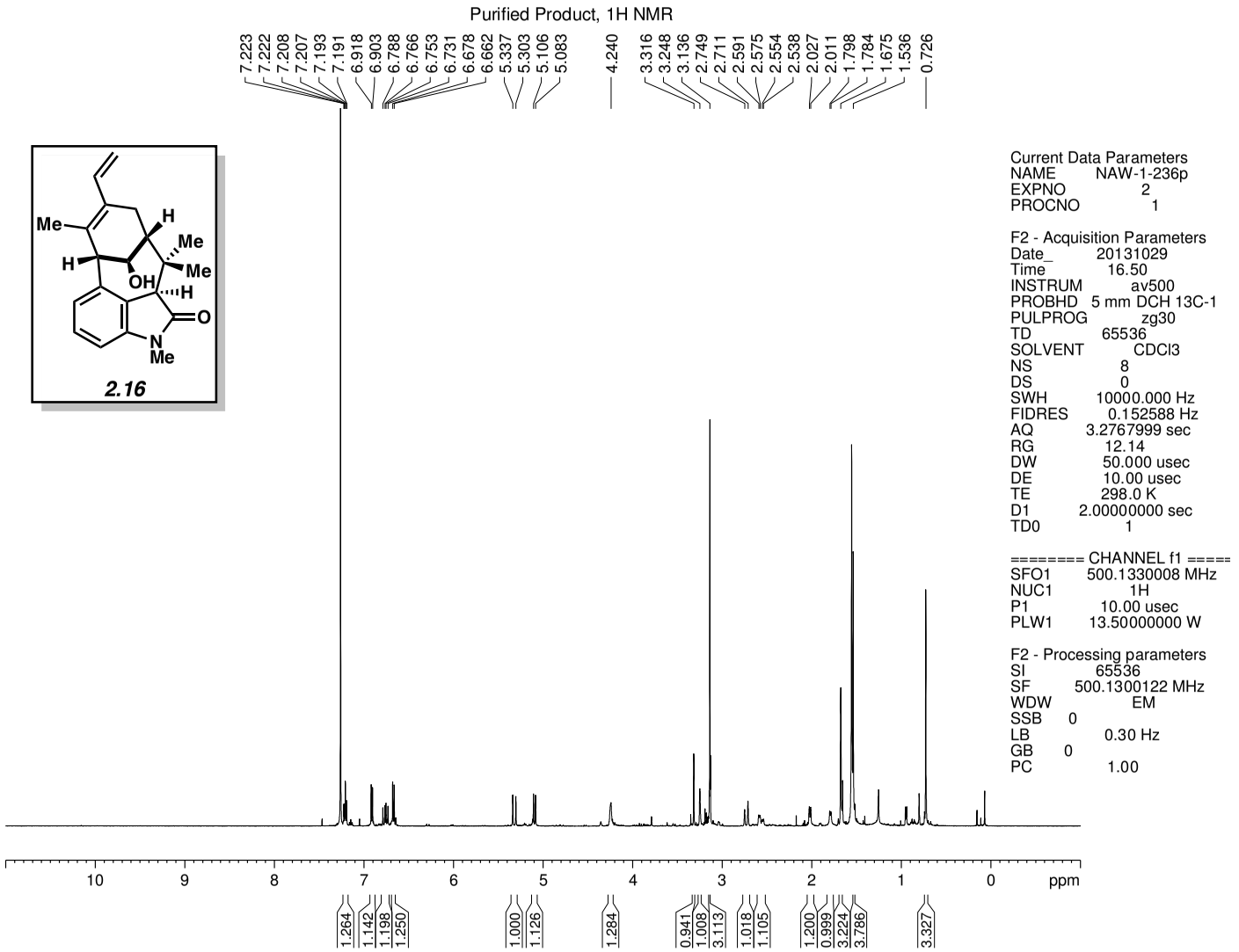

Figure 2.12 ^{1}H NMR (500 MHz, $CDCl_3$) of compound **2.16**.

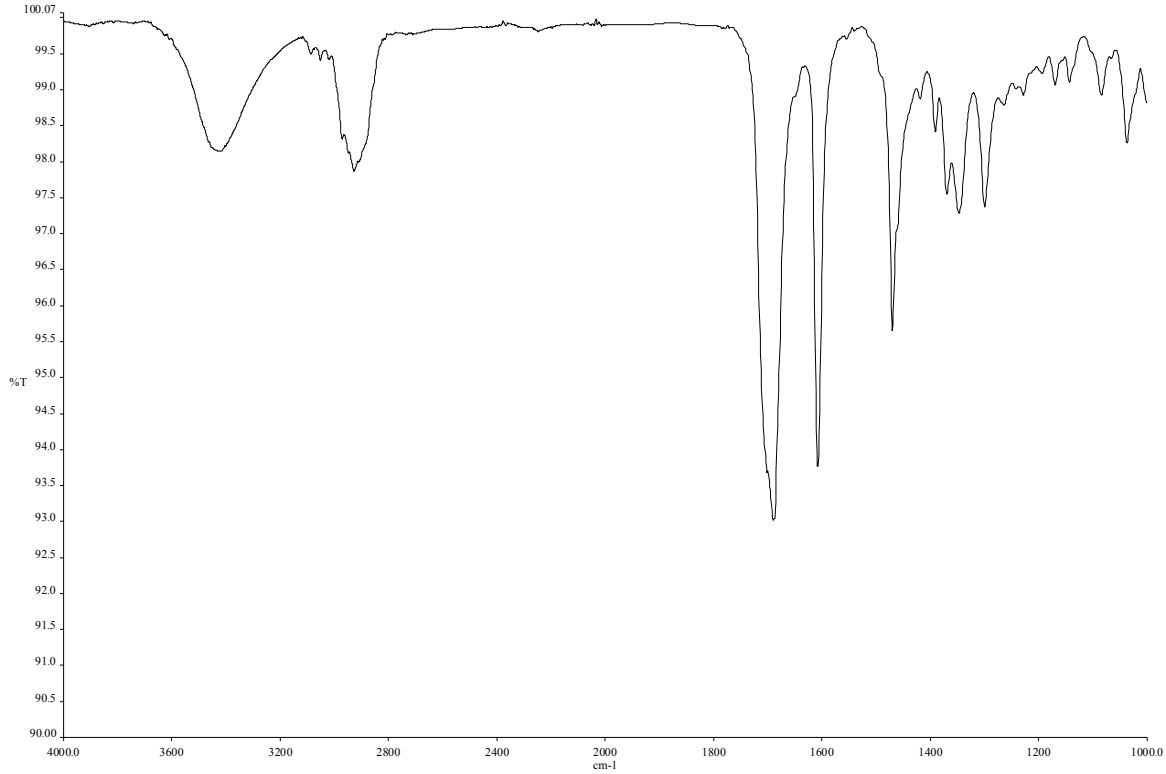

Figure 2.13 Infrared spectrum of compound **2.16**.

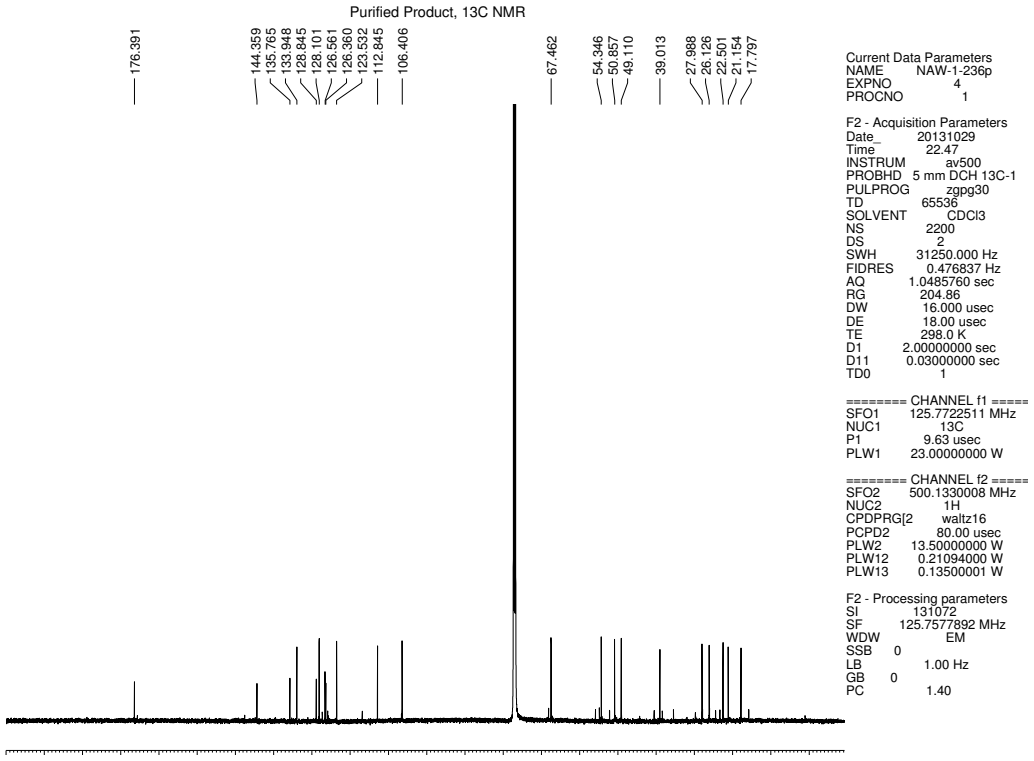

Figure 2.14 ^{13}C NMR (125 MHz, $CDCl_3$) of compound **2.16**.

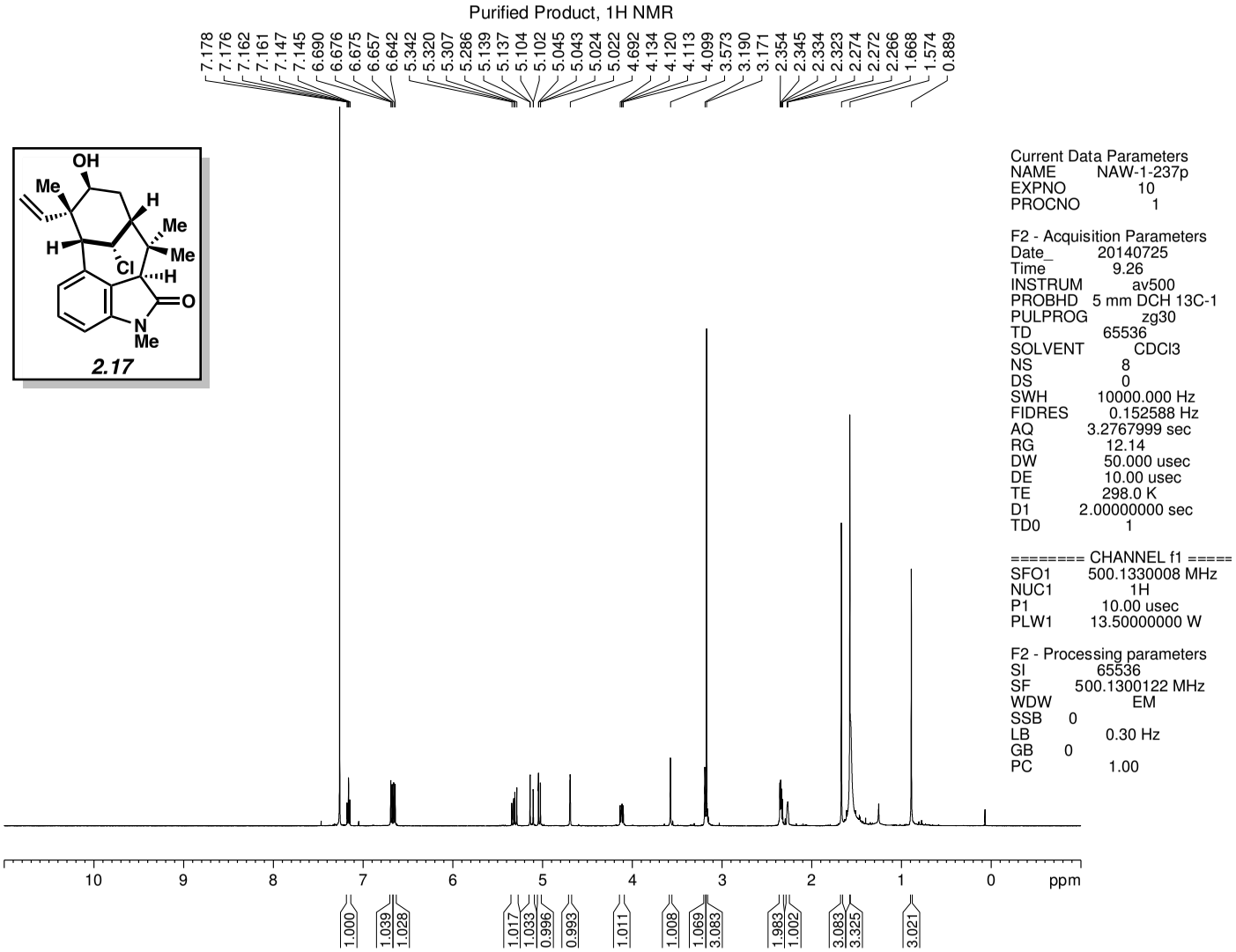

Figure 2.15 ^{1}H NMR (500 MHz, $CDCl_3$) of compound **2.17**.

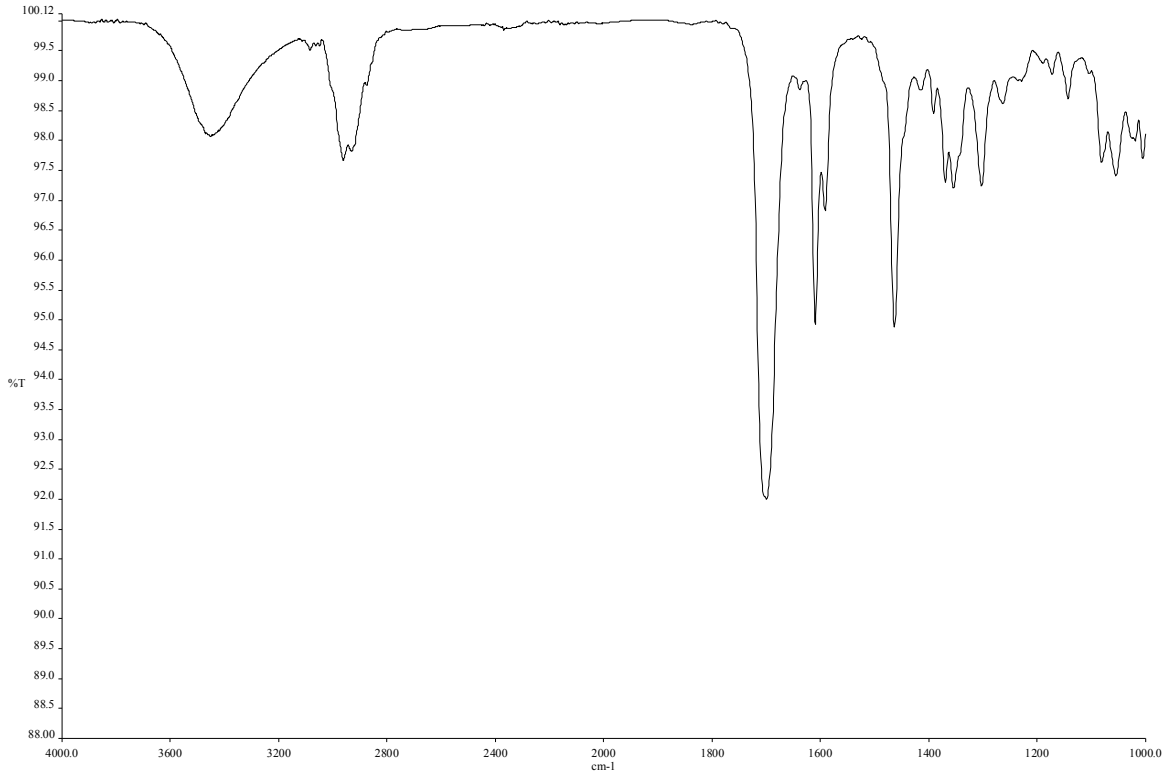

Figure 2.16 Infrared spectrum of compound **2.17**.

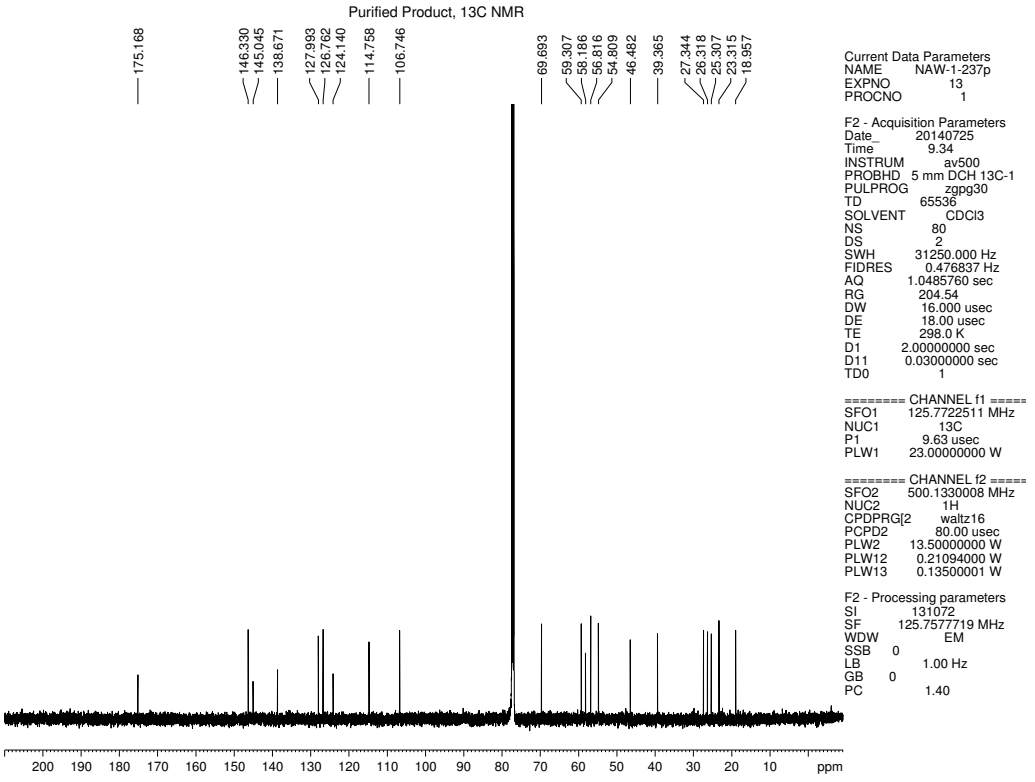

Figure 2.17 ^{13}C NMR (125 MHz, $CDCl_3$) of compound **2.17**.

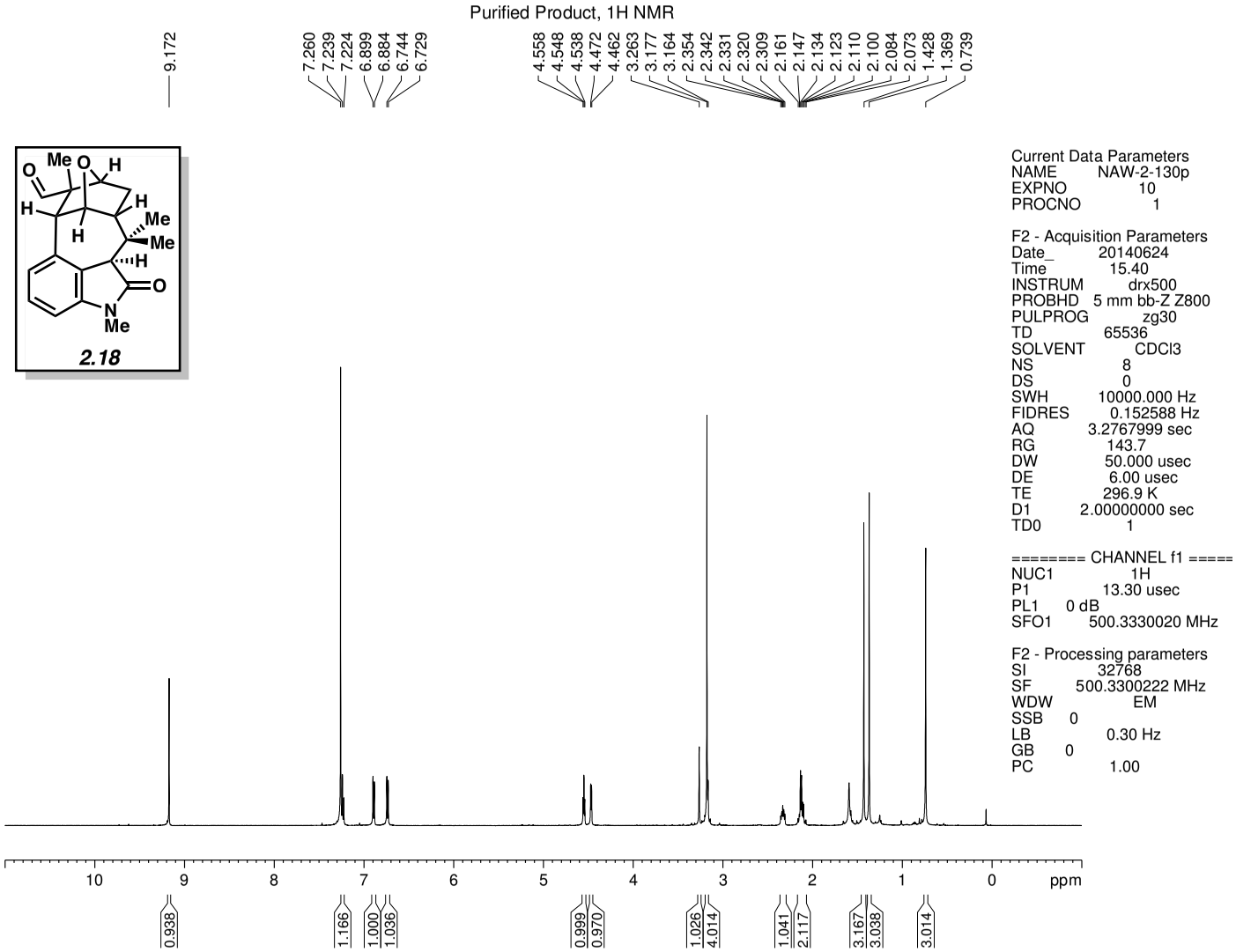

Figure 2.18 ^{1}H NMR (500 MHz, $CDCl_3$) of compound **2.18**.

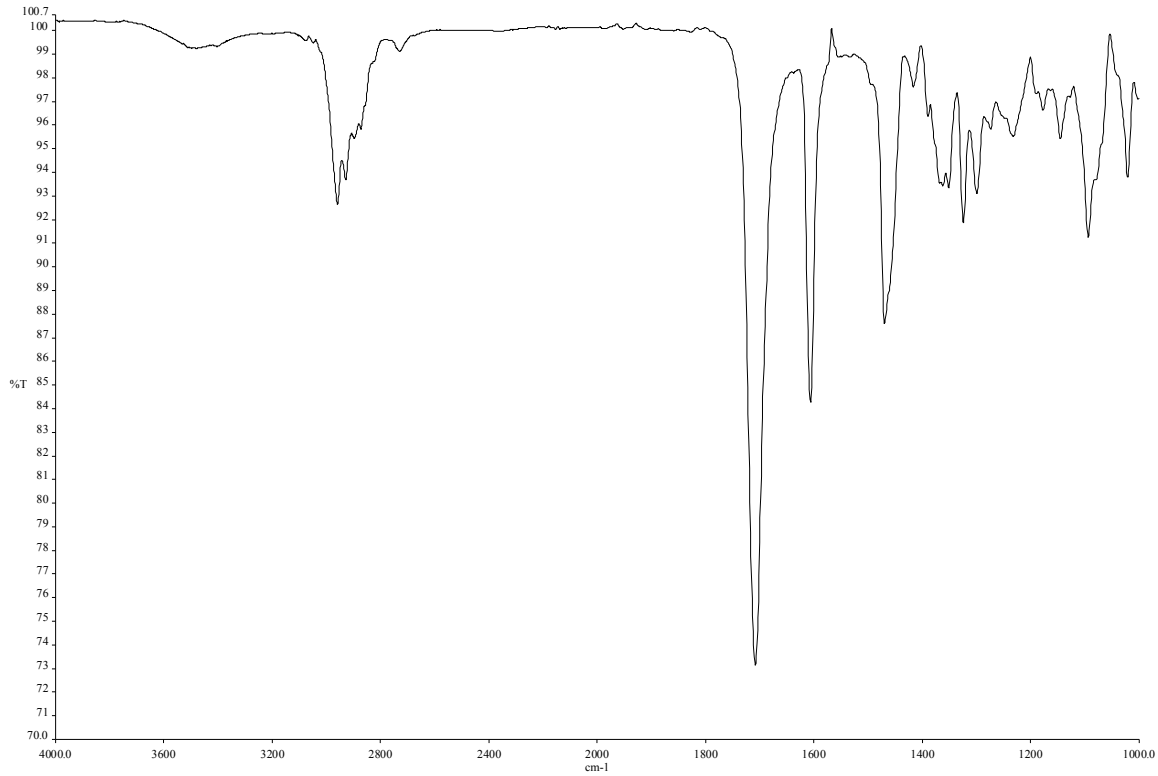

Figure 2.19 Infrared spectrum of compound **2.18**.

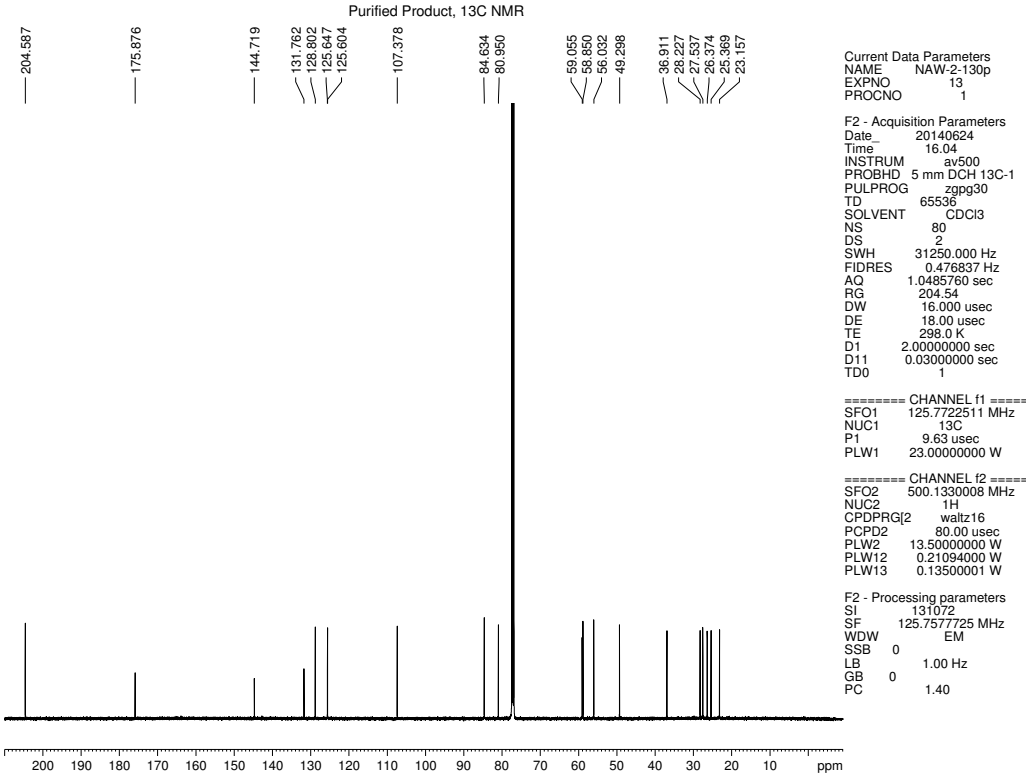

Figure 2.20 ^{13}C NMR (125 MHz, $CDCl_3$) of compound **2.18**.

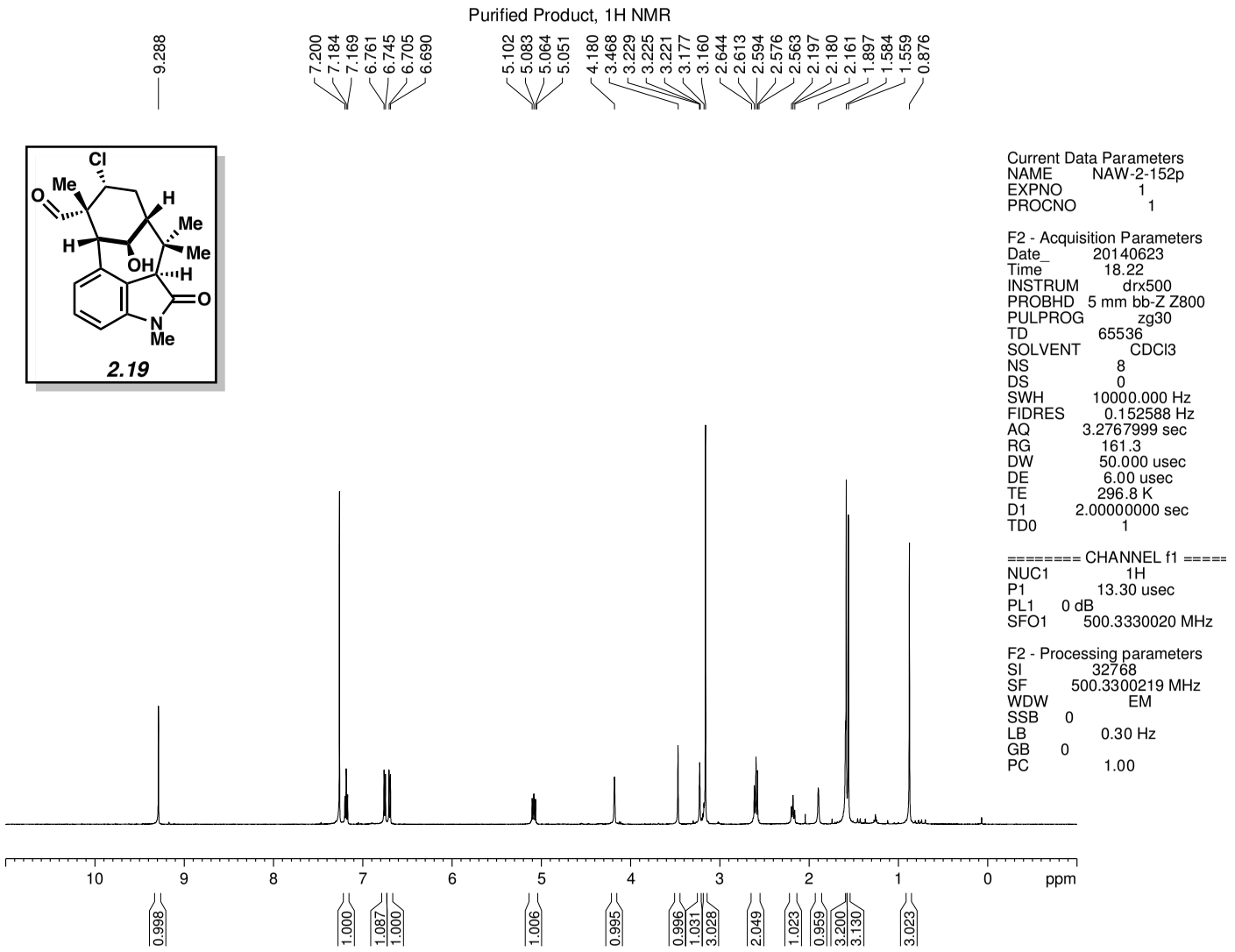

Figure 2.21 ^{1}H NMR (500 MHz, $CDCl_3$) of compound **2.19**.

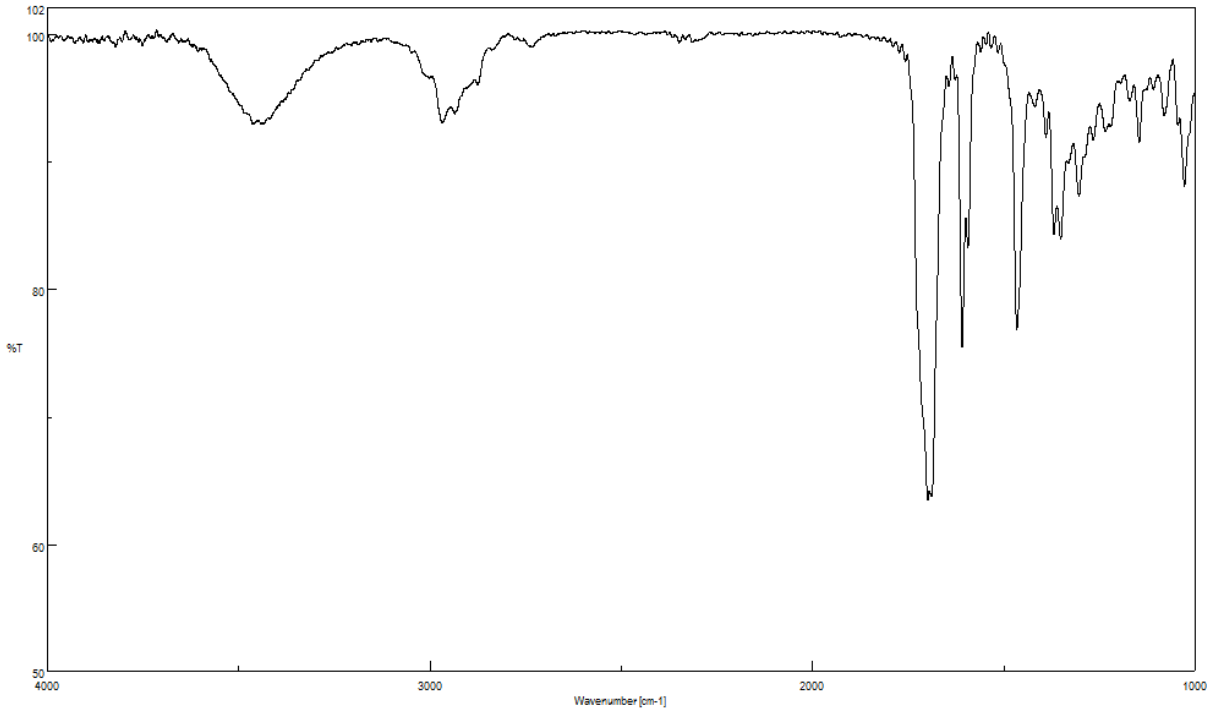

Figure 2.22 Infrared spectrum of compound **2.19**.

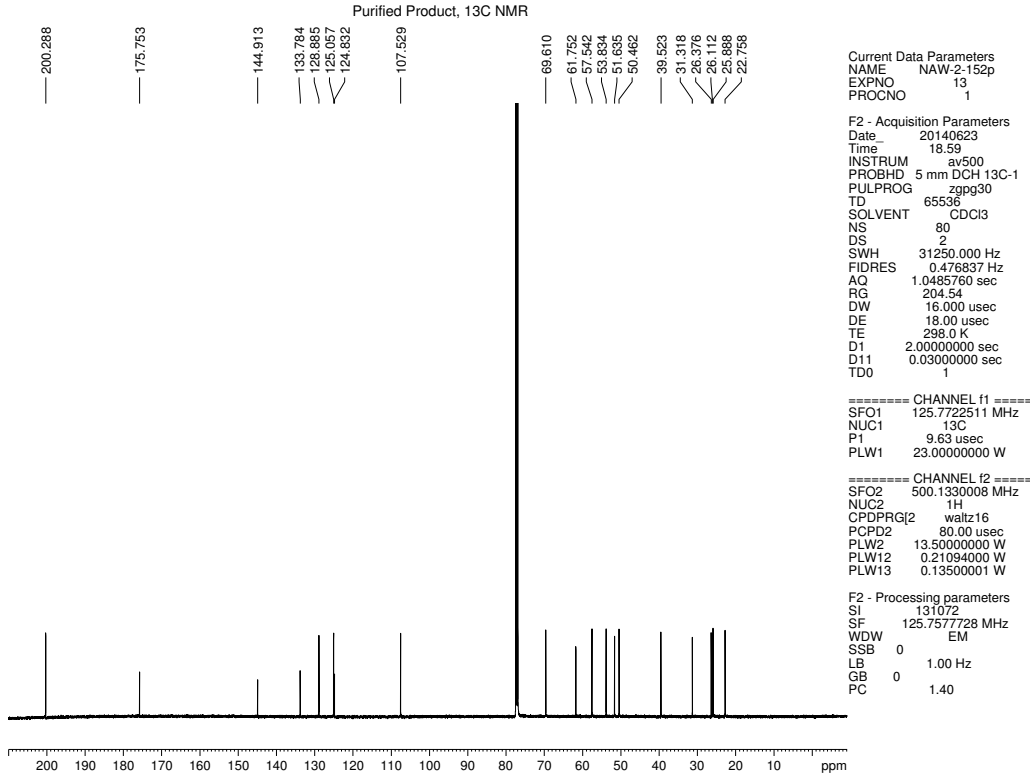

Figure 2.23 ^{13}C NMR (125 MHz, $CDCl_3$) of compound **2.19**.

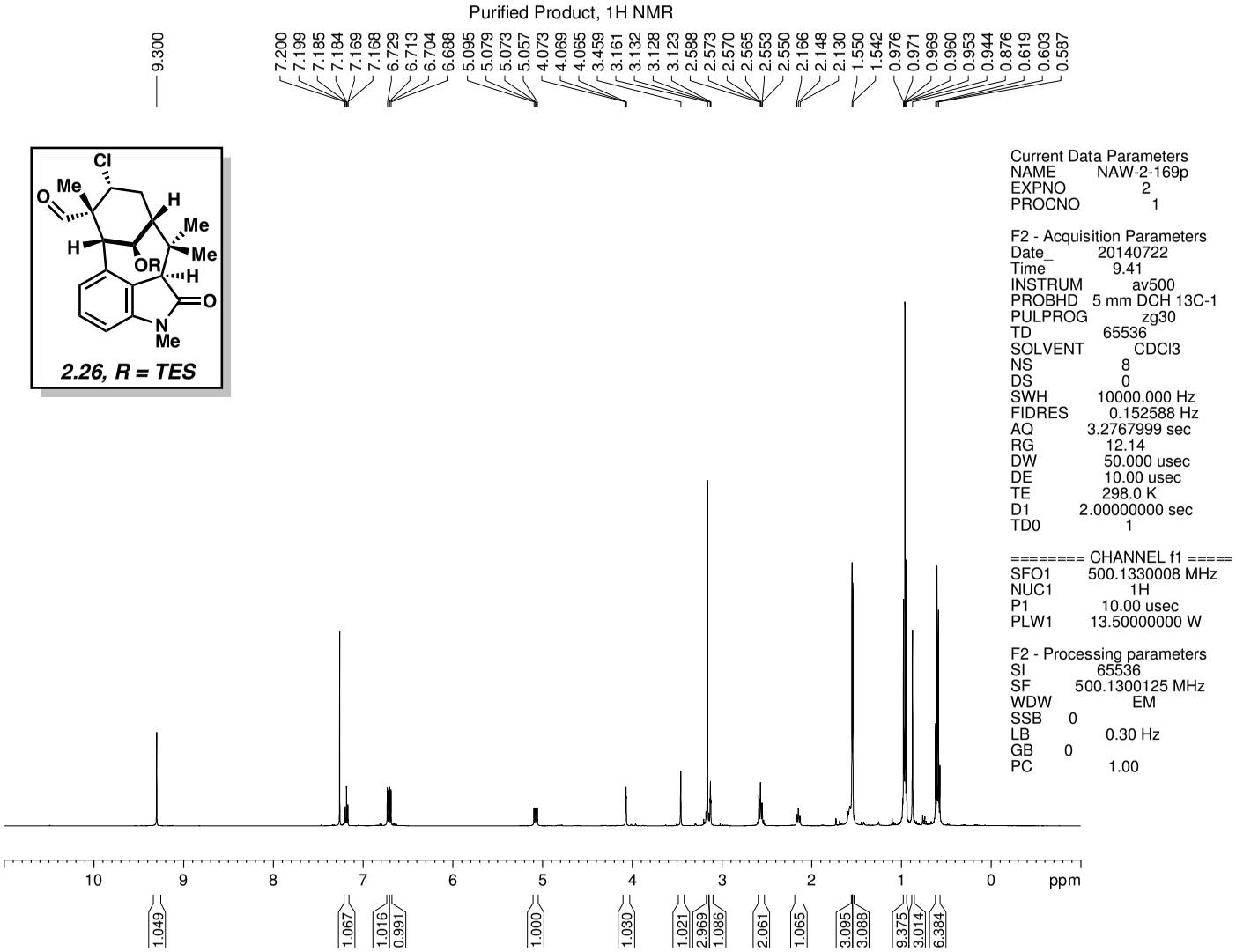

Figure 2.24 ^{1}H NMR (500 MHz, $CDCl_3$) of compound **2.26**.

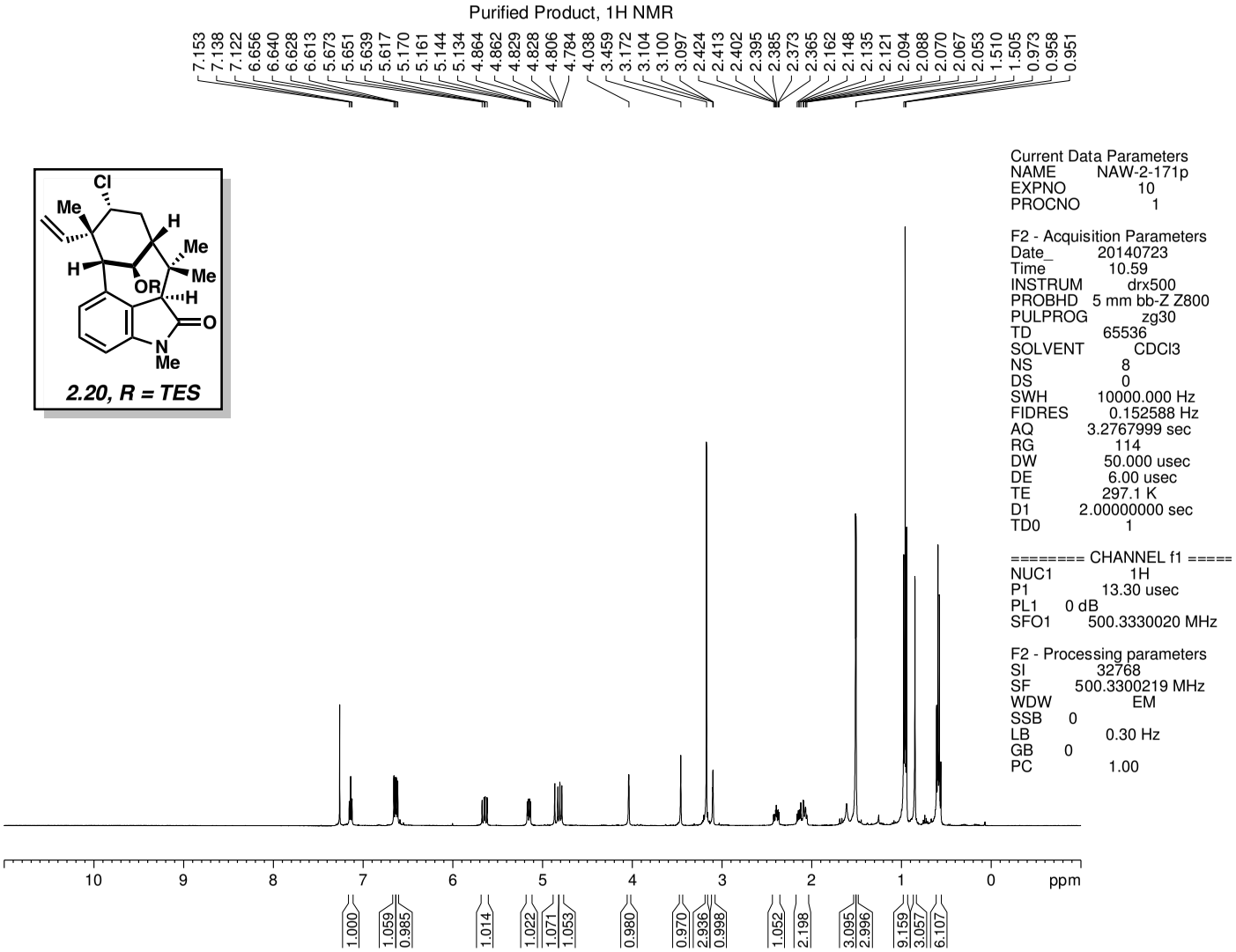

Figure 2.25 ^{1}H NMR (500 MHz, $CDCl_3$) of compound **2.20**.

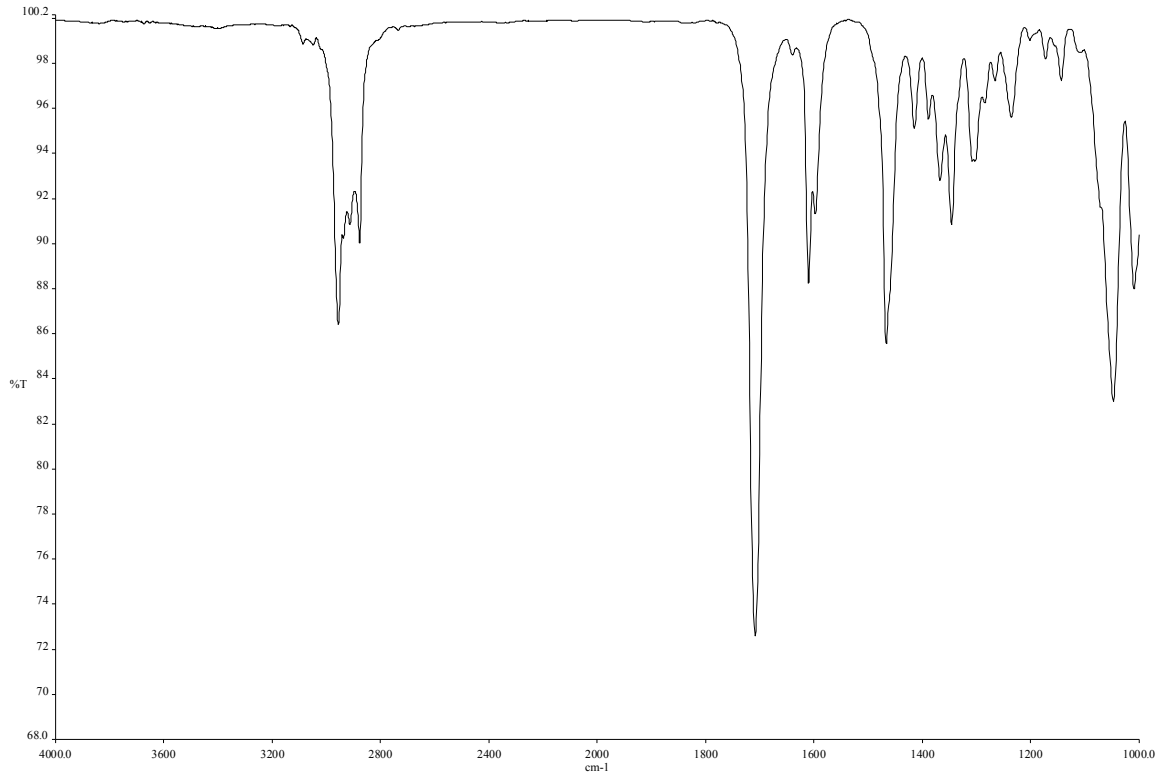

Figure 2.26 Infrared spectrum of compound **2.20**.

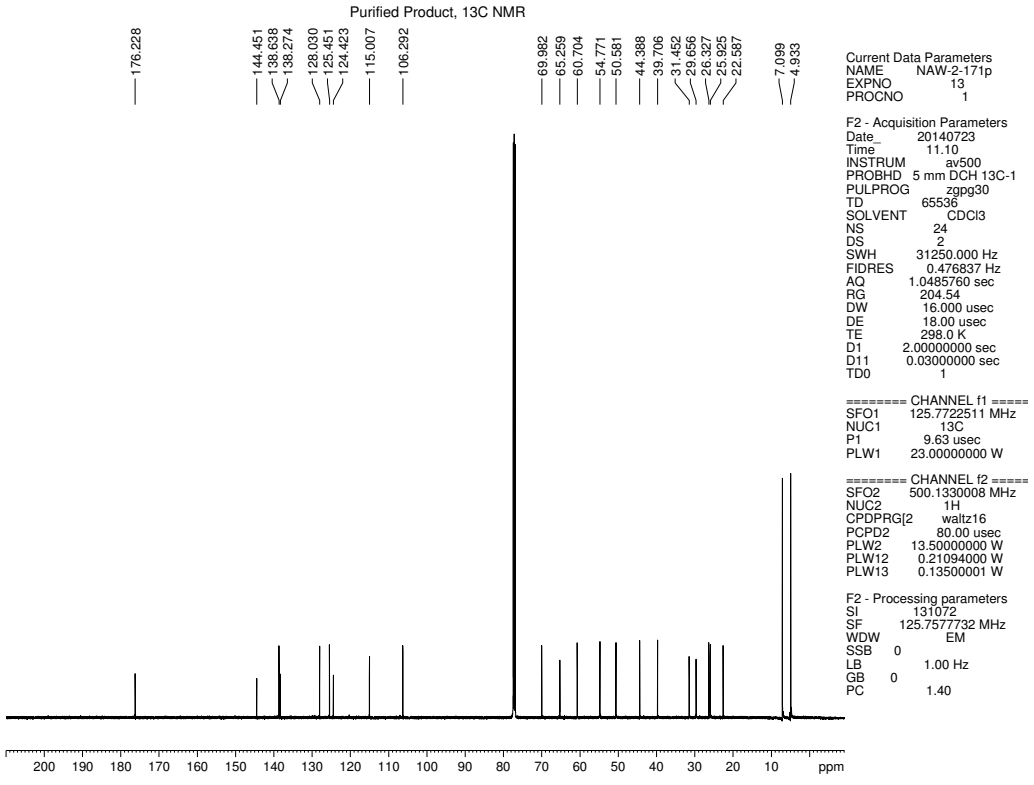

Figure 2.27 ^{13}C NMR (125 MHz, $CDCl_3$) of compound **2.20**.

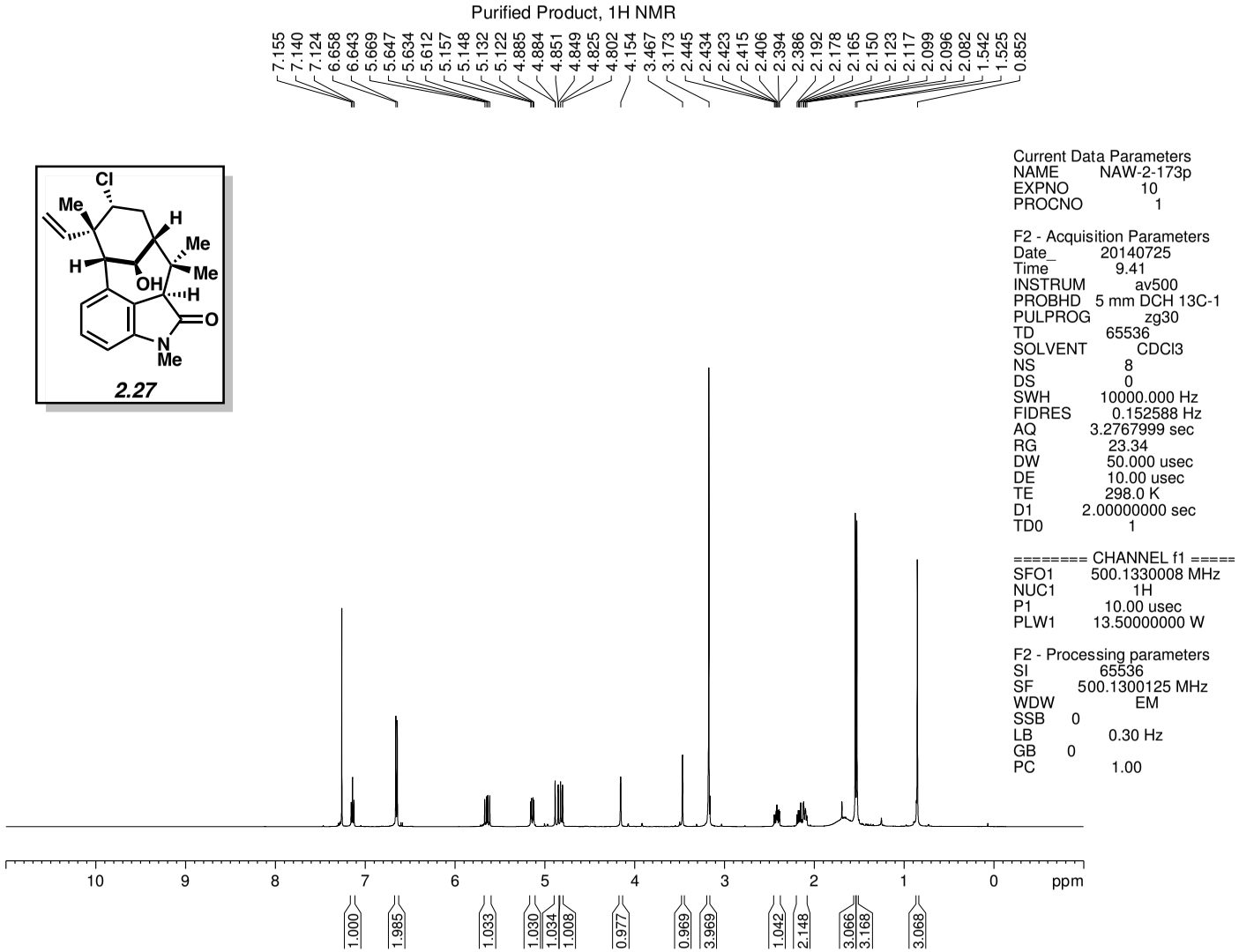

Figure 2.28 ^{1}H NMR (500 MHz, $CDCl_3$) of compound **2.27**.

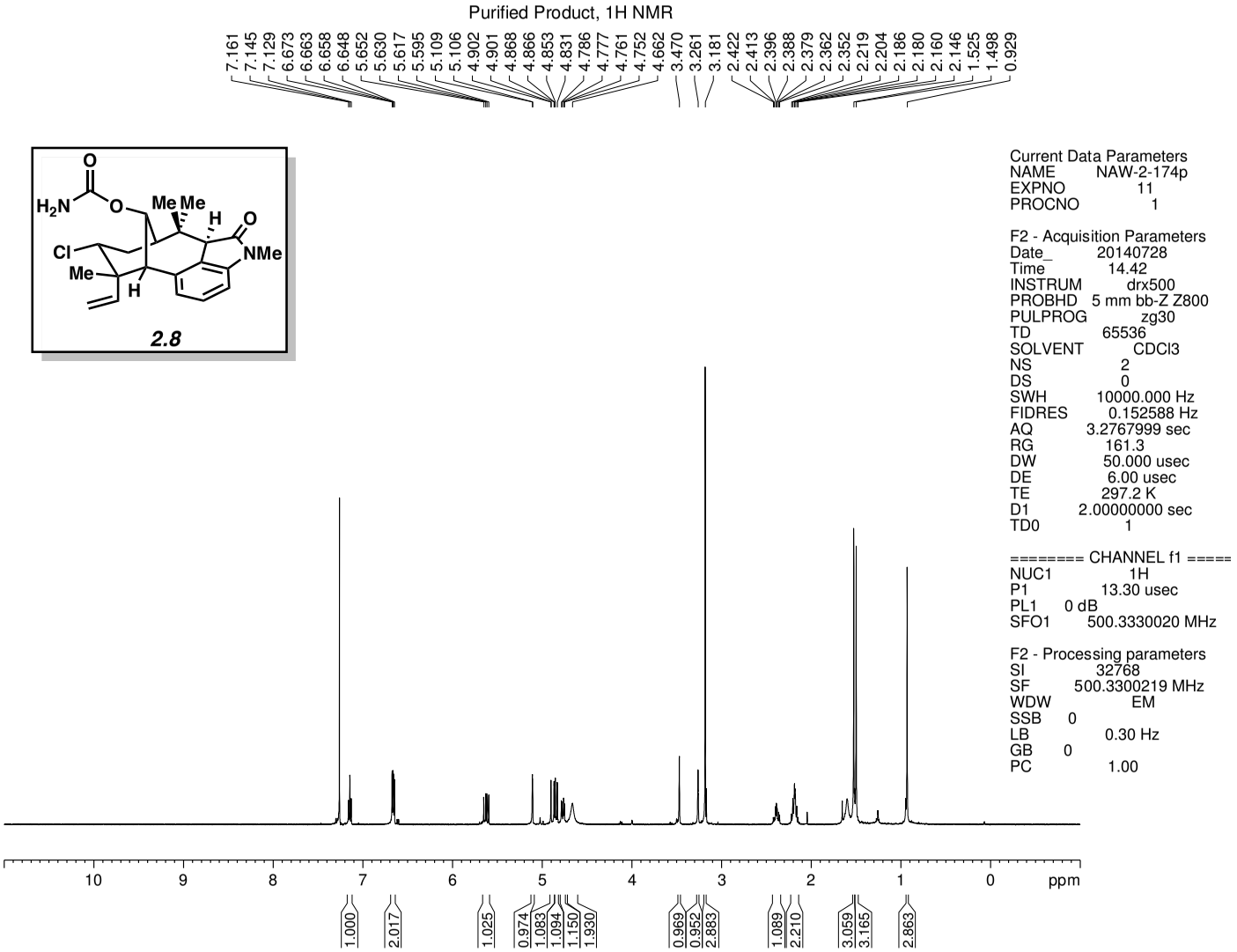

Figure 2.29 ^{1}H NMR (500 MHz, $CDCl_3$) of compound **2.8**.

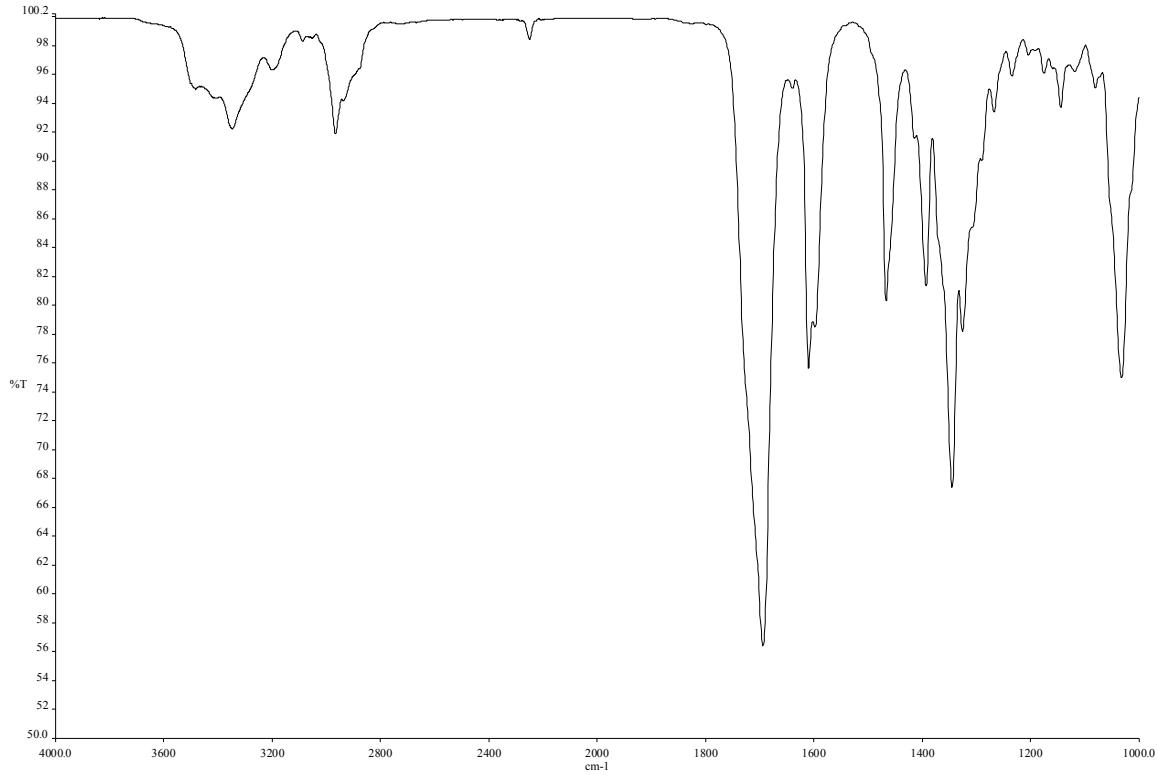

Figure 2.30 Infrared spectrum of compound **2.8**.

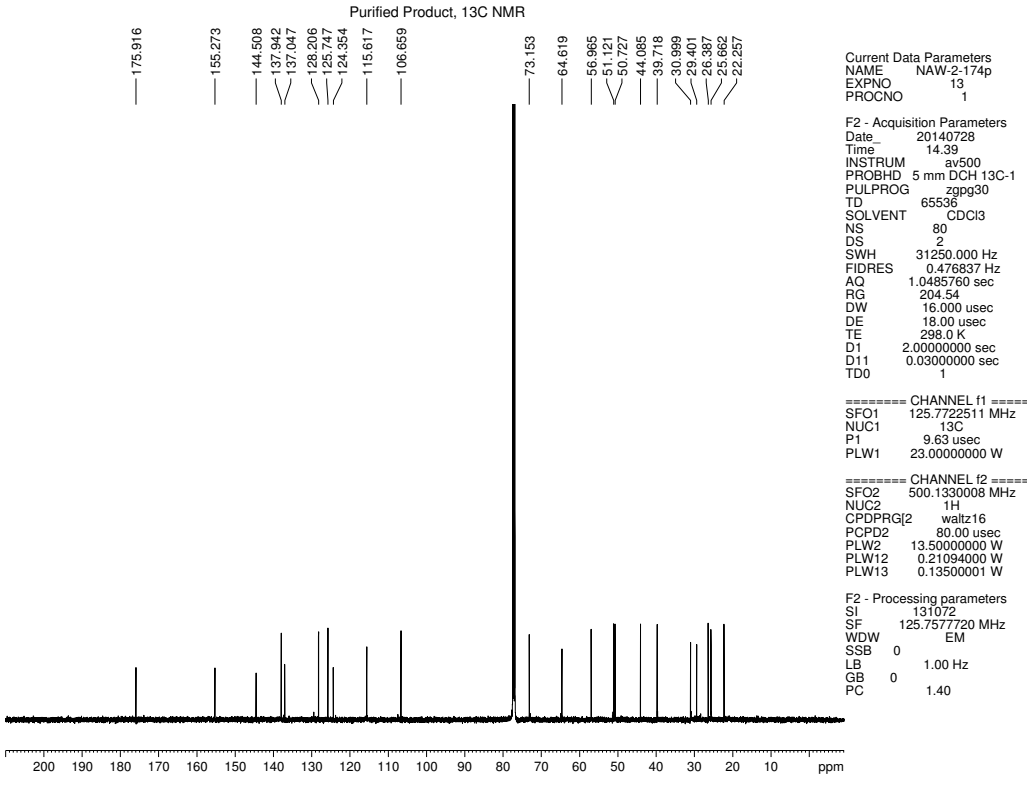

Figure 2.31 ^{13}C NMR (125 MHz, $CDCl_3$) of compound **2.8**.

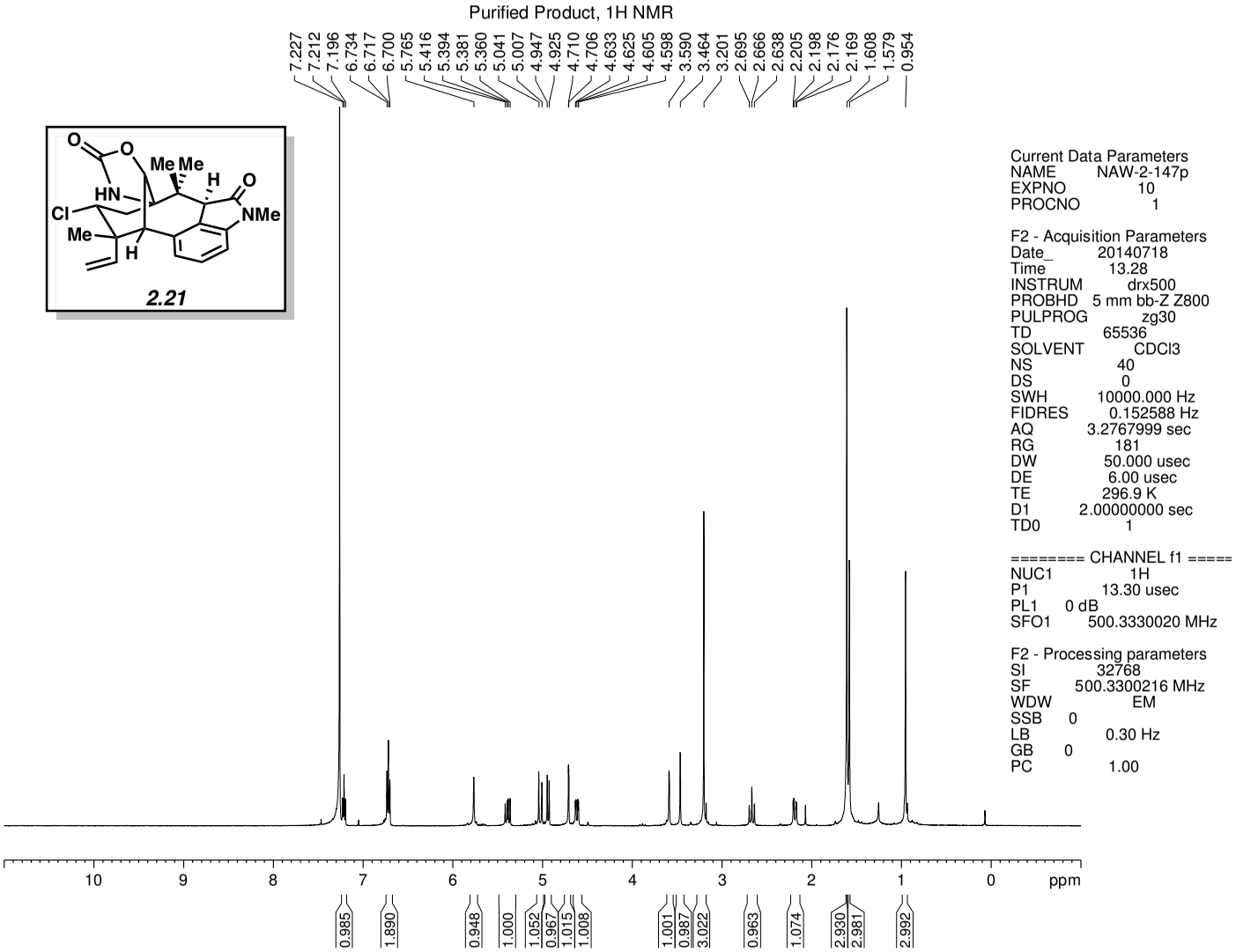

Figure 2.32 ^{1}H NMR (500 MHz, $CDCl_3$) of compound **2.21**.

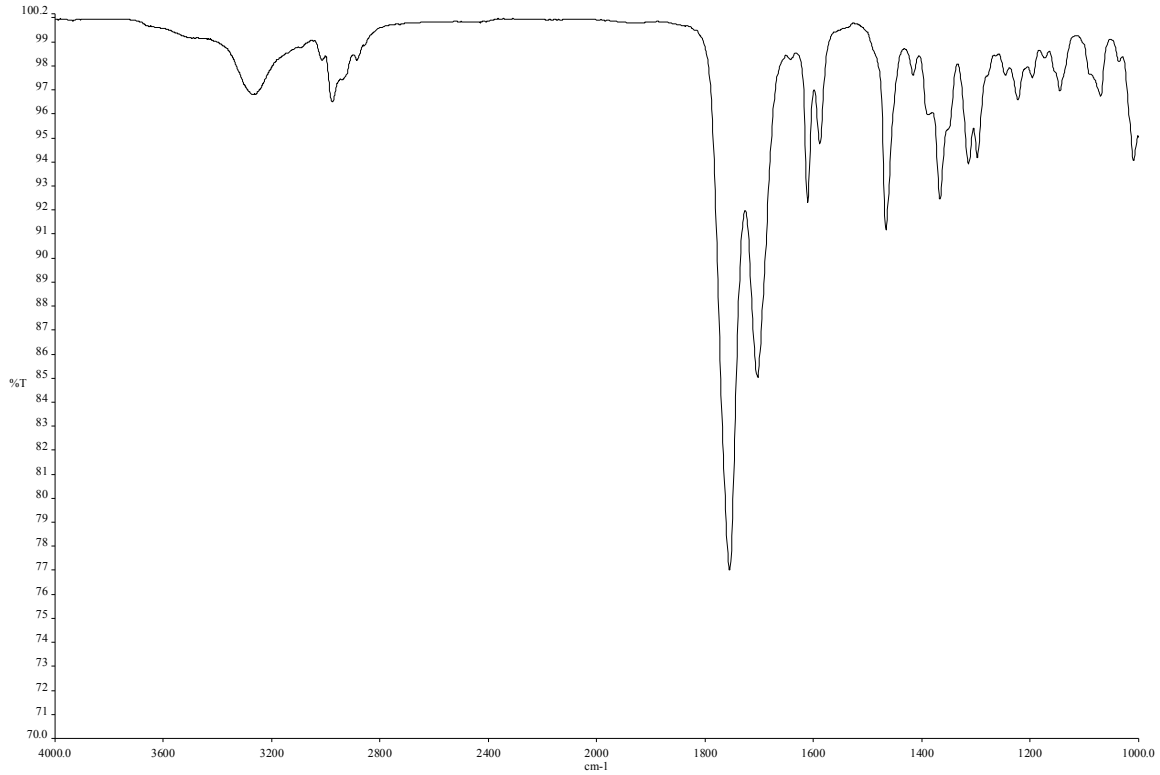

Figure 2.33 Infrared spectrum of compound **2.21**.

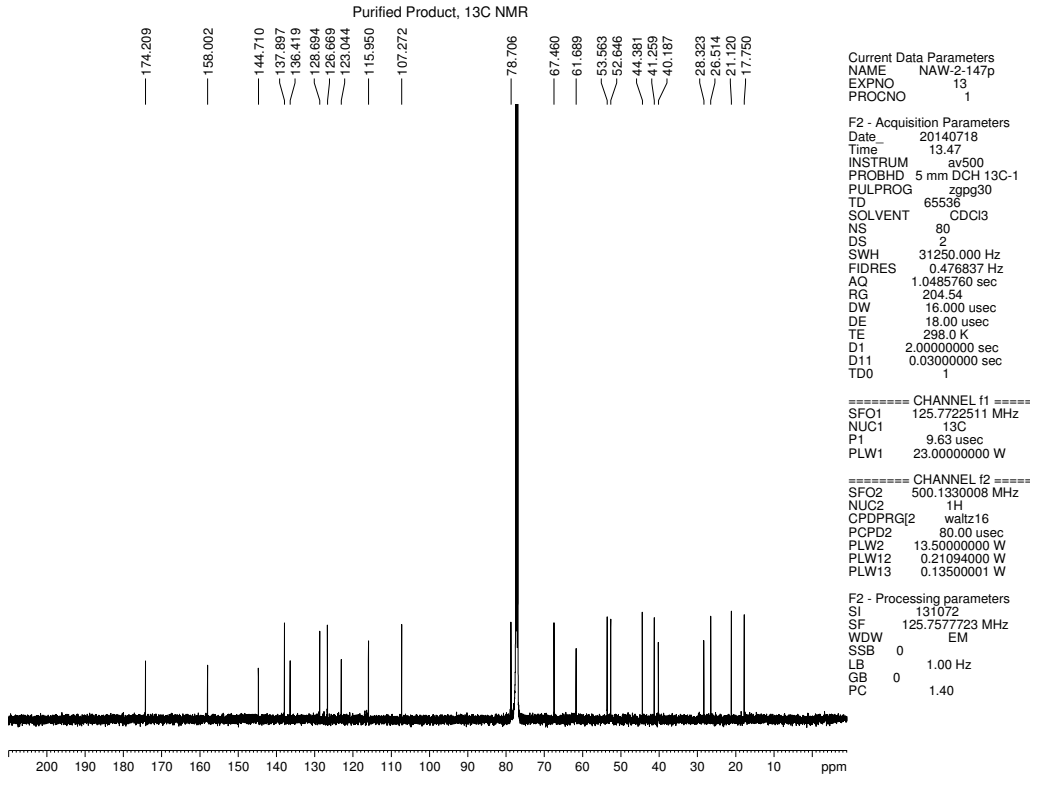

Figure 2.34 ^{13}C NMR (125 MHz, $CDCl_3$) of compound **2.21**.

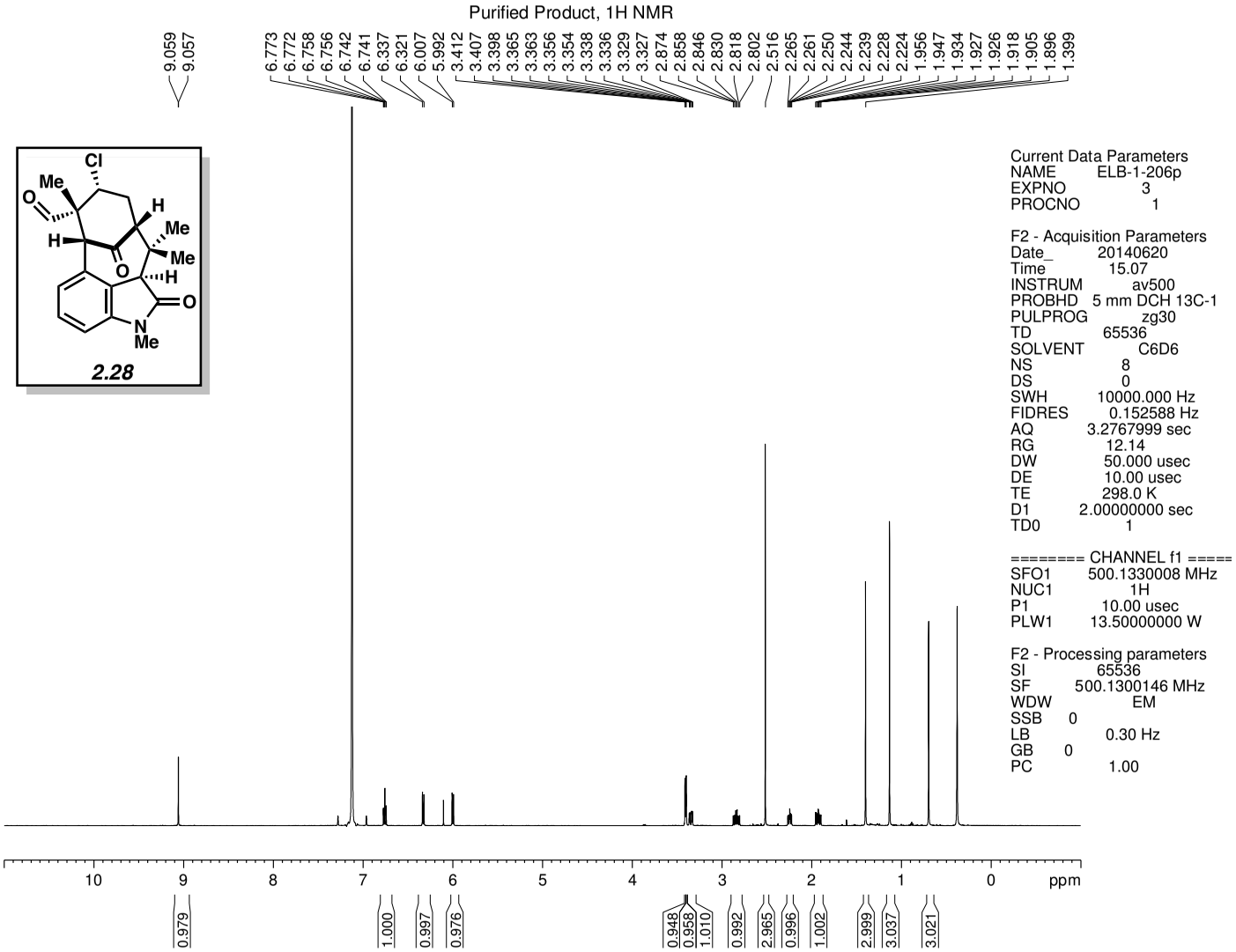

Figure 2.35 ^{1}H NMR (500 MHz, $CDCl_3$) of compound **2.28**.

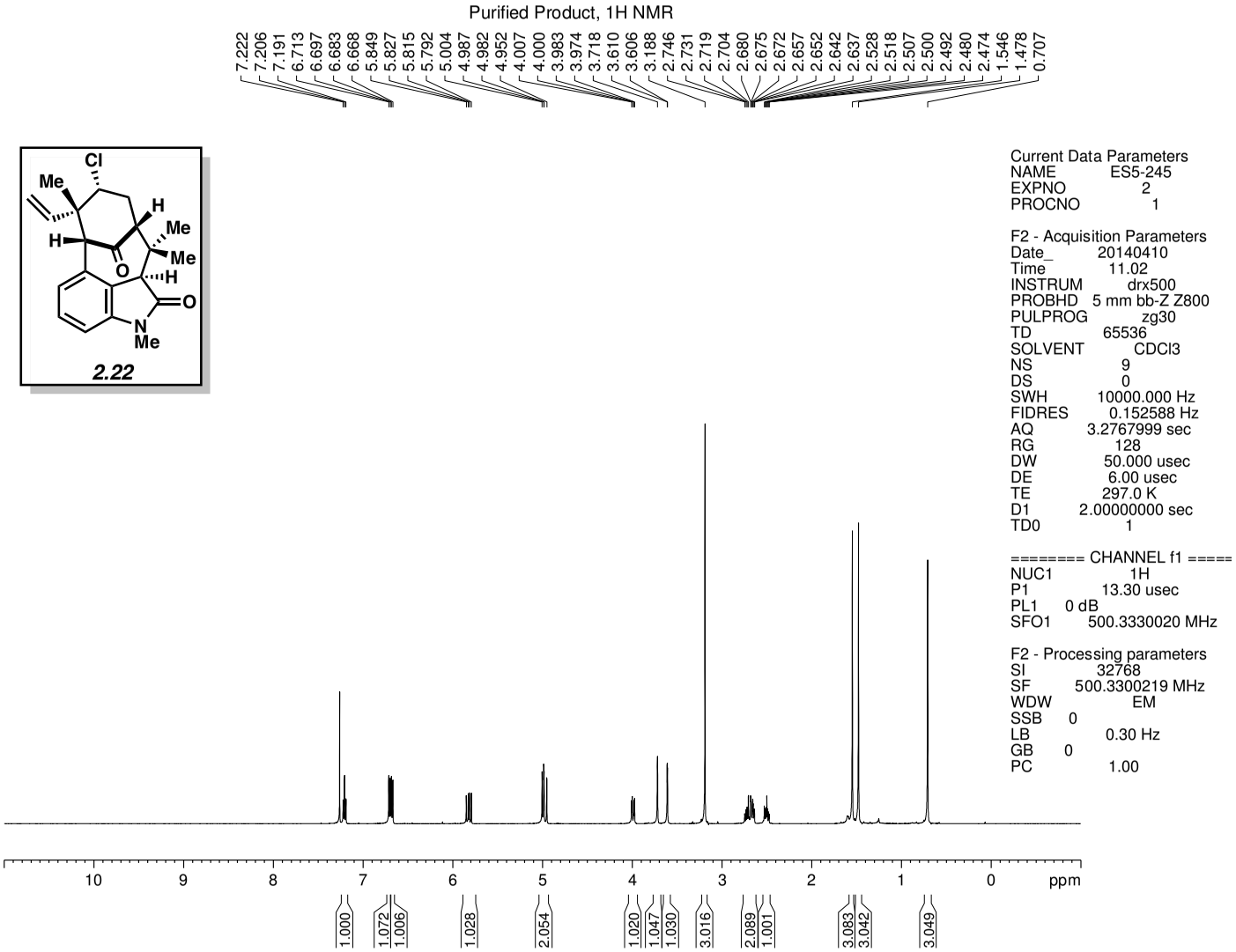

Figure 2.36 ^{1}H NMR (500 MHz, $CDCl_3$) of compound **2.22**.

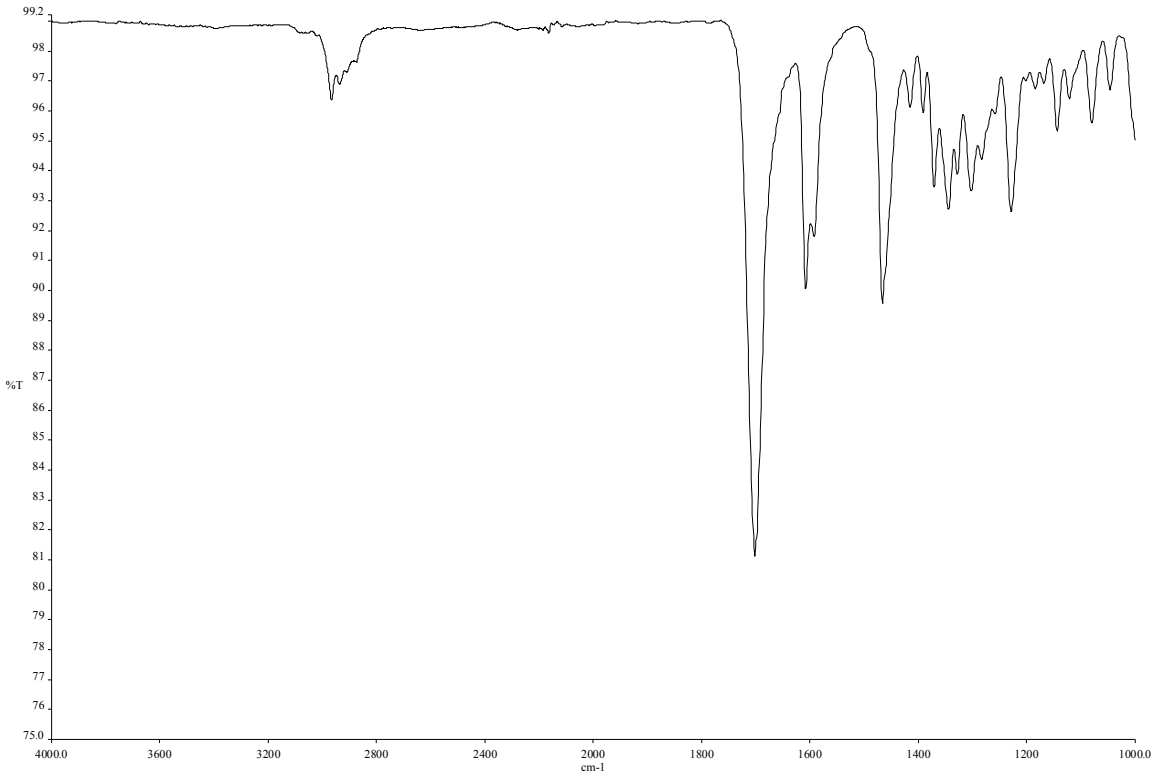

Figure 2.37 Infrared spectrum of compound **2.22**.

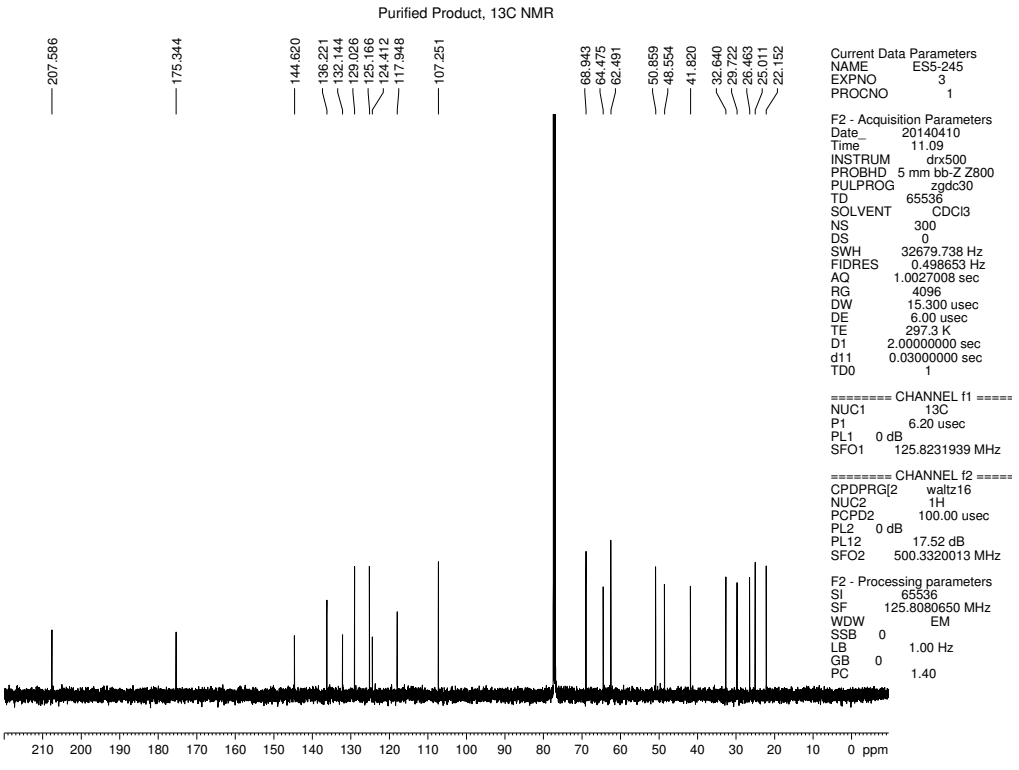

Figure 2.38 ^{13}C NMR (125 MHz, $CDCl_3$) of compound **2.22**.

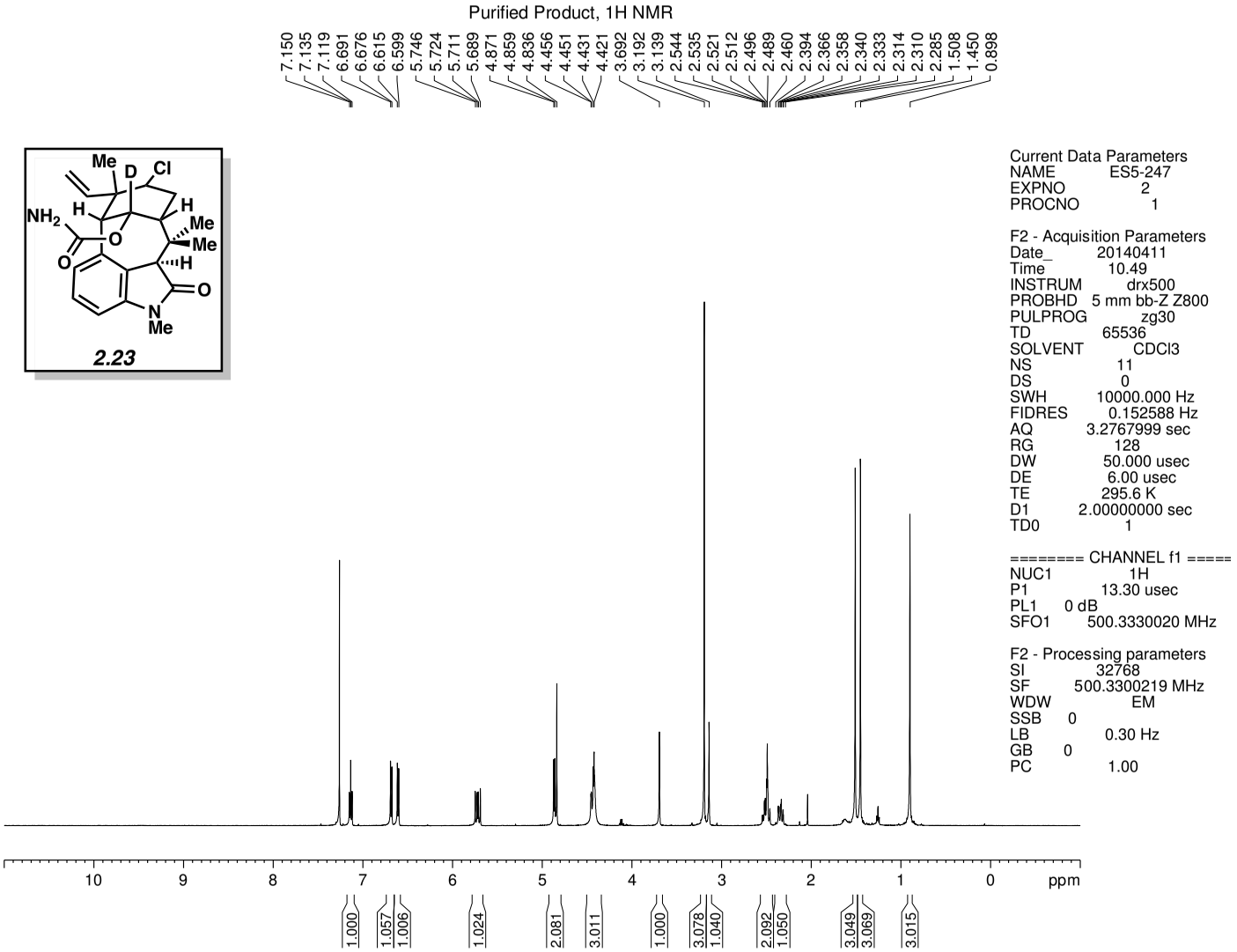

Figure 2.39 ^{1}H NMR (500 MHz, $CDCl_3$) of compound **2.23**.

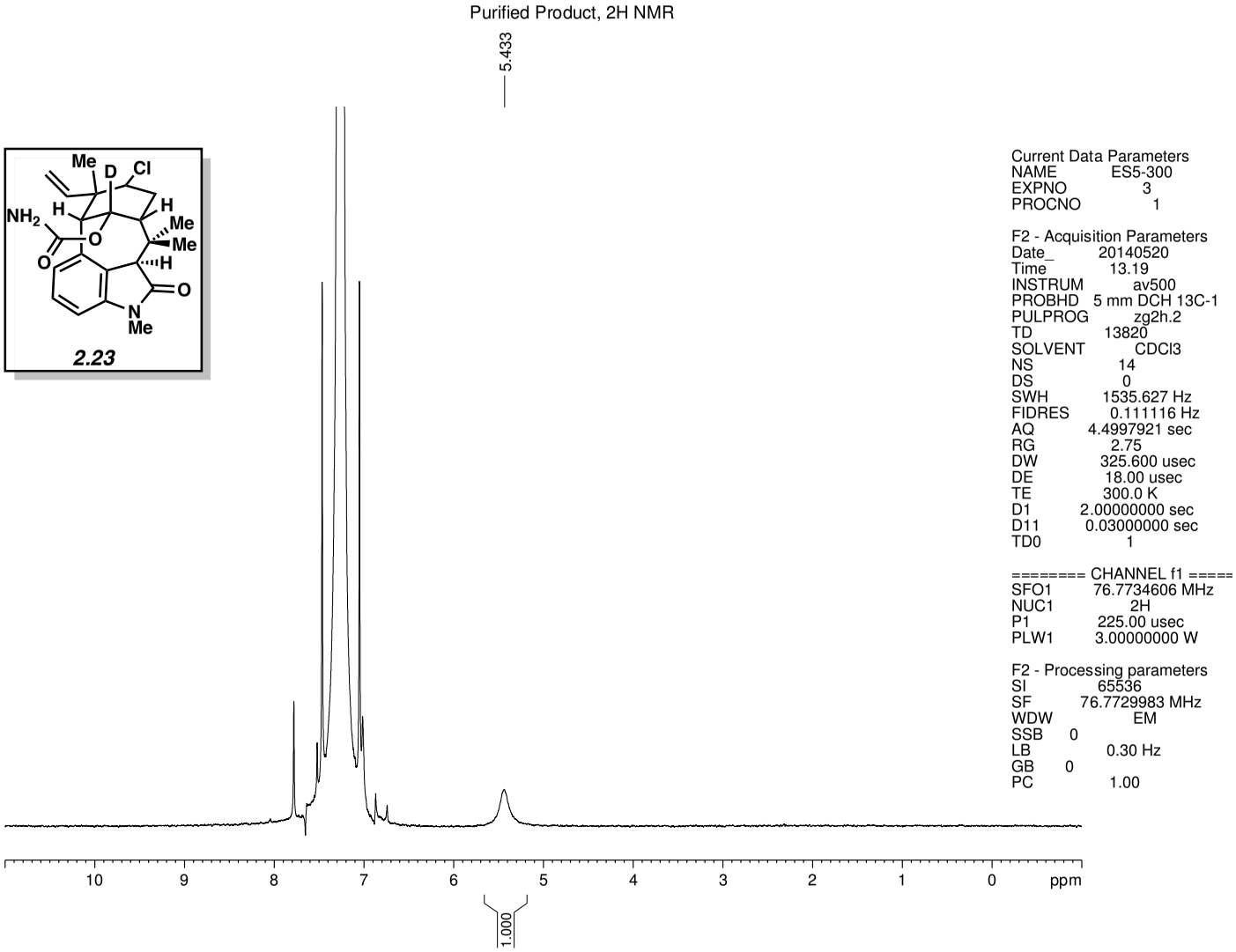

Figure 2.40 ^{2}H NMR (77 MHz, $CDCl_3$) of compound **2.23**.

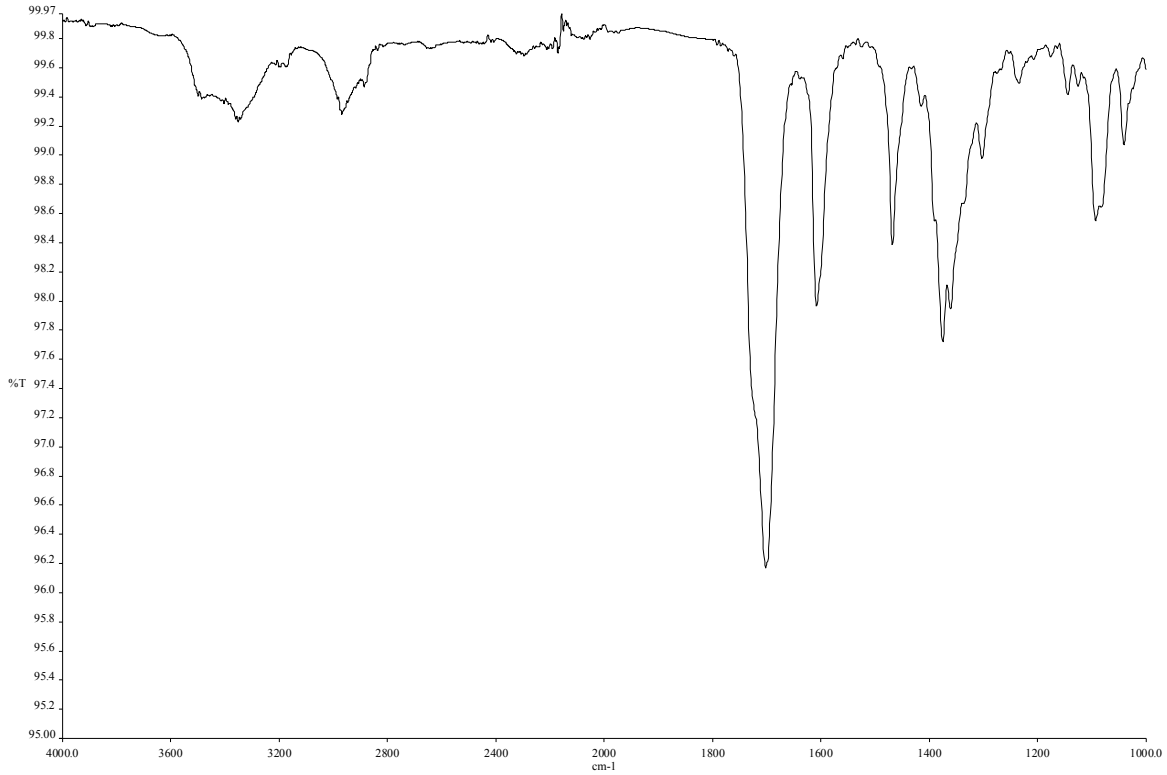

Figure 2.41 Infrared spectrum of compound **2.23**.

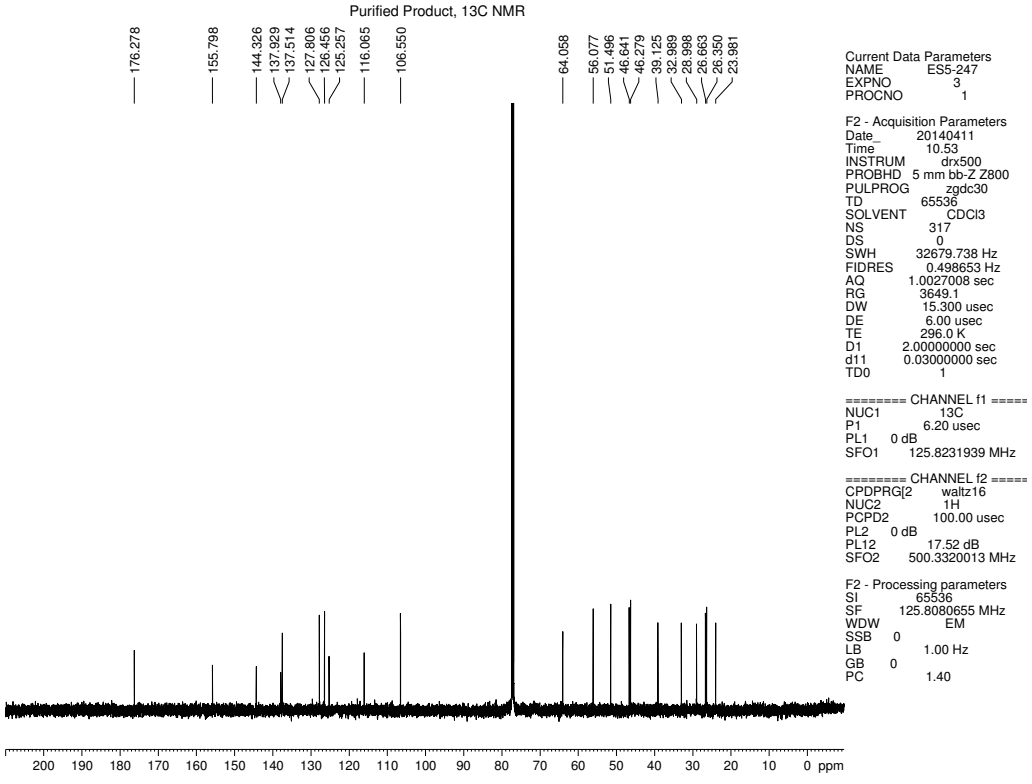

Figure 2.42 ^{13}C NMR (125 MHz, $CDCl_3$) of compound **2.23**.

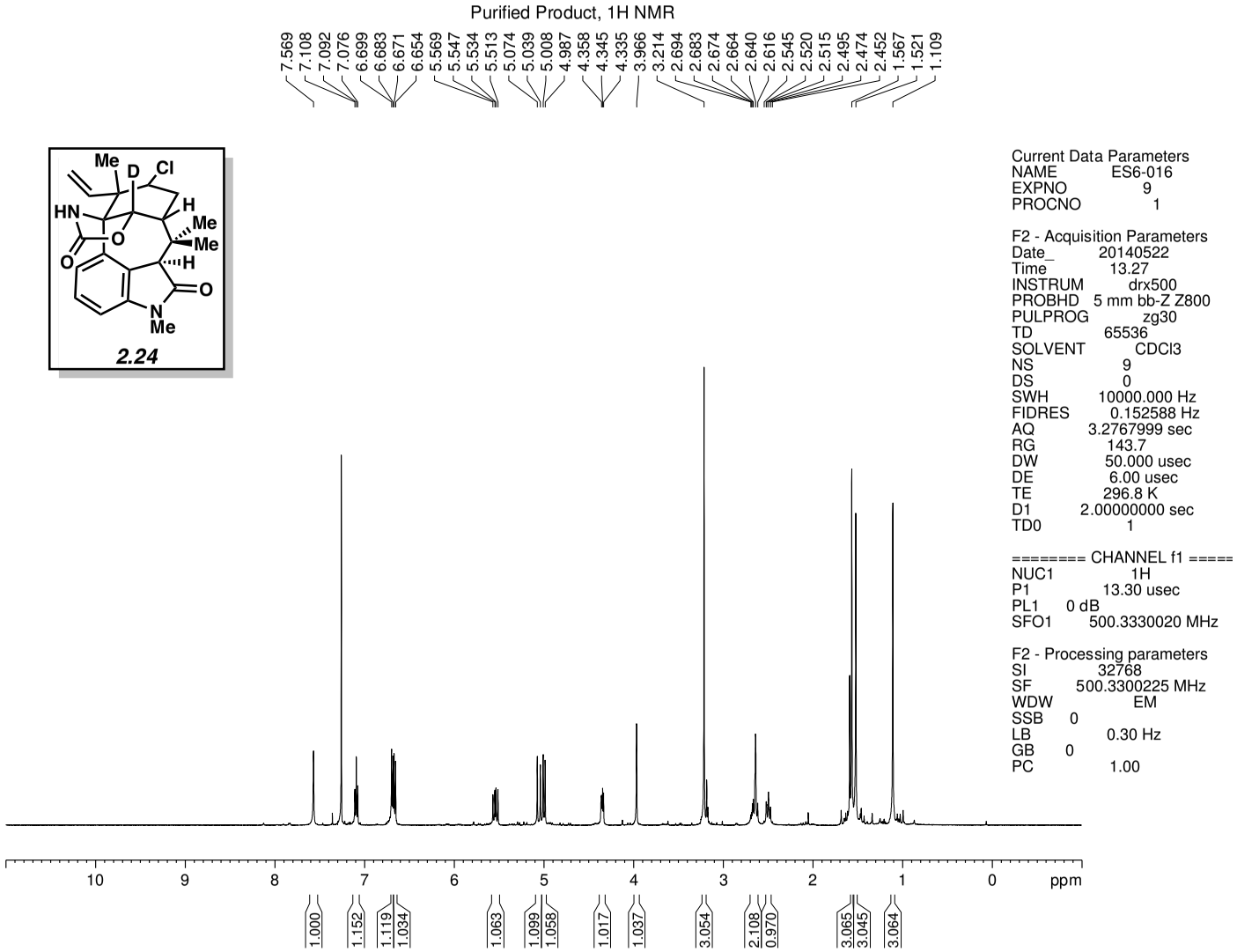

Figure 2.43 ^{1}H NMR (500 MHz, $CDCl_3$) of compound **2.24**.

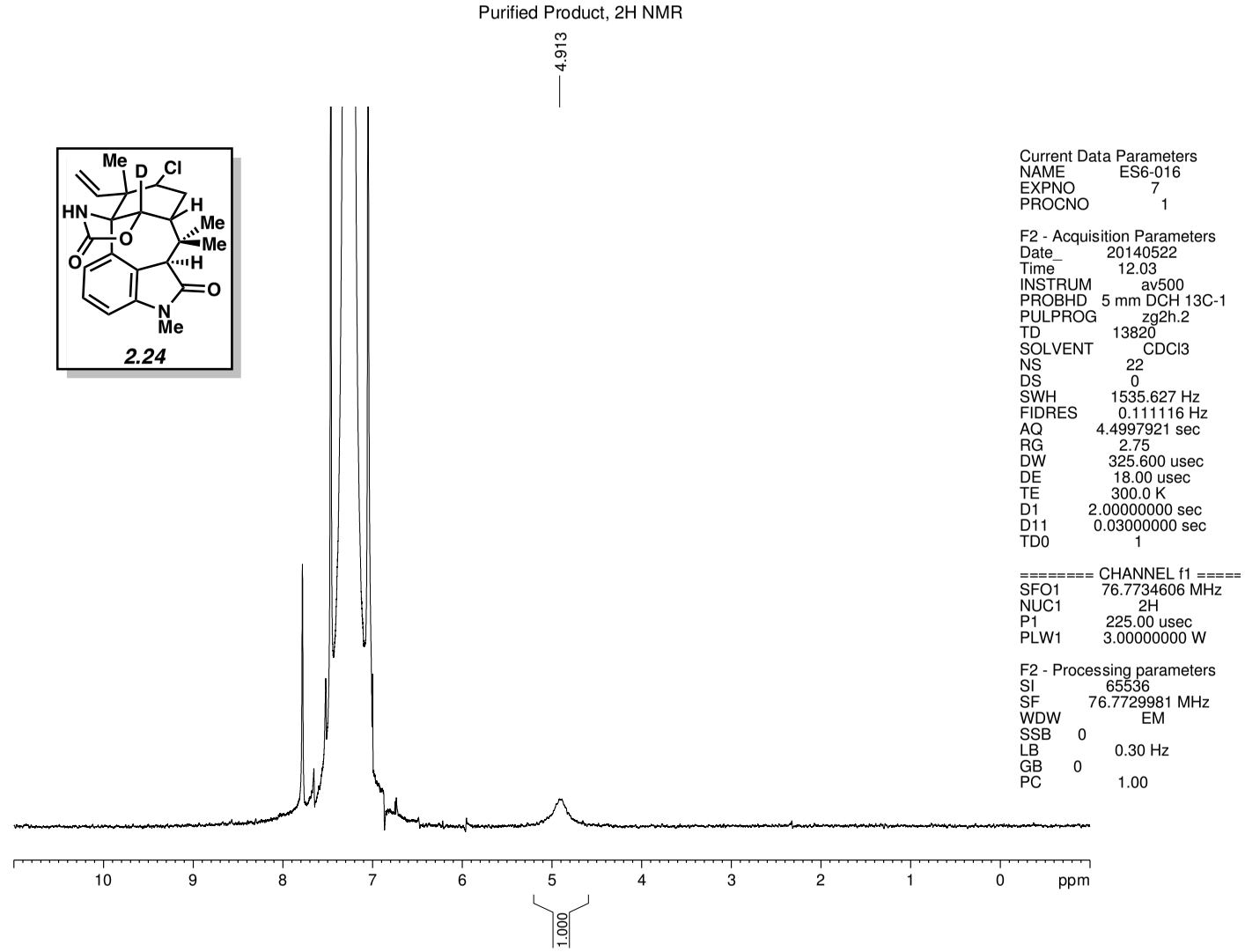

Figure 2.44 ^{2}H NMR (77 MHz, $CDCl_3$) of compound **2.24**.

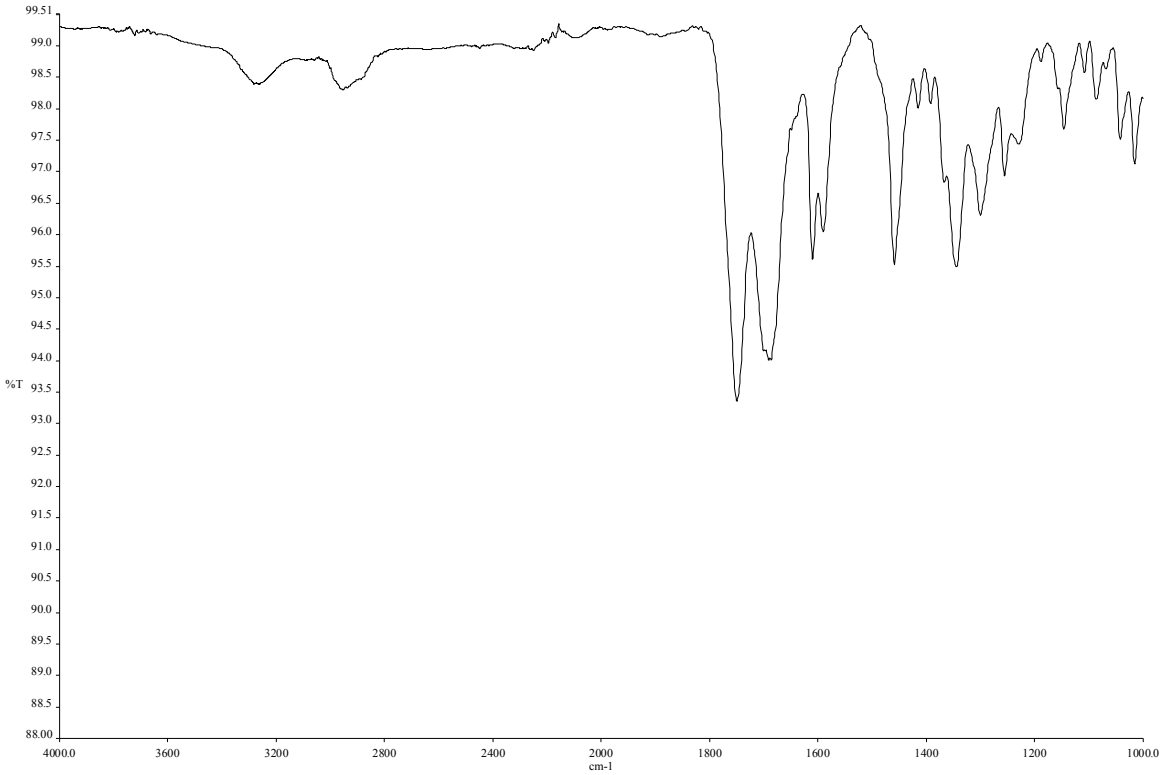

Figure 2.45 Infrared spectrum of compound **2.24**.

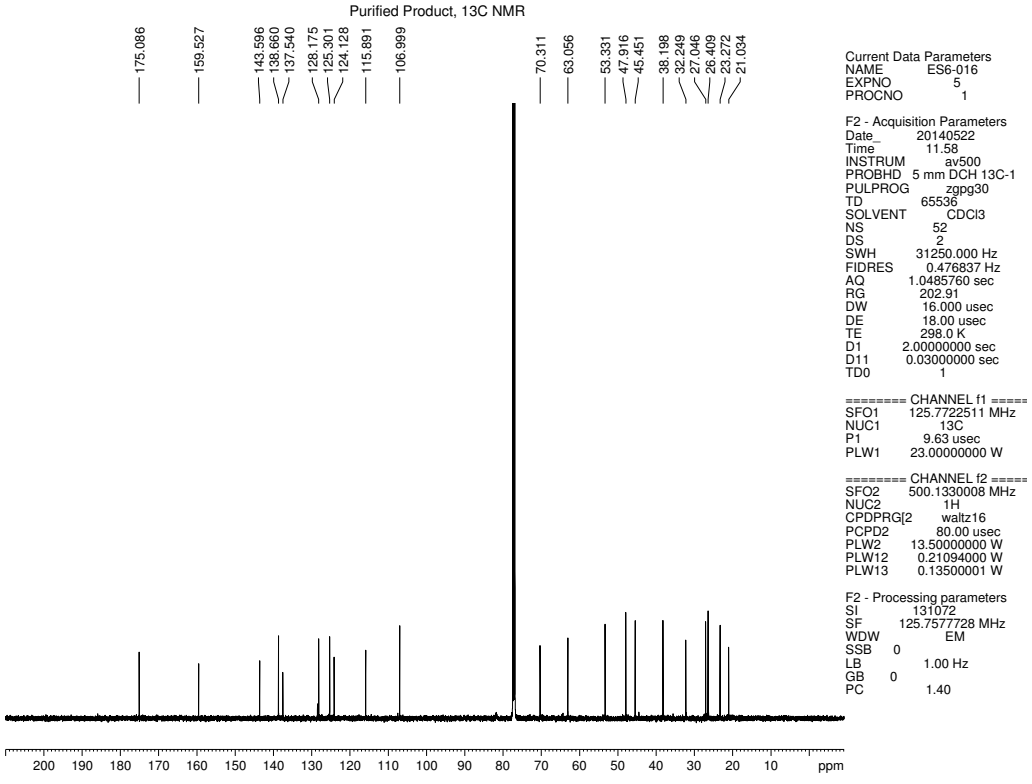

Figure 2.46 ^{13}C NMR (125 MHz, $CDCl_3$) of compound **2.24**.

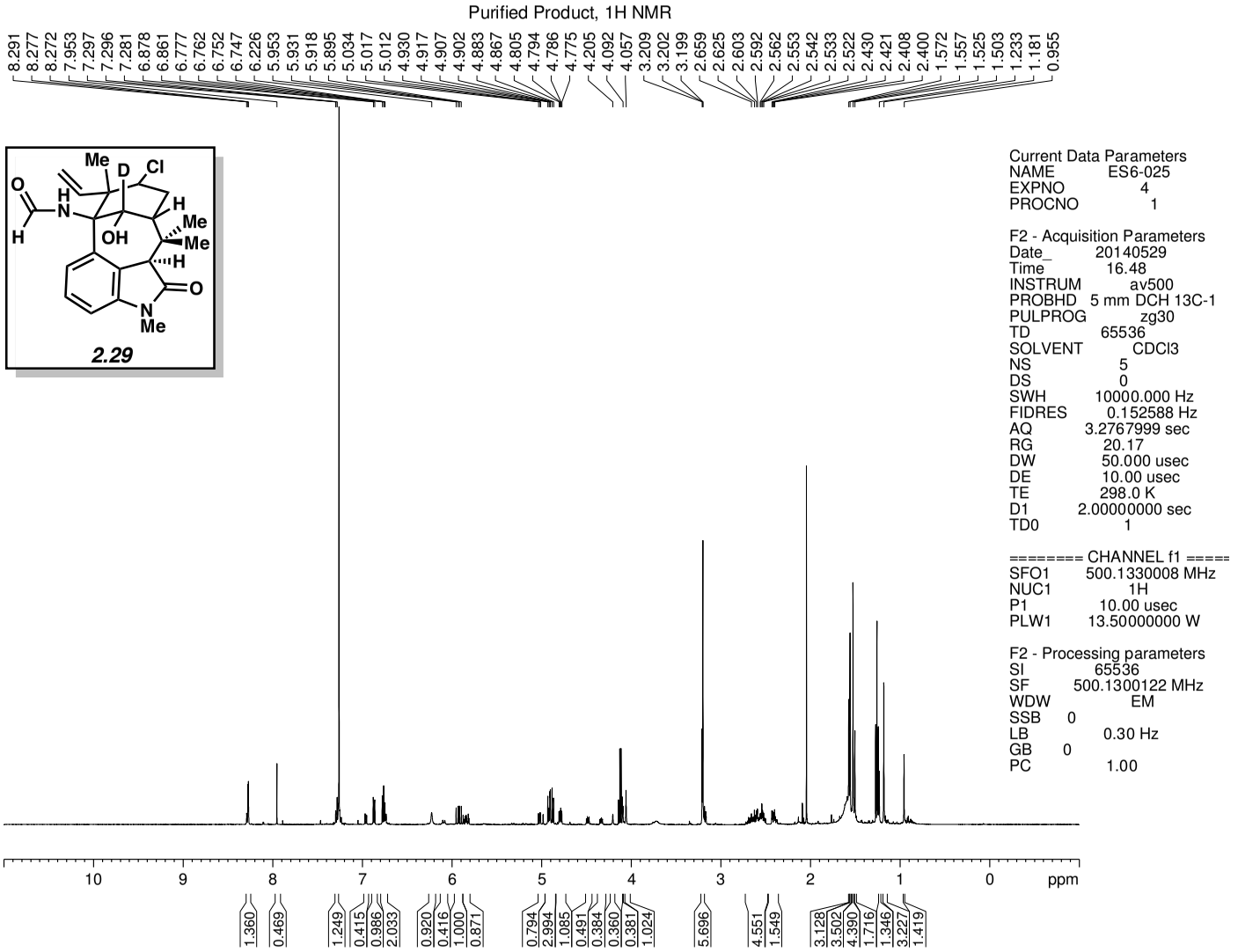

Figure 2.47 ^{1}H NMR (500 MHz, $CDCl_3$) of compound **2.29**.

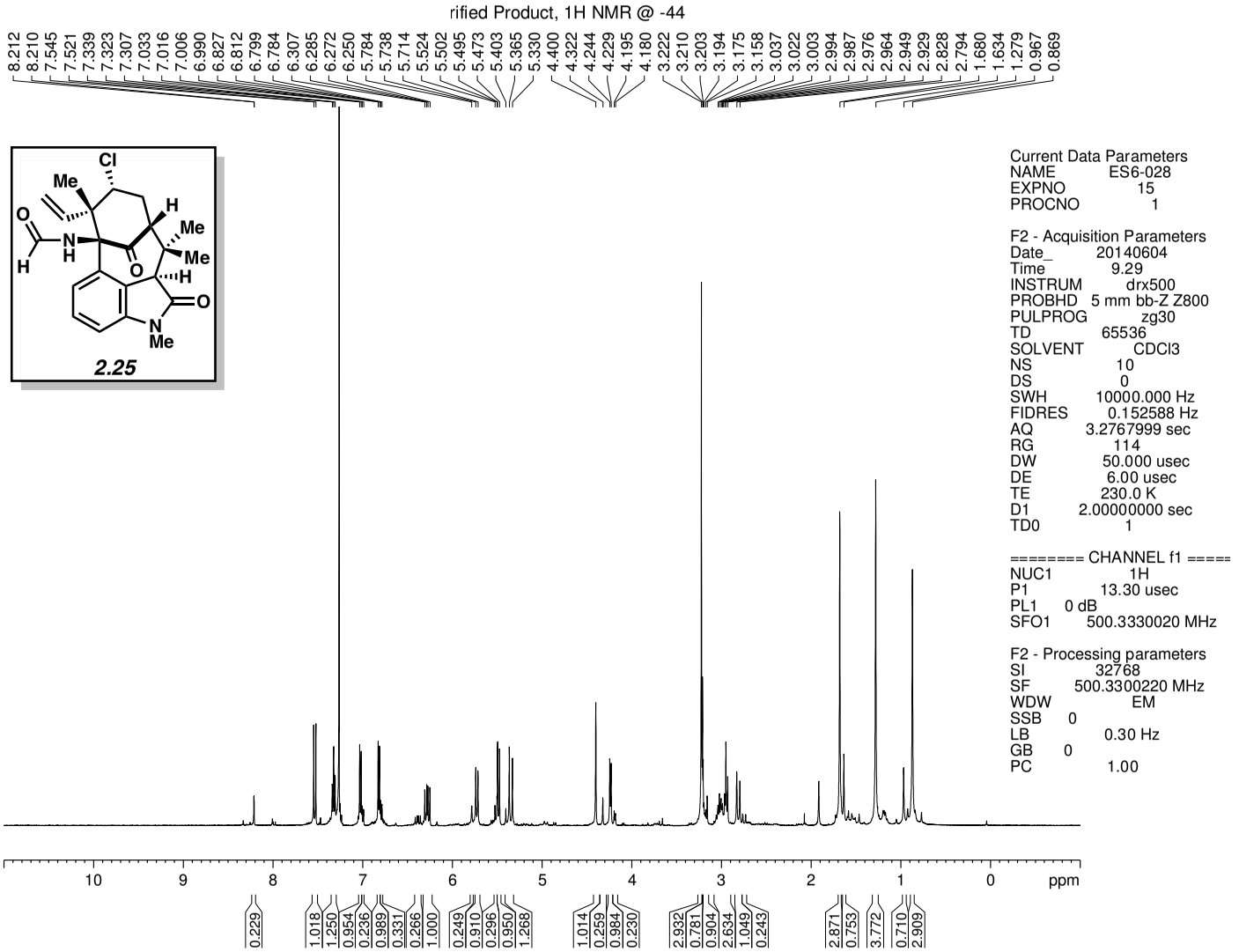

Figure 2.48 ^{1}H NMR (500 MHz, $CDCl_3$) of compound **2.25**.

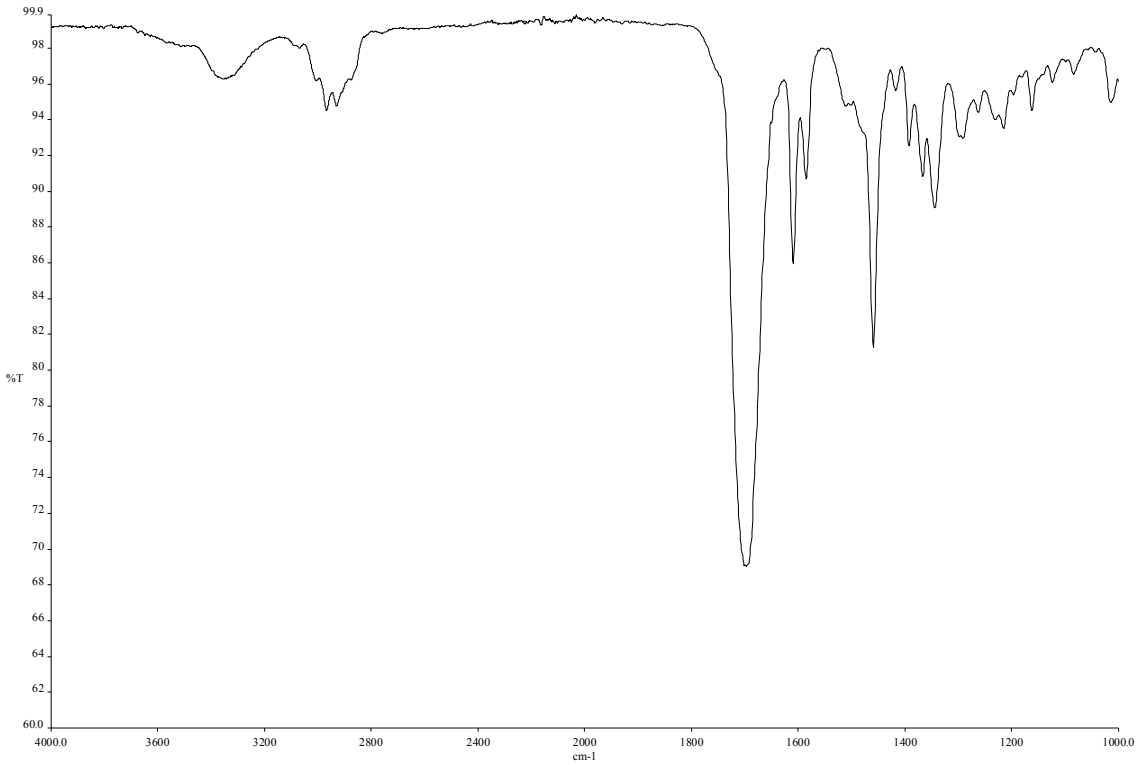

Figure 2.49 Infrared spectrum of compound **2.25**.

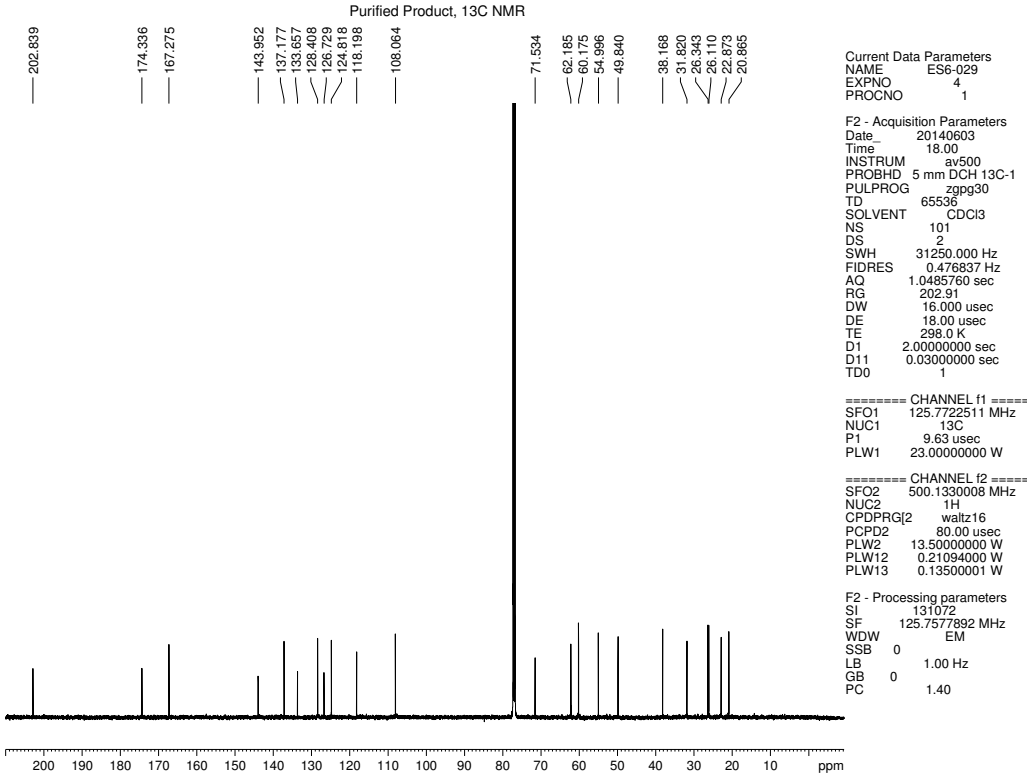

Figure 2.50 ^{13}C NMR (125 MHz, $CDCl_3$) of compound **2.25**.

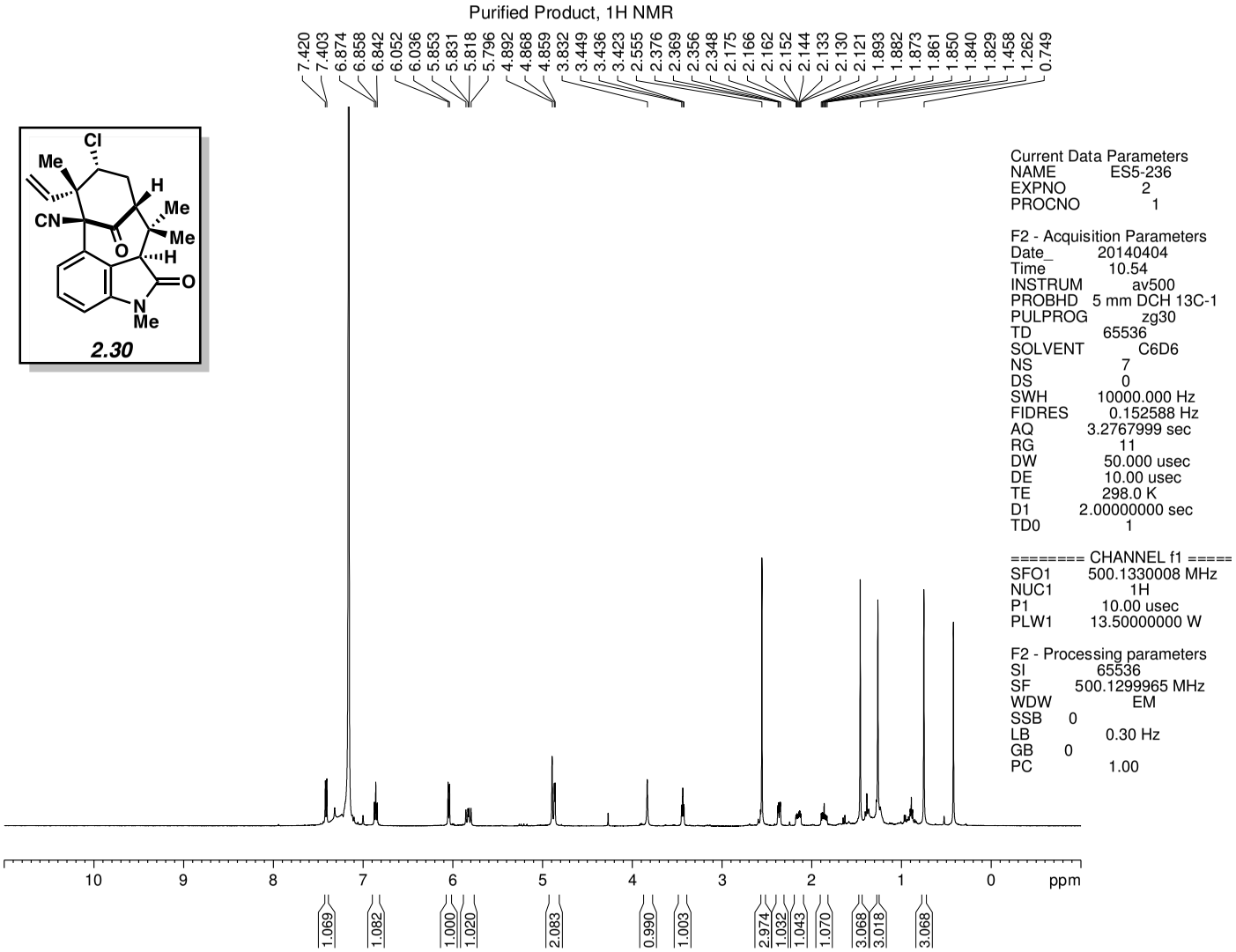

Figure 2.51 ^{1}H NMR (500 MHz, $CDCl_3$) of compound **2.30**.

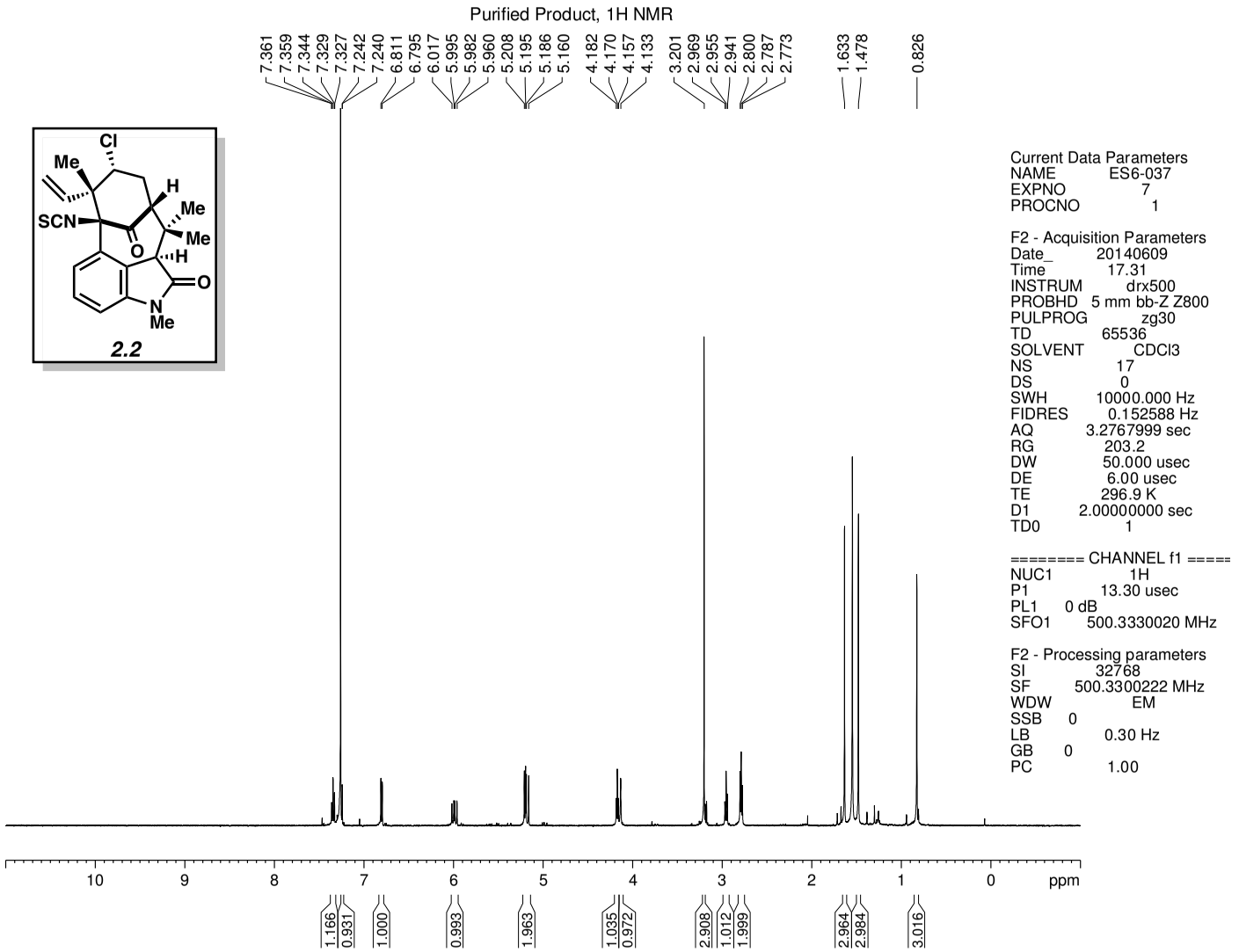

Figure 2.52 ^{1}H NMR (500 MHz, $CDCl_3$) of compound **2.2**.

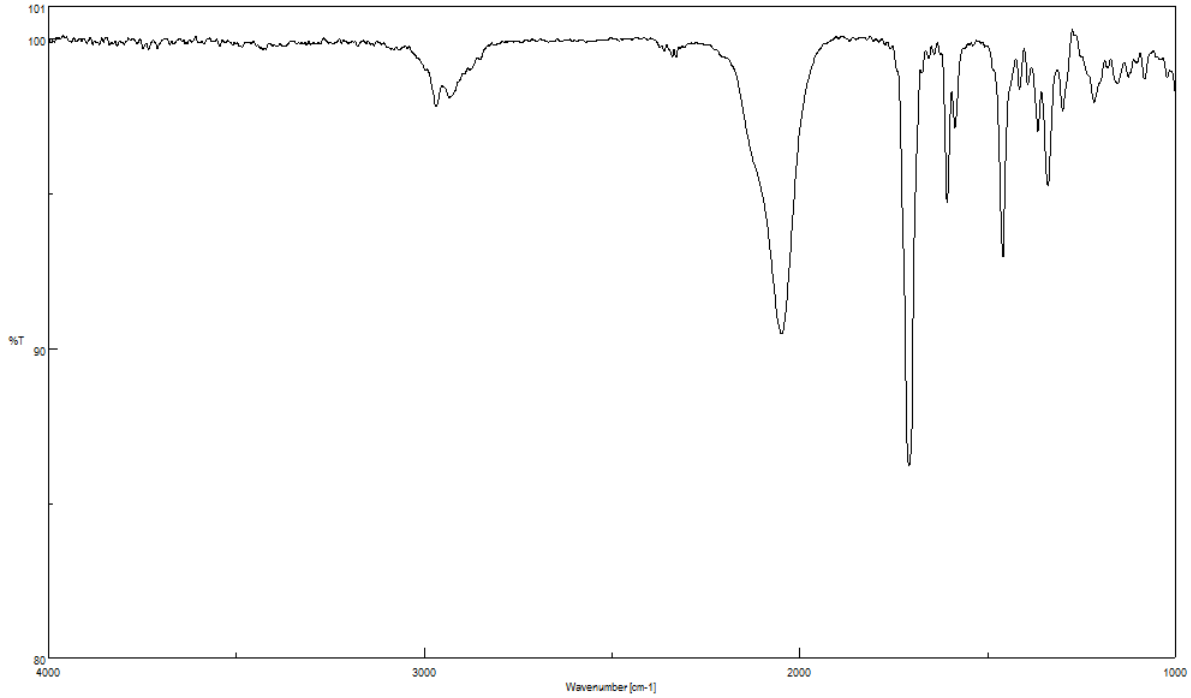

Figure 2.53 Infrared spectrum of compound **2.2**.

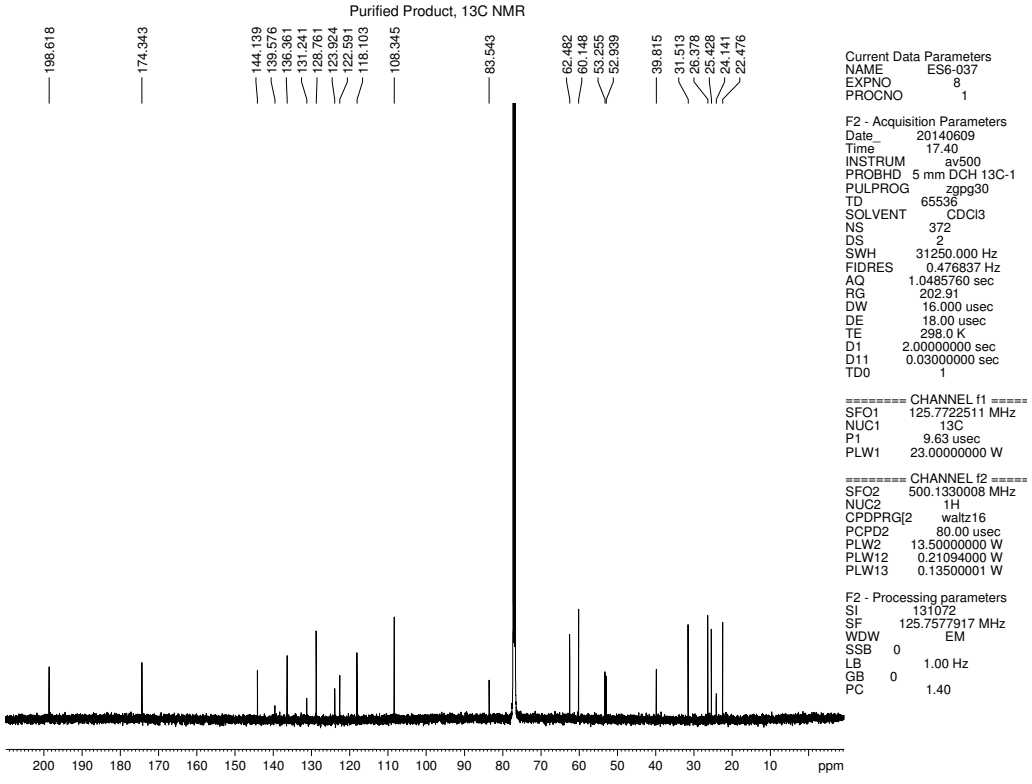

Figure 2.54 ^{13}C NMR (125 MHz, $CDCl_3$) of compound **2.2**.

2.11 Notes and References

(1) For pertinent reviews, see: (a) Wood, J. L. *Nat. Chem.* **2012**, *4*, 341. (b) Huters, A. D.; Styduhar, E. D.; Garg. N. K. *Angew. Chem. Int. Ed.* **2012**, *51*, 3758. (c) Brown, L. E.; Konopelski, J. P. *Org. Prep. Proced. Int.* **2008**, *40*, 411. (d) Avendaño, C.; Menéndez, J. C. *Curr. Org. Synth.* **2004**, *1*, 65.

(2) For completed total syntheses of **2.1**, see: (a) Baran, P. S.; Richter, J. M. *J. Am. Chem. Soc.* **2005**, *127*, 15394. (b) Richter, J. M.; Ishihara, Y.; Masuda, T.; Whitefield, B. W.; Llamas, T.; Pohjakallio, A.; Baran, P. S. *J. Am. Chem. Soc.* **2008**, *130*, 17938. (c) Reisman, S. E.; Ready, J. M.; Hasuoka, A.; Smith, C. J.; Wood, J. L. *J. Am. Chem. Soc.* **2006**, *128*, 1448. (d) Reisman, S. E.; Ready, J. M.; Weiss, M. M.; Hasuoka, A.; Hirata, M.; Tamaki, K.; Ovaska, T. V.; Smith, C. J.; Wood, J. L. *J. Am. Chem. Soc.* **2008**, *130*, 2087.

(3) (a) Stratmann, K.; Moore, R. E.; Bonjouklian, R.; Deeter, J. B.; Patterson, G. M. L.; Shaffer, S.; Smith, C. D.; Smitka, T. A. *J. Am. Chem. Soc.* **1994**, *116*, 9935. (b) Jimenez, J. I.; Huber, U.; Moore, R. E.; Patterson, G. M. L. *J. Nat. Prod.* **1999**, *62*, 569.

(4) For progress toward the synthesis of bicyclo[4.3.1]-welwitindolinones, see: (a) Konopelski, J. P.; Deng, H.; Schiemann, K.; Keane, J. M.; Olmstead, M. M. *Synlett* **1998**, 1105. (b) Wood, J. L.; Holubec, A. A.; Stoltz, B. M.; Weiss, M. M.; Dixon, J. A.; Doan, B. D.; Shamji, M. F.; Chen, J. M.; Heffron, T. P. *J. Am. Chem. Soc.* **1999**, *121*, 6326. (c) Kaoudi, T.; Quiclet-Sire, B.; Seguin, S.; Zard, S. Z. *Angew. Chem. Int. Ed.* **2000**, *39*, 731. (d) Deng, H.; Konopelski, J. P. *Org. Lett.* **2001**, *3*, 3001. (e) Jung, M. E.; Slowinski, F. *Tetrahedron Lett.* **2001**, *42*, 6835. (f) López-Alvarado, P.; García-Granda, S.; Álvarez-Rúa, C.; Avendaño, C. *Eur. J. Org. Chem.* **2002**, 1702. (g) MacKay, J. A.; Bishop, R. L.; Rawal, V. H. *Org. Lett.*

2005, *7*, 3421. (h) Baudoux, J.; Blake, A. J.; Simpkins, N. S. *Org. Lett.* **2005**, *7*, 4087. (i) Greshock, T. J.; Funk, R. L. *Org. Lett.* **2006**, *8*, 2643. (j) Lauchli, R.; Shea, K. J. *Org. Lett.* **2006**, *8*, 5287. (k) Guthikonda, K.; Caliando, B. J.; Du Bois, J. Rh(II)-catalyzed olefin aziridination: Toward the synthesis of *N*-methylwelwitindolinone C. *Abstracts of Papers*, 232nd ACS National Meeting, San Francisco, CA, Sept. 10–14, **2006**; American Chemical Society: Washington, DC, 2006; ORGN-002. (l) Xia, J.; Brown, L. E.; Konopelski, J. P. *J. Org. Chem.* **2007**, *72*, 6885. (m) Boissel, V.; Simpkins, N. S.; Bhalay, G.; Blake, A. J.; Lewis, W. *Chem. Commun.* **2009**, 1398. (n) Boissel, V.; Simpkins, N. S.; Bhalay, G. *Tetrahedron Lett.* **2009**, *50*, 3283. (o) Tian, X.; Huters, A. D.; Douglas, C. J.; Garg, N. K. *Org. Lett.* **2009**, *11*, 2349. (p) Trost, B. M.; McDougall, P. J. *Org. Lett.* **2009**, *11*, 3782. (q) Brailsford, J. A.; Lauchli, R.; Shea, K. J. *Org. Lett.* **2009**, *11*, 5330. (r) Freeman, D. B.; Holubec, A. A.; Weiss, M. W.; Dixon, J. A.; Kafefuda, A.; Ohtsuka, M.; Inoue, M.; Vaswani R. G.; Ohki, H.; Doan, B. D.; Reisman, S. E.; Stoltz, B. M.; Day, J. J.; Tao, R. N.; Dieterich, N. A.; Wood, J. L. *Tetrahedron* **2010**, *66*, 6647–6655. (s) Heidebrecht, R. W., Jr.; Gulledge, B.; Martin, S. F. *Org. Lett.* **2010**, *12*, 2492. (t) Ruiz, M.; López-Alvarado, P.; Menéndez, J. C. *Org. Biomol. Chem.* **2010**, *8*, 4521. (u) Bhat, V.; Rawal, V. H. *Chem. Commun.* **2011**, *47*, 9705. (v) Bhat, V.; MacKay, J. A.; Rawal, V. H. *Org. Lett.* **2011**, *13*, 3214. (w) Bhat, V.; MacKay, J. A.; Rawal, V. H. *Tetrahedron* **2011**, *67*, 10097. (x) Zhang, M.; Tang, W. *Org. Lett.* **2012**, *14*, 3756. (y) Cleary, L.; Pitzen, J.; Brailsford, J. A.; Shea, K. J. *Org. Lett.* **2014**, *16*, 4460–4463.

(5) (a) Fu, T.-h.; McElroy, W. T.; Shamszad, M.; Martin, S. F. *Org. Lett.* **2012**, *14*, 3834. (b) Fu, T.-h.; McElroy, W. T.; Shamszad, M.; Heidebrecht, R. W., Jr.; Gulledge, B.; Martin, S. F. *Tetrahedron* **2013**, *69*, 5588.

(6) (a) Bhat, V.; Allan, K. M.; Rawal, V. H. *J. Am. Chem. Soc.* **2011**, *133*, 5798. (b) Allan, K. M.; Kobayashi, K.; Rawal, V. H. *J. Am. Chem. Soc.* **2012**, *134*, 1392.

(7) (a) Huters, A. D.; Quasdorf, K. W.; Styduhar, E. D.; Garg, N. K. *J. Am. Chem. Soc.* **2011**, *133*, 15797. (b) Quasdorf, K. W.; Huters, A. D.; Lodewyk, M. W.; Tantillo, D. J.; Garg, N. K. *J. Am. Chem. Soc.* **2012**, *134*, 1396. (c) Styduhar, E. D.; Huters, A. D.; Weires, N. A.; Garg, N. K. *Angew. Chem. Int. Ed.* **2013**, *52*, 12422.

(8) The 3D representation of **2.2** was obtained using B3LYP/6-31G* calculations (geometry optimization), using MacSpartan software.

(9) Image prepared using CYLview: Legault, C. Y. CYLview, 1.0b; Université de Sherbrooke: Québec, Montreal, Canada, 2009; http://www.cylview.org.

(10) Related natural products, such as **2.1**, also bear a similar motif where an alkyl chloride resides adjacent to a quaternary center, albeit not on a [4.3.1]-bicyclic scaffold. For elegant approaches to this motif, see ref 2.

(11) Huters, A. D.; Styduhar, E. D.; Weires, N. A.; Garg, N. K. University of California, Los Angeles, CA, **2012**, unpublished work.

(12) In related studies, efforts to reduce the vinyl chloride in compounds lacking the terminal olefin either led to recovery of starting material or over-reduction to cyclohexyl compounds lacking the chloride.

(13) Subjection of **2.6** to Rawal's chlorination conditions resulted in vinyl migration and cyclopropanation products **2.31** and **2.32**; see ref 4u.

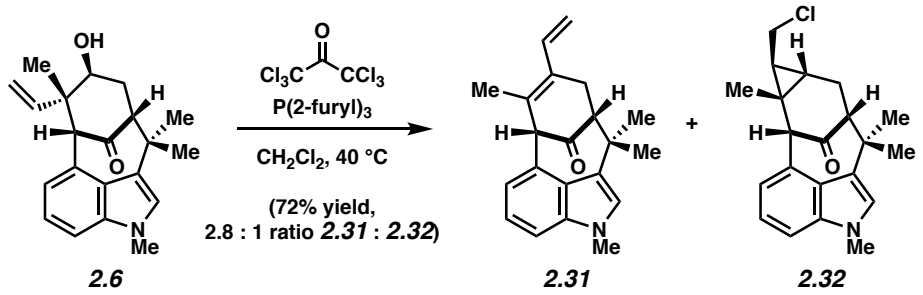

2.6 *2.31* *2.32*

(14) As seen in transition structure **2.33** below, approach of the chloride is obstructed, whereas the vinyl group is poised to react at C13.

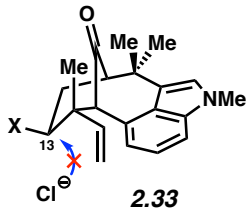

2.33

(15) For a review on C–N bond forming reactions involving C(sp^3)–H bonds, see: Jeffrey, J. L.; Sarpong, R. *Chem. Sci.* **2013**, *4*, 4092.

(16) Although this strategy would not preclude the possibility of vinyl group migration, it was anticipated that the ease of chlorination would be considerably greater. As such, it was hoped that the necessary chlorinative displacement could compete with the undesired vinyl group migration.

(17) For reviews of indolynes and other heterocyclic arynes, see: (a) Bronner, S. M.; Goetz, A. E.; Garg, N. K. *Synlett* **2011**, 2599. (b) Goetz, A. E.; Garg, N. K. *J. Org. Chem.* **2014**, *79*, 846.

(18) Attempts to achieve the chlorinative ring opening of indolo-oxabicycle **2.14** resulted in undesired byproducts and decomposition.

(19) Treatment of **2.15** with $ZnCl_2$ and acetyl chloride resulted in the acetylated derivative of **2.17** in ca. 40% yield; see: Clive, D. L. J.; Sannigrahi, M.; Hisaindee, S. *J. Org. Chem.* **2001**, *66*, 954.

(20) MaloneyHuss, K. E.; Portoghese, P. S. *J. Org. Chem.* **1990**, *55*, 2957.

(21) Delaney, P. A.; Johnstone, R. A. W.; Entwistle, I. D. *J. Chem. Soc., Perkin Trans. 1* **1986**, 1855.

(22) Koreeda, M.; Gopalaswamy, R. *J. Am. Chem. Soc.* **1995**, *117*, 10595.

(23) Wensheng, Y.; Mei, Y.; Kang, Y.; Hua, Z.; Jin, Z. *Org. Lett.* **2004**, *6*, 3217.

(24) Compound **2.34** (single diastereomer, unassigned) commonly forms as a minor byproduct of this transformation, presumably by way of an intramolecular aldol reaction.

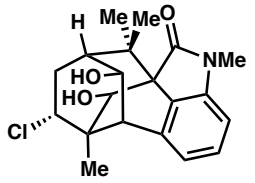

2.34

(25) All attempts to directly olefinate aldehyde **2.19** were unsuccessful. Attempts to olefinate **2.26** using Wittig olefination protocols led to aldol reaction (i.e., the TES ether analog of compound **2.34**; see ref 24).

(26) (a) Li, Z.; Capretto, D. A.; Rahaman, R.; He, C. *Angew. Chem. Int. Ed.* **2007**, *46*, 5184. (b) Cui, Y.; He, C. *Angew. Chem. Int. Ed.* **2004**, *43*, 4210.

(27) Espino, C. G.; Du Bois, J. *Angew. Chem. Int. Ed.* **2001**, *40*, 598.

(28) Use of the sulfamate derivative of **2.8** under Rh-catalysis also facilitated C9 insertion.

(29) We also carried out the corresponding sequence with $LiAlH_4$, which gave the proteo derivative of carbamate **2.23**. When employed in the nitrene insertion reaction, we obtained a

1:1.4 ratio of desired insertion product to ketone **2.22**. Consistent with our previous findings on alternate substrates, the strategic use of deuterium minimizes an undesirable competitive reaction, thus giving synthetically useful yields of the desired nitrene insertion product; see ref 7b, c.

(30) Morin, J.; Zhao, Y.; Snieckus, V. *Org. Lett.* **2013**, *15*, 4102.

(31) Nishikawa, K.; Umezawa, T.; Garson, M. J.; Matsuda, F. *J. Nat. Prod.* **2012**, *75*, 2232.

(32) Payack, J. F.; Hughed, D. L.; Cai, D.; Cottrell, I. F.; Verhoeven, T. R. *Org. Synth.* **2002**, *79*, 19.

(33) Niu, C.; Pettersson, T.; Miller, M. J. *J. Org. Chem.* **1996**, *61*, 1014.

(34) For compound **2.2** the ^{13}C NMR residual solvent peak is set to 77.0 ppm to match the reference values set in the isolation paper.

(35) In our studies, products containing a formamide often assume a mixture of rotamers by ^{1}H NMR.

(36) **2.29** was obtained as a 2.8:1.3:1 mixture of rotamers. These data represent empirically obtained chemical shifts and coupling constants from the ^{1}H NMR spectrum.

(37) Formamide **2.25** was obtained as a 4:1 mixture of rotamers. These data represent empirically obtained chemical shifts and coupling constants from the ^{1}H NMR spectrum.

(38) Reported values for specific rotations can be highly variable, for a pertinent discussion, see: Gawley, R. E. *J. Org. Chem.* **2006**, *71*, 2411.

CHAPTER THREE

Nickel-Catalyzed Suzuki–Miyaura Coupling of Amides

Nicholas A. Weires, Emma L. Baker, and Neil K. Garg.

Nat. Chem. **2016**, *8*, 75–79.

3.1 Abstract

The Suzuki–Miyaura coupling has become one of the most important and prevalent methods for the construction of carbon–carbon bonds. Although palladium catalysis has historically dominated the field, the use of nickel catalysis has become increasingly widespread due to its unique ability to cleave carbon–heteroatom bonds that are unreactive toward other transition metals. We report the first nickel-catalyzed Suzuki–Miyaura coupling of amides, which proceeds by an uncommon cleavage of the amide C–N bond following *N*-Boc activation. The methodology is mild, functional group tolerant, and can be strategically employed in sequential transition metal-catalyzed cross-coupling sequences to unite heterocyclic fragments. These studies demonstrate that amides, despite classically being considered inert substrates, can in fact be harnessed as synthons for use in C–C bond forming reactions through cleavage of the C–N bond using non-precious metal catalysis.

3.2 Introduction

Transition metal-catalyzed cross-coupling reactions have become an indispensable tool for the construction of carbon–carbon bonds.[1] Although palladium catalysis has dominated the field and was the topic of the 2010 Nobel Prize in Chemistry, there has been much interest in the development of complementary nickel-catalyzed processes.[2,3,4] Much of the excitement

surrounding nickel-catalyzed cross-couplings stems from nickel being more abundant and therefore less expensive compared to palladium.[2,3] However, the most striking feature of nickel catalysis is the opportunity to uncover new reactivity. To this end, nickel-catalyzed C–O bond cleavage processes have led to the cross-coupling of unconventional phenol-based electrophiles,[4] such as aryl pivalates and ethers, while C–N bond breaking reactions have allowed for the cross-coupling of aniline derivatives.[5,6,7]

We recently discovered that Ni/SIPr could facilitate the conversion of amides to esters (**3.1→3.2**, Figure 3.1).[8,9,10] Hypothesizing that this transformation occurred by the metal-catalyzed activation of the amide C–N bond, which is typically considered stable and unreactive,[11] we postulated that the putative oxidative addition intermediate **3.4** could be intercepted by carbon-based nucleophiles to ultimately forge carbon–carbon bonds (**3.1→3.3**). Direct acyl couplings of this type have been achieved using acid chlorides, thioesters,[12] carboxylic anhydrides,[13] arylated mixed imides,[14] and geometrically distorted cyclic imides.[15] A nickel-catalyzed process to build acyl carbon–carbon (C–C) bonds from amides would provide a powerful new synthetic tool for ketone synthesis, which would also complement Weinreb's widespread methodology,[16,17] but without the need for strongly basic and pyrophoric organometallic reagents. In this manuscript, we report the first method for building C–C bonds by the catalytic activation of *N*-Boc-activated secondary amides using non-precious transition metal catalysis.

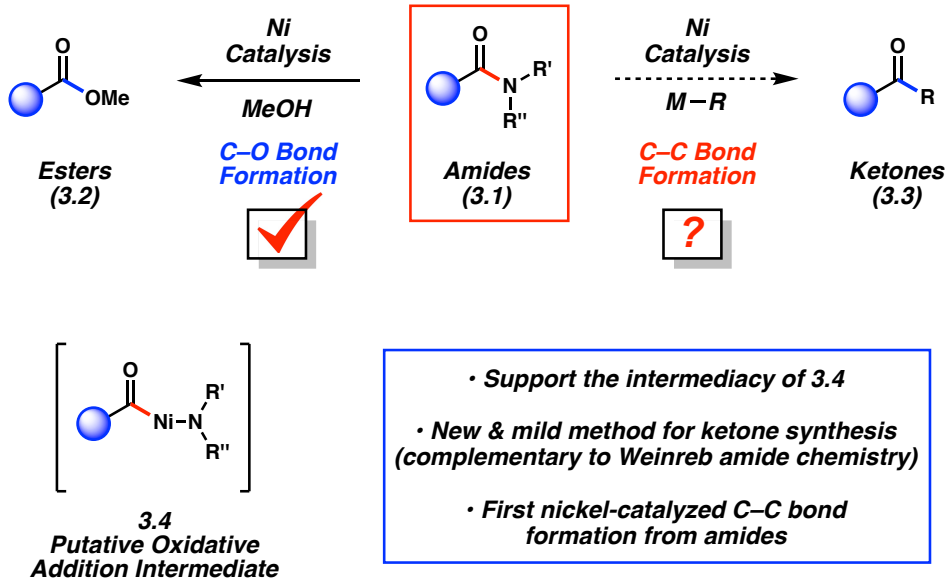

Figure 3.1. Following the discovery of the nickel-catalysed conversion of amides (**3.1**) to esters (**3.2**), the present study seeks to intercept putative oxidative addition intermediate **3.4** with carbon-based nucleophiles to uncover a new methodology for the synthesis of ketones (**3.3**) from amides (**3.1**).

3.3 Discovery and Optimization of Nickel-Catalyzed Suzuki–Miyaura Coupling of Amides

In considering possible amide cross-coupling partners for C–C bond formation, we elected to pursue the use of boron-based coupling partners. Countless boron coupling partners, including heterocycles that serve as building blocks to medicines and natural products, are commercially available and are used pervasively in Suzuki–Miyaura cross-couplings.[18,19] Thus, we examined the coupling of amides **3.5** with phenylboronic acid (**3.6a**) or boronic ester **3.6b**, with several of our key results involving Ni/SIPr, K_3PO_4, and toluene shown in Table 3.1. The use of anilide **3.5a**, which was an excellent coupling partner in our amide to ester conversion,[8] only led to low yields of ketone product **3.7** (entry 1). We also evaluated the use of *N*-Bn-*N*-Boc-derivative **3.5b**. Although the coupling of **3.5b** with boronic acid **3.6a** gave higher yields of the desired ketone, yields were inconsistent (entry 2) and led us to consider the corresponding boronic ester. In turn, the use of pinacolatoboronate **3.6b** gave only trace amounts of the desired

product **3.7** (entry 3). As we, and others, have seen similar inconsistencies in nickel-catalyzed Suzuki–Miyaura couplings that were attributed to variations in water content,[20,21,22,23] we tested the use of boronic ester **3.6b** with added water. We were delighted to find that the coupling proceeded smoothly to give a quantitative yield of ketone **3.7** when 2.0 equiv of water was used (entry 4). Further optimization allowed us to lower the catalyst and ligand loadings to 5 mol% without any loss in yield (entry 5). Of note, no evidence of decarbonylation was observed. This is significant as Yamamoto and, more recently, Itami have reported decarbonylation in acyl C–O bond cleavage processes.[24,25,26] It should be noted that the coupling required $Ni(cod)_2$, SIPr, and K_3PO_4 in order to proceed, as demonstrated by control experiments. Specifically, in the absence of any of these components, conversion to the desired ketone product was not observed.

Table 3.1 Reaction discovery and optimization.[a]

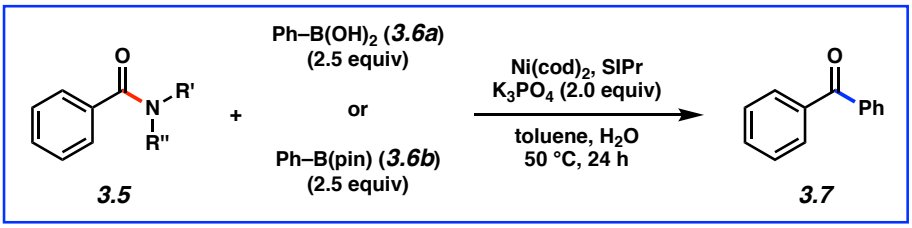

Entry	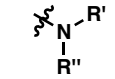	Boron Source	$Ni(cod)_2$ (mol%)	SIPr (mol%)	H_2O (equiv)	Yield[b]
1	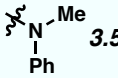 *3.5a*	*3.6a*	10	10	—	*12%*
2	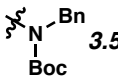 *3.5b*	*3.6a*	10	10	—	*42–89%*
3	 *3.5b*	*3.6b*	10	10	—	*7%*
4	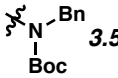 *3.5b*	*3.6b*	10	10	2.0	*>99%*
5	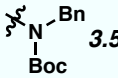 *3.5b*	*3.6b*	5	5	2.0	*>99%*

[a] Conditions: $Ni(cod)_2$ (5 or 10 mol%), SIPr (5 or 10 mol%), substrate **3.5a** or **3.5b** (1.0 equiv), boron source **3.6a** or **3.6b** (2.5 equiv), K_3PO_4 (2.0 equiv), toluene (1.0 M), and H_2O (if applicable, 2.0 equiv) at 50 °C for 24 h. [b] Yields of **3.7** determined by ^1H NMR analysis using 1,3,5-trimethoxybenzene as an internal standard.

3.4 Scope of Methodology

Having identified suitable reaction conditions, we assessed the scope of the nickel-catalyzed Suzuki–Miyaura coupling of amides. Table 3.2 showcases isolated yields for a variety of substrates and boronic esters. Beyond the parent coupling to give **3.7** in 96% isolated yield (entry 1), *para*-, *meta*-, and *ortho*-substitution was tolerated, as shown by the formation of ketones **3.8**–**3.10**, respectively (entries 2–4). Additionally, electron-rich substrates possessing

methoxy or amino substituents underwent the desired coupling to give products **3.11–3.13** (entries 5–7). Substrates with electron-withdrawing substituents, such as –F, $–CF_3$, $–CO_2Me$, and –C(O)Me, were also suitable and gave adducts **3.14–3.17** in synthetically useful yields (entries 8–11). It is notable that ketones and esters are compatible with this methodology (as are tertiary alcohols, nitriles, secondary amides, carboxylic acids, epoxides, and the free NH's of indoles; see Table 3.6 for robustness screen results), as these functional groups often pose challenges for Weinreb amide chemistry.[17] Finally, an extended aromatic system was evaluated, which gave naphthylphenyl ketone **3.18** in 70% yield (entry 12).

The scope with regard to the boronic ester coupling partner, in addition to the tolerance of the methodology toward heterocycles, was also examined (entries 13–25). The use of methyl substituted boronic esters smoothly provided tolyl ketones **3.8–3.10** (entries 13–15), whereas the use of the *para*-methoxy substituted boronic ester gave **3.19** in 95% yield (entry 16). The fluoro and trifluoromethyl substituents were also tolerated to give **3.14** and **3.20**, respectively (entries 17–18). Moreover, a naphthylboronic ester could be employed to provide **3.18** (entry 19). As shown by the formation of **3.21–3.26**, furan, thiophene, indole, pyrrole, and pyrazole heterocycles were all tolerated (entries 20–25), thus demonstrating the potential utility of this methodology for the synthesis of medicinally-relevant scaffolds.[27] In fact, diaryl or hetaryl ketone frameworks are seen in several currently marketed drugs or compounds under clinical evaluation.[28]

Table 3.2 Scope of nickel-catalyzed Suzuki–Miyaura coupling of amides.[a]

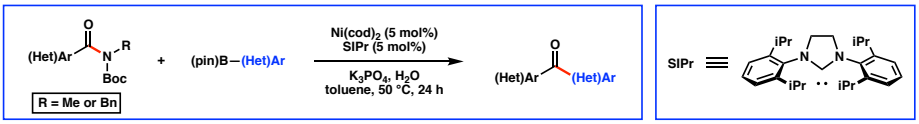

Entry	Ketone Product	Yield[a]	Entry	Ketone Product	Yield[a]	Entry	Ketone Product	Yield[a]	Entry	Ketone Product	Yield[a]
1	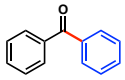 **3.7**	96%	7	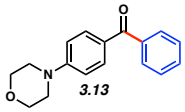 **3.13**	81%	13	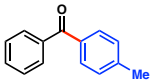 **3.8**	73%	19	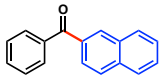 **3.18**	94%
2	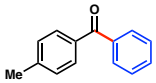 **3.8**	92%	8	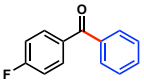 **3.14**	90%	14	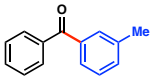 **3.9**	80%[b]	20 21	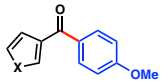 **3.21 (X = O)** **3.22 (X = S)**	64%[b] 66%[b]
3	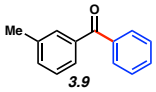 **3.9**	91%	9	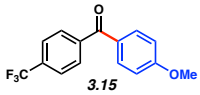 **3.15**	85%	15	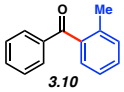 **3.10**	66%[b]	22	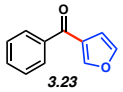 **3.23**	86%[b]
4	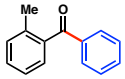 **3.10**	51%[b,c]	10	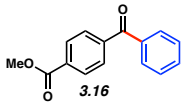 **3.16**	77%[c]	16	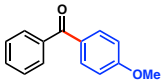 **3.19**	95%	23	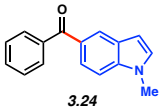 **3.24**	80%
5	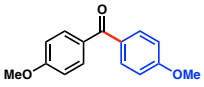 **3.11**	78%	11	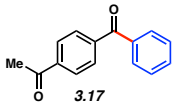 **3.17**	72%[b]	17	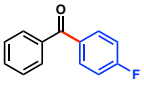 **3.14**	88%	24	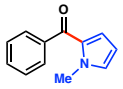 **3.25**	96%
6	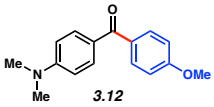 **3.12**	59%	12	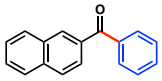 **3.18**	70%	18	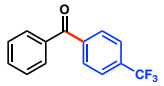 **3.20**	81%	25	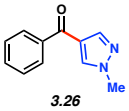 **3.26**	82%[b]

[a] Conditions unless otherwise stated: $Ni(cod)_2$ (5 mol%), SIPr (5 mol%), substrate (1.0 equiv; R = Me or Bn), boron source (1.2–2.5 equiv), K_3PO_4 (2.0 equiv), toluene (1.0 M), and H_2O (2.0 equiv) at 50 °C for 24 h; Yields shown reflect the average of two isolation experiments. [b] $Ni(cod)_2$ (10 mol%) and SIPr (10 mol%) were used. [c] Yields determined by ^1H NMR analysis using 1,3,5-trimethoxybenzene as an internal standard.

3.5 Synthetic Applications Involving Amide Suzuki–Miyaura Coupling Methodology

Several synthetic applications were undertaken to further assess the utility of the amide Suzuki–Miyaura couplings. In the first, we performed the gram-scale coupling of amide **3.27** with indolylboronic ester **3.28** (Figure 3.2a). This smoothly delivered ketone **3.29**, a nanomolar tubulin binding agent,[29] in 83% yield. Next, the potential to carry out sequential palladium- and nickel-catalyzed Suzuki–Miyaura couplings of heterocycles was tested (Figure 3.2b).

Furanylboronic acid **3.30** was first cross-coupled with aryl chloride **3.31** using palladium catalysis.[30] This facilitated *aryl–aryl* coupling to furnish **3.32** in 71% yield, without disturbing the amide. Next, amide **3.32** underwent nickel-catalyzed *aryl–acyl* coupling with pyrazolylboronic ester **3.33** to furnish **3.34**. The ability to unite heterocyclic fragments using such sequences should prove useful in the synthesis of drug candidates, new materials, and natural products.

The recently discovered nickel-catalyzed esterification of amides, paired with the Suzuki–Miyaura coupling of amides, provides opportunities to sequentially construct acyl C–C and acyl C–O bonds, as demonstrated in Figure 3.2c. In one scenario, bis(amide) **3.35** was coupled with furanylboronic ester **3.36** to furnish furanyl ketone **3.37**, without disturbing the secondary amide. Subsequent Boc-activation and Ni-catalyzed esterification[8] of **3.37** furnished menthol ester **3.39**. The coupling sequence can also be reversed. Esterification of bis(amide) **3.35** with (–)-menthol (**3.38**)[8] provided amidoester **3.40**. Boc activation and Suzuki–Miyaura coupling of **3.40** with furanyl boronic ester **3.36** delivered ketoester **3.39**. Of note, the ester of **3.40** withstood the base-mediated reaction conditions and was also not disrupted by the nickel catalyst.

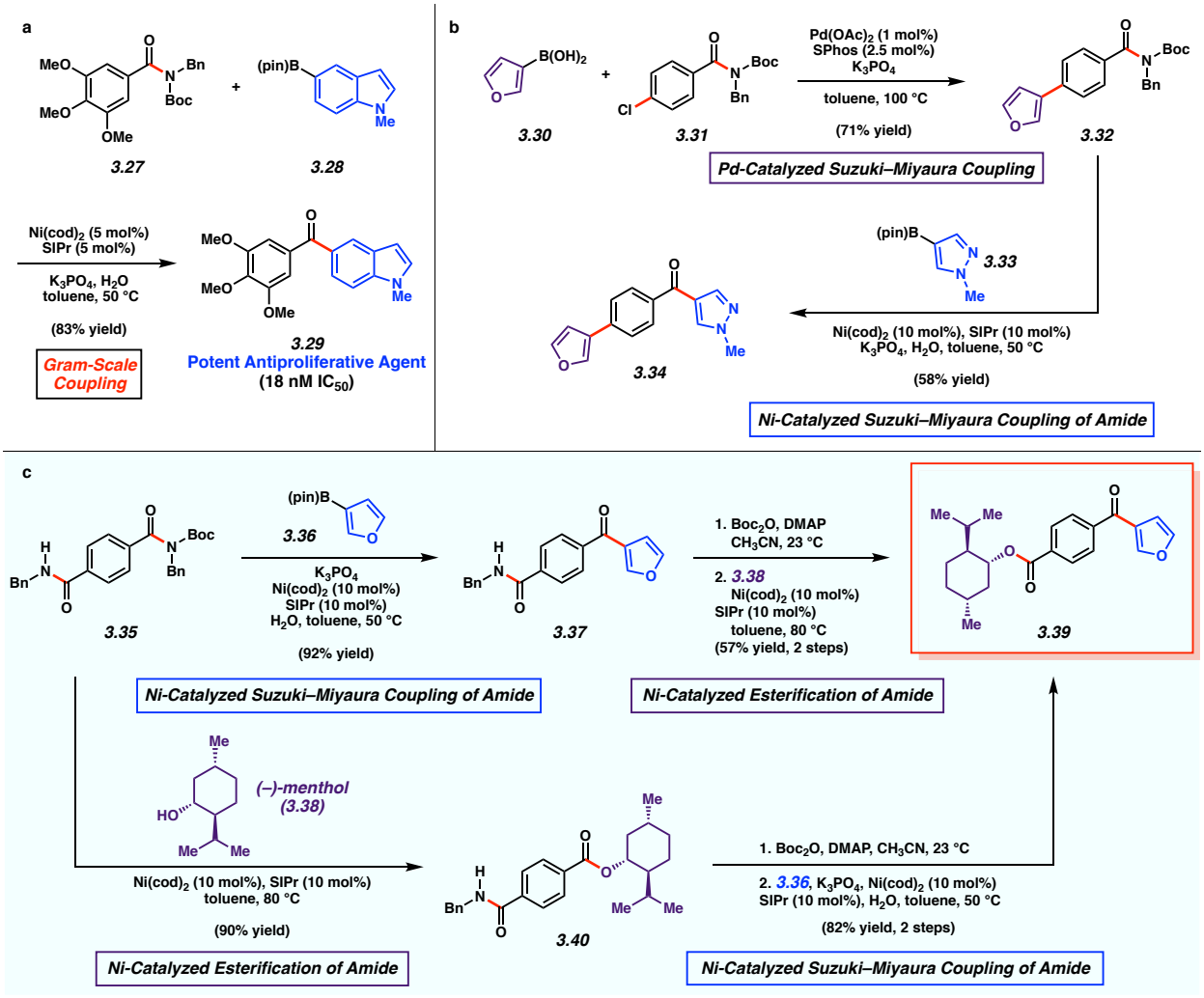

Figure 3.2. Several applications of the Suzuki–Miyaura coupling of amides were carried out in order to assess the synthetic utility of the methodology. **a**, The gram-scale coupling of trimethoxy amide **3.27** and heterocyclic fragment **3.28** was conducted to furnish tubulin binding agent **3.29**, a potent antiproliferative diaryl ketone. **b**, A sequence of Suzuki–Miyaura couplings was performed to access **3.34**, using palladium and nickel catalysis, thus highlighting the capacity of this method to unite heterocyclic frameworks. **c**, Sequential Ni-catalysed esterification and Suzuki–Miyaura couplings of amides were carried out, to illustrate the ability of amides to be used in multi-step synthesis through controlled activation / coupling sequences.

3.6 Conclusion

In summary, we have developed the first nickel-catalyzed method for the construction of C–C bonds from amides. Our approach relies on the use of nickel catalysis to activate the strong C–N bond of amides. In situ coupling of the putative oxidative addition intermediate **3.4** with

(het)arylboronic esters furnishes the products of Suzuki–Miyaura cross-coupling. The methodology is mild and tolerant of a variety of functional groups, including ketones and amines, in addition to several heterocycles and functional groups bearing acidic protons. With the future design and testing of new catalysts, we expect the scope of nickel-catalyzed amide couplings will be further broadened. Nonetheless, we have shown that the present methodology can be used to prepare bioactive molecules (Figure 3.2a), or can be strategically employed in sequential cross-couplings involving palladium or nickel catalysis to unite heterocyclic fragments in controlled ways (Figures 3.2b and 3.2c). Taken together, these studies demonstrate that amides, despite classically being considered inert substrates, can in fact be harnessed as synthons for use in C–C bond forming reactions using non-precious metal catalysis.

3.7 Experimental Section

3.7.1 Materials and Methods

Unless stated otherwise, reactions were conducted in flame-dried glassware under an atmosphere of nitrogen and commercially obtained reagents were used as received. Non-commercially available substrates were synthesized following protocols specified in Section 3.7.2.1 in the Experimental Procedures. Prior to use, toluene was purified by distillation and taken through five freeze-pump-thaw cycles, and (–)-menthol (**3.38**) was recrystallized. Acid chlorides **3.41**, **3.45**, **3.47**, **4.49**, **3.53**, **3.55**, **3.61**, **3.63**, **3.78**, **3.79**, terephthaloyl chloride (**3.80**), carboxylic acids **3.43**, **3.51**, **3.57**, **3.59**, boronate esters **3.6b**, **3.71**, **3.74**, **3.75**, **3.36**, **3.28**, **3.77**, **3.33**, furan-3-boronic acid (**3.30**), and benzylamine were obtained from Sigma–Aldrich. Boronate esters **3.76**, **3.72**, **3.73**, and **3.70** were obtained from Combi-Blocks. Phenylboronic acid (**3.6a**) was obtained from Oakwood Products, Inc. $Ni(cod)_2$ and SIPr were obtained from Strem Chemicals. Amide **3.66** was obtained from Alfa Aesar. K_3PO_4 was obtained from Acros. Reaction temperatures were controlled using an IKAmag temperature modulator, and unless stated otherwise, reactions were performed at room temperature (approximately 23 °C). Thin-layer chromatography (TLC) was conducted with EMD gel 60 F254 pre-coated plates (0.25 mm for analytical chromatography and 0.50 mm for preparative chromatography) and visualized using a combination of UV, anisaldehyde, and potassium permanganate staining techniques. Silicycle Siliaflash P60 (particle size 0.040–0.063 mm) was used for flash column chromatography. ^{1}H NMR spectra were recorded on Bruker spectrometers (at 300, 400 and 500 MHz) and are reported relative to residual solvent signals. Data for ^{1}H NMR spectra are reported as follows: chemical shift (δ ppm), multiplicity, coupling constant (Hz), integration. Data for ^{13}C NMR are reported in terms of chemical shift (at 75 and 125 MHz). IR spectra were recorded on a

Perkin-Elmer 100 spectrometer and are reported in terms of frequency absorption (cm^{-1}). High-resolution mass spectra were obtained on Thermo Scientific™ Exactive Mass Spectrometer with DART ID-CUBE.

3.7.2 Experimental Procedures

3.7.2.1 Syntheses of Amide Substrates

Representative Procedure A for the synthesis of amide substrates from Table 3.2 (synthesis of amide 3.42 is used as an example).

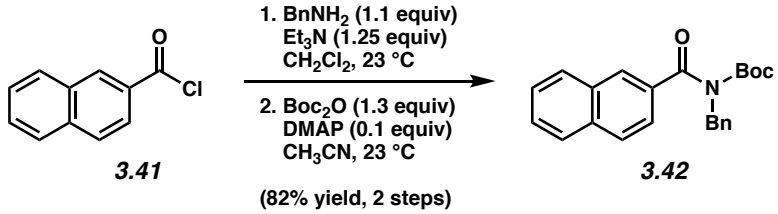

To a solution of acid chloride **3.41** (1.00 g, 5.25 mmol, 1.0 equiv), triethylamine (0.908 mL, 6.56 mmol, 1.25 equiv), and dichloromethane (6.0 mL), was added dropwise a solution of benzylamine (0.629 mL, 5.77 mmol, 1.1 equiv) in dichloromethane (4.5 mL, 0.5 M in total). The reaction mixture was stirred at 23 °C for 1 h, then diluted with EtOAc (50 mL) and washed successively with 1.0 M HCl (50 mL) and brine (50 mL). The organic layer was dried over Na_2SO_4 and concentrated under reduced pressure. The resulting crude solid material was used in the subsequent step without further purification.

To a flask containing the crude material from the previous step was added DMAP (64.1 mg, 0.525 mmol, 0.1 equiv) followed by acetonitrile (26.2 mL, 0.2 M). Boc_2O (1.42 g, 6.83 mmol, 1.3 equiv) was added in one portion and the reaction vessel was flushed with N_2, then the reaction mixture was allowed to stir at 23 °C for 16 h. The reaction was quenched by addition of

10 mL saturated aqueous $NaHCO_3$, transferred to a separatory funnel with EtOAc (30 mL) and H_2O (30 mL), and extracted with EtOAc (3 x 20 mL). The organic layers were combined, dried over Na_2SO_4, and evaporated under reduced pressure. The resulting crude residue was purified by flash chromatography (9:1 Hexanes:EtOAc) to yield amide **3.42** (1.56 g, 82% yield, over two steps) as a white solid. Amide **3.42**: mp: 93–95 °C; R_f 0.58 (2:1 Hexanes:Acetone); ^{1}H NMR (500 MHz, $CDCl_3$): δ 8.04 (s, 1H), 7.90–7.82 (m, 3H), 7.63–7.59 (m, 1H), 7.58–7.50 (m, 2H), 7.50–7.46 (m, 2H), 7.39–7.32 (m, 2H), 7.31–7.26 (m, 1H), 5.05 (s, 2H), 1.06 (s, 9H); ^{13}C NMR (125 MHz, $CDCl_3$, 18 of 19 observed): δ 173.3, 153.7, 138.0, 135.0, 134.6, 132.5, 128.9, 128.6, 128.3, 128.1, 127.9, 127.7, 127.6, 126.9, 124.5, 83.3, 49.2, 27.5; IR (film): 3069, 2978, 1726, 1673, 1324 cm^{-1}; HRMS-ESI (*m/z*) $[M + H]^+$ calcd for $C_{23}H_{24}NO_3$, 362.17562; found 362.17167.

Representative Procedure B for the synthesis of amide substrates from Table 3.2 (synthesis of amide 3.44 is used as an example).

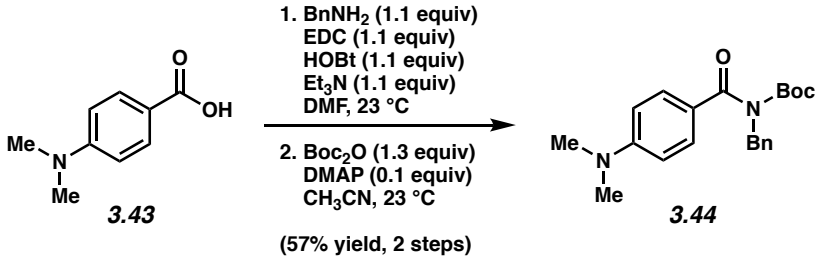

To a mixture of carboxylic acid **3.43** (955 mg, 5.78 mmol, 1.0 equiv), EDC (1.22 g, 6.36 mmol, 1.1 equiv), HOBt (858.0 mg, 6.36 mmol, 1.1 equiv), triethylamine (0.880 mL, 6.36 mmol, 1.1 equiv) and DMF (57.8 mL, 1.0 M) was added benzylamine (0.694 mL, 6.36 mmol, 1.1 equiv). The resulting mixture was stirred at 23 °C for 16 h, and then diluted with deionized water (50 mL) and transferred to a separatory funnel with EtOAc (50 mL) and brine (50 mL). The aqueous layer was extracted with EtOAc (3 x 30 mL), then the organic layers were combined

and washed with deionized water (3 x 50 mL), dried over Na_2SO_4, and evaporated under reduced pressure. The resulting crude solid material was used in the subsequent step without further purification.

To a flask containing the crude material from the previous step was added DMAP (70.5 mg, 0.578 mmol, 0.1 equiv) followed by acetonitrile (28.9 mL, 0.2 M). Boc_2O (1.64 g, 7.51 mmol, 1.3 equiv) was added in one portion and the reaction vessel was flushed with N_2, then the reaction mixture was allowed to stir at 23 °C for 16 h. The reaction was quenched by addition of 10 mL saturated aqueous $NaHCO_3$, transferred to a separatory funnel with EtOAc (30 mL) and H_2O (30 mL), and extracted with EtOAc (3 x 20 mL). The organic layers were combined, dried over Na_2SO_4, and evaporated under reduced pressure. The resulting crude residue was purified by flash chromatography (19:1 Hexanes:EtOAc) to yield amide **3.44** (1.16 g, 57% yield, over two steps) as an off-white solid. Amide **3.44**: mp: 97–99 ºC; R_f 0.39 (5:1 Hexanes:EtOAc); ^{1}H NMR (500 MHz, $CDCl_3$): δ 7.54–7.49 (m, 2H), 7.43–7.38 (m, 2H), 7.33–7.28 (m, 2H), 7.25–7.21 (m, 1H), 6.70–6.60 (m, 2H), 4.93 (s, 2H), 3.02 (s, 6H), 1.21 (s, 9H); ^{13}C NMR (125 MHz, $CDCl_3$): δ 173.1, 154.3, 152.9, 138.7, 130.7, 128.5, 128.2, 127.2, 123.7, 110.6, 82.3, 49.4, 40.3, 27.8; IR (film): 2977, 2933, 2812, 1721, 1663, 1600 cm^{-1}; HRMS-ESI (*m/z*) $[M + H]^+$ calcd for $C_{21}H_{27}N_2O_3$, 355.20217; found 355.20058.

Note: Supporting information for the syntheses of amides shown in Tables 3.1, 3.3, and 3.5 have previously been reported: **3.5a**,[31a] **3.65**,[31b] **3.66, 3.67**,[31c] **3.68**,[31d] and **3.5b**.[31e] In addition, supporting information for the synthesis of amide **3.69**[31e] (Table 3.2) has also previously been reported. Syntheses for the remaining substrates shown in Table 3.2 are as follows:

Any modifications of the conditions shown in the representative procedures above are specified in the following schemes.

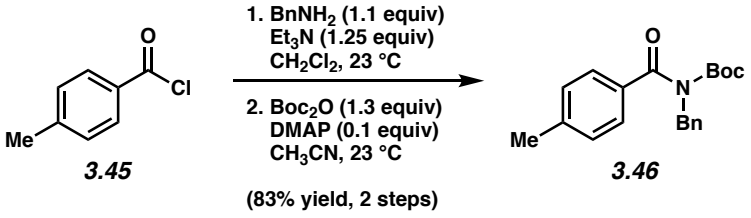

Amide 3.46. Followed representative procedure A. Purification by flash chromatography (19:1 Hexanes:EtOAc) generated amide **3.46** (83% yield, over two steps) as a white solid. Amide **3.46**: mp: 58–60 ºC; R_f 0.58 (5:1 Hexanes:EtOAc); ^{1}H NMR (500 MHz, $CDCl_3$): δ 7.45–7.40 (m, 4H), 7.35–7.30 (m, 2H), 7.28–7.22 (m, 1H), 7.21–7.15 (m, 2H), 4.97 (s, 2H), 2.38 (s, 3H), 1.15 (s, 9H); ^{13}C NMR (125 MHz, $CDCl_3$): δ 173.3, 153.8, 141.8, 138.1, 134.8, 128.8, 128.6, 128.2, 127.9, 127.5, 83.1, 49.1, 27.6, 21.7; IR (film): 3035, 2978, 1725, 1673, 1323 cm^{-1}; HRMS-ESI (*m/z*) $[M + H]^+$ calcd for $C_{20}H_{24}NO_3$, 326.17562; found 326.17342.

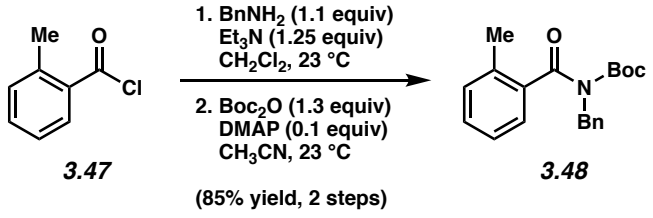

Amide 3.48. Followed representative procedure A. Purification by flash chromatography (9:1 Hexanes:EtOAc) generated amide **3.48** (85% yield, over two steps) as a white solid. Amide **3.48**: mp: 69–71 ºC; R_f 0.50 (5:1 Hexanes:EtOAc); ^{1}H NMR (500 MHz, $CDCl_3$): δ 7.48–7.42 (m, 2H), 7.37–7.32 (m, 2H), 7.31–7.25 (m, 2H), 7.20–7.09 (m, 3H), 5.03 (s, 2H), 2.32 (s, 3H), 1.08 (s, 9H); ^{13}C NMR (125 MHz, $CDCl_3$): δ 172.8, 153.1, 138.7, 137.9, 135.0, 130.6, 129.5, 128.6, 128.5, 127.5, 125.8, 125.5, 83.3, 48.1, 27.4, 19.4; IR (film): 3064, 2982, 1731, 1668, 1334 cm^{-1}; HRMS-ESI (*m/z*) $[M + H]^+$ calcd for $C_{20}H_{24}NO_3$, 326.17562; found 326.17222.

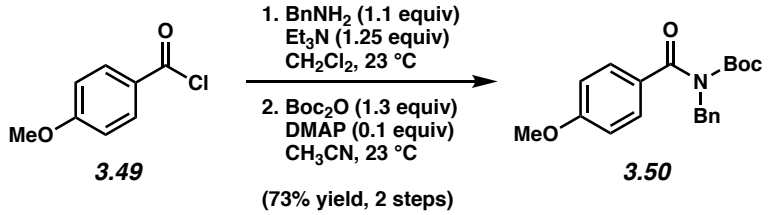

Amide 3.50. Followed representative procedure A. Purification by flash chromatography (19:1 Hexanes:EtOAc → 9:1 Hexanes:EtOAc) generated amide **3.50** (73% yield, over two steps) as an off-white solid. Amide **3.50**: mp: 63–65 ºC; R_f 0.39 (5:1 Hexanes:EtOAc); ^{1}H NMR (500 MHz, $CDCl_3$): δ 7.57–7.50 (m, 2H), 7.44–7.38 (m, 2H), 7.36–7.29 (m, 2H), 7.28–7.22 (m, 1H), 6.92–6.85 (m, 2H), 4.96 (s, 2H), 3.84 (s, 3H), 1.18 (s, 9H); ^{13}C NMR (125 MHz, $CDCl_3$): δ 172.8, 162.4, 153.9, 138.2, 130.1, 129.7, 128.5, 128.2, 127.4, 113.4, 83.0, 55.6, 49.3, 27.6; IR (film): 2982, 1731, 1668, 1605, 1508 cm^{-1}; HRMS-ESI (*m/z*) $[M + H]^+$ calcd for $C_{20}H_{24}NO_4$, 342.17053; found 342.16749.

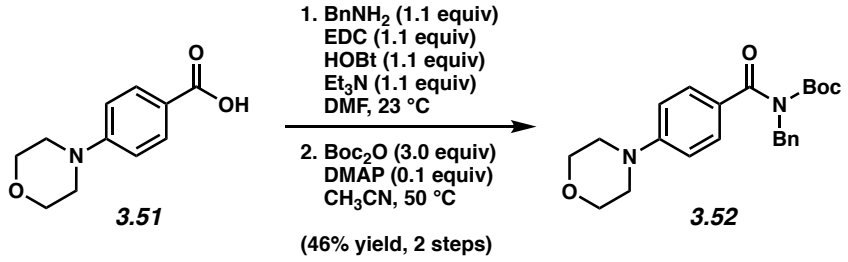

Amide 3.52. Followed representative procedure B. Purification by flash chromatography (10:1 Hexanes:EtOAc → 5:1 Hexanes:EtOAc) generated amide **3.52** (46% yield, over two steps) as an off-white solid. Amide **3.52**: mp: 114–116 ºC; R_f 0.70 (1:1 Hexanes:EtOAc); ^{1}H NMR (500 MHz, $CDCl_3$): δ 7.54–7.49 (m, 2H), 7.43–7.38 (m, 2H), 7.34–7.28 (m, 2H), 7.26–7.21 (m, 1H), 4.94 (s, 2H), 3.89–3.81 (m, 4H), 3.28–3.19 (m, 4H), 1.20 (s, 9H); ^{13}C NMR (125 MHz, $CDCl_3$): δ 172.8, 154.0, 153.7, 138.4, 130.2, 128.5, 128.2, 127.4, 127.4, 113.6, 82.7, 66.8, 49.3, 48.2,

27.7; IR (film): 2977, 2856, 1721, 1663, 1605 cm^{-1}; HRMS-ESI (*m/z*) $[M + H]^+$ calcd for $C_{23}H_{29}N_2O_4$, 397.21273; found 397.20902.

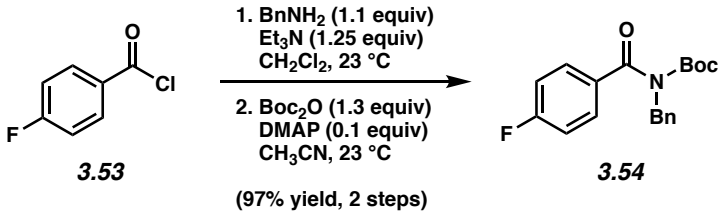

Amide 3.54. Followed representative procedure A. Purification by flash chromatography (19:1 Hexanes:EtOAc) generated amide **3.54** (97% yield, over two steps) as a white solid. Amide **3.54**: mp: 42–44 ºC; R_f 0.56 (5:1 Hexanes:EtOAc); ^{1}H NMR (500 MHz, $CDCl_3$): δ 7.58–7.50 (m, 2H), 7.44–7.38 (m, 2H), 7.36–7.30 (m, 2H), 7.29–7.25 (m, 1H), 7.11–7.03 (m, 2H), 4.97 (s, 2H), 1.17 (s, 9H); ^{13}C NMR (125 MHz, $CDCl_3$): δ 172.1, 165.6, 163.6, 153.5, 137.9, 133.8 (d, J_{C-F} = 3.4), 130.1 (d, J_{C-F} = 8.9), 128.4 (d, J_{C-F} = 48.2), 127.6, 115.3 (d, J_{C-F} = 21.9), 83.5, 49.2, 27.6; IR (film): 3069, 3032, 2981, 2934, 1730, 1674 cm^{-1}; HRMS-ESI (*m/z*) $[M + H]^+$ calcd for $C_{19}H_{20}FNO_3$, 330.15055; found 330.14909.

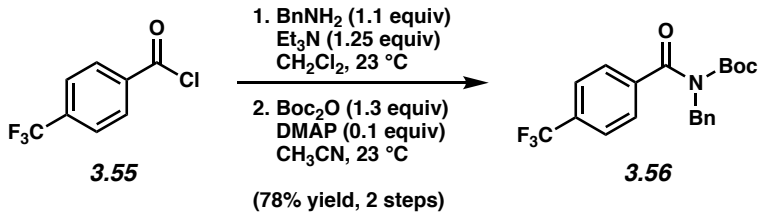

Amide 3.56. Followed representative procedure A. Purification by flash chromatography (24:1 Hexanes:EtOAc) generated amide **3.56** (78% yield, over two steps) as a white solid. Amide **3.56**: mp: 76–78 ºC; R_f 0.57 (5:1 Hexanes:EtOAc); ^{1}H NMR (500 MHz, $CDCl_3$): δ 7.68–7.56 (m, 4H), 7.45–7.39 (m, 2H), 7.37–7.32 (m, 2H), 7.31–7.26 (m, 1H), 5.00 (s, 2H), 1.15 (s, 9H); ^{13}C NMR

(125 MHz, $CDCl_3$): δ 171.9, 153.1, 141.2, 137.6, 132.7 (q, J_{C-F} = 32.8), 128.7, 128.3, 127.75, 127.67, 125.3 (q, J_{C-F} = 3.7), 123.8 (d, J_{C-F} = 272.7), 84.0, 48.9 27.6; IR (film): 3729, 3620, 2987, 2795, 1734, 1672 cm^{-1}; HRMS-ESI (*m/z*) $[M + H]^+$ calcd for $C_{20}H_{20}F_3NO_3$, 380.14735; found 380.14455.

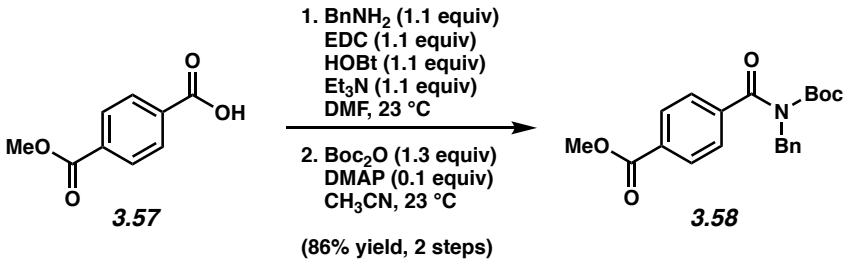

Amide 3.58. Followed representative procedure B. Purification by flash chromatography (20:1 Hexanes:EtOAc → 16:1 Hexanes:EtOAc) generated amide **3.58** (86% yield, over two steps) as a white solid. Amide **3.58**: mp: 94–96 ºC; R_f 0.38 (5:1 Hexanes:EtOAc); ^1H NMR (500 MHz, $CDCl_3$): δ 8.09–8.03 (m, 2H), 7.59–7.53 (m, 2H), 7.45–7.40 (m, 2H), 7.37–7.32 (m, 2H), 7.30–7.27 (m, 1H), 5.00 (s, 2H), 3.94 (s, 3H), 1.13 (s, 9H); ^{13}C NMR (125 MHz, $CDCl_3$): δ 172.3, 166.4, 153.2, 142.0, 137.7, 132.1, 129.5, 128.7, 128.3, 127.7, 127.3, 83.9, 52.5, 8.9, 27.5; IR (film): 2987, 2895, 1731, 1663, 1430 cm^{-1}; HRMS-ESI (m/z) $[M + H]^+$ calcd for $C_{21}H_{24}NO_5$, 370.16545; found 370.16296.

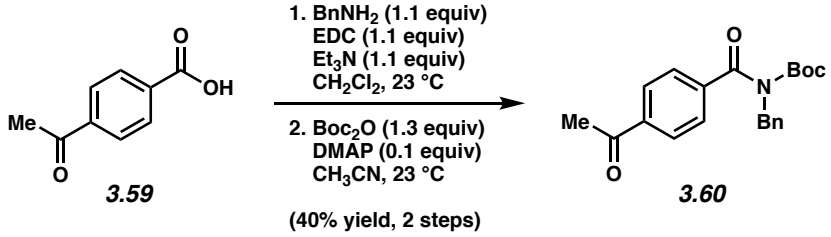

Amide 3.60. Followed representative procedure B. Purification by flash chromatography (24:1 Hexanes:EtOAc → 14:1 Hexanes:EtOAc → 9:1 Hexanes:EtOAc) generated amide **3.60** (40%

yield, over two steps) as a white solid. Amide **3.60**: mp: 91–93 ºC; R_f 0.26 (1:1 Hexanes:EtOAc); ^{1}H NMR (500 MHz, $CDCl_3$): δ 8.00–7.95 (m, 2H), 7.61–7.55 (m, 2H), 7.44–7.40 (m, 2H), 7.37–7.31 (m, 2H), 7.31–7.26 (m, 1H), 5.00 (s, 2H), 2.63 (s, 3H), 1.15 (s, 9H); ^{13}C NMR (125 MHz, $CDCl_3$): δ 197.5, 172.2, 153.2, 141.9, 138.6, 137.7, 128.7, 128.3, 128.2, 127.7, 127.6, 83.9, 48.9, 27.6, 26.9; IR (film): 3064, 2982, 1736, 1687, 1668 cm^{-1}; HRMS-ESI (*m/z*) $[M + H]^+$ calcd for $C_{21}H_{24}NO_4$, 354.17053; found 354.16722.

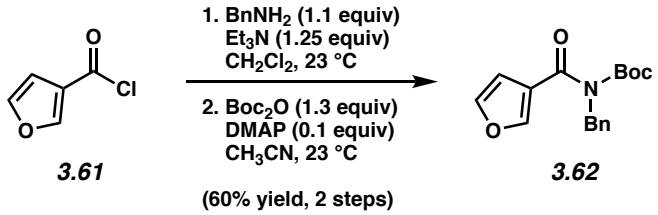

Amide 3.62. Followed representative procedure A. Purification by flash chromatography (24:1 Hexanes:EtOAc) generated amide **3.62** (60% yield, over two steps) as an off-white solid. Amide **3.62**: mp: 72–74 ºC; R_f 0.52 (2:1 Hexanes:Acetone); ^{1}H NMR (500 MHz, $CDCl_3$): δ 7.89 (s, 1H), 7.40–7.37 (m, 1H), 7.37–7.28 (m, 4H), 7.27–7.22 (m, 1H), 6.55 (s, 1H), 4.92 (s, 2H), 1.31 (s, 9H); ^{13}C NMR (125 MHz, $CDCl_3$): δ 166.5, 153.3, 146.4, 142.6, 137.9, 128.4, 127.8, 127.3, 123.9, 110.1, 83.3, 48.9, 27.6; IR (film): 3729, 3629, 1734, 1673, 1507 cm^{-1}; HRMS-ESI (*m/z*) $[M + H]^+$ calcd for $C_{17}H_{20}NO_4$, 302.13923; found 302.13643.

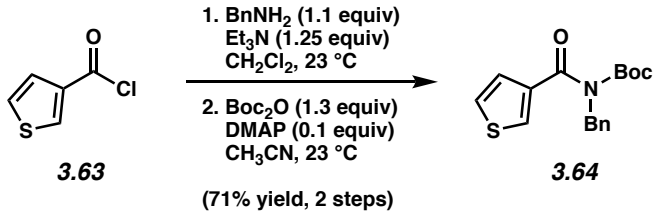

Amide 3.64. Followed representative procedure A. Purification by flash chromatography (9:1 Hexanes:EtOAc) generated amide **3.64** (71% yield, over two steps) as an off-white solid. Amide **3.64**: mp: 85–87 ºC; R_f 0.62 (2:1 Hexanes:Acetone); ^{1}H NMR (500 MHz, $CDCl_3$): δ 7.76–7.70 (m, 1H), 7.42–7.37 (m, 2H), 7.35–7.29 (m, 2H), 7.28–7.20 (m, 3H), 4.95 (s, 2H), 1.23 (s, 9H); ^{13}C NMR (125 MHz, $CDCl_3$): δ 167.8, 153.6, 139.1, 138.0, 129.4, 128.6, 128.1, 127.5, 127.3, 125.3, 83.3, 49.1, 27.6; IR (film): 3108, 2982, 1731, 1673, 1319 cm^{-1}; HRMS-ESI (*m/z*) [M + H]$^+$ calcd for $C_{17}H_{20}NO_3S$, 318.11639; found 318.11328.

3.7.2.2. Initial Survey of Benzamide Substrates with Phenylboronic Acid (3.6a)

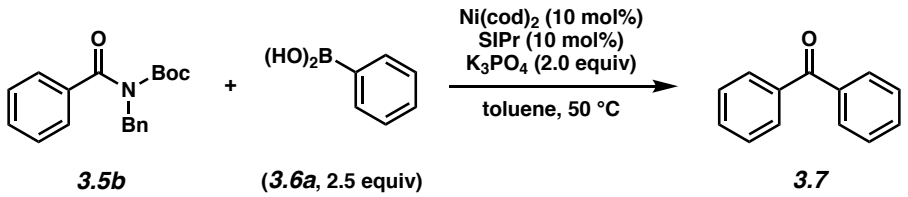

Representative Procedure for Suzuki reactions of benzamides from Table 3.3 (coupling of amide 3.5b and phenylboronic acid (3.6a) is used as an example). A 1-dram vial was charged with anhydrous powdered K_3PO_4 (84.8 mg, 0.400 mmol, 2.0 equiv) and a magnetic stir bar. The vial and contents were flame-dried under reduced pressure, then allowed to cool under N_2. Amide substrate **3.5b** (62.2 mg, 0.200 mmol, 1.0 equiv), phenylboronic acid (**3.6a**) (61.0 mg, 0.500 mmol, 2.5 equiv) and 1,3,5-trimethoxybenzene (10.1 mg, 0.060 mmol, 0.3 equiv) were added, and the vial was flushed with N_2. The vial was taken into a glove box and charged with $Ni(cod)_2$ (5.5 mg, 0.020 mmol, 10 mol%) and SIPr (7.8 mg, 0.020 mmol, 10 mol%).

Subsequently, toluene (0.20 mL, 1.0 M) was added. The vial was sealed with a Teflon-lined screw cap, removed from the glove box, and stirred vigorously (1,000 rpm) at 50 °C for 24 h. After cooling to 23 °C, the mixture was diluted with hexanes (0.5 mL) and filtered over a plug of silica gel (10 mL of EtOAc eluent). The volatiles were removed under reduced pressure, and the yield was determined by ^{1}H NMR analysis with 1,3,5-trimethoxybenzene as an internal standard.

Any modifications of the conditions shown in the representative procedure above are specified below in Table 3.3.

Table 3.3. Initial Survey of Benzamide Substrates with Phenylboronic Acid (**3.6a**)[a]

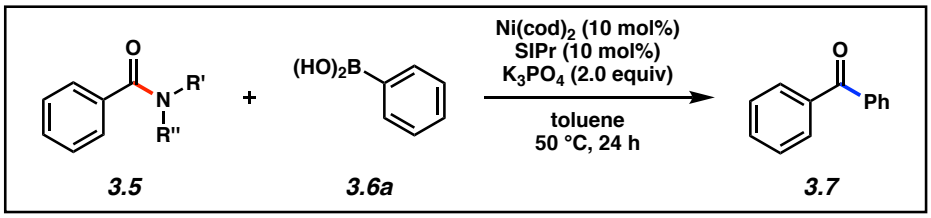

3.5 + *3.6a* → *3.7*

Entry			*Yield of ketone*	*Remainder of the mass*
1		*3.5a*	12%	*3.5a* (88%)
2		*3.65*	<5%	*3.65* (48%)
3		*3.66*	0%	*3.66* (21%)
4		*3.67*	68%	-
5		*3.5b*	42–89%[b]	*3.5b* (7–45%)[b]

[a] Yields were determined by ^{1}H NMR analysis using 1,3,5-trimethoxybenzene as an internal standard. [b] Yield range based on two experiments.

3.7.2.3. Optimization of the Suzuki Reaction and Relevant Control Experiments

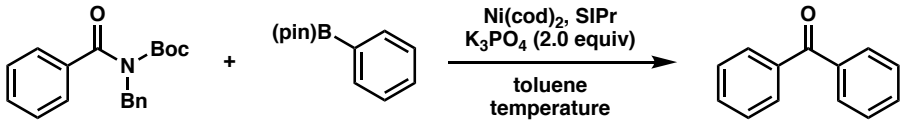

3.5b *3.6b* *3.7*

Representative Procedure for Suzuki reactions of benzamides from Tables 3.3 and 3.4 (coupling of amide 3.5b and phenylboronic acid pinacol ester (3.6b) is used as an example). A 1-dram vial was charged with anhydrous powdered K_3PO_4 (84.8 mg, 0.400 mmol, 2.0 equiv) and a magnetic stir bar. The vial and contents were flame-dried under reduced pressure, then allowed to cool under N_2. Amide substrate **3.5b** (62.2 mg, 0.200 mmol, 1.0 equiv), phenylboronic acid pinacol ester (**3.6b**) (102.0 mg, 0.500 mmol, 2.5 equiv) and 1,3,5-trimethoxybenzene (10.1 mg, 0.060 mmol, 0.3 equiv) were added, and the vial was flushed with N_2. The vial was taken into a glove box and charged with $Ni(cod)_2$ (2.8 mg, 0.010 mmol, 5 mol%) and SIPr (3.9 mg, 0.010 mmol, 5 mol%). Subsequently, toluene (0.20 mL, 1.0 M) was added. The vial was sealed with a Teflon-lined screw cap, removed from the glove box, and stirred vigorously (1,000 rpm) at 50 °C for 24 h. After cooling to 23 °C, the mixture was diluted with hexanes (0.5 mL) and filtered over a plug of silica gel (10 mL of EtOAc eluent). The volatiles were removed under reduced pressure, and the yield was determined by ^1H NMR analysis with 1,3,5-trimethoxybenzene as an internal standard.

Any modifications of the conditions shown in the representative procedure above are specified below in Tables 3.4 and 3.5.

Table 3.4. Optimization of the Suzuki Reaction and Relevant Control Experiments[a]

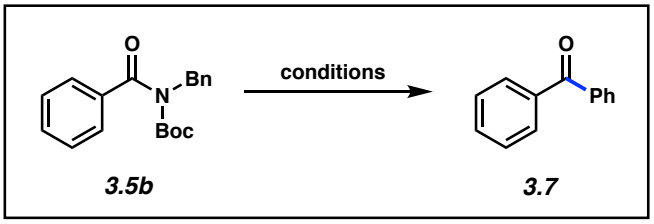

3.5b *3.7*

Reaction Conditions	*Experimental Results* *3.5b*	*3.7*
PhB(pin) (2.5 equiv), K_3PO_4 (2.0 equiv) $Ni(cod)_2$ (10 mol%), SIPr (10 mol%), toluene (1.0 M), 50 °C, 24 h	93%	7%
PhB(pin) (2.5 equiv), K_3PO_4 (2.0 equiv), H_2O (1.0 equiv) $Ni(cod)_2$ (10 mol%), SIPr (10 mol%), toluene (1.0 M), 50 °C, 24 h	0%	100%
PhB(pin) (2.5 equiv), K_3PO_4 (2.0 equiv), H_2O (2.0 equiv) $Ni(cod)_2$ (10 mol%), SIPr (10 mol%), toluene (1.0 M), 50 °C, 24 h	0%	100%
PhB(pin) (2.5 equiv), K_3PO_4 (2.0 equiv), H_2O (2.0 equiv) $Ni(cod)_2$ (5 mol%), SIPr (5 mol%), toluene (1.0 M), 50 °C, 24 h	0%	100%
PhB(pin) (1.2 equiv), K_3PO_4 (2.0 equiv), H_2O (2.0 equiv) $Ni(cod)_2$ (5 mol%), SIPr (5 mol%), toluene (1.0 M), 50 °C, 24 h	0%	100%
PhB(pin) (1.2 equiv), K_3PO_4 (2.0 equiv), H_2O (2.0 equiv) $Ni(cod)_2$ (5 mol%), SIPr (5 mol%), toluene (1.0 M), 23 °C, 24 h	47%	53%
PhB(pin) (1.2 equiv), K_3PO_4 (2.0 equiv), H_2O (2.0 equiv) $Ni(cod)_2$ (5 mol%), SIPr (5 mol%), toluene (1.0 M), 80 °C, 24 h	39%	51%
Control Experiments:		
PhB(pin) (1.2 equiv), K_3PO_4 (2.0 equiv), H_2O (2.0 equiv) toluene (1.0 M), 50 °C, 24 h	100%	0%
PhB(pin) (1.2 equiv), K_3PO_4 (2.0 equiv), H_2O (2.0 equiv) SIPr (5 mol%), toluene (1.0 M), 50 °C, 24 h	100%	0%
PhB(pin) (1.2 equiv), K_3PO_4 (2.0 equiv), H_2O (2.0 equiv) $Ni(cod)_2$ (5 mol%), toluene (1.0 M), 50 °C, 24 h	100%	0%
PhB(pin) (1.2 equiv), H_2O (2.0 equiv) $Ni(cod)_2$ (5 mol%), SIPr (5 mol%), toluene (1.0 M), 50 °C, 24 h	100%	0%

[a] Yields were determined by ^1H NMR analysis using 1,3,5-trimethoxybenzene as an internal standard.

Table 3.5. Survey of Other Benzamide Substrates Under the Optimized Conditions[a]

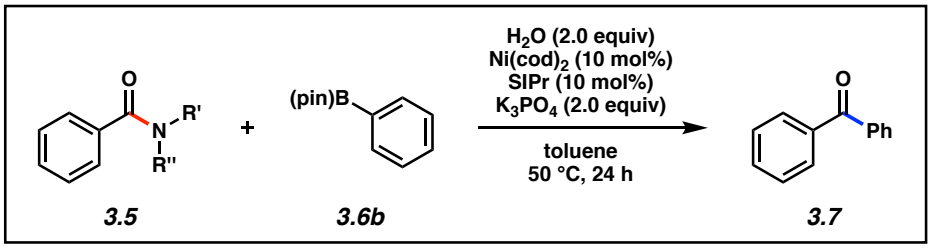

Entry		*Yield of ketone*	*Remainder of the mass*
1	 ***3.5a***	40%	***3.5a*** (58%)
2	 ***3.67***	24%	***3.67*** (75%)
3	 ***3.68***	95%	***3.68*** (4%)

[a] Yields were determined by ^{1}H NMR analysis using 1,3,5-trimethoxybenzene as an internal standard.

3.7.2.4. Evaluation of Functional Group Compatibility in the Suzuki Reaction

In order to provide further insight into functional group tolerance for the Suzuki reaction, a "robustness screen" was performed.[32] The reaction was doped with 1.0 equiv of various additives to determine whether or not certain functionalities would be compatible in the coupling.

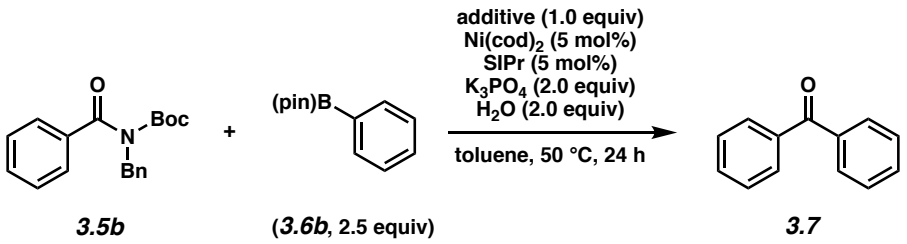

Representative Procedure for Suzuki reactions in the presence of additives from Table 3.6. A 1-dram vial was charged with anhydrous powdered K_3PO_4 (84.8 mg, 0.400 mmol, 2.0 equiv) and a magnetic stir bar. The vial and contents were flame-dried under reduced pressure, then allowed to cool under N_2. Amide substrate **3.5b** (62.2 mg, 0.200 mmol, 1.0 equiv), phenylboronic acid pinacol ester (**3.6b**) (102.0 mg, 0.500 mmol, 2.5 equiv), additive (0.200 mmol, 1.0 equiv) and 1,3,5-trimethoxybenzene (10.1 mg, 0.060 mmol, 0.3 equiv) were added, and the vial was flushed with N_2. The vial was taken into a glove box and charged with $Ni(cod)_2$ (2.8 mg, 0.010 mmol, 5 mol%) and SIPr (3.9 mg, 0.010 mmol, 5 mol%). Subsequently, toluene (0.20 mL, 1.0 M) was added. The vial was sealed with a Teflon-lined screw cap, removed from the glove box, and stirred vigorously (1,000 rpm) at 50 °C for 24 h. After cooling to 23 °C, the mixture was diluted with hexanes (0.5 mL) and filtered over a plug of silica gel (10 mL of EtOAc eluent). The volatiles were removed under reduced pressure, and the yield was determined by ^1H NMR analysis with 1,3,5-trimethoxybenzene as an internal standard.

Any modifications of the conditions shown in the representative procedure above are specified below in Table 3.6.

Table 3.6. Evaluation of Functional Group Compatibility in the Suzuki Reaction[a]

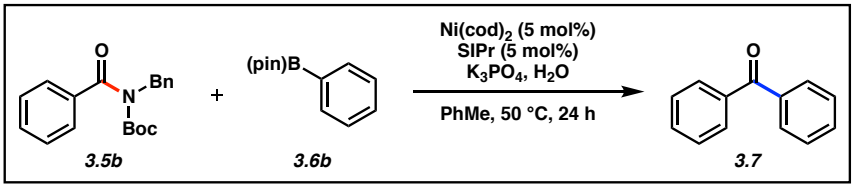

Entry	Additive	Yield of 3.7 (%)	Additive Remaining (%)	SM Remaining (%)	Entry	Additive	Yield of 3.7 (%)	Additive Remaining (%)	SM Remaining (%)
1	None	100	-	0	8	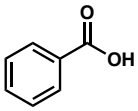	65	2	33
2	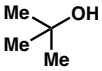	81	N.D.[b]	0	9	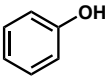	6	60	85
3	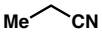	58	N.D.[b]	42	10		0	0	100
4	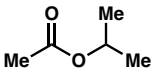	93	N.D.[b]	0	11	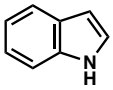	84	80	5
5	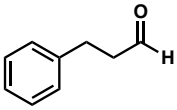	32	0	55	12	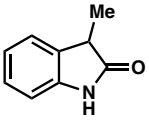	0	88	79
6	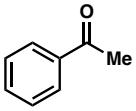	100	90	0	13	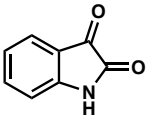	0	0	100
7	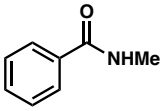	90	50	3	14		96	N.D.[b]	0

[a] Conditions: $Ni(cod)_2$ (5 mol%), SIPr (5 mol%), substrate (1.0 equiv), PhB(pin) (2.5 equiv), K_3PO_4 (2.0 equiv), toluene (1.0 M), H_2O (2.0 equiv), and additive (1.0 equiv) at 50 °C for 24 h. Yields of coupled product, remaining additive, and remaining starting material were determined by ^1H NMR analysis using 1,3,5-trimethoxybenzene as an internal standard. [b] Not determined due to low boiling point.

3.7.2.5. Scope of Methodology

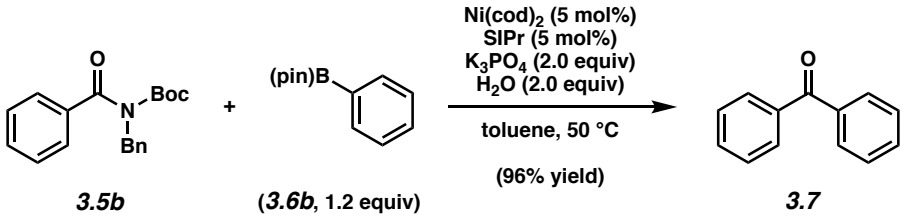

Representative Procedure (coupling of amide 3.5b and phenylboronic acid pinacol ester (3.6b) is used as an example). Ketone 3.7. A 1-dram vial was charged with anhydrous powdered K_3PO_4 (84.8 mg, 0.400 mmol, 2.0 equiv) and a magnetic stir bar. The vial and contents were flame-dried under reduced pressure, then allowed to cool under N_2. Amide substrate **3.5b** (62.2 mg, 0.200 mmol, 1.0 equiv) and phenylboronic acid pinacol ester (**3.6b**) (49.0 mg, 0.240 mmol, 1.2 equiv) were added. The vial was flushed with N_2, then water (7.2 μL, 0.400 mmol, 2.0 equiv), which had been sparged with N_2 for 10 min, was added. The vial was taken into a glove box and charged with $Ni(cod)_2$ (2.8 mg, 0.010 mmol, 5 mol%) and SIPr (3.9 mg, 0.010 mmol, 5 mol%). Subsequently, toluene (0.20 mL, 1.0 M) was added. The vial was sealed with a Teflon-lined screw cap, removed from the glove box, and stirred vigorously (1,000 rpm) at 50 °C for 24 h. After cooling to 23 °C, the mixture was diluted with hexanes (0.5 mL) and filtered over a plug of silica gel (10 mL of EtOAc eluent). The volatiles were removed under reduced pressure, and the crude residue was purified by preparative thin-layer chromatography (5:1 Hexanes:EtOAc) to yield ketone product **7** (96% yield, average of two experiments) as a white solid. Ketone **3.7**: R_f 0.56 (5:1 Hexanes:EtOAc). Spectral data match those previously reported.[33]

Any modifications of the conditions shown in the representative procedure above are specified in the following schemes, which depict all of the results shown in Table 3.2. Note: N-Me,Boc and N-Bn,Boc amides were used in a variable manner, but only as a means to facilitate purification of reactions (i.e., separation of the N-Boc-amine byproduct from the desired product).

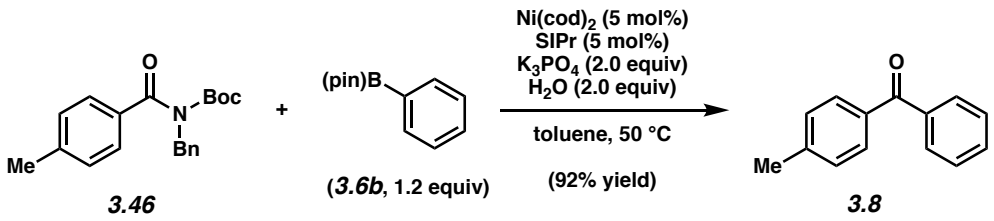

Ketone 3.8. Purification by preparative thin-layer chromatography (5:1 Hexanes:EtOAc) generated ketone **3.8** (92% yield, average of two experiments) as a white solid. Ketone **3.8**: R_f 0.49 (5:1 Hexanes:EtOAc). Spectral data match those previously reported.[33]

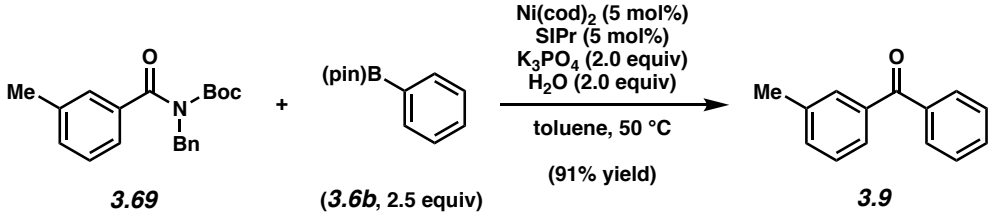

Ketone 3.9. Purification by flash chromatography (49:1 Hexanes:EtOAc) generated ketone **3.9** (90% yield, average of two experiments) as a clear oil. Ketone **3.9**: R_f 0.49 (5:1 Hexanes:EtOAc). Spectral data match those previously reported.[33]

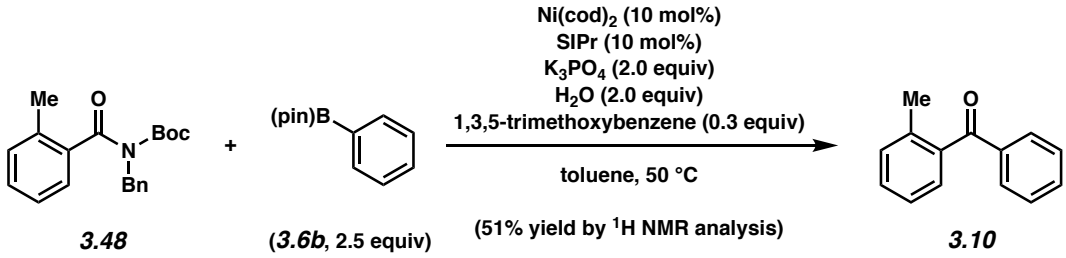

Ketone 3.10. ^{1}H NMR analysis of the crude reaction mixture indicated a 51% yield (average of two experiments) of ketone **3.10** relative to 1,3,5-trimethoxybenzene internal standard. Iterative purification by preparative thin-layer chromatography (5:1 Hexanes:EtOAc then 100% benzene) generated ketone **3.10** as a clear oil. Ketone **3.10**: R_f 0.58 (5:1 Hexanes:EtOAc). Spectral data match those previously reported.[33]

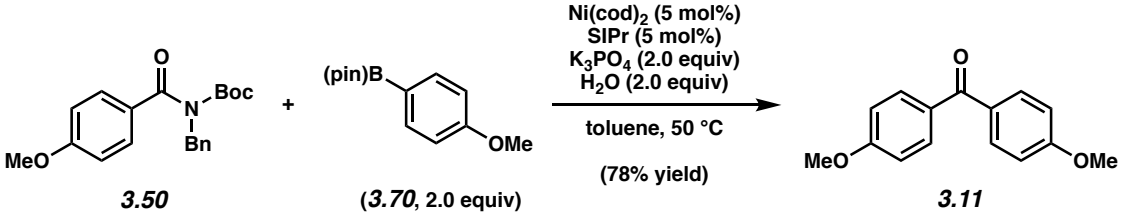

Ketone 3.11. Purification by preparative thin-layer chromatography (5:1 Hexanes:EtOAc) generated ketone **3.11** (78% yield, average of two experiments) as a white solid. Ketone **3.11**: R_f 0.20 (5:1 Hexanes:EtOAc). Spectral data match those previously reported.[34]

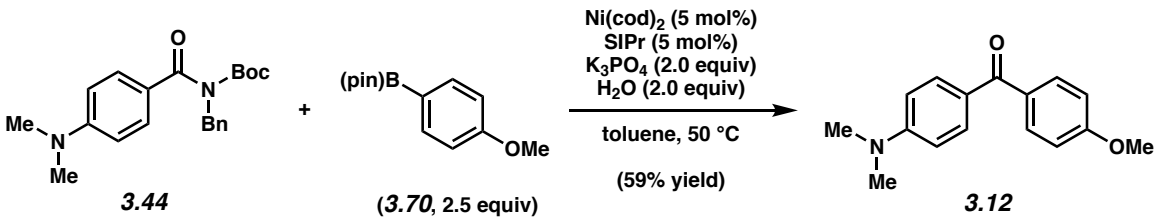

Ketone 3.12. Purification by preparative thin-layer chromatography (5:1 Hexanes:EtOAc) generated ketone **3.12** (59% yield, average of two experiments) as an off-white solid. Ketone **3.12**: R_f 0.17 (5:1 Hexanes:EtOAc). Spectral data match those previously reported.[34]

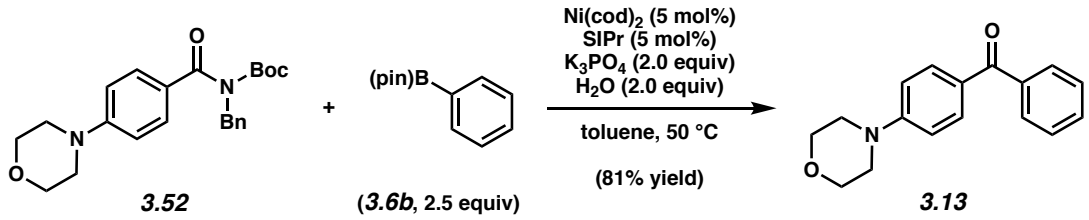

Ketone 3.13. Purification by flash chromatography (29:1 Hexanes:EtOAc → 19:1 Hexanes:EtOAc → 100% EtOAc) generated ketone **3.13** (81% yield, average of two

experiments) as an off-white solid. Ketone **3.13**: R_f 0.56 (1:1 Hexanes:EtOAc). Spectral data match those previously reported.[35]

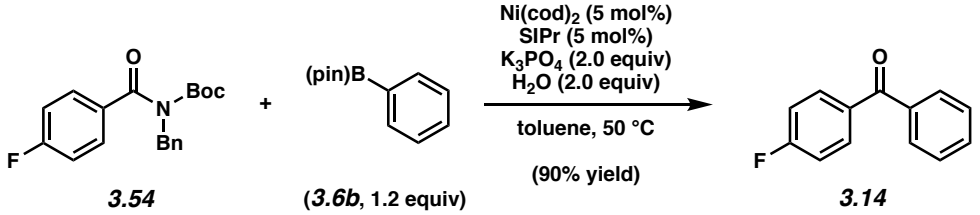

Ketone 3.14. Purification by preparative thin-layer chromatography (6:1 Hexanes:EtOAc) generated ketone **3.14** (90% yield, average of two experiments) as a white solid. Ketone **3.14**: R_f 0.58 (5:1 Hexanes:EtOAc). Spectral data match those previously reported.[33]

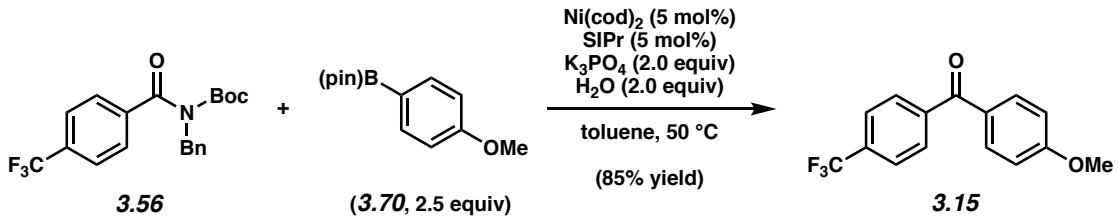

Ketone 3.15. Purification by flash chromatography (49:1 Hexanes:EtOAc) generated ketone **3.15** (85% yield, average of two experiments) as a white solid. Ketone **3.15**: R_f 0.47 (5:1 Hexanes:EtOAc). Spectral data match those previously reported.[34]

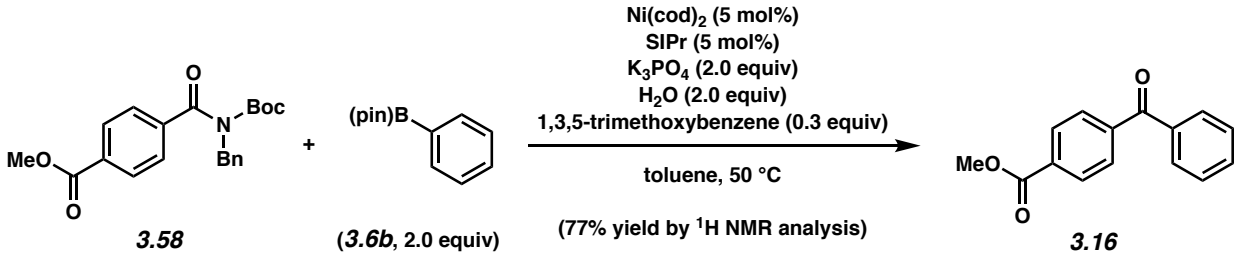

Ketone 3.16. ^{1}H NMR analysis of the crude reaction mixture indicated a 77% yield (average of two experiments) of ketone **3.16** relative to 1,3,5-trimethoxybenzene internal standard. Trituration of the crude material with 5 mL Hexanes and purification by preparative thin-layer

chromatography (5:1 Hexanes:EtOAc) generated ketone **3.16** as a white solid. Ketone **3.16**: R_f 0.40 (5:1 Hexanes:EtOAc). Spectral data match those previously reported.[36]

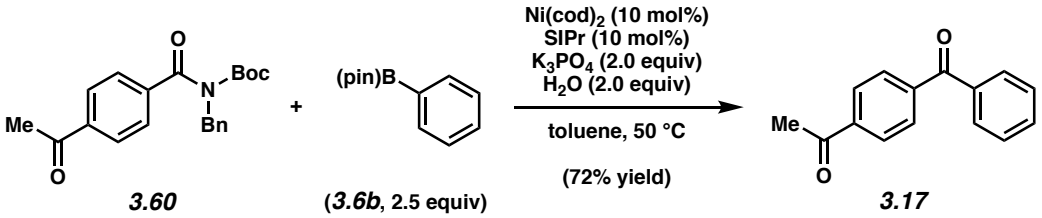

Ketone 3.17. Purification by flash chromatography (24:1 Hexanes:EtOAc) generated ketone **3.17** (72% yield, average of two experiments) as a white solid. Ketone **3.17**: R_f 0.29 (5:1 Hexanes:EtOAc). Spectral data match those previously reported.[33]

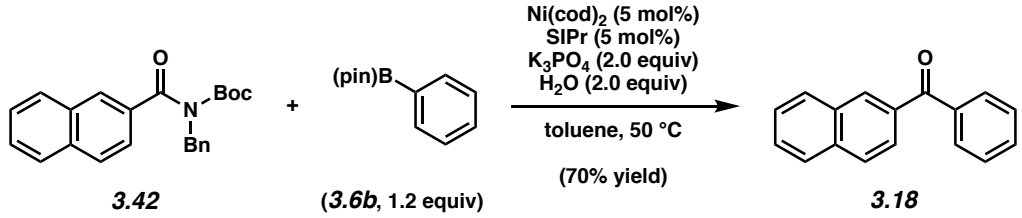

Ketone 3.18. Purification by preparative thin-layer chromatography (6:1 Hexanes:EtOAc) generated ketone **3.18** (70% yield, average of two experiments) as a white solid. Ketone **3.18**: R_f 0.45 (5:1 Hexanes:EtOAc). Spectral data match those previously reported.[33]

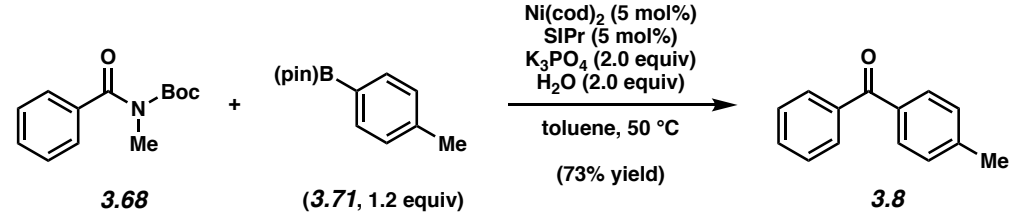

Ketone 3.8. Purification by preparative thin-layer chromatography (6:1 Hexanes:EtOAc) generated ketone **3.8** (73% yield, average of two experiments) as a white solid. Ketone **3.8**: R_f 0.49 (5:1 Hexanes:EtOAc). Spectral data match those previously reported.[33]

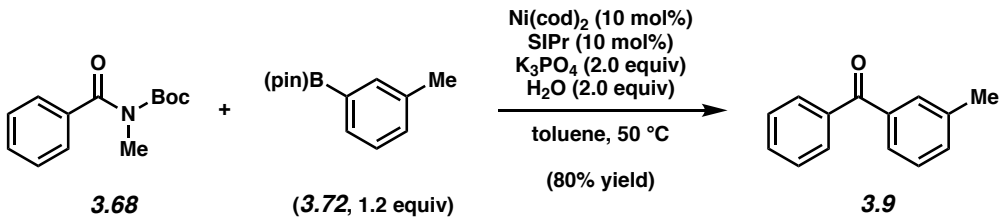

3.68 (*3.72*, 1.2 equiv) *3.9*

Ketone 3.9. Purification by preparative thin-layer chromatography (6:1 Hexanes:EtOAc) generated ketone **3.9** (80% yield, average of two experiments) as a clear oil. Ketone **3.9**: R_f 0.49 (5:1 Hexanes:EtOAc). Spectral data match those previously reported.[33]

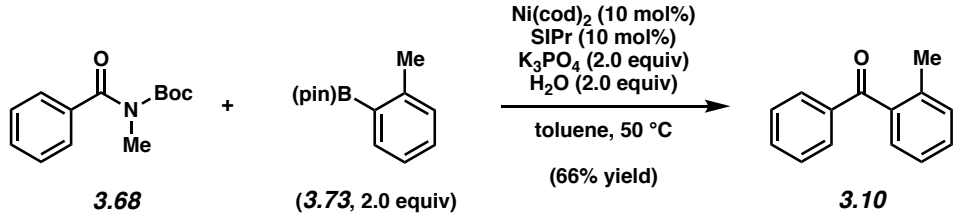

3.68 (*3.73*, 2.0 equiv) *3.10*

Ketone 3.10. Purification by preparative thin-layer chromatography (5:1 Hexanes:EtOAc) generated ketone **3.10** (66% yield, average of two experiments) as a clear oil. Ketone **3.10**: R_f 0.58 (5:1 Hexanes:EtOAc). Spectral data match those previously reported.[33]

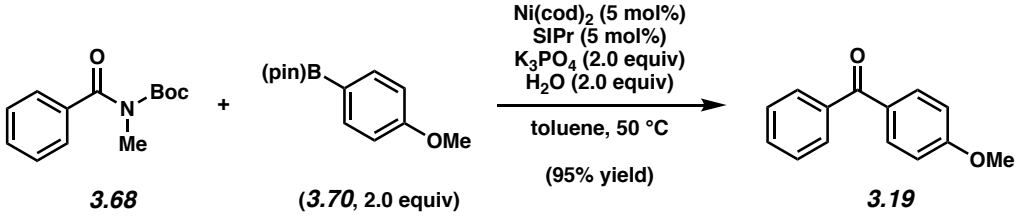

3.68 (*3.70*, 2.0 equiv) *3.19*

Ketone 3.19. Purification by preparative thin-layer chromatography (5:1 Hexanes:EtOAc) generated ketone **3.19** (95% yield, average of two experiments) as a white solid. Ketone **3.19**: R_f 0.35 (5:1 Hexanes:EtOAc). Spectral data match those previously reported.[33]

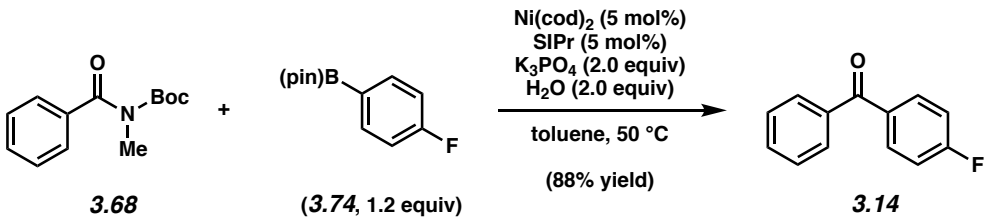

Ketone 3.14. Purification by preparative thin-layer chromatography (5:1 Hexanes:EtOAc) generated ketone **3.14** (88% yield, average of two experiments) as a white solid. Ketone **3.14**: R_f 0.58 (5:1 Hexanes:EtOAc). Spectral data match those previously reported.[33]

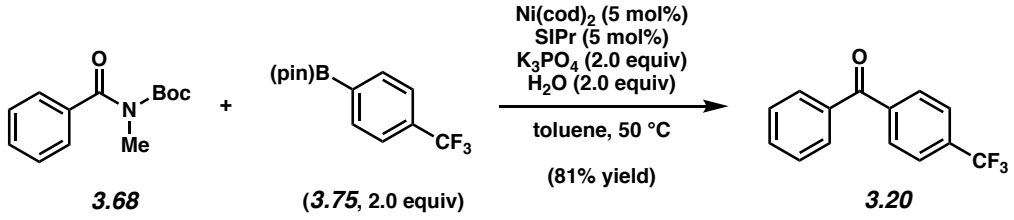

Ketone 3.20. Purification by flash chromatography (24:1 Hexanes:EtOAc) generated ketone **3.20** (81% yield, average of two experiments) as a white solid. Ketone **3.20**: R_f 0.63 (5:1 Hexanes:EtOAc). Spectral data match those previously reported.[33]

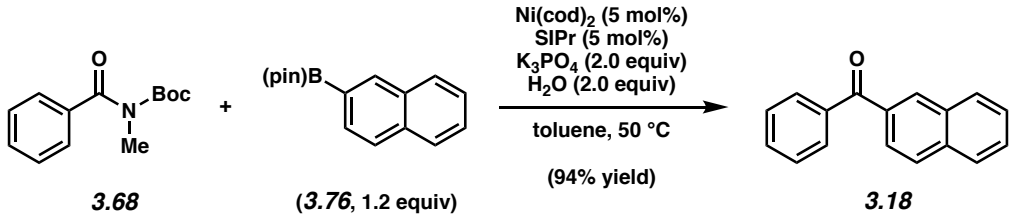

Ketone 3.18. Purification by preparative thin-layer chromatography (6:1 Hexanes:EtOAc) generated ketone **3.18** (94% yield, average of two experiments) as a white solid. Ketone **3.18**: R_f 0.45 (5:1 Hexanes:EtOAc). Spectral data match those previously reported.[33]

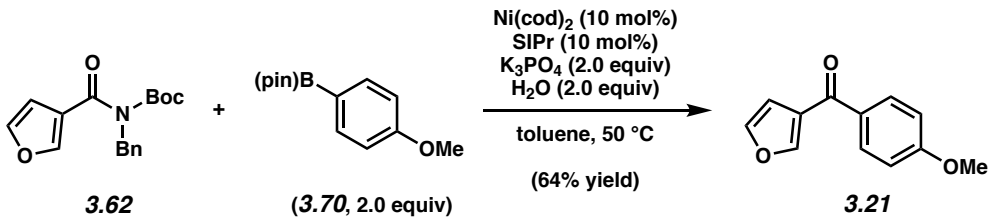

Ketone 3.21. Purification by preparative thin-layer chromatography (5:1 Hexanes:EtOAc) generated ketone **3.21** (64% yield, average of two experiments) as a white solid. Ketone **3.21**: R_f 0.61 (1:1 Hexanes:EtOAc). Spectral data match those previously reported.[37]

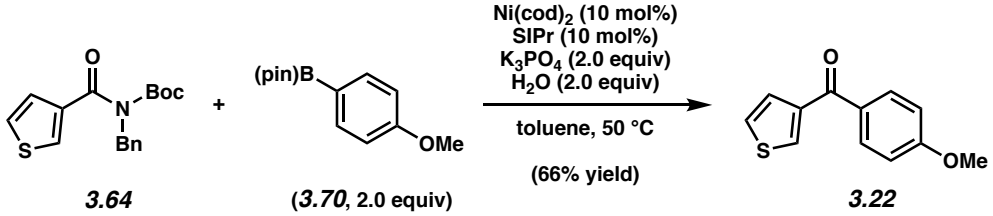

Ketone 3.22. Purification by preparative-thin layer chromatography (6:1 Hexanes:EtOAc) generated ketone **3.22** (66% yield, average of two experiments) as a white solid. Ketone **3.22**: R_f 0.32 (5:1 Hexanes:EtOAc). Spectral data match those previously reported.[38]

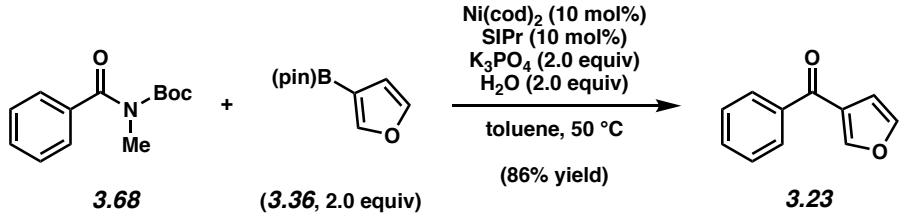

Ketone 3.23. Purification by preparative thin-layer chromatography (5:1 Hexanes:EtOAc) generated ketone **3.23** (86% yield, average of two experiments) as a tan solid. Ketone **3.23**: mp: 38–40 °C; R_f 0.51 (5:1 Hexanes:EtOAc); ^{1}H NMR (500 MHz, $CDCl_3$): δ 7.92 (dd, J = 1.4, 0.8, 1H), 7.88–7.82 (m, 2H), 7.62–7.57 (m, 1H), 7.53–7.46 (m, 3H), 6.91 (dd, J = 1.9, 0.8, 1H); ^{13}C NMR (125 MHz, $CDCl_3$): δ 189.6, 148.7, 144.1, 139.0, 132.6, 129.0, 128.7, 126.7, 110.4; IR

(film): 3142, 3060, 1649 cm^{-1}; HRMS-ESI (*m/z*) $[M + H]^+$ calcd for $C_{11}H_8O_2$, 173.06025; found 173.05927.

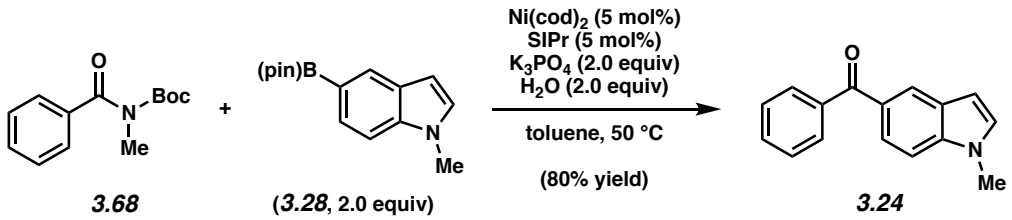

Ketone 3.24. Purification by preparative thin-layer chromatography (3:1 Hexanes:EtOAc) generated ketone **3.24** (80% yield, average of two experiments) as an off-white solid. Ketone **3.24**: mp: 83–85 °C; R_f 0.19 (5:1 Hexanes:EtOAc); ^{1}H NMR (500 MHz, $CDCl_3$): δ 8.14–8.10 (m, 1H, 7.86–7.77 (m, 3H), 7.60–7.54 (m, 1H), 7.52–7.46 (m, 2H), 7.42–7.37 (m, 1H), 7.14 (d, *J* = 3.2, 1H), 6.59 (dd, *J* = 3.2, 0.8, 1H), 3.85 (s, 3H); ^{13}C NMR (125 MHz, $CDCl_3$, 13 of 14 observed): δ 197.4, 139.3, 131.1, 130.5, 130.0, 129.3, 128.2, 127.8, 125.6, 124.0, 109.2, 103.1, 33.2; IR (film): 3103, 3060, 2943, 1731, 1644, 1605 cm^{-1}; HRMS-ESI (*m/z*) $[M + H]^+$ calcd for $C_{16}H_{14}NO$, 236.10754; found 236.10624.

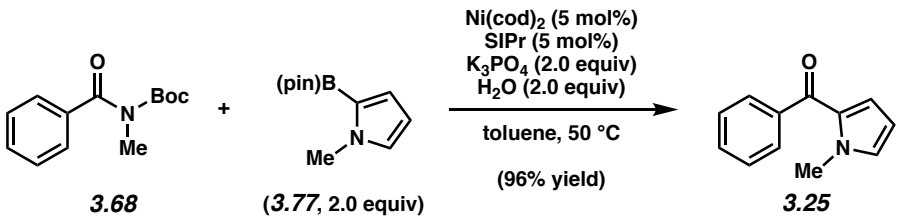

Ketone 3.25. Purification by preparative thin-layer chromatography (5:1 Hexanes:EtOAc) generated ketone **3.25** (96% yield, average of two experiments) as a clear oil. Ketone **3.25**: R_f 0.39 (5:1 Hexanes:EtOAc). Spectral data match those previously reported.[39]

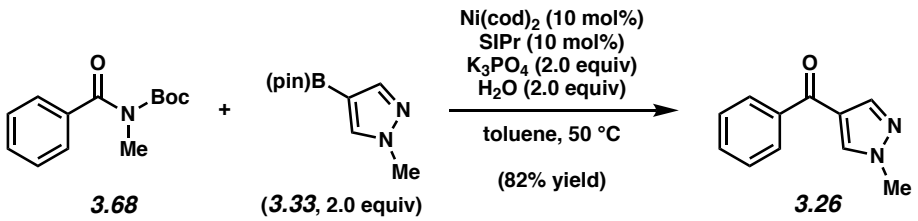

Ketone 3.26. Purification by preparative thin-layer chromatography (1:1 Hexanes:EtOAc) generated ketone **3.26** (82% yield, average of two experiments) as a white solid. Ketone **3.26**: mp: 85–87 °C; R_f 0.24 (1:1 Hexanes:EtOAc); ^{1}H NMR (500 MHz, $CDCl_3$): δ 7.97–7.91 (m, 2H), 7.88–7.82 (m, 2H), 7.62–7.54 (m, 1H), 7.53–7.46 (m, 2H), 3.98 (s, 3H); ^{13}C NMR (125 MHz, $CDCl_3$): δ 188.9, 141.9, 139.3, 134.3, 132.3, 128.9, 128.6, 123.0, 39.5; IR (film): 3122, 2942, 1639, 1595, 1542 cm^{-1}; HRMS-ESI (*m/z*) $[M + H]^+$ calcd for $C_{11}H_{11}N_2O$, 187.08714; found 187.08568.

3.7.2.6. Gram Scale Synthesis of Tubulin Binding Agent 3.29

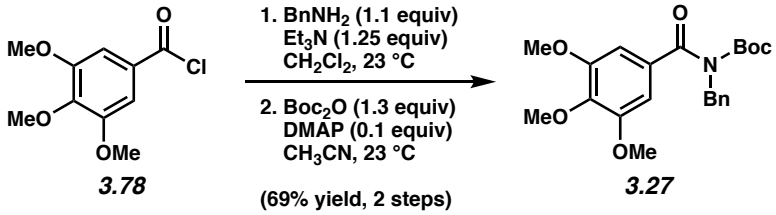

Amide 3.27. To a solution of acid chloride **3.78** (5.00 g, 21.7 mmol, 1.0 equiv), triethylamine (3.74 mL, 27.1 mmol, 1.25 equiv), and dichloromethane (21.5 mL), was added dropwise a solution of benzylamine (2.60 mL, 23.9 mmol, 1.1 equiv) in dichloromethane (21.9 mL, 0.5 M in total). The reaction mixture was stirred at 23 °C for 1 h, then transferred to a separatory funnel with EtOAc (50 mL) and H_2O (50 mL), and extracted with EtOAc (3 x 50 mL). The organic

layers were combined, dried over Na_2SO_4, and evaporated under reduced pressure. The resulting crude solid material was used in the subsequent step without further purification.

To a flask containing the crude material from the previous step was added DMAP (270.0 mg, 2.22 mmol, 0.1 equiv) followed by acetonitrile (111 mL, 0.2 M). Boc_2O (6.30 g, 28.9 mmol, 1.3 equiv) was added in one portion and the reaction vessel was flushed with N_2, then the reaction mixture was allowed to stir at 23 °C for 16 h. The reaction was quenched by addition of 100 mL saturated aqueous $NaHCO_3$, transferred to a separatory funnel with EtOAc (100 mL) and H_2O (100 mL), and extracted with EtOAc (3 x 80 mL). The organic layers were combined, dried over Na_2SO_4, and evaporated under reduced pressure. The resulting crude residue was purified by flash chromatography (7:1 → 4:1 Hexanes:EtOAc) to yield amide **3.27** (6.00 g, 69% yield, over two steps) as a white solid. Amide **3.27**: mp: 94–96 ºC; R_f 0.24 (5:1 Hexanes:EtOAc); ^{1}H NMR (500 MHz, $CDCl_3$): δ 7.44–7.39 (m, 2H), 7.36–7.30 (m, 2H), 7.29–7.25 (m, 1H), 6.77 (s, 2H), 4.95 (s, 2H), 3.86 (s, 3H), 3.83 (s, 6H), 1.18 (s, 9H); ^{13}C NMR (125 MHz, $CDCl_3$): δ 173.0, 153.7, 153.0, 140.9, 137.9, 132.8, 128.6, 128.3, 127.6, 105.2, 83.3, 61.1, 56.3, 49.4, 27.6; IR (film): 2987, 2933, 2837, 1731, 1668 cm^{-1}; HRMS-ESI (*m/z*) $[M + H]^+$ calcd for $C_{22}H_{28}NO_6$, 402.19166; found 402.18970.

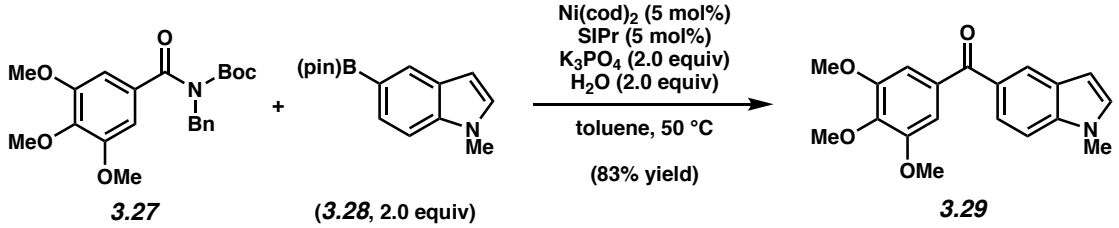

Ketone 3.29. A 20 mL scintillation vial was charged with anhydrous powdered K_3PO_4 (1.06 g, 4.98 mmol, 2.0 equiv) and a magnetic stir bar. The vial and contents were flame-dried under reduced pressure, then allowed to cool under N_2. Amide substrate **3.27** (1.00 g, 2.49 mmol, 1.0

equiv) and *N*-methylindole-5-boronic acid pinacol ester (**3.28**) (1.28 g, 4.98 mmol, 2.0 equiv) were added. The vial was flushed with N_2, then water (88.8 μL, 4.98 mmol, 2.0 equiv), which had been sparged with N_2 for 10 min, was added. The vial was taken into a glove box and charged with $Ni(cod)_2$ (34.2 mg, 0.125 mmol, 5 mol%) and SIPr (48.9 mg, 0.125 mmol, 5 mol%). Subsequently, toluene (2.5 mL, 1.0 M) was added. The vial was sealed with a Teflon-lined screw cap, removed from the glove box, and stirred vigorously (1,000 rpm) at 50 °C for 24 h. After cooling to 23 °C, the mixture was diluted with hexanes (7 mL) and filtered over a plug of silica gel (75 mL of EtOAc eluent). The volatiles were removed under reduced pressure, and the crude residue was purified by flash chromatography (6:1 → 3:1 Hexanes:EtOAc) to yield ketone **3.29** (676.0 mg, 83% yield) as an off-white solid. Ketone **3.29**: mp: 125–127 ºC; R_f 0.40 (1:1 Hexanes:EtOAc); ^{1}H NMR (500 MHz, $CDCl_3$): δ 8.16–8.11 (m, 1H), 7.80 (dd, *J* = 8.6, 1.6, 1H), 7.40 (d, *J* = 8.6, 1H), 7.15 (d, *J* = 3.2, 1H), 7.08 (s, 2H), 6.61 (dd, *J* = 3.2, 0.7, 1H), 3.95 (s, 3H), 3.87 (s, 6H), 3.86 (s, 3H); ^{13}C NMR (125 MHz, $CDCl_3$): δ 196.5, 152.9, 141.4, 139.0, 134.4, 130.6, 129.4, 127.8, 125.3, 124.0, 109.2, 107.7, 103.1, 61.1, 56.4, 33.2; IR (film): 2943, 2827, 1644, 1581, 1503 cm^{-1}; HRMS-ESI (*m/z*) $[M + H]^+$ calcd for $C_{19}H_{20}NO_4$, 326.13923; found 326.13731.

3.7.2.7. Sequential Palladium- and Nickel-Catalysed Suzuki Reactions

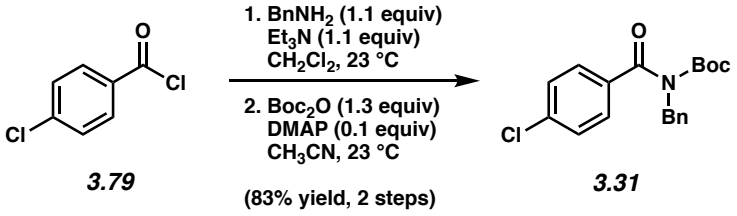

Amide 3.31. To a solution of acid chloride **3.79** (5.00 g, 28.6 mmol, 1.0 equiv), triethylamine (4.35 mL, 31.4 mmol, 1.1 equiv), and dichloromethane (28.5 mL), was added dropwise a

solution of benzylamine (4.30 mL, 31.4 mmol, 1.1 equiv) in dichloromethane (28.7 mL, 0.5 M in total). The reaction mixture was stirred at 23 °C for 1 h, then quenched by addition of 30 mL 1 M aq. HCl, transferred to a separatory funnel with EtOAc (100 mL) and H_2O (100 mL), and extracted with EtOAc (3 x 80 mL). The organic layers were combined, dried over Na_2SO_4, and evaporated under reduced pressure. The resulting crude solid material was used in the subsequent step without further purification.

To a flask containing the crude material from the previous step was added DMAP (351.0 mg, 2.88 mmol, 0.1 equiv) followed by acetonitrile (144 mL, 0.2 M). Boc_2O (8.20 g, 37.4 mmol, 1.3 equiv) was added in one portion and the reaction vessel was flushed with N_2, then the reaction mixture was allowed to stir at 23 °C for 16 h. The reaction was quenched by addition of 100 mL saturated aqueous $NaHCO_3$, transferred to a separatory funnel with EtOAc (100 mL) and H_2O (100 mL), and extracted with EtOAc (3 x 80 mL). The organic layers were combined, dried over Na_2SO_4, and evaporated under reduced pressure. The resulting crude residue was purified by flash chromatography (27:1 Hexanes:EtOAc) to yield amide **3.31** (8.25 g, 83% yield, over two steps) as a white solid. Amide **3.31**: mp: 59–61 ºC; R_f 0.36 (5:1 Hexanes:EtOAc); ^{1}H NMR (500 MHz, $CDCl_3$): δ 7.49–7.44 (m, 2H), 7.43–7.39 (m, 2H), 7.39–7.30 (m, 4H), 7.30–7.25 (m, 1H), 4.97 (s, 2H), 1.17 (s, 9H); ^{13}C NMR (125 MHz, $CDCl_3$): δ 172.17, 153.38, 137.81, 137.37, 136.11, 129.06, 128.64, 128.49, 128.25, 127.64, 83.69, 49.09, 27.59; IR (film): 3068.67, 2980.69, 2934.4, 1729.59, 1673.91 cm^{-1}; HRMS-ESI (*m/z*) $[M + H]^+$ calcd for $C_{19}H_{21}ClNO_3$, 346.12100; found 346.11931.

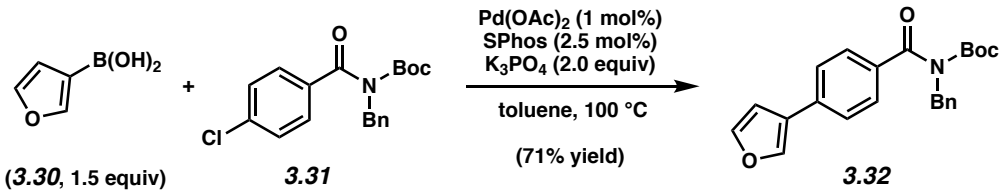

Amide 3.32: A 1-dram vial was charged with anhydrous powdered K_3PO_4 (339.2 mg, 1.60 mmol, 2.0 equiv) and a magnetic stir bar. The vial and contents were flame-dried under reduced pressure, then allowed to cool under N_2. Amide substrate **3.31** (276.6 mg, 0.800 mmol, 1.0 equiv), furan-3-boronic acid (**3.30**) (134.3 mg, 1.20 mmol, 1.5 equiv), and $Pd(OAc)_2$ (1.8 mg, 0.008 mmol, 1 mol%) were added, and the vial was flushed with N_2. The vial was taken into a glove box and charged with SPhos (8.2 mg, 0.020 mmol, 2.5 mol%). Subsequently, toluene (0.80 mL, 1.0 M) was added. The vial was sealed with a Teflon-lined screw cap, removed from the glove box, and stirred vigorously (1,000 rpm) at 100 °C for 16 h. After cooling to 23 °C, the mixture was diluted with Et_2O (0.5 mL) and filtered over a plug of silica gel (10 mL of Et_2O eluent). The volatiles were removed under reduced pressure, and the resulting crude residue was purified by flash chromatography (19:1 Hexanes:EtOAc) to yield amide **3.32** (214.0 mg, 71% yield) as a white solid. Amide **3.32**: mp: 114–116 ºC; R_f 0.44 (5:1 Hexanes:EtOAc); ^{1}H NMR (500 MHz, $CDCl_3$): δ 7.80–7.77 (m, 1H), 7.57–7.53 (m, 2H), 7.52–7.48 (m, 3H), 7.45–7.41 (m, 2H), 7.36–7.31 (m, 2H), 7.30–7.24 (m, 1H), 6.72 (dd, J = 1.9, 0.9, 1H), 4.99 (s, 2H), 1.17 (s, 9H); ^{13}C NMR (125 MHz, $CDCl_3$): δ 172.9, 153.7, 144.1, 139.4, 138.0, 136.0, 135.5, 128.6, 128.5, 128.3, 127.5, 125.9, 125.4, 108.8, 83.4, 49.1, 27.6; IR (film): 3134, 3032, 2976, 1730, 1669 cm^{-1}; HRMS-ESI (*m/z*) $[M + H]^+$ calcd for $C_{23}H_{24}NO_4$, 378.17053; found 378.16889.

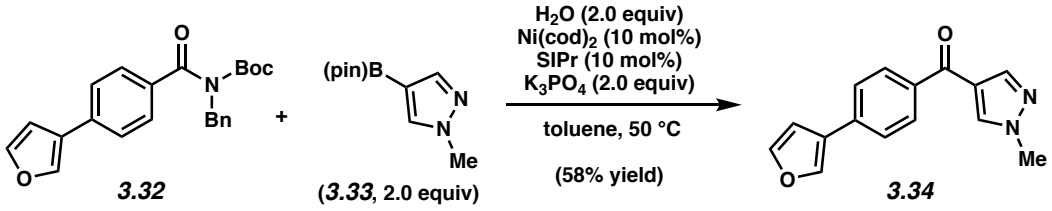

3.32 (*3.33*, 2.0 equiv) *3.34*

Ketone 3.34: A 1-dram vial was charged with anhydrous powdered K_3PO_4 (84.8 mg, 0.400 mmol, 2.0 equiv) and a magnetic stir bar. The vial and contents were flame-dried under reduced pressure, then allowed to cool under N_2. Amide **3.32** (75.5 mg, 0.200 mmol, 1.0 equiv) and *N*-methylpyrazole-4-boronic acid pinacol ester (**3.33**) (82.8 mg, 0.400 mmol, 2.0 equiv) were added. The vial was flushed with N_2, then water (7.2 μL, 0.400 mmol, 2.0 equiv), which had been sparged with N_2 for 10 min, was added. The vial was taken into a glove box and charged with $Ni(cod)_2$ (5.5 mg, 0.020 mmol, 10 mol%) and SIPr (7.8 mg, 0.020 mmol, 10 mol%). Subsequently, toluene (0.20 mL, 1.0 M) was added. The vial was sealed with a Teflon-lined screw cap, removed from the glove box, and stirred vigorously (1,000 rpm) at 50 °C for 24 h. After cooling to 23 °C, the mixture was diluted with hexanes (0.5 mL) and filtered over a plug of silica gel (10 mL of EtOAc eluent). The volatiles were removed under reduced pressure, and the crude residue was purified by preparative thin-layer chromatography (1:1 Hexanes:EtOAc) to yield ketone **3.34** (29.1 mg, 58% yield) as a white solid. Ketone **3.34**: mp: 161–163 ºC; R_f 0.26 (1:1 Hexanes:EtOAc); ^{1}H NMR (500 MHz, $CDCl_3$): δ 7.95 (app s, 2H), 2.88 (d, J = 8.3, 2H), 7.83 (app s, 1H), 7.60 (d, J = 8.3, 2H), 7.52 (app s, 1H), 6.76 (app s, 1H), 3.99 (s, 3H); ^{13}C NMR (125 MHz, $CDCl_3$): δ 188.2, 144.3, 141.9, 139.6, 137.6, 136.6, 134.2, 129.7, 125.9, 125.8, 123.1, 108.8, 39.5; IR (film): 3137, 3113, 2982, 2944, 1631, 1603, 1546 cm^{-1}; HRMS-ESI (*m/z*) [M + H]$^+$ calcd for $C_{15}H_{13}N_2O_2$, 253.09770; found 253.09624.

3.7.2.8. Chemoselective Sequential Suzuki and Esterification Reactions

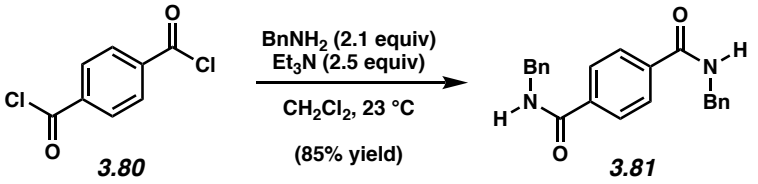

***N*,*N*-dibenzylterephthalamide (3.81).** To a solution of terephthaloyl chloride (**3.80**) (2.00 g, 9.85 mmol, 1.0 equiv), triethylamine (3.41 mL, 24.6 mmol, 2.5 equiv), and dichloromethane (14.7 mL), was added dropwise a solution of benzylamine (2.26 mL, 20.7 mmol, 2.1 equiv) in dichloromethane (5.0 mL, 0.5 M in total). During the addition of the benzylamine solution, the reaction mixture thickened into a slurry, which was stirred at 23 °C for 1 h. The reaction mixture was filtered, and the filtrate was washed with MeOH and dried under reduced pressure to yield *N*,*N*-dibenzylterephthalamide (**3.81**) (2.88 g, 85% yield) as a white solid. *N*,*N*-dibenzylterephthalamide (**3.81**): mp: 260–262 ºC; R_f 0.16 (1:1 Hexanes:EtOAc); ^{1}H NMR (500 MHz, DMSO-d_6): δ 7.52 (s, 4H), 7.42–7.25 (m, 10H), 4.96 (s, 4H), 1.17 (s, 18H); ^{13}C NMR (125 MHz, DMSO-d_6): δ 165.6, 139.5, 136.6, 128.3, 127.28, 127.26, 126.8, 42.7; IR (solid): 3282, 3069, 3030, 1629, 1542 cm^{-1}; HRMS-ESI (*m/z*) $[M + H]^+$ calcd for $C_{22}H_{21}N_2O_2$, 345.16030; found 345.15838.

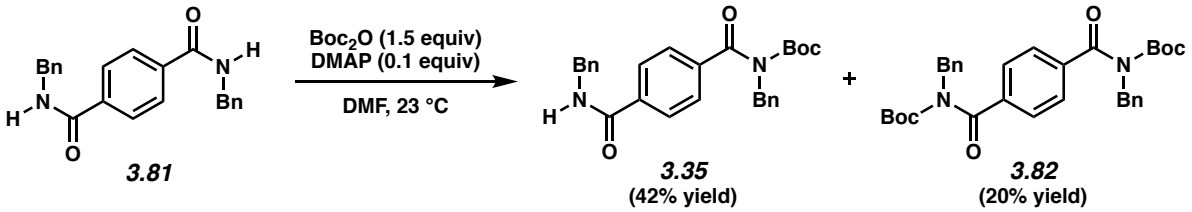

Diamide 3.35 and diamide 3.82. To a flask containing *N*,*N*-dibenzylterephthalamide (**3.81**) (770.0 mg, 2.24 mmol, 1.0 equiv) was added DMAP (27.3 mg, 0.224 mmol, 0.1 equiv) followed

by DMF (44.8 mL, 0.05 M). Boc_2O (731.9 mg, 3.36 mmol, 1.5 equiv) was added in one portion and the reaction vessel was flushed with N_2, then the reaction mixture was allowed to stir at 23 °C for 19 h. The reaction was diluted with 25 mL deionized water, transferred to a separatory funnel with EtOAc (50 mL) and H_2O (50 mL), and extracted with EtOAc (3 x 25 mL). The organic layers were combined and washed with deionized water (3 x 50 mL), dried over Na_2SO_4, and evaporated under reduced pressure. The resulting crude residue was purified by flash chromatography (9:1 → 5:1 → 3:1 Hexanes:EtOAc) to yield diamide **3.35** (420.3 mg, 42% yield) as a white solid and diamide **3.82** (243.7 mg, 20% yield) as a white solid. Diamide **3.35**: mp: 38–40 ºC; R_f 0.52 (1:1 Hexanes:EtOAc); ^{1}H NMR (500 MHz, $CDCl_3$): δ 7.84–7.77 (m, 2H), 7.59–7.53 (m, 2H), 7.44–7.26 (m, 10H), 6.50–6.32 (t, J = 5.6, 1H), 4.98 (s, 2H), 4.65 (d, J = 5.6, 2H), 1.15 (s, 9H); ^{13}C NMR (125 MHz, $CDCl_3$): δ 172.3, 166.4, 153.2, 140.6, 138.0, 137.7, 136.4, 129.0, 128.7 128.3, 128.2, 127.9, 127.7, 127.68, 126.9, 83.9, 49.0, 44.5, 27.6; IR (film): 3332, 2978, 1738, 1672, 1651 cm^{-1}; HRMS-ESI (*m/z*) $[M + H]^+$ calcd for $C_{27}H_{29}N_2O_4$, 445.21273; found 445.21156. Diamide **3.82**: mp: 180–182 ºC; R_f 0.33 (5:1 Hexanes:EtOAc); ^{1}H NMR (500 MHz, CD_2Cl_2): δ 7.52 (s, 4H), 7.41–7.25 (m, 10H), 4.96 (s, 4H), 1.17 (s, 18H); ^{13}C NMR (125 MHz, CD_2Cl_2): δ 172.5, 153.5, 140.2, 138.4, 128.8, 128.2, 127.7, 127.4, 84.0, 49.1, 27.6; IR (film): 3069, 2977, 2933, 1731, 1673 cm^{-1}; HRMS-ESI (*m/z*) $[M + H]^+$ calcd for $C_{32}H_{37}N_2O_6$, 545.26516; found 545.26452.

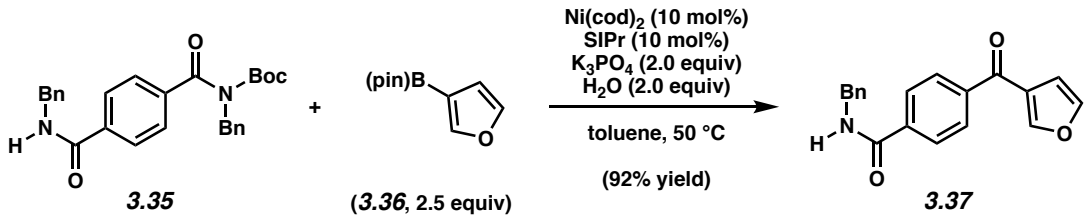

Ketone 3.37. A 1-dram vial was charged with anhydrous powdered K_3PO_4 (95.5 mg, 0.451 mmol, 2.0 equiv) and a magnetic stir bar. The vial and contents were flame-dried under reduced pressure, then allowed to cool under N_2. Diamide substrate **3.35** (100.0 mg, 0.225 mmol, 1.0 equiv) and furan-3-boronic acid pinacol ester (**3.36**) (109.2 mg, 0.563 mmol, 2.5 equiv) were added. The vial was flushed with N_2, then water (8.1 μL, 0.451 mmol, 2.0 equiv), which had been sparged with N_2 for 10 min, was added. The vial was taken into a glove box and charged with $Ni(cod)_2$ (6.2 mg, 0.023 mmol, 10 mol%) and SIPr (8.8 mg, 0.023 mmol, 10 mol%). Subsequently, toluene (0.23 mL, 1.0 M) was added. The vial was sealed with a Teflon-lined screw cap, removed from the glove box, and stirred vigorously (1,000 rpm) at 50 °C for 16 h. After cooling to 23 °C, the mixture was diluted with hexanes (0.5 mL) and filtered over a plug of silica gel (10 mL of EtOAc eluent). The volatiles were removed under reduced pressure, and the crude residue was purified by flash chromatography (9:1 → 5:1 → 3:1 Hexanes:EtOAc) to yield ketone **3.37** (63.0 mg, 92% yield) as a white solid. Ketone **3.37**: mp: 135–137 ºC; R_f 0.41 (1:1 Hexanes:EtOAc); ^{1}H NMR (500 MHz, $CDCl_3$): δ 7.93–7.87 (m, 5H), 7.53–7.51 (m, 1H), 7.40–7.29 (m, 5H), 6.90 (dd, J = 1.9, 0.7, 1H), 6.45 (br s, 1H), 4.68 (d, J = 5.6, 2H); ^{13}C NMR (125 MHz, $CDCl_3$): δ 188.8, 166.5, 148.9, 144.4, 141.4, 137.93, 137.9, 129.2, 129.1, 128.2, 128.0, 127.4, 126.6, 110.2, 44.5; IR (film): 3360, 2953, 2870, 1713, 1647 cm^{-1}; HRMS-ESI (*m/z*) [M + H]$^+$ calcd for $C_{19}H_{16}NO_3$, 306.11302; found 306.10982.

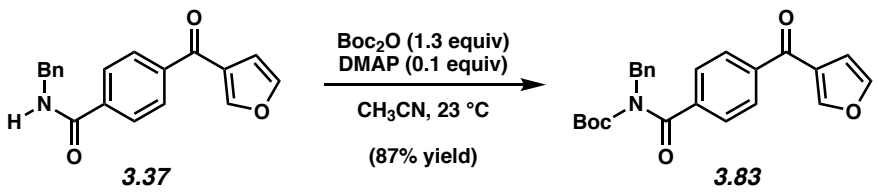

Ketone 3.83. To a flask containing ketone **3.37** (100.0 mg, 0.328 mmol, 1.0 equiv) was added DMAP (4.0 mg, 0.033 mmol, 0.1 equiv) followed by acetonitrile (3.28 mL, 0.1 M). Boc_2O (92.9 mg, 0.426 mmol, 1.3 equiv) was added in one portion and the reaction vessel was flushed with N_2, then the reaction mixture was allowed to stir at 23 °C for 30 h. The reaction was diluted with 5 mL deionized water, transferred to a separatory funnel with EtOAc (10 mL) and H_2O (10 mL), and extracted with EtOAc (3 x 20 mL). The organic layers were combined, dried over Na_2SO_4, and evaporated under reduced pressure. The resulting crude residue was purified by flash chromatography (19:1 → 14:1 → 9:1 Hexanes:EtOAc) to yield ketone **3.83** (115.5 mg, 87% yield) as a white solid. Ketone **3.83**: mp: 119–121 ºC; R_f 0.75 (1:1 Hexanes:EtOAc); ^{1}H NMR (500 MHz, $CDCl_3$): δ 7.92–7.84 (m, 3H), 7.65–7.58 (m, 2H), 7.52 (dd, *J* = 1.8, 1.5, 1H), 7.46–7.41 (m, 2H), 7.38–7.32 (m, 2H), 7.31–7.27 (m, 1H), 6.90 (dd, *J* = 1.8, 0.8, 1H), 5.01 (s, 2H), 1.16 (s, 9H); ^{13}C NMR (125 MHz, $CDCl_3$): δ 188.6, 172.2, 153.2, 148.7, 144.4, 141.5, 140.6, 137.7, 128.71, 128.68 128.3, 127.7, 127.5, 126.6, 110.2, 83.9, 48.9, 27.6; IR (film): 3137, 2977, 1736, 1673, 1654 cm^{-1}; HRMS-ESI (*m/z*) $[M + H]^+$ calcd for $C_{24}H_{24}NO_5$, 406.16545; found 406.16429.

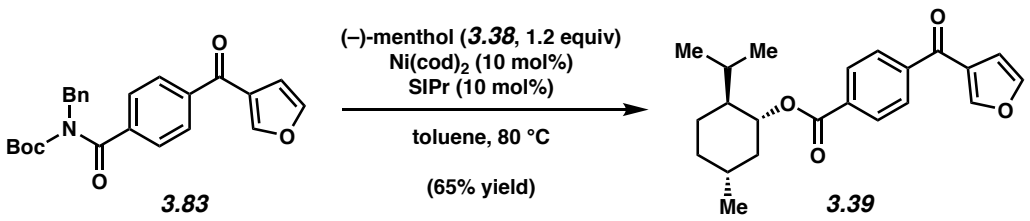

Ester 3.39. A 1-dram vial containing ketone **3.83** (66.0 mg, 0.163 mmol, 1.0 equiv) and a magnetic stir bar was charged with $Ni(cod)_2$ (4.5 mg, 0.016 mmol, 10 mol%) and SIPr (6.4 mg, 0.016 mmol, 10 mol%) in a glove box. Subsequently, toluene (0.20 mL, 0.82 M) and then (–)-menthol (**3.38**, 30.5 mg, 0.196 mmol, 1.2 equiv) were added. The vial was sealed with a Teflon-lined screw cap, removed from the glove box, and stirred at 80 °C for 15 h. After cooling to 23 °C, the mixture was diluted with hexanes (0.5 mL) and filtered over a plug of silica gel (10 mL of EtOAc eluent). The volatiles were removed under reduced pressure, and the crude residue was purified by preparative thin-layer chromatography (5:1 Hexanes:EtOAc) to yield ester **3.39** (37.5 mg, 65% yield) as a colorless amorphous solid. Ester **3.39**: R_f 0.48 (5:1 Hexanes:EtOAc); ^{1}H NMR (500 MHz, $CDCl_3$): δ 8.18–8.13 (m, 2H), 7.94–7.86 (m, 3H), 7.55–7.52 (m, 1H), 6.93–6.90 (m, 1), 4.97 (dt, J = 10.9, 4.4, 1H), 2.19–2.11 (m, 1H), 2.00–1.91 (m, 1H), 1.79–1.71 (m, 2H), 1.63–1.55 (m, 2H), 1.20–1.08 (m, 2H), 1.00–0.90 (m, 7H), 0.81 (d, J = 7.0, 3H); ^{13}C NMR (125 MHz, $CDCl_3$): δ 189.0, 165.4, 149.0, 144.4, 142.3, 134.3, 129.9, 128.8, 126.6, 110.2, 75.6, 47.4, 41.1, 34.4, 31.6, 26.7, 23.8, 22.2, 20.9, 16.7; IR (film): 2955, 2929, 2870, 1714, 1653 cm^{-1}; HRMS-ESI (*m/z*) $[M + H]^+$ calcd for $C_{22}H_{27}O_4$, 355.19093; found 355.18780; $[a]^{21.9}_D$ –69.20° (*c* = 0.500, $CHCl_3$).

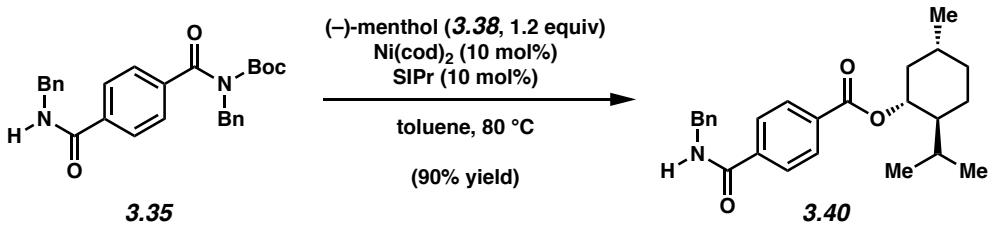

Ester 3.40. A 1-dram vial containing diamide **3.35** (100.0 mg, 0.225 mmol, 1.0 equiv) and a magnetic stir bar was charged with $Ni(cod)_2$ (6.2 mg, 0.023 mmol, 10 mol%) and SIPr (8.8 mg, 0.023 mmol, 10 mol%) in a glove box. Subsequently, toluene (0.23 mL, 1.0 M) and then (–)-menthol (**3.38**, 42.2 mg, 0.270 mmol, 1.2 equiv) were added. The vial was sealed with a Teflon-lined screw cap, removed from the glove box, and stirred at 80 °C for 15 h. After cooling to 23 °C, the mixture was diluted with hexanes (0.5 mL) and filtered over a plug of silica gel (10 mL of EtOAc eluent). The volatiles were removed under reduced pressure, and the crude residue was purified by flash chromatography (24:1 → 14:1 → 9:1 Hexanes:EtOAc) to yield ester **3.40** (80.1 mg, 90% yield) as a colorless amorphous solid. Ester **3.40**: R_f 0.70 (1:1 Hexanes:EtOAc); ^{1}H NMR (500 MHz, $CDCl_3$): δ 8.12–8.07 (m, 2H), 7.87–7.82 (m, 2H), 7.41–7.29 (m, 5H), 6.41 (t, *J* = 5.7, 1H), 4.94 (dt, *J* = 10.9, 4.5, 1H), 4.67 (d, *J* = 5.7, 2H), 2.17–2.08 (m, 1H), 1.98–1.88 (m, 1H), 1.79–1.68 (m, 2H), 1.62–1.51 (m, 2H), 1.19–1.06 (m, 2H), 0.99–0.87 (m, 7H), 0.79 (d, *J* = 6.9, 3H);^{13}C NMR (125 MHz, $CDCl_3$): δ 166.6, 165.4, 138.2, 138.0, 133.7, 130.0, 129.0, 128.1, 128.0, 127.1, 75.5, 47.4, 44.5, 41.0, 34.4, 31.6, 26.7, 23.8, 22.2, 20.9, 16.7; IR (film): 3331, 3064, 3030, 2958, 2929, 2871, 1731, 1717, 1644 cm^{-1}; HRMS-ESI (*m/z*) $[M + H]^+$ calcd for $C_{25}H_{31}NO_3$, 394.23822; found 394.23619; $[a]^{24.4}_D$ –47.80° (*c* = 1.00, $CHCl_3$).

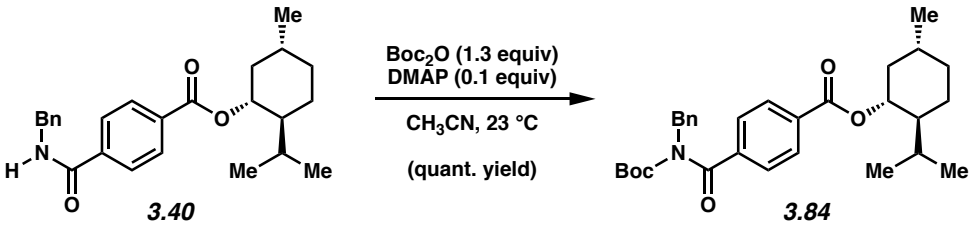

Ester 3.84. To a flask containing ester **3.40** (80.1 mg, 0.203 mmol, 1.0 equiv) was added DMAP (2.5 mg, 0.020 mmol, 0.1 equiv) followed by acetonitrile (2.0 mL, 0.1 M). Boc_2O (57.6 mg, 0.264 mmol, 1.3 equiv) was added in one portion and the reaction vessel was flushed with N_2, then the reaction mixture was allowed to stir at 23 °C for 48 h. The reaction was diluted with 5 mL deionized water, transferred to a separatory funnel with EtOAc (10 mL) and H_2O (10 mL), and extracted with EtOAc (3 x 20 mL). The organic layers were combined, dried over Na_2SO_4, and evaporated under reduced pressure. The resulting crude residue was purified by flash chromatography (24:1 Hexanes:EtOAc) to yield ester **3.84** (100.4 mg, quant. yield) as a colorless amorphous solid. Ester **3.84**: R_f 0.54 (5:1 Hexanes:EtOAc); ^{1}H NMR (500 MHz, $CDCl_3$): δ 8.09–8.02 (m, 2H), 7.59–7.52 (m, 2H), 7.45–7.38 (m, 2H), 7.37–7.31 (m, 2H), 7.31–7.27 (m, 1H), 5.00 (s, 2H), 4.93 (dt, *J* = 6.5, 4.4, 1H), 2.16–2.09 (m, 1H), 1.97–1.86 (m, 1H), 1.78–1.69 (m, 2H), 1.62–1.50 (m, 2H), 1.18–1.07 (m, 11H), 0.98–0.89 (m, 7H), 0.80–0.76 (m, 3H); ^{13}C NMR (125 MHz, $CDCl_3$): δ 172.4, 165.4, 153.2, 141.6, 137.7, 132.9, 129.5, 128.7, 128.3, 127.8, 127.3, 83.9, 75.5, 48.9, 47.4, 41.0, 34.4, 31.6, 27.6, 26.8, 23.9, 22.2, 20.8, 16.8; IR (film): 3064, 3036, 2958, 2930, 2874, 1734, 1716, 1679 cm^{-1}; HRMS-ESI (*m/z*) $[M + H]^+$ calcd for $C_{30}H_{40}NO_5$, 494.29065; found 494.28699; $[a]^{20.9}_D$ –37.80° (*c* = 1.00, $CHCl_3$).

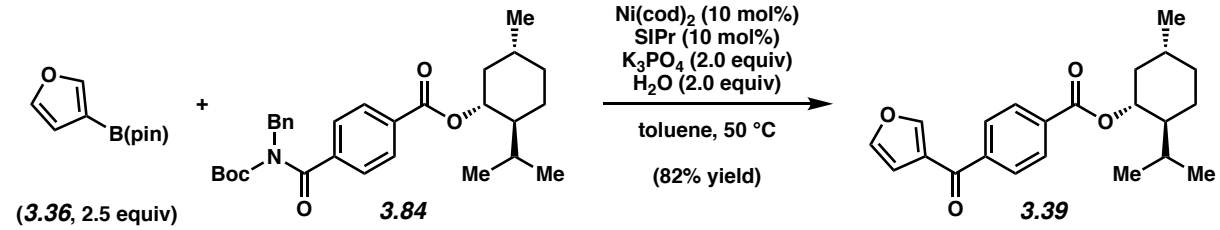

Ester 3.39. A 1-dram vial was charged with anhydrous powdered K_3PO_4 (86.2 mg, 0.407 mmol, 2.0 equiv) and a magnetic stir bar. The vial and contents were flame-dried under reduced pressure, then allowed to cool under N_2. Ester substrate **3.84** (100.4 mg, 0.203 mmol, 1.0 equiv) and furan-3-boronic acid pinacol ester (**3.36**) (98.6 mg, 0.508 mmol, 2.5 equiv) were added. The vial was flushed with N_2, then water (7.3 μL, 0.407 mmol, 2.0 equiv), which had been sparged with N_2 for 10 min, was added. The vial was taken into a glove box and charged with $Ni(cod)_2$ (5.6 mg, 0.020 mmol, 10 mol%) and SIPr (7.9 mg, 0.020 mmol, 10 mol%). Subsequently, toluene (0.20 mL, 1.0 M) was added. The vial was sealed with a Teflon-lined screw cap, removed from the glove box, and stirred vigorously (1,000 rpm) at 50 °C for 16 h. After cooling to 23 °C, the mixture was diluted with hexanes (0.5 mL) and filtered over a plug of silica gel (10 mL of EtOAc eluent). The volatiles were removed under reduced pressure, and the crude residue was purified by preparative thin-layer chromatography (5:1 Hexanes:EtOAc) to yield ester **3.39** (59.2 mg, 82% yield) as a white solid. Ester **3.39**: R_f 0.48 (5:1 Hexanes:EtOAc); ^{1}H NMR (500 MHz, $CDCl_3$): δ 8.18–8.13 (m, 2H), 7.94–7.86 (m, 3H), 7.55–7.52 (m, 1H), 6.93–6.90 (m, 1), 4.97 (dt, J = 10.9, 4.4, 1H), 2.19–2.11 (m, 1H), 2.00–1.91 (m, 1H), 1.79–1.71 (m, 2H), 1.63–1.55 (m, 2H), 1.20–1.08 (m, 2H), 1.00–0.90 (m, 7H), 0.81 (d, J = 7.0, 3H); ^{13}C NMR (125 MHz, $CDCl_3$): δ 189.0, 165.4, 149.0, 144.4, 142.3, 134.3, 129.9, 128.8, 126.6, 110.2, 75.6, 47.4, 41.1, 34.4, 31.6, 26.7, 23.8, 22.2, 20.9, 16.7; IR (film): 2955, 2929, 2870, 1714, 1653 cm^{-1}; HRMS-ESI (*m/z*) $[M + H]^+$ calcd for $C_{22}H_{27}O_4$, 355.19093; found 355.18780; $[a]^{21.9}_D$ –69.20° (c = 0.500, $CHCl_3$).

3.8 Spectra Relevant to Chapter Three:

Nickel-Catalyzed Suzuki–Miyaura Coupling of Amides

Nicholas A. Weires, Emma L. Baker, and Neil K. Garg.

Nat. Chem. **2016**, *8*, 75–79.

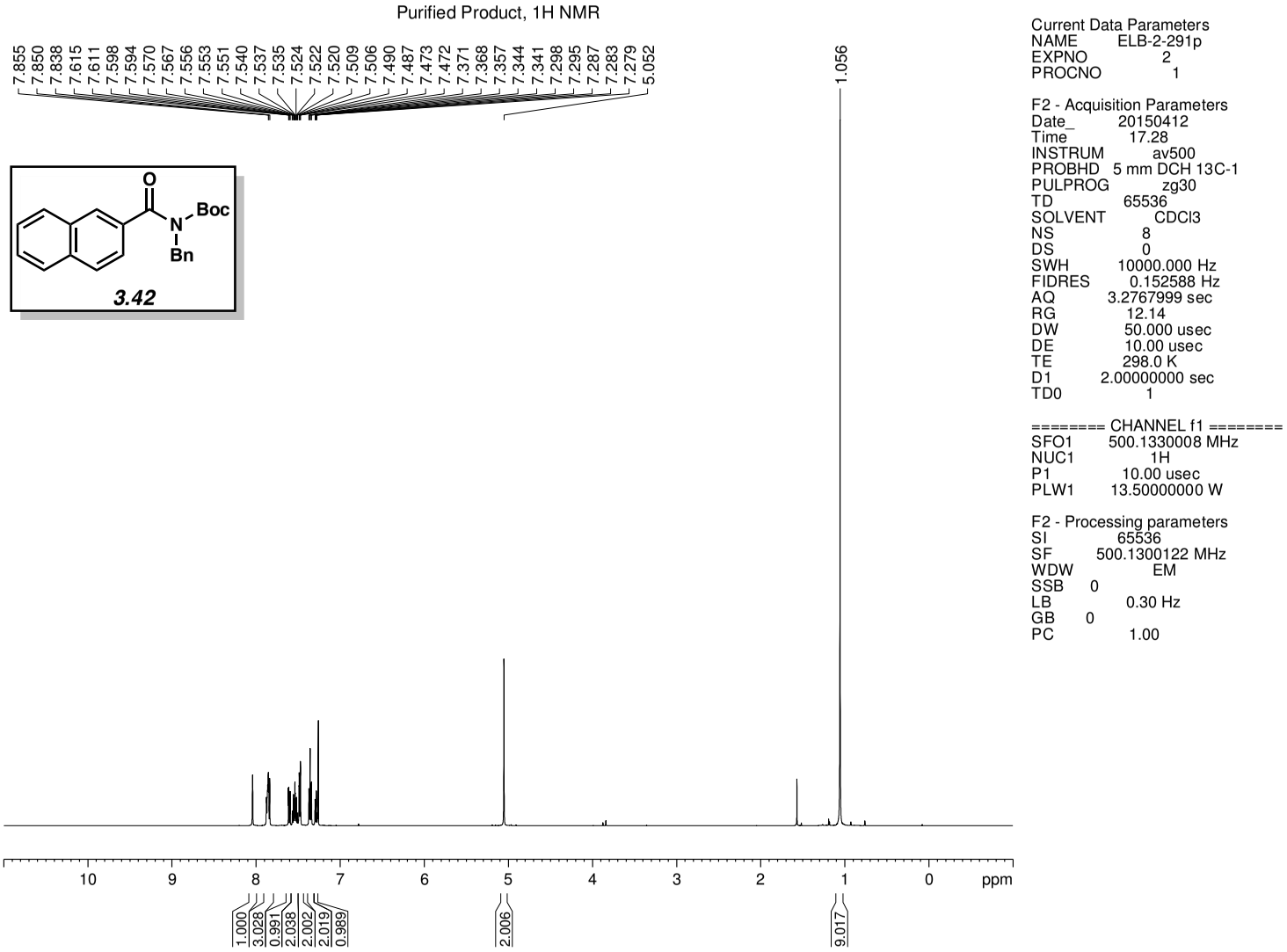

Figure 3.3 ^{1}H NMR (500 MHz, $CDCl_3$) of compound **3.42**.

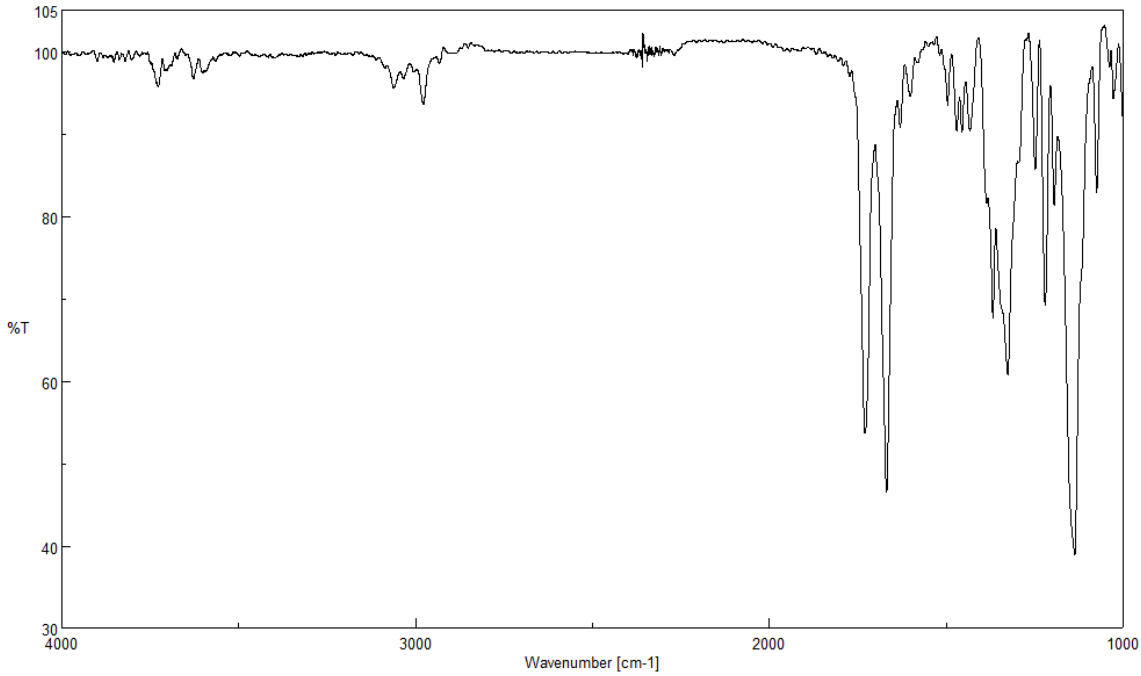

Figure 3.4 Infrared spectrum of compound **3.42**.

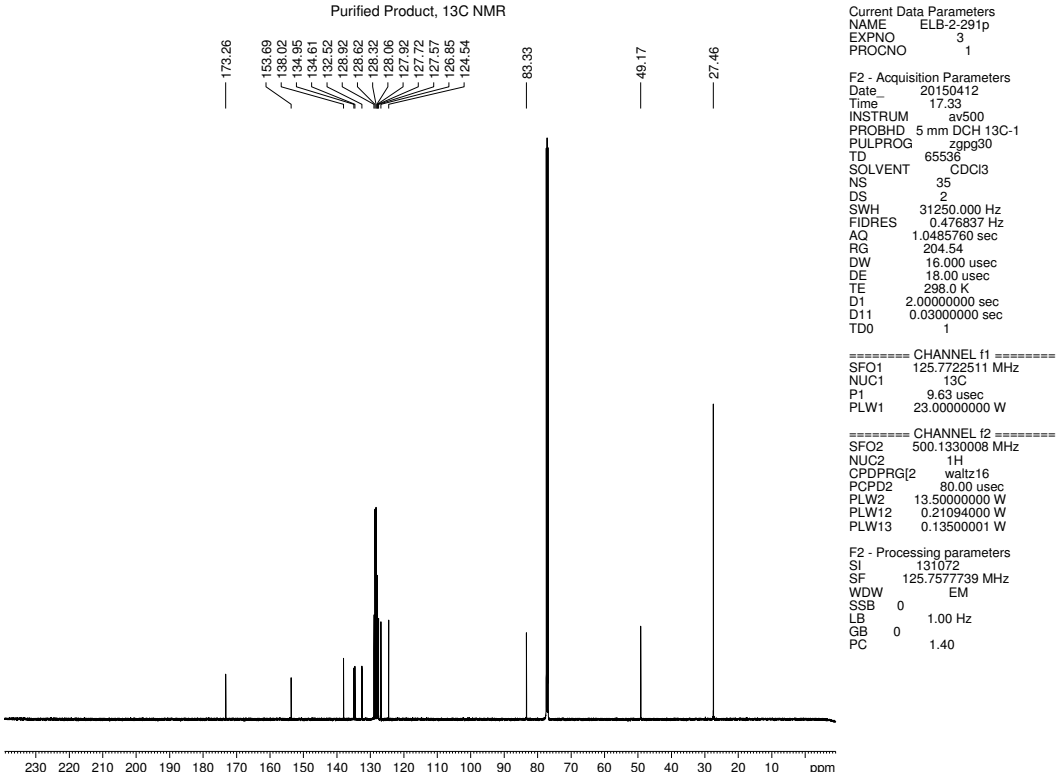

Figure 3.5 ^{13}C NMR (125 MHz, $CDCl_3$) of compound **3.42**.

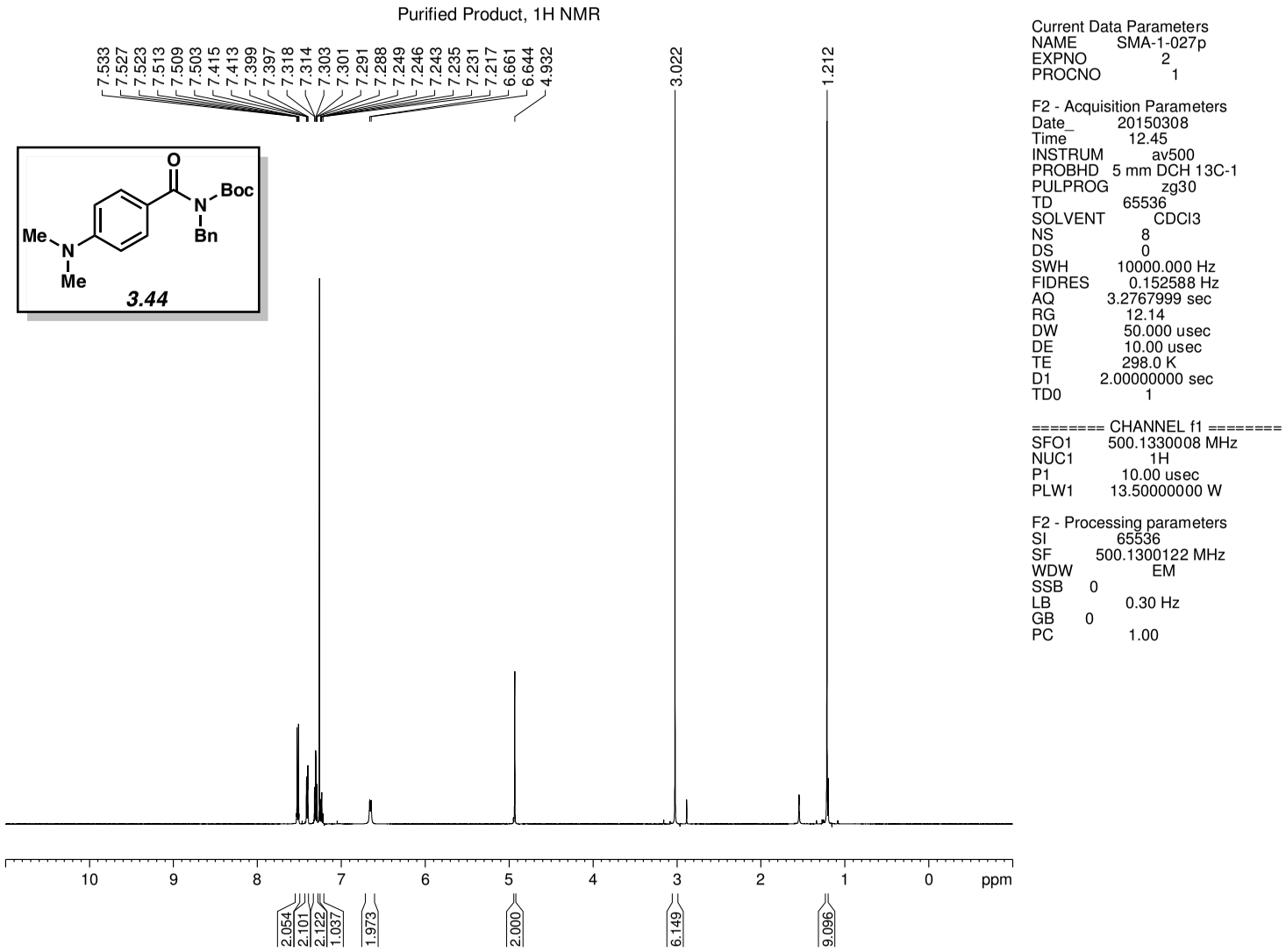

Figure 3.6 ^{1}H NMR (500 MHz, $CDCl_3$) of compound **3.44**.

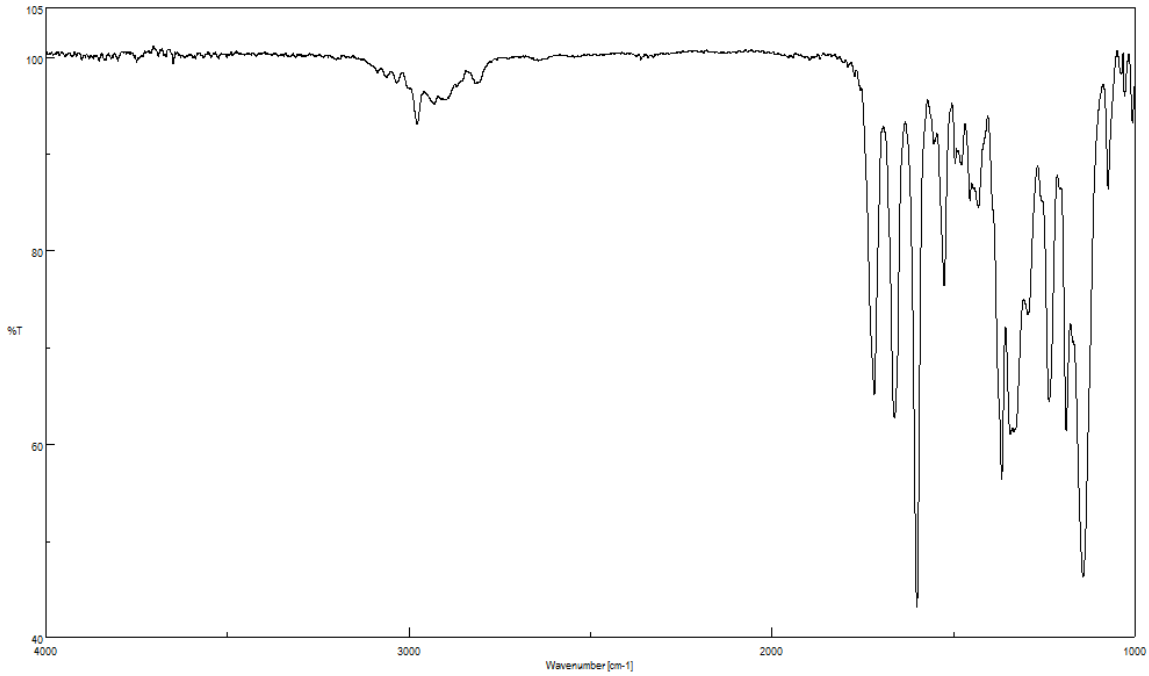

Figure 3.7 Infrared spectrum of compound **3.44**.

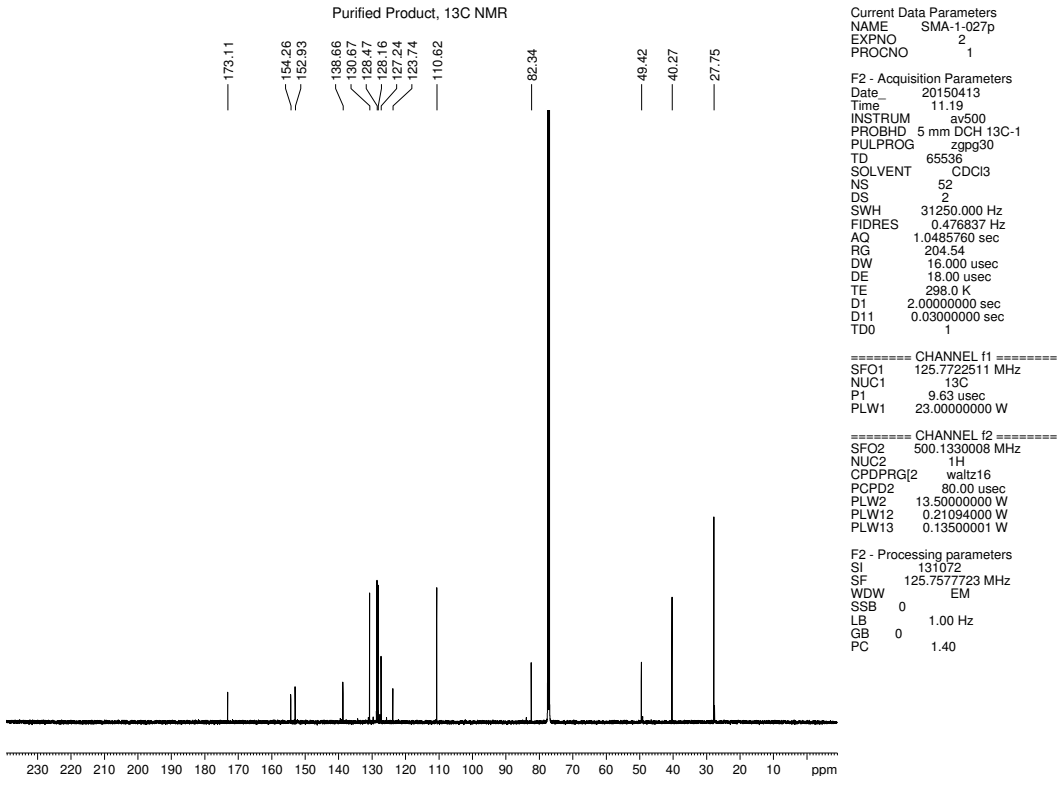

Figure 3.8 ^{13}C NMR (125 MHz, $CDCl_3$) of compound **3.44**.

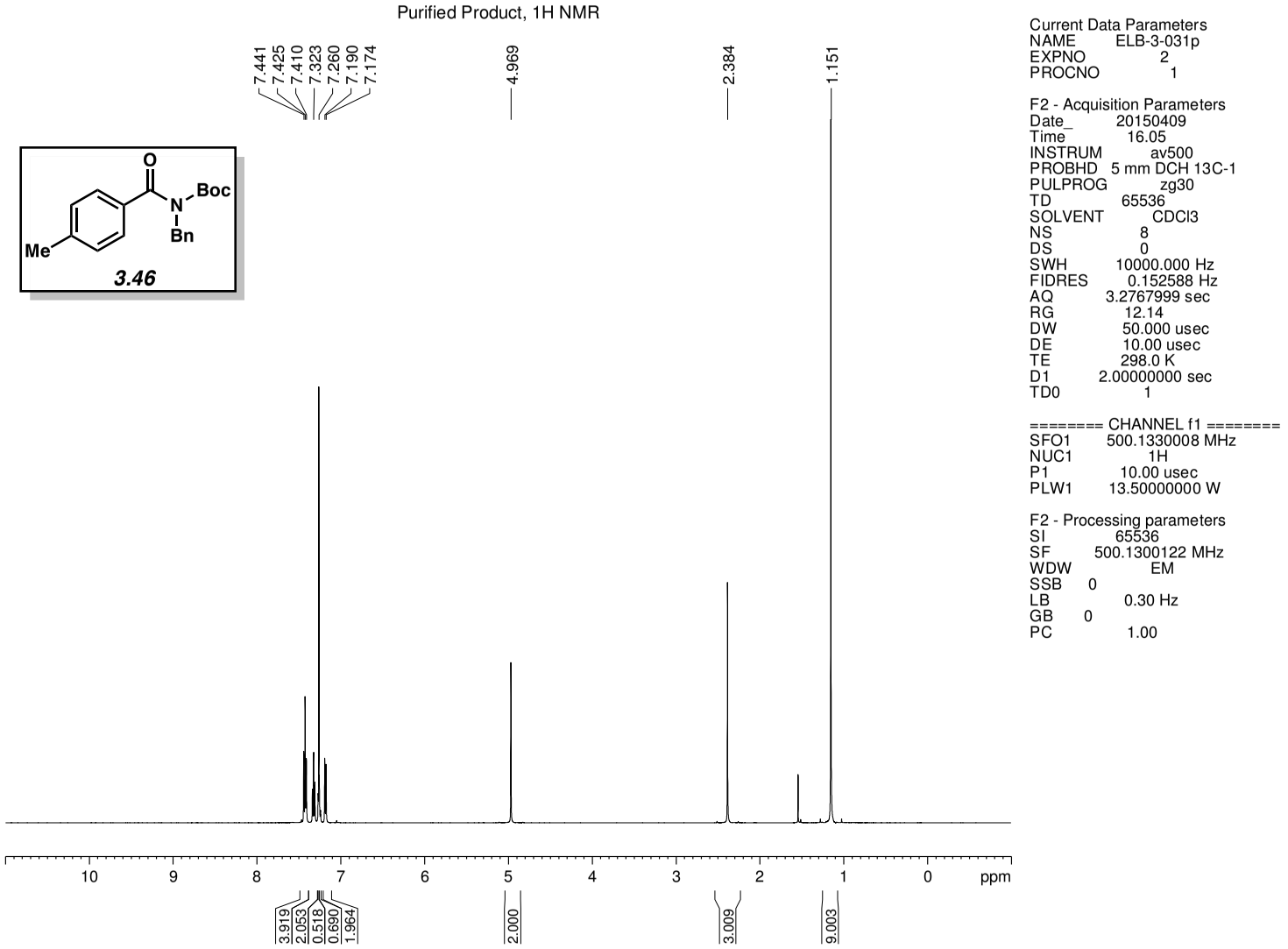

Figure 3.9 ^{1}H NMR (500 MHz, $CDCl_3$) of compound **3.46**.

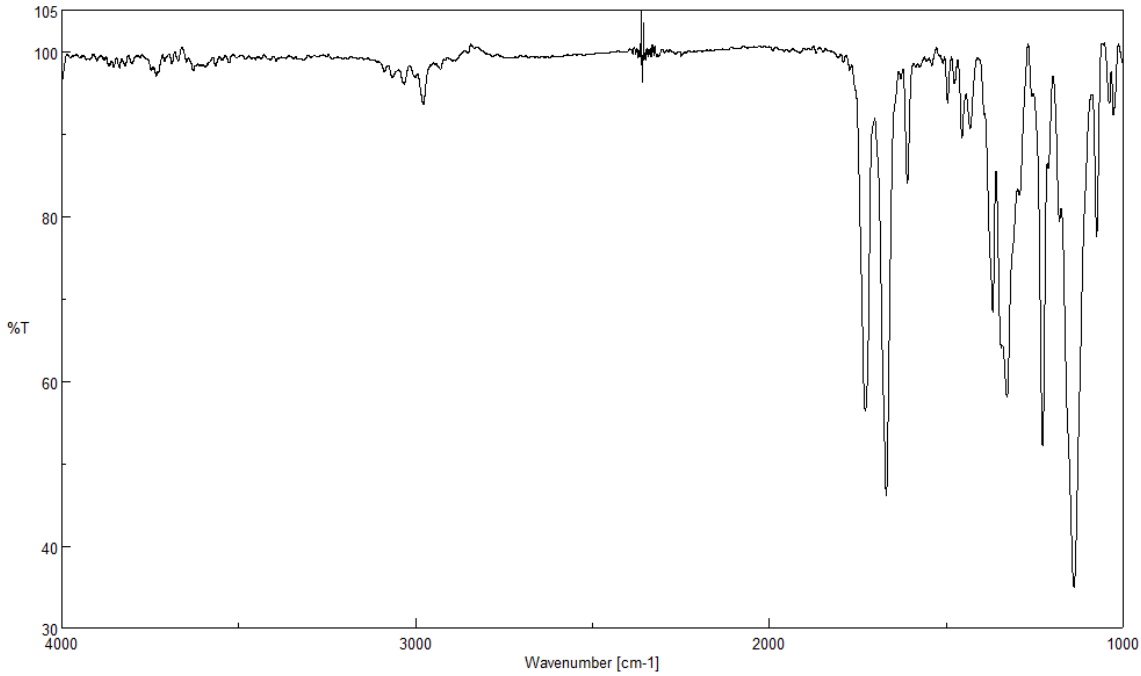

Figure 3.10 Infrared spectrum of compound **3.46**.

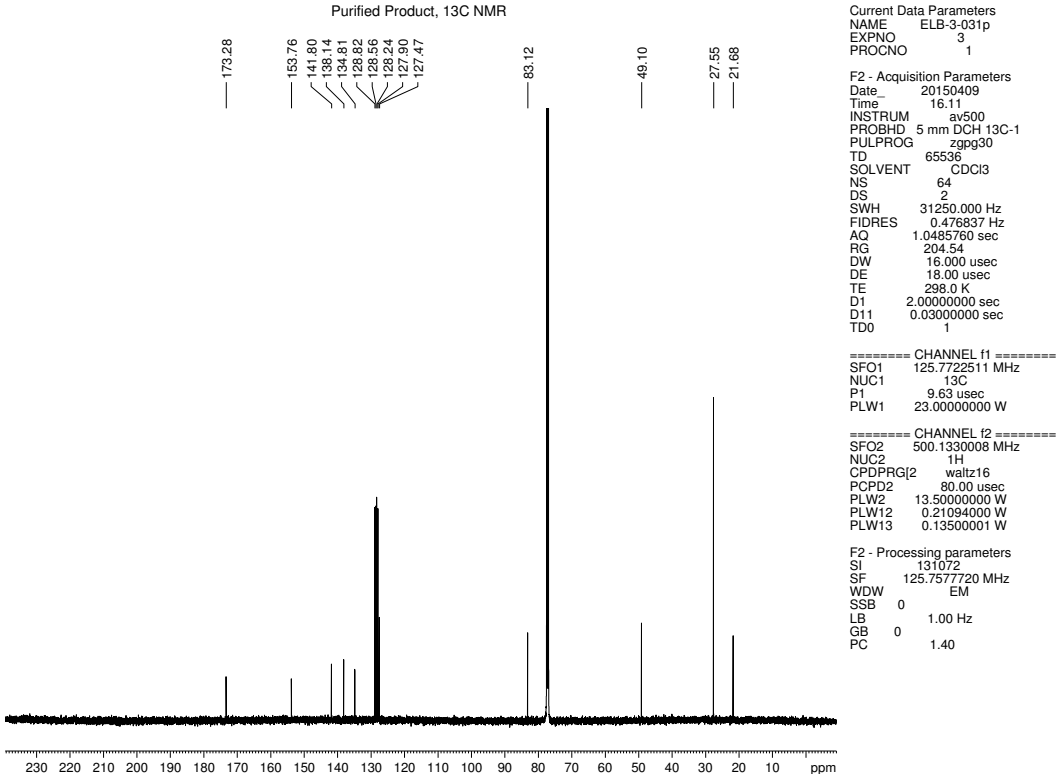

Figure 3.11 ^{13}C NMR (125 MHz, $CDCl_3$) of compound **3.46**.

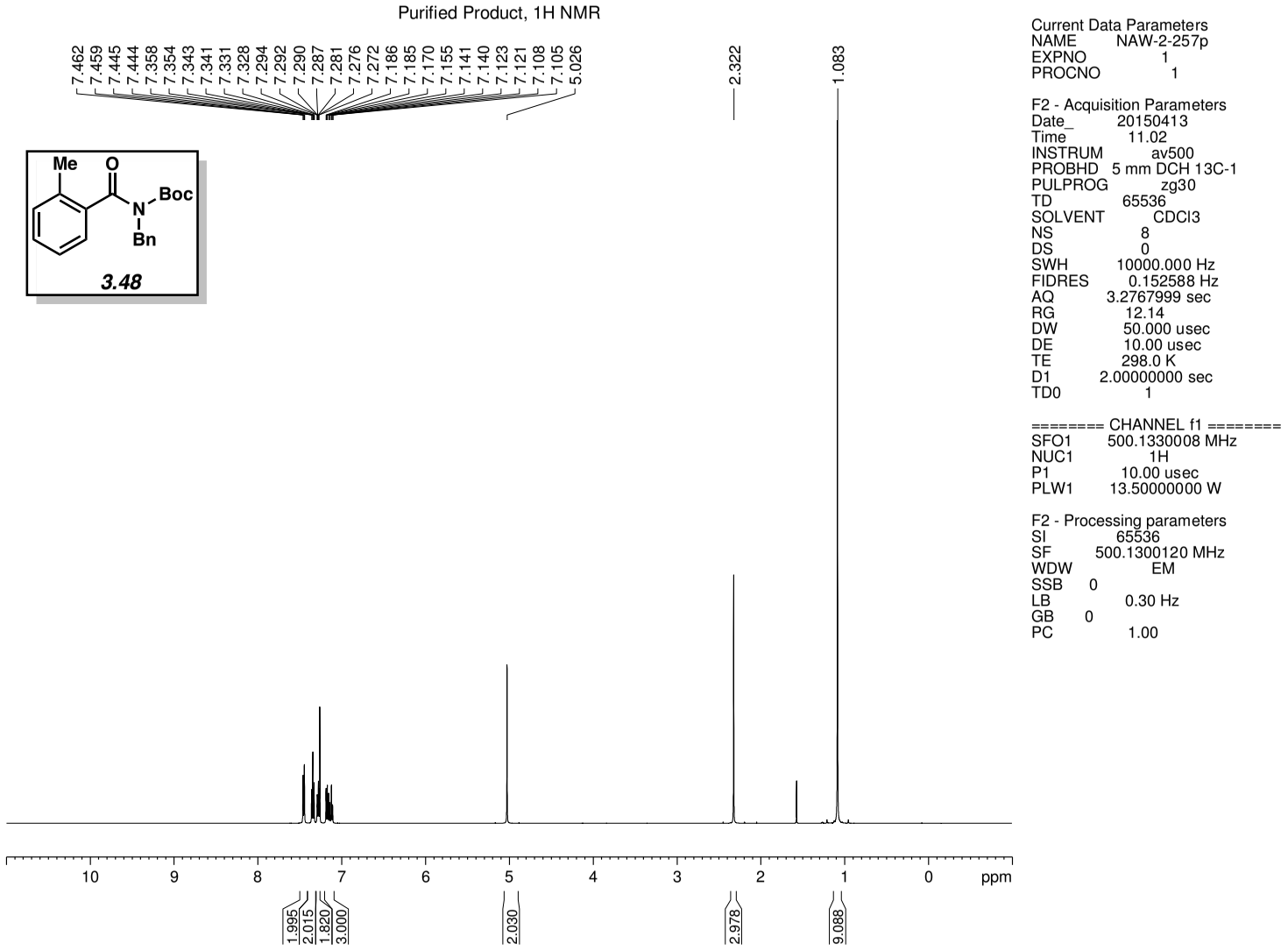

Figure 3.12 ^{1}H NMR (500 MHz, $CDCl_3$) of compound **3.48**.

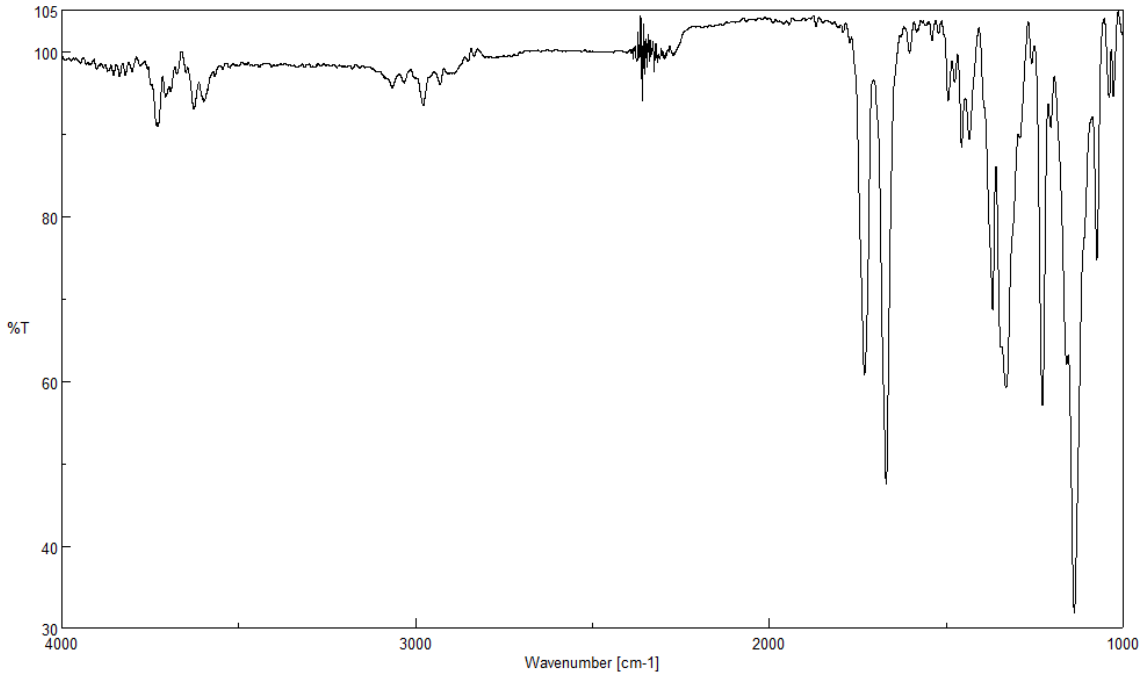

Figure 3.13 Infrared spectrum of compound **3.48**.

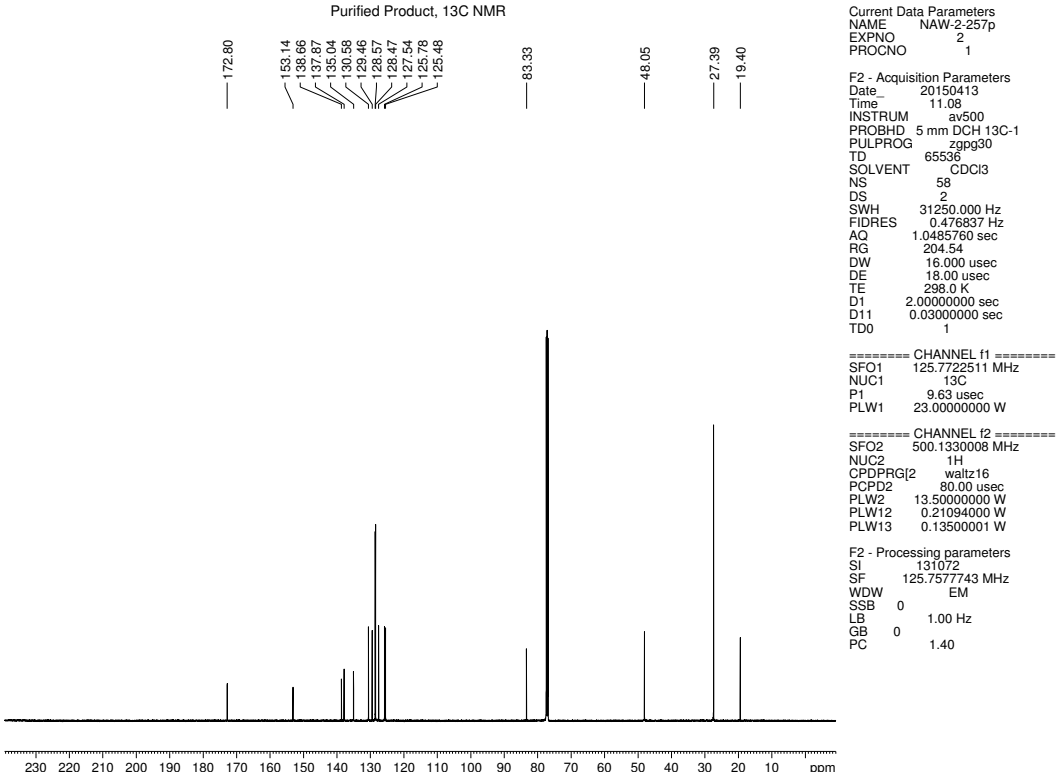

Figure 3.14 ^{13}C NMR (125 MHz, $CDCl_3$) of compound **3.48**.

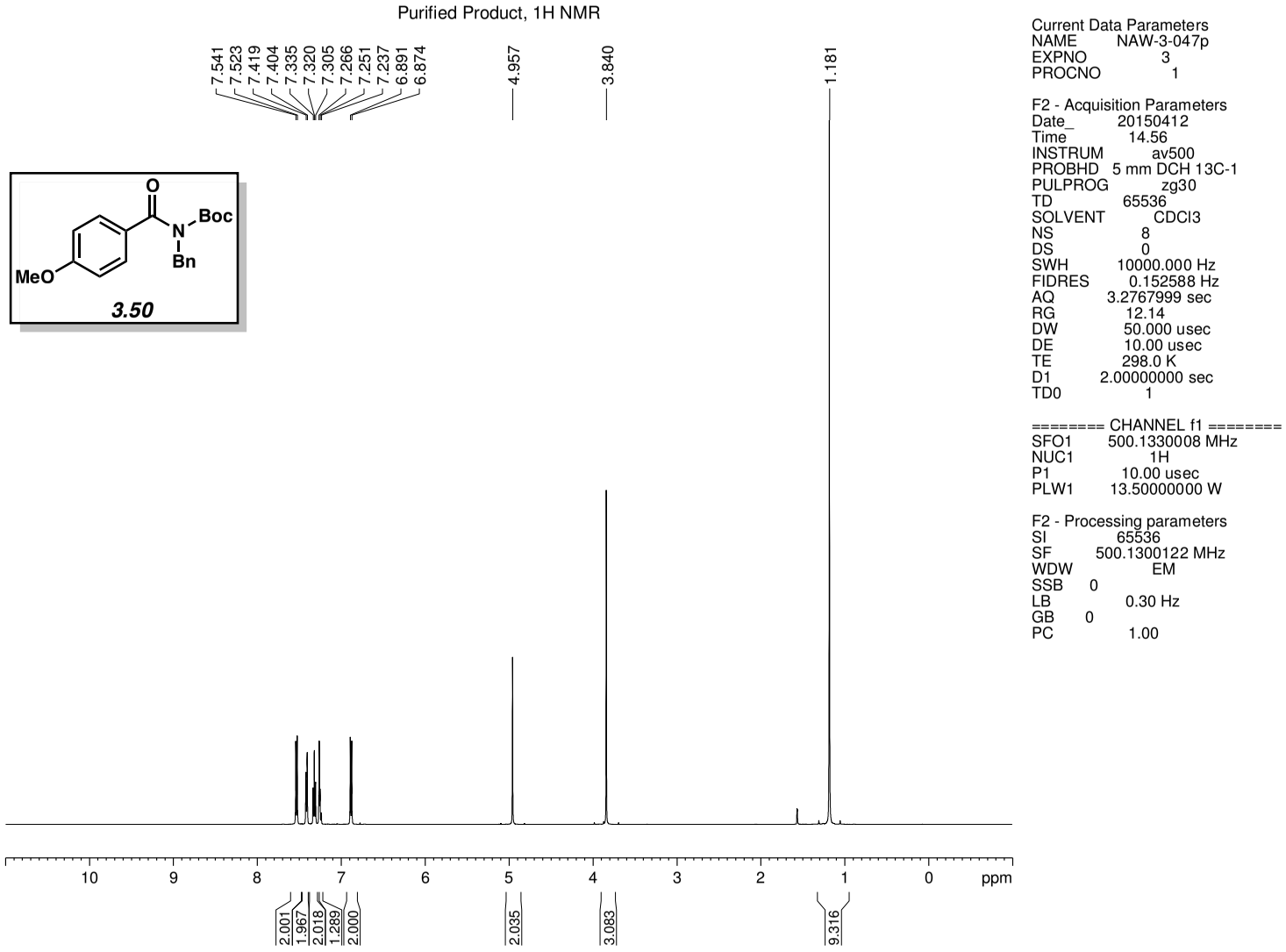

Figure 3.15 ^{1}H NMR (500 MHz, $CDCl_3$) of compound **3.50**.

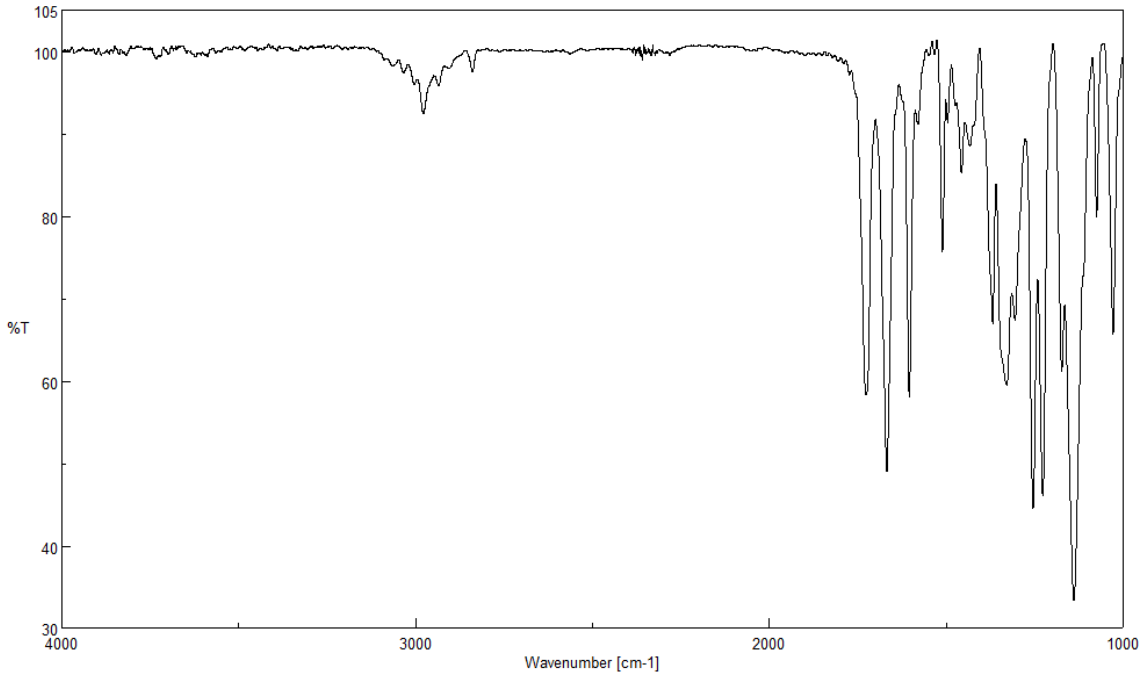

Figure 3.16 Infrared spectrum of compound **3.50**.

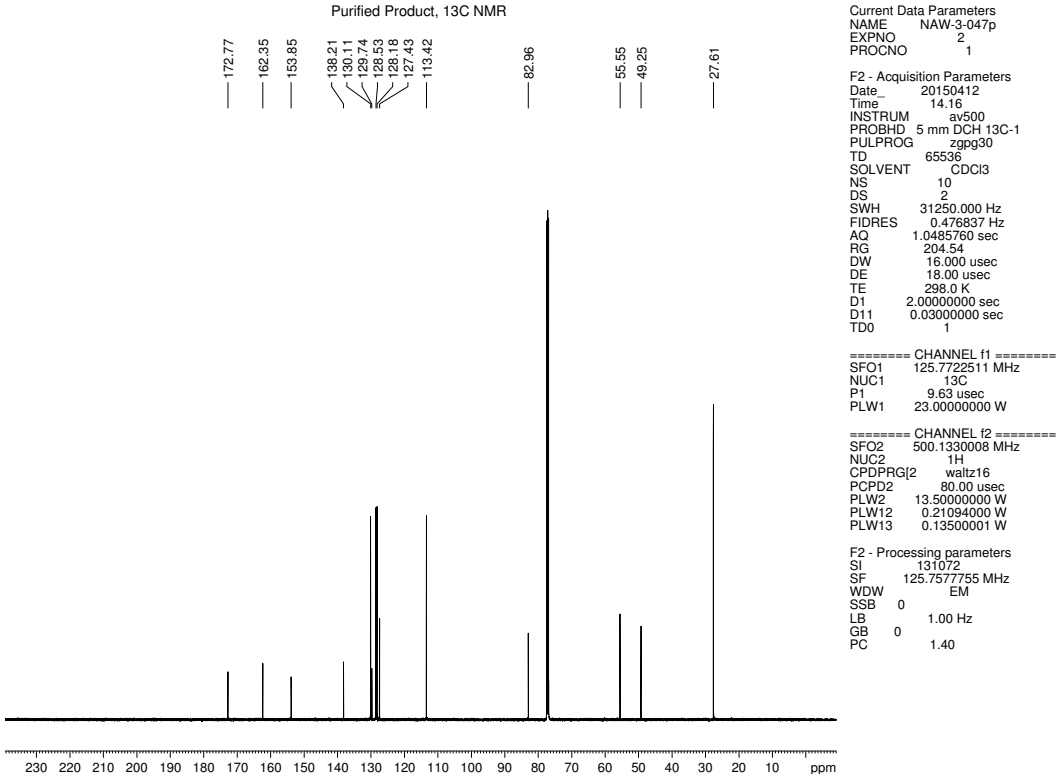

Figure 3.17 ^{13}C NMR (125 MHz, $CDCl_3$) of compound **3.50**.

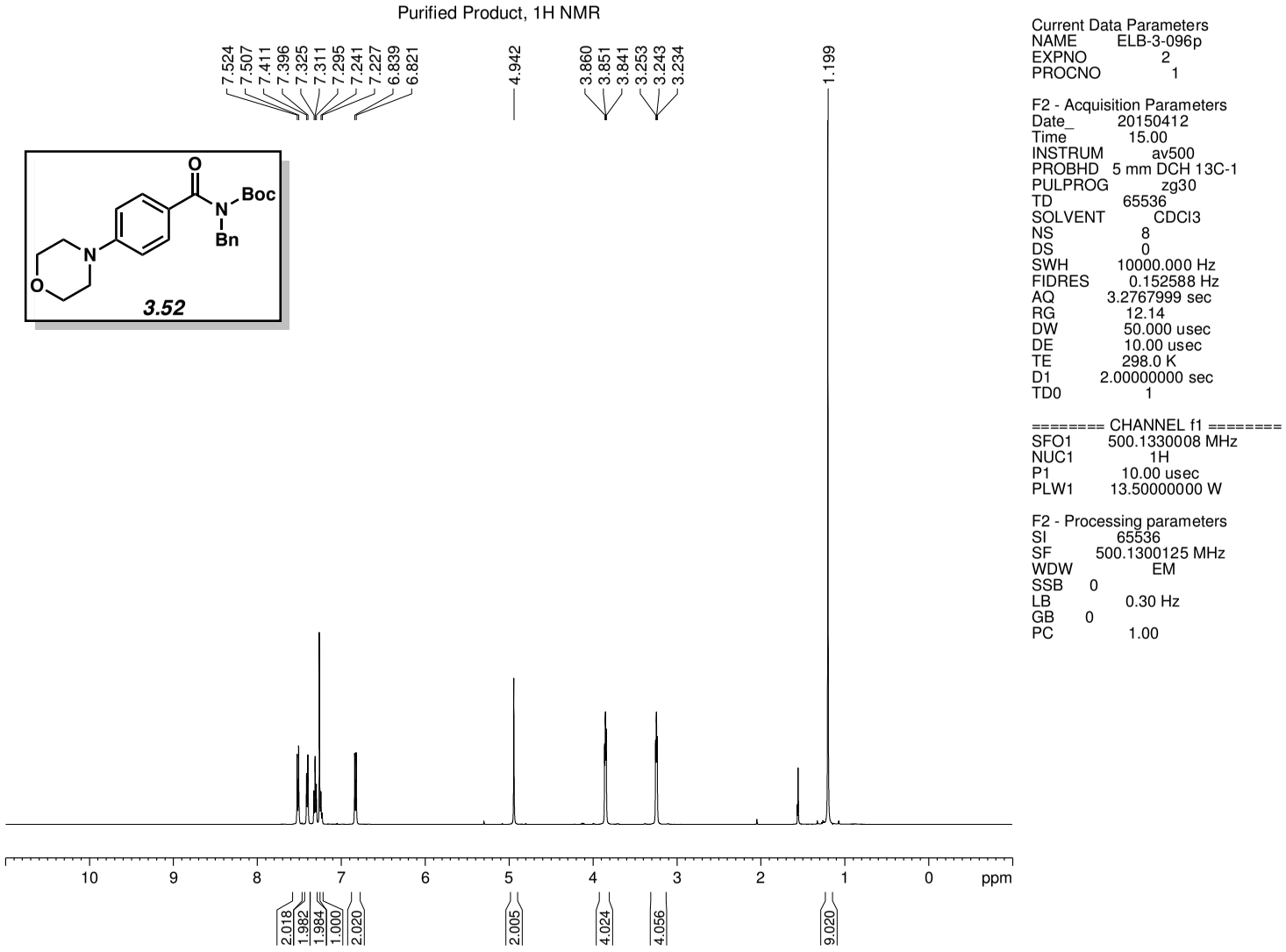

Figure 3.18 ^{1}H NMR (500 MHz, $CDCl_3$) of compound **3.52**.

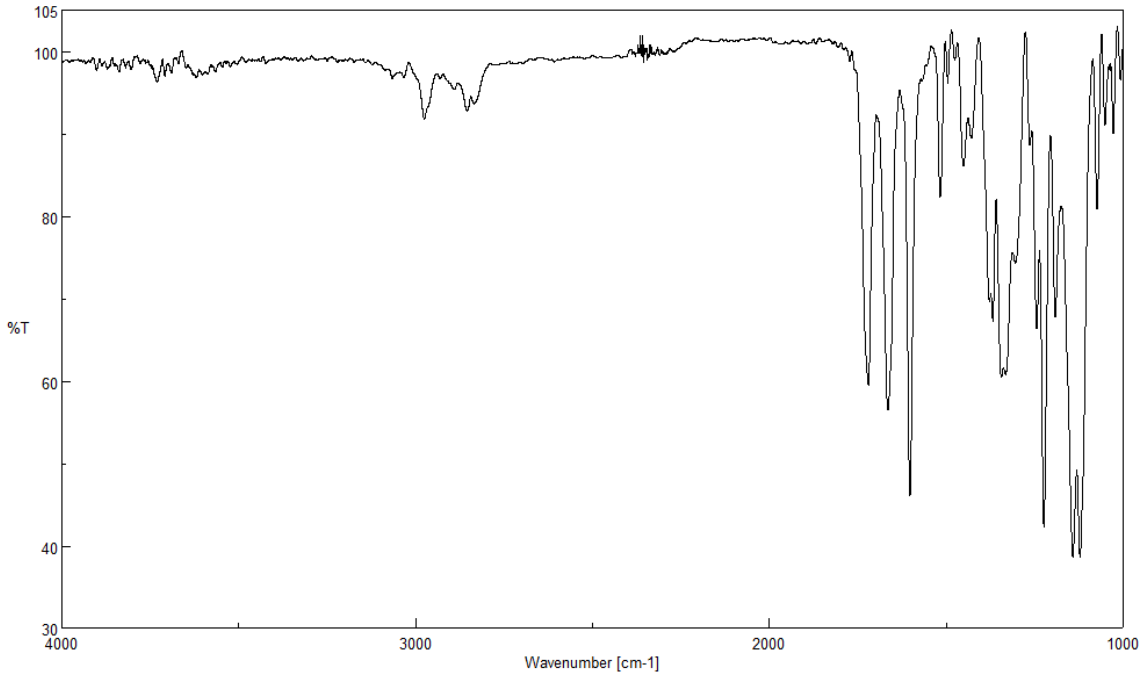

Figure 3.19 Infrared spectrum of compound **3.52**.

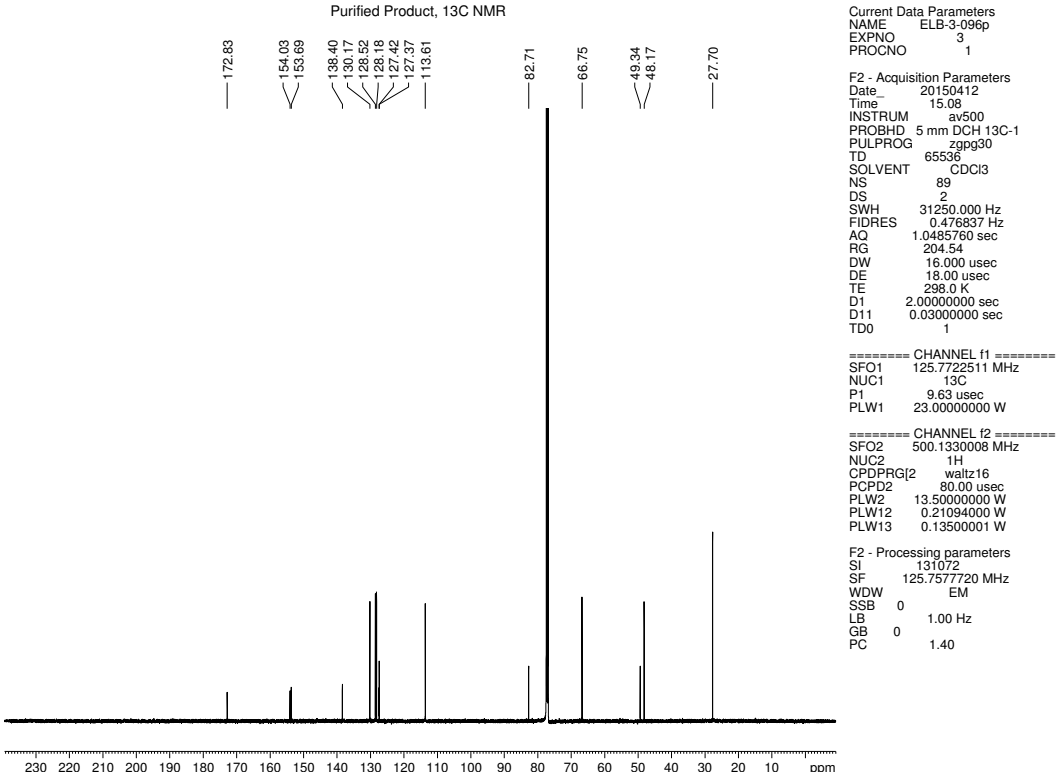

Figure 3.20 ^{13}C NMR (125 MHz, $CDCl_3$) of compound **3.52**.

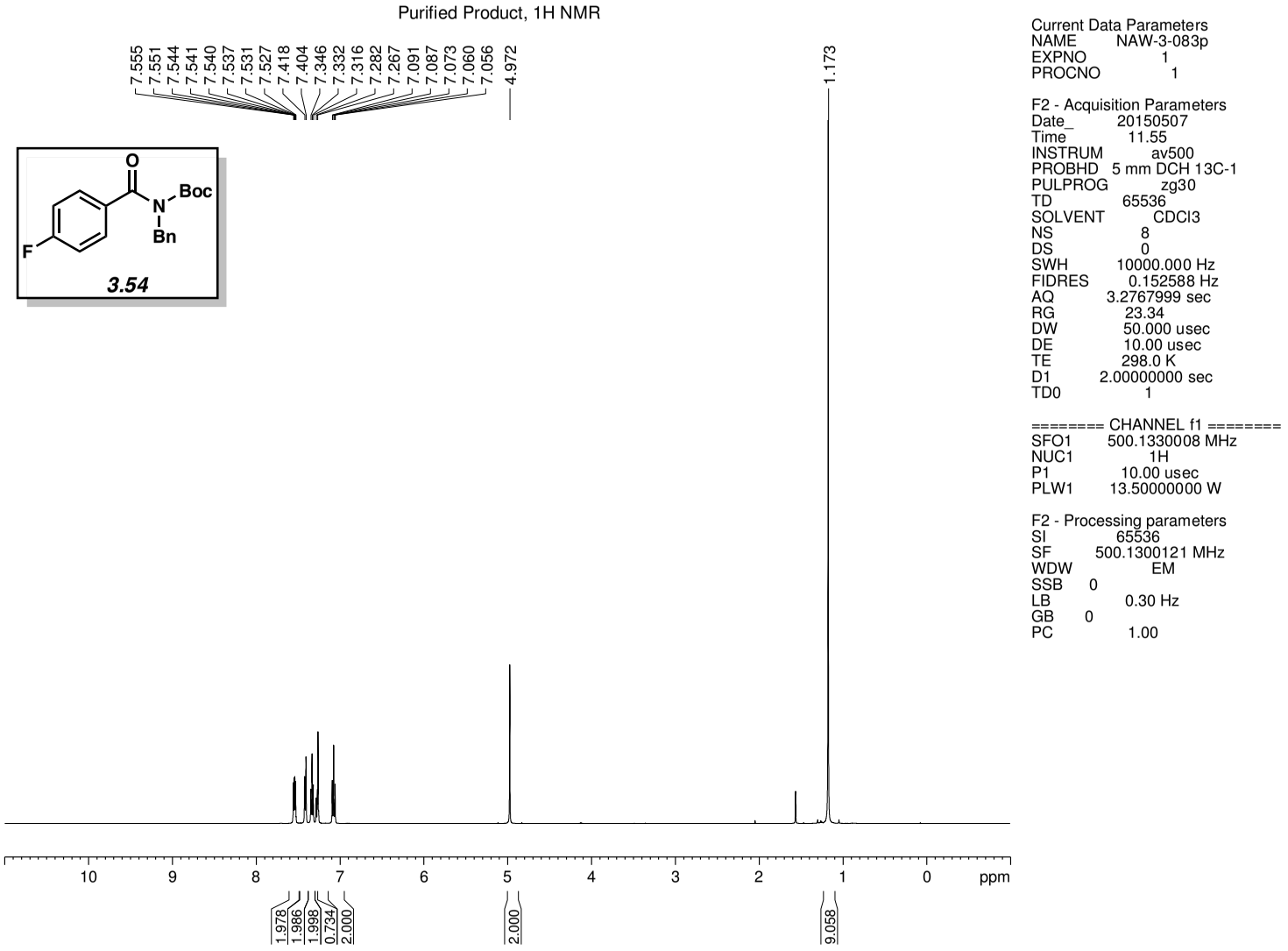

Figure 3.21 ^{1}H NMR (500 MHz, $CDCl_3$) of compound **3.54**.

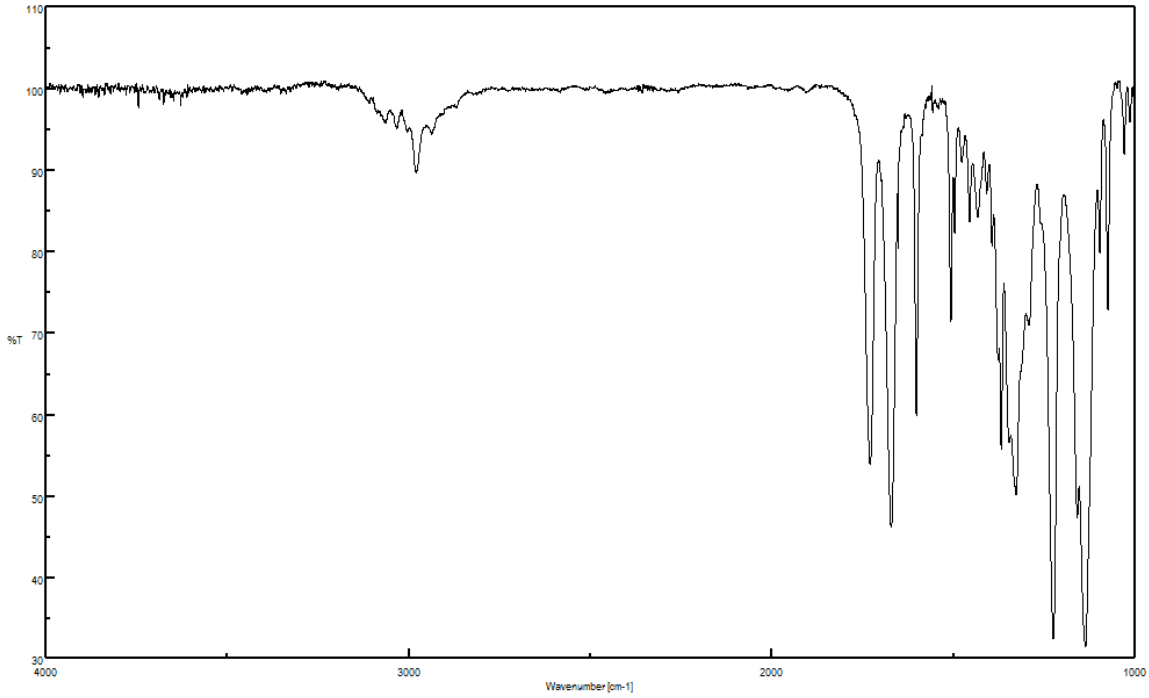

Figure 3.22 Infrared spectrum of compound **3.54**.

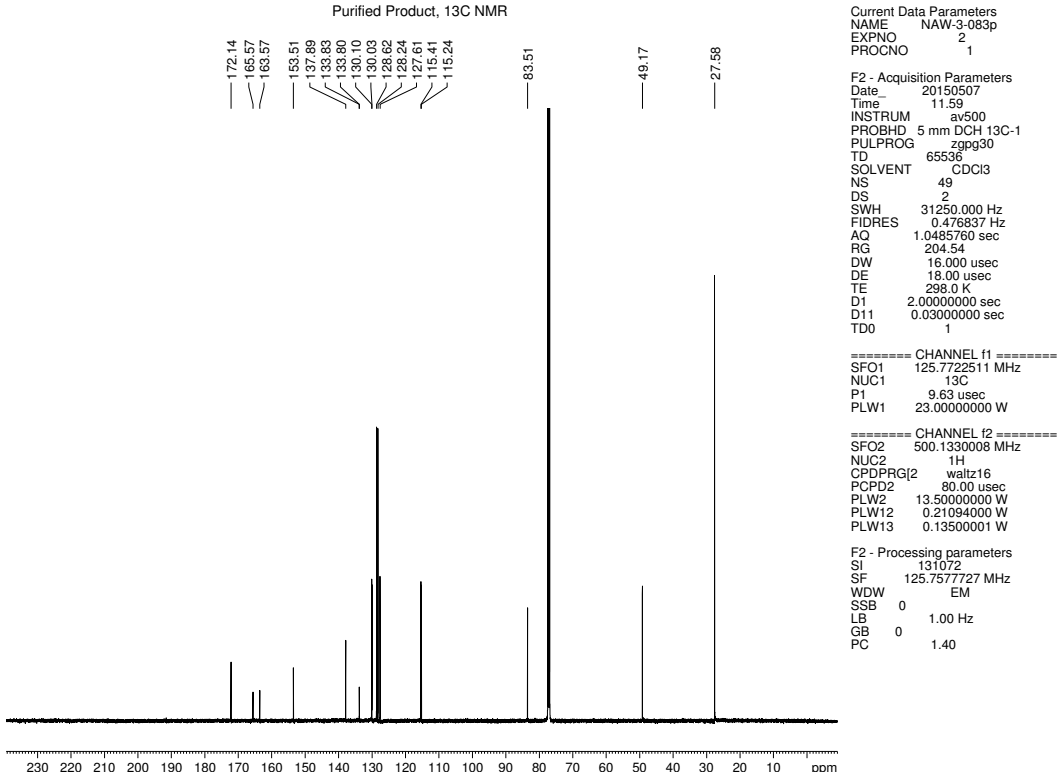

Figure 3.23 ^{13}C NMR (125 MHz, $CDCl_3$) of compound **3.54**.

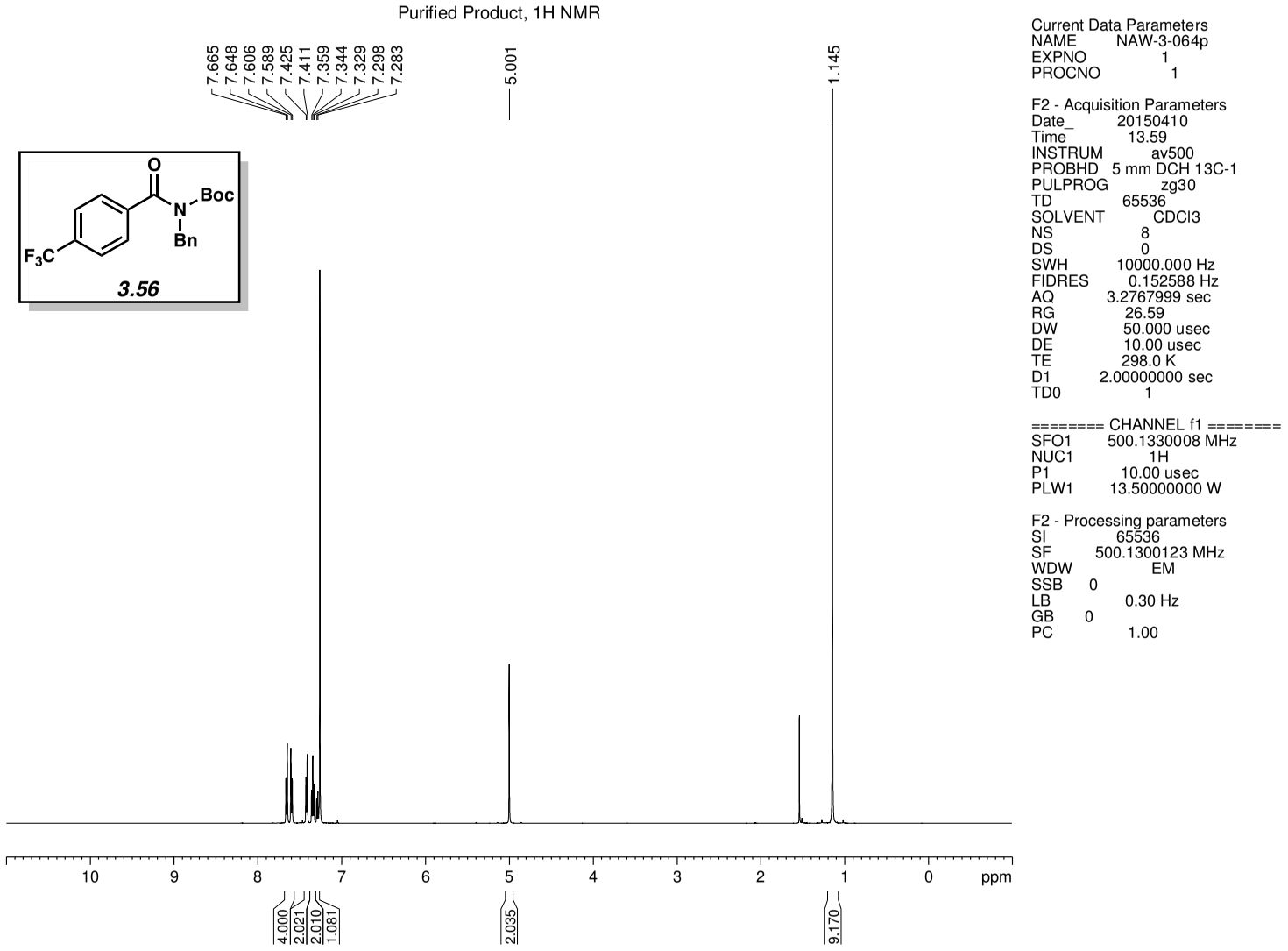

Figure 3.24 ^{1}H NMR (500 MHz, $CDCl_3$) of compound **3.56**.

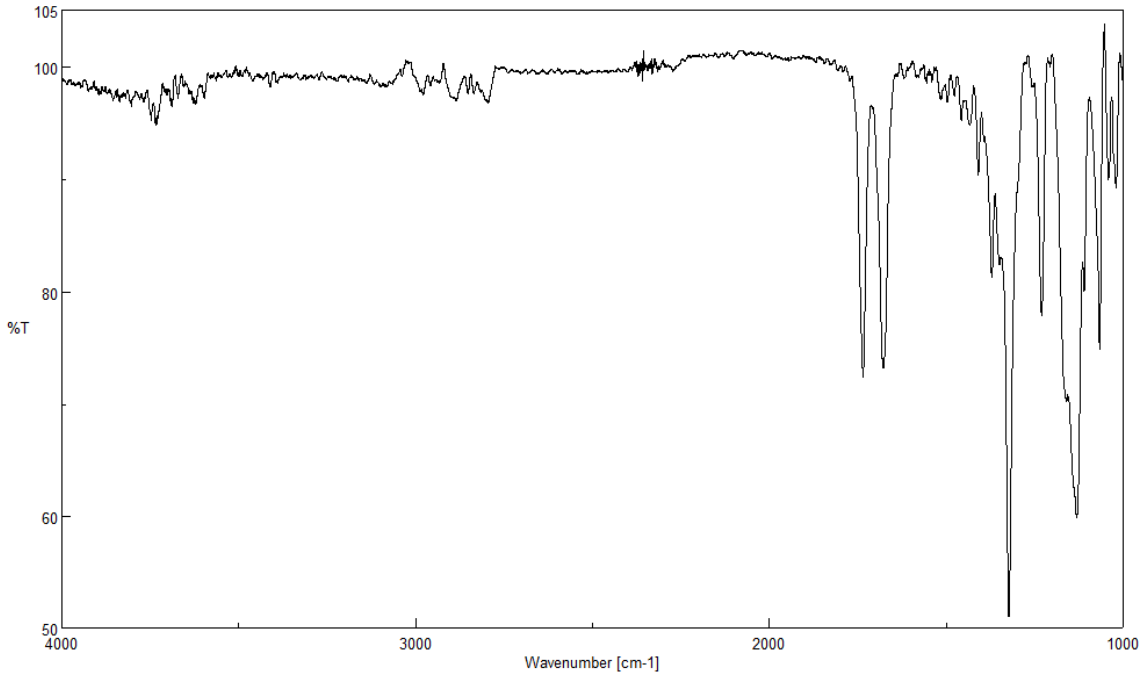

Figure 3.25 Infrared spectrum of compound **3.56**.

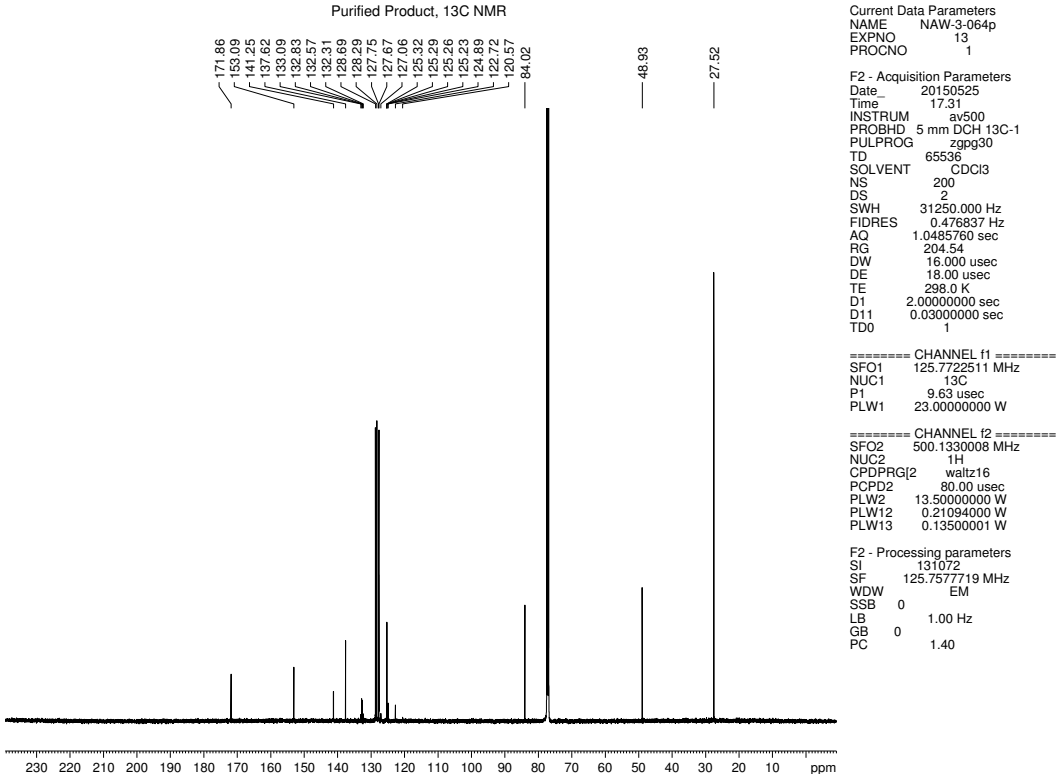

Figure 3.26 ^{13}C NMR (125 MHz, $CDCl_3$) of compound **3.56**.

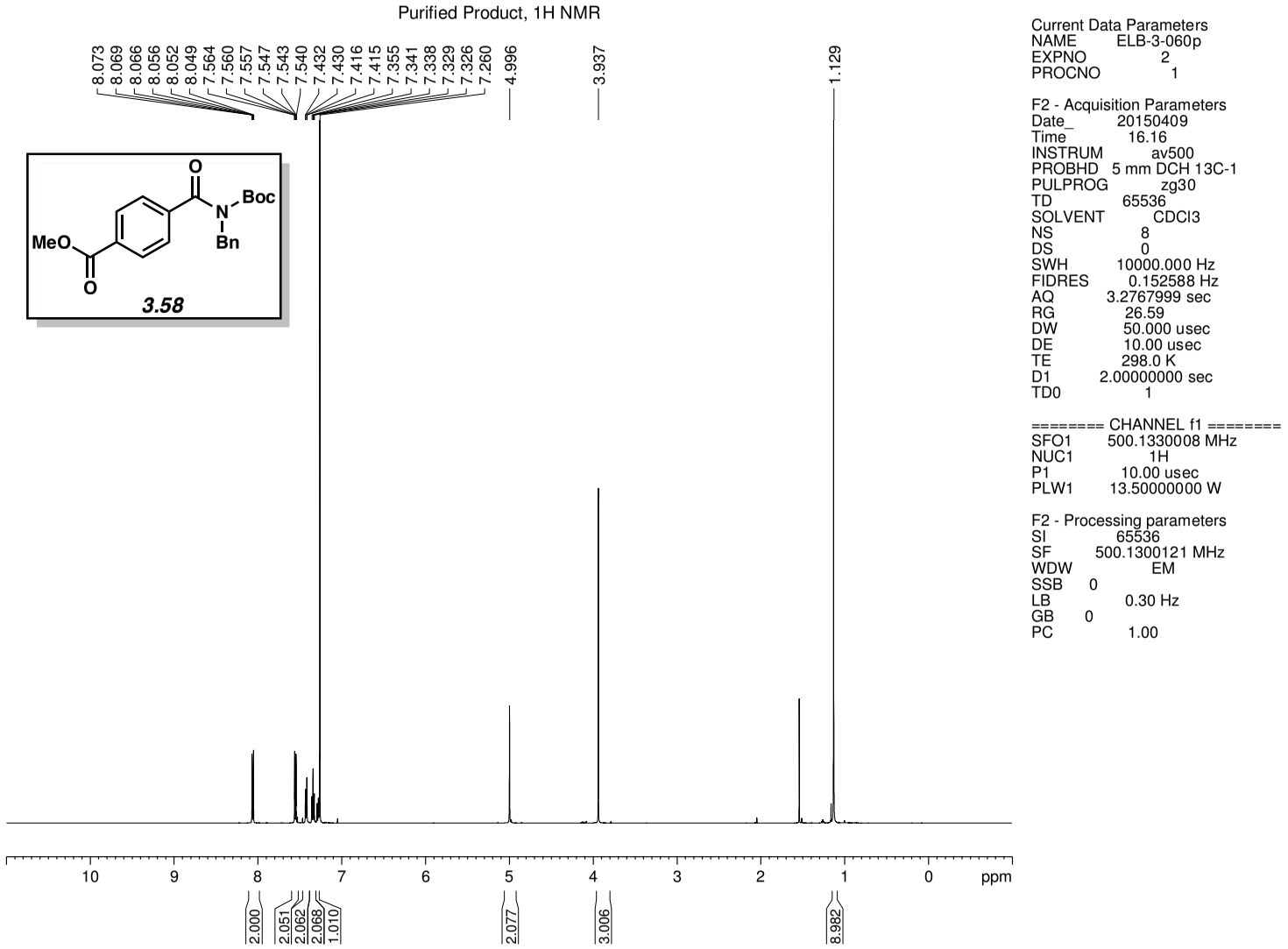

Figure 3.27 ^{1}H NMR (500 MHz, $CDCl_3$) of compound **3.58**.

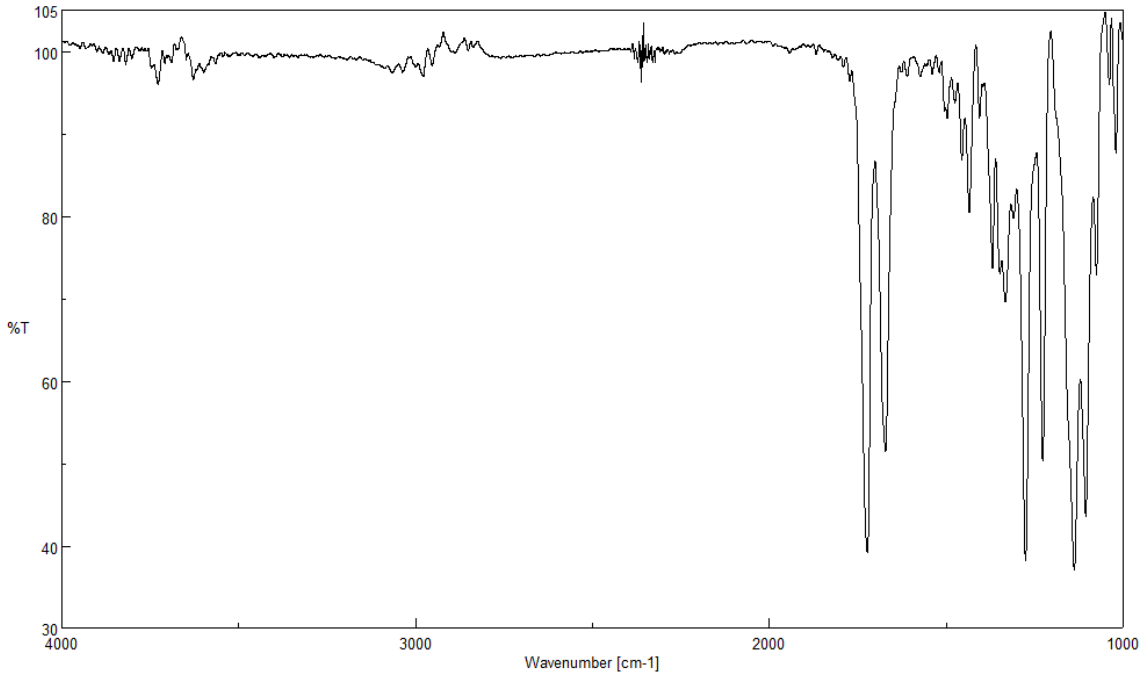

Figure 3.28 Infrared spectrum of compound **3.58**.

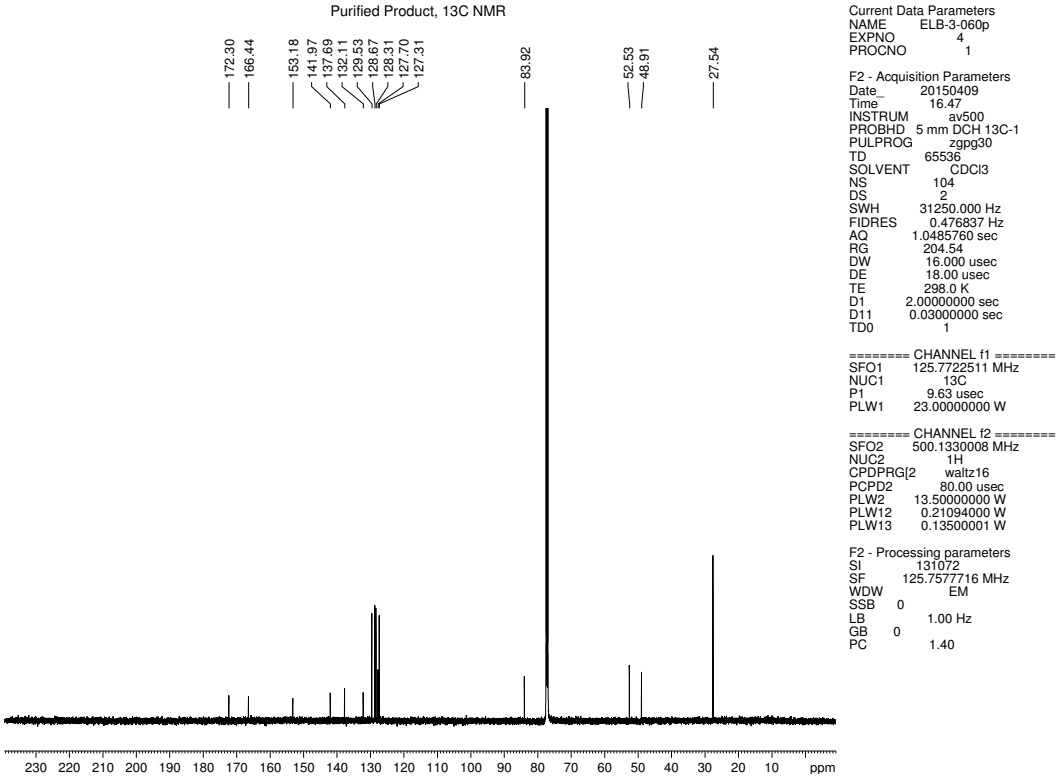

Figure 3.29 ^{13}C NMR (125 MHz, $CDCl_3$) of compound **3.58**.

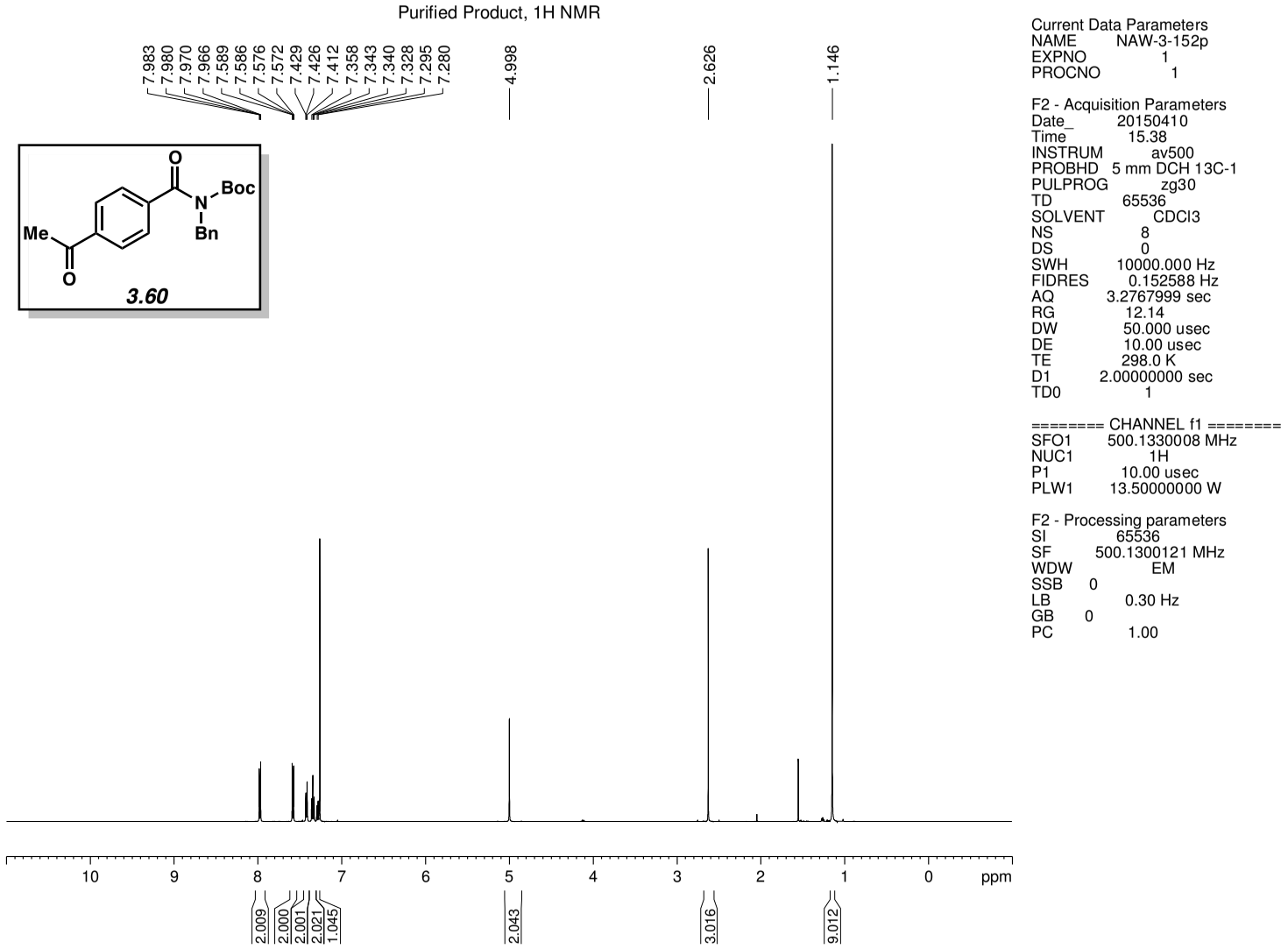

Figure 3.30 ^{1}H NMR (500 MHz, $CDCl_3$) of compound **3.60**.

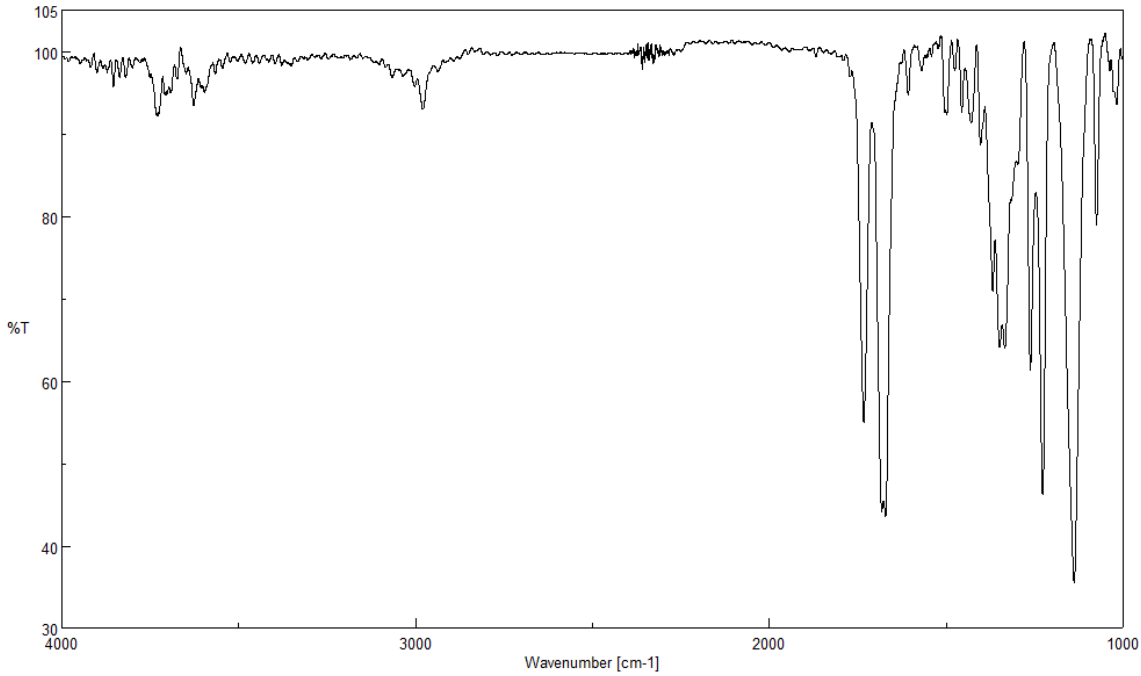

Figure 3.31 Infrared spectrum of compound **3.60**.

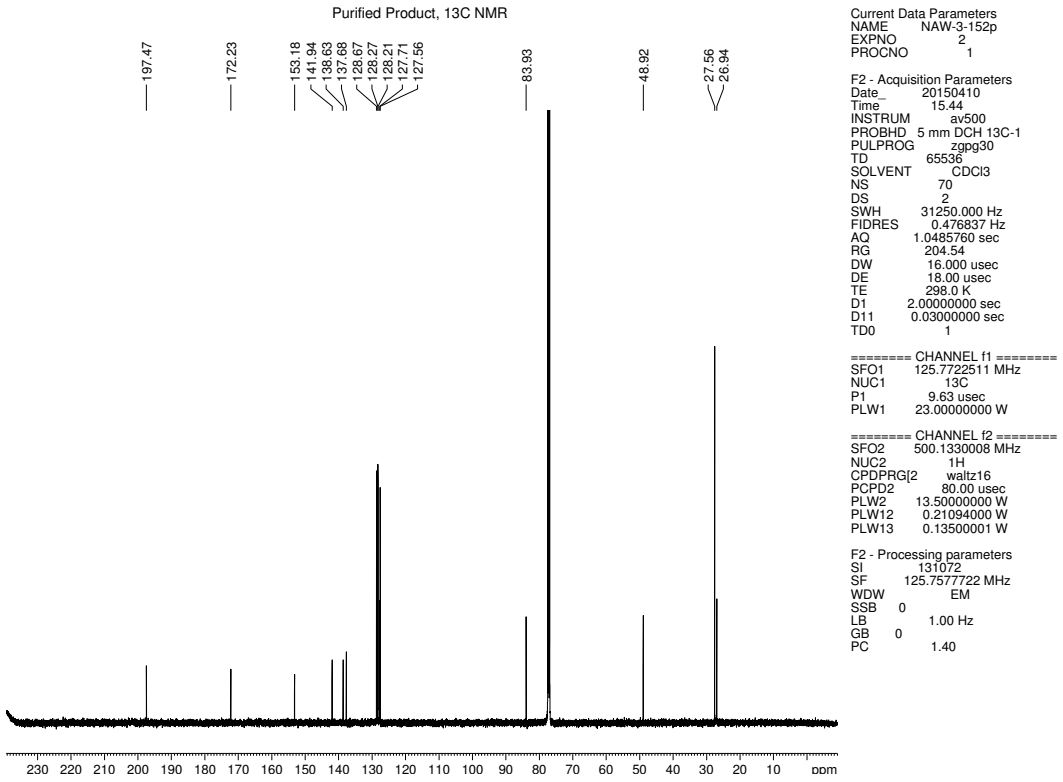

Figure 3.32 ^{13}C NMR (125 MHz, $CDCl_3$) of compound **3.60**.

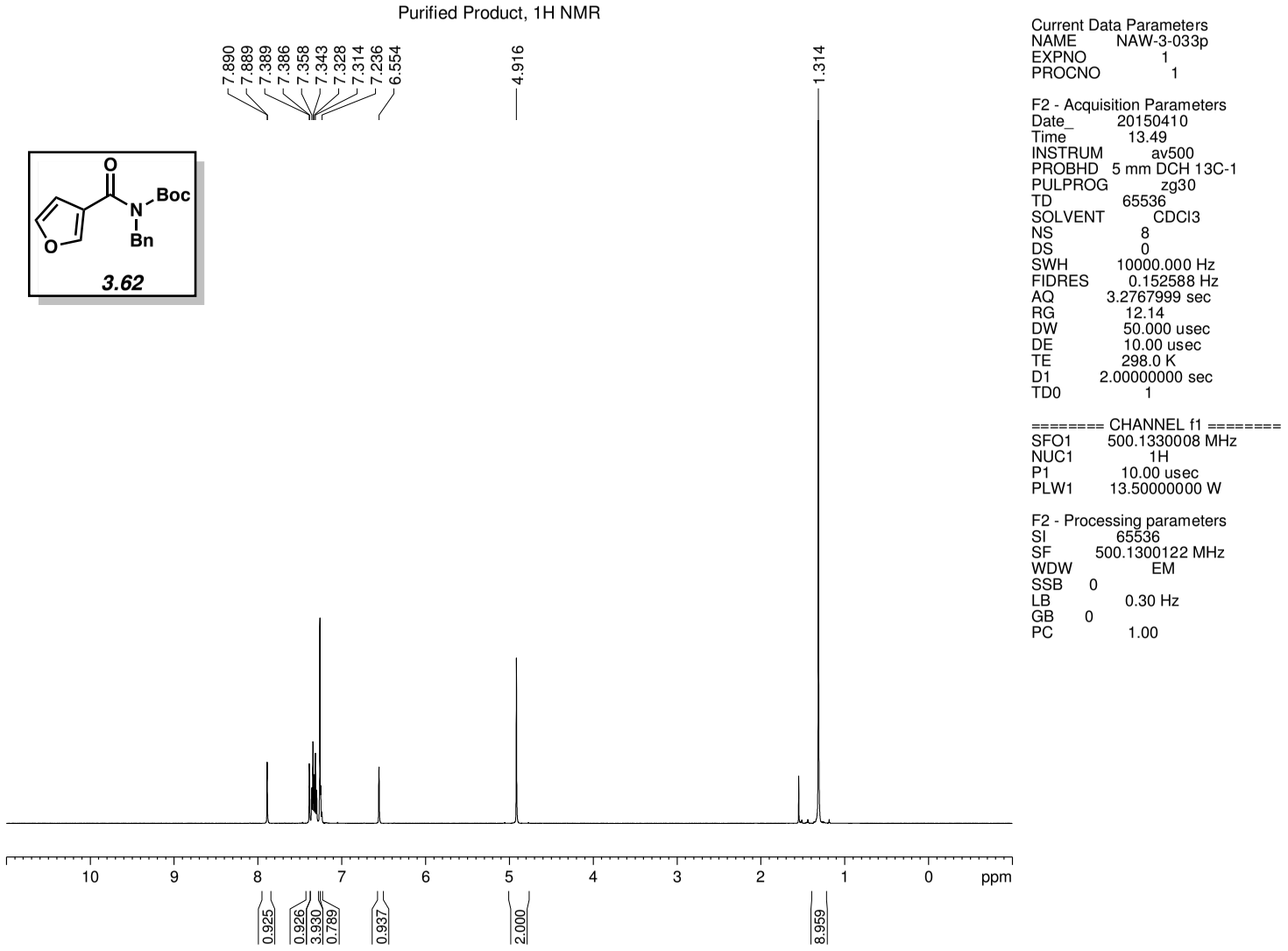

Figure 3.33 ^{1}H NMR (500 MHz, $CDCl_3$) of compound **3.62**.

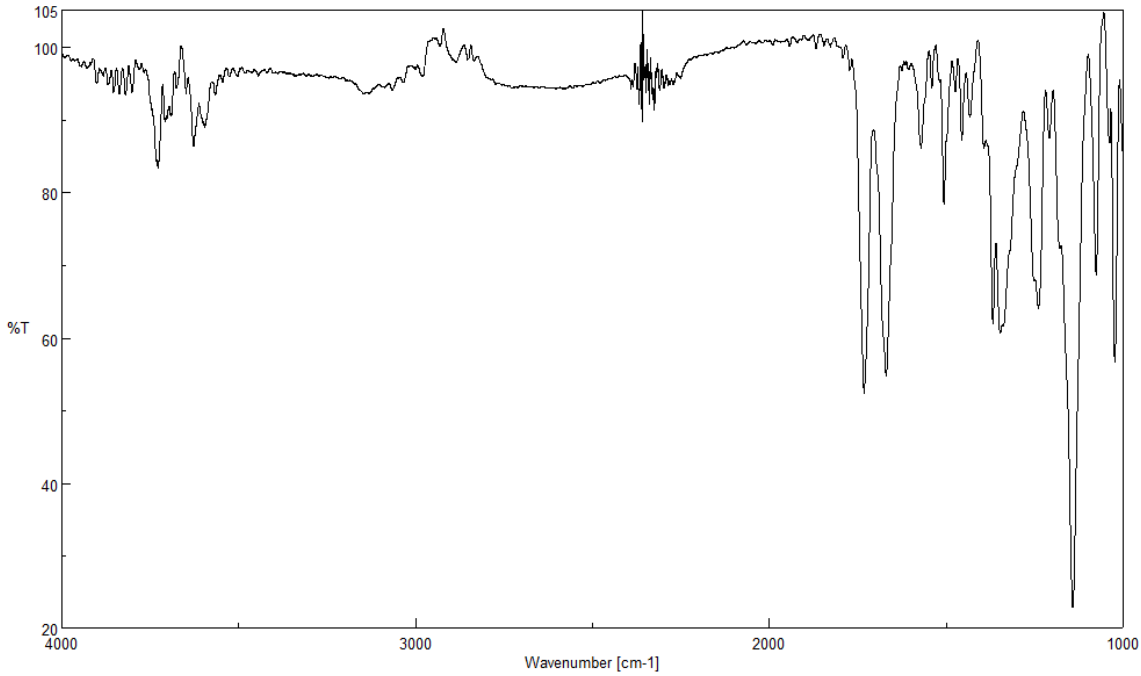

Figure 3.34 Infrared spectrum of compound **3.62**.

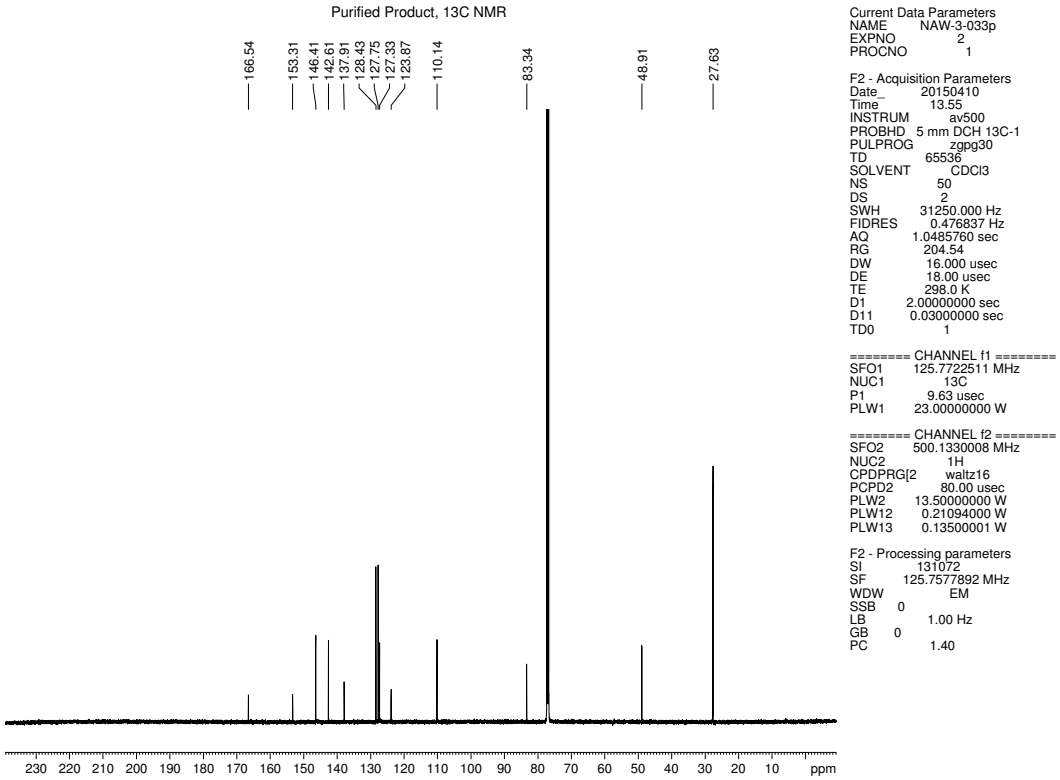

Figure 3.35 ^{13}C NMR (125 MHz, $CDCl_3$) of compound **3.62**.

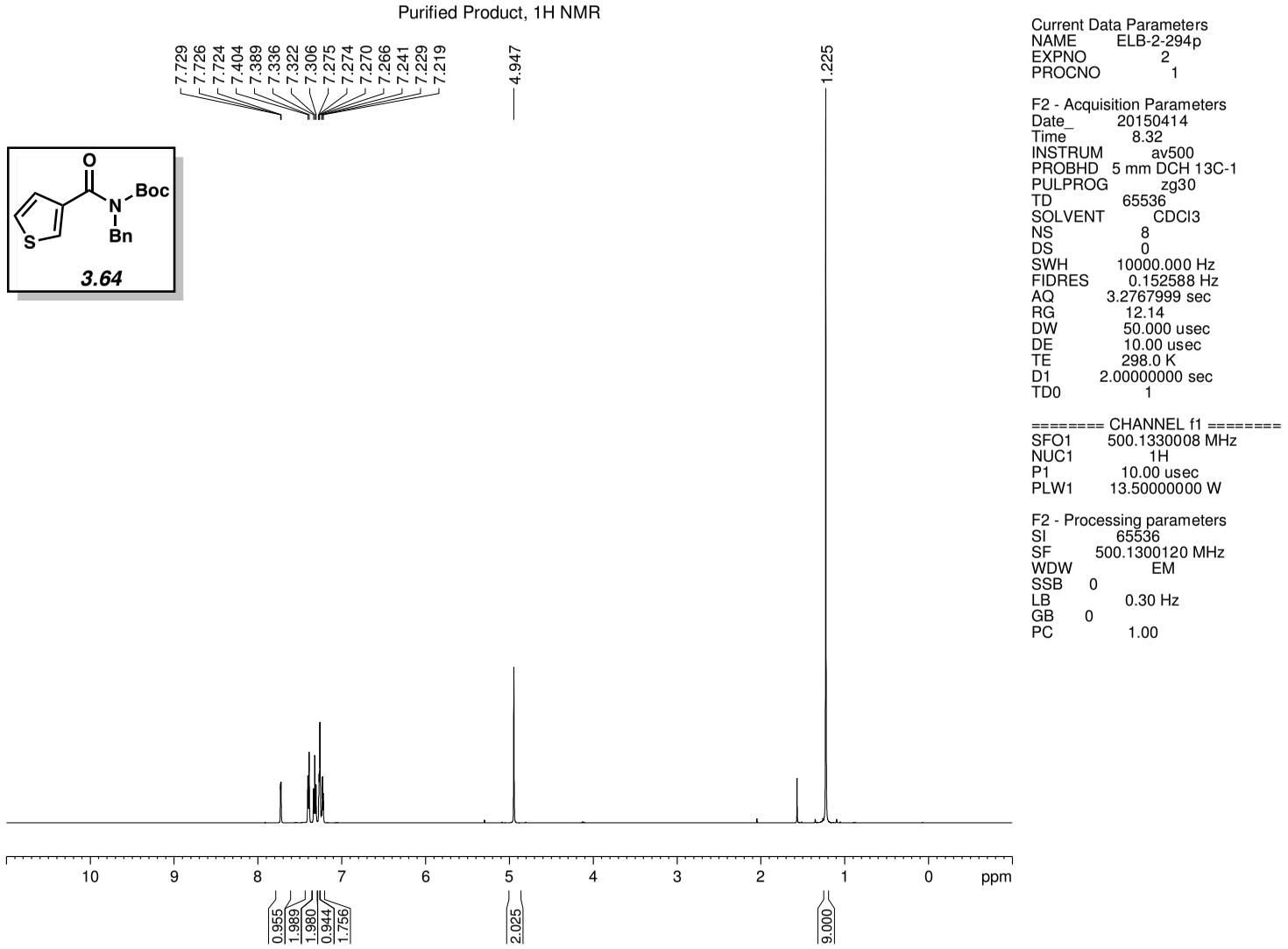

Figure 3.36 ^{1}H NMR (500 MHz, $CDCl_3$) of compound **3.64**.

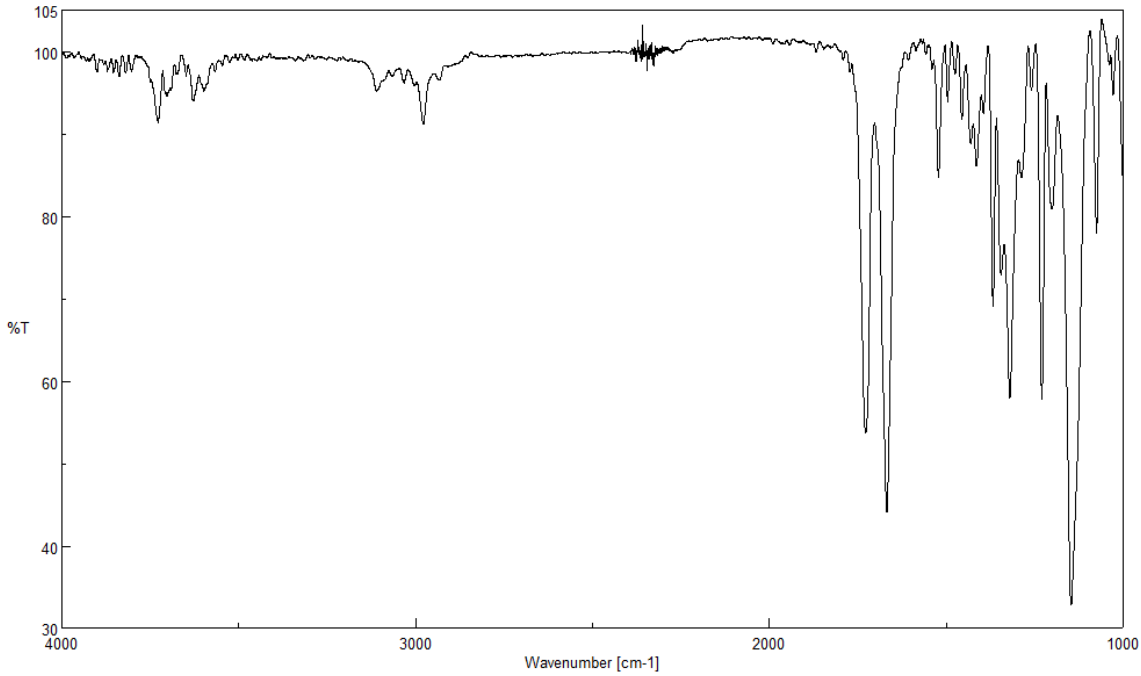

Figure 3.37 Infrared spectrum of compound **3.64**.

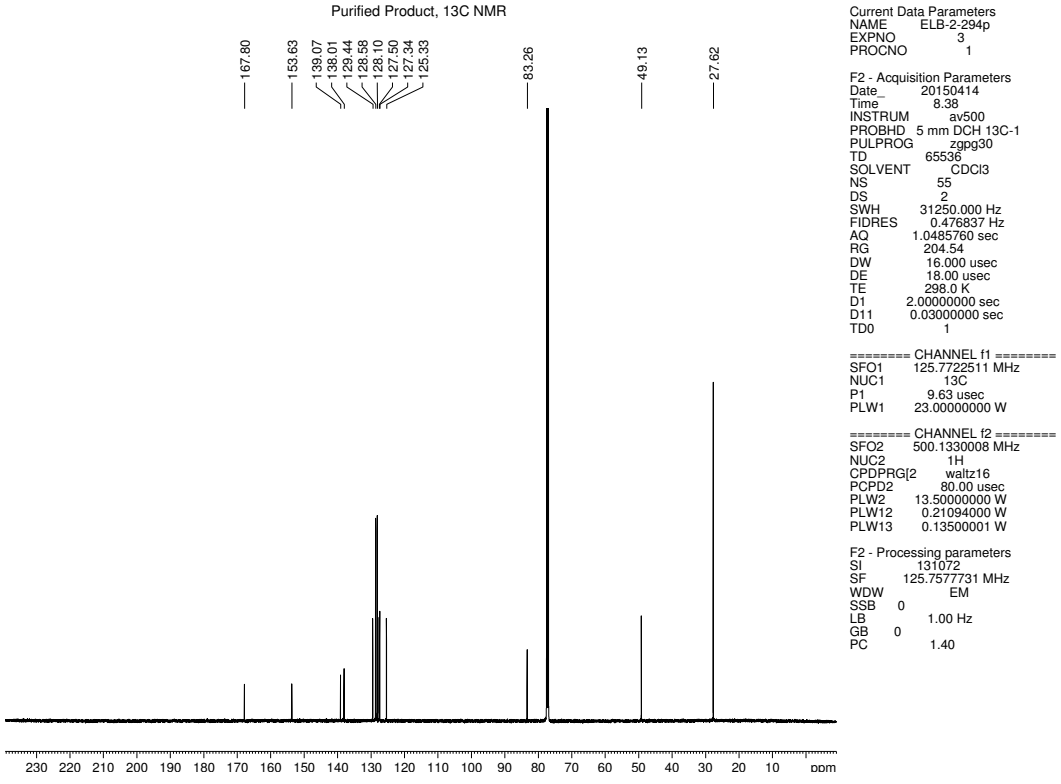

Figure 3.38 ^{13}C NMR (125 MHz, $CDCl_3$) of compound **3.64**.

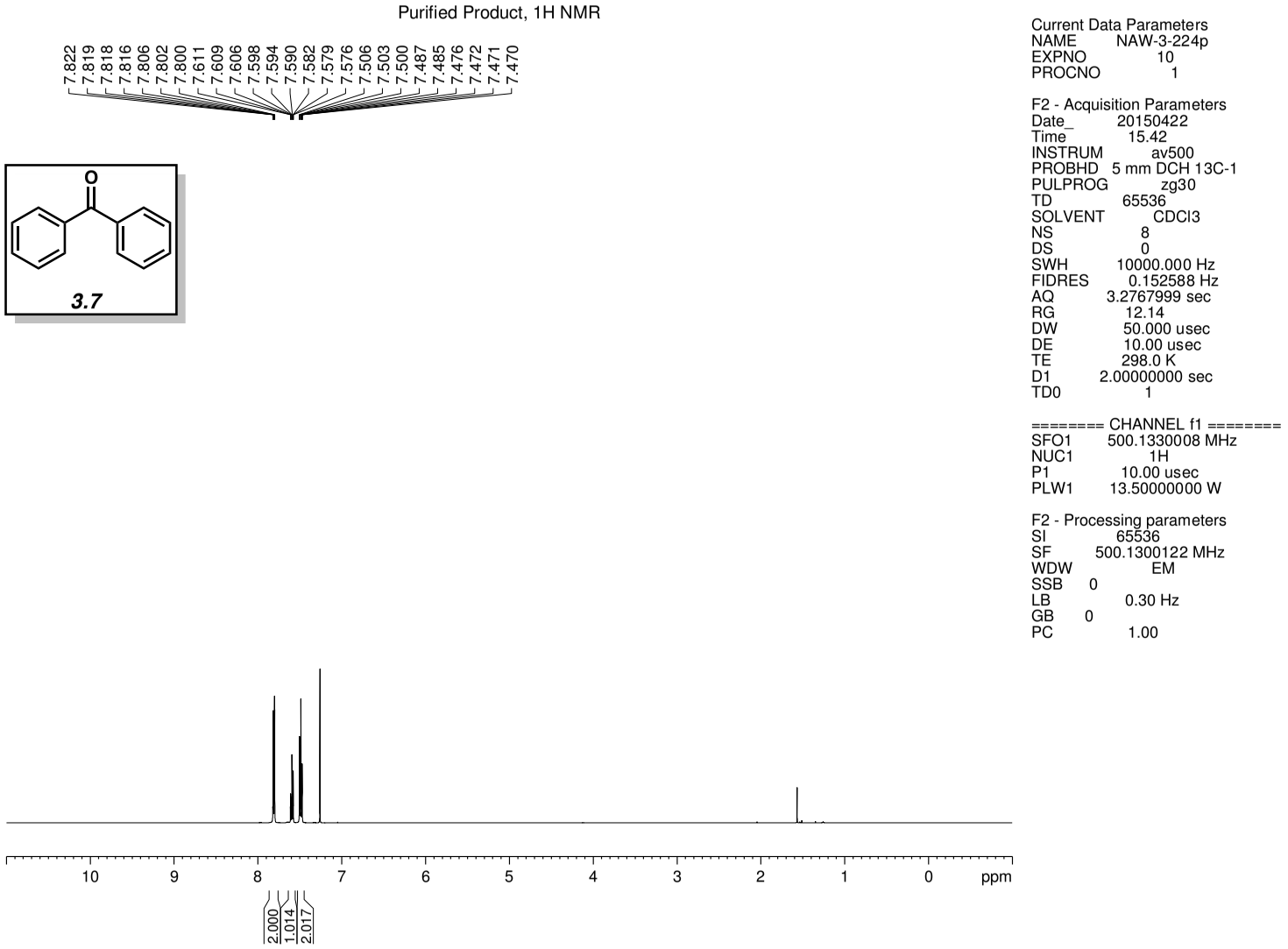

Figure 3.39 ^{1}H NMR (500 MHz, $CDCl_3$) of compound **3.7**.

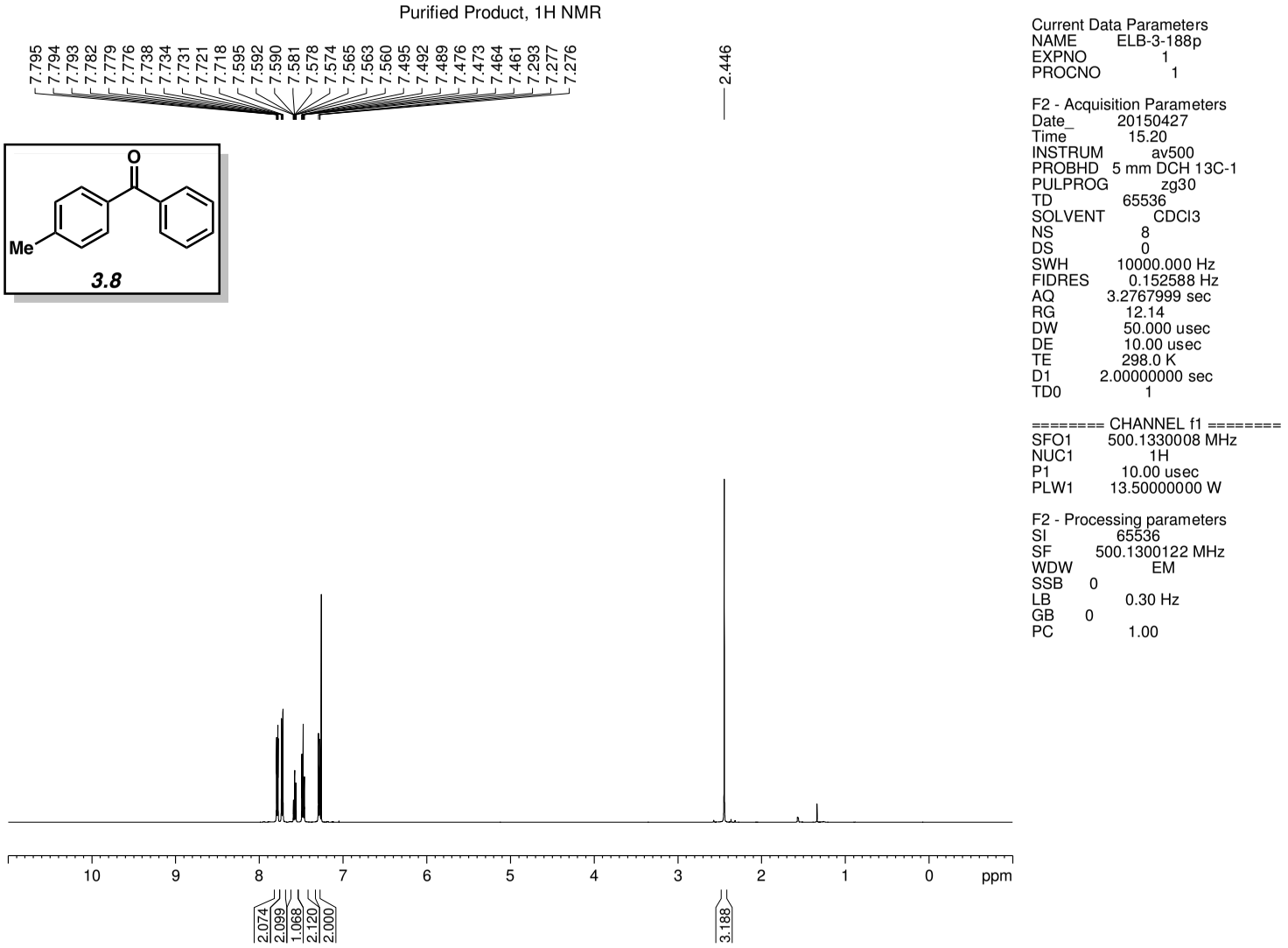

Figure 3.40 ^{1}H NMR (500 MHz, $CDCl_3$) of compound **3.8**.

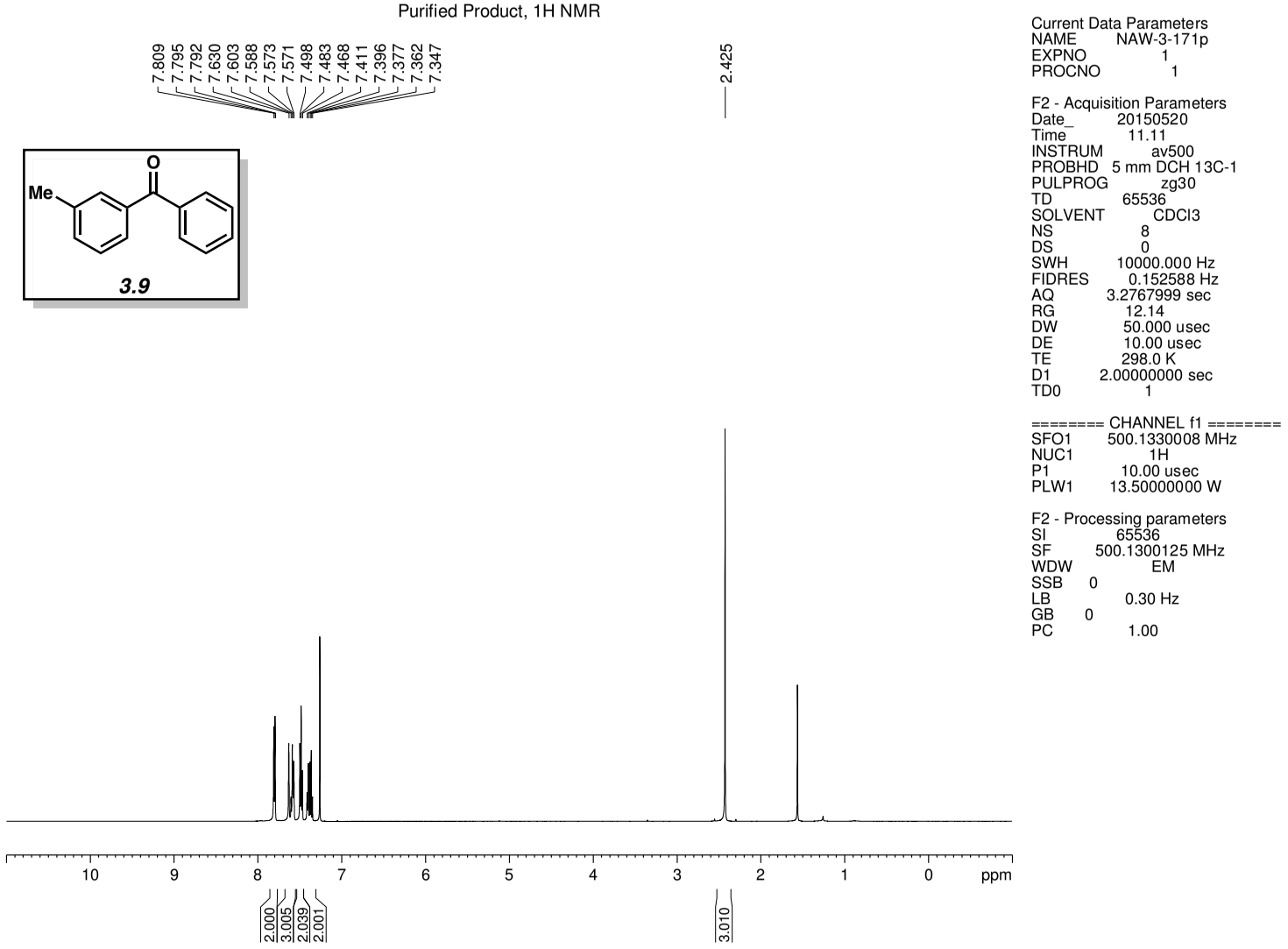

Figure 3.41 ^{1}H NMR (500 MHz, $CDCl_3$) of compound **3.9**.

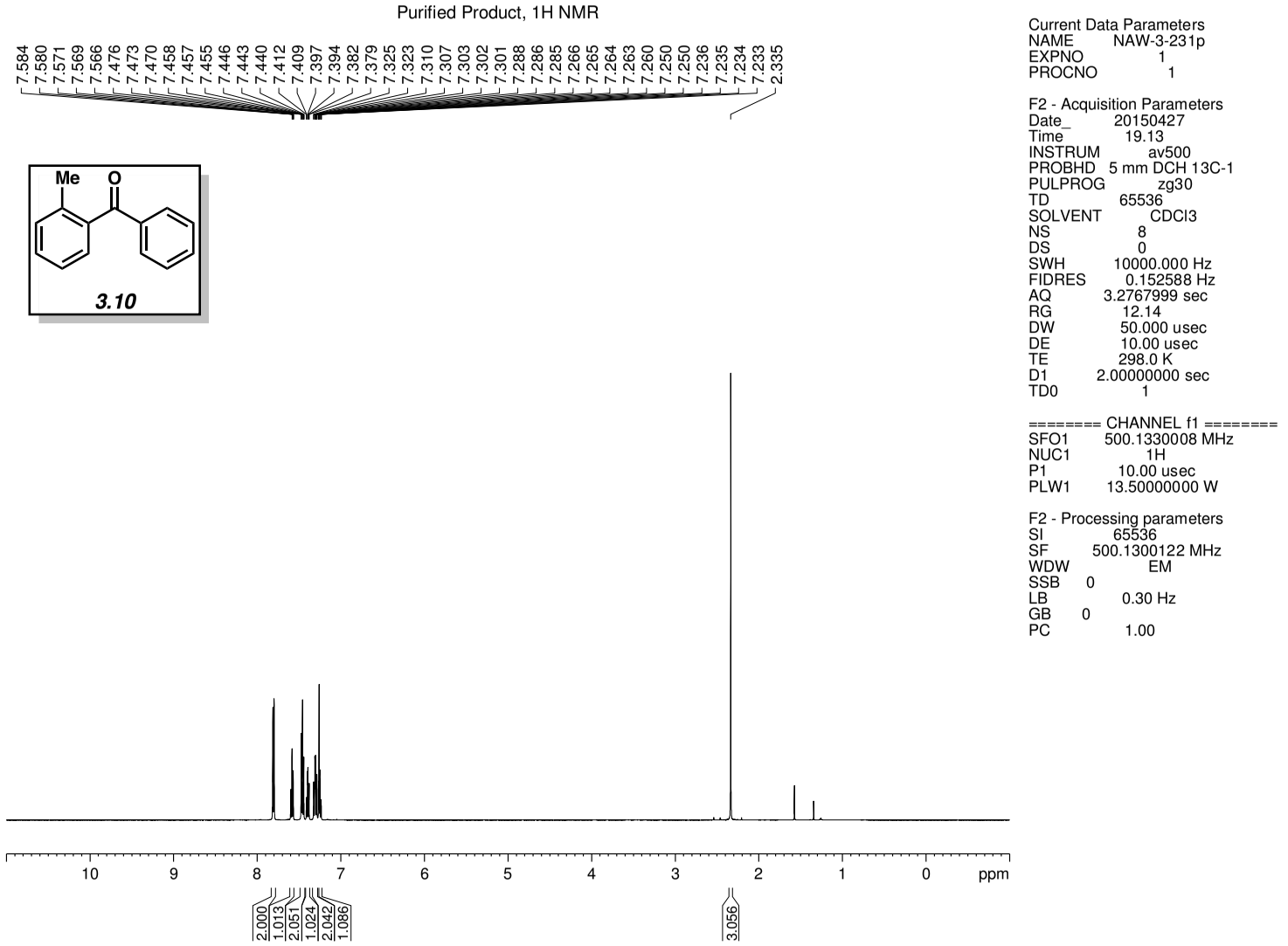

Current Data Parameters
NAME NAW-3-231p
EXPNO 1
PROCNO 1

F2 - Acquisition Parameters
Date_ 20150427
Time 19.13
INSTRUM av500
PROBHD 5 mm DCH 13C-1
PULPROG zg30
TD 65536
SOLVENT CDCl3
NS 8
DS 0
SWH 10000.000 Hz
FIDRES 0.152588 Hz
AQ 3.2767999 sec
RG 12.14
DW 50.000 usec
DE 10.00 usec
TE 298.0 K
D1 2.00000000 sec
TD0 1

======== CHANNEL f1 ========
SFO1 500.1330008 MHz
NUC1 1H
P1 10.00 usec
PLW1 13.50000000 W

F2 - Processing parameters
SI 65536
SF 500.1300122 MHz
WDW EM
SSB 0
LB 0.30 Hz
GB 0
PC 1.00

Figure 3.42 ^{1}H NMR (500 MHz, $CDCl_3$) of compound **3.10**.

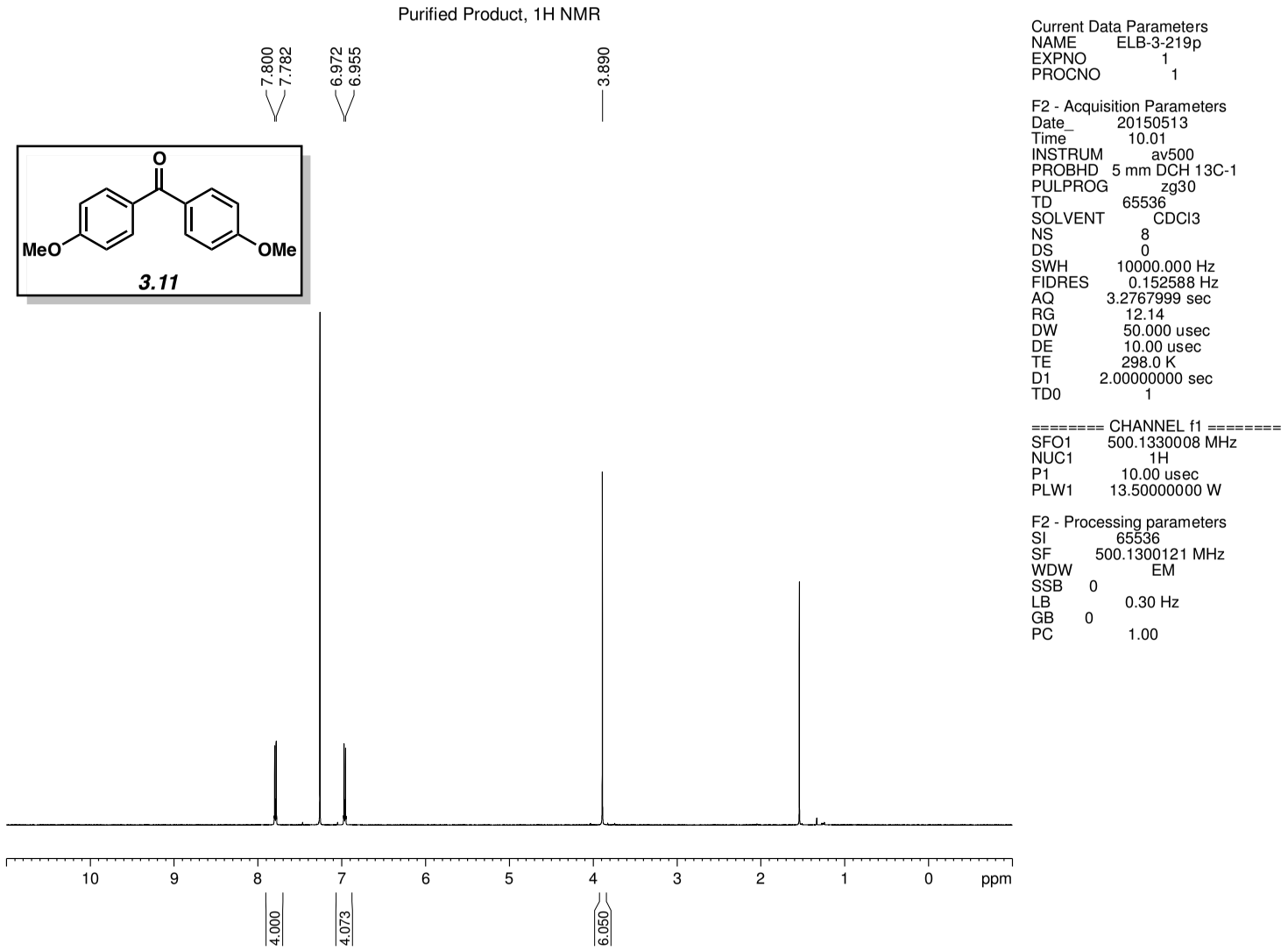

Figure 3.43 ^{1}H NMR (500 MHz, $CDCl_3$) of compound **3.11**.

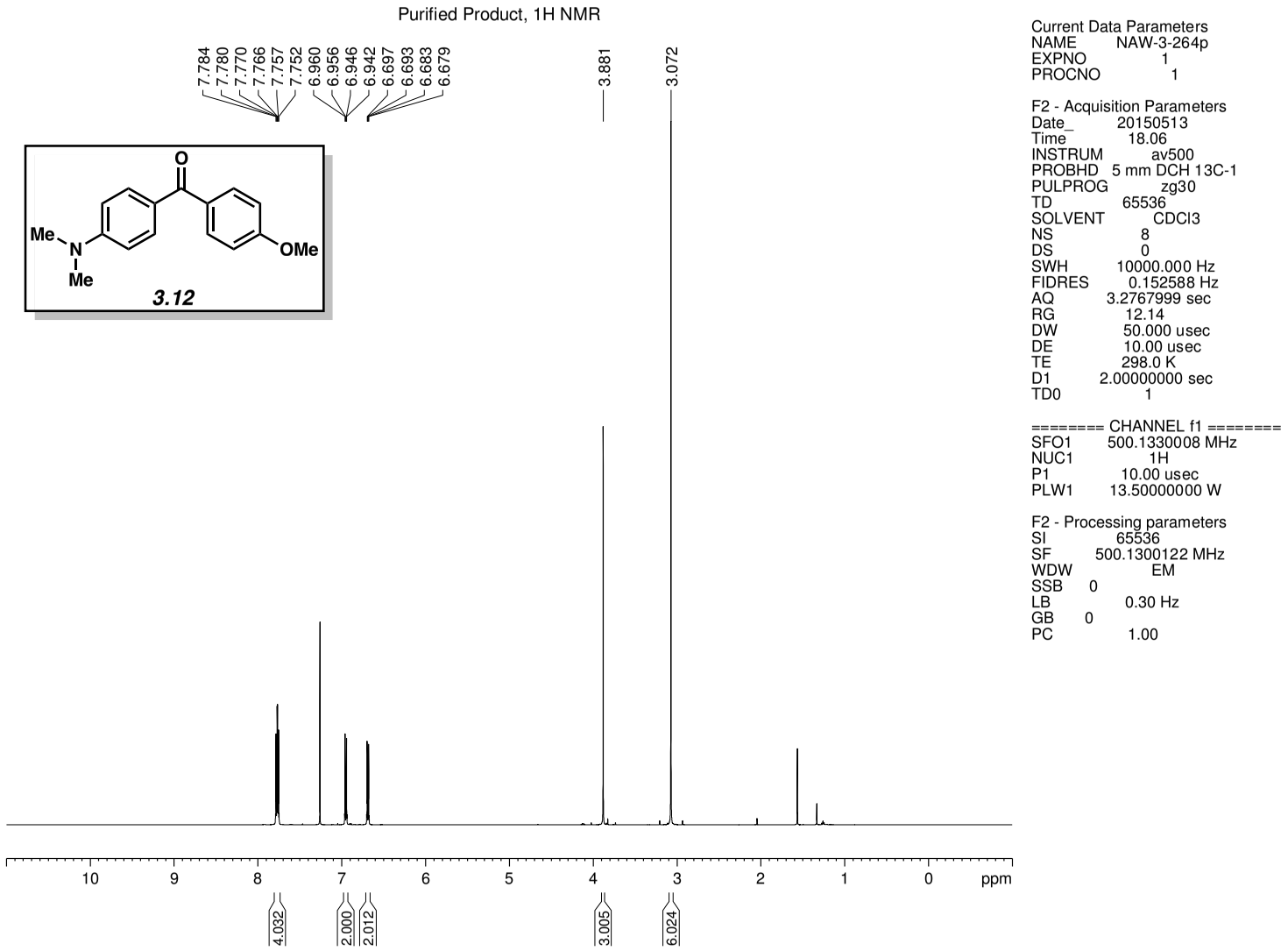

Figure 3.44 ^{1}H NMR (500 MHz, $CDCl_3$) of compound **3.12**.

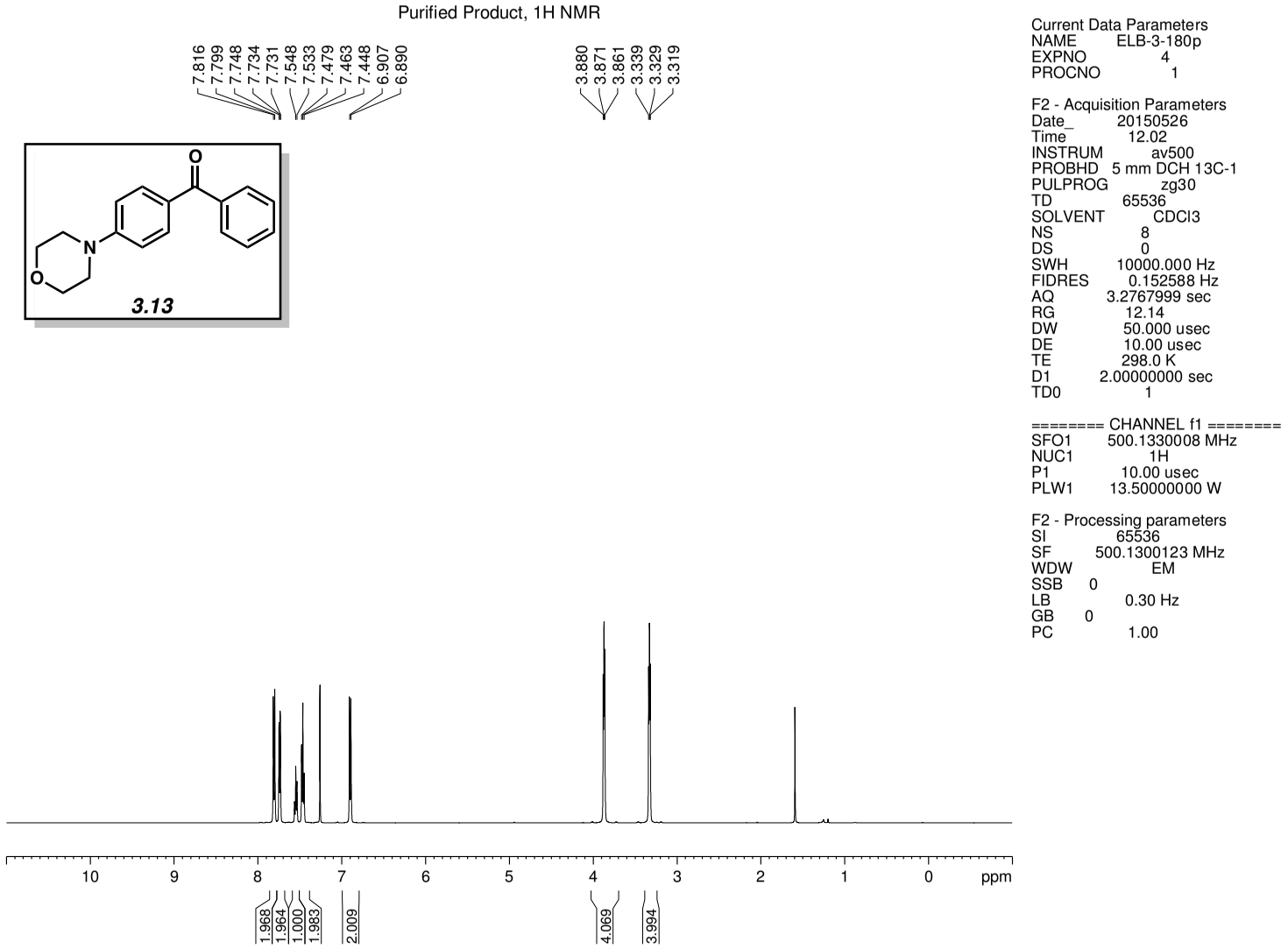

Figure 3.45 ^{1}H NMR (500 MHz, $CDCl_3$) of compound **3.13**.

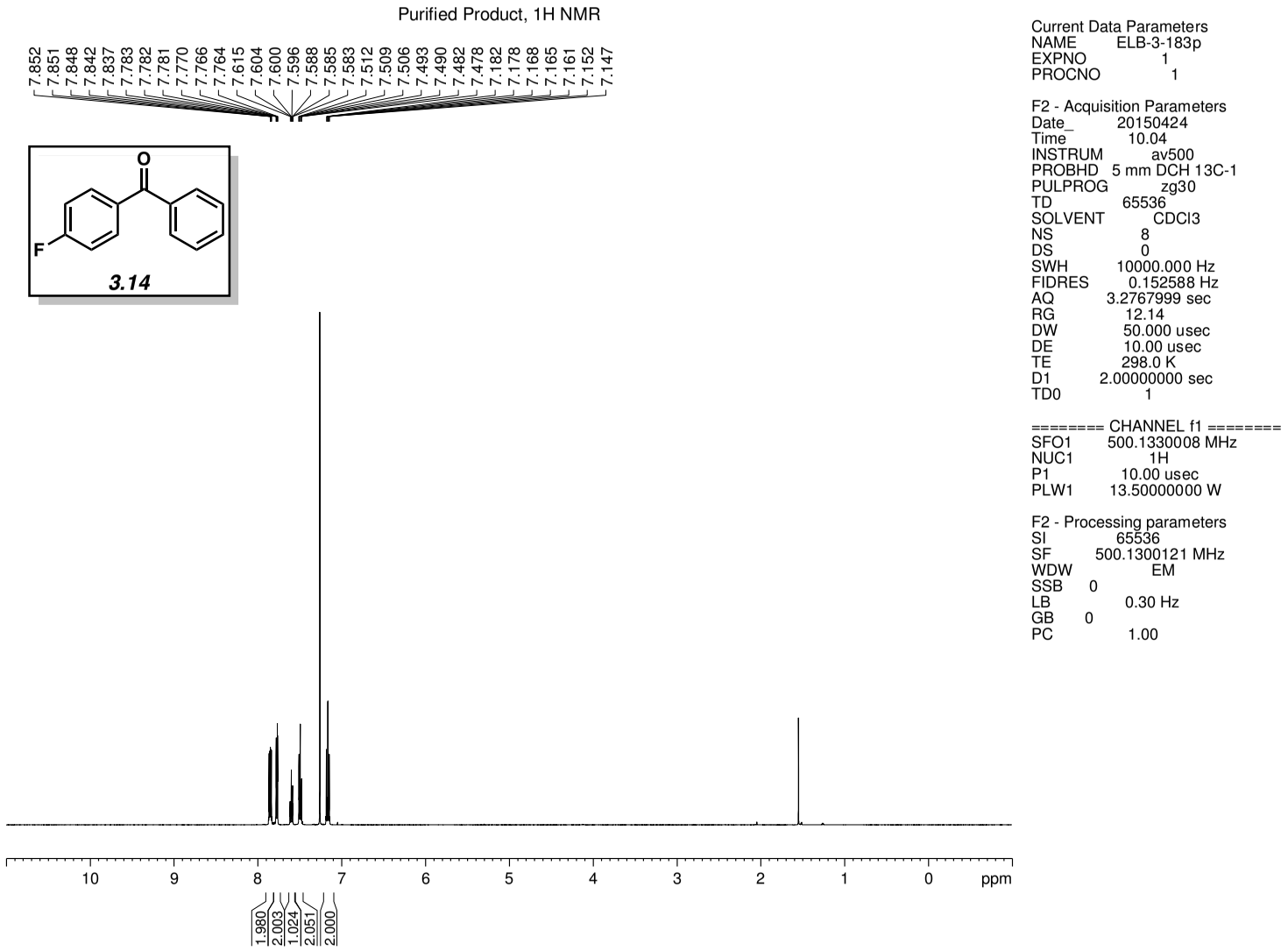

Figure 3.46 ^{1}H NMR (500 MHz, $CDCl_3$) of compound **3.14**.

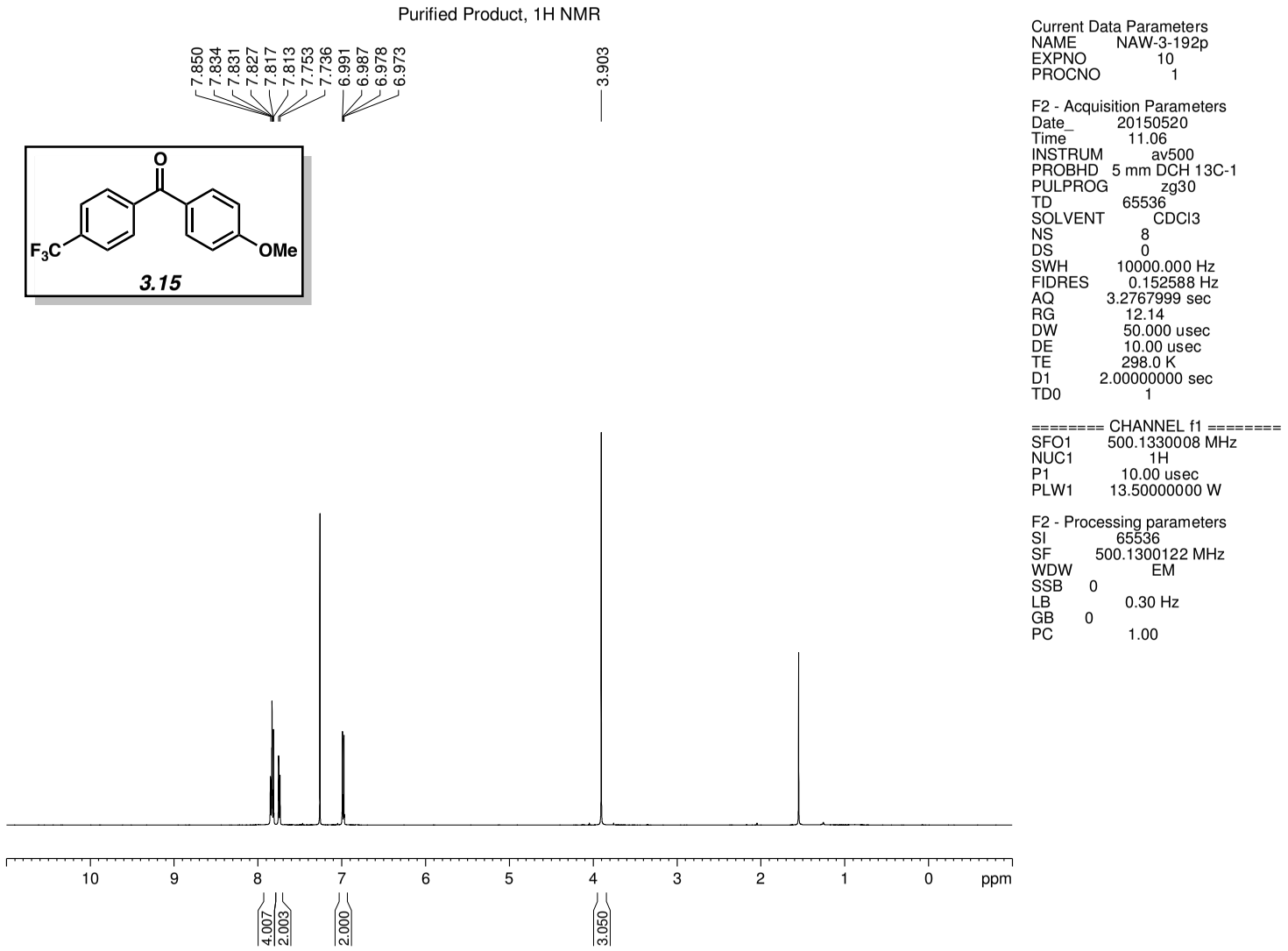

Figure 3.47 ^{1}H NMR (500 MHz, $CDCl_3$) of compound **3.15**.

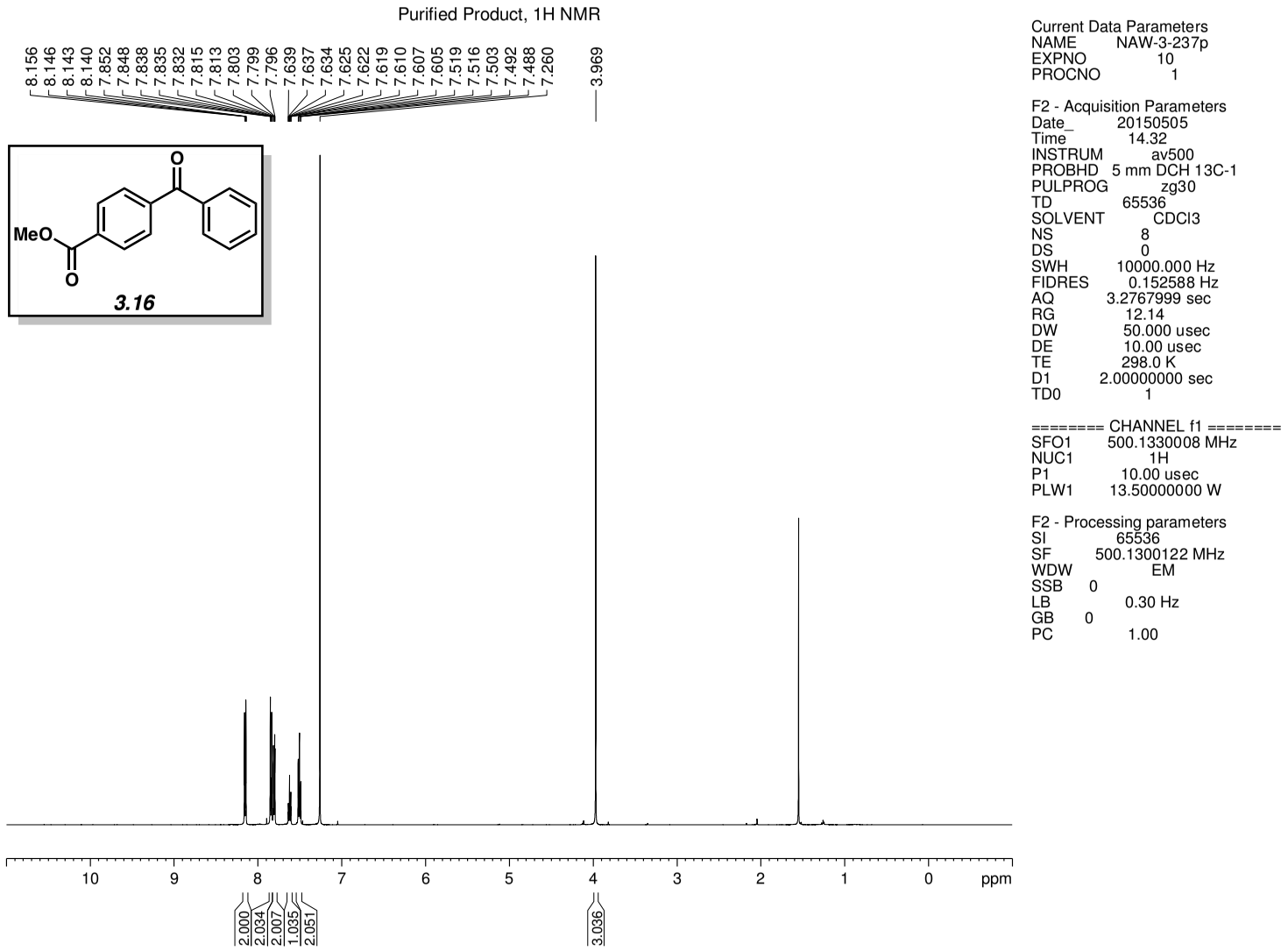

Figure 3.48 ^{1}H NMR (500 MHz, $CDCl_3$) of compound **3.16**.

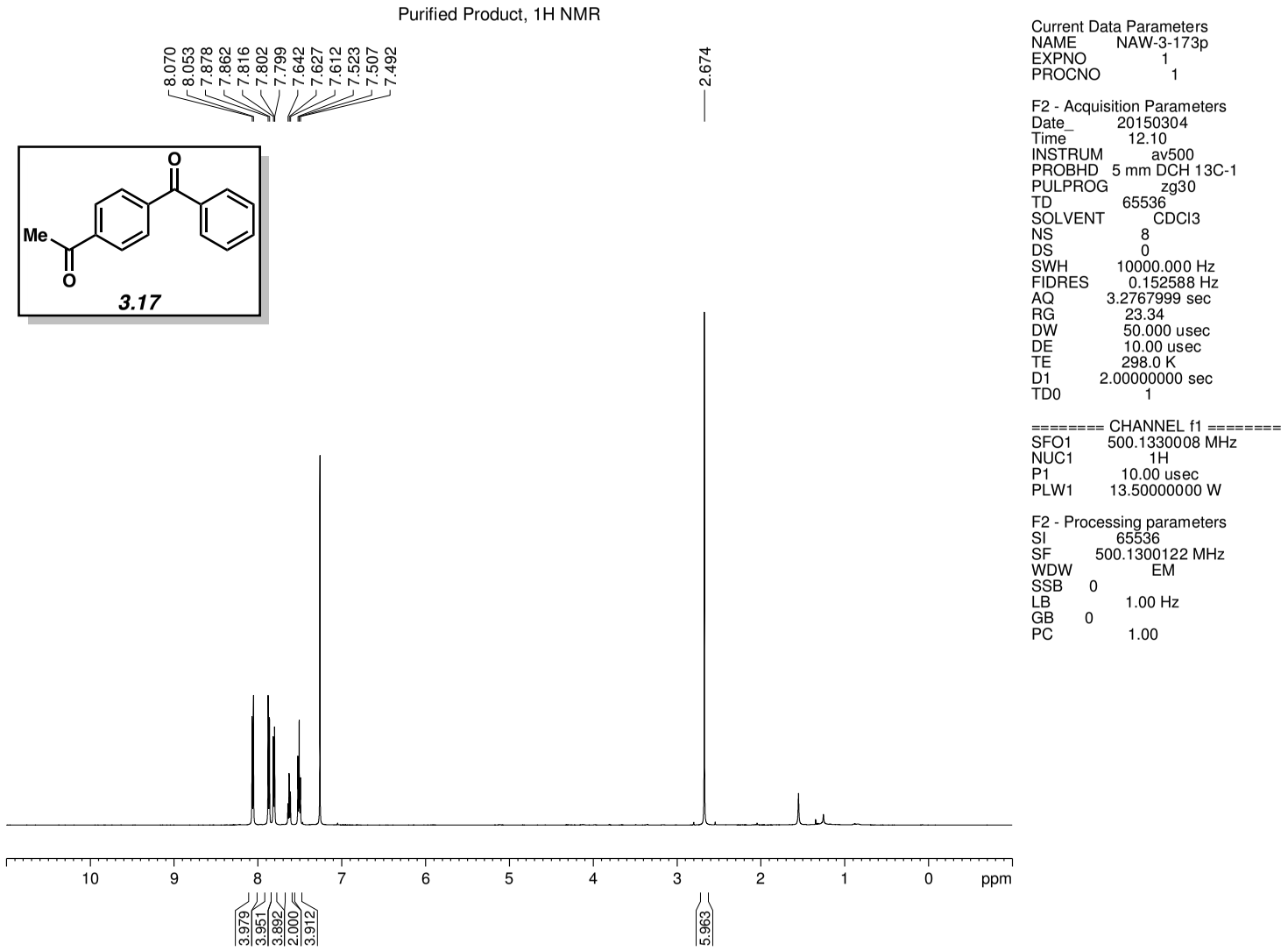

Figure 3.49 ^{1}H NMR (500 MHz, $CDCl_3$) of compound **3.17**.

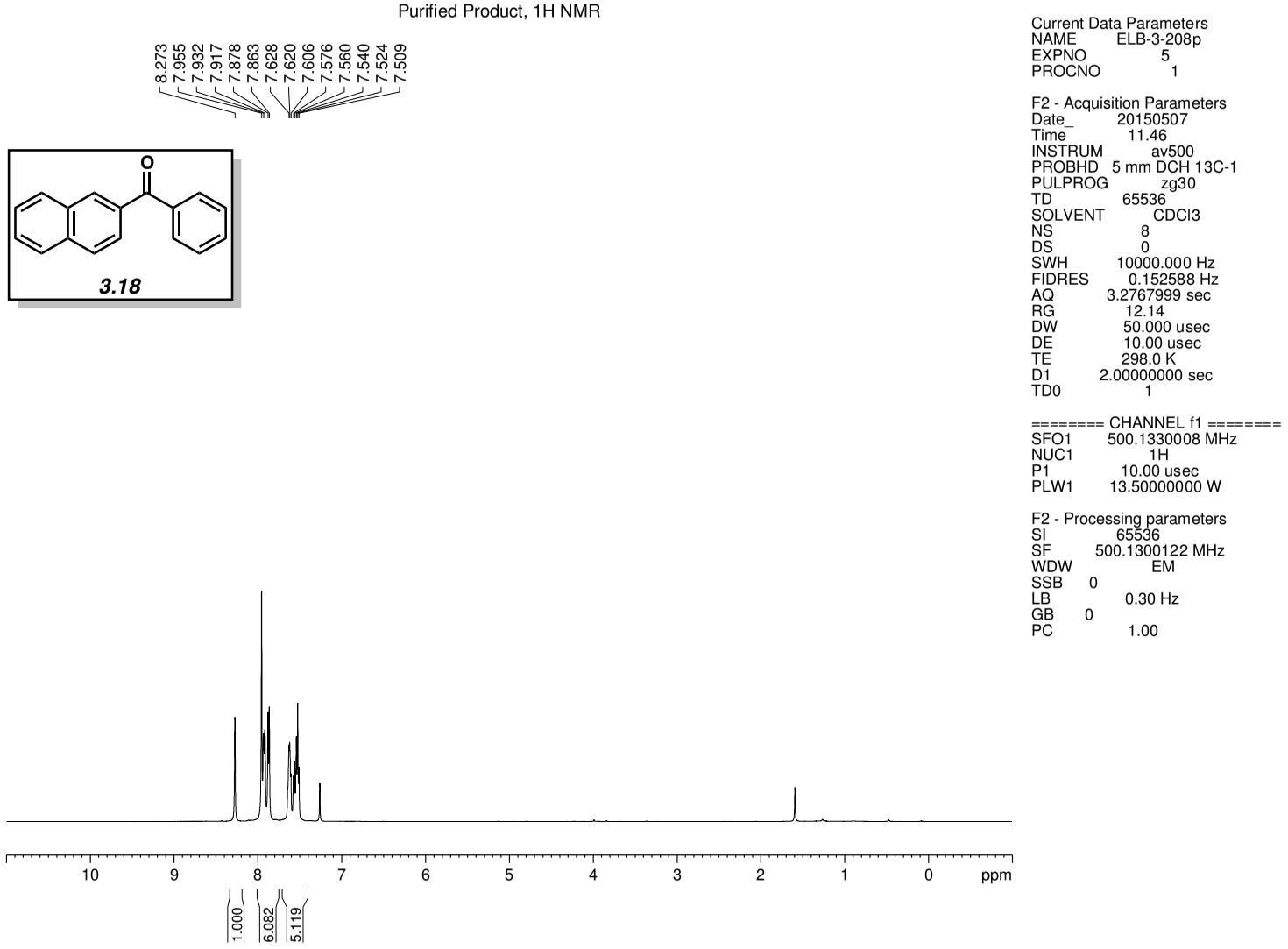

Figure 3.50 ^{1}H NMR (500 MHz, $CDCl_3$) of compound **3.18**.

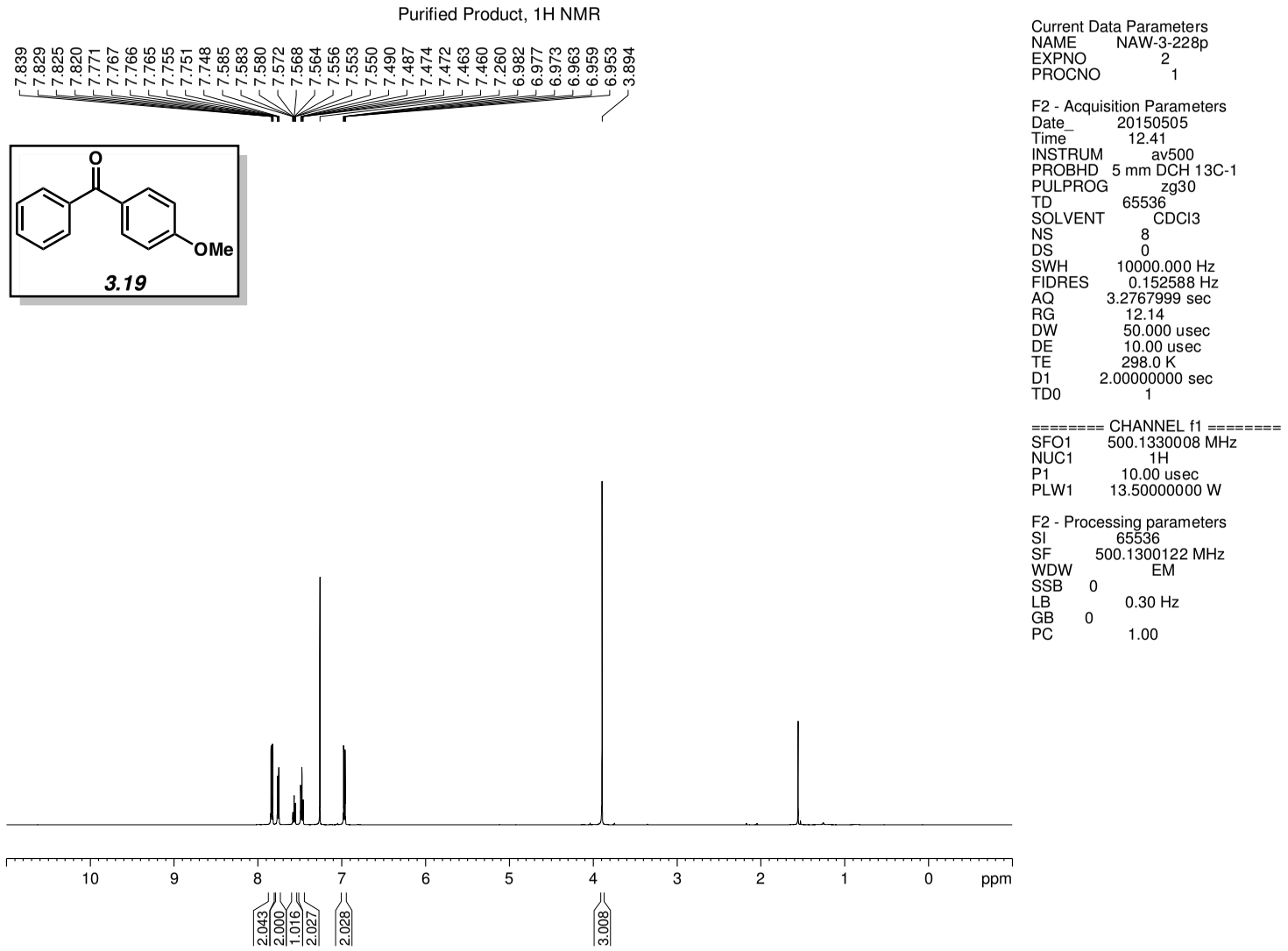

Figure 3.51 ^{1}H NMR (500 MHz, $CDCl_3$) of compound **3.19**.

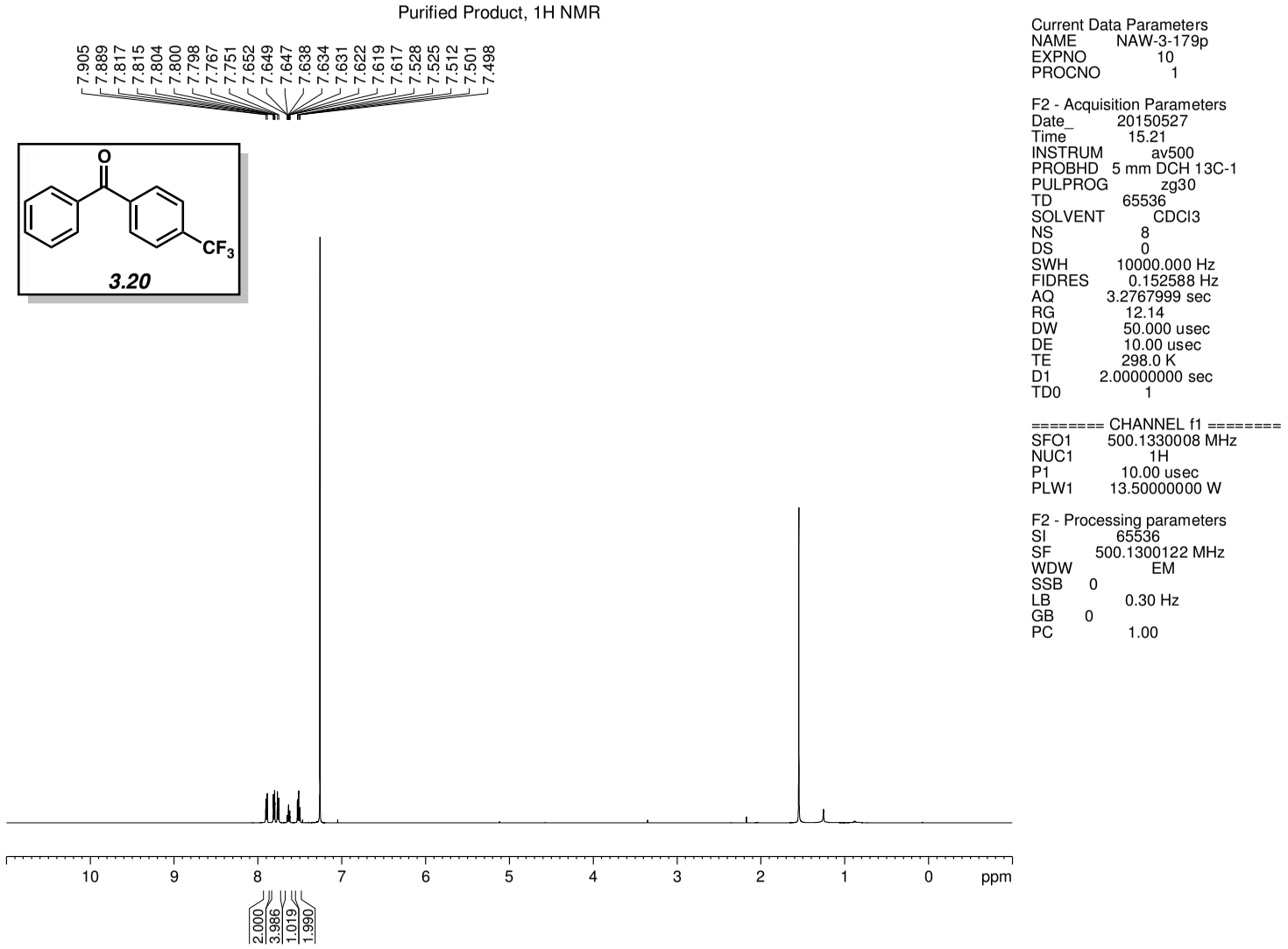

Figure 3.52 ^{1}H NMR (500 MHz, $CDCl_3$) of compound **3.20**.

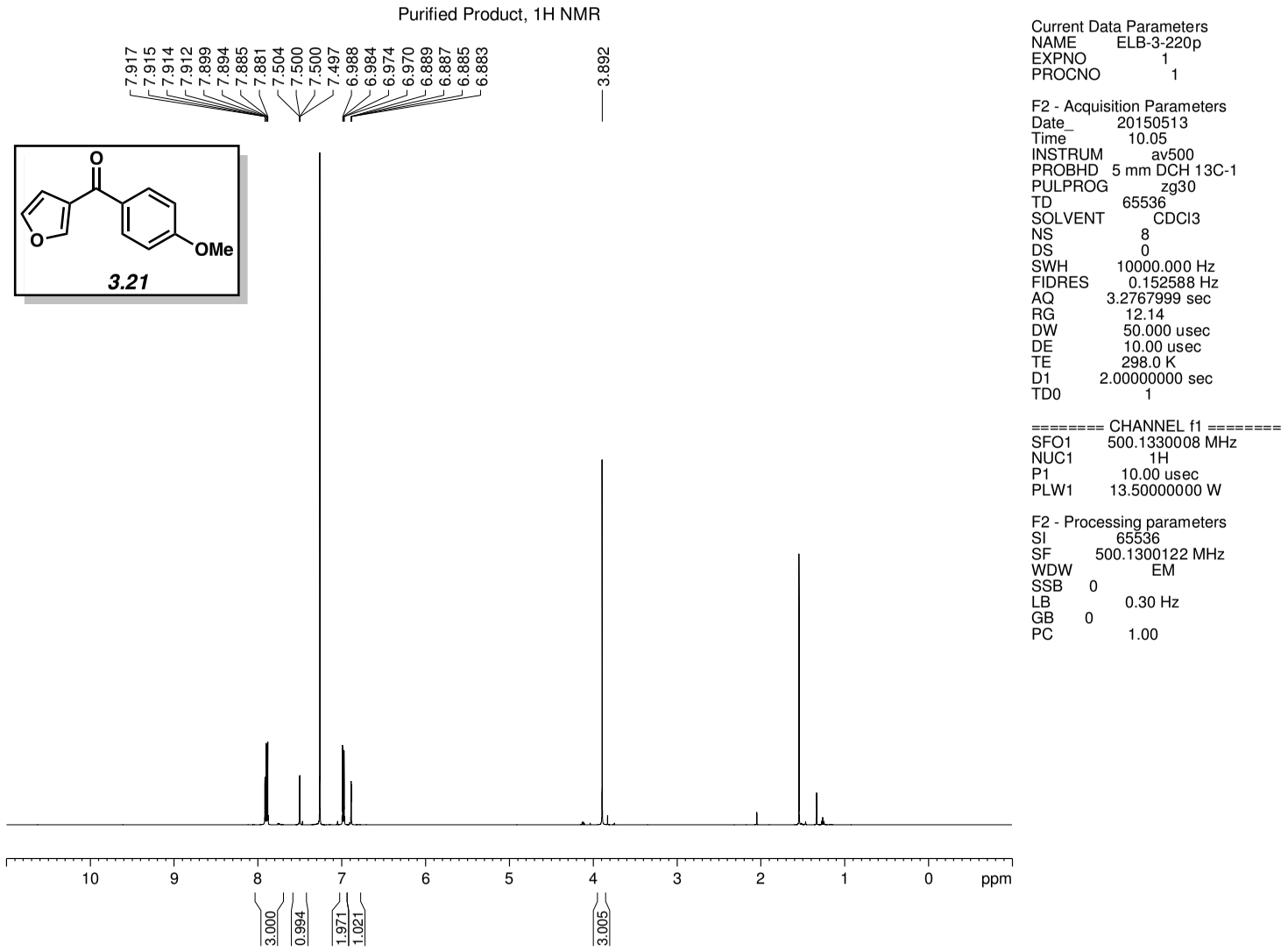

Figure 3.53 ^{1}H NMR (500 MHz, $CDCl_3$) of compound **3.21**.

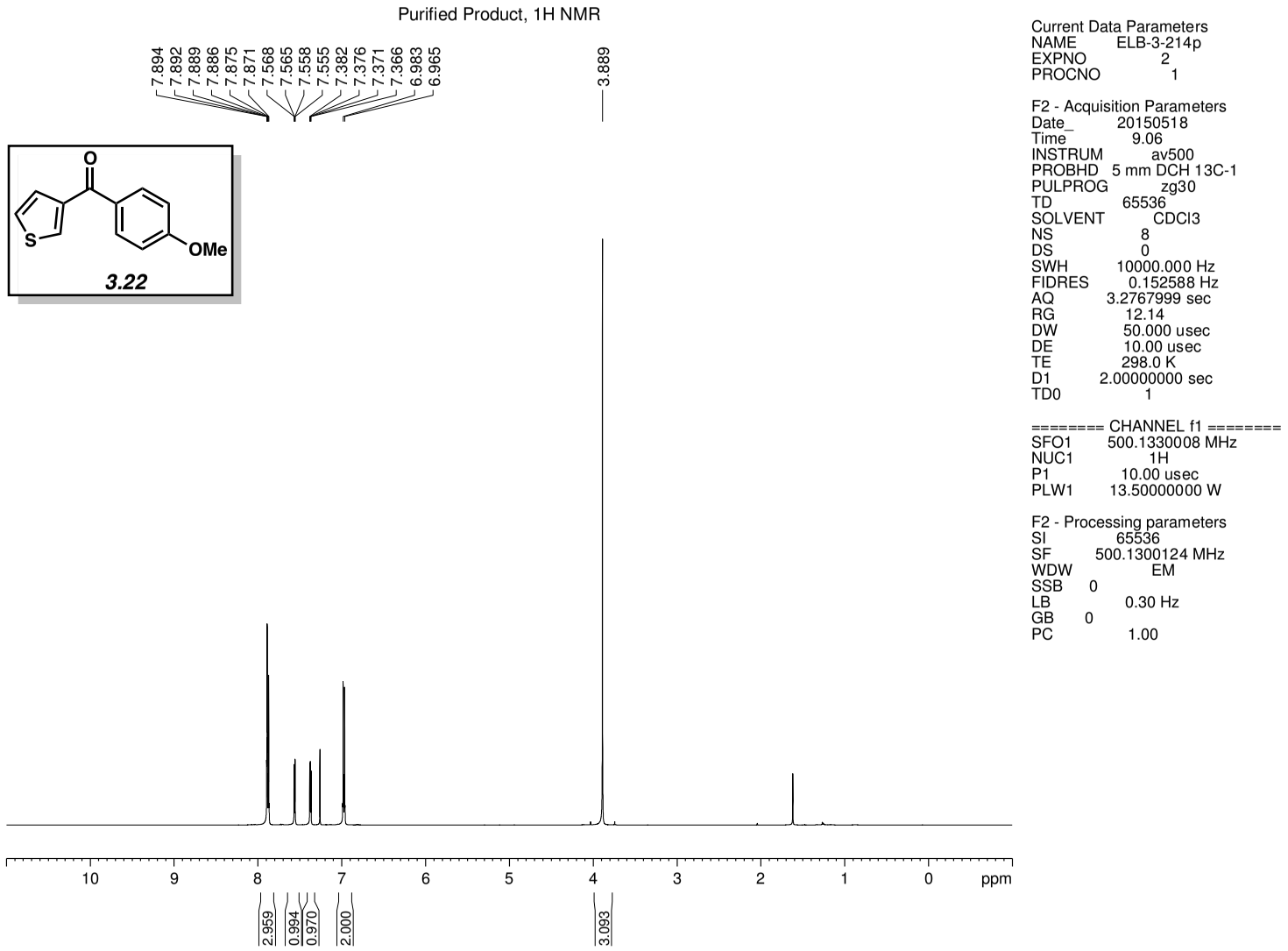

Figure 3.54 ^{1}H NMR (500 MHz, $CDCl_3$) of compound **3.22**.

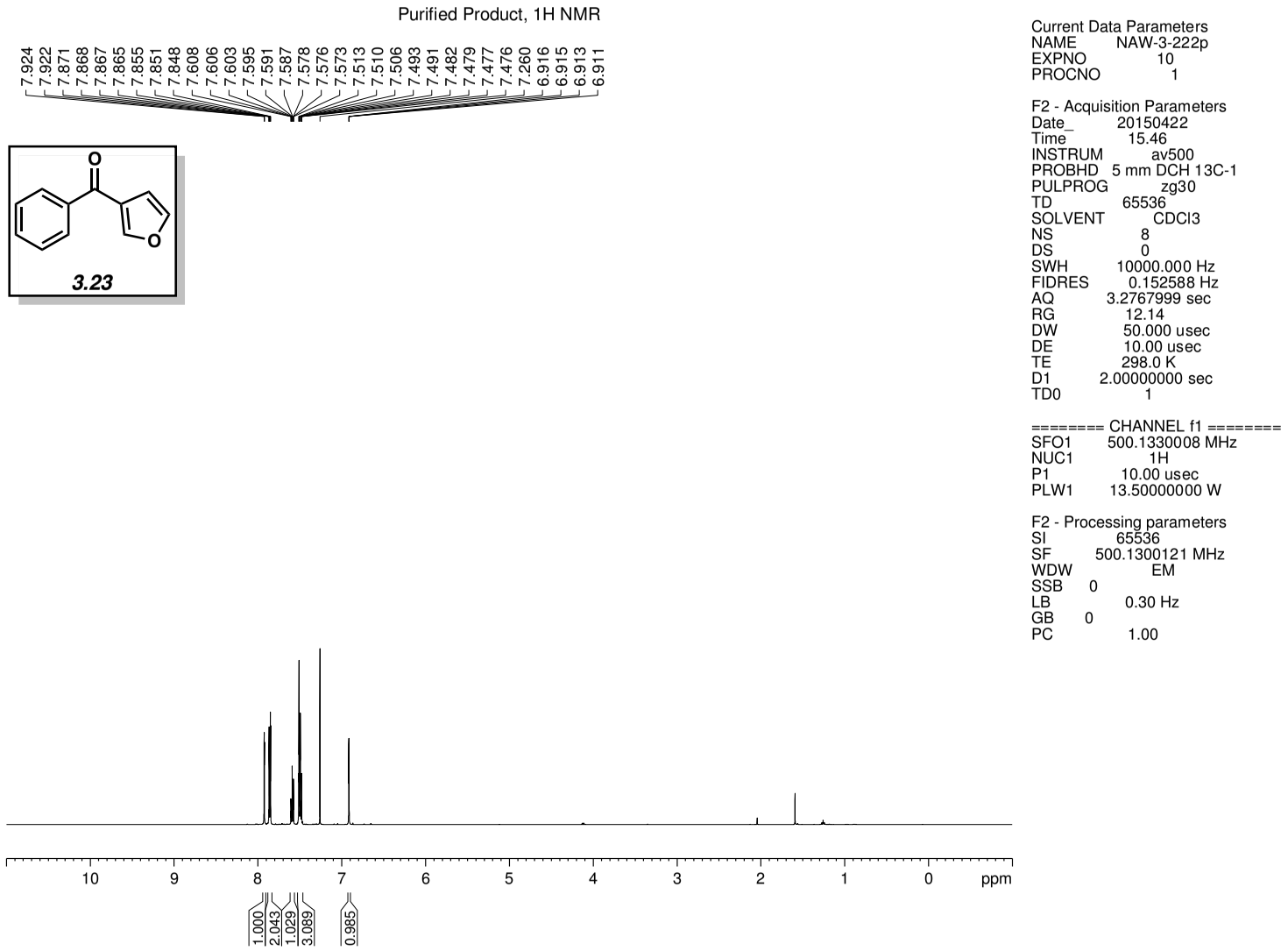

Figure 3.55 ^{1}H NMR (500 MHz, $CDCl_3$) of compound **3.23**.

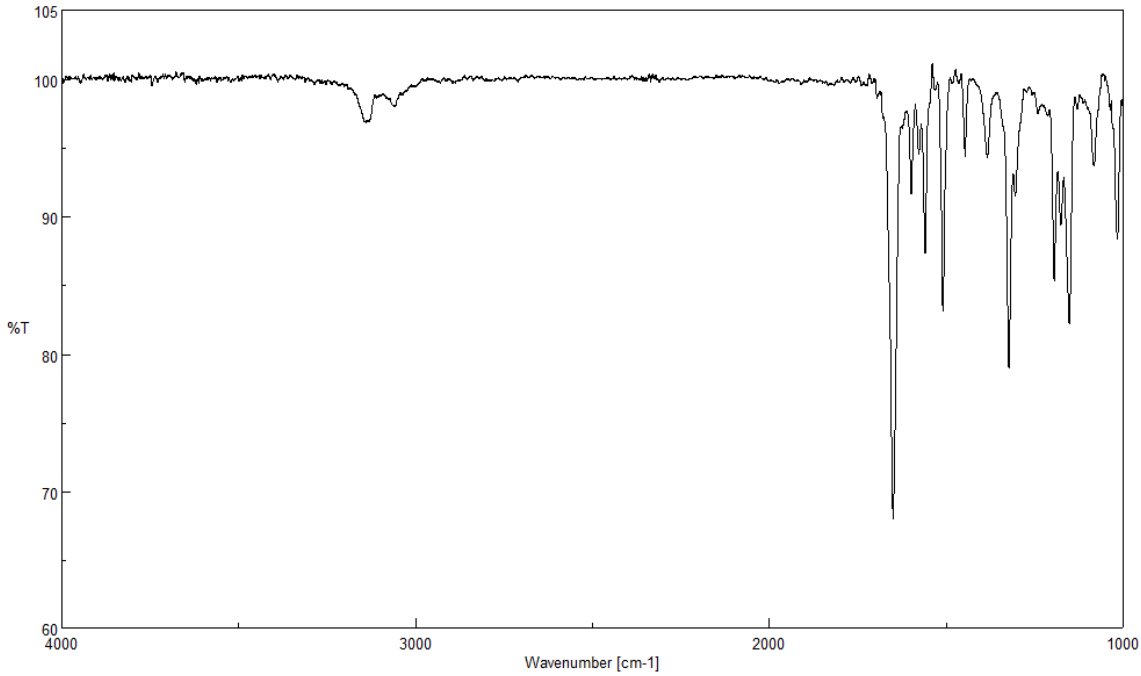

Figure 3.56 Infrared spectrum of compound **3.23**.

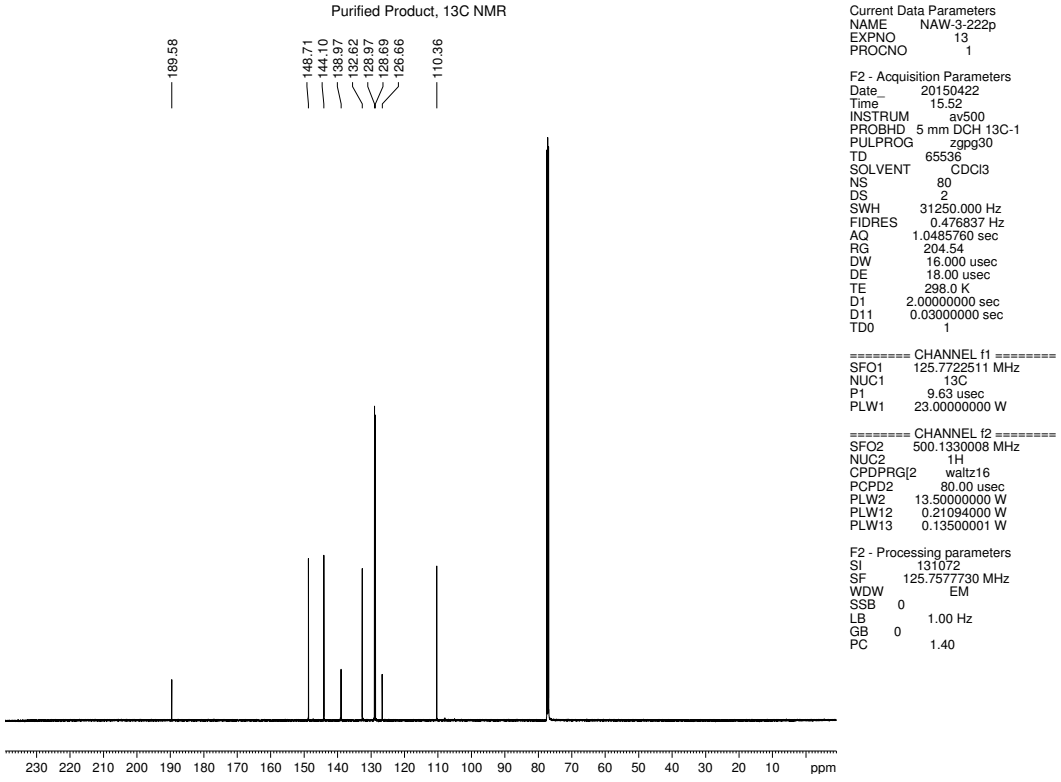

Figure 3.57 ^{13}C NMR (125 MHz, $CDCl_3$) of compound **3.23**.

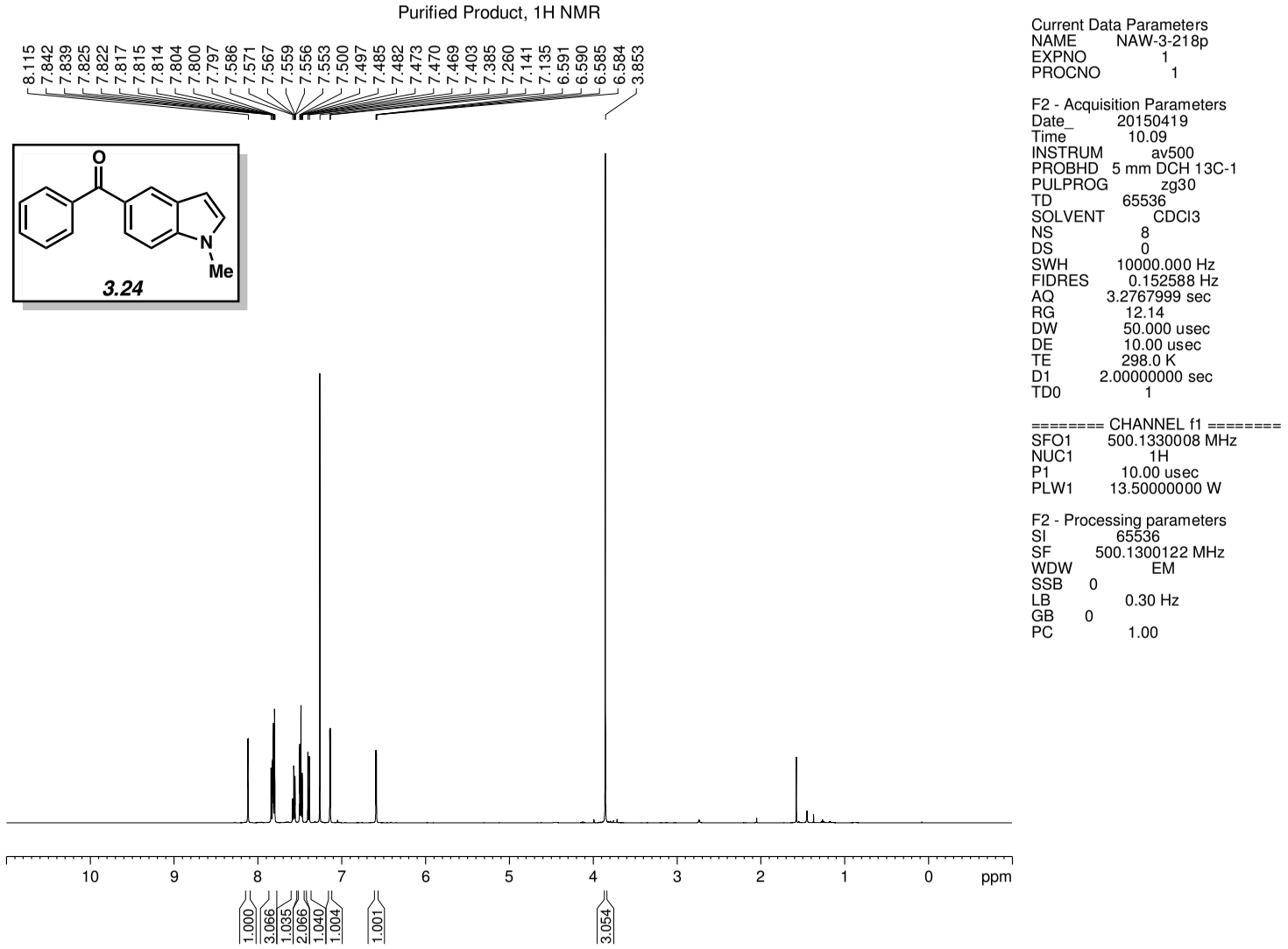

Figure 3.58 ^{1}H NMR (500 MHz, $CDCl_3$) of compound **3.24**.

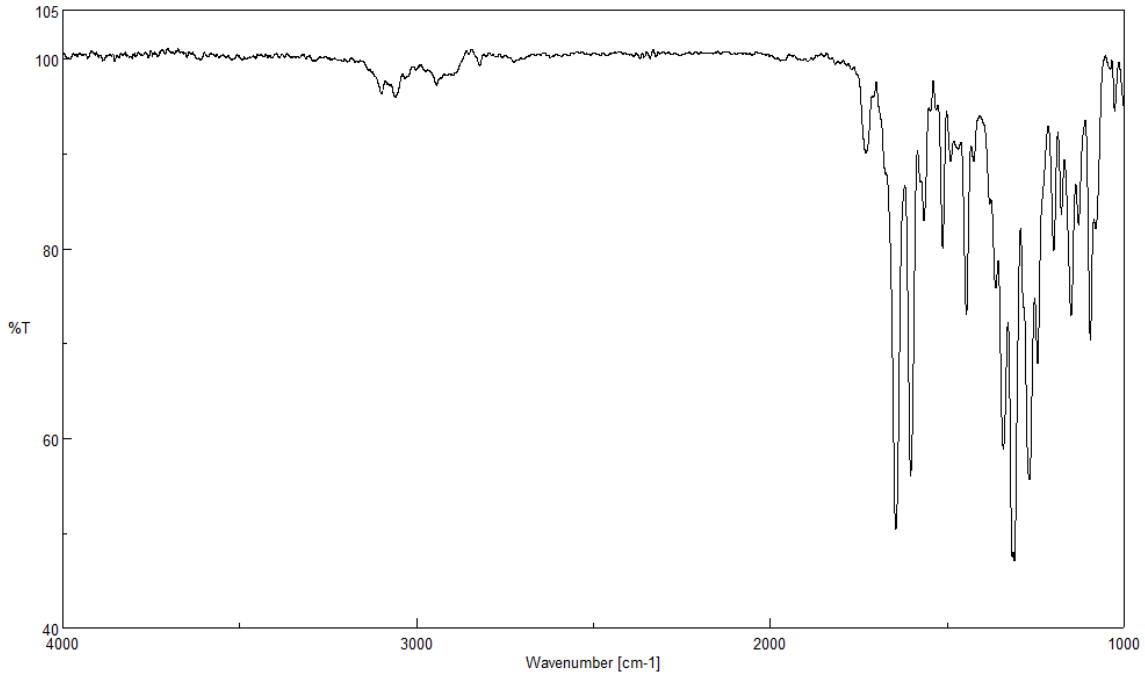

Figure 3.59 Infrared spectrum of compound **3.24**.

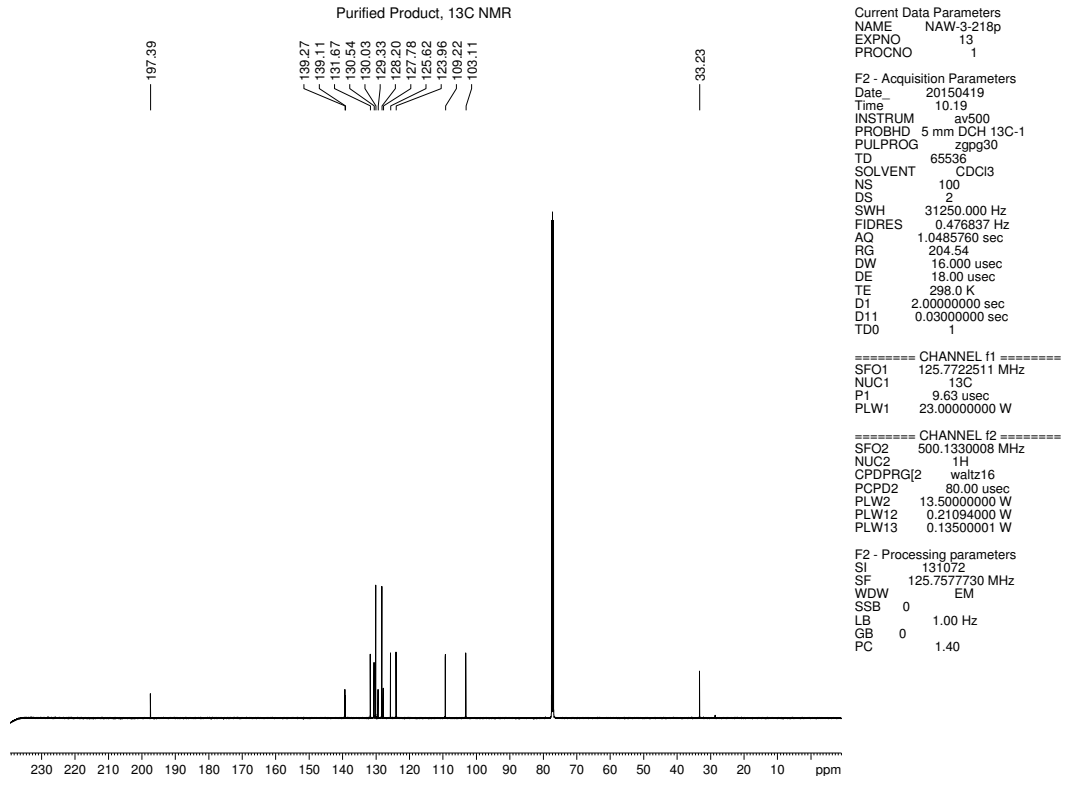

Figure 3.60 ^{13}C NMR (125 MHz, $CDCl_3$) of compound **3.24**.

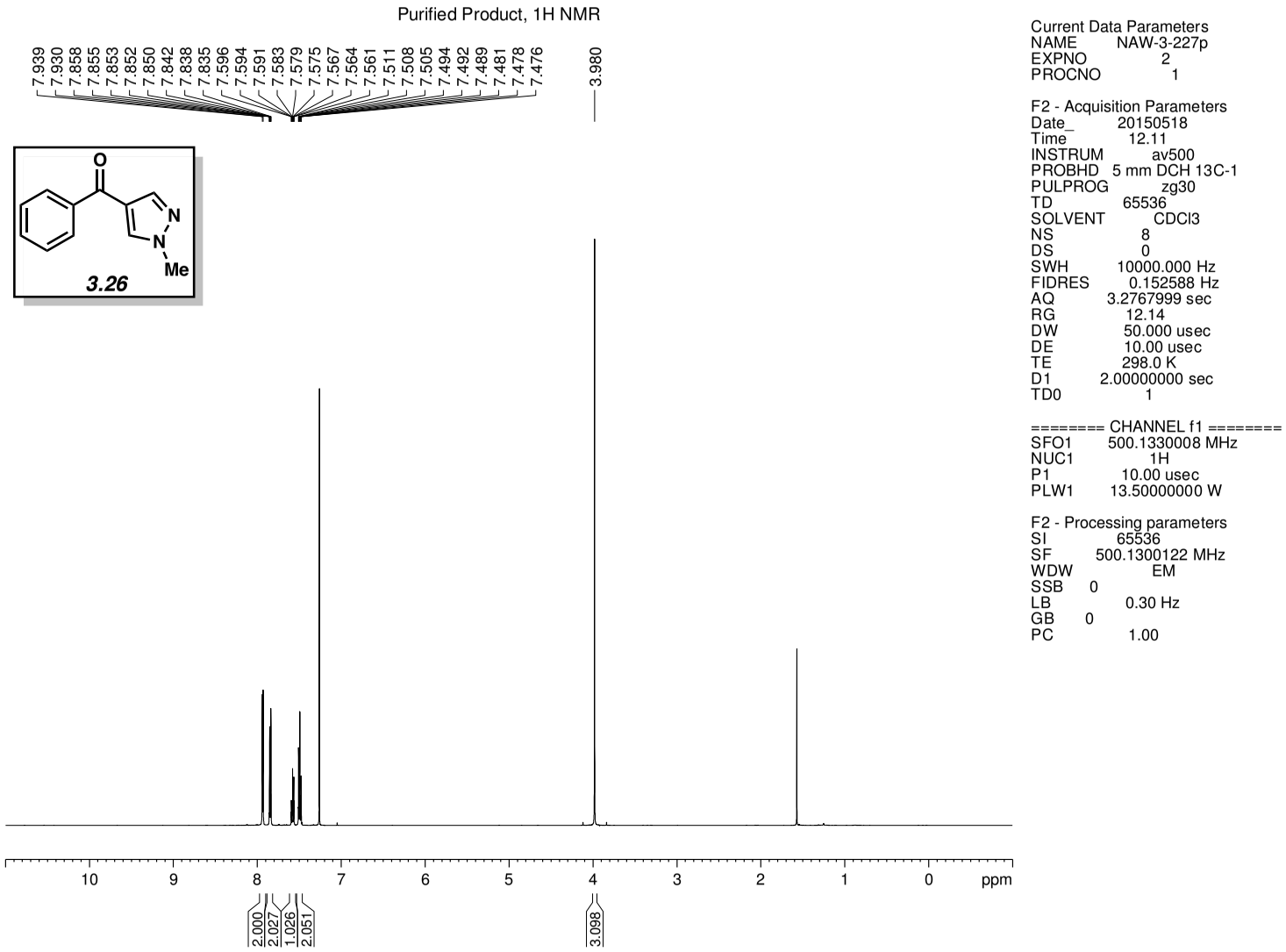

Figure 3.61 ^{1}H NMR (500 MHz, $CDCl_3$) of compound **3.26**.

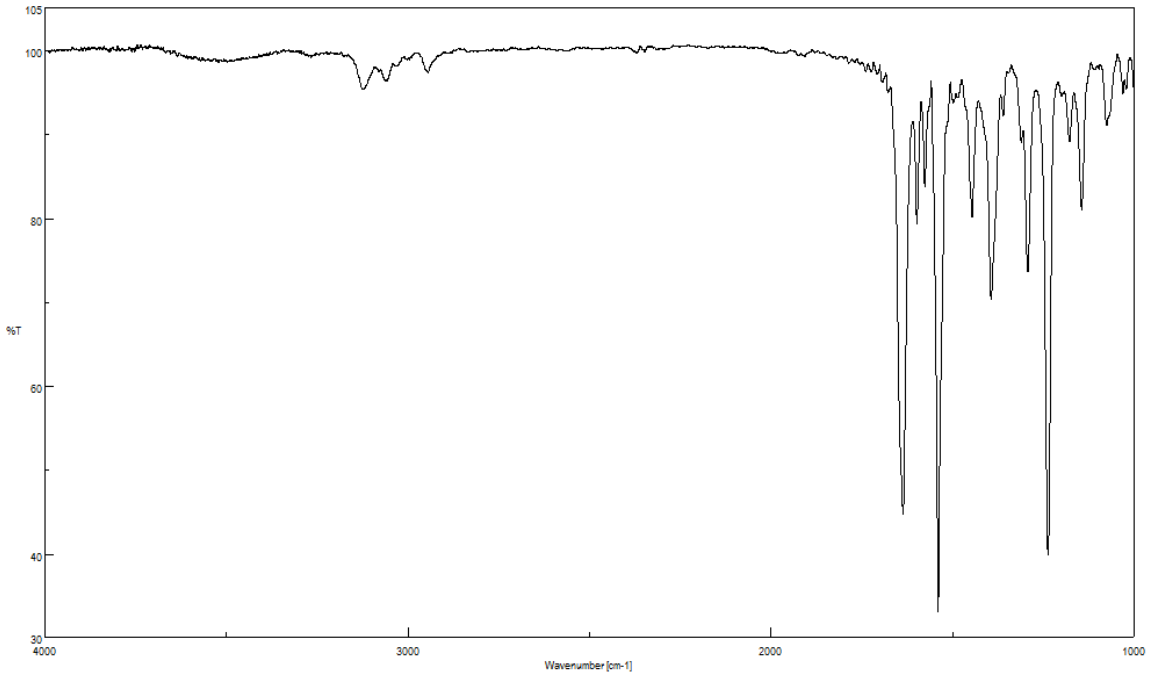

Figure 3.62 Infrared spectrum of compound **3.26**.

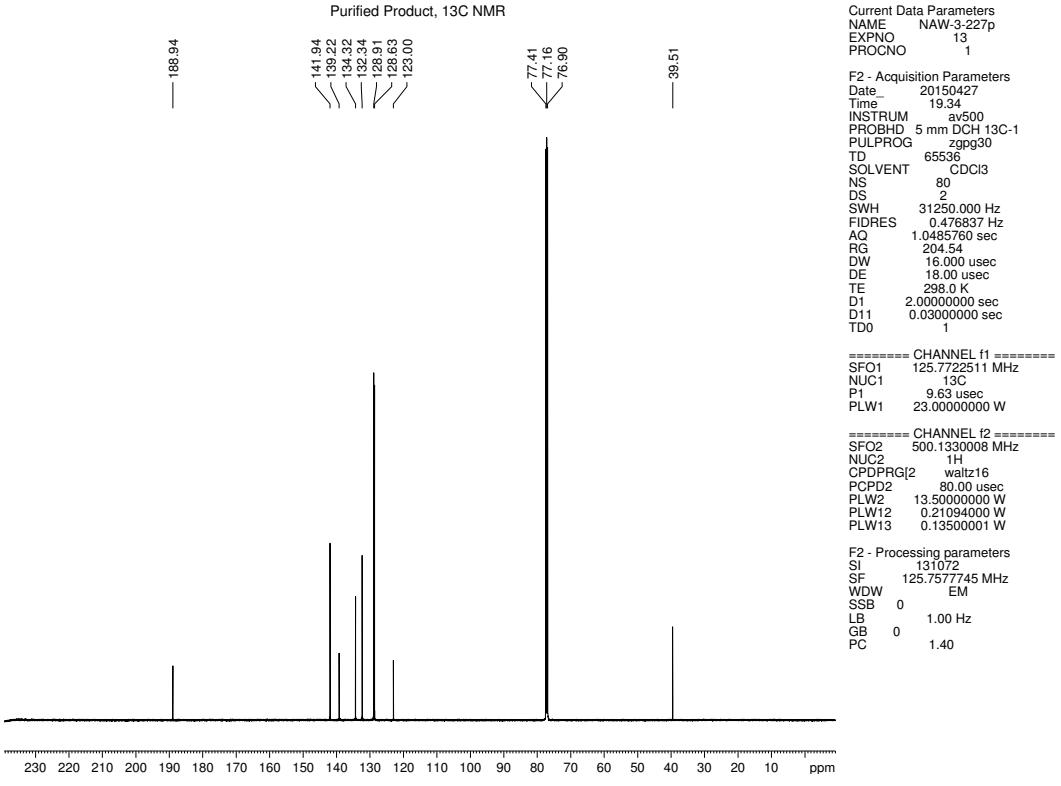

Figure 3.63 ^{13}C NMR (125 MHz, $CDCl_3$) of compound **3.26**.

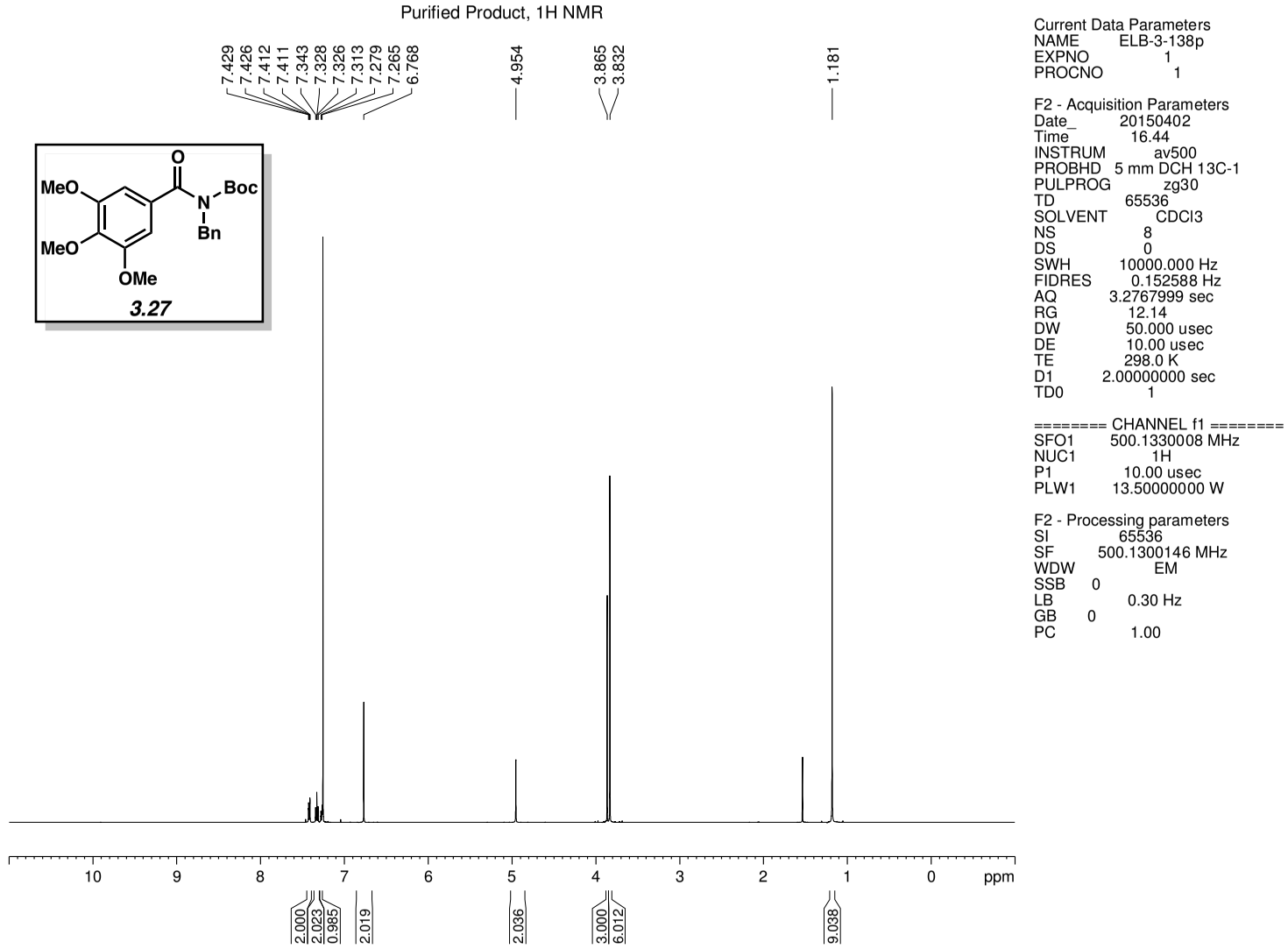

Figure 3.64 ^{1}H NMR (500 MHz, $CDCl_3$) of compound **3.27**.

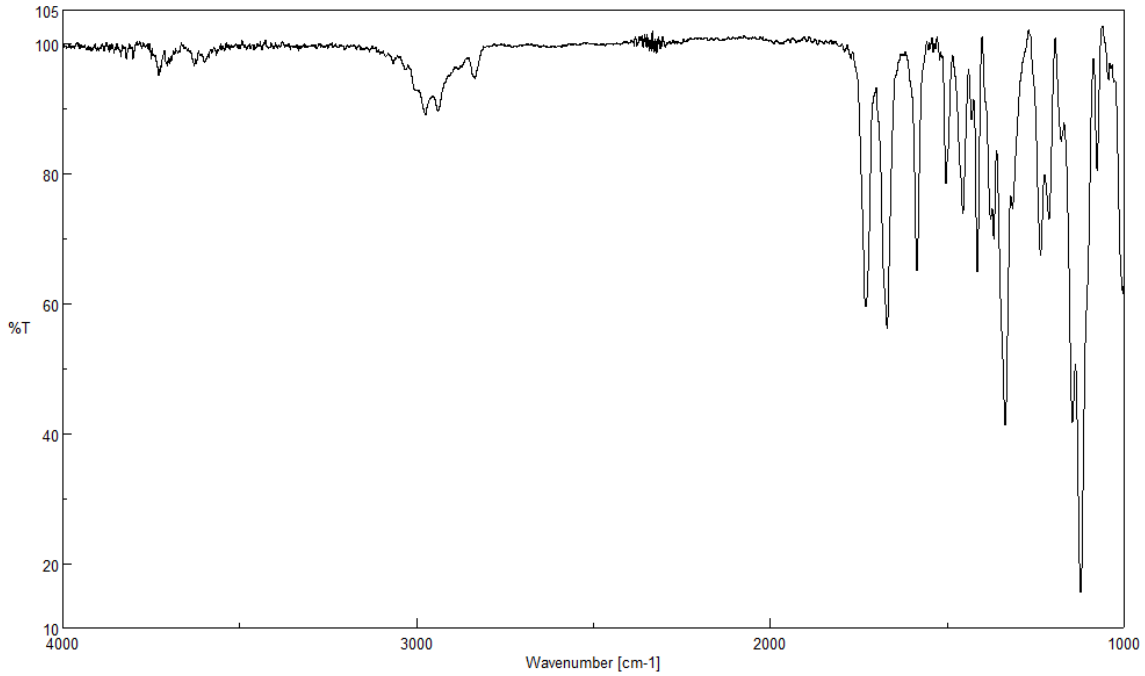

Figure 3.65 Infrared spectrum of compound **3.27**.

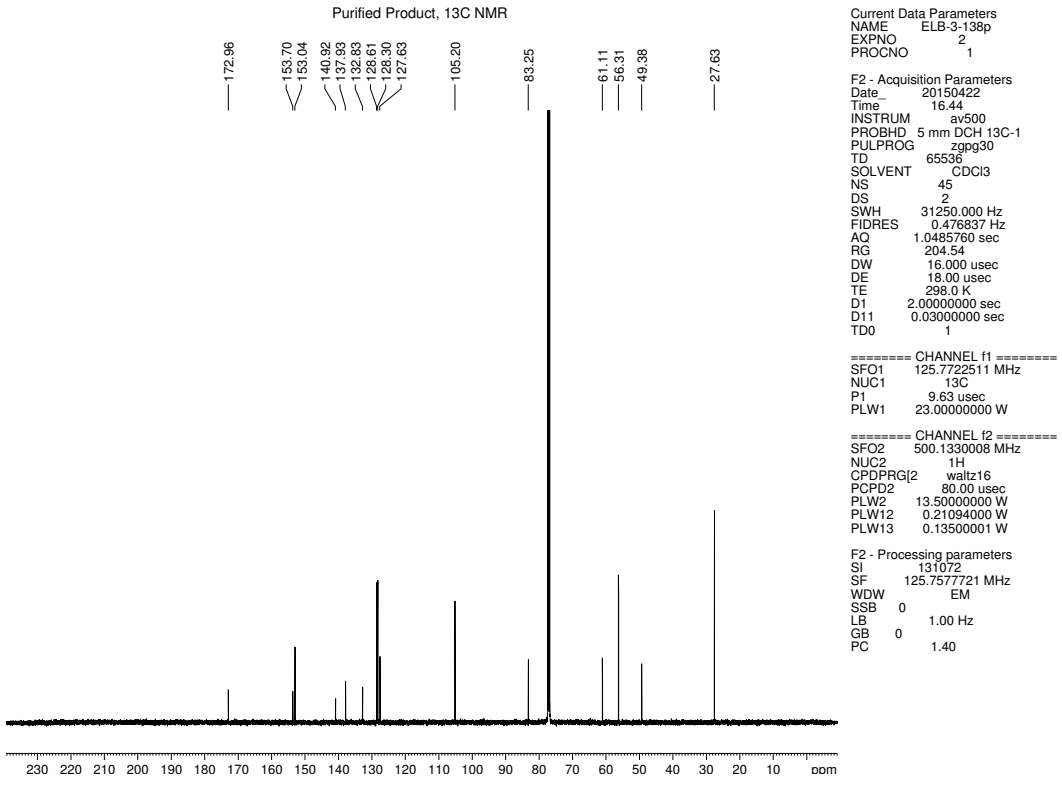

Figure 3.66 ^{13}C NMR (125 MHz, $CDCl_3$) of compound **3.27**.

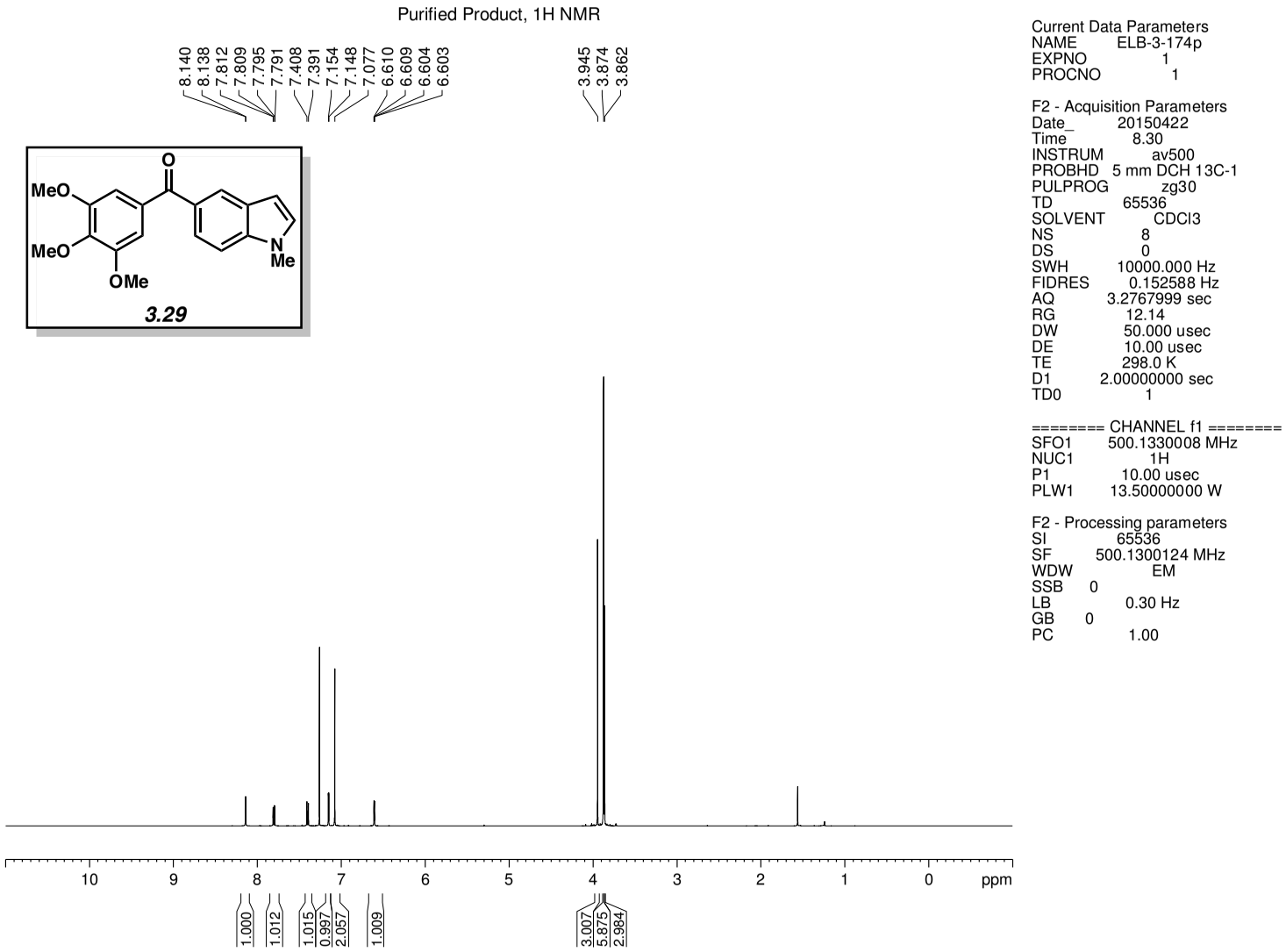

Figure 3.67 ^{1}H NMR (500 MHz, $CDCl_3$) of compound **3.29**.

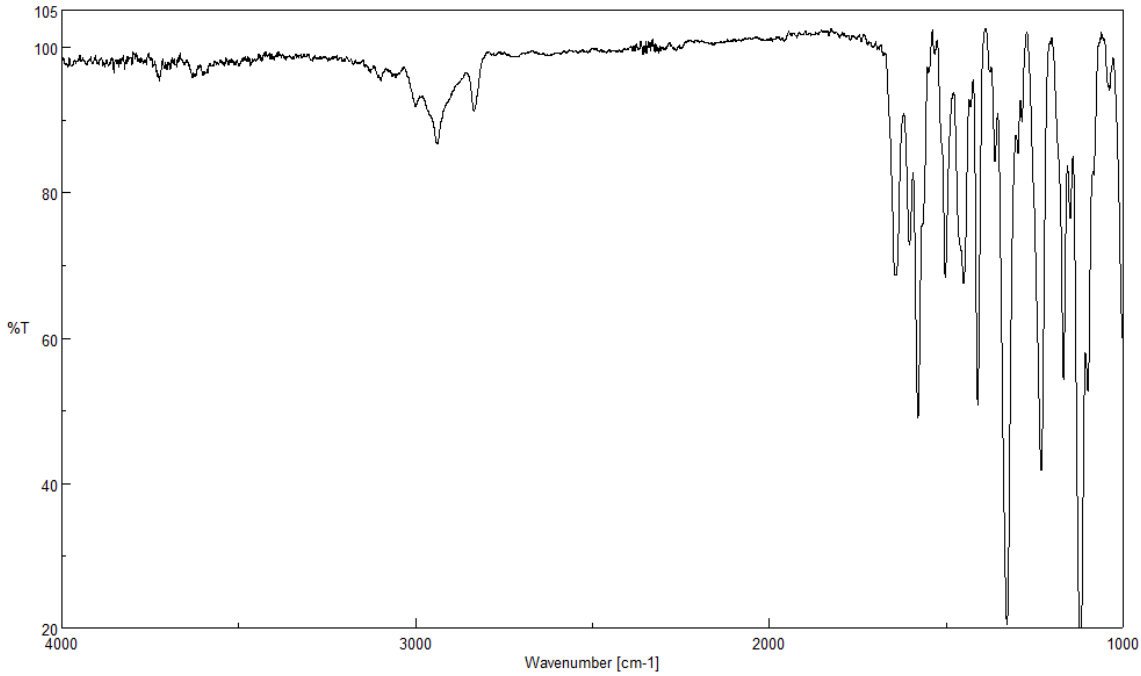

Figure 3.68 Infrared spectrum of compound **3.29**.

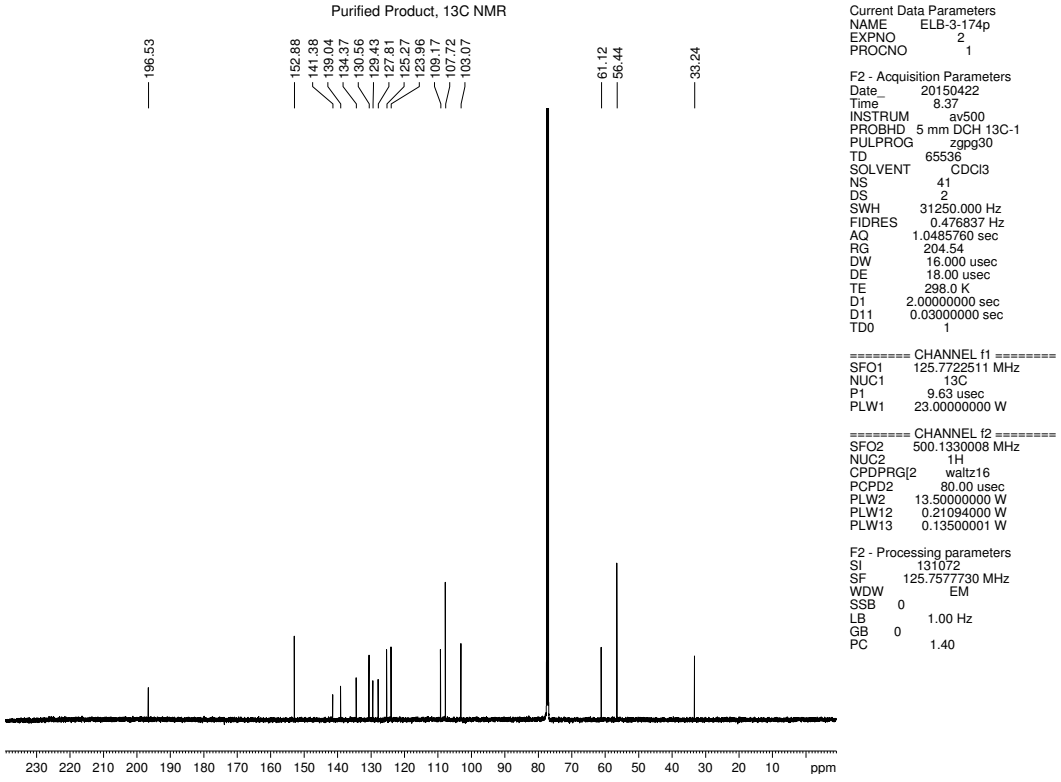

Figure 3.69 ^{13}C NMR (125 MHz, $CDCl_3$) of compound **3.29**.

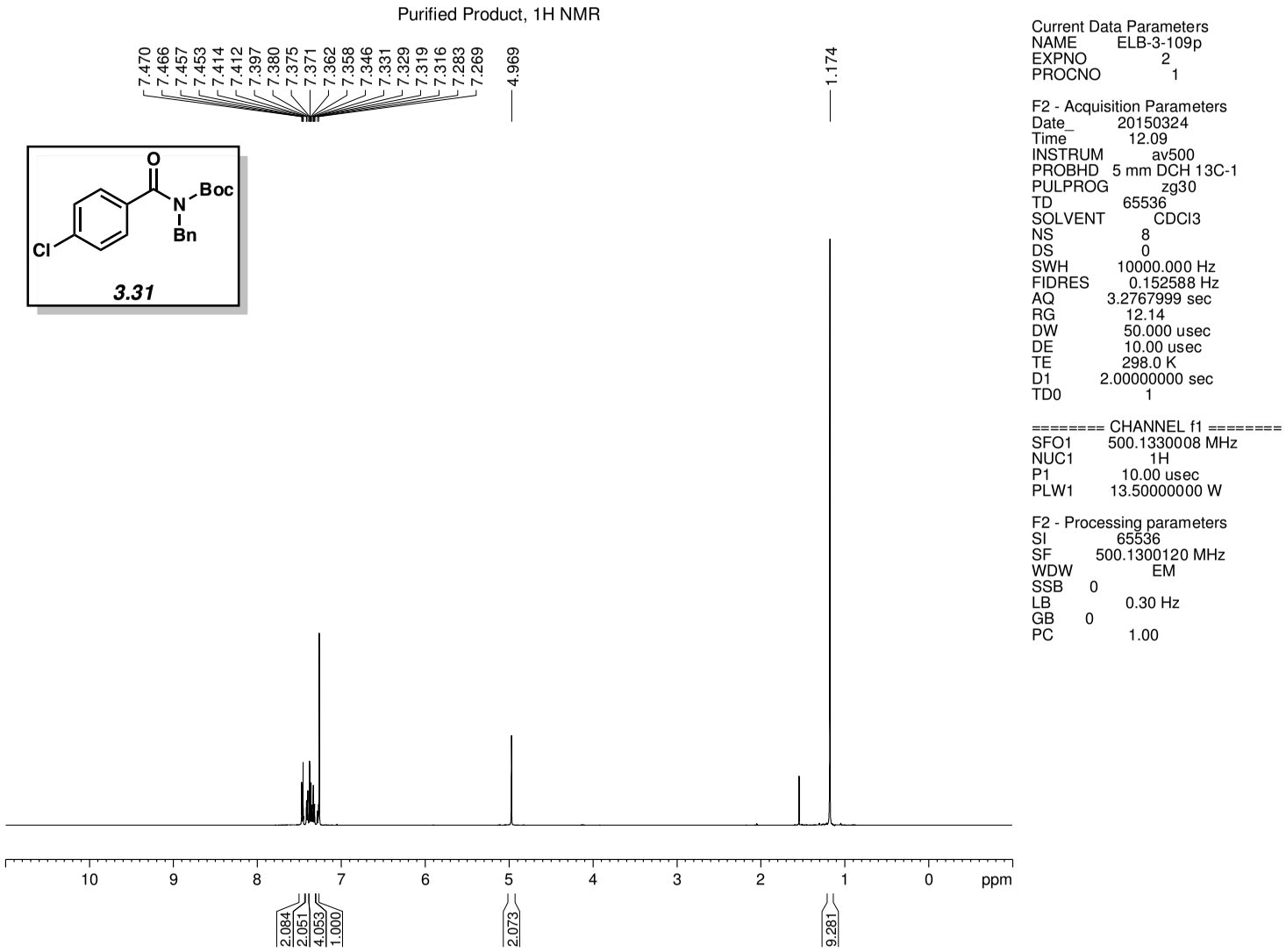

Figure 3.70 ^{1}H NMR (500 MHz, $CDCl_3$) of compound **3.31**.

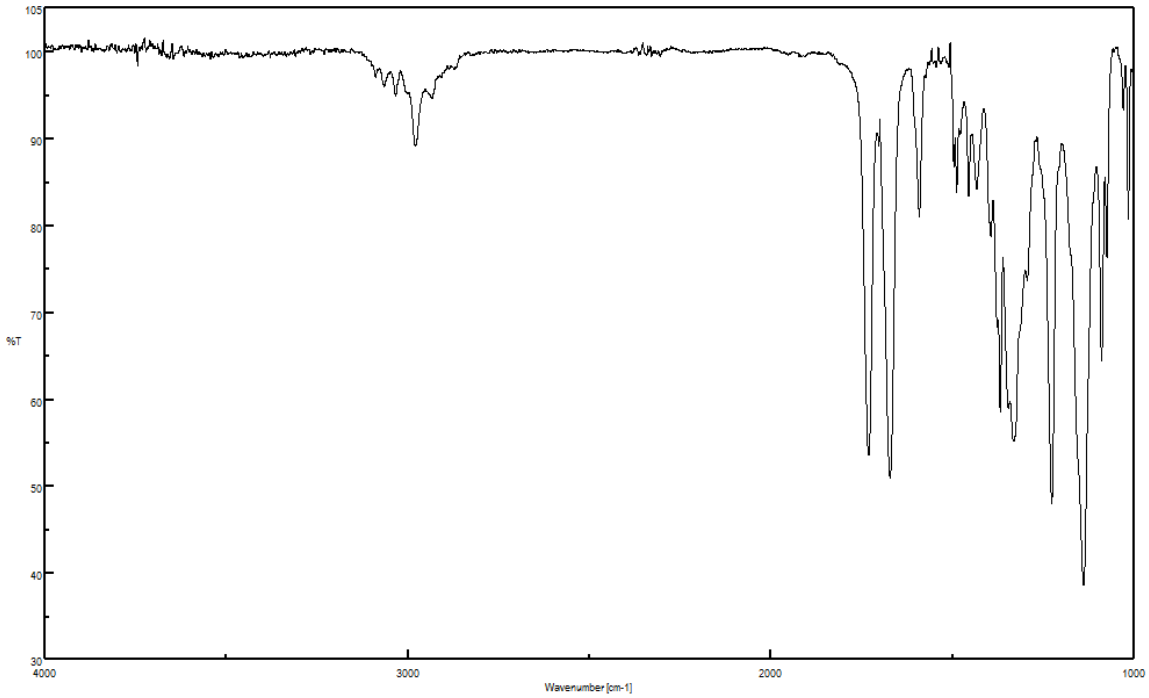

Figure 3.71 Infrared spectrum of compound **3.31**.

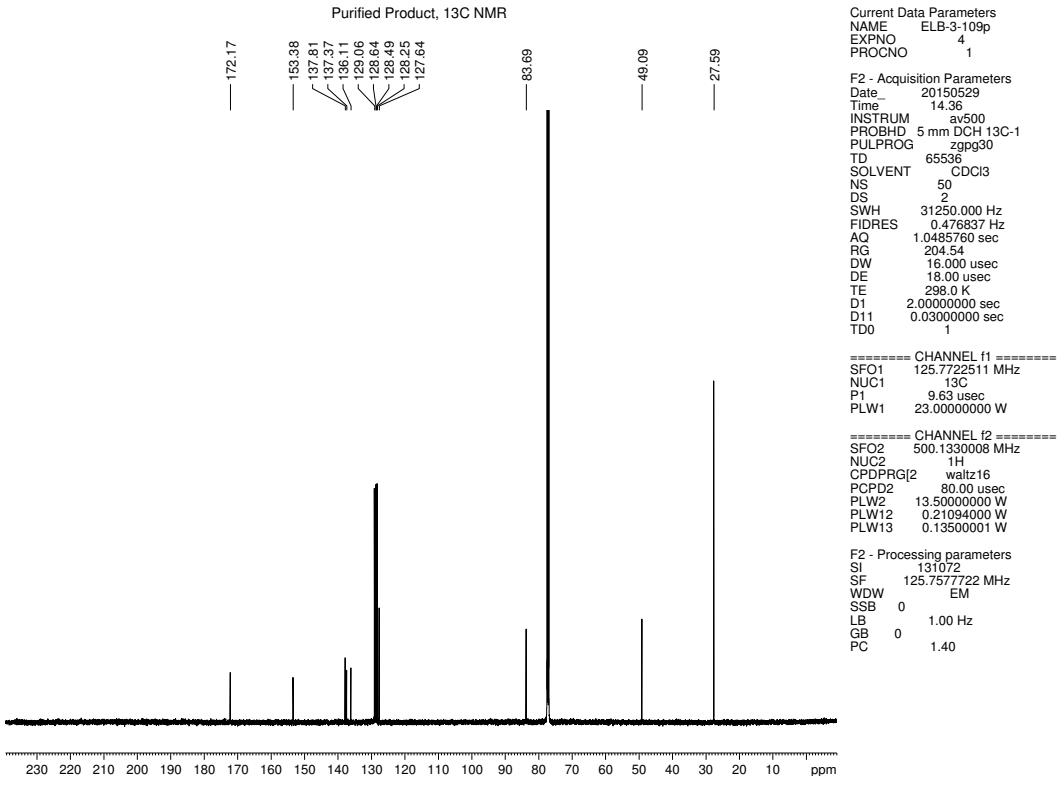

Figure 3.72 ^{13}C NMR (125 MHz, $CDCl_3$) of compound **3.31**.

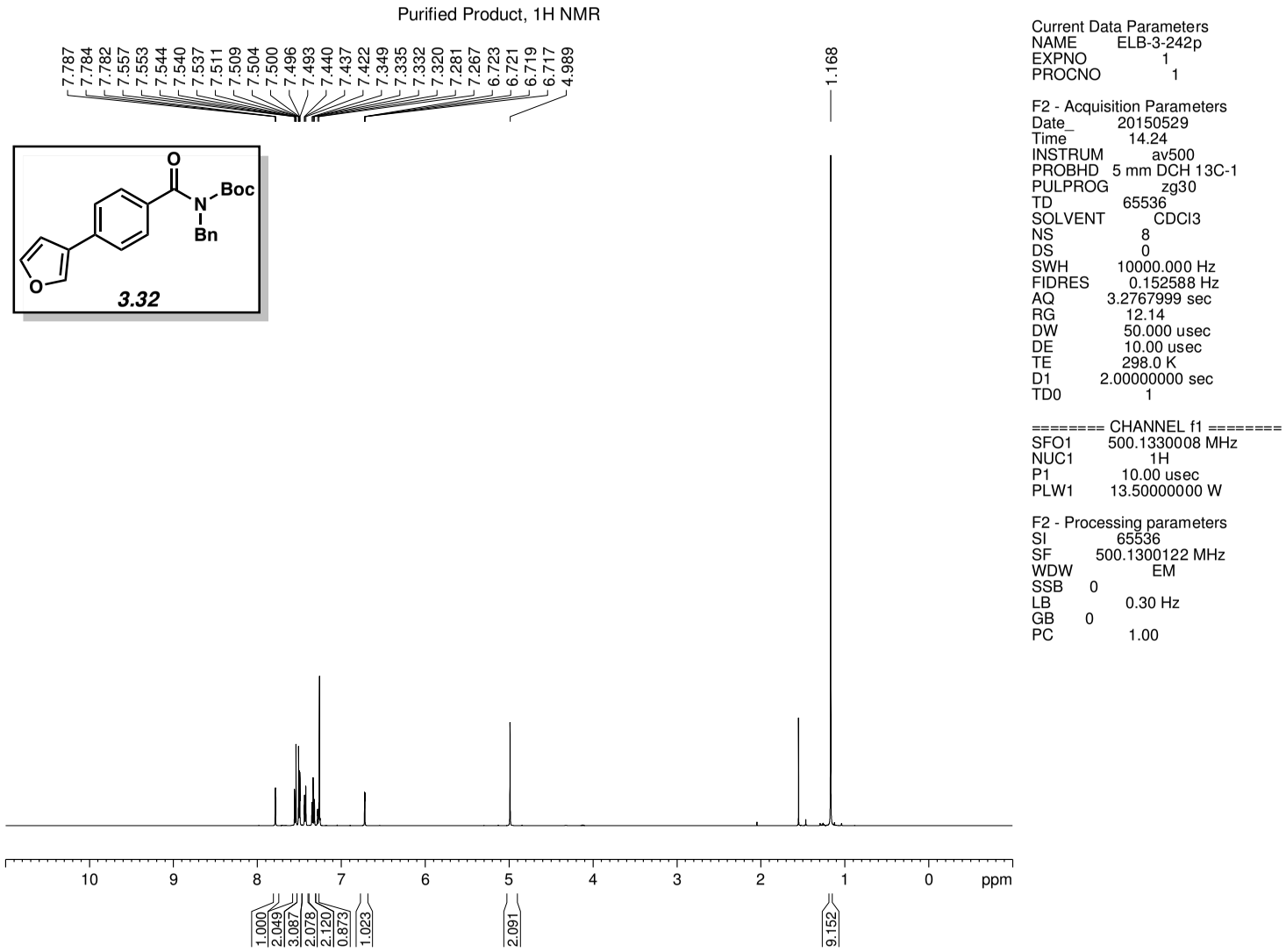

Figure 3.73 ^{1}H NMR (500 MHz, $CDCl_3$) of compound **3.32**.

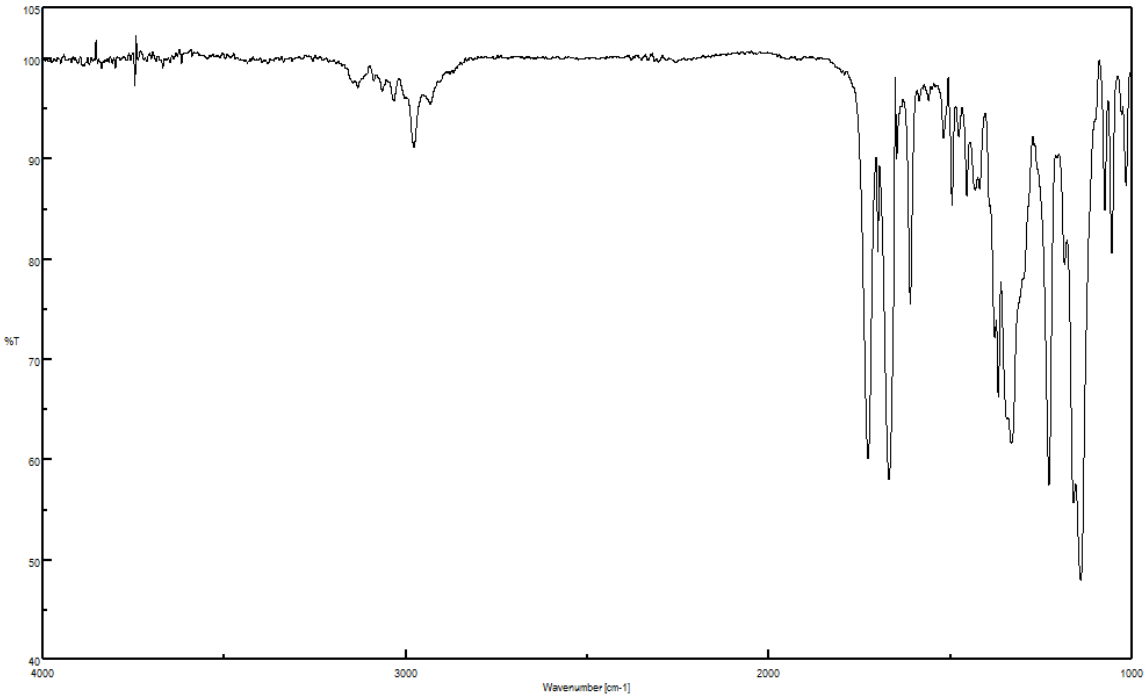

Figure 3.74 Infrared spectrum of compound **3.32**.

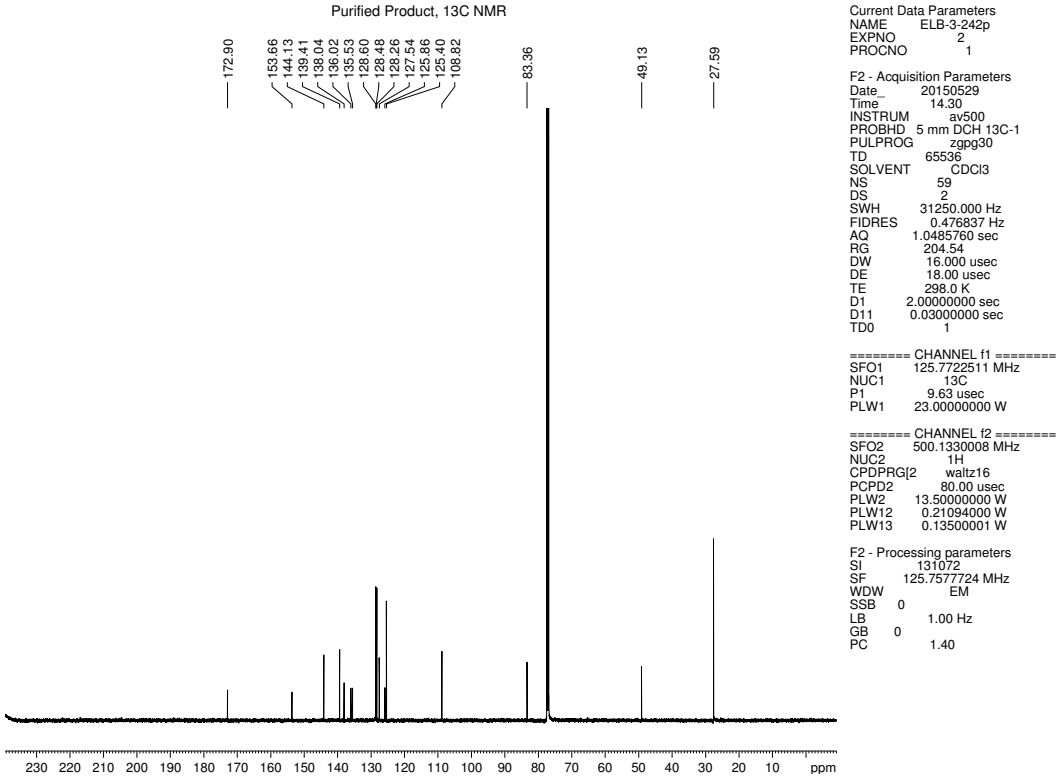

Figure 3.75 ^{13}C NMR (125 MHz, $CDCl_3$) of compound **3.32**.

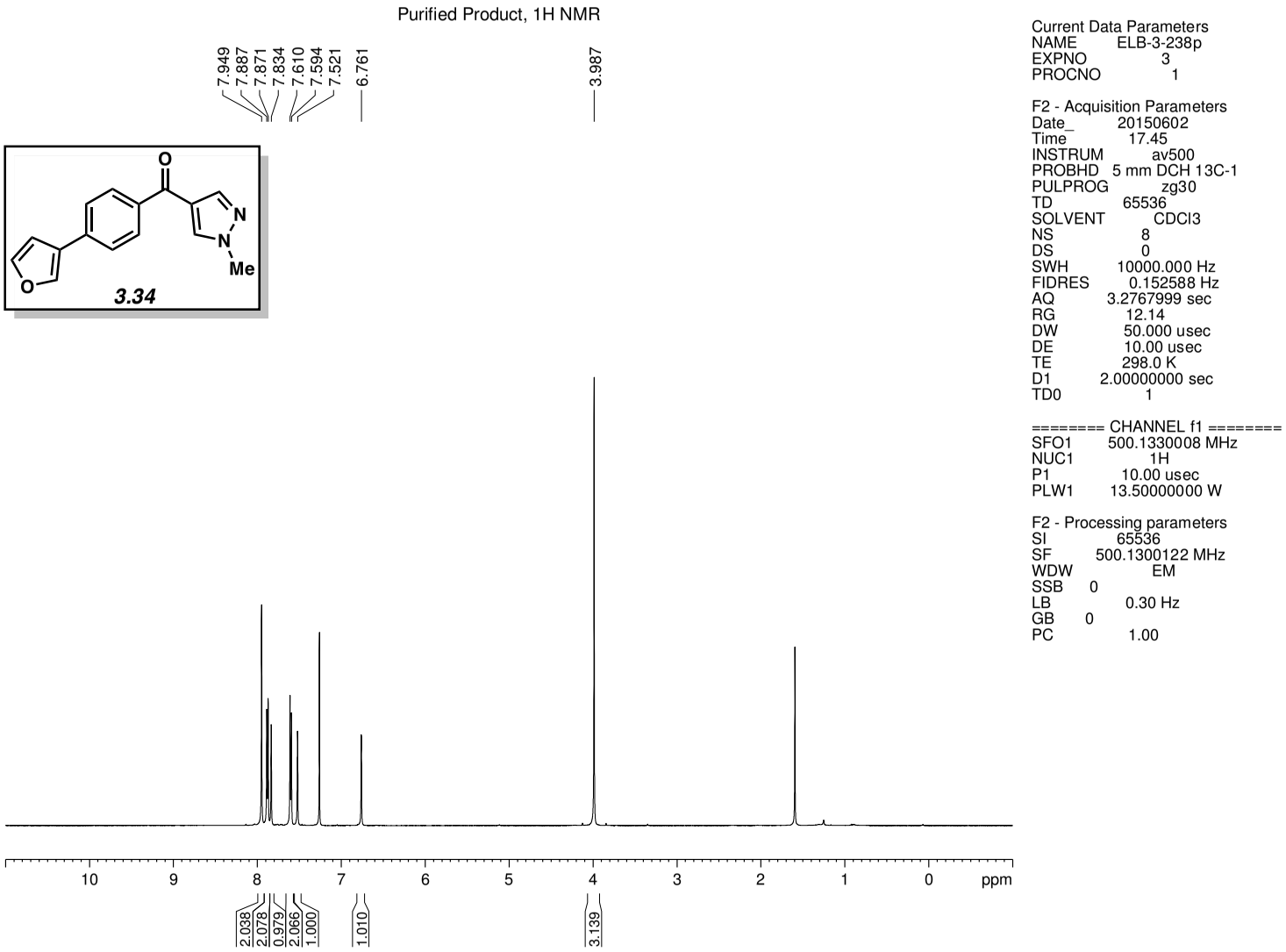

Figure 3.76 ^{1}H NMR (500 MHz, $CDCl_3$) of compound **3.34**.

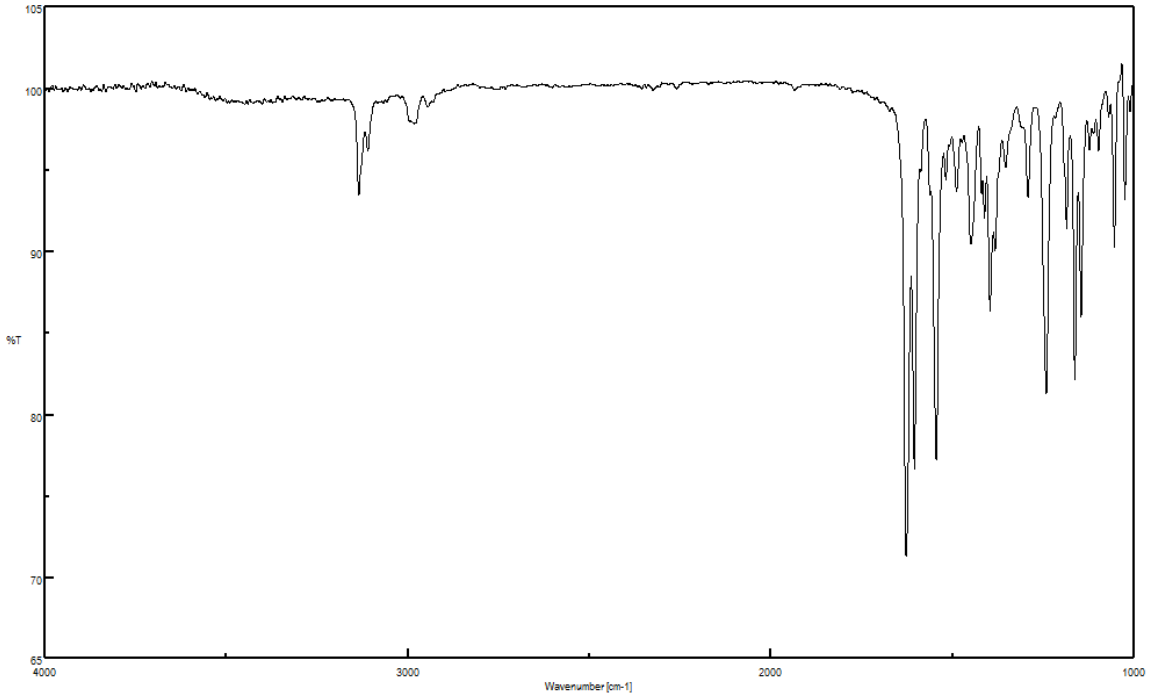

Figure 3.77 Infrared spectrum of compound **3.34**.

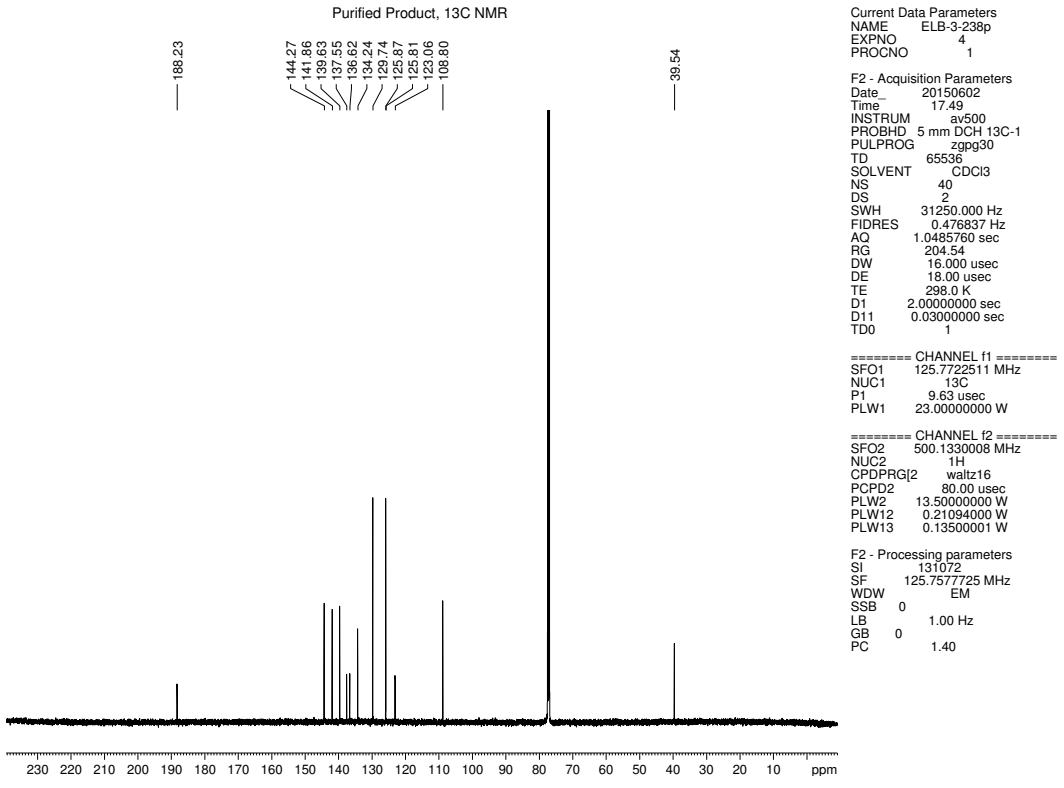

Figure 3.78 ^{13}C NMR (125 MHz, $CDCl_3$) of compound **3.34**.

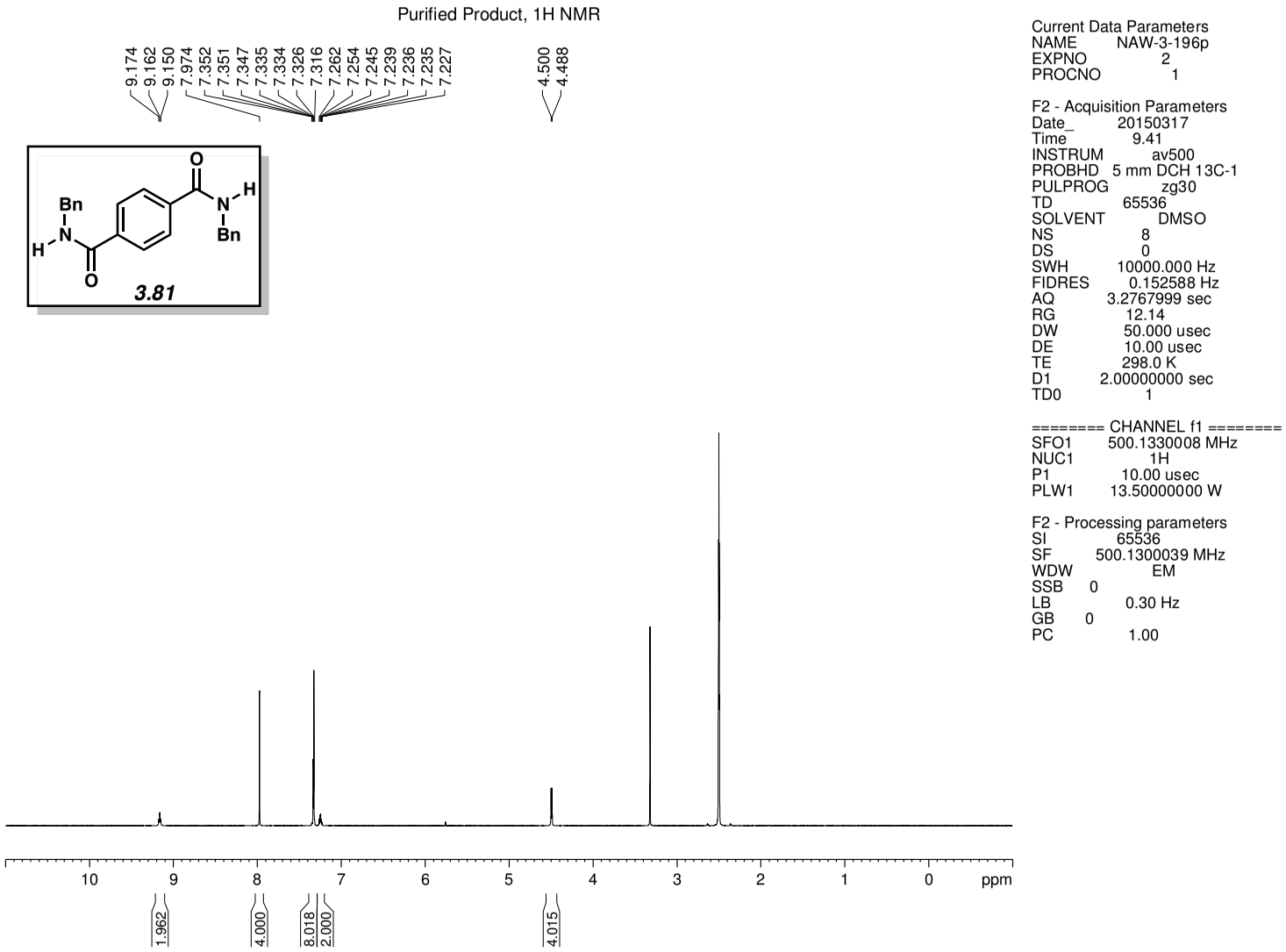

Figure 3.79 ^{1}H NMR (500 MHz, DMSO-d_6) of compound **3.81**.

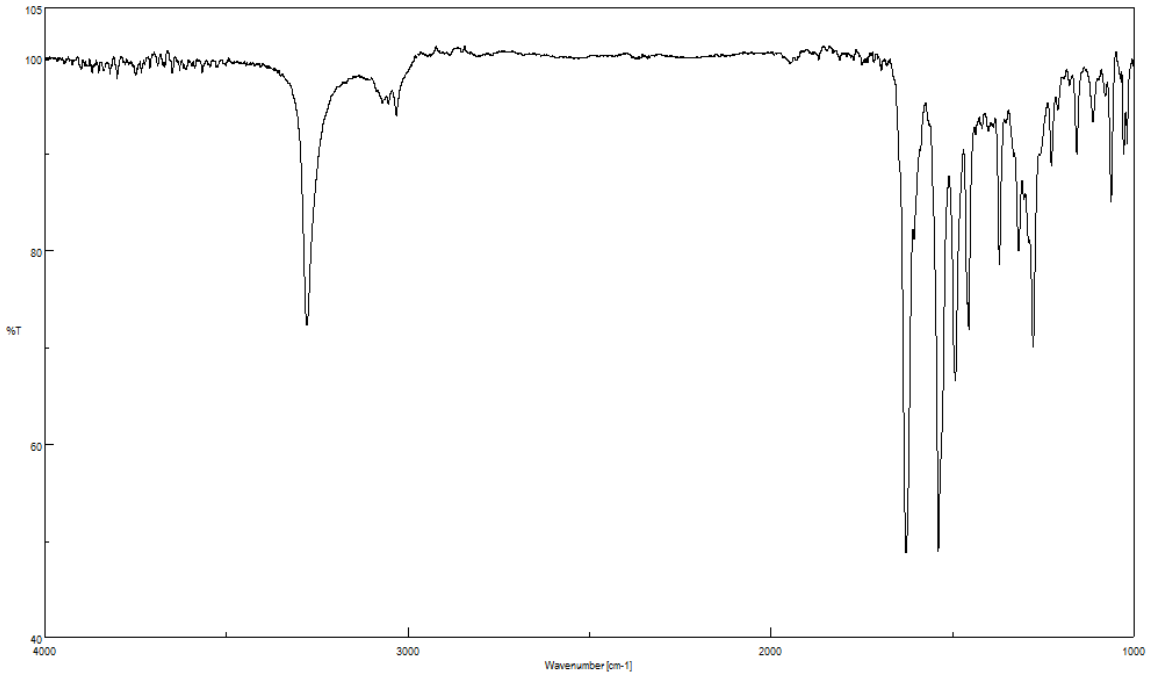

Figure 3.80 Infrared spectrum of compound **3.81**.

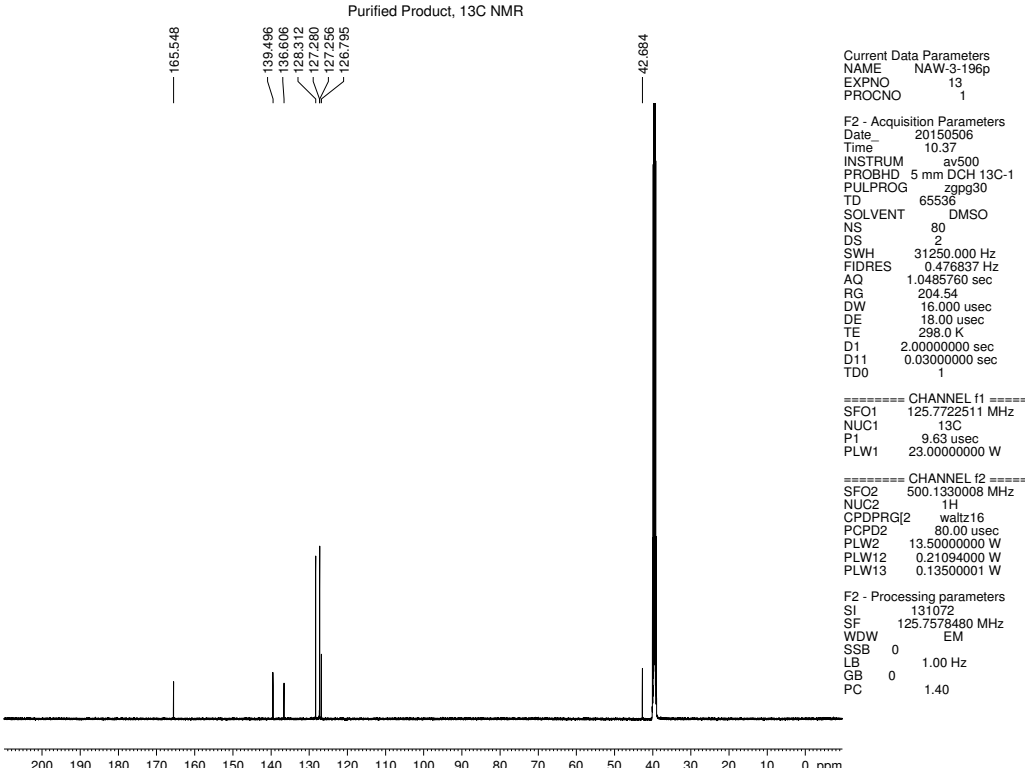

Figure 3.81 ^{13}C NMR (125 MHz, DMSO-d_6) of compound **3.81**.

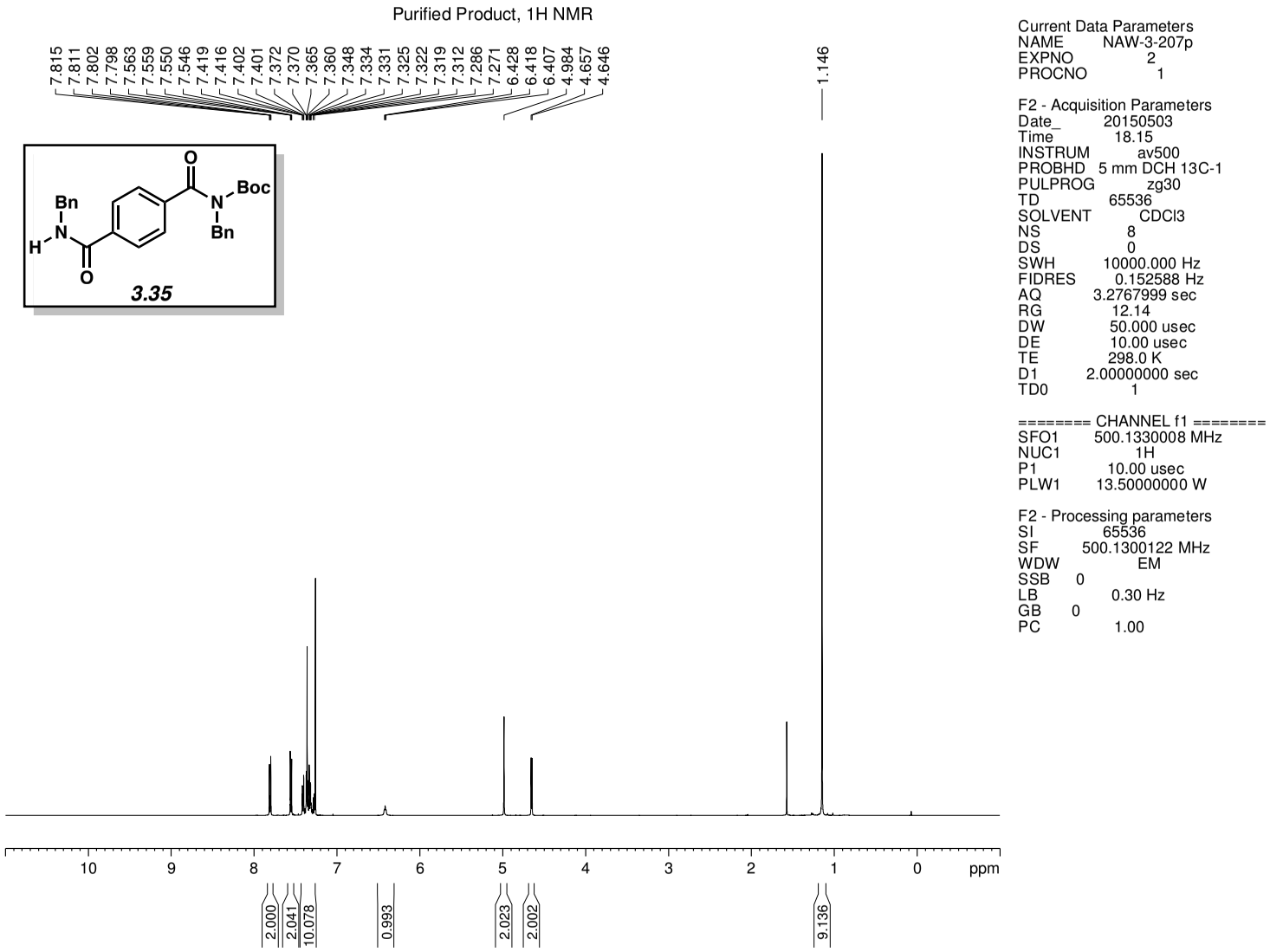

Figure 3.82 ^{1}H NMR (500 MHz, $CDCl_3$) of compound **3.35**.

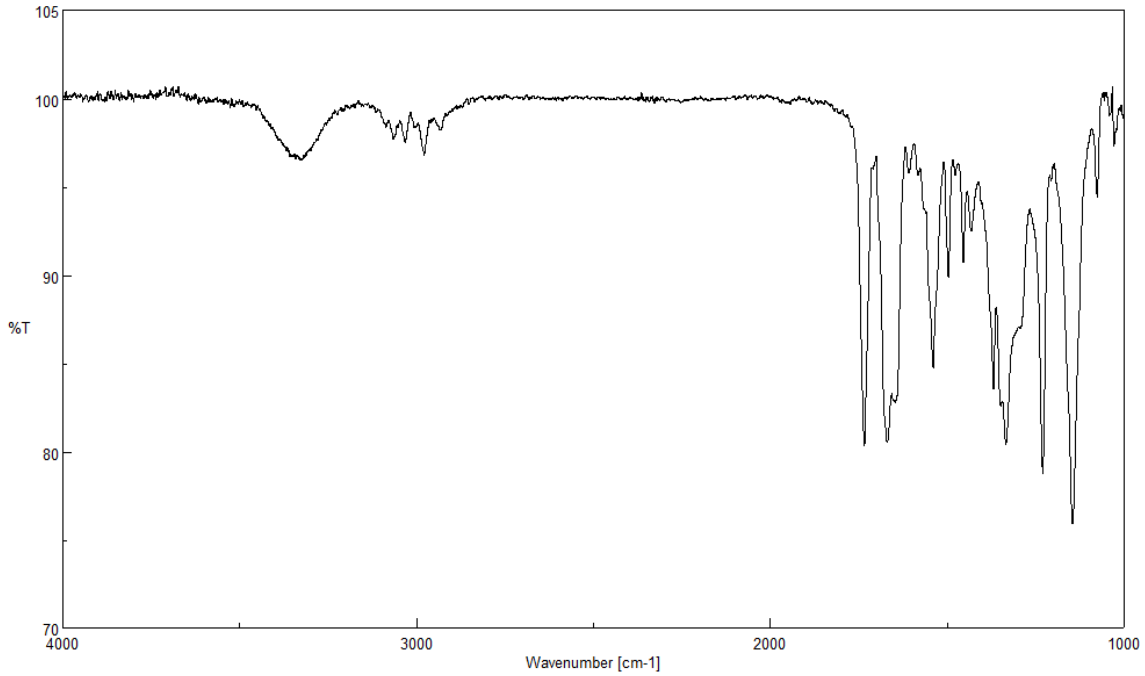

Figure 3.83 Infrared spectrum of compound **3.35**.

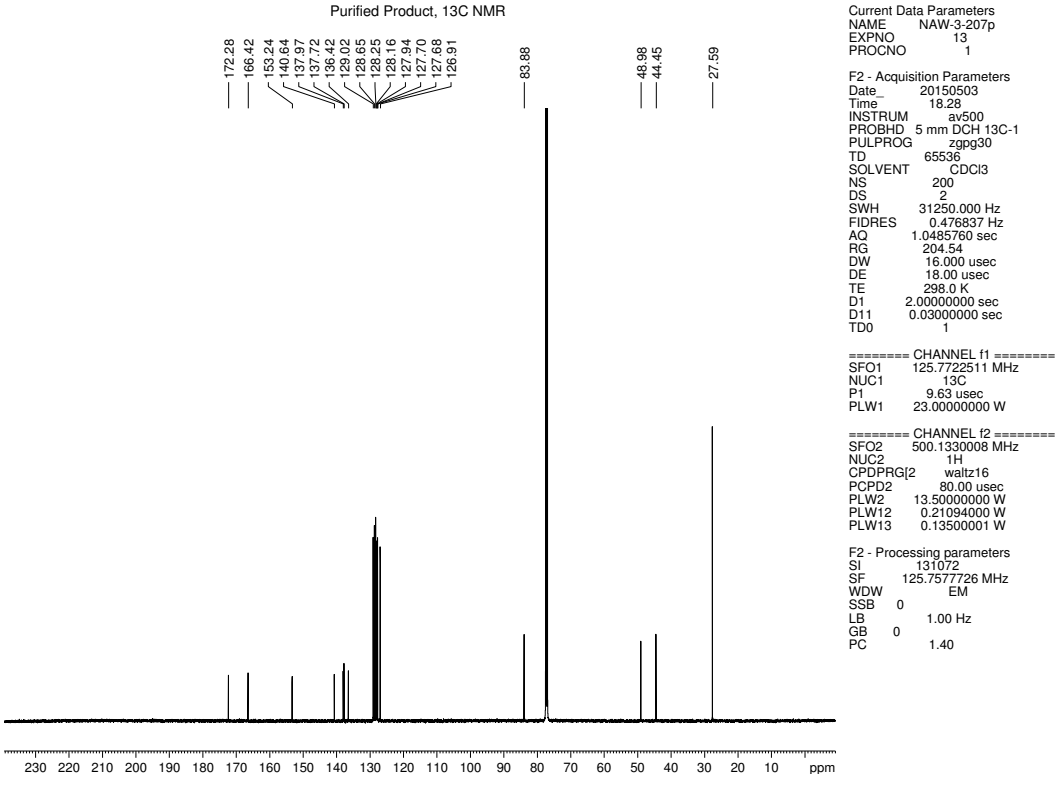

Figure 3.84 ^{13}C NMR (125 MHz, $CDCl_3$) of compound **3.35**.

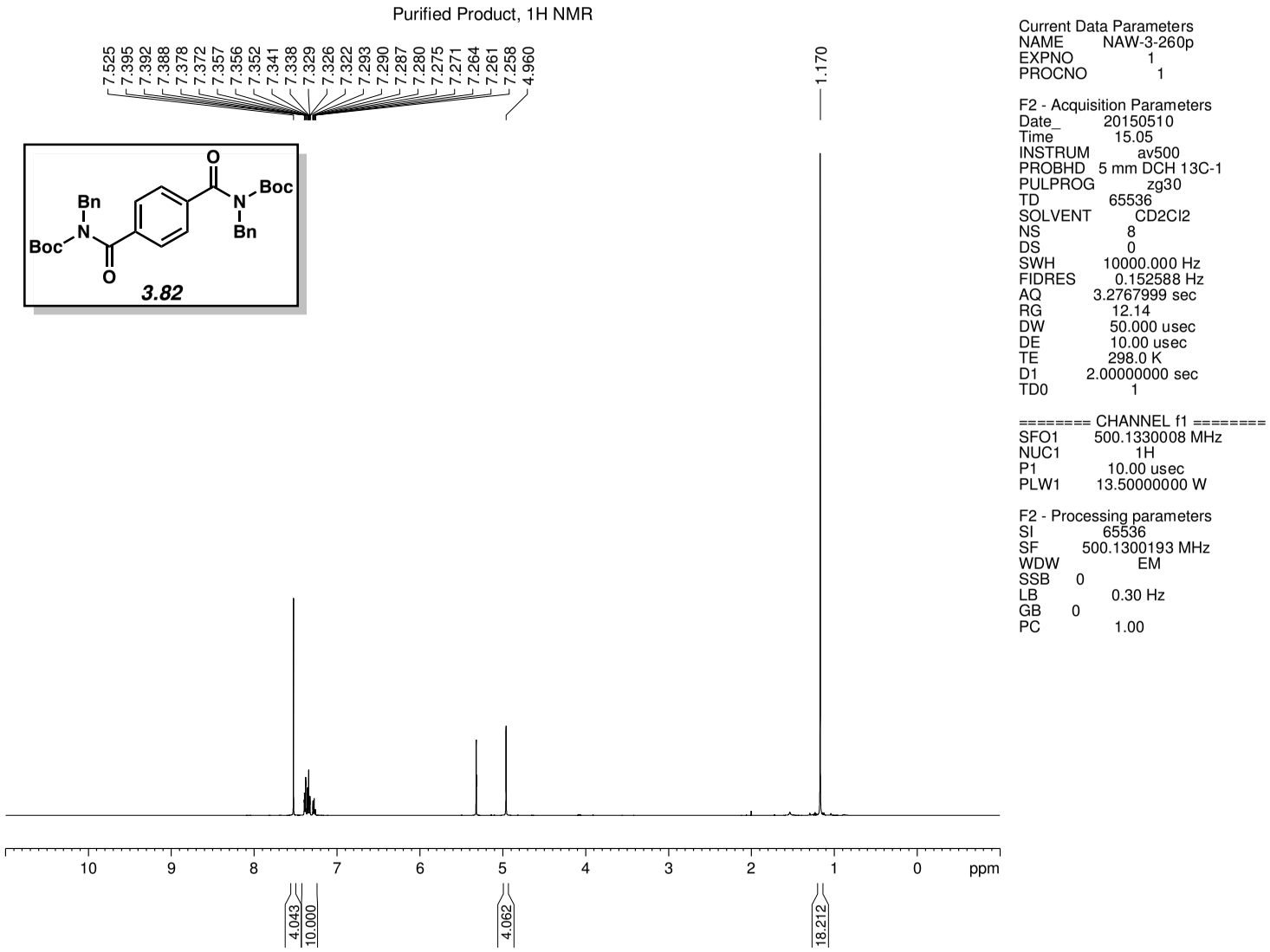

Figure 3.85 ^{1}H NMR (500 MHz, CD_2Cl_2) of compound **3.82**.

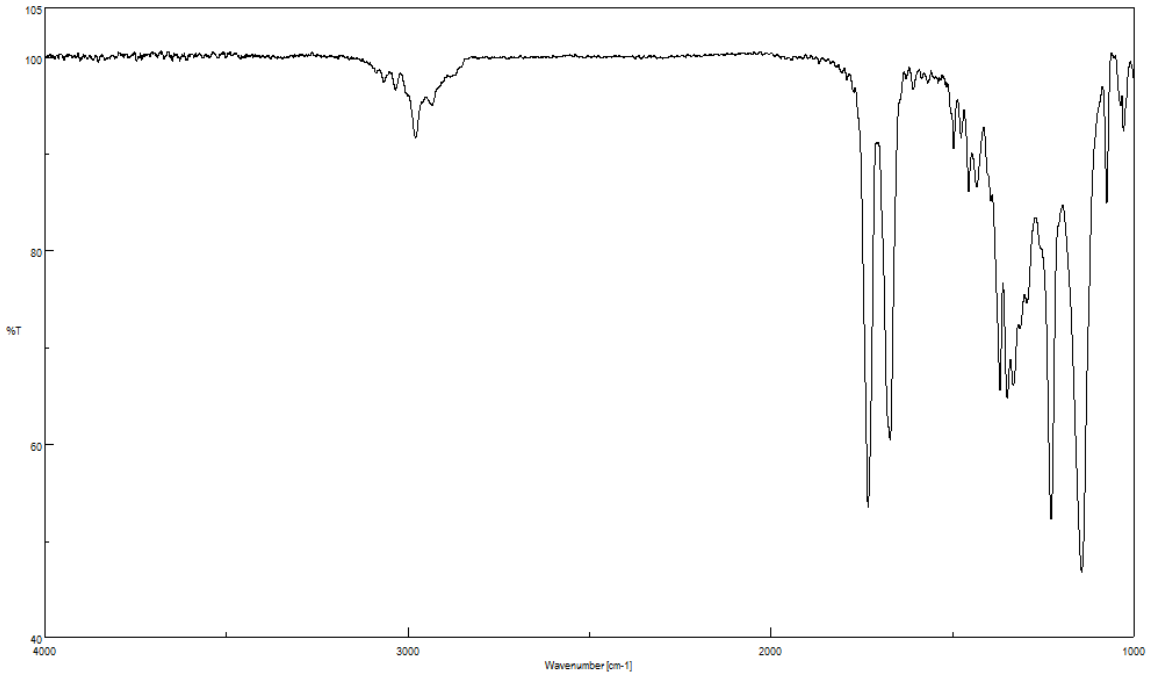

Figure 3.86 Infrared spectrum of compound **3.82**.

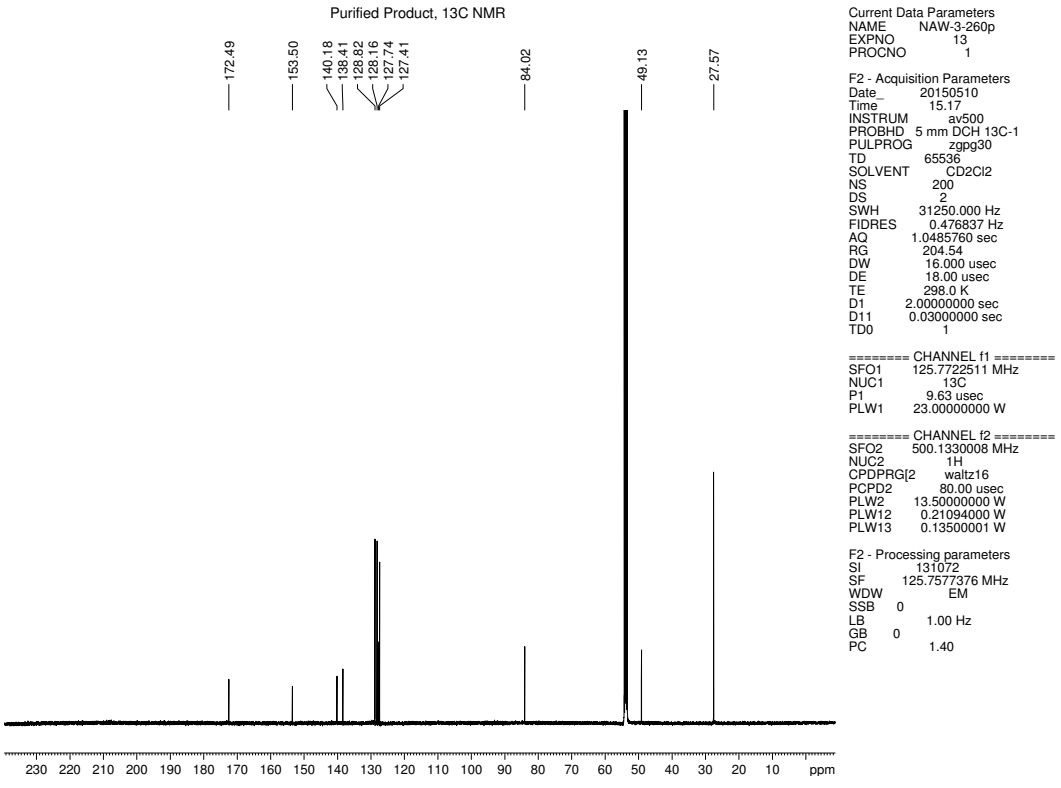

Figure 3.87 ^{13}C NMR (125 MHz, CD_2Cl_2) of compound **3.82**.

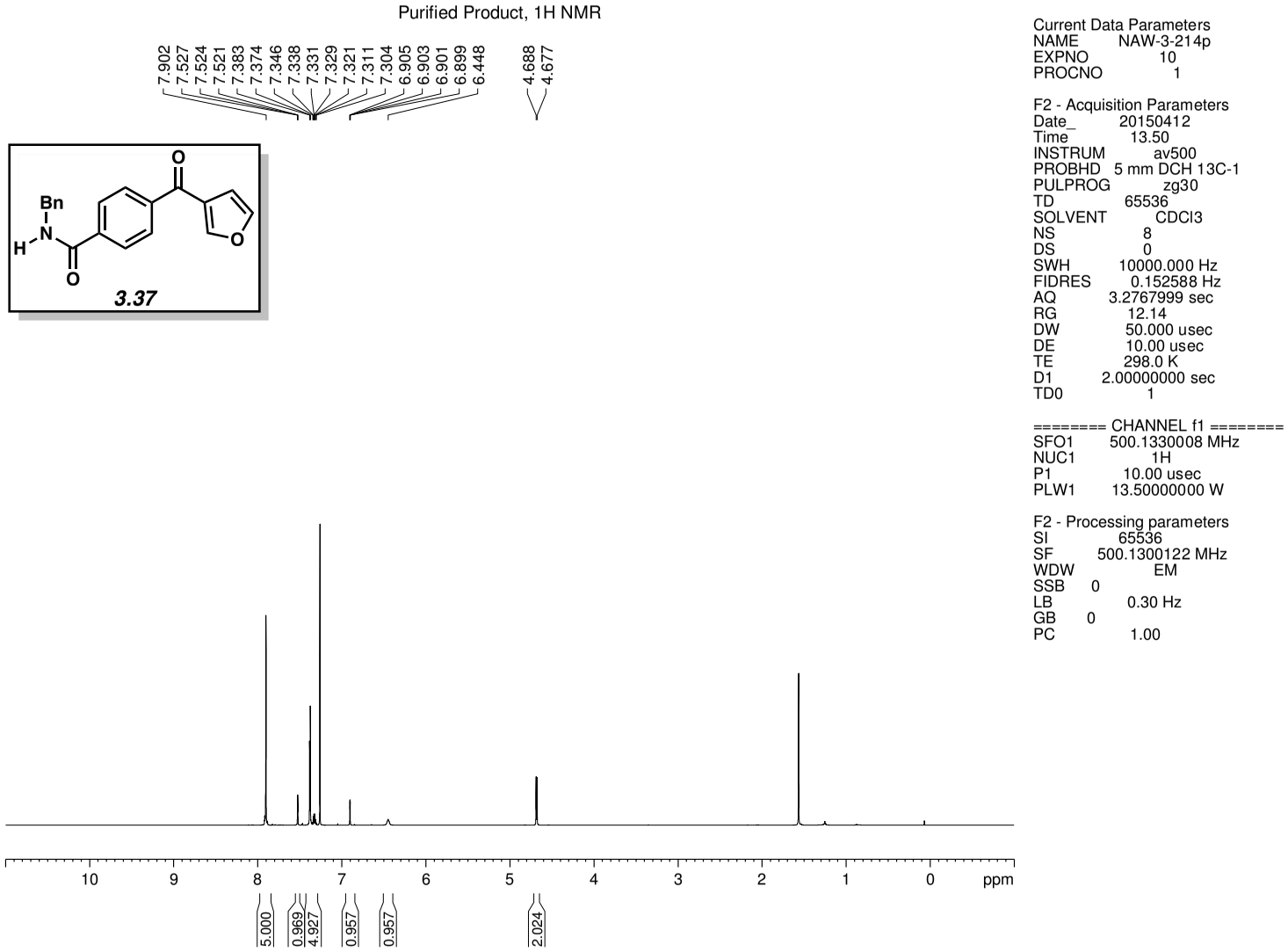

Figure 3.88 ^{1}H NMR (500 MHz, $CDCl_3$) of compound **3.37**.

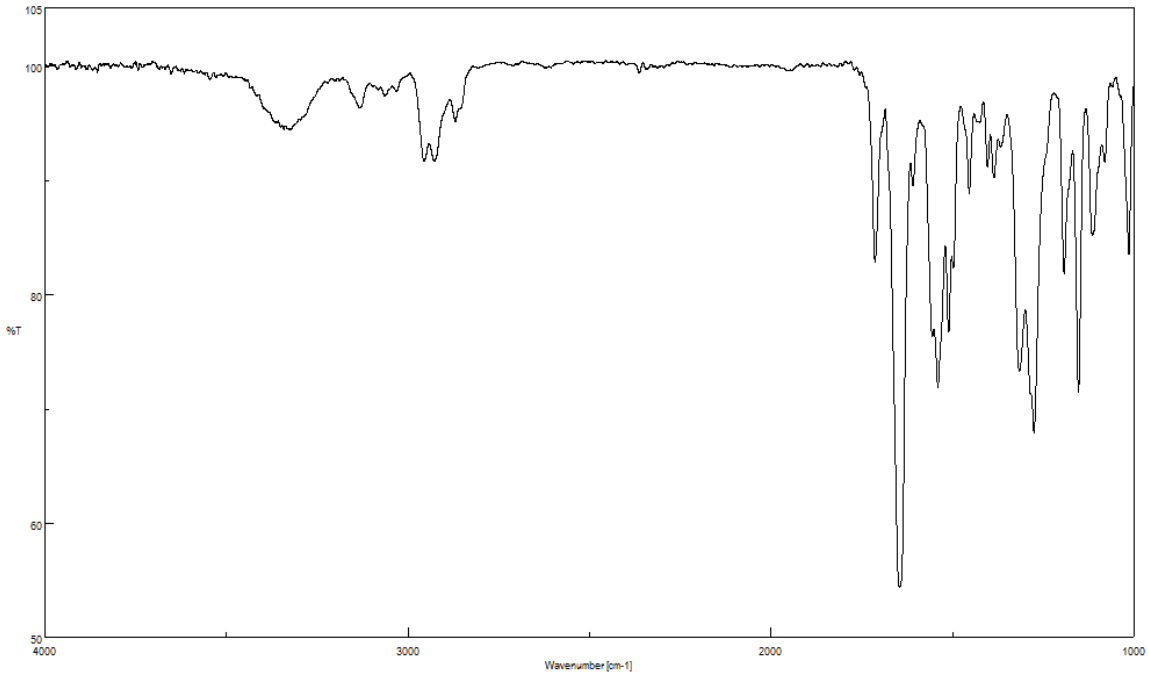

Figure 3.89 Infrared spectrum of compound **3.37**.

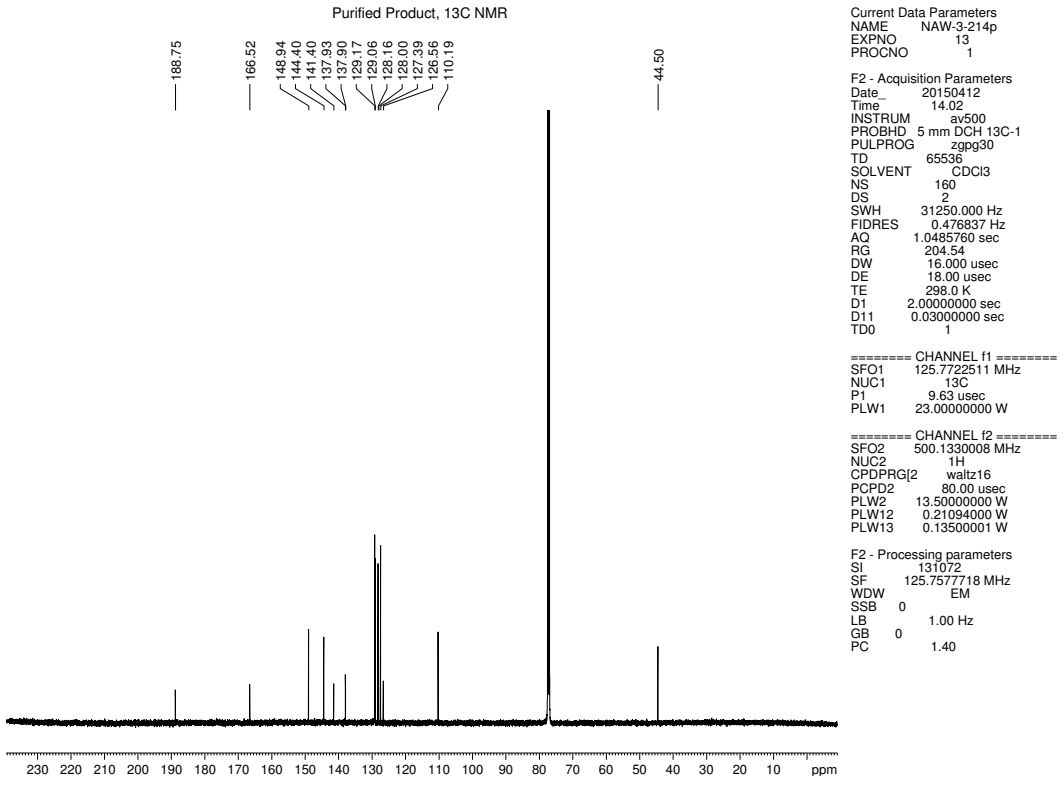

Figure 3.90 ^{13}C NMR (125 MHz, $CDCl_3$) of compound **3.37**.

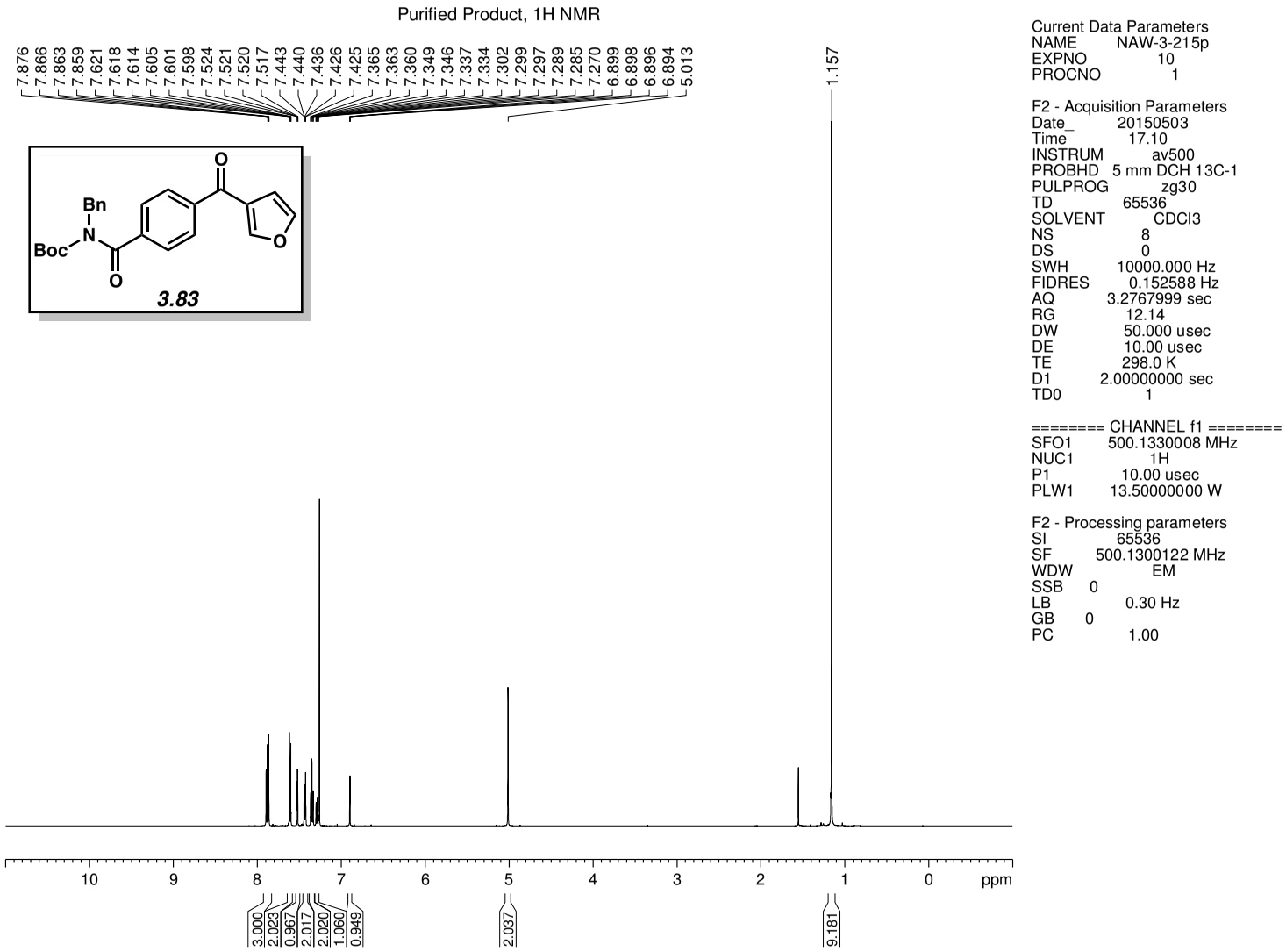

Figure 3.91 ^{1}H NMR (500 MHz, $CDCl_3$) of compound **3.83**.

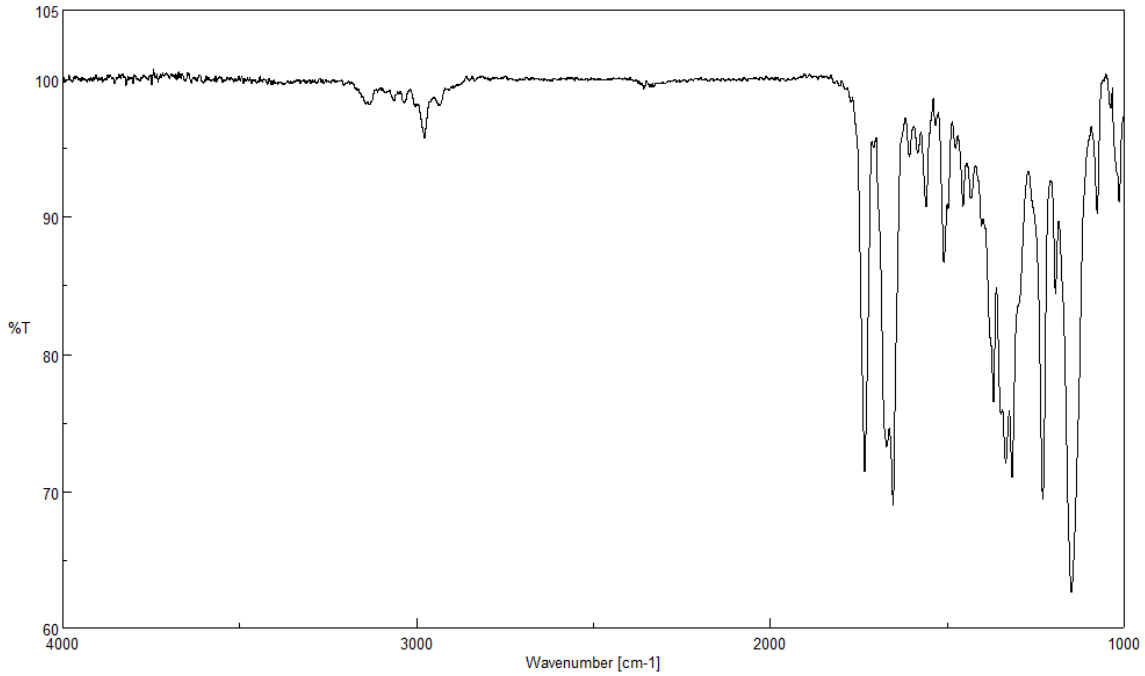

Figure 3.92 Infrared spectrum of compound **3.83**.

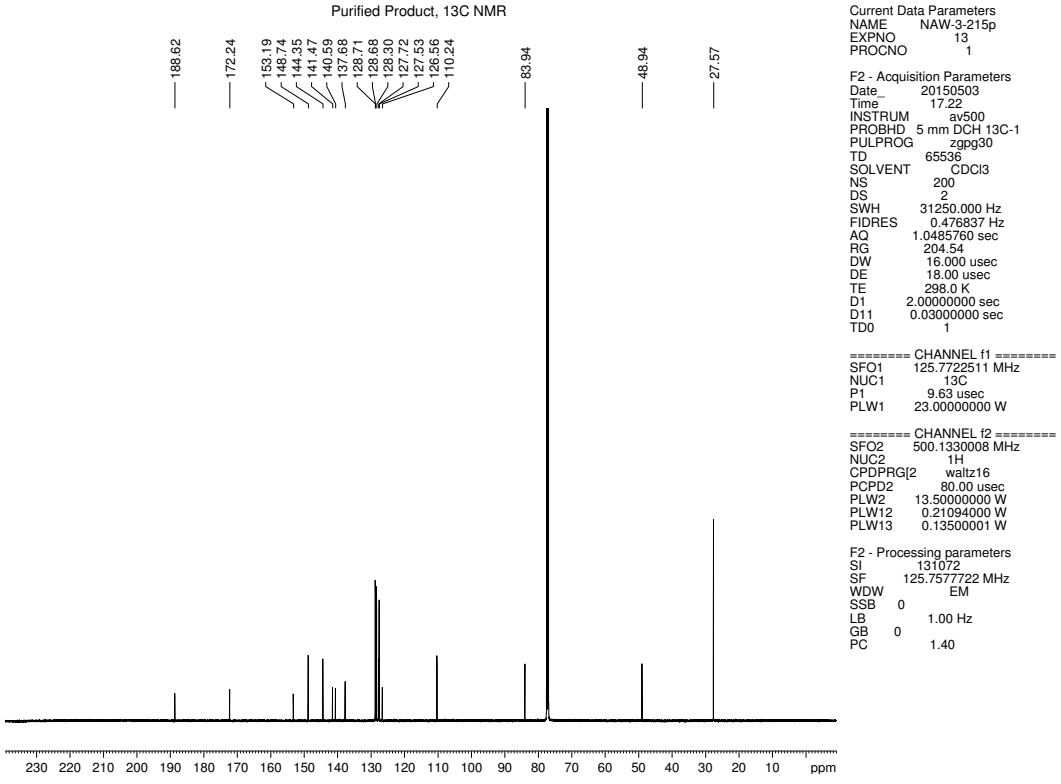

Figure 3.93 ^{13}C NMR (125 MHz, $CDCl_3$) of compound **3.83**.

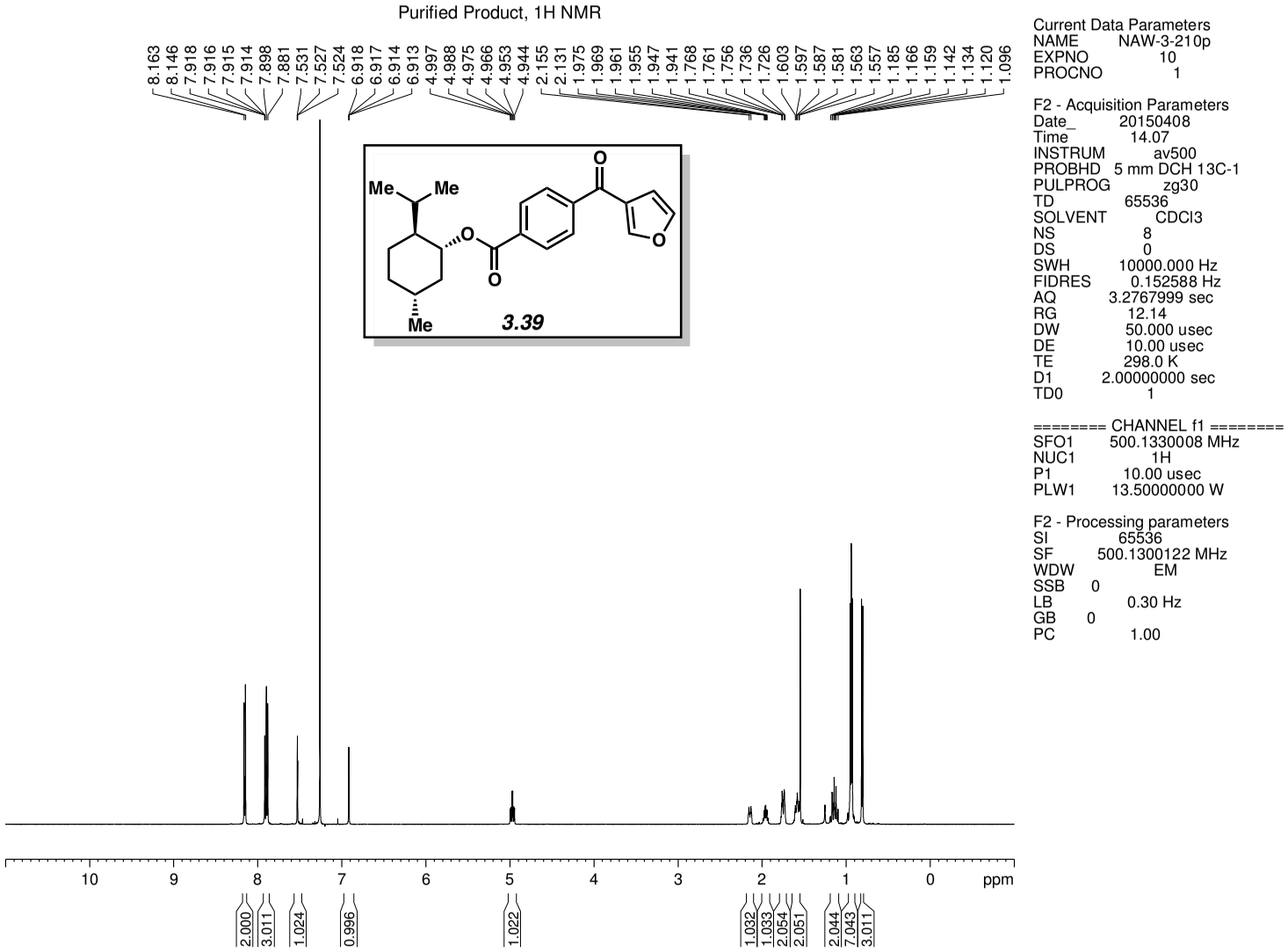

Figure 3.94 ^{1}H NMR (500 MHz, $CDCl_3$) of compound **3.39**.

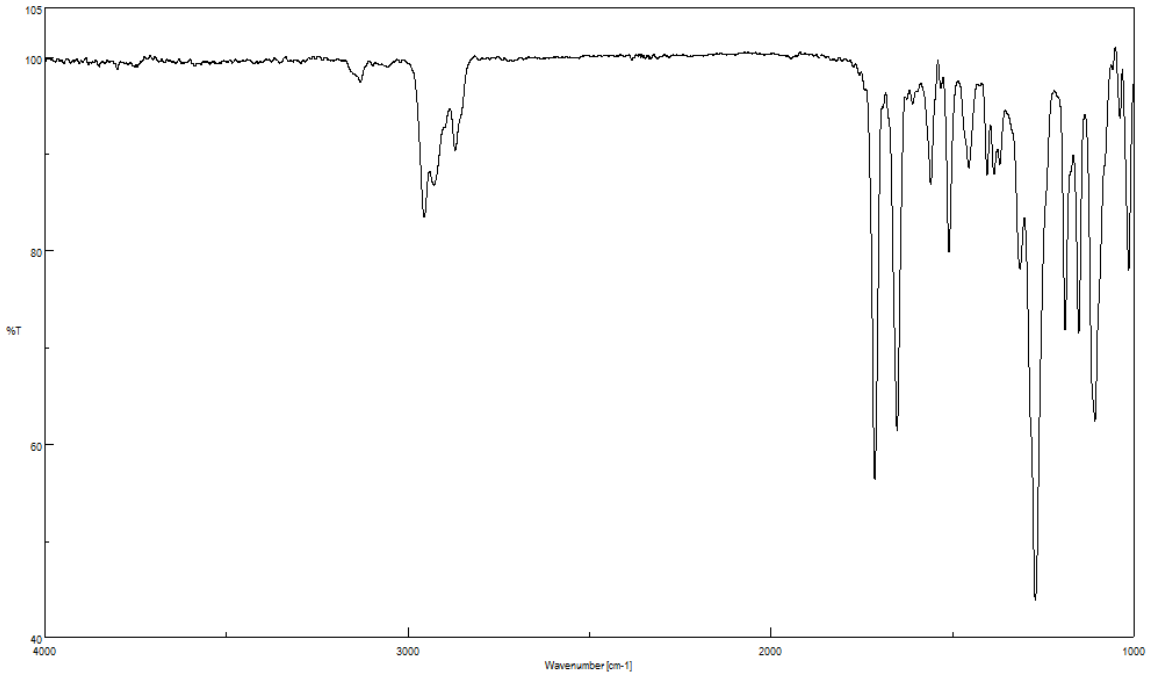

Figure 3.95 Infrared spectrum of compound **3.39**.

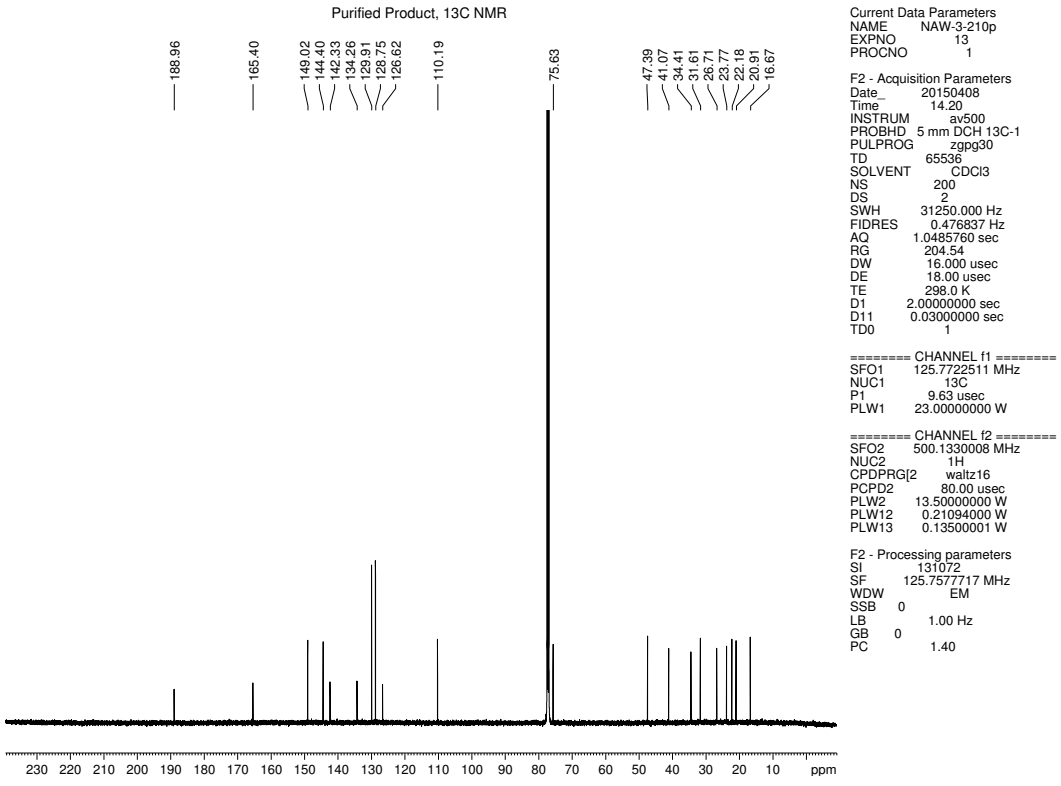

Figure 3.96 ^{13}C NMR (125 MHz, $CDCl_3$) of compound **3.39**.

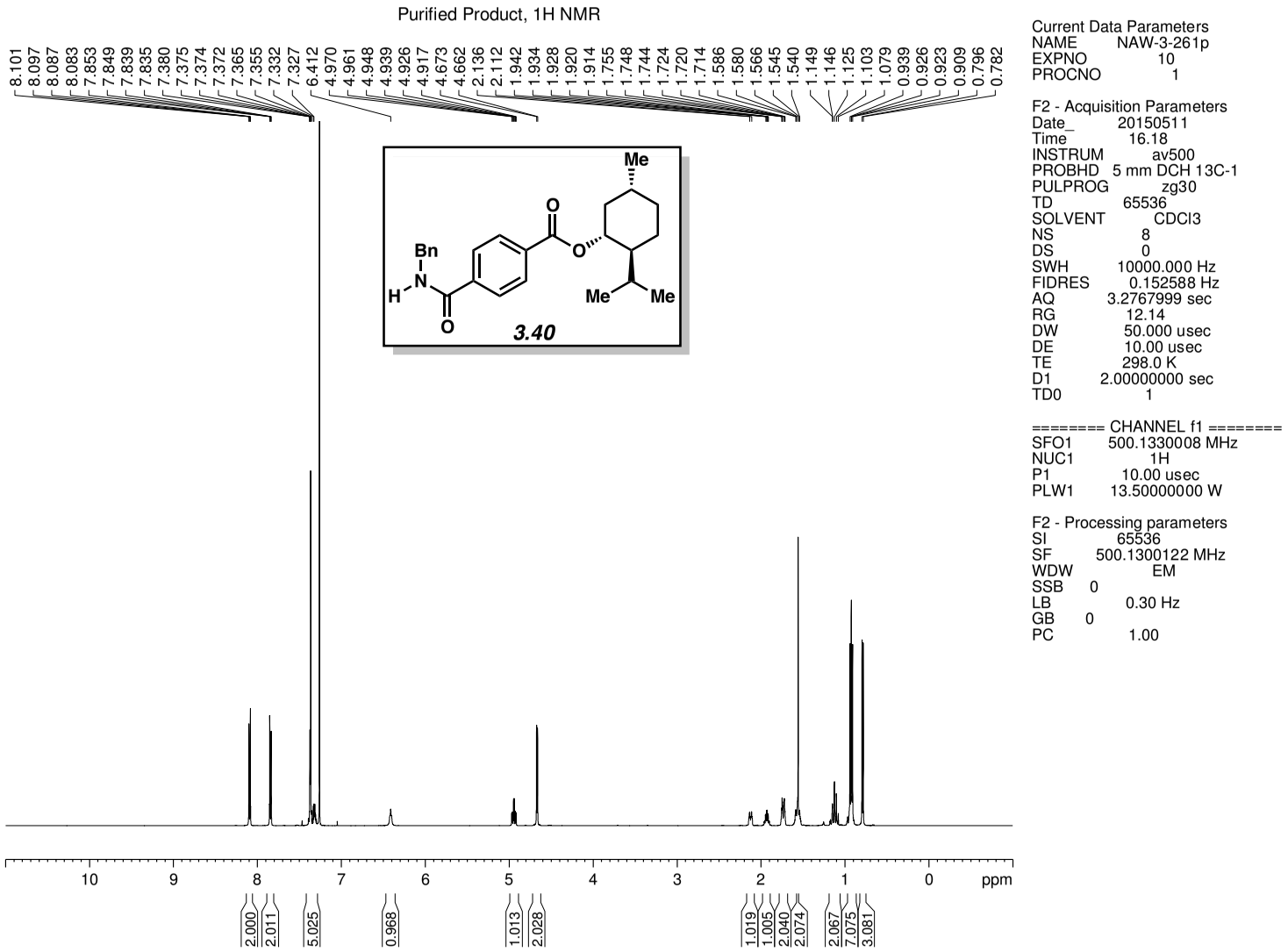

Figure 3.97 ^{1}H NMR (500 MHz, $CDCl_3$) of compound **3.40**.

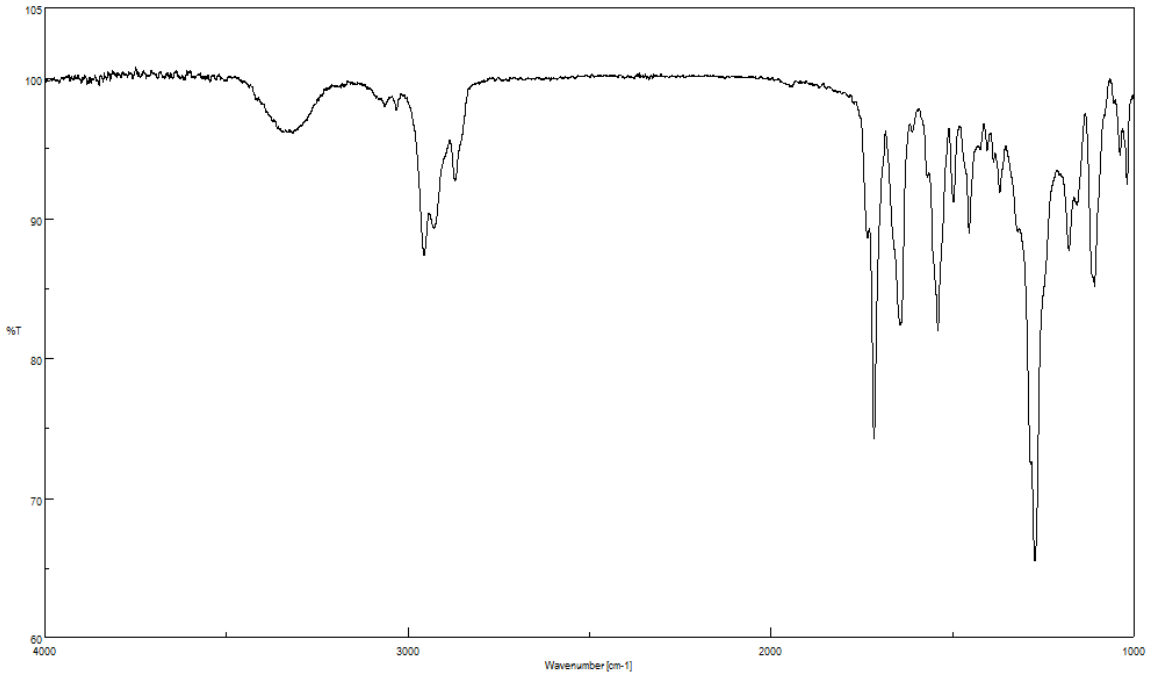

Figure 3.98 Infrared spectrum of compound **3.40**.

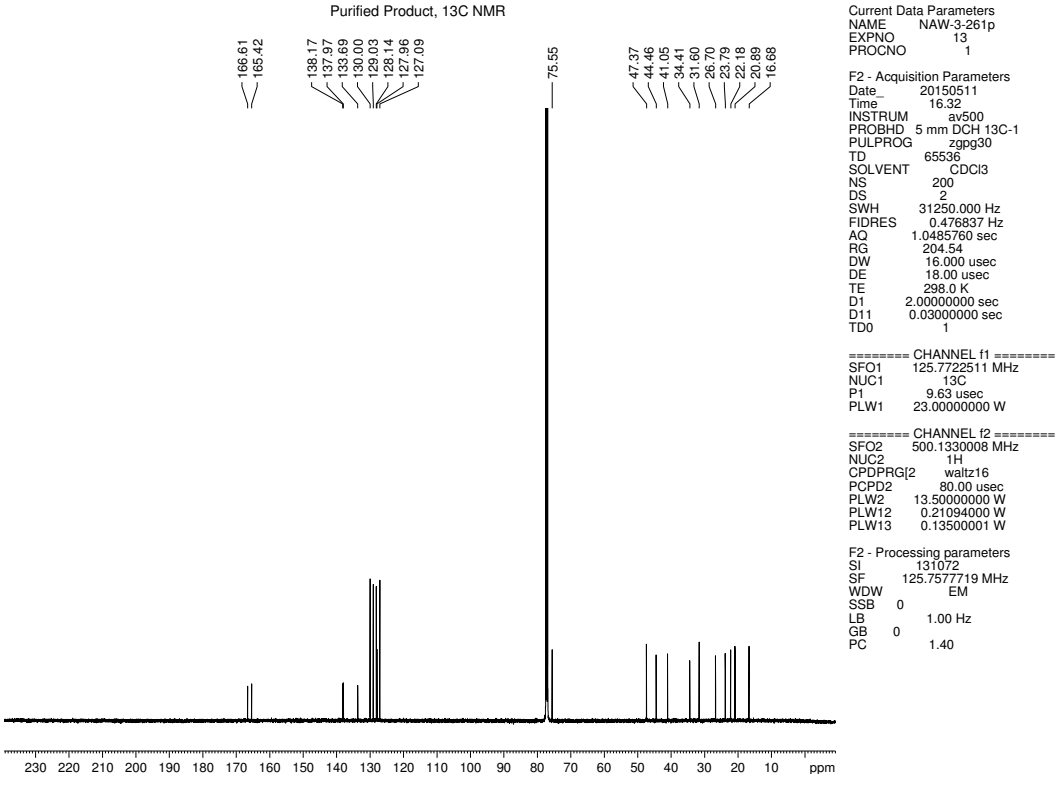

Figure 3.99 ^{13}C NMR (125 MHz, $CDCl_3$) of compound **3.40**.

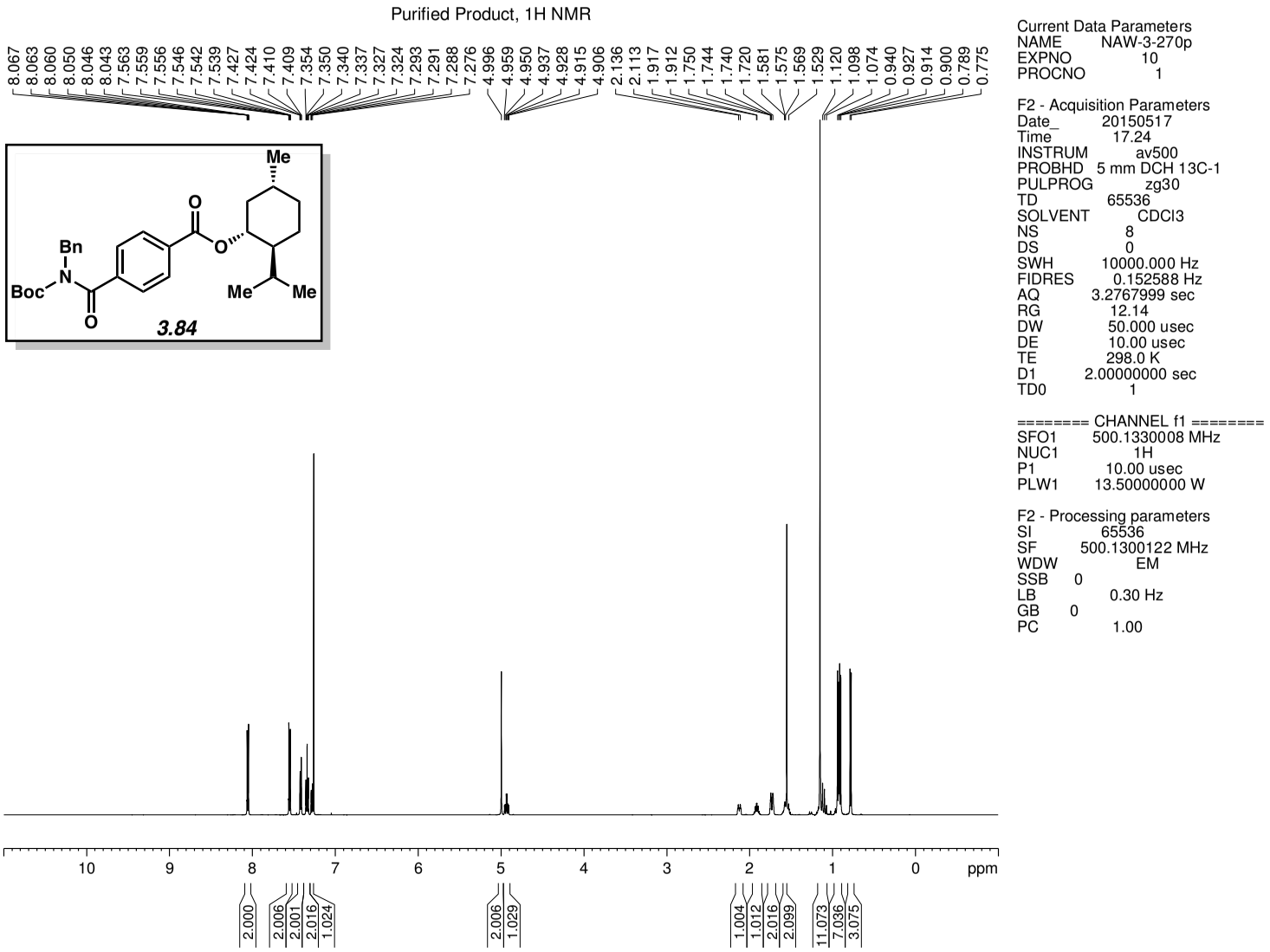

Figure 3.100 ^{1}H NMR (500 MHz, $CDCl_3$) of compound **3.84**.

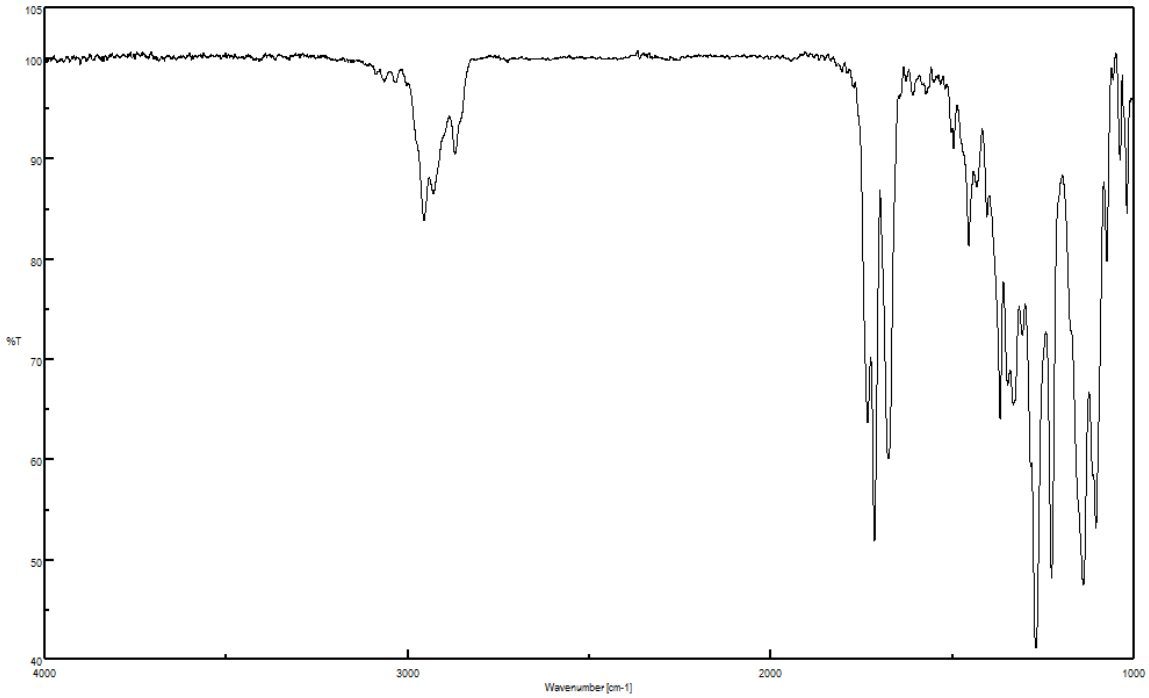

Figure 3.101 Infrared spectrum of compound **3.84**.

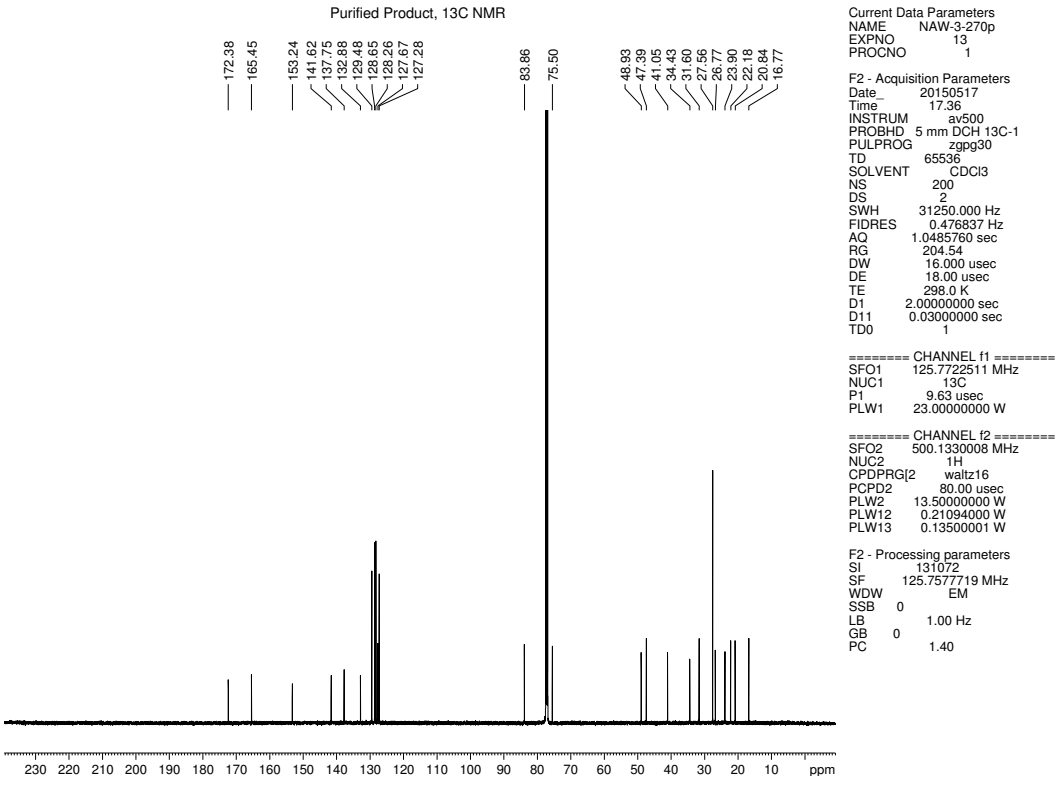

Figure 3.102 ^{13}C NMR (125 MHz, $CDCl_3$) of compound **3.84**.

3.9 Notes and References

(1) Muci, A. R., Buchwald, S. L. In *Topics in Current Chemistry*; Miyaura, N., Ed.; Springer Verlag: New York, 2002; Vol. *219*; 131–209.

(2) Tasker, S. Z.; Standley, E. A.; Jamison, T. F. *Nature* **2014**, *509*, 299–309.

(3) Mesganaw, T.; Garg, N. K. *Org. Process. Res. Dev.* **2013**, *17*, 29–39.

(4) Rosen, B. M.; Quasdorf, K. W.; Wilson, D. A.; Zhang, N.; Resmerita, A.-M.; Garg, N. K.; Percec, V. *Chem. Rev.* **2011**, *111*, 1346–1416.

(5) Blakey, S. B.; MacMillan, D. W. C. *J. Am. Chem. Soc.* **2003**, *125*, 6046–6047.

(6) Zhang, X.-Q.; Wang, Z.-X. *Org. Biomol. Chem.* **2014**, *12*, 1448–1453.

(7) Tobisu, M.; Nakamura, K.; Chatani, N. *J. Am. Chem. Soc.* **2014**, *136*, 5587–5590.

(8) Hie, L.; Fine Nathel, N. F.; Shah, T. K.; Baker, E. L.; Hong, X.; Yang, Y.-F.; Liu, P.; Houk, K. N.; Garg, N. K. *Nature* **2015**, *524*, 79–83.

(9) Louie, J. In *N-Heterocyclic Carbenes in Synthesis*; Nolan, S. P., Ed.; Wiley VCH Verlag: Weinheim, 2006; 163–182.

(10) Hoshimoto, Y.; Hayashi, Y.; Suzuki, H.; Ohashi, M.; Ogoshi, S. *Organometallics* **2014**, *33*, 1276–1282.

(11) Greenberg, A., Breneman, C. M., Liebman, J. F., Eds. *The Amide Linkage: Structural Significance in Chemistry, Biochemistry, and Materials Science*; Wiley: New York, 2003; 1–672.

(12) Blangetti, M.; Rosso, H.; Prandi, C.; Deagostino, A.; Venturello, P. *Molecules* **2013**, *18*, 1188–1213.

(13) Chen, Q.; Fan, X.-H.; Zhang, L.-P.; Yang, L.-M. *RSC Adv.* **2014**, *4*, 53885–53890.

(14) Li, X.; Zou, G. *Chem. Commun.* **2015**, *51*, 5089–5092.

(15) Meng, G.; Szostak, M. *Org. Lett.* **2015**, *17*, 4364–4367.

(16) Nahm, S.; Weinreb, S. M. *Tetrahedron Lett.* **1981**, *22*, 3815–3818.

(17) Balasubramaniam, S.; Aidhen, I. S. *Synthesis* **2008**, 3707–3738.

(18) Lennox, J. J. A.; Lloyd-Jones, G. C. *Chem. Soc. Rev.* **2014**, *43*, 412–443.

(19) Miyaura, N.; Suzuki, A. *Chem. Rev.* **1995**, *95*, 2457–2483.

(20) Quasdorf, K. W.; Antoft-Finch, A.; Liu, P.; Silberstein, A. L.; Komaromi, A.; Blackburn, T.; Ramgren, S. D.; Houk, K. N.; Snieckus, V.; Garg, N. K. *J. Am. Chem. Soc.* **2011**, *133*, 6352–6363.

(21) Guan, B.-T.; Wang, Y.; Li, B.-J.; Yu, D.-G.; Shi, Z.-J. *J. Am. Chem. Soc.* **2008**, *130*, 14468–14470.

(22) Antoft-Finch, A.; Blackburn, T.; Snieckus, V. *J. Am. Chem. Soc.* **2009**, *131*, 17750–17752.

(23) Jezorek, R. L.; Zhang, N.; Leowanawat, P.; Bunner, M. H.; Gutsche, N.; Pesti, A. K. R.; Olsen, J. T.; Percec, V. *Org. Lett.* **2014**, *16*, 6326–6329.

(24) Yamamoto, T.; Ishizu, J.; Kohara, T.; Komiya, S.; Yamamoto, A. *J. Am. Chem. Soc.* **1980**, *102*, 3758–3764.

(25) Amaike, K.; Muto, K.; Yamaguchi, J.; Itami, K. *J. Am. Chem. Soc.* **2012**, *134*, 13573–13576.

(26) Muto, K.; Yamaguchi, J.; Musaev, D. G.; Itami, K. *Nat. Commun.* **2015**, *6*, 7508.

(27) Vitaku, E.; Smith, D. T.; Njardarson, J. T. *J. Med. Chem.* **2014**, *57*, 10257–10274.

(28) *DrugBank Version 4.3*; Wishart Research Group: Alberta, Canada.

(29) Hu, L.; Jiang, J.-d.; Qu, J.; Li, Y.; Jin, J.; Li, Z.-r.; Boykin, D. W. *Bioorg. Med. Chem. Lett.* **2007**, *17*, 3613–3617.

(30) Billingsley, K.; Buchwald, S. L. *J. Am. Chem. Soc.* **2007**, *129*, 3358–3366.

(31) (a) Li, Y.; Jia, F.; Li, Z. *Chem. Eur. J.* **2013**, *19*, 82–86. (b) Friel, D. K.; Snapper, M. L.; Hoveyda, A. H. *J. Am. Chem. Soc.* **2008**, *130*, 9942–9951. (c) Yates, M. H.; Kallman, N. J.; Ley, C. P.; Wei, J. N. *Org. Process. Rev. Dev.* **2009**, *13*, 255–262. (d) Oishi, S.; Saito, S. *Angew. Chem. Int. Ed.* **2012**, *51*, 5395–5399. (e) Johnson II, D. C.; Widlanski, T. S. *Tetrahedron Lett.* **2004**, *45*, 8483–8487.

(32) Collins, K. D.; Glorius, F. *Nature Chem.* **2013**, *5*, 597–601.

(33) Li, M.; Wang, C.; Ge, H. *Org. Lett.* **2011**, *13*, 2062–2064.

(34) Li, H.; Xu, Y.; Shi, E.; Wei, W.; Suo, X.; Wan, X. *Chem. Commun.* **2011**, *47*, 7880–7882.

(35) Huang, J.-H.; Yang, L.-M. *Org. Lett.* **2011**, *13*, 3750–3753.

(36) Biju, A. T.; Glorius, F. *Angew. Chem. Int. Ed.* **2010**, *49*, 9761–9764.

(37) Satoh, T.; Itaya, T.; Okuro, K.; Miura, M.; Nomura, M. *J. Org. Chem.* **1995**, *60*, 7267–7271.

(38) Hartman, G. D.; Halczenko, W. *J. Heterocyclic Chem.* **1989**, *26*, 1793–1798.

(39) Taylor, J. E.; Jones, M. D.; Williams, J. M. J.; Bull, S. D. *Org. Lett.* **2010**, *12*, 5740–5743.

CHAPTER FOUR

Aliphatic Amides as Acyl Donors for the Union of Heterocycles

Nicholas A. Weires, Timothy B. Boit, Junyong Kim, and Neil K. Garg.

Manuscript in Preparation

4.1 Abstract

We report the nickel-catalyzed Suzuki–Miyaura coupling of aliphatic amide derivatives, which offers a facile means to unite heterocyclic fragments. The coupling is tolerant of considerable variation with respect to both the amide-based substrate and the boronate coupling partner. Moreover, a gram-scale Suzuki–Miyaura coupling / Fischer indolization sequence demonstrates the ease with which unique poly-heterocyclic scaffolds can be constructed, particularly by taking advantage of the ketone functionality present in the cross-coupled product. These studies provide a simple means to link heterocyclic compounds together, while further expanding the repertoire of synthetic transformations involving amide derivatives and non-precious metal catalysis.

4.2 Introduction

The unification of heterocyclic fragments via C–C bond formation represents an important and challenging objective in the field of transition metal catalysis.[1] Interest in this area is driven by the fact that biologically active molecules are frequently decorated with heterocycles, especially those containing nitrogen, such as piperidine, pyrrolidine, pyrrole, pyrazole, indole, and pyridine rings.[2] In fact, nearly 60% of all small-molecule drugs that have been approved by the U.S. Food and Drug Administration possess heterocycles containing one or

more nitrogen atom.[3] However, the use of heterocyclic groups in metal-mediated cross-couplings can prove challenging, as certain heterocycles can ligate metal catalysts and inhibit reactivity.[1]

One particularly underdeveloped transformation is the hetero-arylation of aliphatic acyl electrophiles. In contrast to the more traditional aryl-aryl cross-coupling motifs,[1b] the products of such acylation reactions possess a valuable enolizable ketone functionality, which can be utilized in further manipulations. Although some examples of aliphatic acyl electrophile cross-couplings with heteroaryl zinc[4] and heteroaryl stannane[5] nucleophiles are known, the corresponding couplings with the much more widely commercially available, stable, and less toxic heteroaryl boronate nucleophiles remains limited. Indeed, only a handful of isolated examples of hetero-arylative Suzuki–Miyaura couplings of aliphatic acyl electrophiles exist,[6] including couplings of anhydrides,[6a,b] thioesters,[6c,d] and acid chlorides.[6e,f] A more general platform for the hetero-arylation of aliphatic acyl electrophiles would enable the rapid construction of valuable heterocyclic aliphatic ketones, and is thus highly desirable.

Recently, amides have emerged as useful synthetic building blocks in a variety of cross-coupling manifolds involving nickel-catalyzed C–N bond activation.[7,8,9,10] However, although cross-coupling platforms have been disclosed for the efficient coupling of *aryl* amide electrophiles using nickel, the corresponding activation of *aliphatic* amides has proven more challenging.[11,12] Moreover, the field of nickel-catalyzed cross-couplings has gained tremendous interest in recent years due not only to the high natural abundance, low cost, and low CO_2 footprint of nickel, but also because of its ability to effect new or challenging transformations,[13] including those involving activation of the amide C–N bond.[7,8,9,11,12] We therefore postulated that it might be feasible to address the challenge of C–N bond activation of hetero-aliphatic amides (**4.1**) by leveraging the unique reactivity of nickel to facilitate a cross-coupling with hetero-aryl

boronate nucleophiles (**4.2**), thus forging poly-heterocyclic ketones (**4.3**, Figure 4.1). Such a reaction would provide a valuable alternative to the venerable Weinreb ketone synthesis.[14] In this manuscript, we describe the first nickel-catalyzed Suzuki–Miyaura coupling of aliphatic amides. This methodology provides a simple means to unite heterocyclic fragments, while further expanding the repertoire of synthetic transformations involving amide derivatives and non-precious metal catalysis.

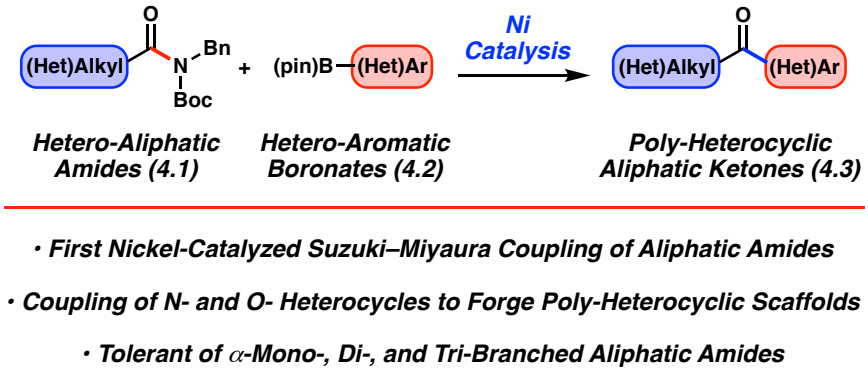

Figure 4.1. Suzuki–Miyaura hetero-arylation of aliphatic amides to construct poly-heterocyclic scaffolds.

4.3 Evaluation of Ligand Effects in the Suzuki–Miyaura Coupling

To initiate our study, we examined the coupling of piperidine derivative **4.4** with *N*-methylpyrrole-2-boronic acid pinacol ester (**4.5**) as shown in Table 4.1. Our initial attempts to employ the *N*-heterocyclic carbene (NHC) ligand SIPr (**4.7**), which we had previously shown to be competent in the Suzuki–Miyaura coupling of aromatic amide derivatives,[7b] were met with difficulty, as no trace of the desired ketone product **4.6** was formed at 50 °C (entry 1). Moreover, increasing the temperature to 120 °C only led to partial decomposition of substrate **4.4** (entry 2).

Interestingly, efforts to utilize the ligand terpyridine (**4.8**), which had been shown to facilitate the nickel-catalyzed esterification of aliphatic amide derivatives,[11] were also unfruitful (entry 3). Gratifyingly, however, use of the NHC precursor ICy•HBF_4 (**4.9**) was found to promote the desired Suzuki–Miyaura coupling, and delivered ketone **4.6** in 95% yield (entry 4). Finally, the related NHC precursor Benz-ICy•HCl (**4.10**) was evaluated and found to give similarly useful results (entry 5). As NHC precursor **4.10** was found to be broadly effective in subsequent scouting experiments, it was used in our further studies.

Table 4.1. Evaluation of reaction conditions for the coupling of aliphatic amides.[a]

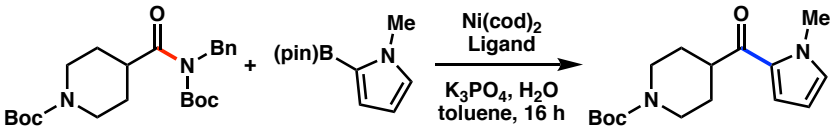

4.4 | *4.5* (2.5 equiv) | *4.6*

Entry	*Temp.*	*Ni(cod)$_2$*	*Ligand*	*Remaining 4.4*	*Yield of 4.6*
1	50 °C	5 mol%	*4.7* (10 mol%)	100%	0%
2	120 °C	5 mol%	*4.7* (10 mol%)	52%	0%
3	120 °C	5 mol%	*4.8* (10 mol%)	50%	0%
4	120 °C	5 mol%	*4.9* (10 mol%)	0%	95%
5	120 °C	5 mol%	*4.10* (10 mol%)	0%	95%

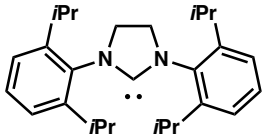

SIPr (4.7)

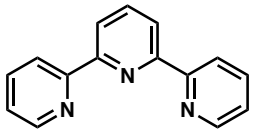

terpyridine (4.8)

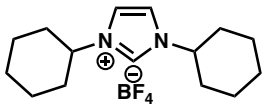

ICy·HBF$_4$ (4.9)

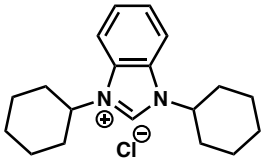

Benz-ICy·HCl (4.10)

[a] Conditions: Ni(cod)$_2$ (5 mol%), **4.7**–**4.10** (10 mol%), substrate **4.4** (1.0 equiv), boronate **4.5** (2.5 equiv), K_3PO_4 (4.0 equiv), toluene (1.0 M), and H_2O (2.0 equiv) heated at the indicated temperature for 16 h. Yields were determined by ^{1}H NMR analysis using hexamethylbenzene as an internal standard.

4.4 Scope of the Coupling with Hetero-Aliphatic Amides and Hetero-Aryl Boronates

With optimized conditions in hand, we explored the scope of the coupling with respect to both the hetero-aliphatic amide-derived substrate and the hetero-aryl boronate, producing a variety of bis-heterocyclic ketone products (Figure 4.2). The reaction was found to be widely tolerant of *N*-heterocycles on the boronate nucleophile, including pyrrole, pyrazole, indole, and

morpholino-pyridine moieties, as demonstrated by the formation of **4.6** and **4.11–4.13**, all in good yields. Moreover, an isomeric piperidine amide substrate could be utilized, allowing for the formation of pyrrolo- and pyrazolo-ketones **4.14** and **4.15**, respectively. Alternatively, the pyrrolidine heterocycle could also be employed to generate ketones **4.16** and **4.17** in 82% and 90% yields, respectively. Finally, substrates derived from both 4- and 3-isomers of tetrahydropyran carboxylic acid were shown to be competent in the coupling, furnishing ketones **4.18–4.21** in good to excellent yields. It is worth noting that non-heterocyclic aryl boronates could also be employed in the Suzuki–Miyaura coupling; see section 4.8.2.3 for details.

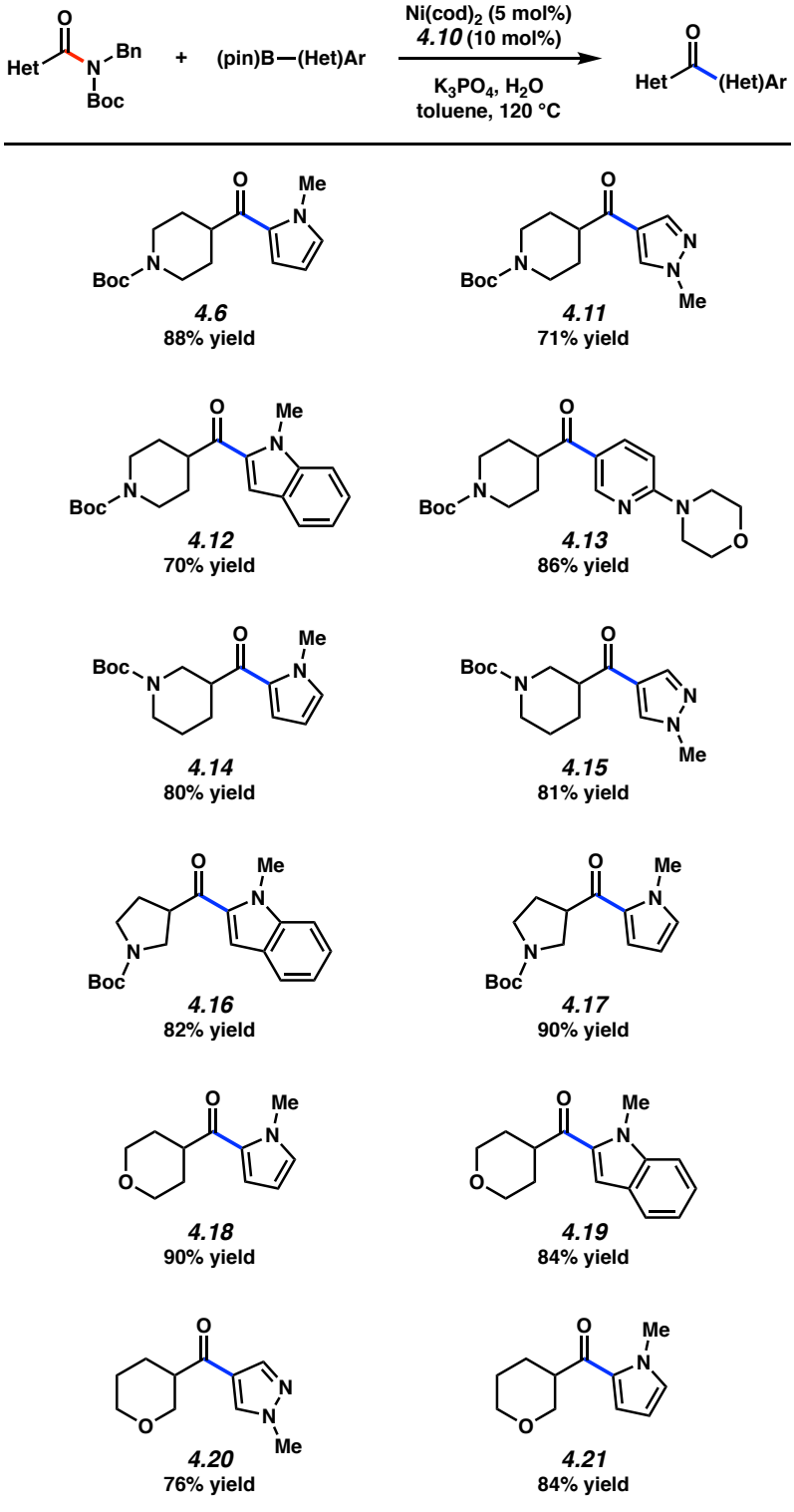

Figure 4.2. Scope of the Suzuki–Miyaura coupling with hetero-aliphatic amide substrates and hetero-aryl boronates. Conditions: $Ni(cod)_2$ (5 mol%), **4.10** (10 mol%), substrate (1.0 equiv), boronate (2.5 equiv), K_3PO_4 (4.0 equiv), toluene (1.0 M), and H_2O (2.0 equiv) heated at 120 °C for 16 h. Yields reflect the average of two isolation experiments.

4.5 Scope of the Coupling with Non-Heterocyclic Aliphatic Amide Substrates

The scope of the hetero-arylative coupling with boronate **4.5** was also evaluated with respect to several non-heterocyclic aliphatic amide derivatives (Figure 4.3). Substrates derived from dihydrocinnamic and decanoic acids coupled in high yields to furnish ketones **4.22** and **4.23**, respectively. Additionally, alpha-branched carbocyclic amides also underwent efficient couplings, forging pyrrolo-ketones **4.24** and **4.25**. Notably, sensitive functional groups such as olefins and esters were well tolerated in the coupling, allowing for the formation of ketones **4.26** and **4.27** in good yields. It is worth noting that electrophilic functional groups such as esters would likely not be tolerated in the Weinreb ketone synthesis, which relies on the use of highly nucleophilic and basic Grignard reagents.[14] Lastly, sterically encumbered carboxamides could also be employed in the coupling, as demonstrated by the production of *tert*-butyl ketone **4.28** in excellent yield.

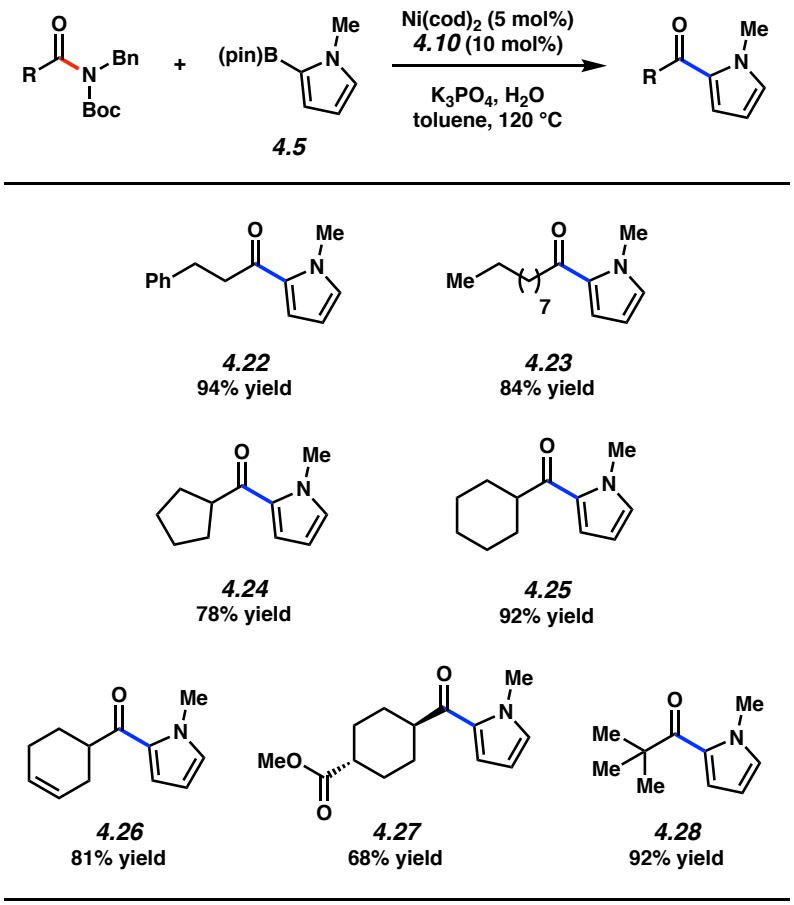

Figure 4.3. Scope of the coupling with non-heterocyclic aliphatic amide substrates and boronate **4.5**. Conditions: $Ni(cod)_2$ (5 mol%), **4.10** (10 mol%), substrate (1.0 equiv), boronate **4.5** (2.5 equiv), K_3PO_4 (4.0 equiv), toluene (1.0 M), and H_2O (2.0 equiv) heated at 120 °C for 16 h. Yields reflect the average of two isolation experiments.

4.6 Gram-Scale Suzuki–Miyaura Coupling and Subsequent Fischer Indolization

The synthetic utility of the Suzuki–Miyaura reaction was further substantiated via a gram-scale coupling and subsequent Fischer indolization reaction to construct poly-heterocyclic indolenine scaffold **4.33** (Figure 4.4). In the event, Suzuki–Miyaura coupling of tetrahydropyran carboxamide **4.29** with boronate **4.30** took place on gram scale under conditions employing reduced boronate, catalyst, and ligand loadings to furnish ketone **4.31** in 82% yield. Enolizable ketone **4.31** was further manipulated by taking advantage of a more classical method for the

construction of heterocycles, namely the Fischer indole synthesis.[15] Ketone **4.31** was thus transformed into pentacyclic indolenine **4.33** in 61% yield by reaction with phenylhydrazine (**4.32**) in the presence of TFA. The rapid construction of poly-heterocyclic indolenine **4.33**, hinging upon the classical reactivity of enolizable ketones, underscores the utility of the Suzuki–Miyaura coupling of aliphatic amides and further demonstrates the ease with which a variety of unique heterocyclic compounds can be fashioned.

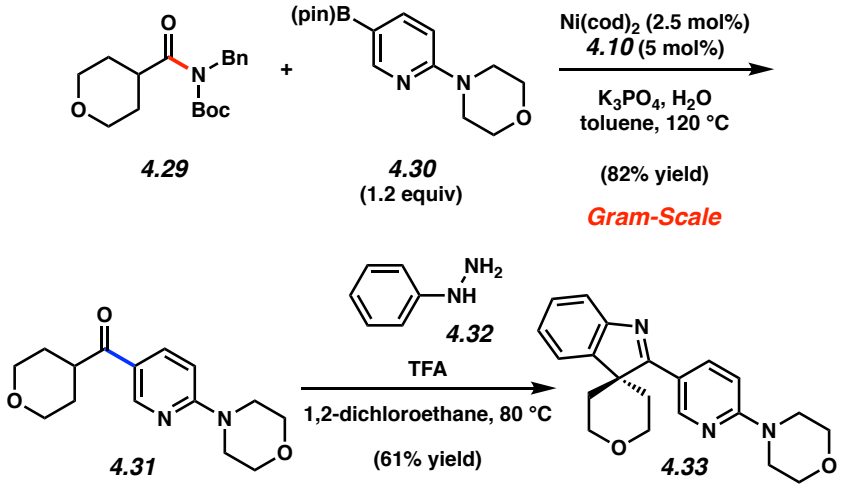

Figure 4.4. Sequential gram-scale Suzuki–Miyaura coupling and Fischer indolization to forge indolenine **4.33**.

4.7 Conclusion

We have developed the first nickel-catalyzed Suzuki–Miyaura coupling of aliphatic amides. The coupling was found to be tolerant of a wide variety of heterocyclic building blocks, thus allowing for the construction of valuable heterocyclic aliphatic ketone products. The synthetic utility of this methodology was further demonstrated on gram-scale via a Suzuki–Miyaura coupling / Fischer indolization sequence to form poly-heterocyclic indolenine **4.33**. We

expect that these studies will provide chemists with a simple means to unite heterocyclic fragments, while further expanding the repertoire of synthetic transformations involving amide derivatives and non-precious metal catalysis.

4.8 Experimental Section

4.8.1 Materials and Methods

Unless stated otherwise, reactions were conducted in flame-dried glassware under an atmosphere of nitrogen or argon and commercially obtained reagents were used as received. Non-commercially available substrates were synthesized following protocols specified in Section 4.8.2.1 in the Experimental Procedures. Prior to use, toluene was purified by distillation and taken through five freeze-pump-thaw cycles, and phenylhydrazine (**4.32**) was passed over a plug of basic alumina. Benzylamine was obtained from Sigma–Aldrich. Boronate esters **4.5**, **4.44**, **4.50**, **4.51**, **4.52**, **4.53**, **4.54**, **4.55**, and **4.30** and carboxylic acids **4.34**, **4.35**, **4.37**, **4.39**, **4.40**, **4.42** were obtained from Combi-Blocks. $Ni(cod)_2$, SIPr (**4.7**), terpyridine (**4.8**), ICy•HBF_4 (**4.9**), and Benz-ICy•HCl (**4.10**) were obtained from Strem Chemicals. K_3PO_4 was obtained from Acros. Reaction temperatures were controlled using an IKAmag temperature modulator, and unless stated otherwise, reactions were performed at room temperature (approximately 23 °C). Thin-layer chromatography (TLC) was conducted with EMD gel 60 F254 pre-coated plates (0.25 mm for analytical chromatography and 0.50 mm for preparative chromatography) and visualized using a combination of UV, anisaldehyde, iodine, and potassium permanganate staining techniques. Silicycle Siliaflash P60 (particle size 0.040–0.063 mm) was used for flash column chromatography. ^{1}H NMR spectra were recorded on Bruker spectrometers (at 300, 400 and 500 MHz) and are reported relative to residual solvent signals. Data for ^{1}H NMR spectra are reported as follows: chemical shift (δ ppm), multiplicity, coupling constant (Hz), integration. Data for ^{13}C NMR are reported in terms of chemical shift (at 75 and 125 MHz). IR spectra were recorded on a Perkin-Elmer UATR Two FT-IR spectrometer and are reported in terms of frequency absorption (cm^{-1}). DART-MS spectra were collected on a Thermo Exactive Plus MSD (Thermo Scientific)

equipped with an ID-CUBE ion source and a Vapur Interface (IonSense Inc.). Both the source and MSD were controlled by Excalibur software v. 3.0. The analyte was spotted onto OpenSpot sampling cards (IonSense Inc.) using $CHCl_3$ as the solvent. Ionization was accomplished using UHP He (Airgas Inc.) plasma with no additional ionization agents. The mass calibration was carried out using Pierce LTQ Velos ESI (+) and (–) Ion calibration solutions (Thermo Fisher Scientific).

4.8.2 Experimental Procedures

4.8.2.1 Syntheses of Amide Substrates

Representative Procedure for the synthesis of amide substrates from Tables 4.1 and 4.2 and Figures 4.2, 4.3, 4.4, and 4.5 (synthesis of amide 4.4 is used as an example).

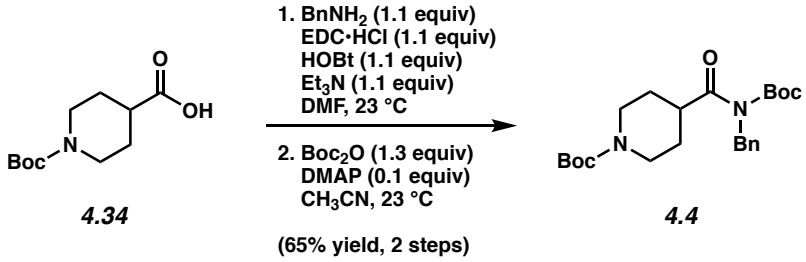

To a mixture of carboxylic acid **4.34** (3.00 g, 13.1 mmol, 1.0 equiv), EDC•HCl (2.76 g, 14.4 mmol, 1.1 equiv), HOBt (1.94 g, 14.4 mmol, 1.1 equiv), triethylamine (1.99 mL, 14.4 mmol, 1.1 equiv) and DMF (131 mL, 0.1 M) was added benzylamine (1.57 mL, 14.4 mmol, 1.1 equiv). The resulting mixture was stirred at 23 °C for 16 h, and then diluted with deionized water (250 mL) and transferred to a separatory funnel with EtOAc (150 mL) and brine (50 mL). The aqueous layer was extracted with EtOAc (3 x 150 mL), then the organic layers were combined and washed with deionized water (3 x 125 mL), dried over Na_2SO_4, and evaporated under

reduced pressure. The resulting crude solid material was used in the subsequent step without further purification.

To a flask containing the crude material from the previous step was added DMAP (148 mg, 1.21 mmol, 0.1 equiv) followed by acetonitrile (60.0 mL, 0.2 M). Boc_2O (3.43 g, 15.7 mmol, 1.3 equiv) was added in one portion and the reaction vessel was flushed with N_2, then the reaction mixture was allowed to stir at 23 °C for 16 h. The reaction was quenched by addition of 200 mL saturated aqueous $NaHCO_3$, transferred to a separatory funnel with EtOAc (200 mL) and H_2O (200 mL), and extracted with EtOAc (3 x 100 mL). The organic layers were combined, dried over Na_2SO_4, and evaporated under reduced pressure. The resulting crude residue was purified by flash chromatography (9:1 Hexanes:EtOAc) to yield amide **4.4** (3.59 g, 65% yield, over two steps) as white solid. Amide **4.4**: mp: 83–85 ºC; R_f 0.39 (5:1 Hexanes:EtOAc); ^{1}H NMR (500 MHz, $CDCl_3$): δ 7.31–7.26 (m, 2H), 7.24–7.18 (m, 3H), 4.86 (s, 2H), 4.12 (br s, 2H), 3.59 (tt, *J* = 11.2, 3.6, 1H), 2.88–2.70 (m, 2H), 1.91–1.79 (m, 2H), 1.65 (qd, *J* = 12.2, 4.0, 2H), 1.45 (s, 9H), 1.40 (s, 9H); ^{13}C NMR (125 MHz, $CDCl_3$): δ 178.2, 154.8, 153.1, 138.4, 128.5, 127.5, 127.2, 83.5, 79.6, 47.8, 43.8, 43.0, 29.0, 28.6, 28.0; IR (film): 2976, 2932, 2861, 1731, 1689 cm^{-1}; HRMS-APCI (*m/z*) $[M + H]^+$ calcd for $C_{23}H_{35}N_2O_5$, 419.25460; found 419.25413.

Note: Supporting information for the syntheses of amides shown in Figure 4.3 have previously been reported: **4.56**,[11] **4.57**,[11] **4.58,**[11] **4.59**,[11] **4.60**,[11] and **4.61**.[11] Syntheses for the remaining substrates shown in Figures 4.2, 4.3, and 4.4 are as follows:

Any modifications of the conditions shown in the representative procedure above are specified in the following schemes.

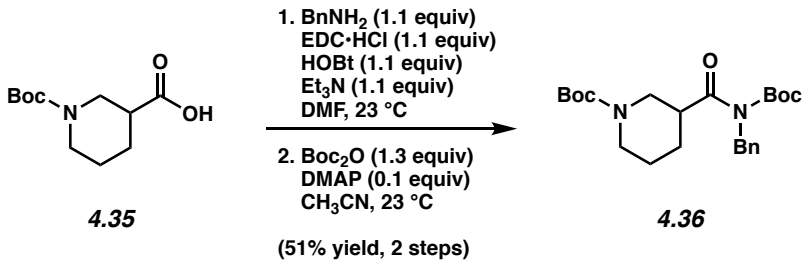

4.35 *4.36*

Amide 4.36. Purification by flash chromatography (9:1 Hexanes:EtOAc) generated amide **4.36** (51% yield, over two steps) as a white solid. Amide **4.36**: mp: 73–75 ºC; R_f 0.43 (5:1 Hexanes:EtOAc); ^{1}H NMR (500 MHz, $CDCl_3$): δ 7.31–7.26 (m, 2H), 7.24–7.19 (m, 3H), 4.92–4.78 (m, 2H), 4.26–3.94 (m, 2H), 3.51 (tt, *J* = 10.6, 3.6, 1H), 2.75 (br s, 1H), 2.10 (br s, 1H), 1.74–1.68 (m, 1H), 1.62–1.48 (m, 2H), 1.45 (s, 9H), 1.40 (s, 9H); ^{13}C NMR (125 MHz, $CDCl_3$, 15 of 17 observed): δ 177.2, 154.8, 152.9, 138.3, 128.5, 127.5, 127.3, 83.6, 79.7, 47.7, 43.5, 28.7, 28.6, 28.0, 24.7; IR (film): 2977, 2935, 2862, 1732, 1687 cm^{-1}; HRMS-APCI (*m/z*) [M + H]$^+$ calcd for $C_{23}H_{35}N_2O_5$, 419.25460; found 419.25304.

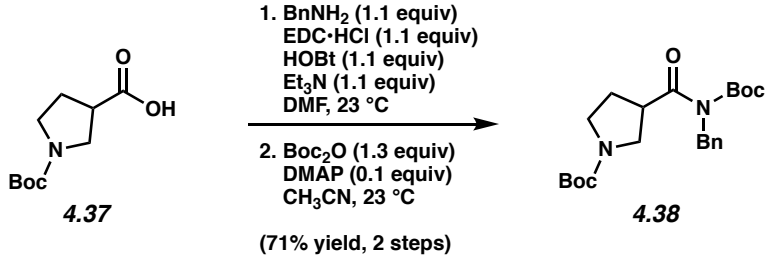

4.37 *4.38*

Amide 4.38. Purification by flash chromatography (9:1 Hexanes:EtOAc) generated amide **4.38** (71% yield, over two steps) as a colorless oil. Amide **4.38**: R_f 0.47 (5:1 Hexanes:EtOAc); ^{1}H NMR (500 MHz, $CDCl_3$): δ 7.32–7.27 (m, 2H), 7.25–7.19 (m, 3H), 4.88 (s, 2H), 4.08 (p, *J* = 7.1, 1H), 3.67 (br s, 1H), 3.56 (dd, *J* = 10.8, 6.3, 1H), 3.53–3.45 (m, 1H), 3.43–3.33 (m, 1H), 2.15 (br s, 2H), 1.46 (s, 9H), 1.42 (s, 9H); ^{13}C NMR (125 MHz, $CDCl_3$, 15 of 16 observed): δ 176.2, 154.6, 153.2, 138.3, 128.5, 127.6, 127.4, 83.8, 79.4, 49.3, 48.0, 45.6, 29.4, 28.7, 28.1; IR (film):

2979, 2887, 1731, 1693, 1366, 1143 cm^{-1}; HRMS-APCI (*m/z*) $[M + H]^+$ calcd for $C_{22}H_{33}N_2O_5$, 405.23840; found 405.23794.

*Note: ^1H and ^{13}C NMR spectra of amide **4.38** were obtained at 57 °C.*

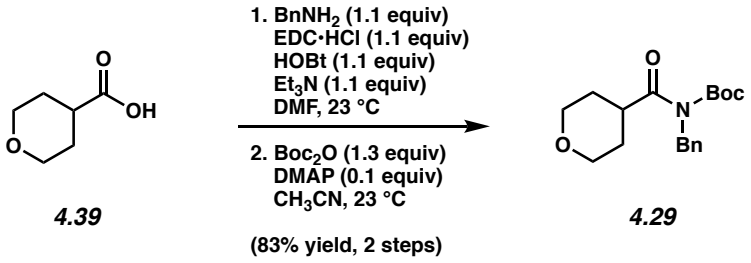

Amide 4.29. Purification by flash chromatography (14:1 Hexanes:EtOAc) generated amide **4.29** (83% yield, over two steps) as a white solid. Amide **4.29**: mp: 52–54 ºC; R_f 0.59 (5:1 Hexanes:EtOAc); ^1H NMR (500 MHz, $CDCl_3$): δ 7.32–7.27 (m, 2H), 7.25–7.19 (m, 3H), 4.87 (s, 2H), 4.03–3.97 (m, 2H), 3.74–3.65 (m, 1H), 3.48 (td, *J* = 11.5, 2.4, 2H), 1.91–1.75 (m, 4H), 1.40 (s, 9H); ^{13}C NMR (125 MHz, $CDCl_3$): δ 178.1, 153.1, 138.4, 128.5, 127.5, 127.3, 83.4, 67.5, 47.8, 42.2, 29.7, 28.0; IR (film): 2962, 2842, 1728, 1688, 1366, 1143 cm^{-1}; HRMS-APCI (*m/z*) $[M + H]^+$ calcd for $C_{18}H_{26}NO_4$, 320.18563; found 320.18538.

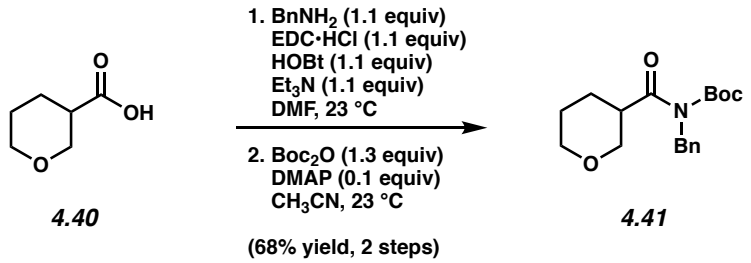

Amide 4.41. Purification by flash chromatography (14:1 Hexanes:EtOAc) generated amide **4.41** (68% yield, over two steps) as a white solid. Amide **4.41**: mp: 49–50 ºC; R_f 0.38 (5:1 Hexanes:EtOAc); ^1H NMR (500 MHz, $CDCl_3$): δ 7.31–7.26 (m, 2H), 7.25–7.18 (m, 3H), 4.87 (d,

J = 14.9, 1H), 4.81 (d, J = 14.9, 1H), 4.10–4.01 (m, 1H), 3.95–3.87 (m, 1H), 3.72–3.63 (m, 1H), 3.55 (t, J = 10.4, 1H), 3.44 (td, J = 10.8, 3.4, 1H), 2.13–2.04 (m, 1H), 1.81–1.63 (m, 3H), 1.42 (s, 9H); ^{13}C NMR (125 MHz, $CDCl_3$): δ 176.7, 153.0, 138.3, 128.5, 127.6, 127.3, 83.7, 70.1, 68.4, 47.7, 44.0, 28.0, 27.3, 25.3; IR (film): 2977, 2847, 1732, 1685, 1371, 1146 cm^{-1}; HRMS-APCI (*m*/*z*) [M + H]$^+$ calcd for $C_{18}H_{26}NO_4$, 320.18563; found 320.18577.

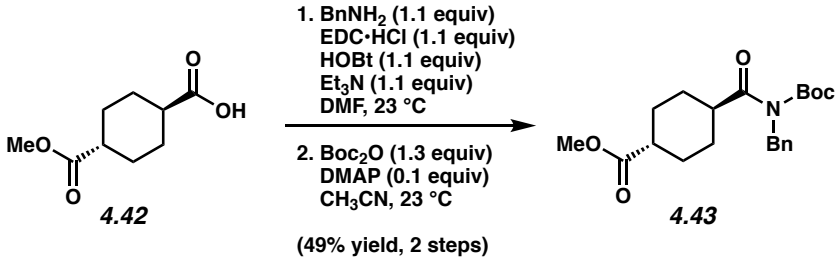

Amide 4.43. Purification by flash chromatography (9:1 Hexanes:EtOAc) generated amide **4.43** (49% yield, over two steps) as a white solid. Amide **4.43**: mp: 65–67 ºC; R_f 0.49 (5:1 Hexanes:EtOAc); ^{1}H NMR (500 MHz, $CDCl_3$): δ 7.31–7.26 (m, 2H), 7.24–7.20 (m, 3H), 4.85 (s, 2H), 3.67 (s, 3H), 3.43–3.36 (m, 1H), 2.37–2.30 (m, 1H), 2.10–1.96 (m, 4H), 1.58–1.46 (m, 4H), 1.41 (s, 9H); ^{13}C NMR (125 MHz, $CDCl_3$): δ 179.1, 176.2, 153.1, 138.5, 128.5, 127.6, 127.2, 83.4, 51.7, 47.8, 44.1, 42.8, 29.0, 28.4, 28.0; IR (film): 2977, 2946, 2865, 1728, 1689 cm^{-1}; HRMS-APCI (*m*/*z*) [M + H]$^+$ calcd for $C_{21}H_{30}NO_5$, 376.21240; found 376.21140.

4.8.2.2 Initial Survey of Ligands and Relevant Control Experiments

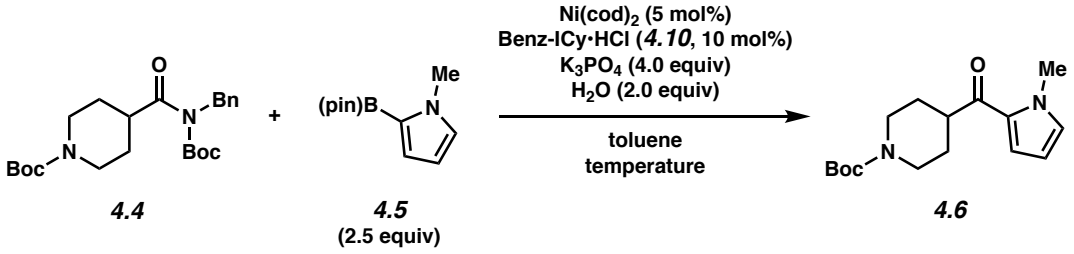

4.4 *4.5* (2.5 equiv) *4.6*

Representative Procedure for Suzuki reactions from Table 4.2 (coupling of amide 4.4 and *N*-methylpyrrole-2-boronic acid pinacol ester (4.5) is used as an example). A 1-dram vial was charged with anhydrous powdered K_3PO_4 (170 mg, 0.800 mmol, 4.0 equiv) and a magnetic stir bar. The vial and contents were flame-dried under reduced pressure, then allowed to cool under N_2. Amide substrate **4.4** (83.8 mg, 0.200 mmol, 1.0 equiv), *N*-methylpyrrole-2-boronic acid pinacol ester (**4.5**) (104 mg, 0.500 mmol, 2.5 equiv), and hexamethylbenzene (9.6 mg, 0.59 mmol, 0.30 equiv) were added. The vial was flushed with N_2, then water (7.2 μL, 0.400 mmol, 2.0 equiv), which had been sparged with N_2 for 10 min, was added. The vial was taken into a glove box and charged with $Ni(cod)_2$ (2.8 mg, 0.010 mmol, 5 mol%) and Benz-ICy•HCl (**4.10**, 6.4 mg, 0.020 mmol, 10 mol%). Subsequently, toluene (0.20 mL, 1.0 M) was added. The vial was sealed with a Teflon-lined screw cap, removed from the glove box, and stirred vigorously (800 rpm) at 120 °C for 16 h. After cooling to 23 °C, the mixture was diluted with hexanes (0.5 mL) and filtered over a plug of silica gel (10 mL of EtOAc eluent). The volatiles were removed under reduced pressure, and the yield was determined by ^{1}H NMR analysis with hexamethylbenzene as an internal standard.

Any modifications of the conditions shown in the representative procedure above are specified below in Table 4.2.

Table 4.2. Initial Survey of Ligands and Relevant Control Experiments.[a]

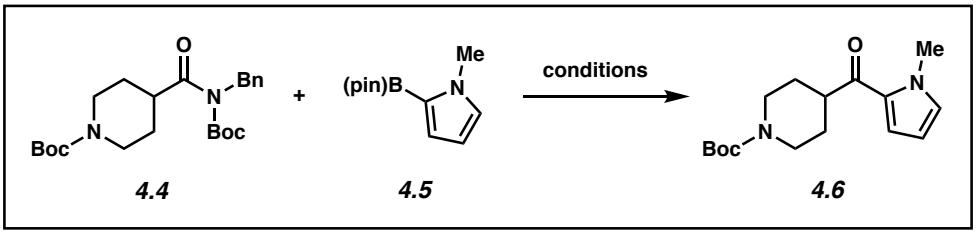

4.4 ***4.5*** ***4.6***

Reaction Conditions	***Experimental Results*** ***4.4***	***4.6***
4.5 (2.5 equiv), K_3PO_4 (4.0 equiv), H_2O (2.0 equiv) $Ni(cod)_2$ (5 mol%), SIPr (***4.7***,10 mol%), toluene (1.0 M), 50 °C, 16 h	100%	0%
4.5 (2.5 equiv), K_3PO_4 (4.0 equiv), H_2O (2.0 equiv) $Ni(cod)_2$ (5 mol%), SIPr (***4.7***,10 mol%), toluene (1.0 M), 120 °C, 16 h	52%[b]	0%
4.5 (2.5 equiv), K_3PO_4 (4.0 equiv), H_2O (2.0 equiv) $Ni(cod)_2$ (5 mol%), terpyridine (***4.8***,10 mol%), toluene (1.0 M), 120 °C, 16 h	50%[b]	0%
4.5 (2.5 equiv), K_3PO_4 (4.0 equiv), H_2O (2.0 equiv) $Ni(cod)_2$ (5 mol%), ICy·HBF_4 (***4.9***,10 mol%), toluene (1.0 M), 120 °C, 16 h	0%	95%
4.5 (2.5 equiv), K_3PO_4 (4.0 equiv), H_2O (2.0 equiv) $Ni(cod)_2$ (5 mol%), Benz-ICy·HCl (***4.10***,10 mol%), toluene (1.0 M), 120 °C, 16 h	0%	95%
Control Experiments:		
4.5 (2.5 equiv), K_3PO_4 (4.0 equiv), H_2O (2.0 equiv) toluene (1.0 M), 120 °C, 16 h	25%[b]	0%
4.5 (2.5 equiv), K_3PO_4 (4.0 equiv), H_2O (2.0 equiv) Benz-ICy·HCl (***4.10***,10 mol%), toluene (1.0 M), 120 °C, 16 h	25%[b]	0%
4.5 (2.5 equiv), K_3PO_4 (4.0 equiv), H_2O (2.0 equiv) $Ni(cod)_2$ (5 mol%), toluene (1.0 M), 120 °C, 16 h	5%[b]	0%

[a] Yields were determined by ^1H NMR analysis using hexamethylbenzene as an internal standard. [b] Substantial amounts of the corresponding Boc-cleavage product (des-Boc amide starting material) were observed due to the elevated reaction temperature.

4.8.2.3 Suzuki Reactions with Non-Heterocyclic Boronates

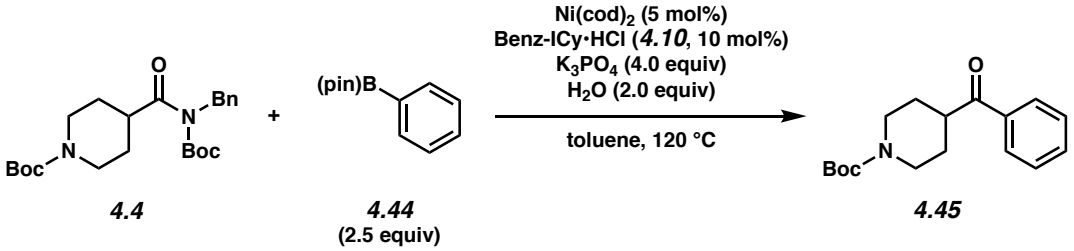

4.4 *4.44* (2.5 equiv) *4.45*

Representative Procedure for Suzuki reactions from Figure 4.5 (coupling of amide 4.4 and phenylboronic acid pinacol ester (4.44) is used as an example). A 1-dram vial was charged with anhydrous powdered K_3PO_4 (170 mg, 0.800 mmol, 4.0 equiv) and a magnetic stir bar. The vial and contents were flame-dried under reduced pressure, then allowed to cool under N_2. Amide substrate **4.4** (83.8 mg, 0.200 mmol, 1.0 equiv), phenylboronic acid pinacol ester (**4.44**) (102 mg, 0.500 mmol, 2.5 equiv), and hexamethylbenzene (9.6 mg, 0.59 mmol, 0.30 equiv) were added. The vial was flushed with N_2, then water (7.2 μL, 0.400 mmol, 2.0 equiv), which had been sparged with N_2 for 10 min, was added. The vial was taken into a glove box and charged with $Ni(cod)_2$ (2.8 mg, 0.010 mmol, 5 mol%) and Benz-ICy•HCl (**4.10**, 6.4 mg, 0.020 mmol, 10 mol%). Subsequently, toluene (0.20 mL, 1.0 M) was added. The vial was sealed with a Teflon-lined screw cap, removed from the glove box, and stirred vigorously (800 rpm) at 120 °C for 16 h. After cooling to 23 °C, the mixture was diluted with hexanes (0.5 mL) and filtered over a plug of silica gel (10 mL of EtOAc eluent). The volatiles were removed under reduced pressure, and the yield was determined by ^{1}H NMR analysis with hexamethylbenzene as an internal standard.

Any modifications of the conditions shown in the representative procedure above are specified in the schemes that follow Figure 4.5, which depict all of the results shown in Figure 4.5.

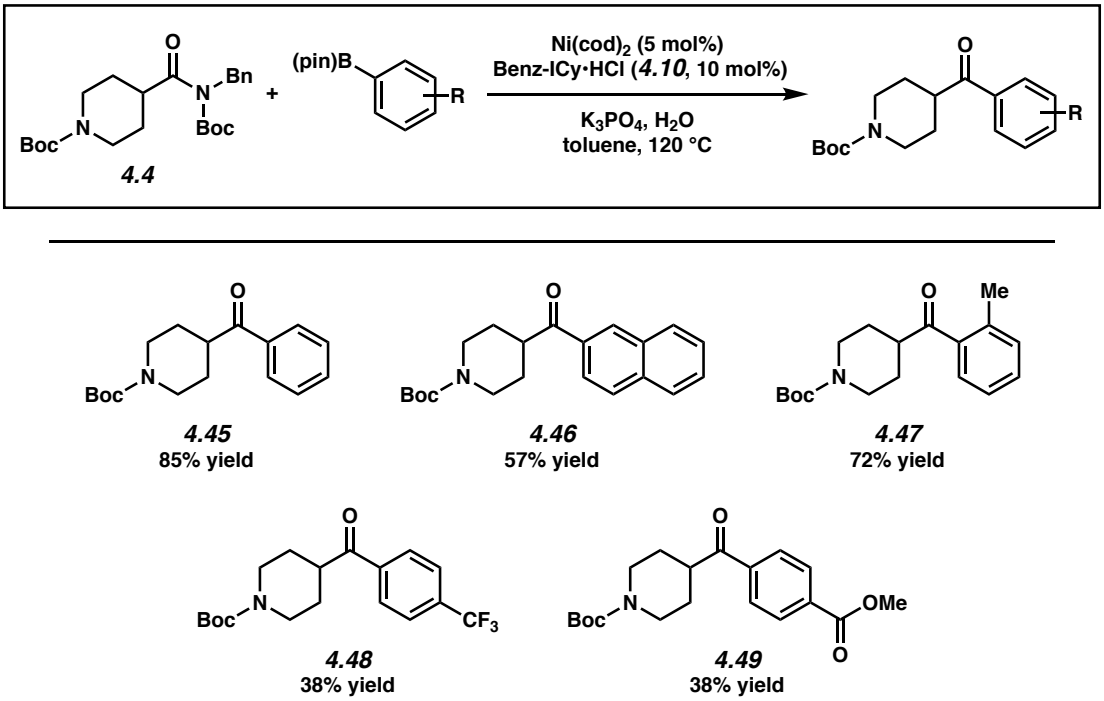

[a] Yields were determined by ^{1}H NMR analysis using hexamethylbenzene as an internal standard.

Figure 4.5. Suzuki Reactions with Non-Heterocyclic Boronates.[a]

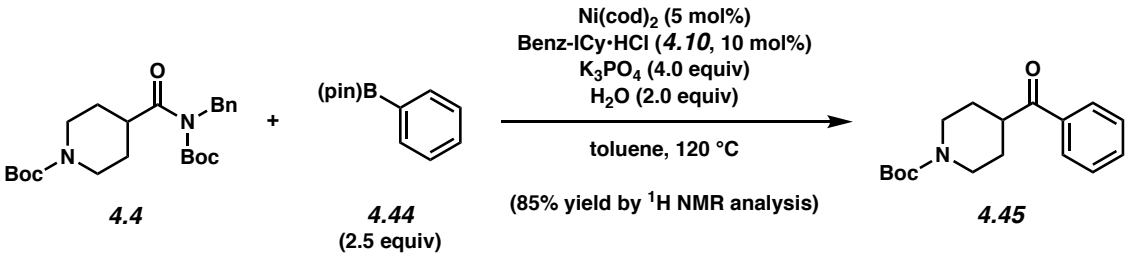

Ketone 4.45. ^{1}H NMR analysis of the crude reaction mixture indicated an 85% yield of ketone **4.45** relative to hexamethylbenzene internal standard. Purification by preparative thin-layer chromatography (3:1 Hexanes:EtOAc) generated ketone **4.45** as a white amorphous solid. Ketone **4.45**: R_f 0.21 (5:1 Hexanes:EtOAc). Spectral data match those previously reported.[16]

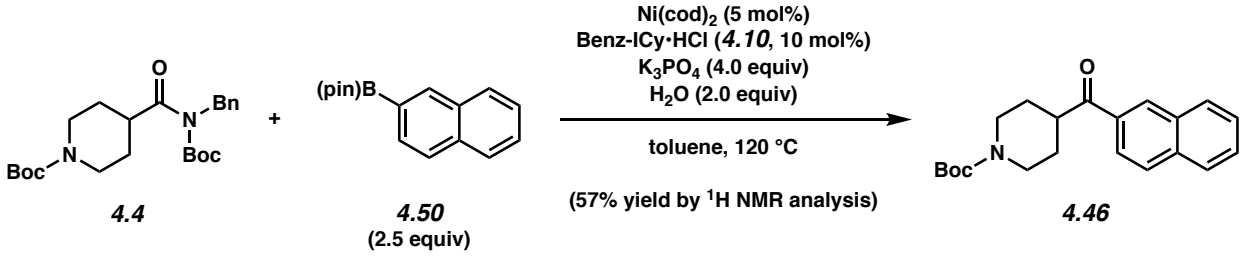

Ketone 4.46. ^{1}H NMR analysis of the crude reaction mixture indicated a 57% yield of ketone **4.46** relative to hexamethylbenzene internal standard. Purification by preparative thin-layer chromatography (4:1 Hexanes:EtOAc) generated ketone **4.46** as a white amorphous solid. Ketone **4.46**: R_f 0.29 (4:1 Hexanes:EtOAc); ^{1}H NMR (500 MHz, $CDCl_3$): δ 8.45 (s, 1H), 8.02–7.96 (m, 2H), 7.93–7.86 (m, 2H), 7.63–7.54 (m, 2H), 4.20 (br s, 2H), 3.58 (tt, J = 11.1, 3.7, 1H), 3.04–2.87 (m, 2H), 1.97–1.84 (m, 2H), 1.82–1.71 (m, 2H), 1.48 (s, 9H); ^{13}C NMR (125 MHz, $CDCl_3$): δ 202.2, 154.9, 135.7, 133.3, 132.7, 129.8, 129.7, 128.8, 128.7, 127.9, 127.0, 124.3, 79.8, 43.7, 43.3, 28.7, 28.6; IR (film): 3060, 2975, 2930, 2858, 1682 cm^{-1}; HRMS-APCI (*m/z*) $[M + H]^+$ calcd for $C_{21}H_{26}NO_3$, 340.19127; found 340.19041.

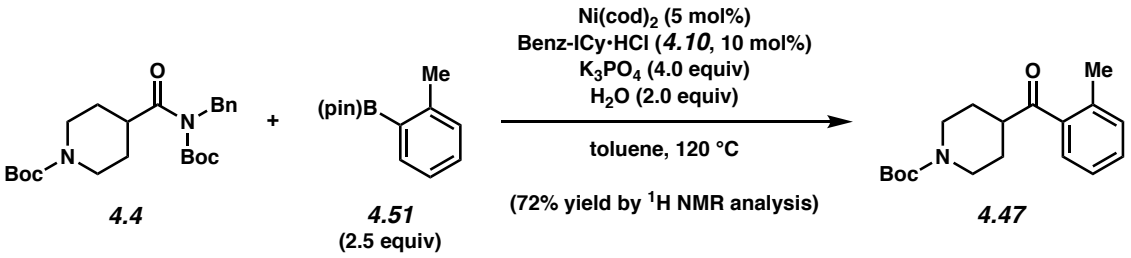

4.4 *4.51* (2.5 equiv) *4.47*

Ketone 4.47. ^{1}H NMR analysis of the crude reaction mixture indicated a 72% yield of ketone **4.47** relative to hexamethylbenzene internal standard. Purification by preparative thin-layer chromatography (4:1 Hexanes:EtOAc) generated ketone **4.47** as a clear oil. Ketone **4.47**: R_f 0.42 (3:1 Hexanes:EtOAc). Spectral data match those previously reported.[16]

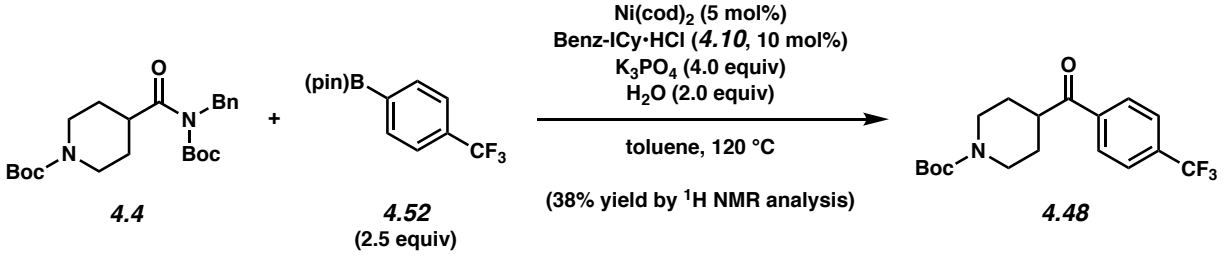

4.4 *4.52* (2.5 equiv) *4.48*

Ketone 4.48. ^{1}H NMR analysis of the crude reaction mixture indicated a 38% yield of ketone **4.48** relative to hexamethylbenzene internal standard. Purification by preparative thin-layer chromatography (4:1 Hexanes:EtOAc) generated ketone **4.48** as a white solid. Ketone **4.48**: R_f 0.38 (3:1 Hexanes:EtOAc). Spectral data match those previously reported.[16]

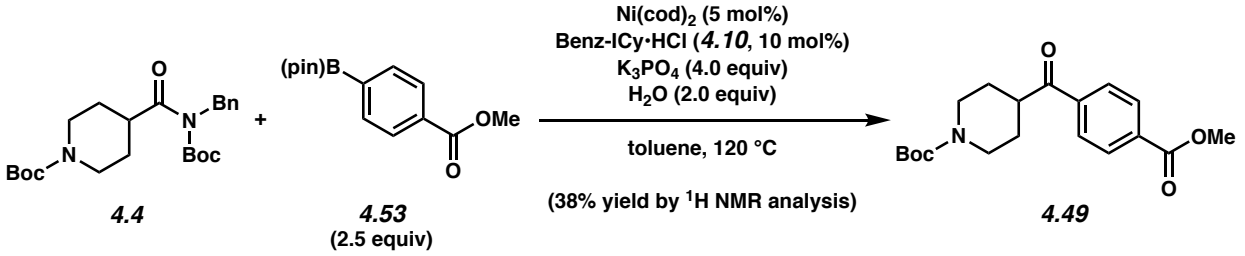

Ketone 4.49. ^{1}H NMR analysis of the crude reaction mixture indicated a 38% yield of ketone **4.49** relative to hexamethylbenzene internal standard. Purification by preparative thin-layer chromatography (3:1 Hexanes:EtOAc) generated ketone **4.49** as a white amorphous solid. Ketone **4.49**: R_f 0.25 (3:1 Hexanes:EtOAc). Spectral data match those previously reported.[16]

4.8.2.4 Scope of Methodology

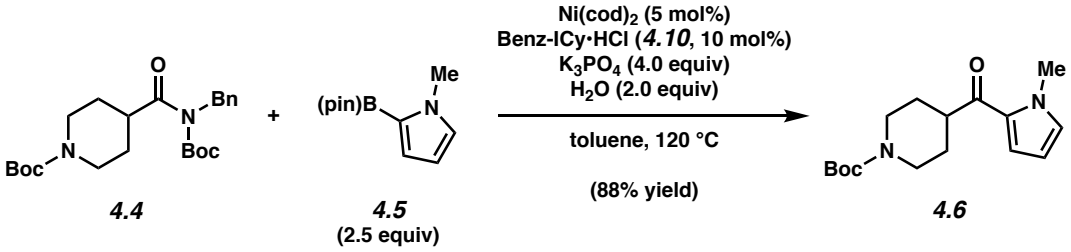

Representative Procedure (coupling of amide 4.4 and *N*-methylpyrrole-2-boronic acid pinacol ester (4.5) is used as an example). Ketone 4.6. A 1-dram vial was charged with anhydrous powdered K_3PO_4 (170 mg, 0.800 mmol, 4.0 equiv) and a magnetic stir bar. The vial and contents were flame-dried under reduced pressure, then allowed to cool under N_2. Amide substrate **4.4** (83.8 mg, 0.200 mmol, 1.0 equiv) and *N*-methylpyrrole-2-boronic acid pinacol ester (**4.5**) (104 mg, 0.500 mmol, 2.5 equiv) were added. The vial was flushed with N_2, then water (7.2 μL, 0.400 mmol, 2.0 equiv), which had been sparged with N_2 for 10 min, was added. The vial was taken into a glove box and charged with $Ni(cod)_2$ (2.8 mg, 0.010 mmol, 5 mol%) and Benz-ICy•HCl (**4.10**, 6.4 mg, 0.020 mmol, 10 mol%). Subsequently, toluene (0.20 mL, 1.0 M) was added. The vial was sealed with a Teflon-lined screw cap, removed from the glove box, and

stirred vigorously (800 rpm) at 120 °C for 16 h. After cooling to 23 °C, the mixture was diluted with hexanes (0.5 mL) and filtered over a plug of silica gel (10 mL of EtOAc eluent). The volatiles were removed under reduced pressure, and the crude residue was purified by flash chromatography (19:1 Hexanes:EtOAc → 14:1 Hexanes:EtOAc → 9:1 Hexanes:EtOAc) to yield ketone product **4.6** (88% yield, average of two experiments) as a white solid. Ketone **4.6**: mp: 77–80 ºC; R_f 0.18 (5:1 Hexanes:EtOAc); ^{1}H NMR (500 MHz, $CDCl_3$): δ 7.00–6.95 (m, 1H), 6.85–6.80 (m, 1H), 6.16–6.11 (m, 1H), 4.18 (br s, 2H), 3.93 (s, 3H), 3.20–3.10 (m, 1H), 2.93–2.70 (m, 2H), 1.85–1.66 (m, 4H), 1.46 (s, 9H); ^{13}C NMR (125 MHz, $CDCl_3$): δ 193.1, 154.9, 131.6, 129.8, 118.9, 108.1, 79.7, 44.8, 43.6, 38.0, 29.1, 28.6; IR (film): 2929, 2859, 1686, 1646, 1408, 1168 cm^{-1}; HRMS-APCI (*m/z*) [M + H]$^+$ calcd for $C_{16}H_{25}N_2O_3$, 293.18597; found 293.18535.

Any modifications of the conditions shown in the representative procedure above are specified in the following schemes, which depict all of the results shown in Figures 4.2 and 4.3.

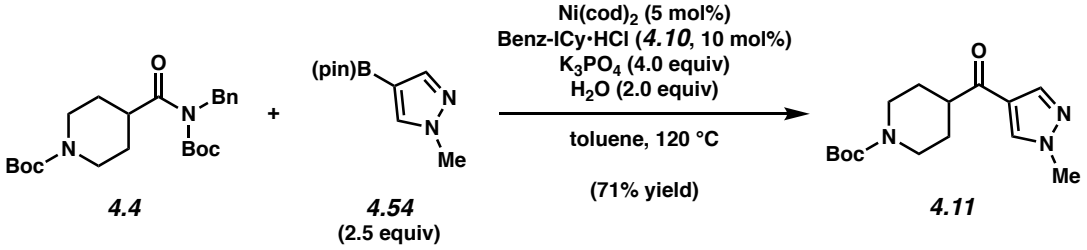

4.4 *4.54* (2.5 equiv) *4.11*

Ketone 4.11. Purification by flash chromatography (49:1 PhH:CH_3CN → 19:1 PhH:CH_3CN → 1:1 Hexanes:EtOAc → 1:3 Hexanes:EtOAc) generated ketone **4.11** (71% yield, average of two experiments) as a white solid. Ketone **4.11**: mp: 99–101 ºC; R_f 0.24 (1:3 Hexanes:EtOAc); ^{1}H NMR (500 MHz, $CDCl_3$): δ 7.89 (s, 1H), 7.88 (s, 1H), 4.15 (br s, 2H), 3.94 (s, 3H), 3.27 (tt, *J* = 11.1, 3.9, 1H), 2.93–2.73 (m, 2H), 1.93–1.63 (m, 4H), 1.46 (s, 9H); ^{13}C NMR (125 MHz, $CDCl_3$,

10 of 11 observed): δ 196.4, 154.8, 140.4, 132.8, 123.0, 79.8, 46.3, 39.6, 28.6, 28.4; IR (film): 2977, 2937, 2859, 1671, 1540, 1168 cm^{-1}; HRMS-APCI (*m/z*) $[M + H]^+$ calcd for $C_{15}H_{24}N_3O_3$, 294.18122; found 294.18073.

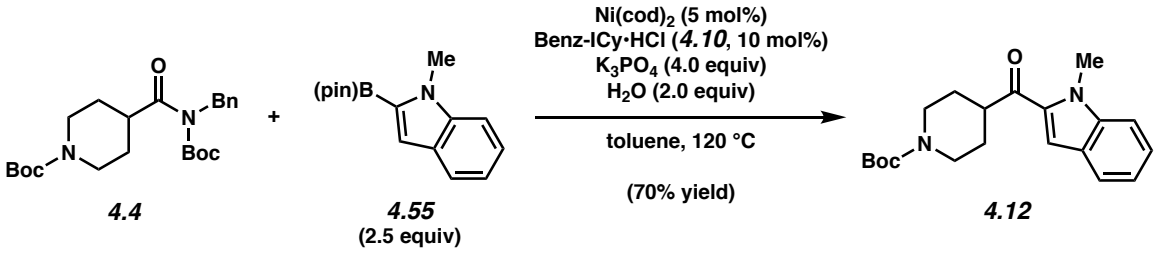

Ketone 4.12. Purification by flash chromatography (19:1 Hexanes:EtOAc → 14:1 Hexanes:EtOAc → 9:1 Hexanes:EtOAc) generated ketone **4.12** (70% yield, average of two experiments) as a white solid. Ketone **4.12**: R_f 0.25 (5:1 Hexanes:EtOAc). Spectral data match those previously reported.[16]

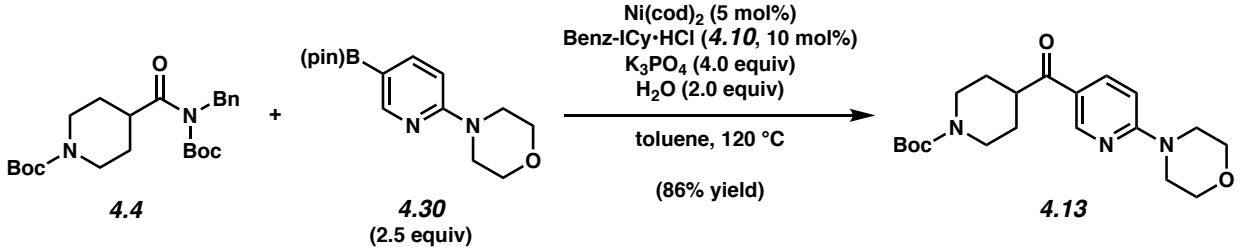

Ketone 4.13. Purification by flash chromatography (5:1 Hexanes:EtOAc → 9:1 CH_2Cl_2:MeOH) generated ketone **4.13** (86% yield, average of two experiments) as a white solid. Ketone **4.13**: mp: 131–133 ºC; R_f 0.52 (1:3 Hexanes:EtOAc); ^1H NMR (500 MHz, $CDCl_3$): δ 8.82–8.72 (m, 1H), 3.26 (dd, *J* = 9.1, 2.5, 1H), 6.69–6.58 (m, 1H), 4.17 (br s, 2H), 3.86–3.77 (m, 4H), 3.73–3.64 (m, 4H), 3.27 (tt, *J* = 11.1, 3.8, 1H), 2.99–2.71 (m, 2H), 1.94–1.64 (m, 4H), 1.46 (s, 9H); ^{13}C NMR (125 MHz, $CDCl_3$, 12 of 14 observed): δ 199.4, 160.9, 154.9, 150.4, 137.9, 121.5,

105.9, 79.8, 66.7, 45.0, 43.3, 28.6; IR (film): 2969, 2857, 1686, 1593, 1418, 1216, 1168 cm^{-1}; HRMS-APCI (*m/z*) $[M + H]^+$ calcd for $C_{20}H_{30}N_3O_4$, 376.22308; found 376.22247.

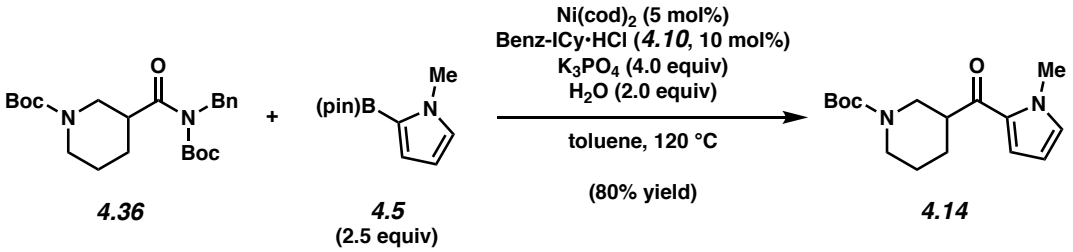

Ketone 4.14. Purification by flash chromatography (19:1 Hexanes:EtOAc → 14:1 Hexanes:EtOAc → 9:1 Hexanes:EtOAc) generated ketone **4.14** (80% yield, average of two experiments) as a white solid. Ketone **4.14**: mp: 86–88 ºC; R_f 0.19 (5:1 Hexanes:EtOAc); ^1H NMR (500 MHz, $CDCl_3$): δ 7.08–7.02 (m, 1H), 6.82 (br s, 1H), 6.17–6.12 (m, 1H), 4.40–4.00 (m, 2H), 3.93 (s, 3H), 3.22–3.09 (m, 1H), 2.99–2.78 (m, 1H), 2.76–2.61 (m, 1H), 2.02–1.92 (m, 1H), 1.78–1.69 (m, 2H), 1.57–1.50 (m, 1H), 1.47 (s, 9H); ^{13}C NMR (125 MHz, $CDCl_3$): δ 192.0, 154.9, 131.7, 129.9, 119.5, 108.3, 79.7, 47.8, 47.1, 45.3, 44.0, 37.9, 28.6, 28.4, 24.8; IR (film): 2937, 2862, 1690, 1645, 1408 cm^{-1}; HRMS-APCI (*m/z*) $[M + H]^+$ calcd for $C_{16}H_{25}N_2O_3$, 293.18597; found 293.18458.

*Note: Ketone **4.14** was obtained as a mixture of conformers. These data represent empirically observed chemical shifts from the ^{13}C NMR spectrum.*

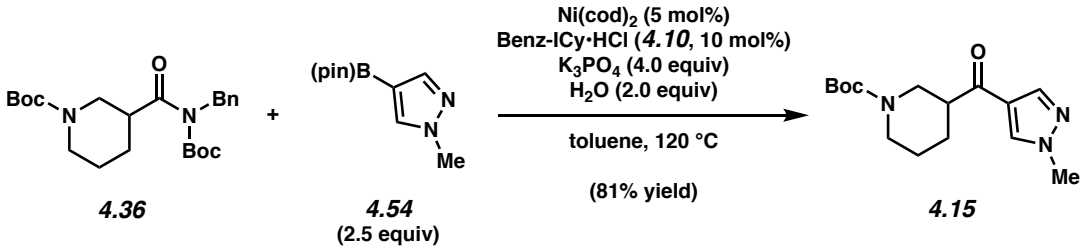

Ketone 4.15. Purification by flash chromatography (9:1 Hexanes:EtOAc → 5:1 Hexanes:EtOAc → 2:1 Hexanes:EtOAc → 1:1 Hexanes:EtOAc) generated ketone **4.15** (81% yield, average of two experiments) as a white solid. Ketone **4.15**: mp: 96–97 ºC; R_f 0.19 (1:1 Hexanes:EtOAc); ^{1}H NMR (500 MHz, $CDCl_3$): δ 7.93 (s, 1H), 7.91 (br s, 1H), 4.40–4.01 (m, 2H), 3.94 (s, 3H), 3.05–2.65 (m, 3H), 2.03–1.95 (m, 1H), 1.79–1.64 (m, 2H), 1.55–1.43 (m, 10H); ^{13}C NMR (125 MHz, $CDCl_3$): δ 195.3, 154.8, 140.6, 132.8, 123.1, 79.9, 46.7, 45.0, 43.9, 39.5, 28.6, 27.8, 24.8; IR (film): 2939, 2862, 1683, 1663, 1540, 1148 cm^{-1}; HRMS-APCI (*m/z*) $[M + H]^+$ calcd for $C_{15}H_{24}N_3O_3$, 294.18122; found 294.17877.

*Note: Ketone **4.15** was obtained as a mixture of conformers. These data represent empirically observed chemical shifts from the ^{13}C NMR spectrum.*

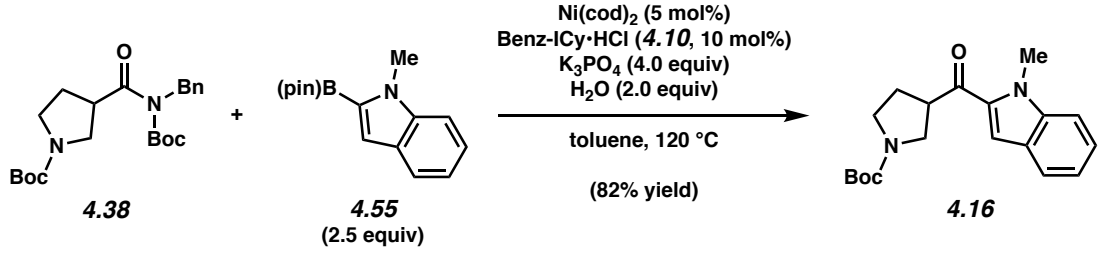

Ketone 4.16. Purification by flash chromatography (4:1 Hexanes:EtOAc) generated ketone **4.16** (82% yield, average of two experiments) as a clear oil. Ketone **4.16**: R_f 0.26 (4:1 Hexanes:EtOAc); ^{1}H NMR (500 MHz, $CDCl_3$): δ 7.70 (br s, 1H), 7.39 (br s, 2H), 7.33 (br s, 1H), 7.17 (br s, 1H), 4.08 (s, 3H), 4.04–3.91 (m, 1H), 3.82–3.65 (m, 1H), 3.65–3.39 (m, 3H), 2.35–

2.12 (m, 2H), 1.47 (s, 9H); ^{13}C NMR (125 MHz, $CDCl_3$): δ 193.1, 192.9, 154.5, 140.5, 134.2, 126.4, 125.9, 123.1, 121.1, 112.0, 110.6, 79.5, 49.0, 48.9, 47.3, 46.3, 45.8, 45.6, 32.4, 29.7, 29.4, 28.6; IR (film): 2974, 2882, 1688, 1658, 1393, 1166, 1118 cm^{-1}; HRMS-APCI (*m/z*) $[M + H]^+$ calcd for $C_{19}H_{25}N_2O_3$, 329.18597; found 329.18463.

*Note: Ketone **4.16** was obtained as a mixture of conformers. These data represent empirically observed chemical shifts from the ^{13}C NMR spectrum.*

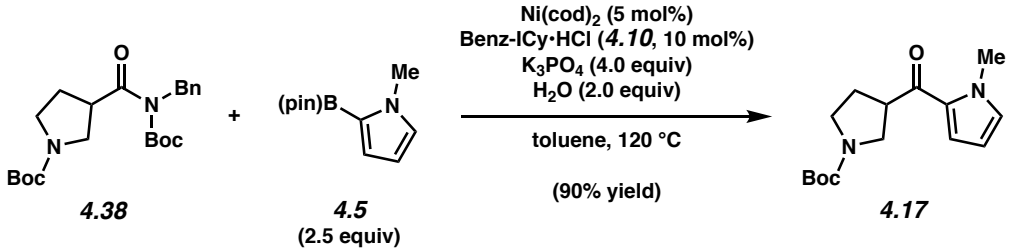

Ketone 4.17. Purification by flash chromatography (4:1 Hexanes:EtOAc) generated ketone **4.17** (82% yield, average of two experiments) as a clear oil. Ketone **4.17**: R_f 0.18 (4:1 Hexanes:EtOAc); ^{1}H NMR (500 MHz, $CDCl_3$): δ 6.97 (br s, 1H), 6.83 (br s, 1H), 6.14 (br s, 1H), 3.93 (s, 3H), 3.83–3.44 (m, 4H), 3.38 (br s, 1H), 2.28–2.12 (m, 1H), 2.08 (br s, 1H), 1.45 (s, 9H); ^{13}C NMR (125 MHz, $CDCl_3$): δ 189.9, 189.7, 154.5, 131.9, 130.2, 119.6, 108.4, 79.4, 49.0, 48.9, 46.4, 45.9, 45.6, 45.5, 37.9, 29.5, 29.4, 28.6; IR (film): 2977, 2882, 1686, 1643, 1401, 1366, 1118 cm^{-1}; HRMS-APCI (*m/z*) $[M + H]^+$ calcd for $C_{15}H_{23}N_2O_3$, 279.17032; found 279.17976.

*Note: Ketone **4.17** was obtained as a mixture of conformers. These data represent empirically observed chemical shifts from the ^{13}C NMR spectrum.*

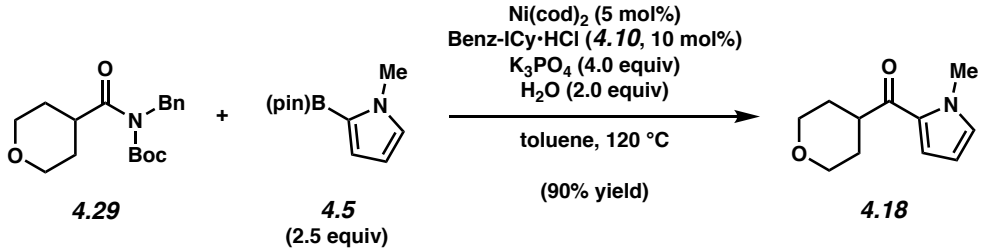

Ketone 4.18. Purification by flash chromatography (5:1 Hexanes:EtOAc) generated ketone **4.18** (90% yield, average of two experiments) as a white solid. Ketone **4.18**: mp: 72–74 ºC; R_f 0.21 (4:1 Hexanes:EtOAc); ^{1}H NMR (500 MHz, $CDCl_3$): δ 7.00–6.95 (m, 1H), 6.82 (s, 1H), 6.15–6.10 (m, 1H), 4.09–4.00 (m, 2H), 3.94 (s, 3H), 3.51 (t, *J* = 11.8, 2H), 3.26 (tt, *J* = 11.5, 3.8, 1H), 1.91 (qd, *J* = 12.4, 4.3, 2H), 1.70 (d, *J* = 13.4, 2H); ^{13}C NMR (125 MHz, $CDCl_3$): δ 192.9, 131.6, 129.8, 118.9, 108.1, 67.6, 43.8, 38.0, 29.7; IR (film): 2952, 2847, 1642, 1408, 1306, 1094 cm^{-1}; HRMS-APCI (*m/z*) $[M + H]^+$ calcd for $C_{11}H_{16}NO_2$, 194.11756; found 194.11707.

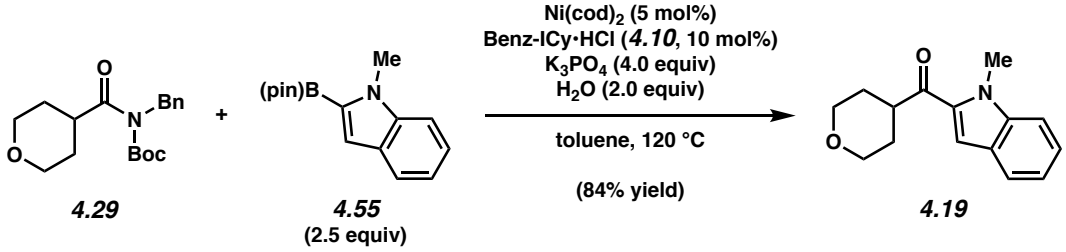

Ketone 4.19. Purification by flash chromatography (5:1 Hexanes:EtOAc) generated ketone **4.19** (84% yield, average of two experiments) as a white solid. Ketone **4.19**: mp: 63–66 ºC; R_f 0.35 (4:1 Hexanes:EtOAc); ^{1}H NMR (500 MHz, $CDCl_3$): δ 7.70 (d, *J* = 8.1, 1H), 7.39 (d, *J* = 3.6, 2H), 7.33 (s, 1H), 7.19–7.14 (m, 1H), 4.12–4.09 (m, 1H), 4.07 (s, 4H), 3.57 (t, *J* = 11.7, 2H), 3.48 (tt, *J* = 11.5, 3.6, 1H), 1.96 (qd, *J* = 12.4, 4.2, 2H), 1.81 (d, *J* = 13.2, 2H); ^{13}C NMR (125 MHz, $CDCl_3$): δ 196.0, 140.4, 133.8, 126.1, 125.9, 123.0, 120.9, 111.1, 110.6, 67.5, 44.7, 32.4, 29.8;

IR (film): 2954, 2844, 1656, 1511, 1386, 1118 cm^{-1}; HRMS-APCI (*m/z*) $[M + H]^+$ calcd for $C_{15}H_{18}NO_2$, 244.13321; found 244.13264.

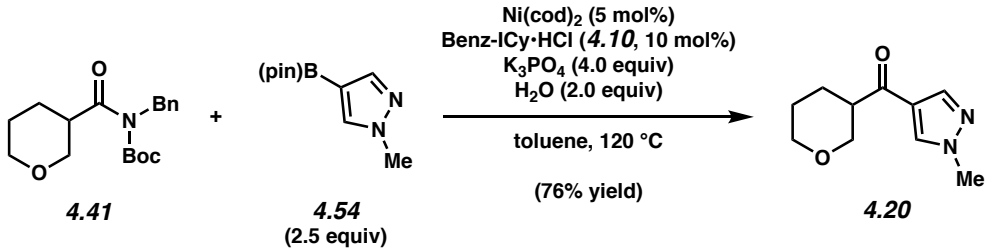

Ketone 4.20. Purification by flash chromatography (1:2 Hexanes:EtOAc) generated ketone **4.20** (76% yield, average of two experiments) as a yellow solid. Ketone **4.20**: mp: 83–84 ºC; R_f 0.25 (1:2 Hexanes:EtOAc); ^{1}H NMR (500 MHz, $CDCl_3$): δ 7.89 (s, 1H), 7.87 (s, 1H), 4.04 (d, J = 11.1, 1H), 3.96–3.86 (m, 4H), 3.50 (t, *J* = 10.9, 1H), 3.43–3.34 (m, 1H), 3.20–3.11 (m, 1H), 1.97 (d, *J* = 12.7, 1H), 1.86–1.73 (m, 1H), 1.73–1.63 (m, 2H); ^{13}C NMR (125 MHz, $CDCl_3$): δ 195.2, 140.4, 132.8, 123.3, 69.8, 68.2, 47.2, 39.5, 26.6, 25.2; IR (film): 2947, 2852, 1656, 1541, 1401, 1188, 1080 cm^{-1}; HRMS-APCI (*m/z*) $[M + H]^+$ calcd for $C_{10}H_{15}N_2O_2$, 165.11280; found 165.11223.

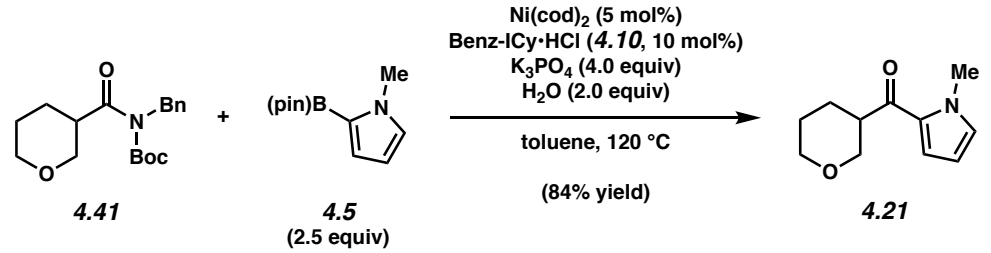

Ketone 4.21. Purification by flash chromatography (4:1 Hexanes:EtOAc) generated ketone **4.21** (84% yield, average of two experiments) as a clear oil. Ketone **4.21**: R_f 0.30 (4:1 Hexanes:EtOAc); ^{1}H NMR (500 MHz, $CDCl_3$): δ 7.04–7.00 (m, 1H), 6.81 (s, 1H), 6.15–6.10 (m,

1H), 4.09–4.02 (m, 1H), 3.98–3.92 (m, 1H), 3.91 (s, 3H), 3.52 (t, *J* = 10.9, 1H), 3.44–3.33 (m, 2H), 2.00–1.93 (m, 1H), 1.84 (qd, *J* = 12.1, 4.3, 1H), 1.78–1.65 (m, 2H); ^{13}C NMR (125 MHz, $CDCl_3$): δ 191.8, 131.7, 130.1, 119.5, 108.2, 70.6, 68.3, 45.7, 37.9, 27.1, 25.4; IR (film): 2947, 2849, 1638, 1406, 1201, 1065 cm^{-1}; HRMS-APCI (*m/z*) [M + H]$^+$ calcd for $C_{11}H_{16}NO_2$, 194.11756; found 194.11699.

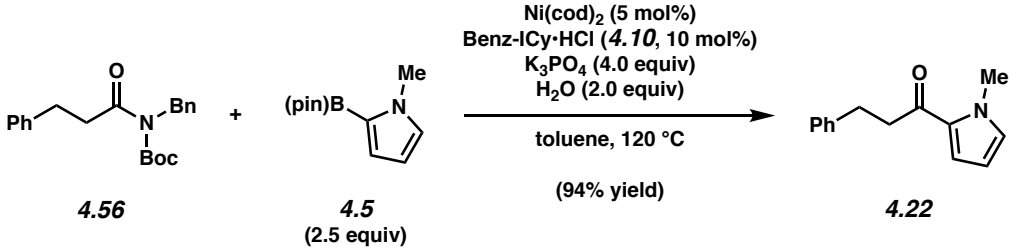

Ketone 4.22. Purification by flash chromatography (19:1 Hexanes:EtOAc → 14:1 Hexanes:EtOAc → 9:1 Hexanes:EtOAc) generated ketone **4.22** (94% yield, average of two experiments) as a clear oil. Ketone **4.22**: R_f 0.43 (5:1 Hexanes:EtOAc). Spectral data match those previously reported.[17]

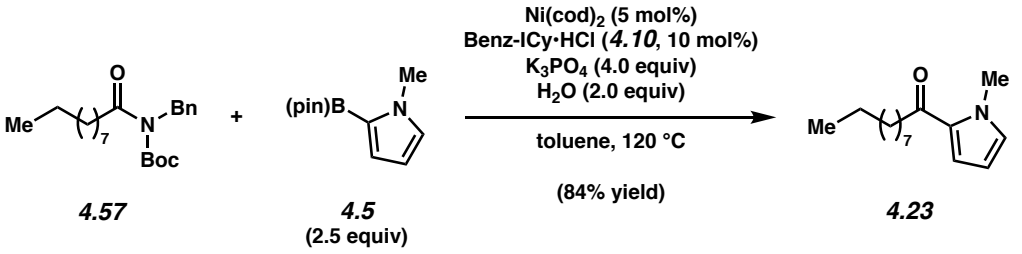

Ketone 4.23. Purification by flash chromatography (24:1 Hexanes:EtOAc) generated ketone **4.23** (84% yield, average of two experiments) as a clear oil. Ketone **4.23**: R_f 0.52 (5:1 Hexanes:EtOAc); ^{1}H NMR (500 MHz, $CDCl_3$): δ 6.95 (dd, *J* = 4.1, 1.7, 1H), 6.80–6.77 (m, 1H), 6.11 (dd, *J* = 4.1, 2.5, 1H), 3.94 (s, 3H), 2.77–2.73 (m, 2H), 1.69 (p, *J* = 7.5, 2H), 1.39–1.20 (m,

12H), 0.88 (t, J = 7.1, 3H); ^{13}C NMR (125 MHz, $CDCl_3$): δ 192.0, 131.0, 130.9, 119.0, 107.9, 39.3, 37.9, 32.0, 29.7, 29.633, 29.627, 29.5, 25.5, 22.8, 14.3; IR (film): 2955, 2923, 2853, 1649, 1528 cm^{-1}; HRMS-APCI (m/z) $[M + H]^+$ calcd for $C_{15}H_{26}NO$, 236.20144; found 236.20080.

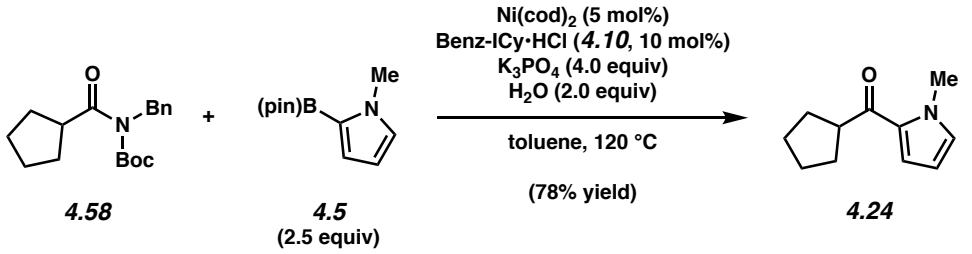

Ketone 4.24. Purification by flash chromatography (24:1 Hexanes:EtOAc → 19:1 Hexanes:EtOAc) generated ketone **4.24** (78% yield, average of two experiments) as a clear oil. Ketone **4.24**: R_f 0.50 (5:1 Hexanes:EtOAc). Spectral data match those previously reported.[18]

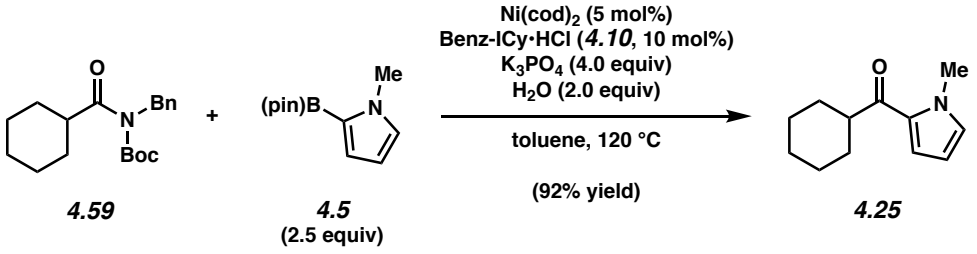

Ketone 4.25. Purification by flash chromatography (14:1 Hexanes:EtOAc) generated ketone **4.25** (92% yield, average of two experiments) as a clear oil. Ketone **4.25**: R_f 0.28 (14:1 Hexanes:EtOAc). Spectral data match those previously reported.[19]

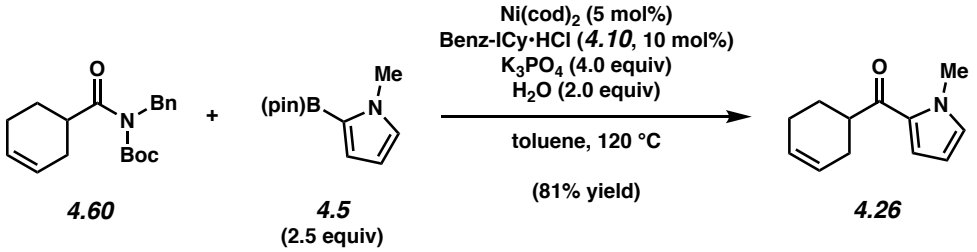

Ketone 4.26. Purification by flash chromatography (24:1 Hexanes:EtOAc → 19:1 Hexanes:EtOAc) generated ketone **4.26** (81% yield, average of two experiments) as a clear oil. Ketone **4.26**: R_f 0.46 (5:1 Hexanes:EtOAc); ^{1}H NMR (500 MHz, $CDCl_3$): δ 6.99 (dd, J = 4.1, 1.6, 1H), 6.83–6.80 (m, 1H), 6.13 (dd, J = 4.1, 2.4, 1H), 5.79–5.70 (m, 2H), 3.95 (s, 3H), 3.32–3.25 (m, 1H), 2.39–2.30 (m, 1H), 2.20–2.11 (m, 3H), 1.96–1.90 (m, 1H), 1.79–1.69 (m, 1H); ^{13}C NMR (125 MHz, $CDCl_3$): δ 194.8, 131.3, 130.3, 126.6, 126.2, 119.0, 108.0, 42.7, 38.0, 28.6, 26.4, 25.2; IR (film): 3107, 3023, 2931, 2838, 1643, 1527 cm^{-1}; HRMS-APCI (*m/z*) $[M + H]^+$ calcd for $C_{12}H_{16}NO$, 190.12319; found 190.12245.

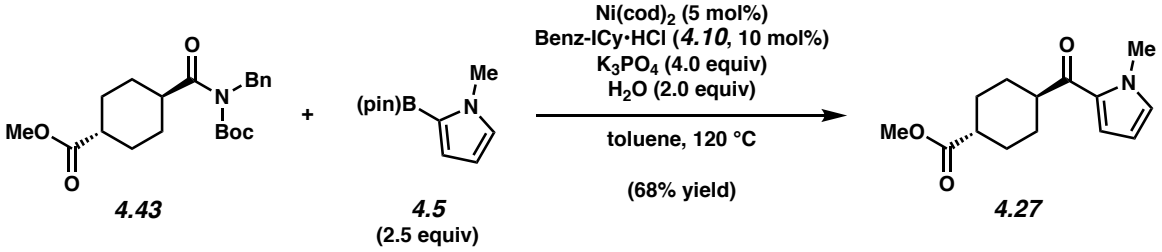

Ketone 4.27. Purification by flash chromatography (49:1 $CHCl_3$:CH_3CN) generated ketone **4.27** (68% yield, average of two experiments) as a white solid. Ketone **4.27**: R_f 0.48 (19:1 $CHCl_3$:CH_3CN); ^{1}H NMR (500 MHz, $CDCl_3$): δ 6.97 (dd, J = 4.1, 1.7, 1H), 6.83–6.80 (m, 1H), 6.13 (dd, J = 4.1, 2.5, 1H), 3.93 (s, 3H), 3.68 (s, 3H), 3.06–2.99 (m, 1H), 2.38–2.30 (m, 1H), 2.14–2.05 (m, 2H), 1.98–1.88 (m, 2H), 1.63–1.49 (m, 4H); ^{13}C NMR (125 MHz, $CDCl_3$): δ 194.3, 176.3, 131.5, 130.0, 118.9, 108.0, 51.7, 45.9, 42.7, 37.9, 29.0, 28.5; IR (film): 2942, 2862,

1730, 1645, 1408, 1251 cm^{-1}; HRMS-APCI (*m/z*) $[M + H]^+$ calcd for $C_{14}H_{20}NO_3$, 250.14377; found 250.14273.

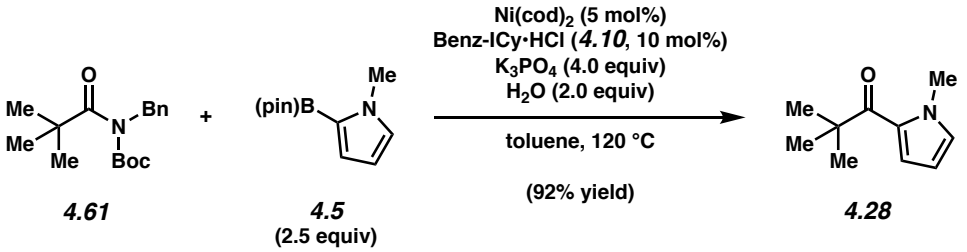

Ketone 4.28. Purification by flash chromatography (19:1 Hexanes:EtOAc) generated ketone **4.28** (92% yield, average of two experiments) as a clear oil. Ketone **4.28**: R_f 0.66 (4:1 Hexanes:EtOAc). Spectral data match those previously reported.[20]

4.8.2.5 Gram Scale Suzuki Reaction and Subsequent Fischer Indolization

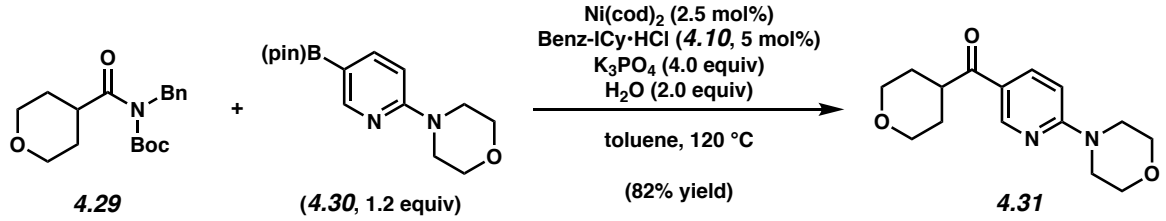

Ketone 4.31. A 20 mL scintillation vial was charged with anhydrous powdered K_3PO_4 (2.66 g, 12.5 mmol, 4.0 equiv) and a magnetic stir bar. The vial and contents were flame-dried under reduced pressure, then allowed to cool under N_2. Amide substrate **4.29** (1.00 g, 3.14 mmol, 1.0 equiv) and 2-morpholinopyridine-5-boronic acid pinacol ester (**4.30**) (1.09 g, 3.76 mmol, 1.2 equiv) were added. The vial was flushed with N_2, then water (113 μL, 6.27 mmol, 2.0 equiv), which had been sparged with N_2 for 10 min, was added. The vial was taken into a glove box and charged with $Ni(cod)_2$ (21.6 mg, 0.0784 mmol, 2.5 mol%) and Benz-ICy•HCl (**4.10**, 50.0 mg, 0.157 mmol, 5 mol%). Subsequently, toluene (3.14 mL, 1.0 M) was added. The vial was sealed

with a Teflon-lined screw cap, removed from the glove box, and stirred vigorously (800 rpm) at 120 °C for 16 h. After cooling to 23 °C, the mixture was diluted with hexanes (7 mL) and filtered over a plug of silica gel (100 mL of EtOAc eluent). The volatiles were removed under reduced pressure, and the crude residue was purified by flash chromatography (3:1 Hexanes:EtOAc → 19:1 CH_2Cl_2:MeOH) to yield ketone product **4.31** (707 mg, 82% yield) as an off-white solid. Ketone **4.31**: mp: 122–124 ºC; R_f 0.36 (4:1 PhH:CH_3CN); ^{1}H NMR (500 MHz, $CDCl_3$): δ 8.79 (d, *J* = 2.2, 1H), 8.06 (dd, *J* = 9.1, 2.4, 1H), 6.63 (d, *J* = 9.1, 1H), 4.09–4.02 (m, 2H), 3.84–3.78 (m, 4H), 3.71–3.65 (m, 4H), 3.54 (td, *J* = 11.7, 2.2, 2H), 3.37 (tt, *J* = 11.2, 3.8, 1H), 1.96–1.84 (m, 2H), 1.79–1.71 (m, 2H); ^{13}C NMR (125 MHz, $CDCl_3$): δ 199.2, 160.7, 150.4, 137.9, 121.5, 105.9, 67.5, 66.7, 45.0, 42.4, 29.3; IR (film): 2955, 2920, 2850, 1663, 1596 cm^{-1}; HRMS-APCI (*m/z*) $[M + H]^+$ calcd for $C_{15}H_{21}N_2O_3$, 277.15522; found 277.15256.

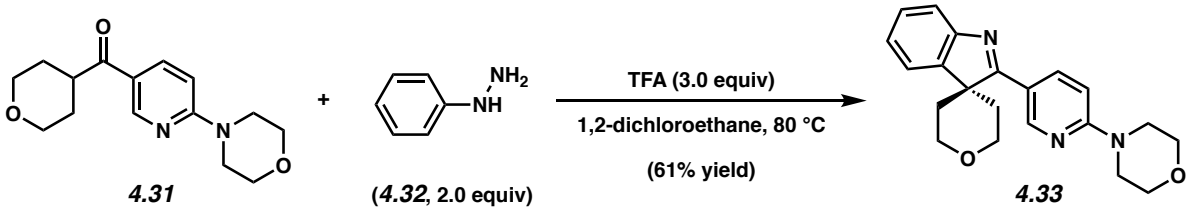

Indolenine 4.33. A 20 mL scintillation vial was charged with ketone **4.31** (707 mg, 2.56 mmol, 1.0 equiv) and a magnetic stir bar. Subsequently, 1,2-dichloroethane (12.0 mL, 0.21 M), phenylhydrazine (**4.32**, 503 μL, 5.12 mmol, 2.0 equiv), and TFA (588 μL, 7.69 mmol, 3.0 equiv) were added. The vial was sealed with a Teflon-lined screw cap and stirred at 80 °C for 16 h. After cooling to 23 °C, the volatiles were removed under reduced pressure, and the crude residue was purified by flash chromatography (3:1 Hexanes:EtOAc → 1:1 Hexanes:EtOAc → 100% EtOAc) to yield indolenine **4.33** (546 mg, 61% yield) as a tan solid. Indolenine **4.33**: mp: 186–189 ºC; R_f 0.26 (4:1 PhH:CH_3CN); ^{1}H NMR (500 MHz, $CDCl_3$): δ 9.11 (d, *J* = 2.2, 1H), 8.49

(dd, J = 9.1, 2.5, 1H), 7.92 (d, J = 7.4, 1H), 7.69 (d, J = 7.3, 1H), 7.41 (td, J = 7.6, 1.1, 1H), 7.22 (td, J = 7.5, 1.1, 1H), 6.73 (d, J = 9.1, 1H), 4.23–4.08 (m, 4H), 3.87–3.81 (m, 4H), 3.70–3.64 (m, 4H), 2.77–2.67 (m, 2H), 1.36 (d, J = 14.1, 2H); ^{13}C NMR (125 MHz, $CDCl_3$): δ 179.2, 159.5, 154.1, 148.9, 145.9, 138.2, 128.3, 124.8, 123.6, 121.2, 118.4, 106.4, 66.8, 64.0, 54.5, 45.2, 31.6; IR (film): 2960, 2921, 2858, 1596, 1499 cm^{-1}; HRMS-APCI (m/z) $[M + H]^+$ calcd for $C_{21}H_{24}N_3O_2$, 350.18685; found 350.18529.

4.9 Spectra Relevant to Chapter Four:

Aliphatic Amides as Acyl Donors for the Union of Heterocycles

Nicholas A. Weires, Timothy B. Boit, Junyong Kim, and Neil K. Garg.

Manuscript in Preparation

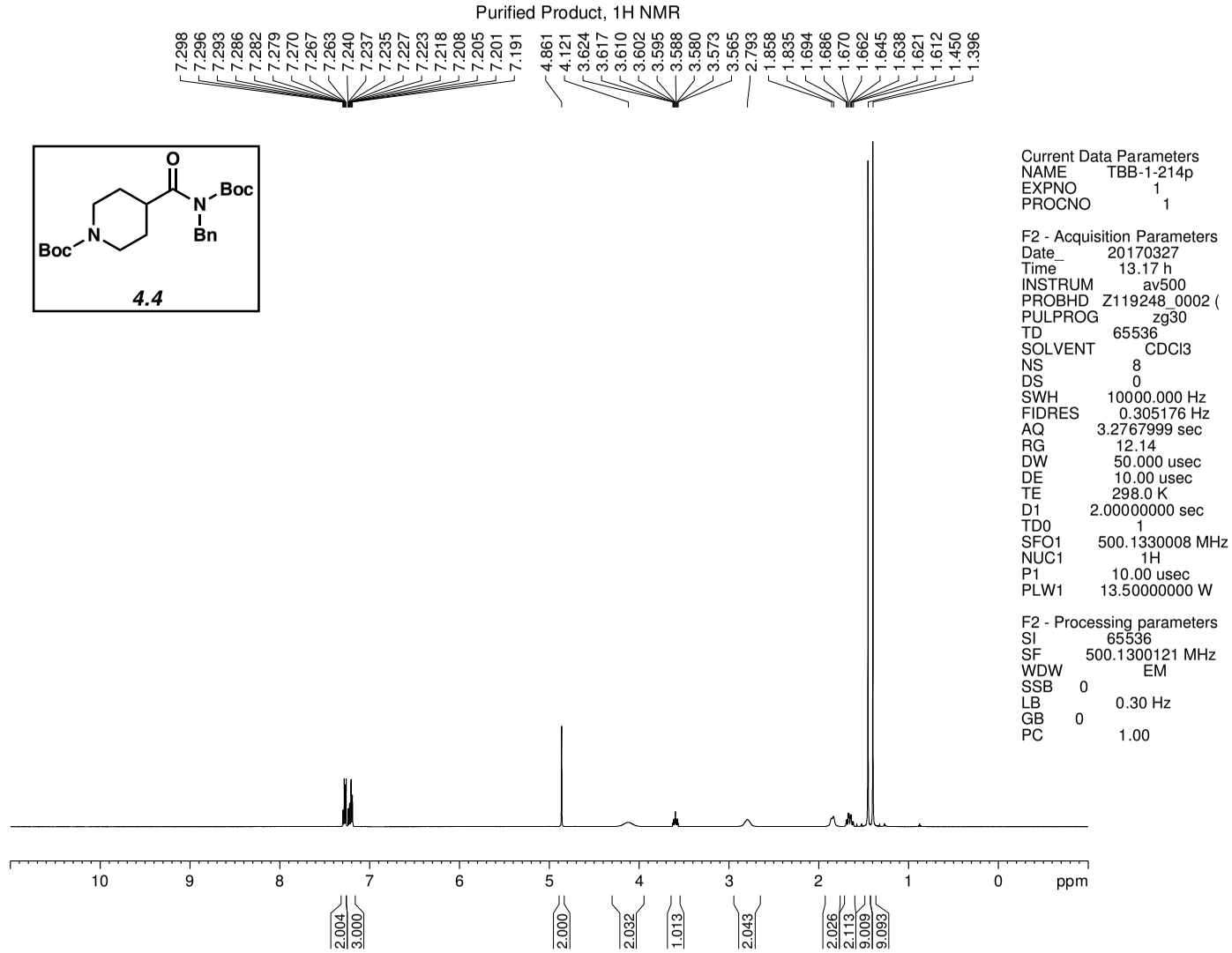

Figure 4.6 ^{1}H NMR (500 MHz, $CDCl_3$) of compound **4.4**.

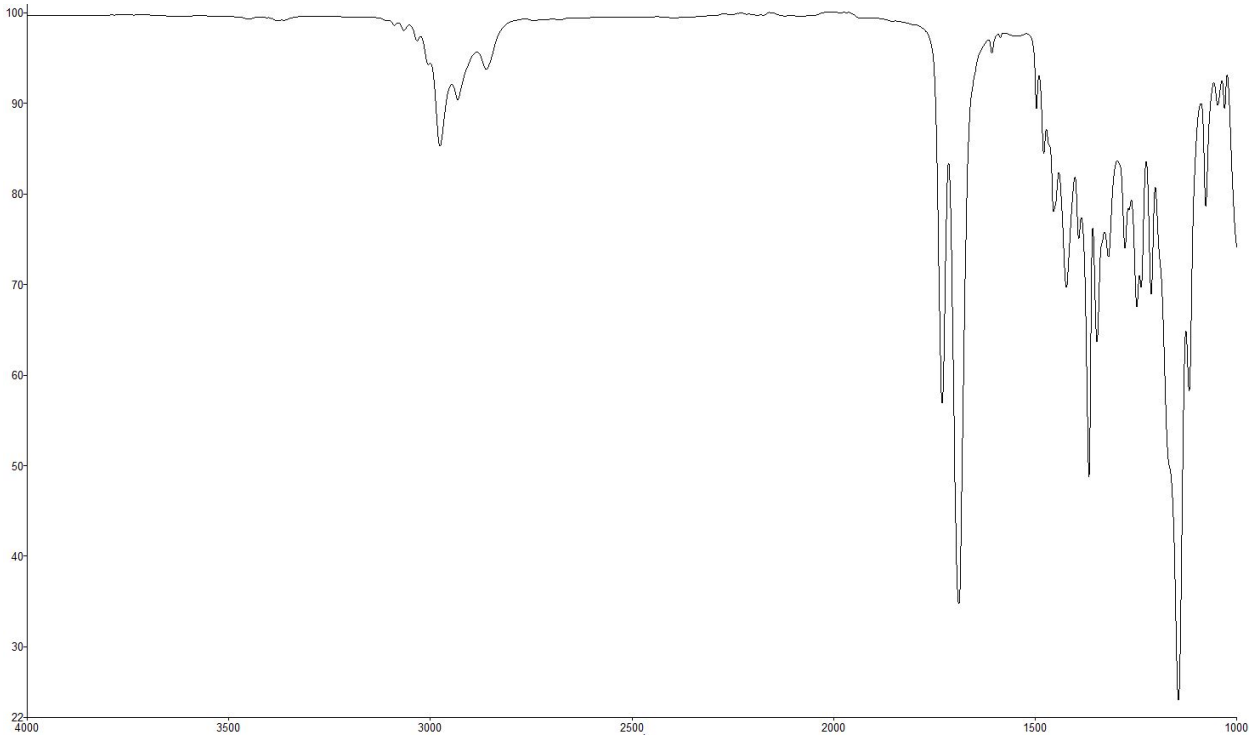

Figure 4.7 Infrared spectrum of compound **4.4**.

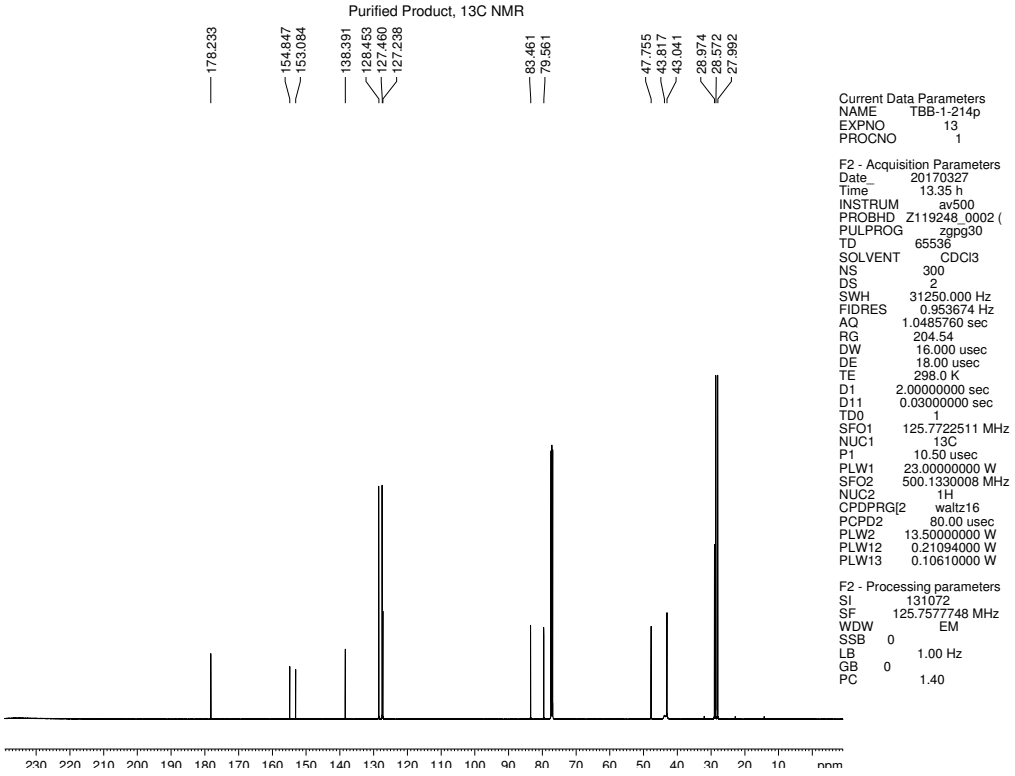

Figure 4.8 ^{13}C NMR (125 MHz, $CDCl_3$) of compound **4.4**.

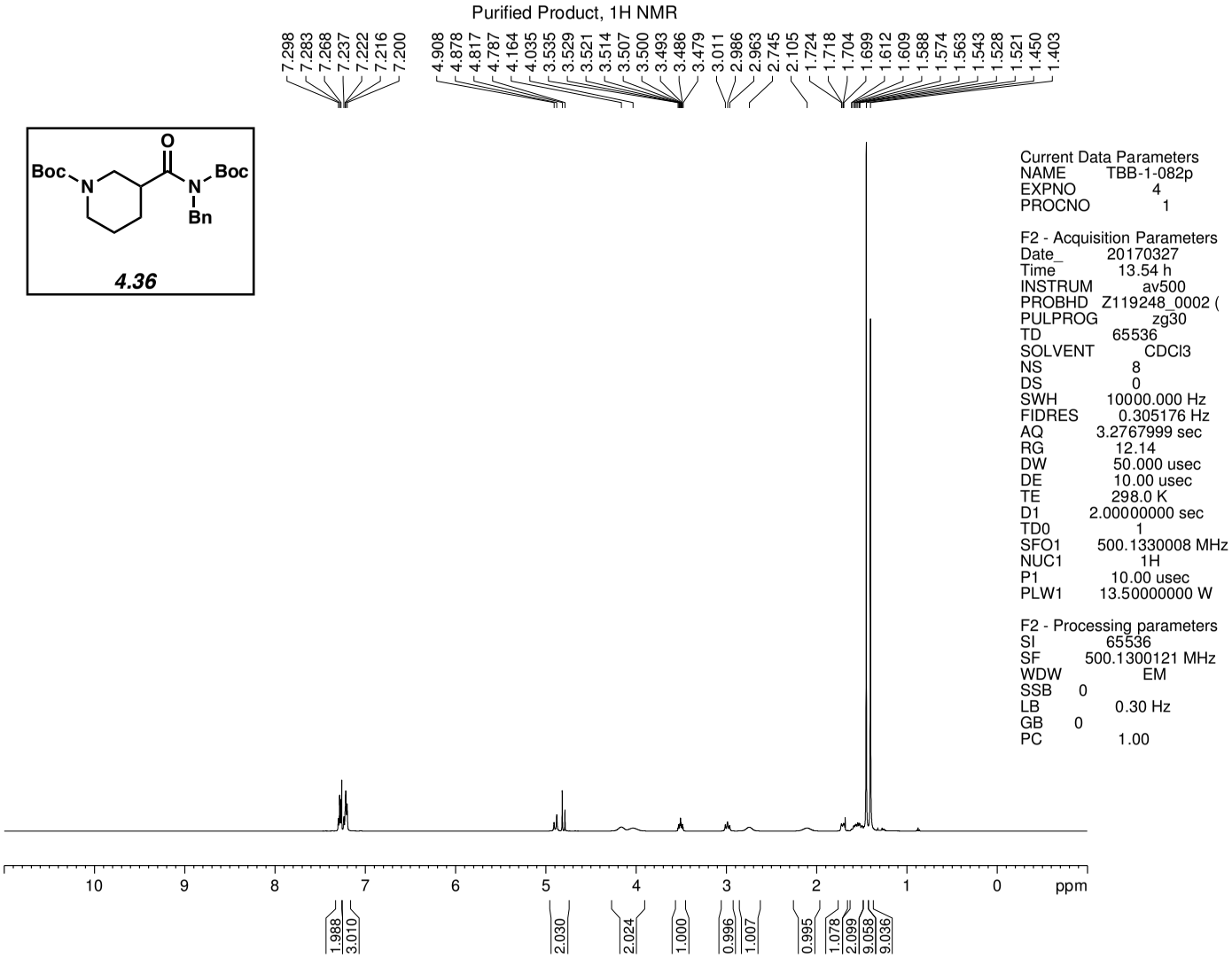

Figure 4.9 ^{1}H NMR (500 MHz, $CDCl_3$) of compound **4.36**.

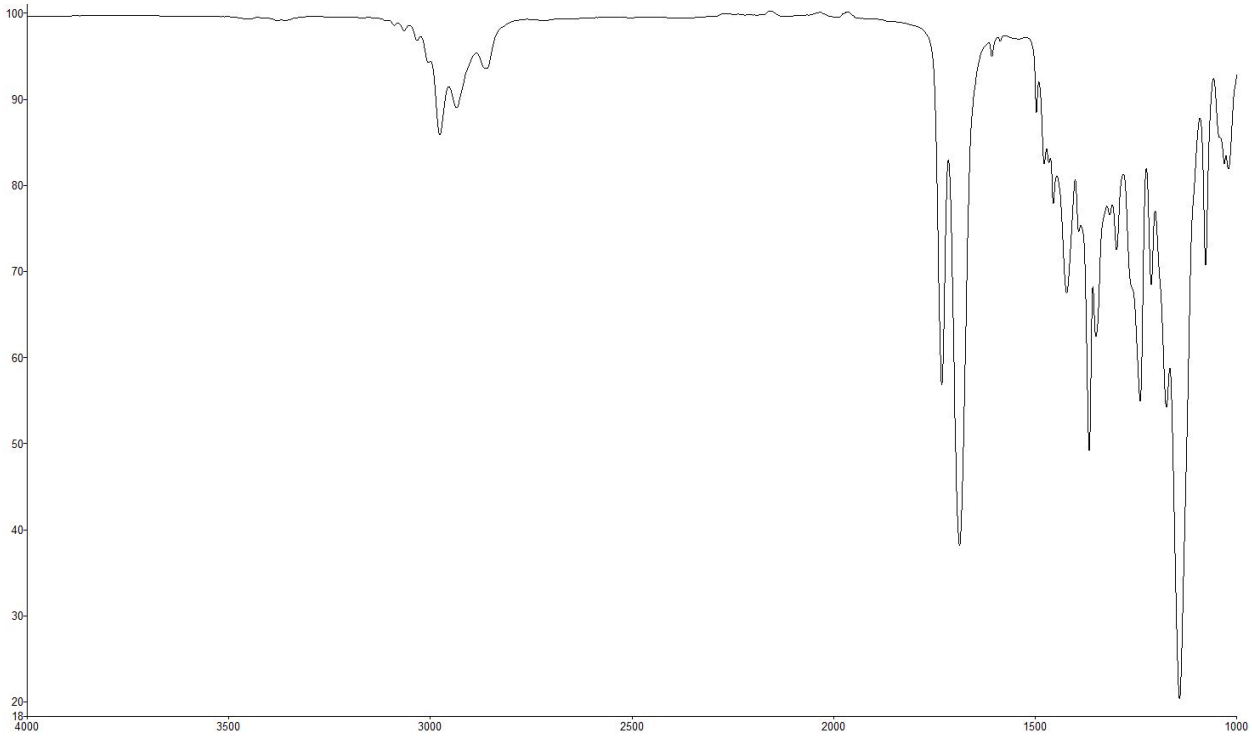

Figure 4.10 Infrared spectrum of compound **4.36**.

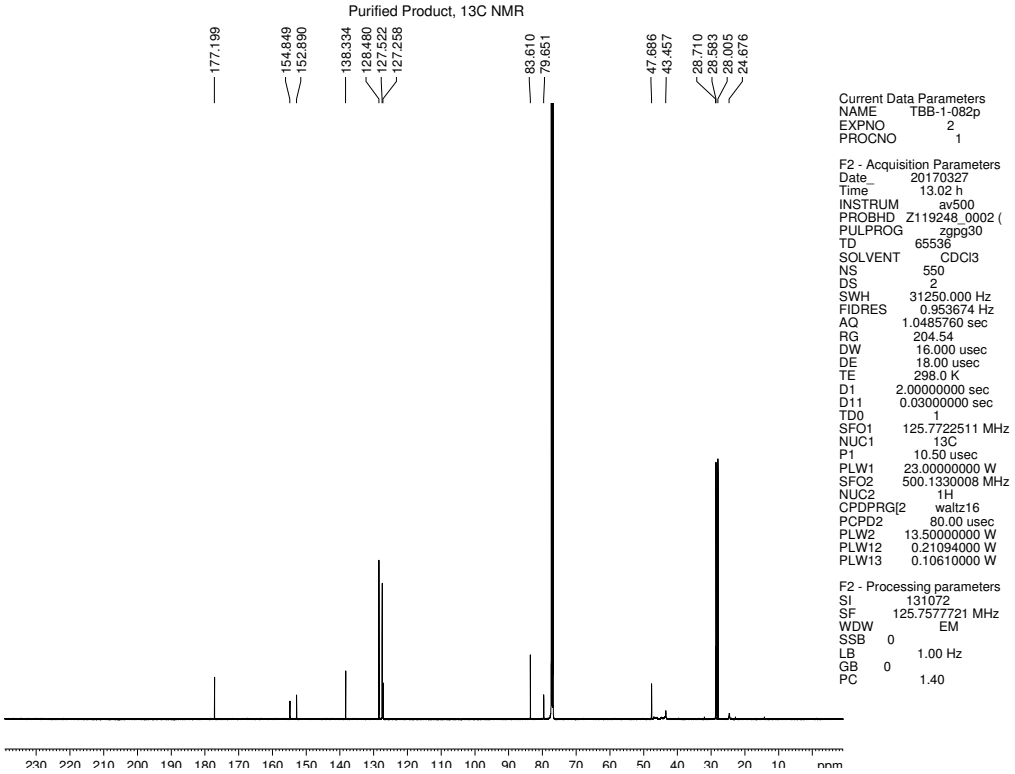

Figure 4.11 ^{13}C NMR (125 MHz, $CDCl_3$) of compound **4.36**.

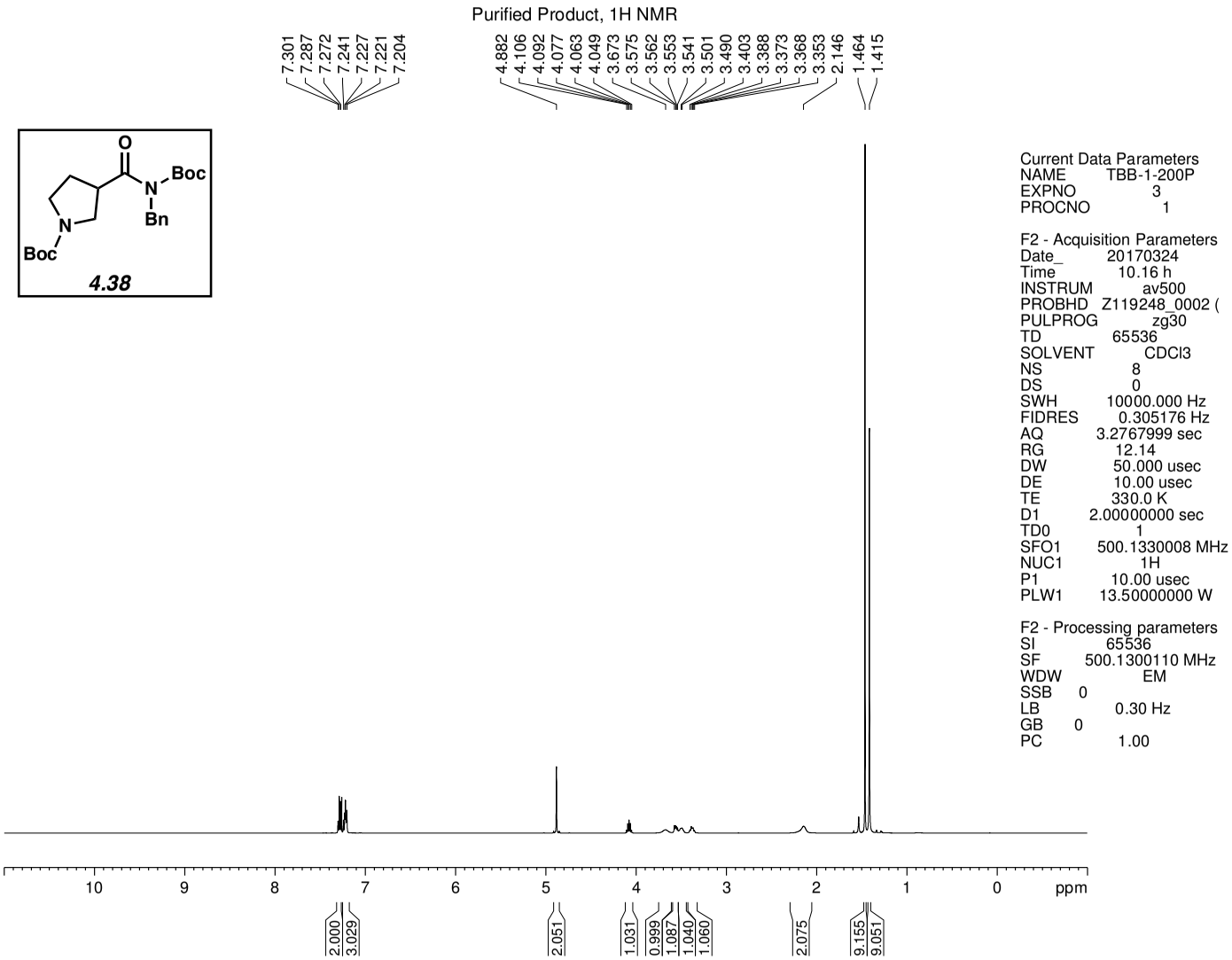

Figure 4.12 ^{1}H NMR (500 MHz, $CDCl_3$) of compound **4.38**.

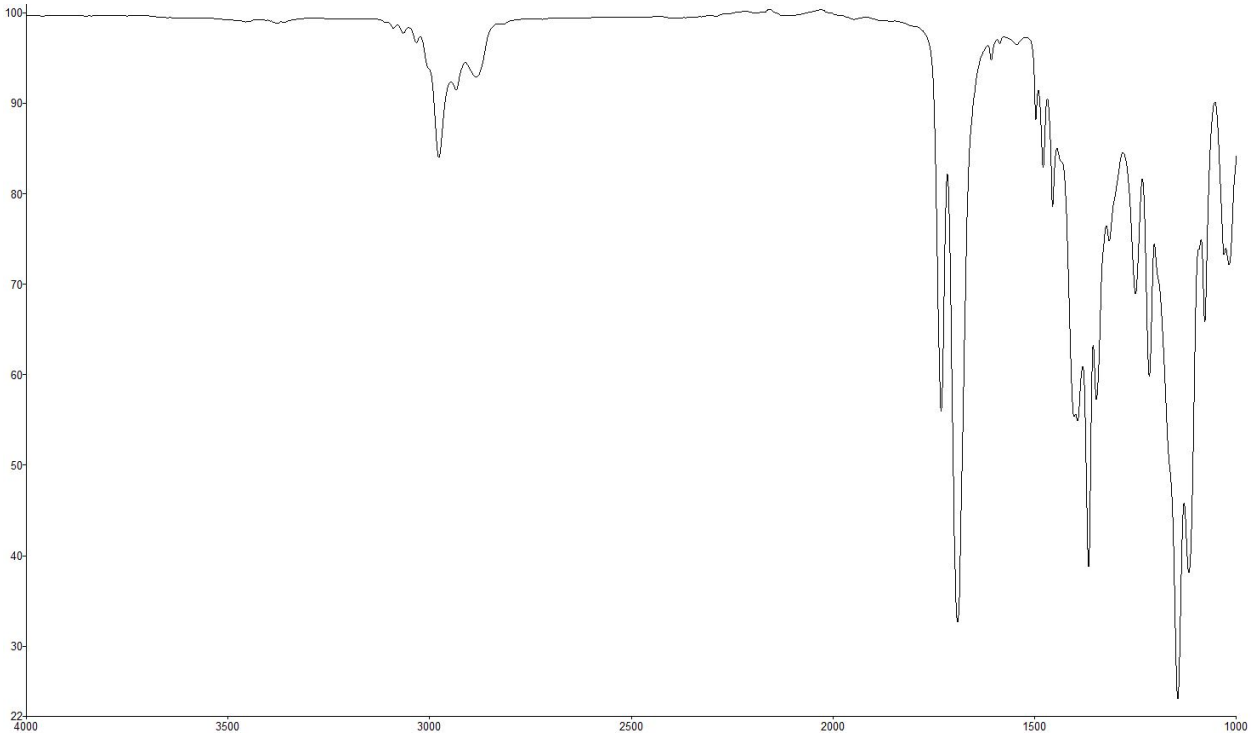

Figure 4.13 Infrared spectrum of compound **4.38**.

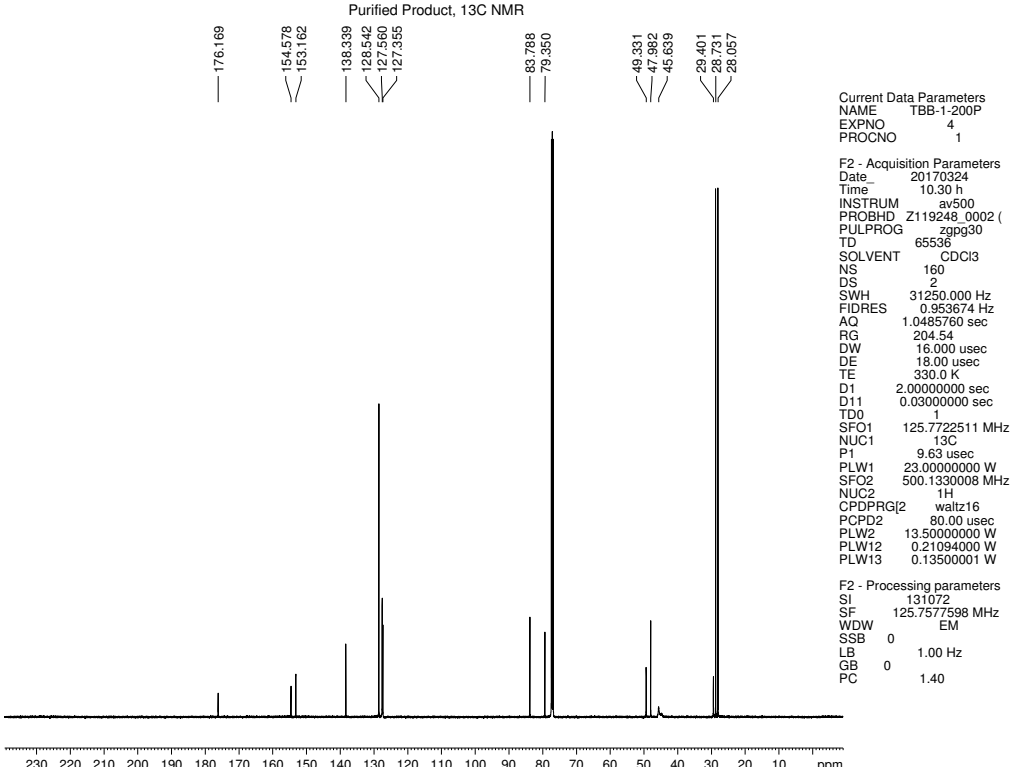

Figure 4.14 ^{13}C NMR (125 MHz, $CDCl_3$) of compound **4.38**.

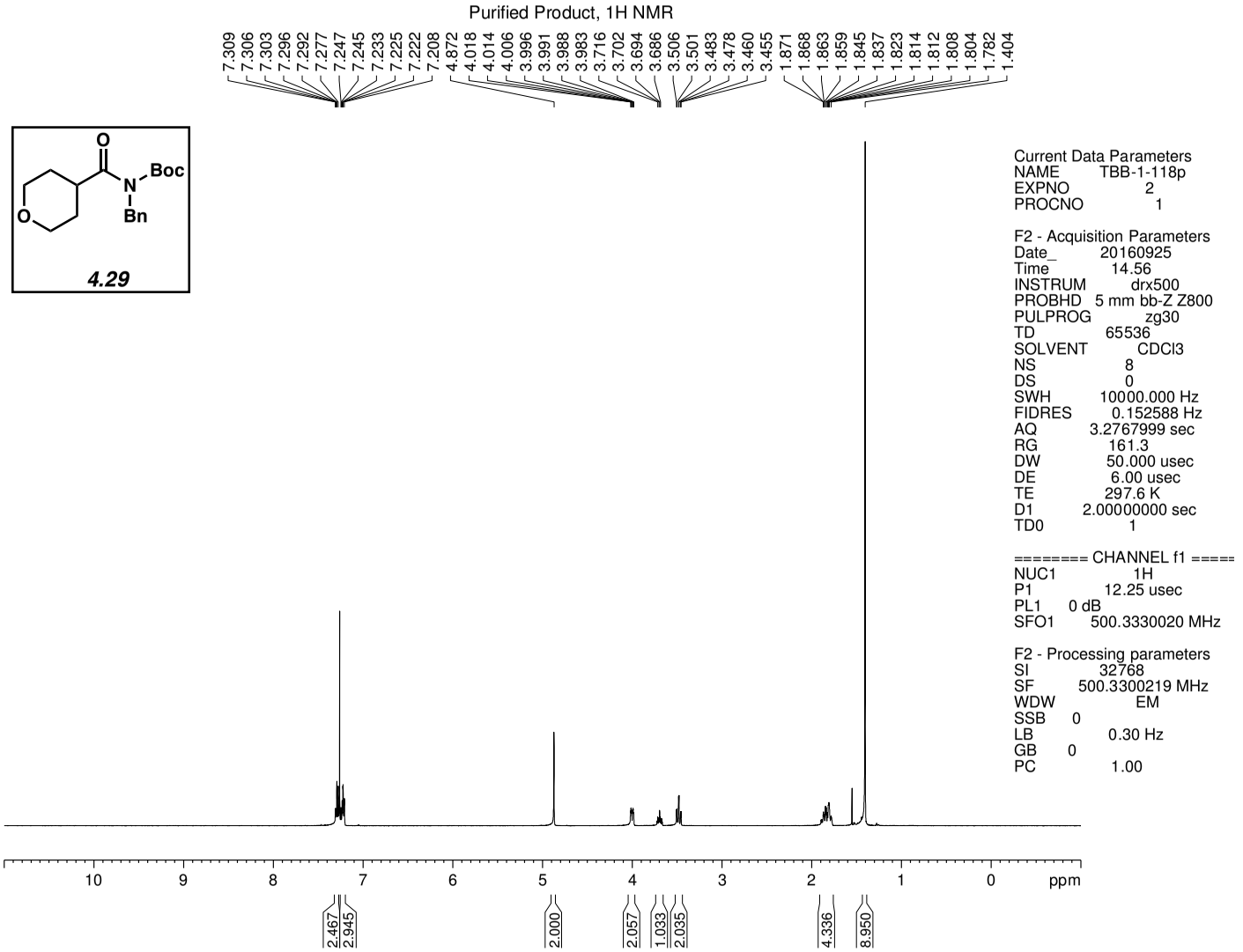

Figure 4.15 ^{1}H NMR (500 MHz, $CDCl_3$) of compound **4.29**.

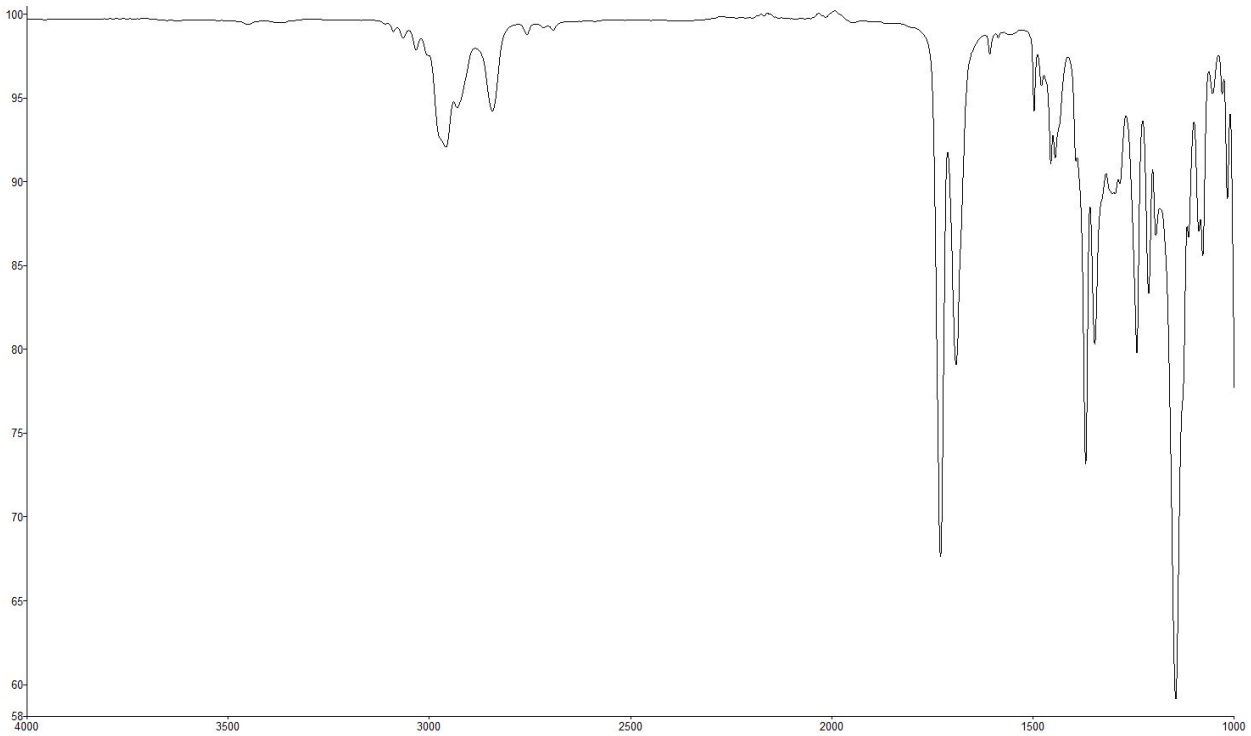

Figure 4.16 Infrared spectrum of compound **4.29**.

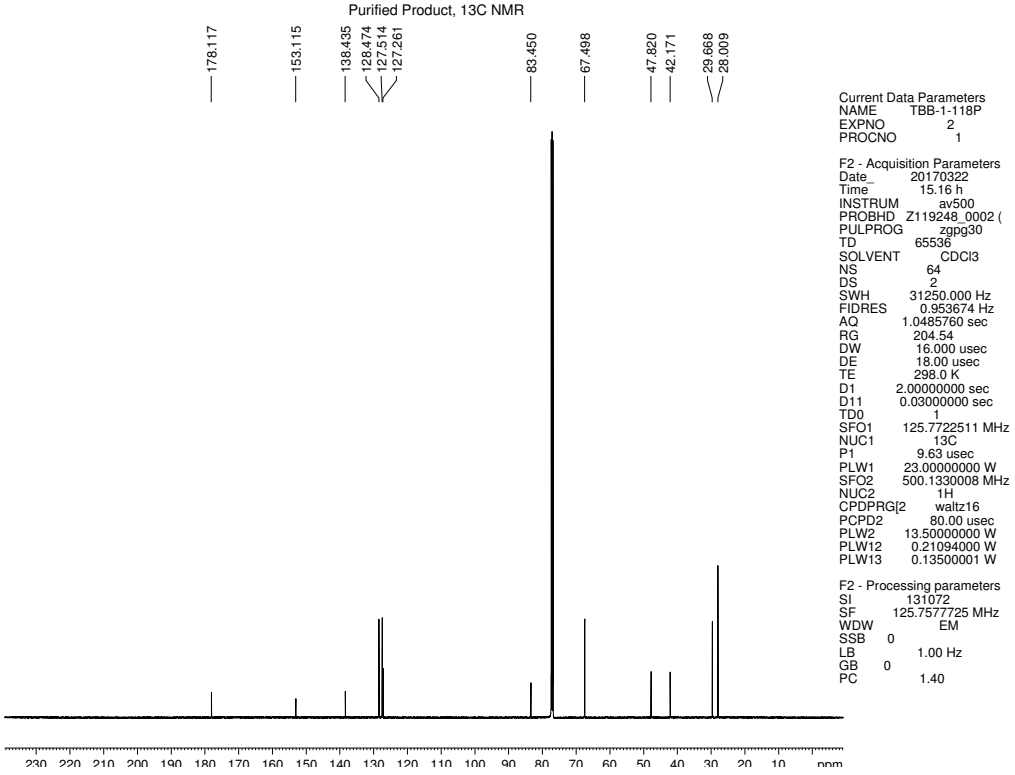

Figure 4.17 ^{13}C NMR (125 MHz, $CDCl_3$) of compound **4.29**.

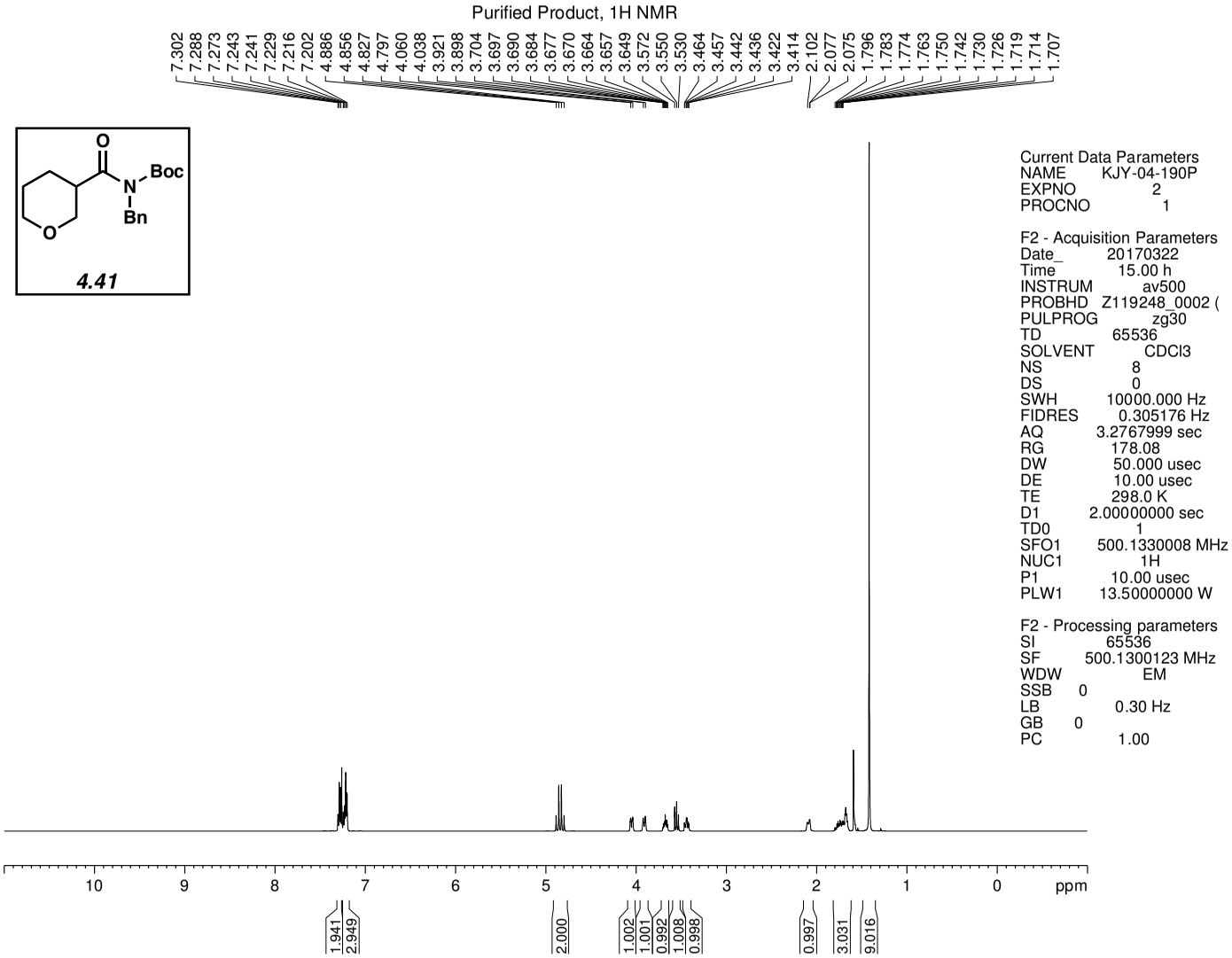

Figure 4.18 ^{1}H NMR (500 MHz, $CDCl_3$) of compound **4.41**.

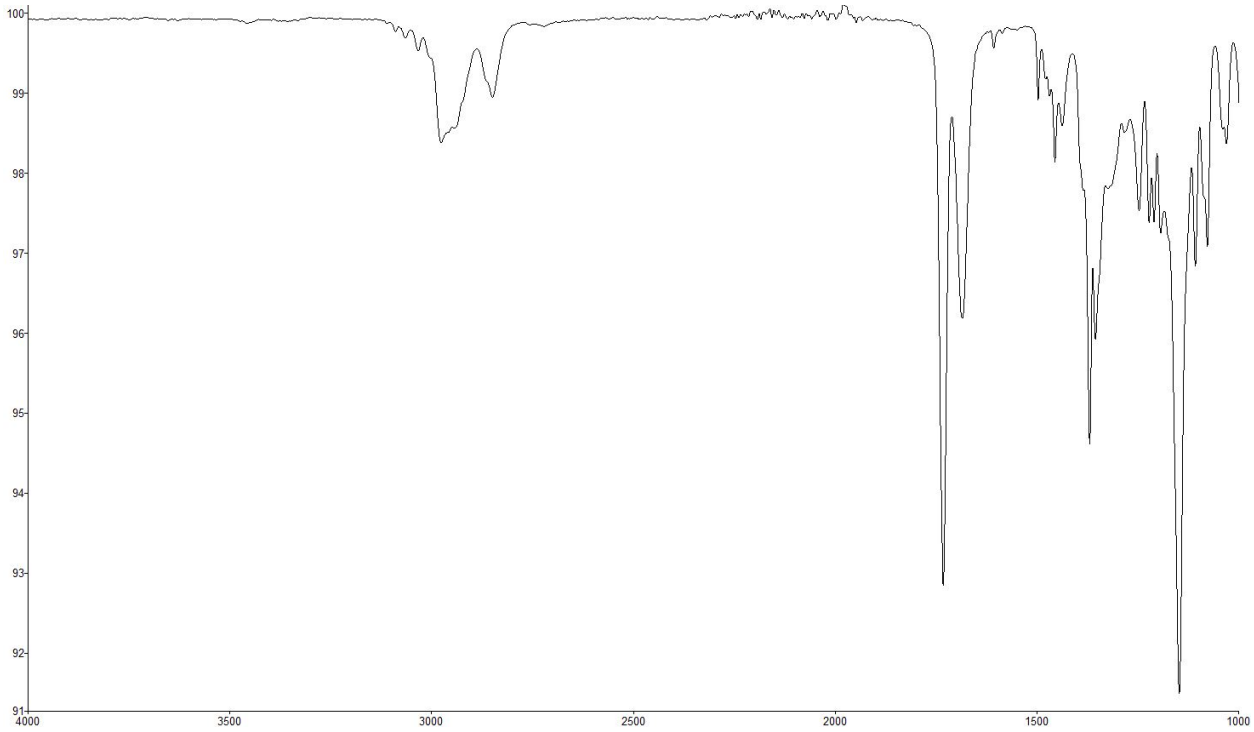

Figure 4.19 Infrared spectrum of compound **4.41**.

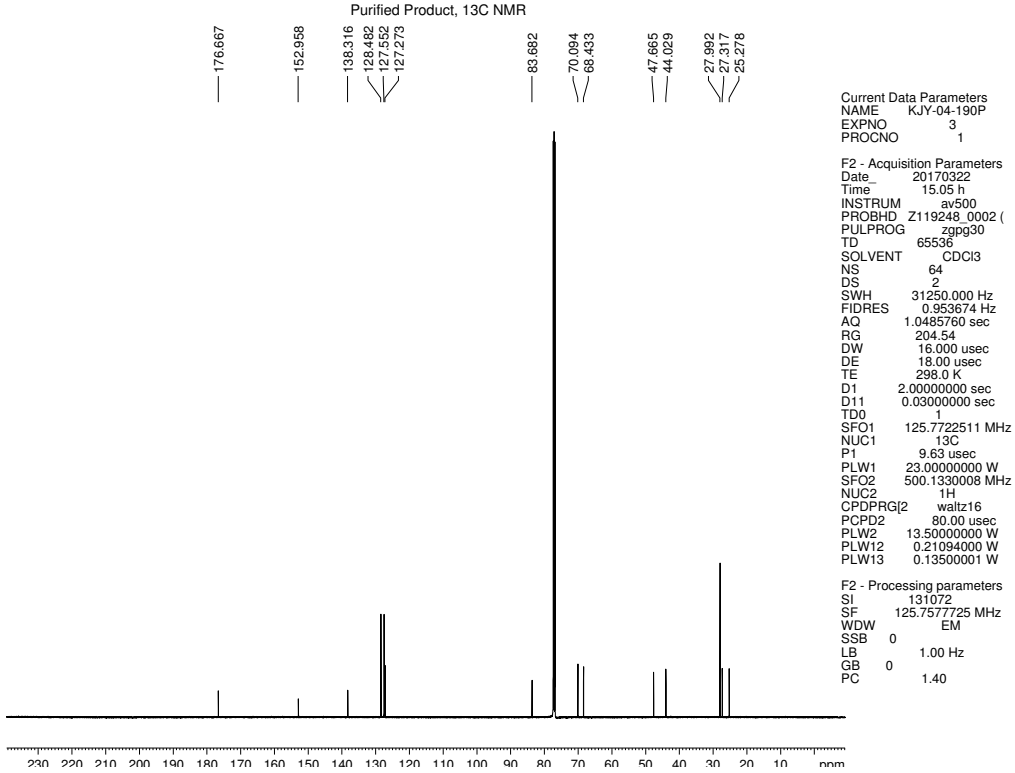

Figure 4.20 ^{13}C NMR (125 MHz, $CDCl_3$) of compound **4.41**.

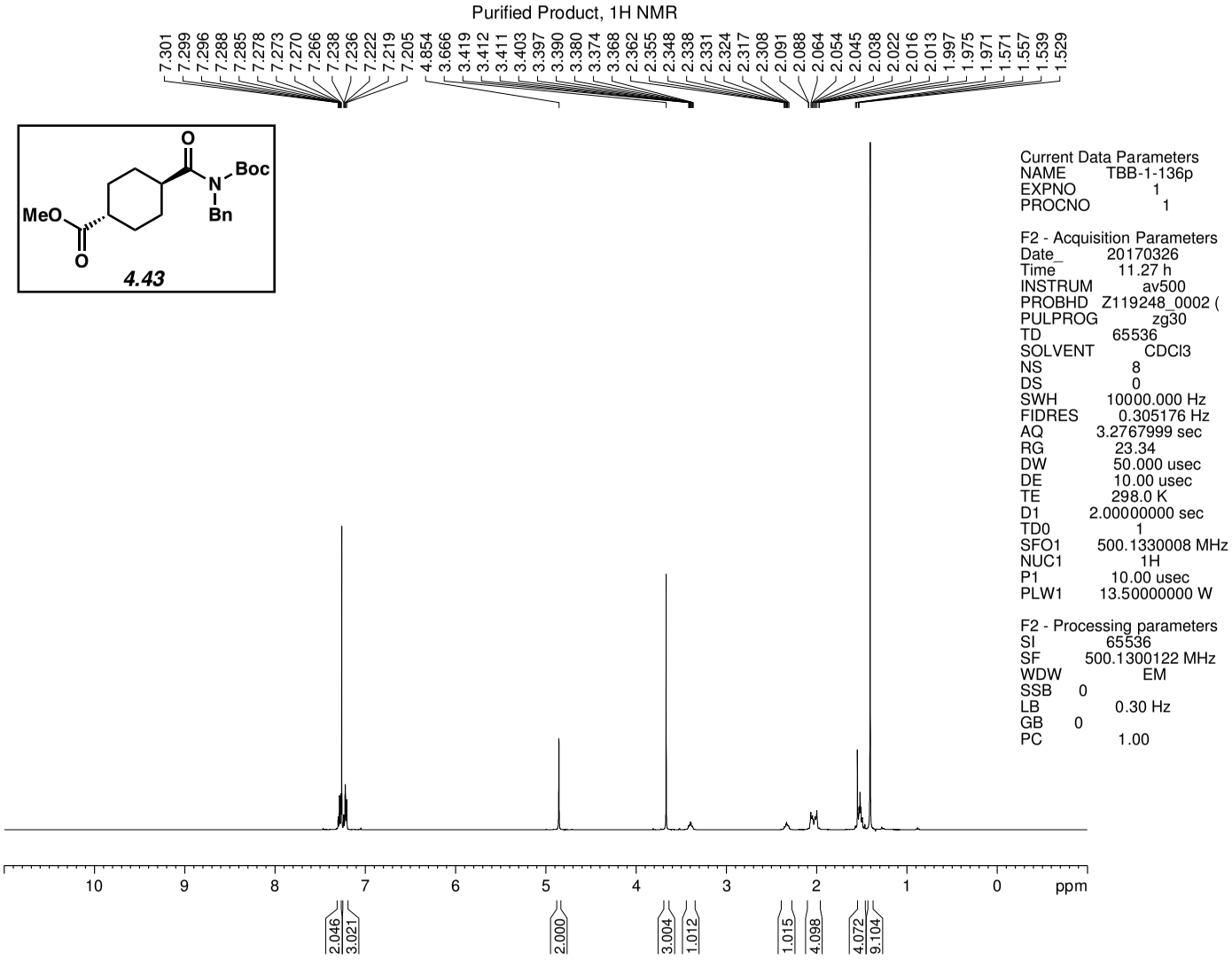

Figure 4.21 ^{1}H NMR (500 MHz, $CDCl_3$) of compound **4.43**.

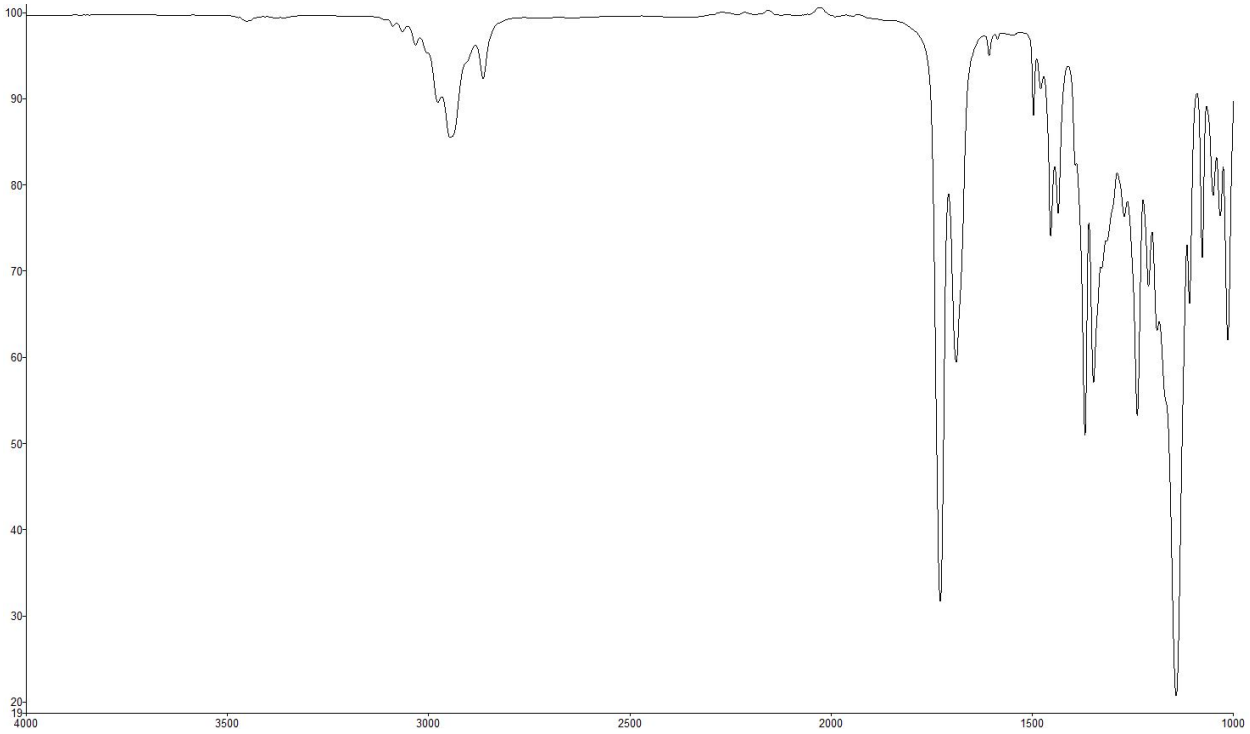

Figure 4.22 Infrared spectrum of compound **4.43**.

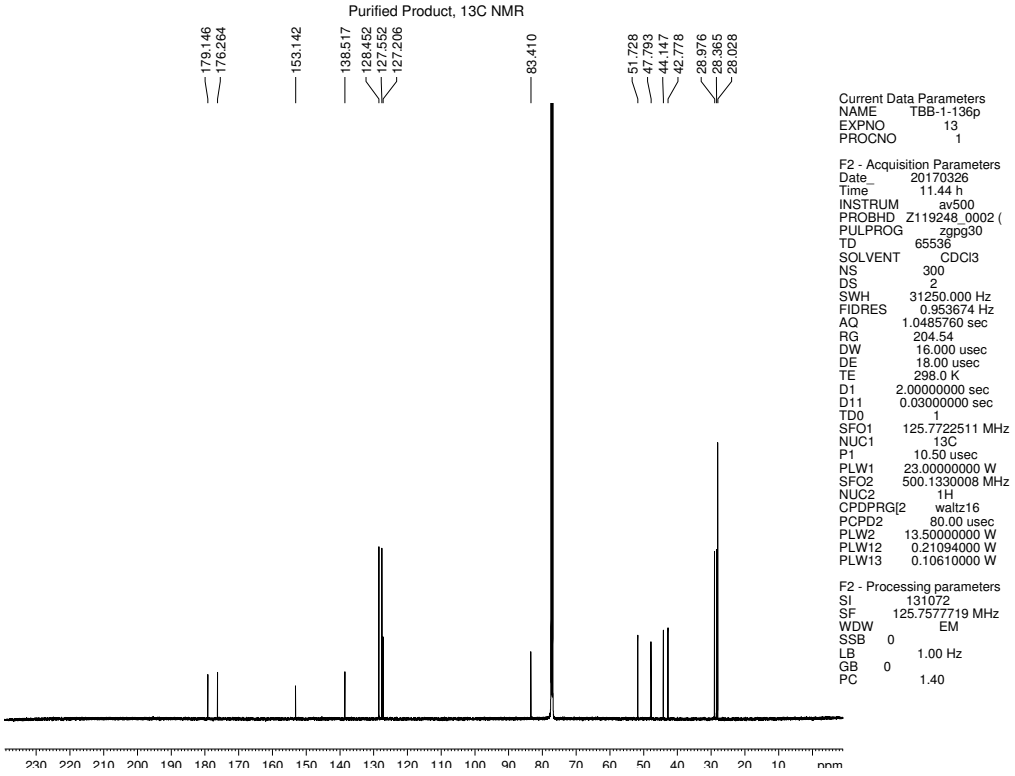

Figure 4.23 ^{13}C NMR (125 MHz, $CDCl_3$) of compound **4.43**.

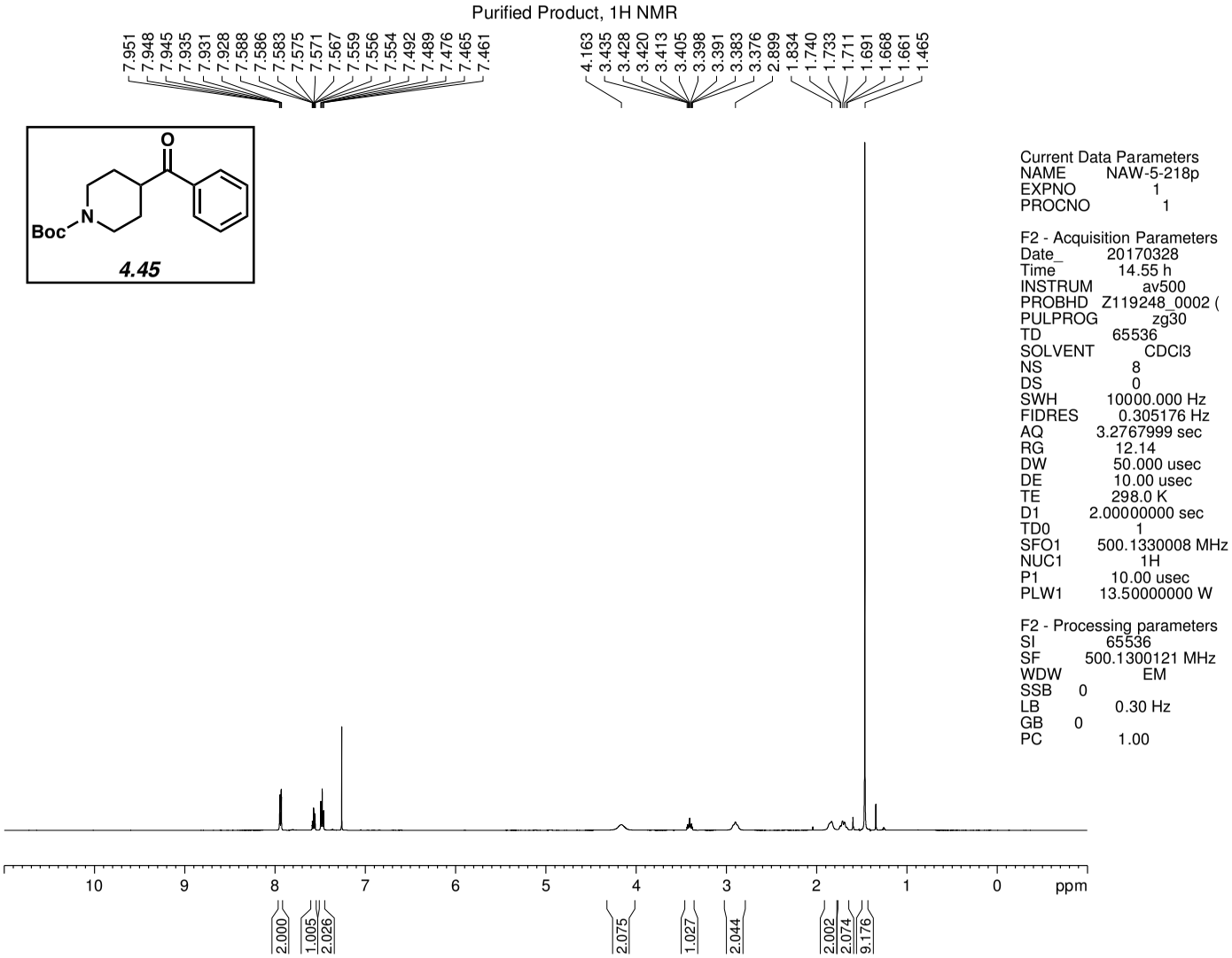

Figure 4.24 ^{1}H NMR (500 MHz, $CDCl_3$) of compound **4.45**.

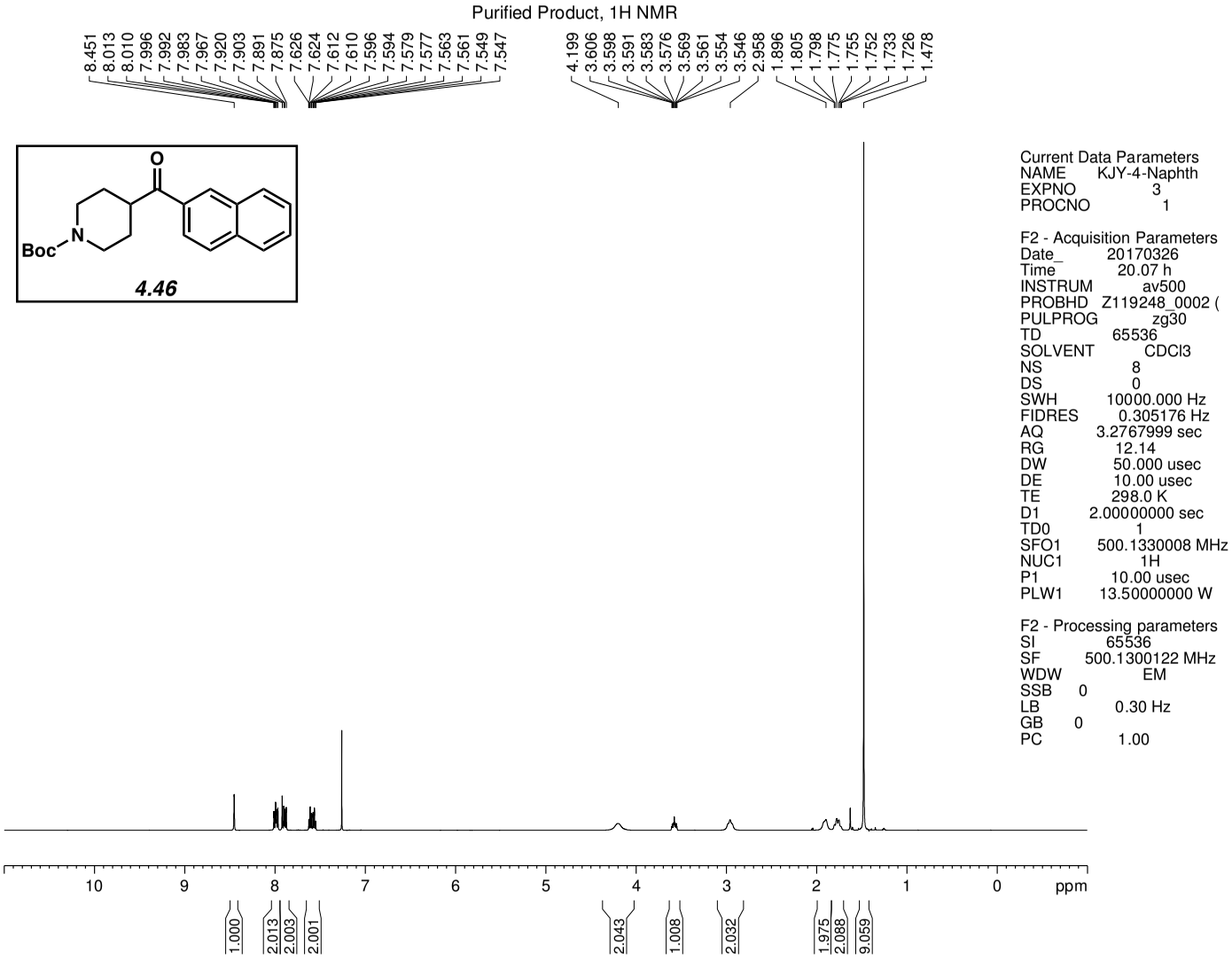

Figure 4.25 ^{1}H NMR (500 MHz, $CDCl_3$) of compound **4.46**.

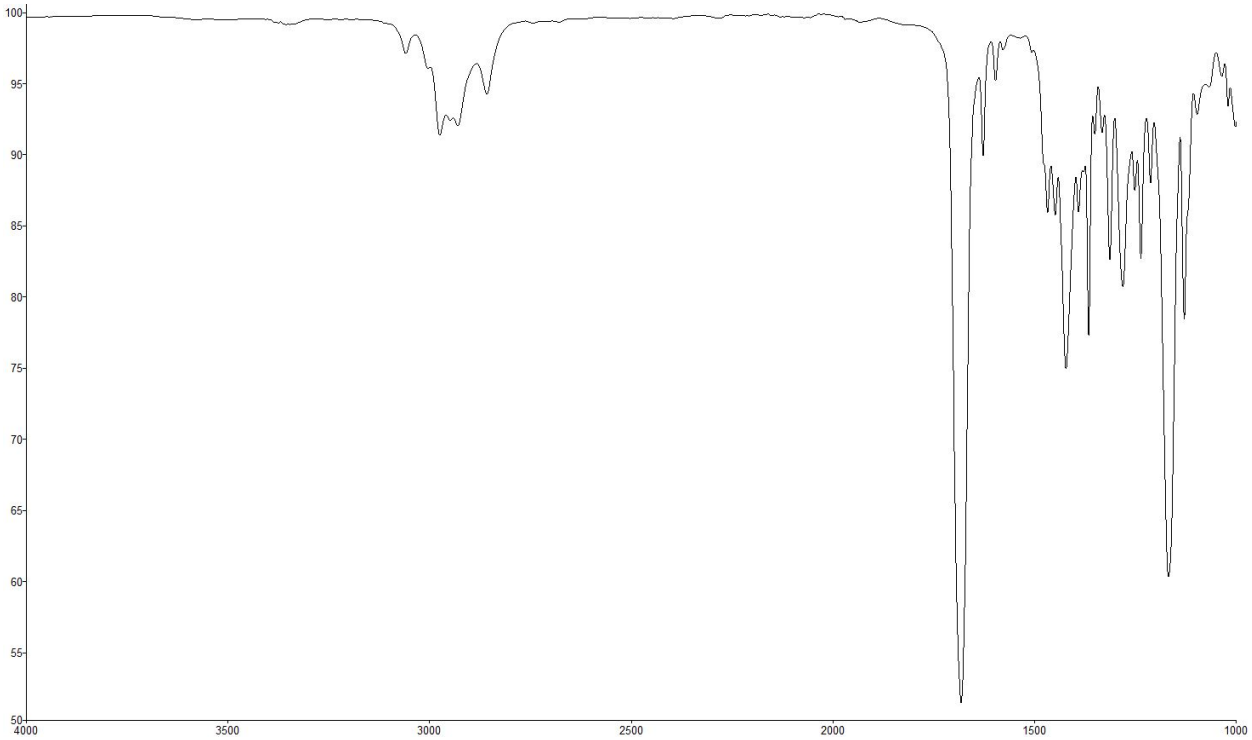

Figure 4.26 Infrared spectrum of compound **4.46**.

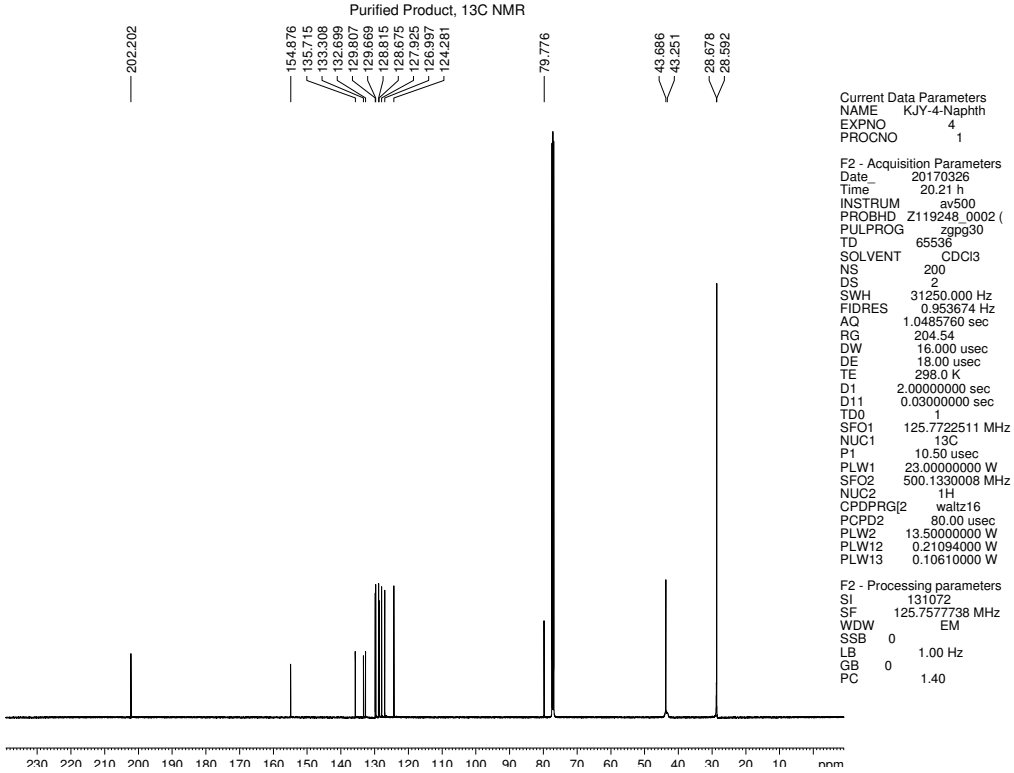

Figure 4.27 ^{13}C NMR (125 MHz, $CDCl_3$) of compound **4.46**.

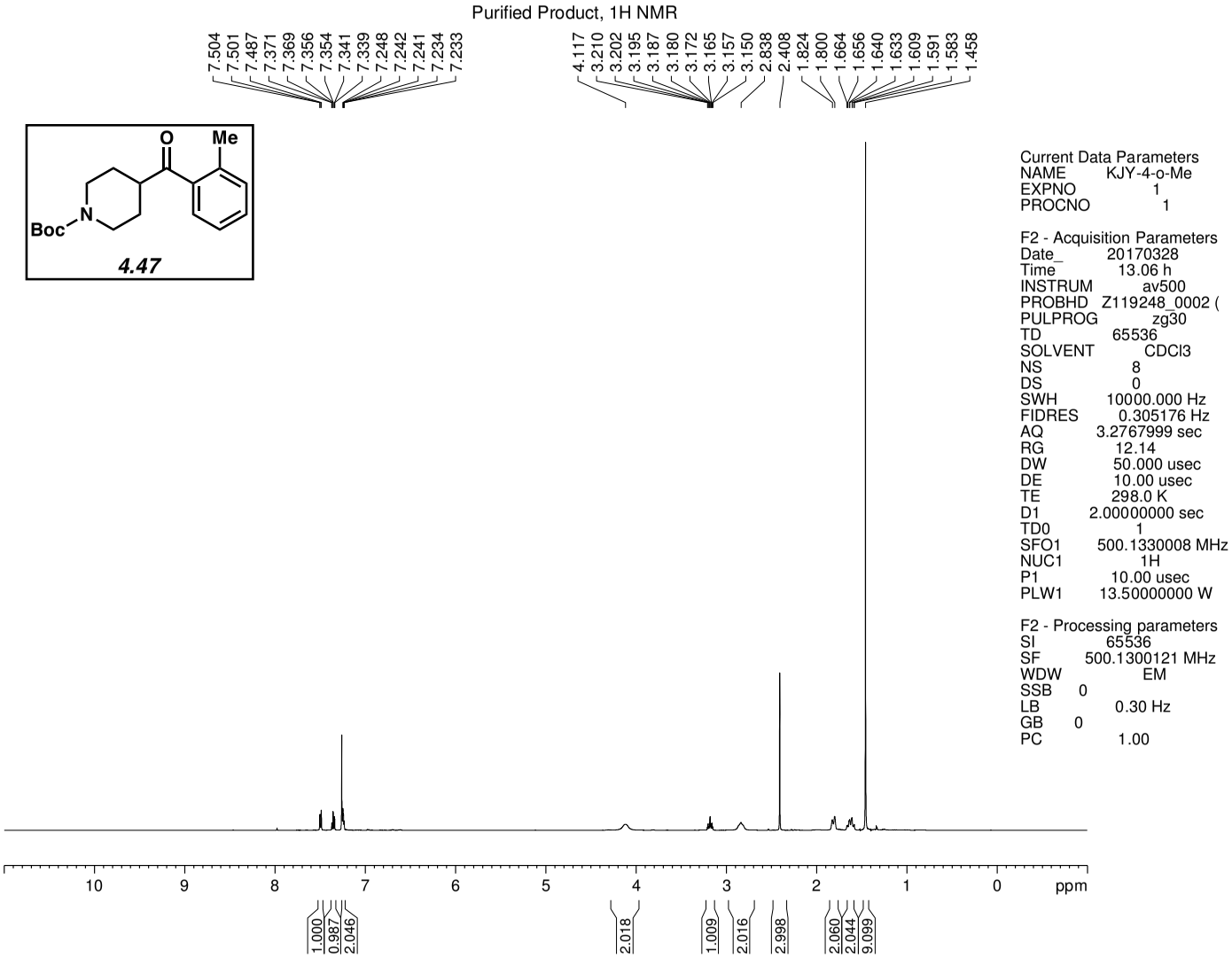

Figure 4.28 ^{1}H NMR (500 MHz, $CDCl_3$) of compound **4.47**.

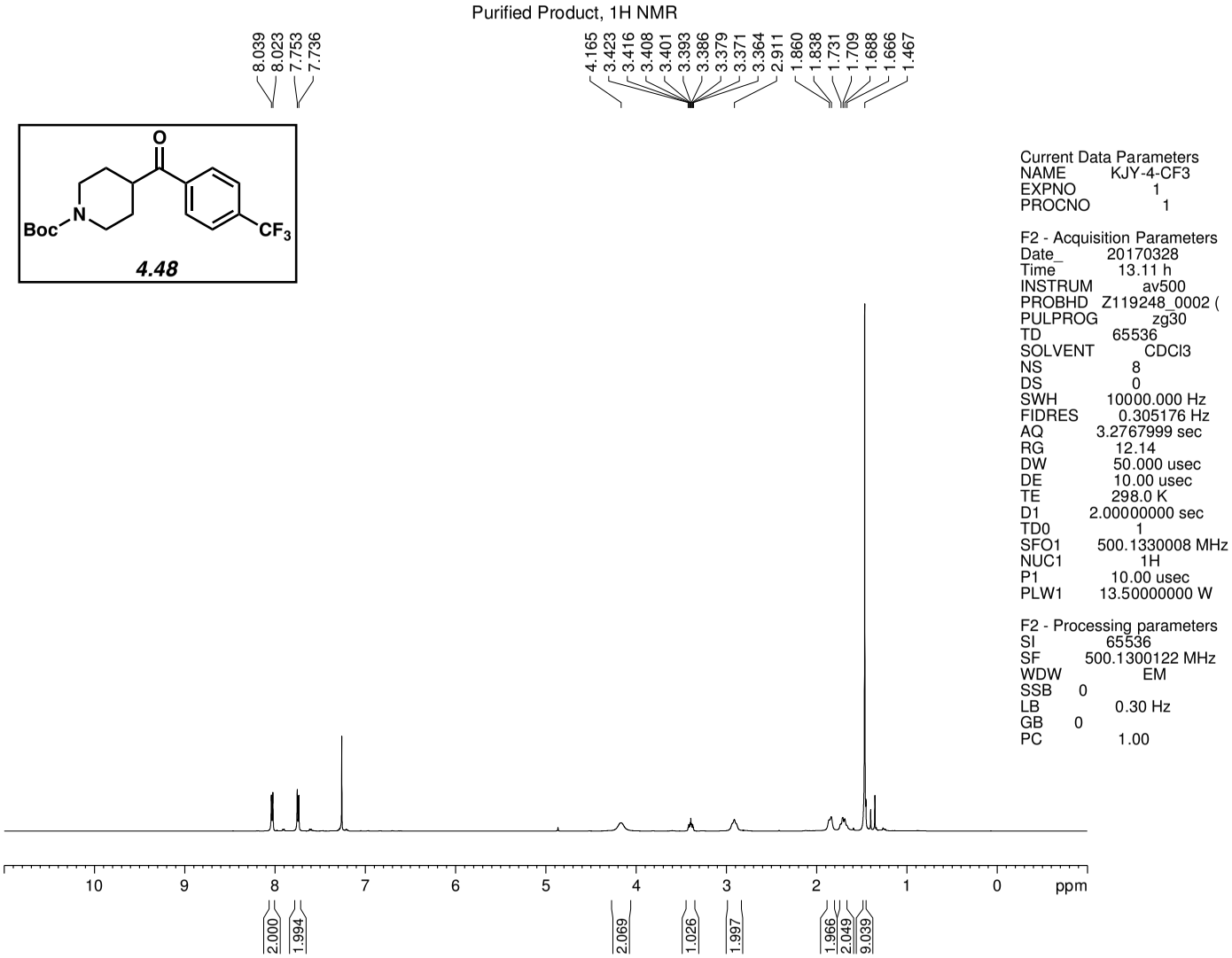

Figure 4.29 ^{1}H NMR (500 MHz, $CDCl_3$) of compound **4.48**.

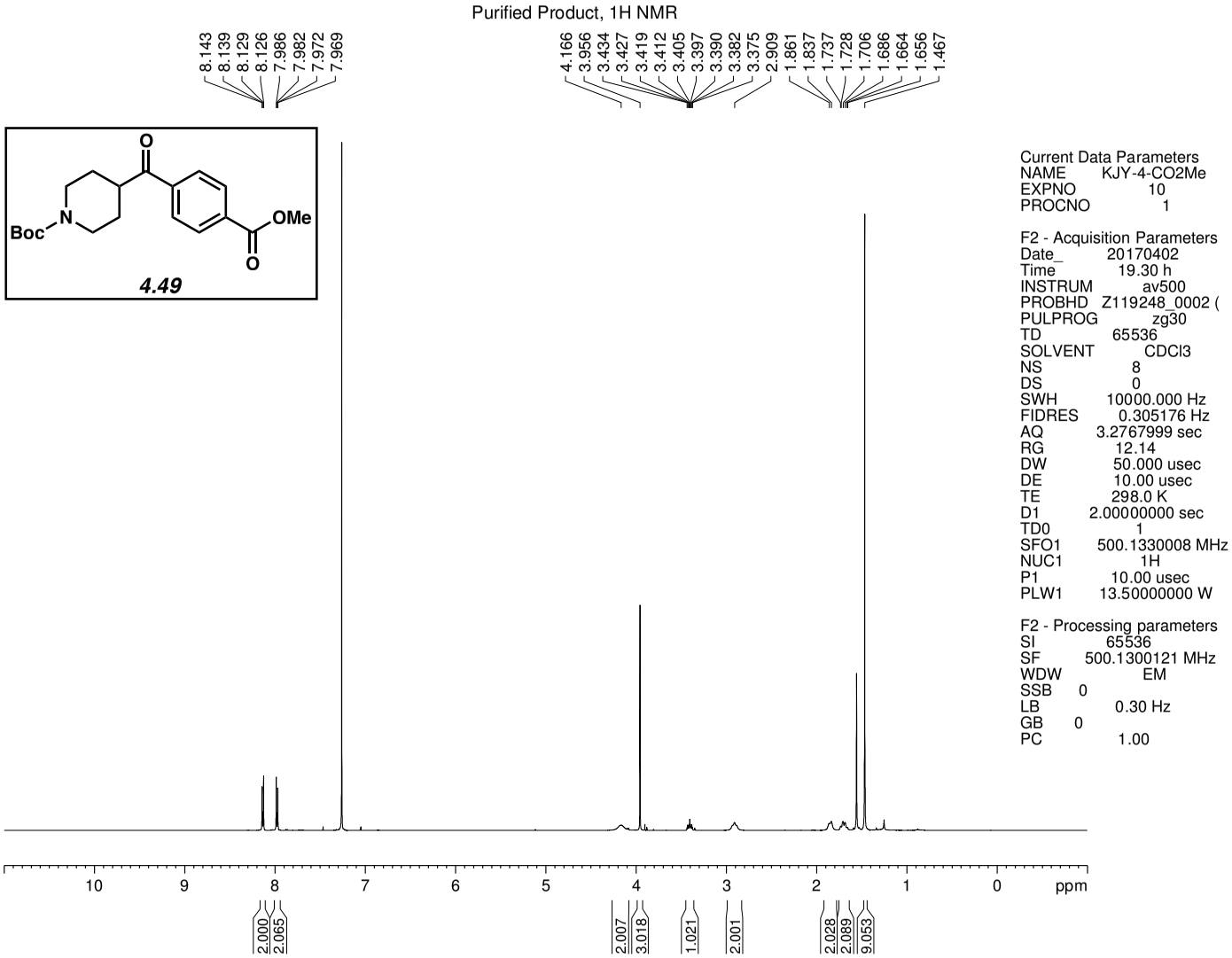

Figure 4.30 ^{1}H NMR (500 MHz, $CDCl_3$) of compound **4.49**.

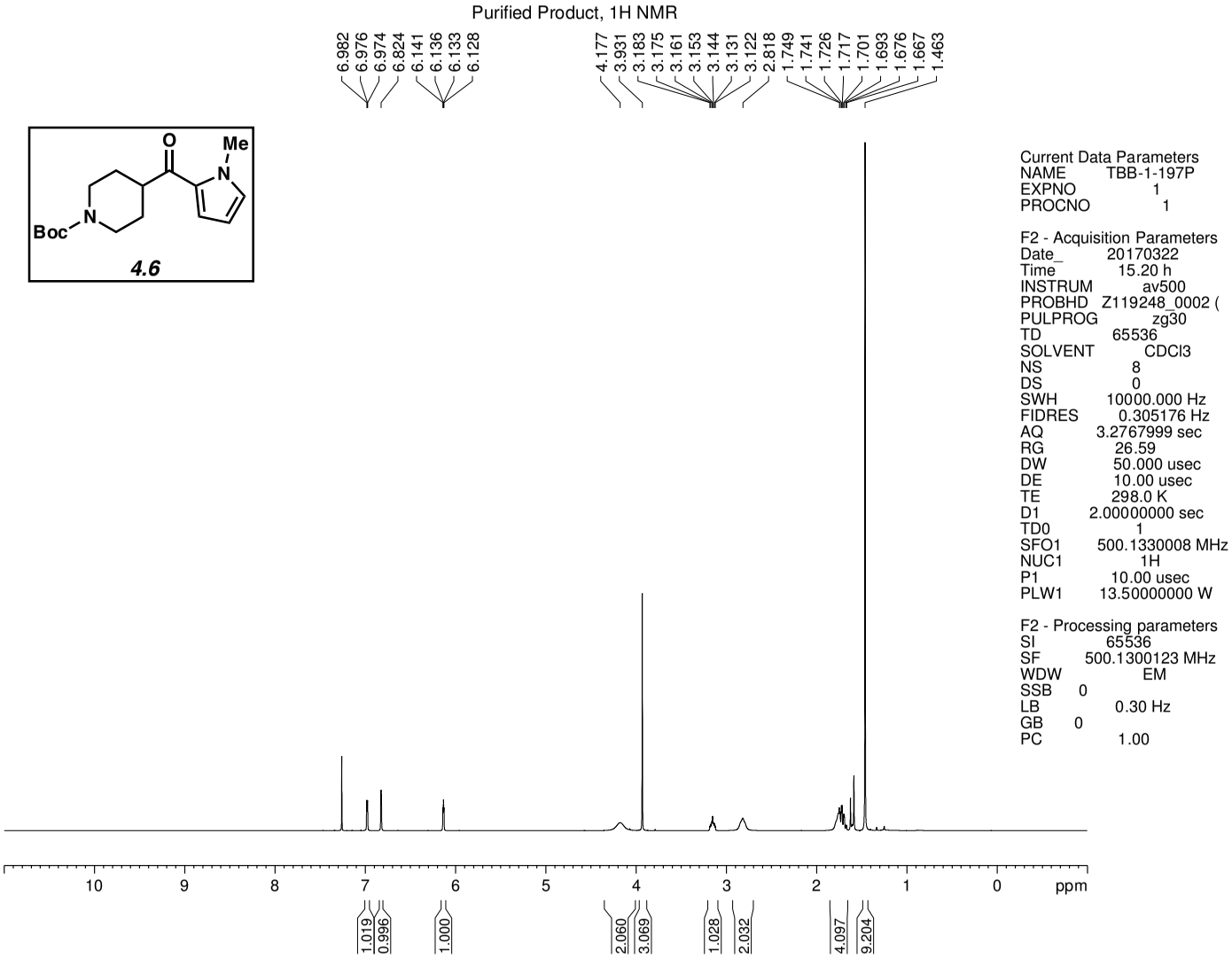

Figure 4.31 ^{1}H NMR (500 MHz, $CDCl_3$) of compound **4.6**.

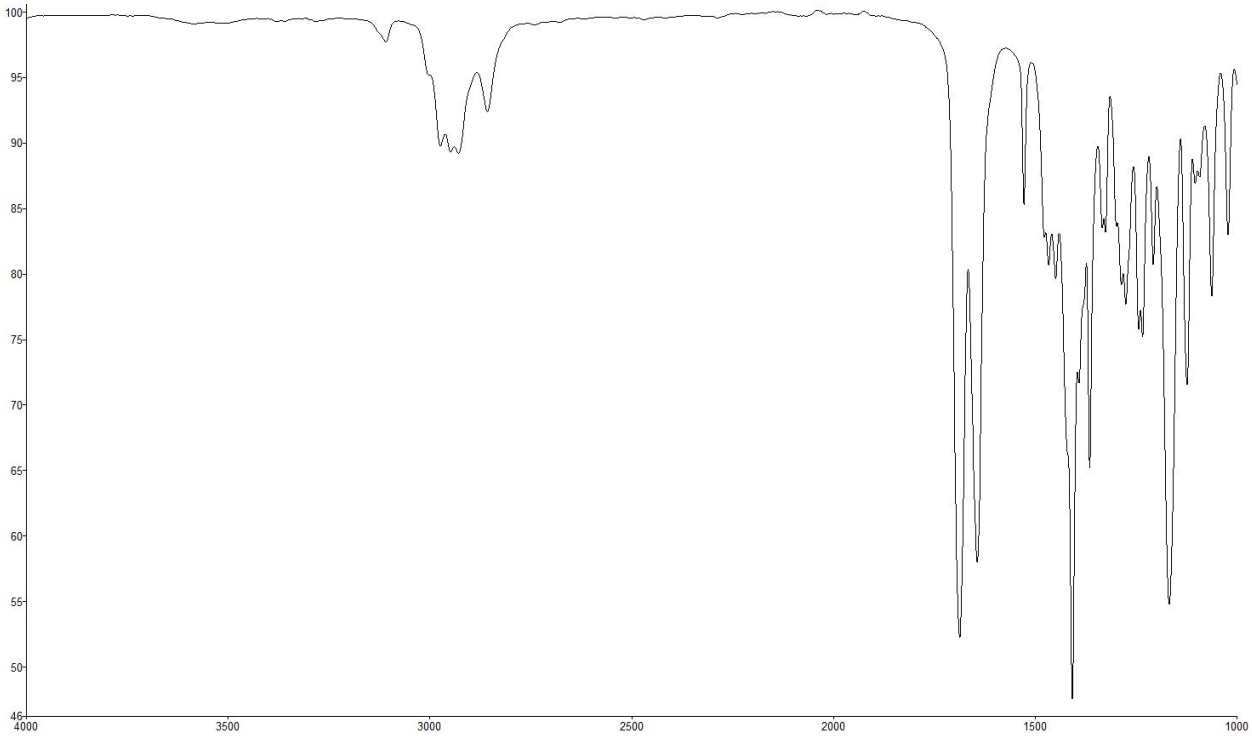

Figure 4.32 Infrared spectrum of compound **4.6**.

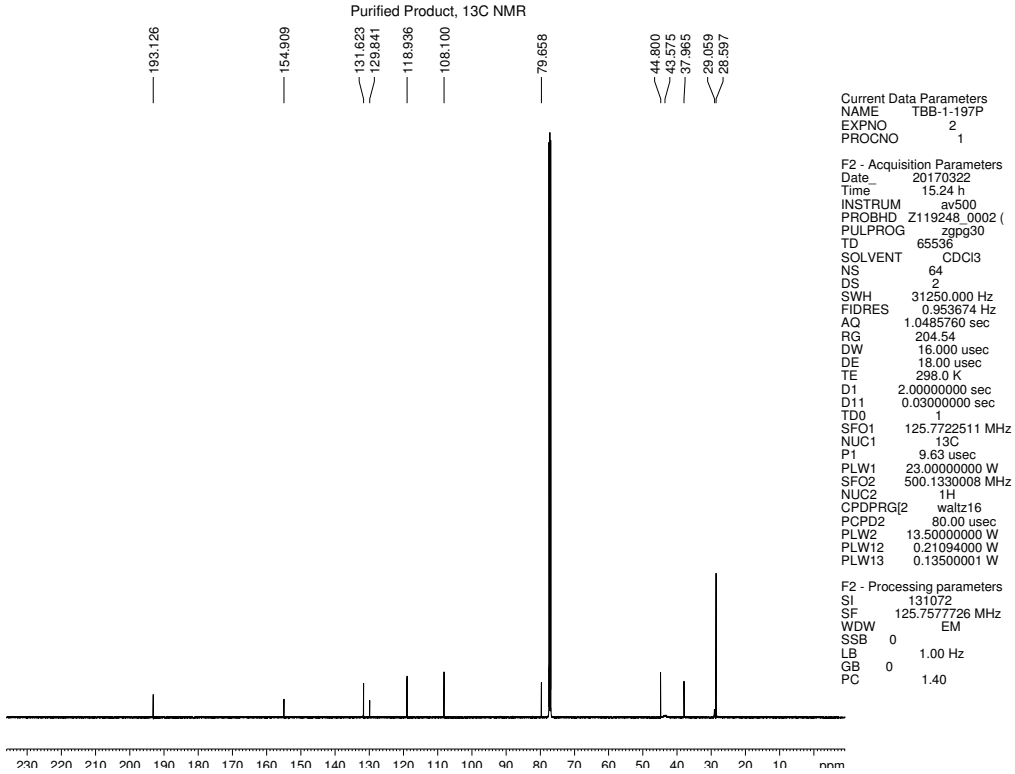

Figure 4.33 ^{13}C NMR (125 MHz, $CDCl_3$) of compound **4.6**.

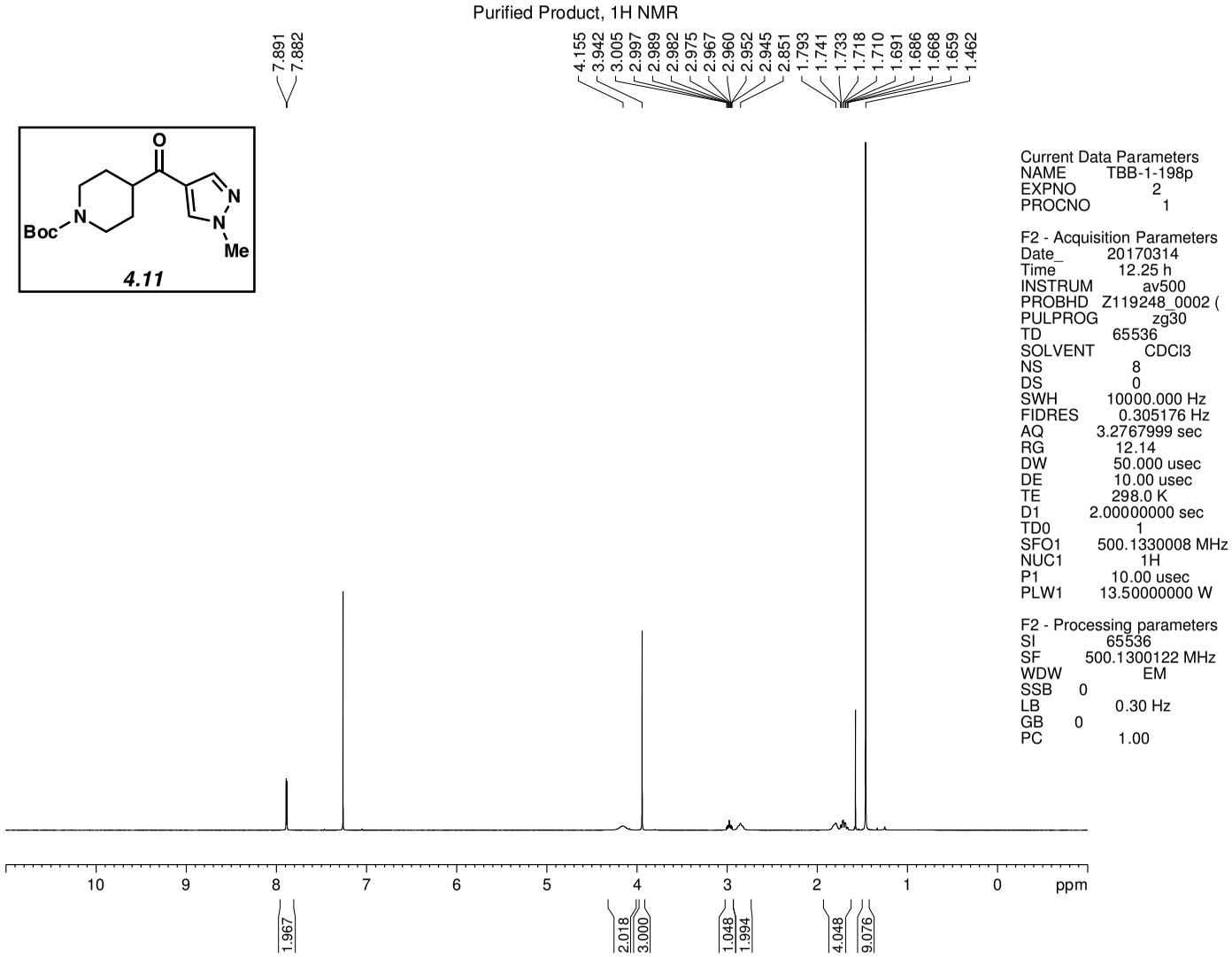

Figure 4.34 ^{1}H NMR (500 MHz, $CDCl_3$) of compound **4.11**.

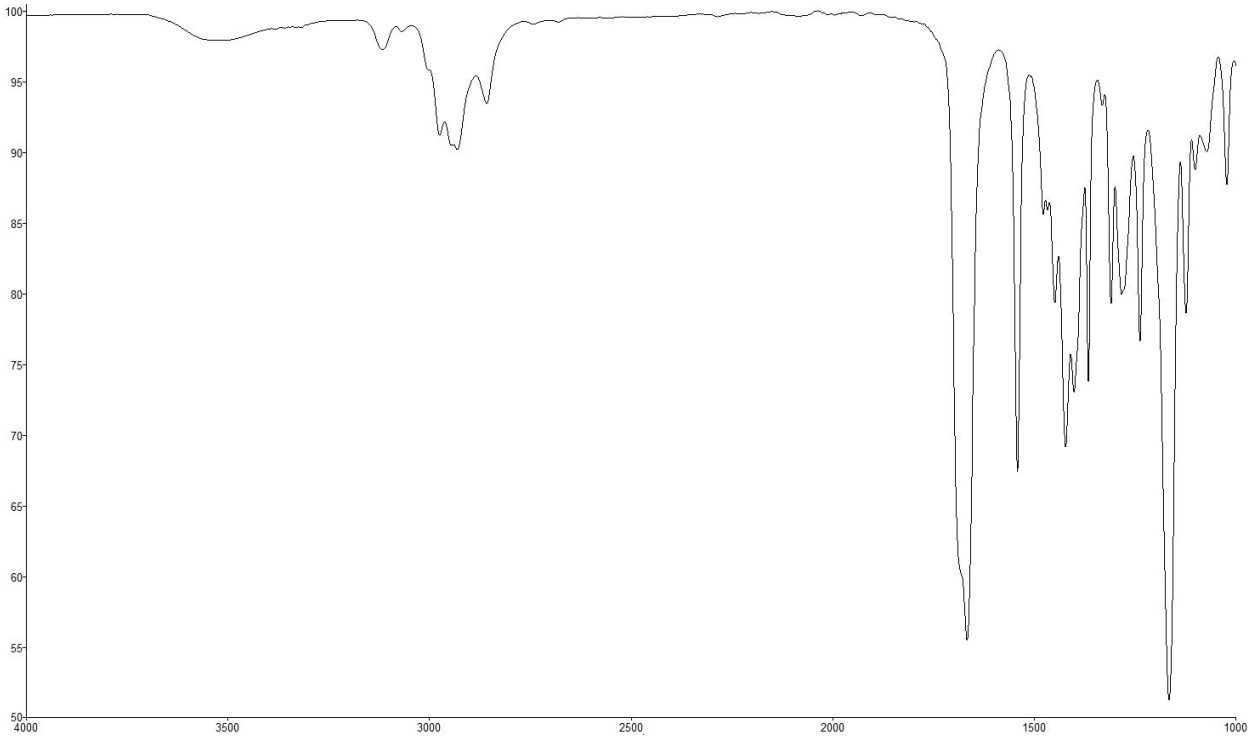

Figure 4.35 Infrared spectrum of compound **4.11**.

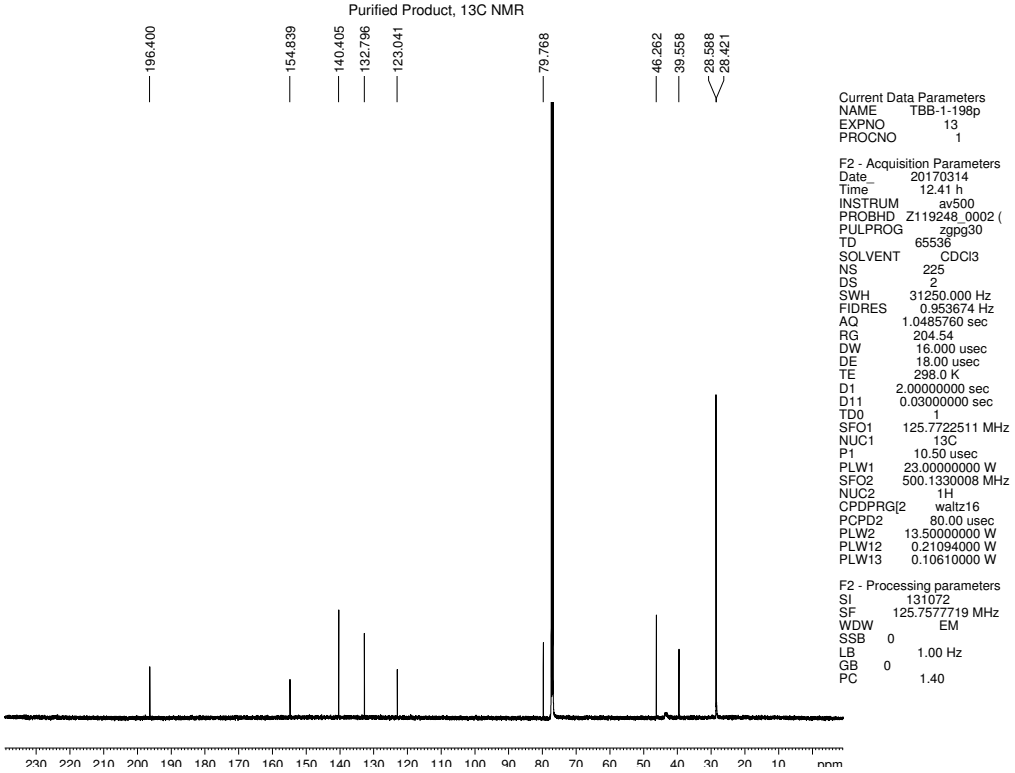

Figure 4.36 ^{13}C NMR (125 MHz, $CDCl_3$) of compound **4.11**.

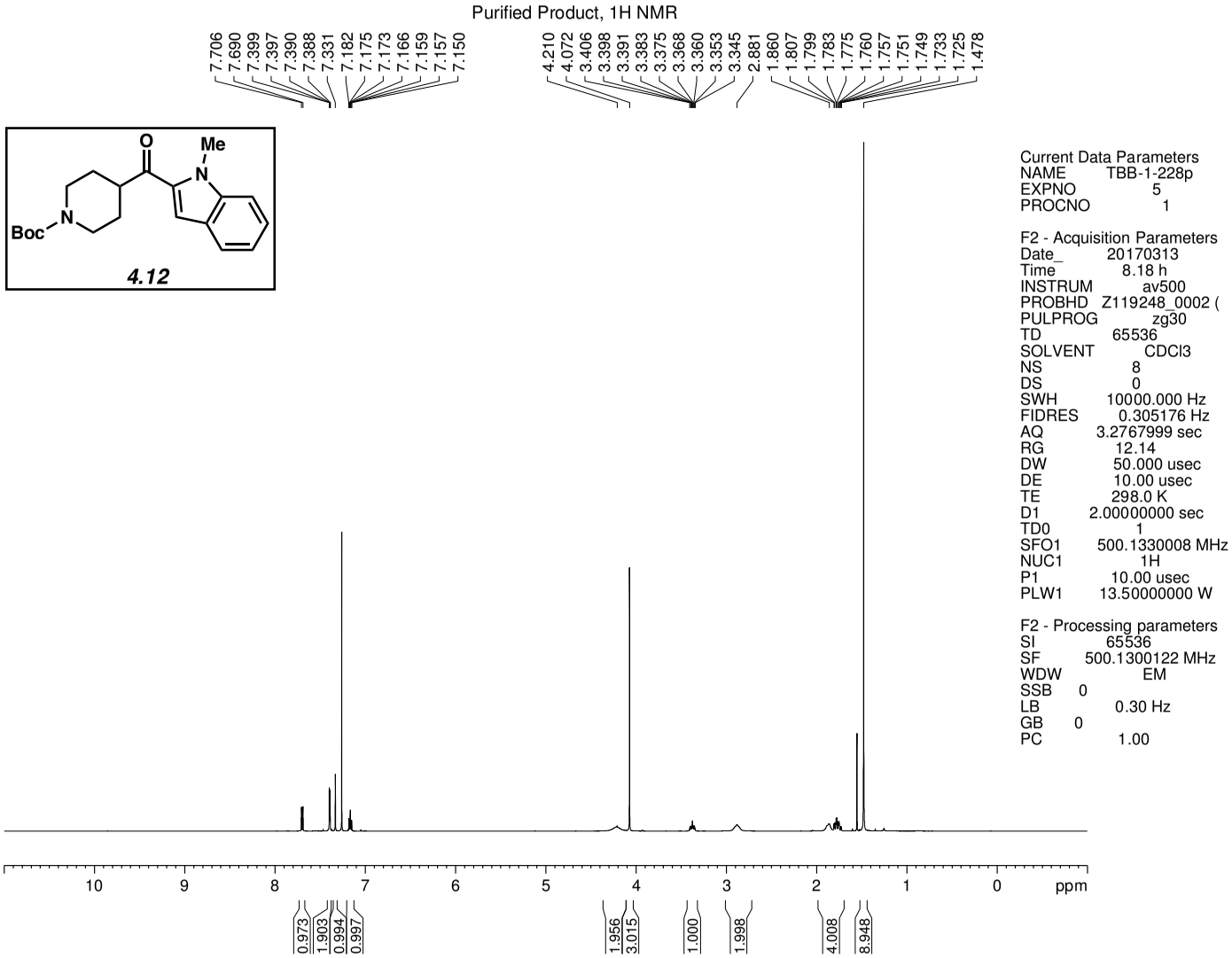

Figure 4.37 ^{1}H NMR (500 MHz, $CDCl_3$) of compound **4.12**.

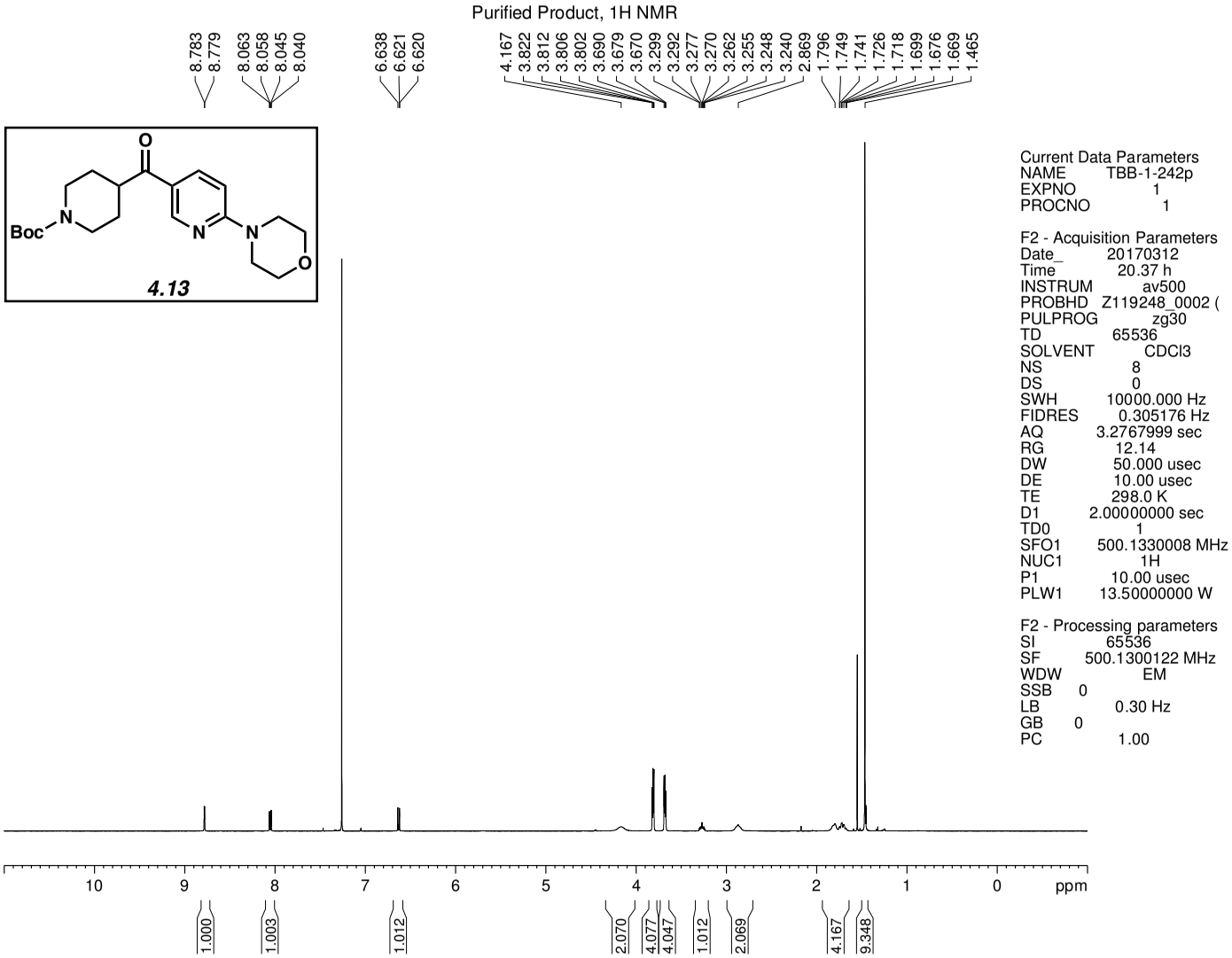

Figure 4.38 ^{1}H NMR (500 MHz, $CDCl_3$) of compound **4.13**.

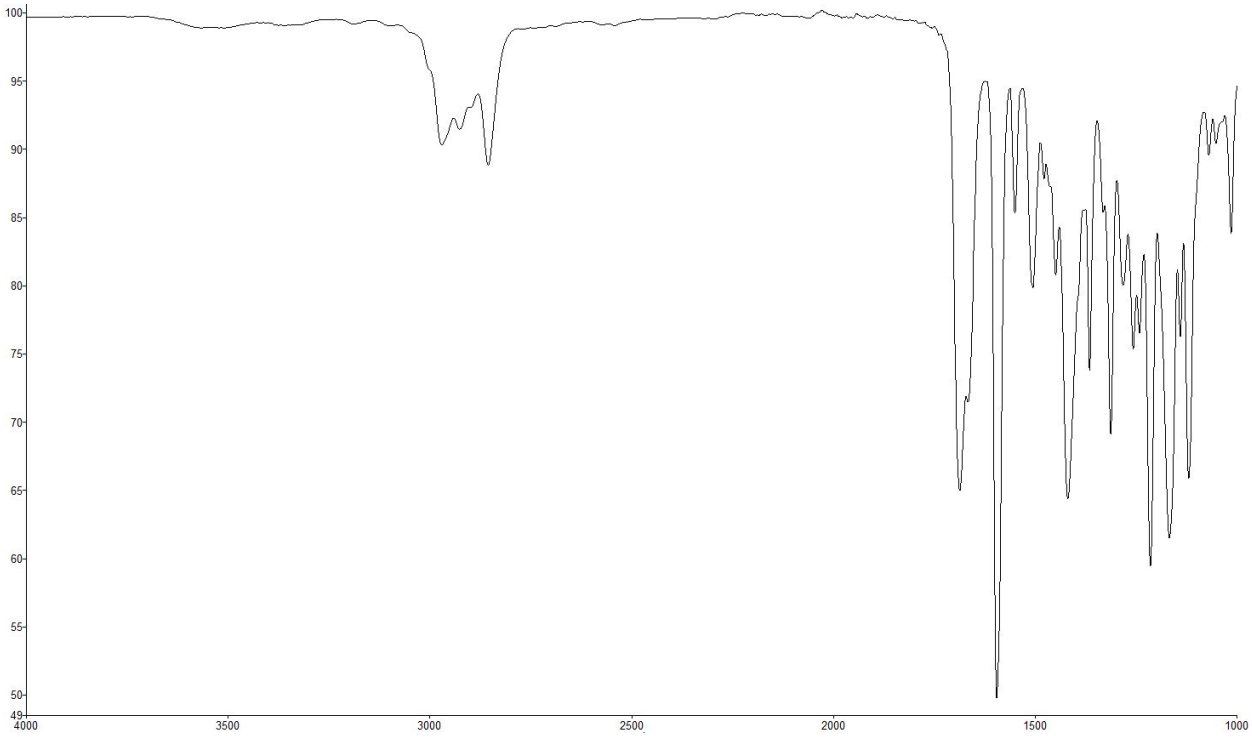

Figure 4.39 Infrared spectrum of compound **4.13**.

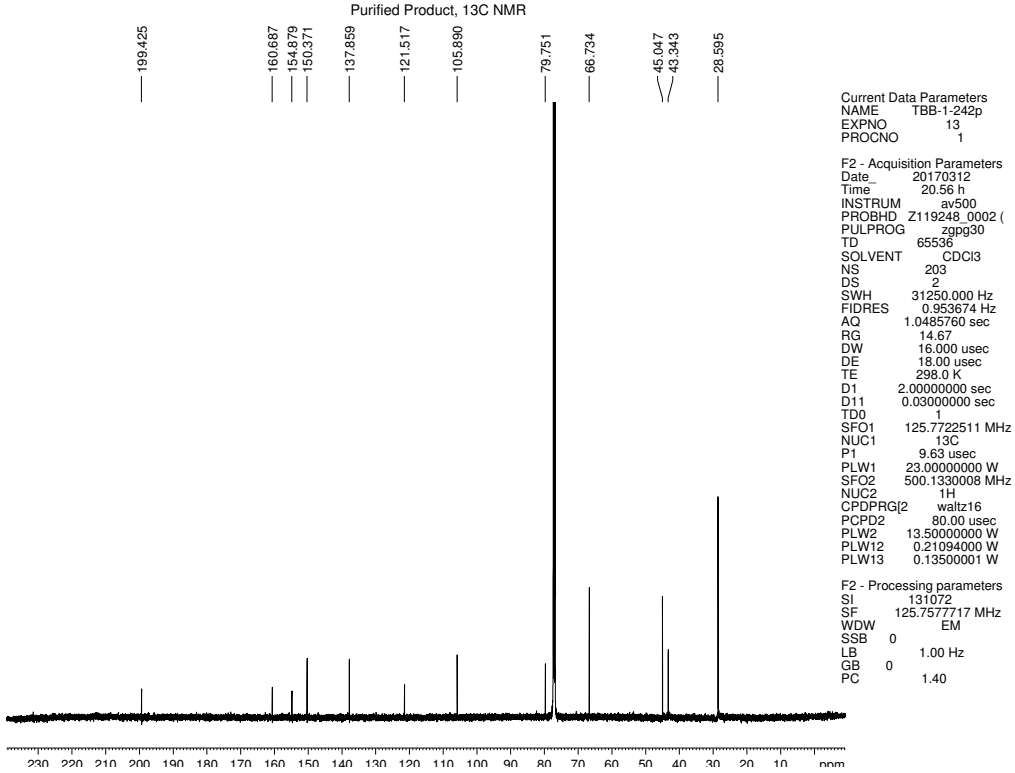

Figure 4.40 ^{13}C NMR (125 MHz, $CDCl_3$) of compound **4.13**.

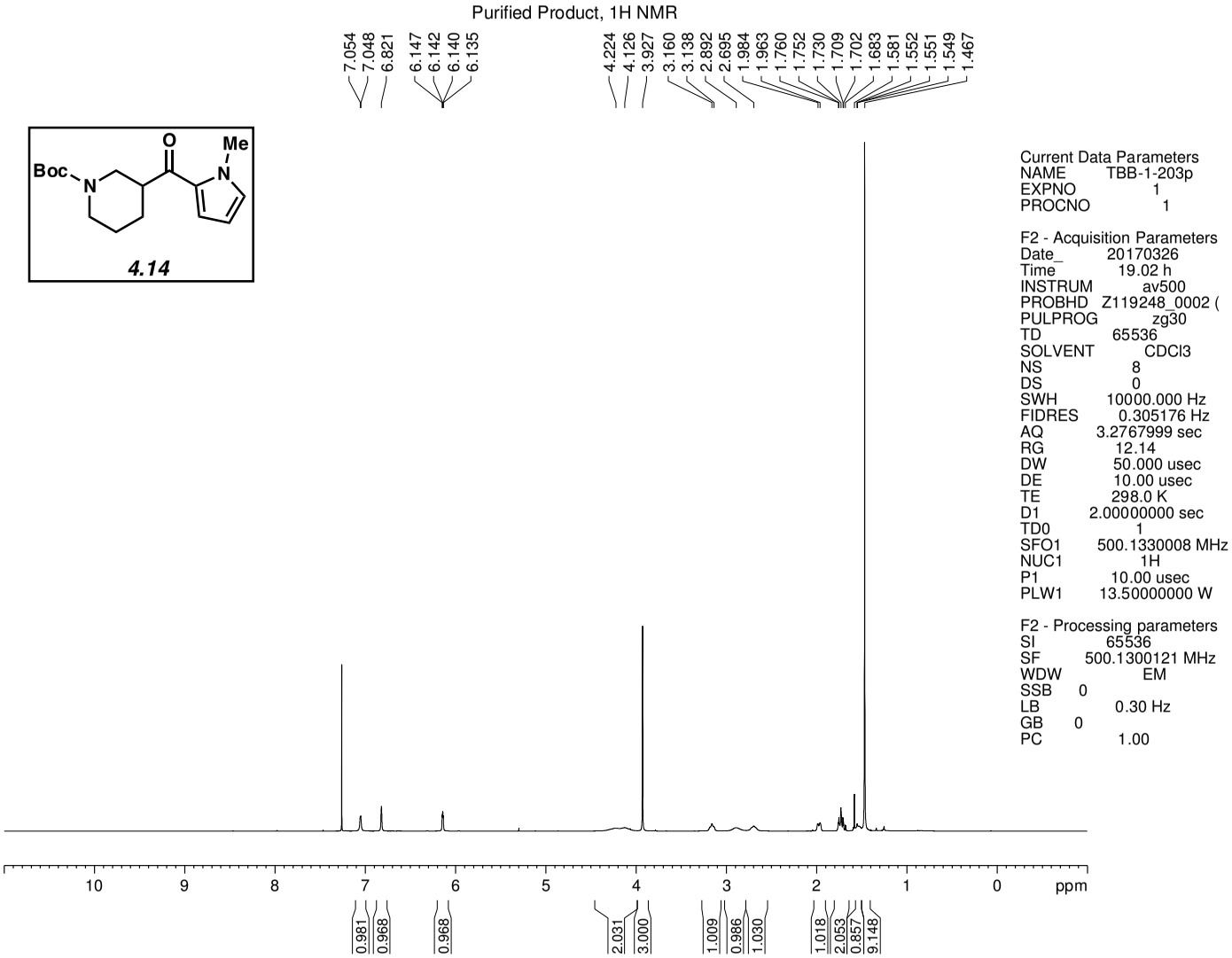

Figure 4.41 ^{1}H NMR (500 MHz, $CDCl_3$) of compound **4.14**.

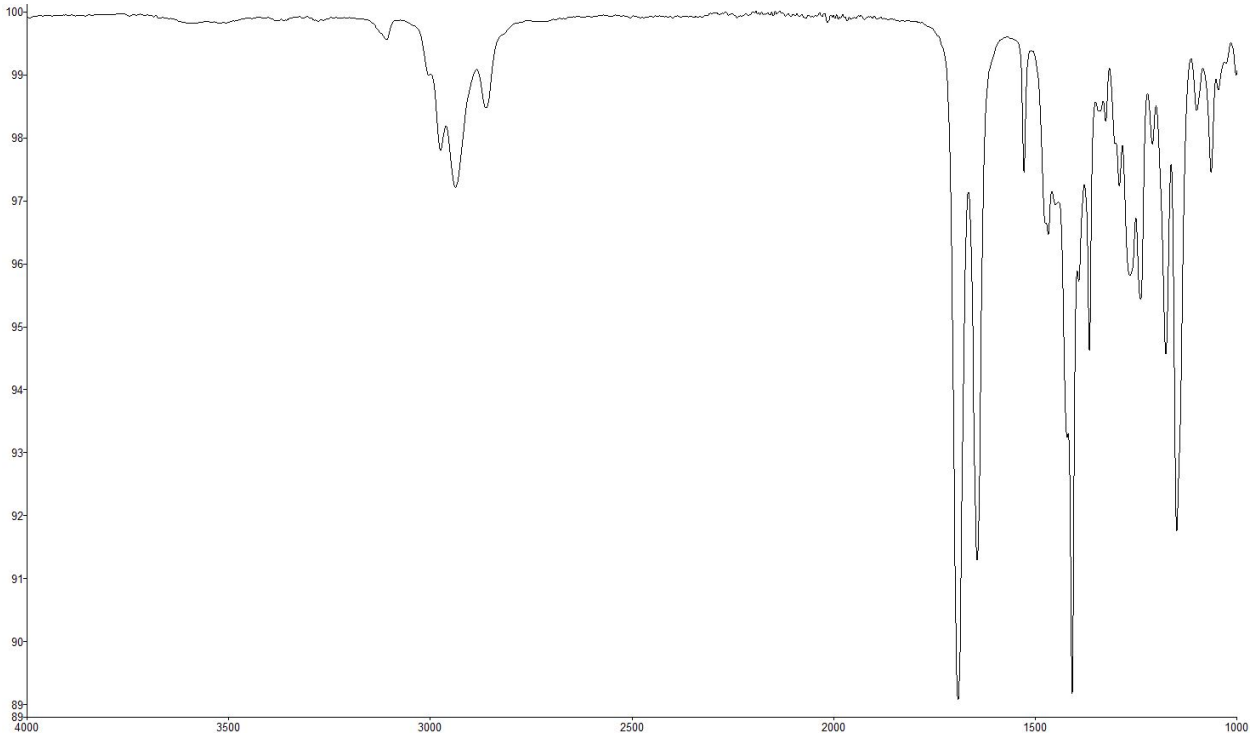

Figure 4.42 Infrared spectrum of compound **4.14**.

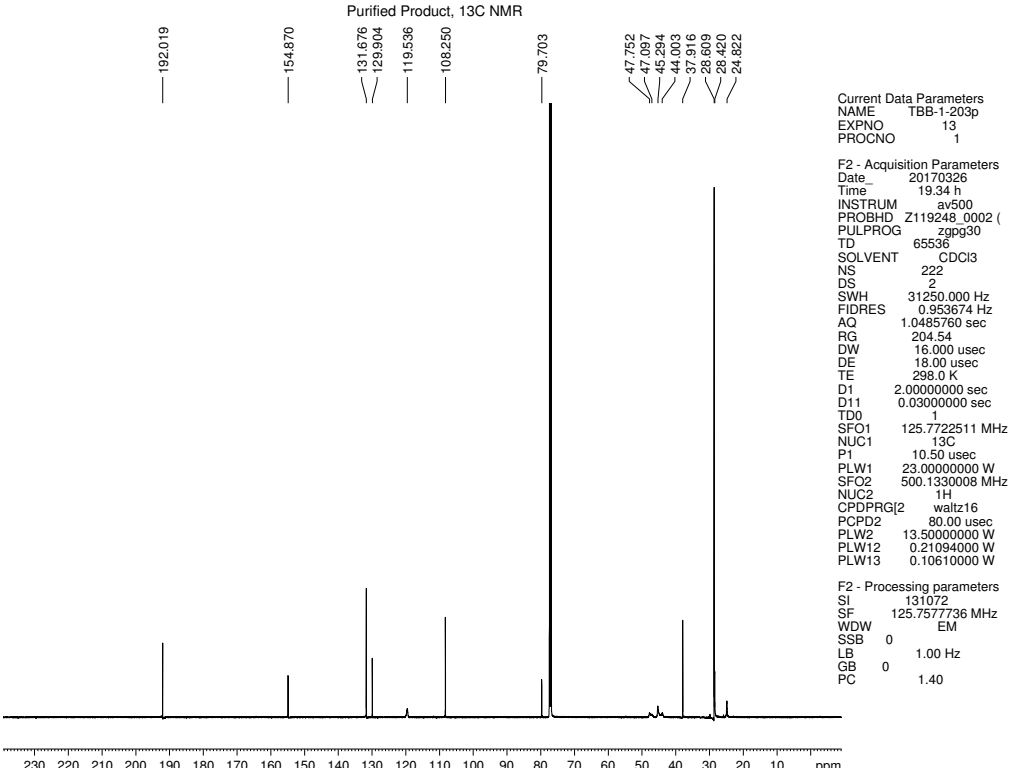

Figure 4.43 ^{13}C NMR (125 MHz, $CDCl_3$) of compound **4.14**.

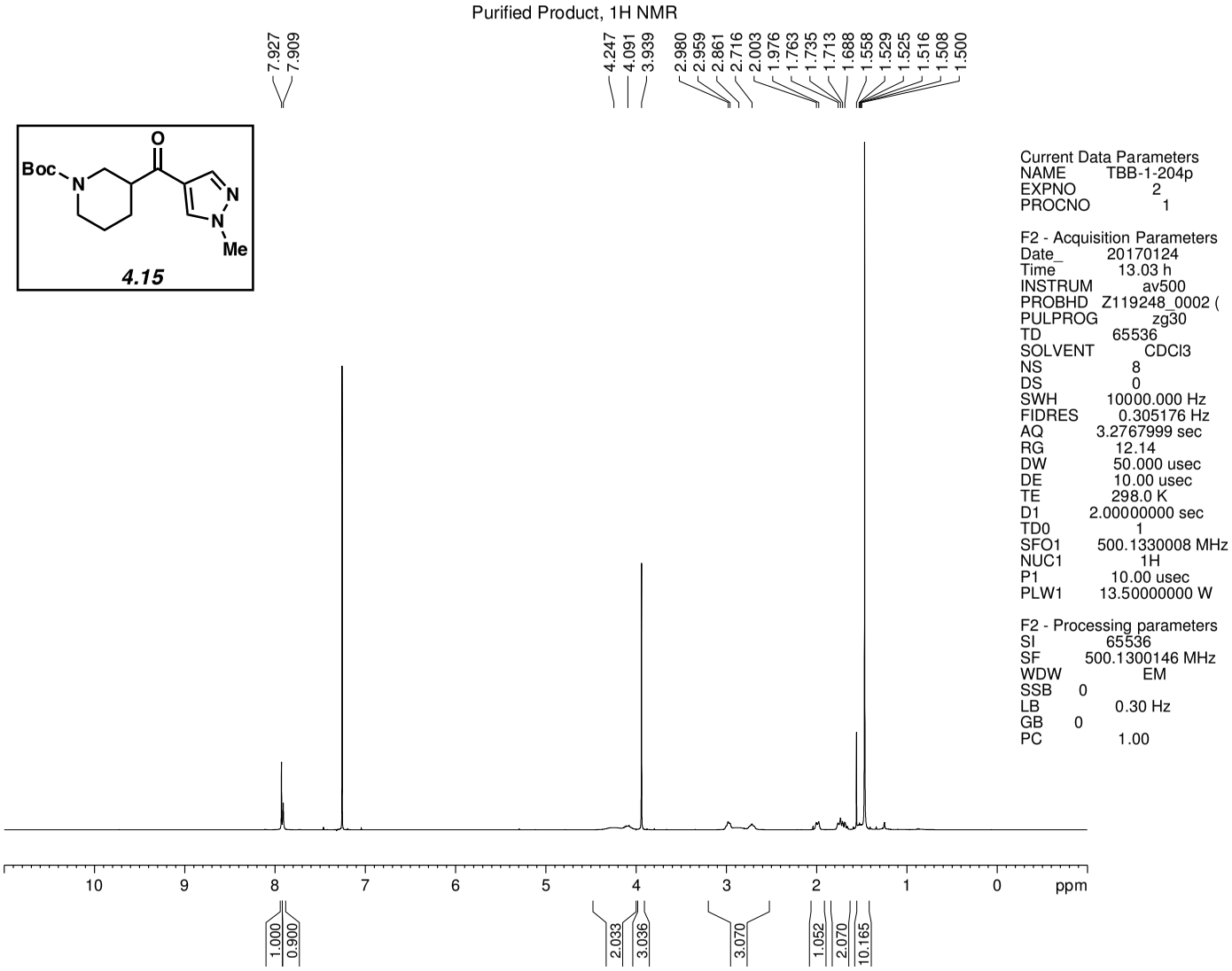

Figure 4.44 ^{1}H NMR (500 MHz, $CDCl_3$) of compound **4.15**.

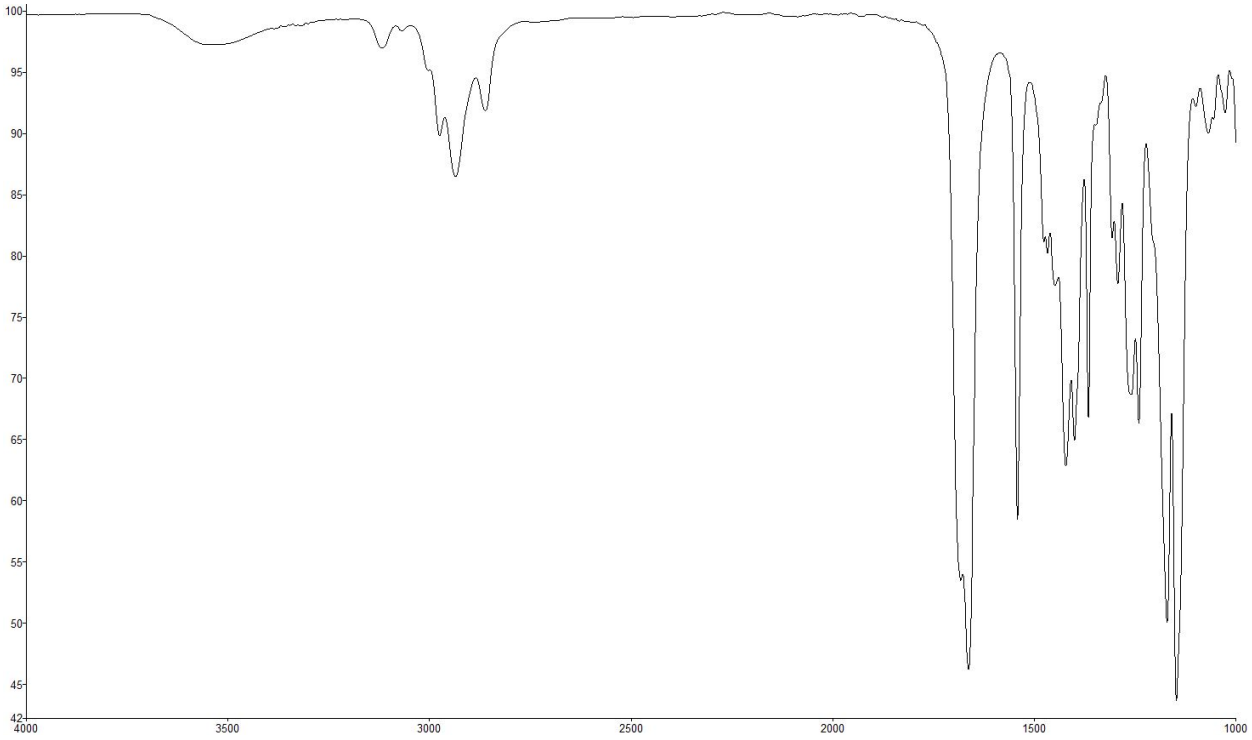

Figure 4.45 Infrared spectrum of compound **4.15**.

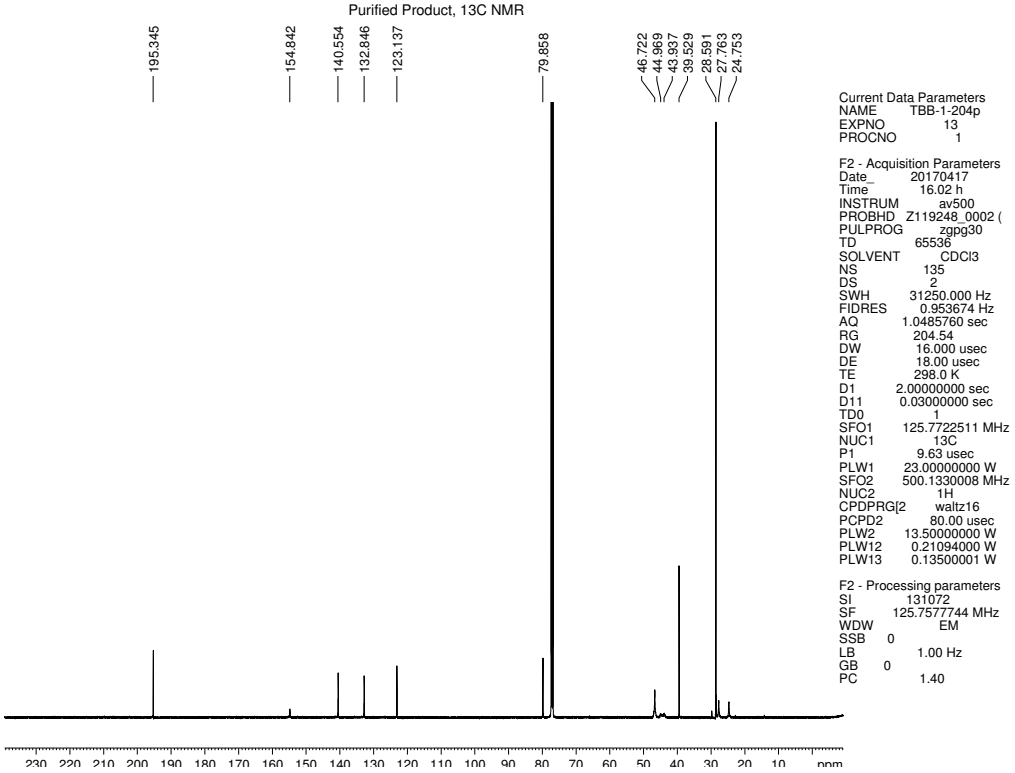

Figure 4.46 ^{13}C NMR (125 MHz, $CDCl_3$) of compound **4.15**.

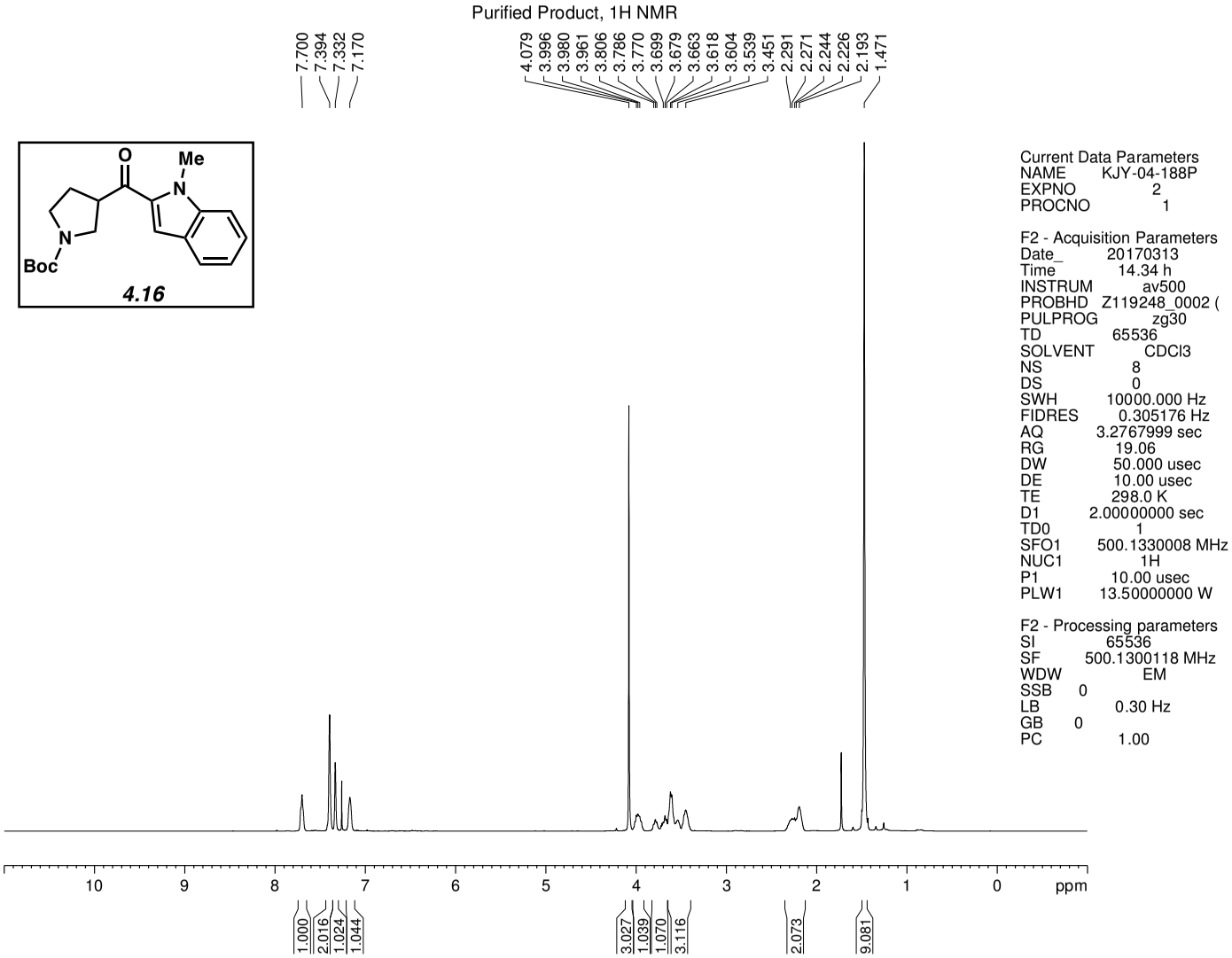

Figure 4.47 ^{1}H NMR (500 MHz, $CDCl_3$) of compound **4.16**.

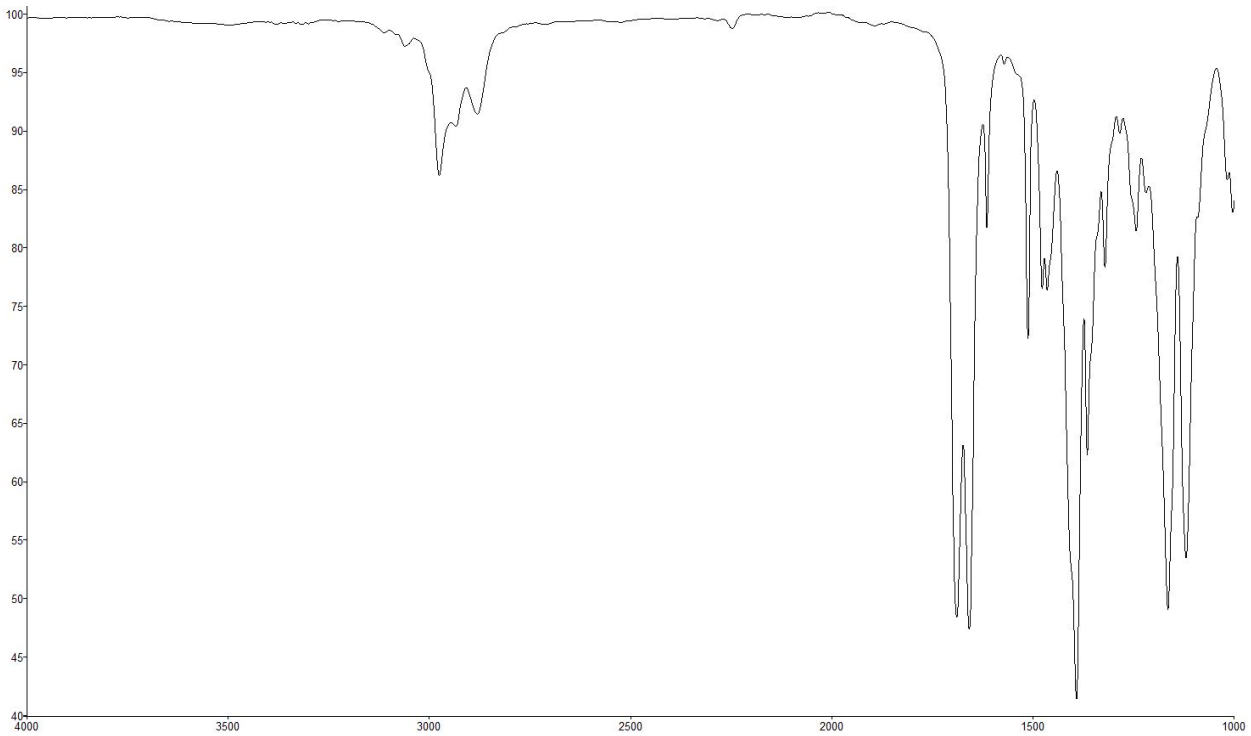

Figure 4.48 Infrared spectrum of compound **4.16**.

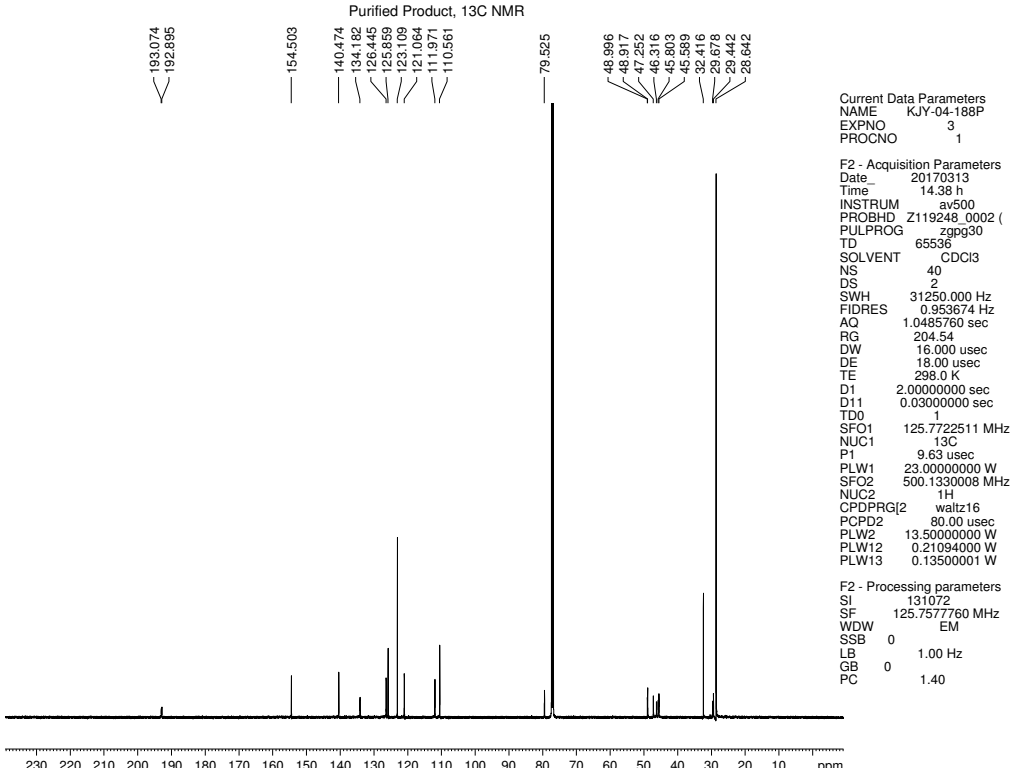

Figure 4.49 ^{13}C NMR (125 MHz, $CDCl_3$) of compound **4.16**.

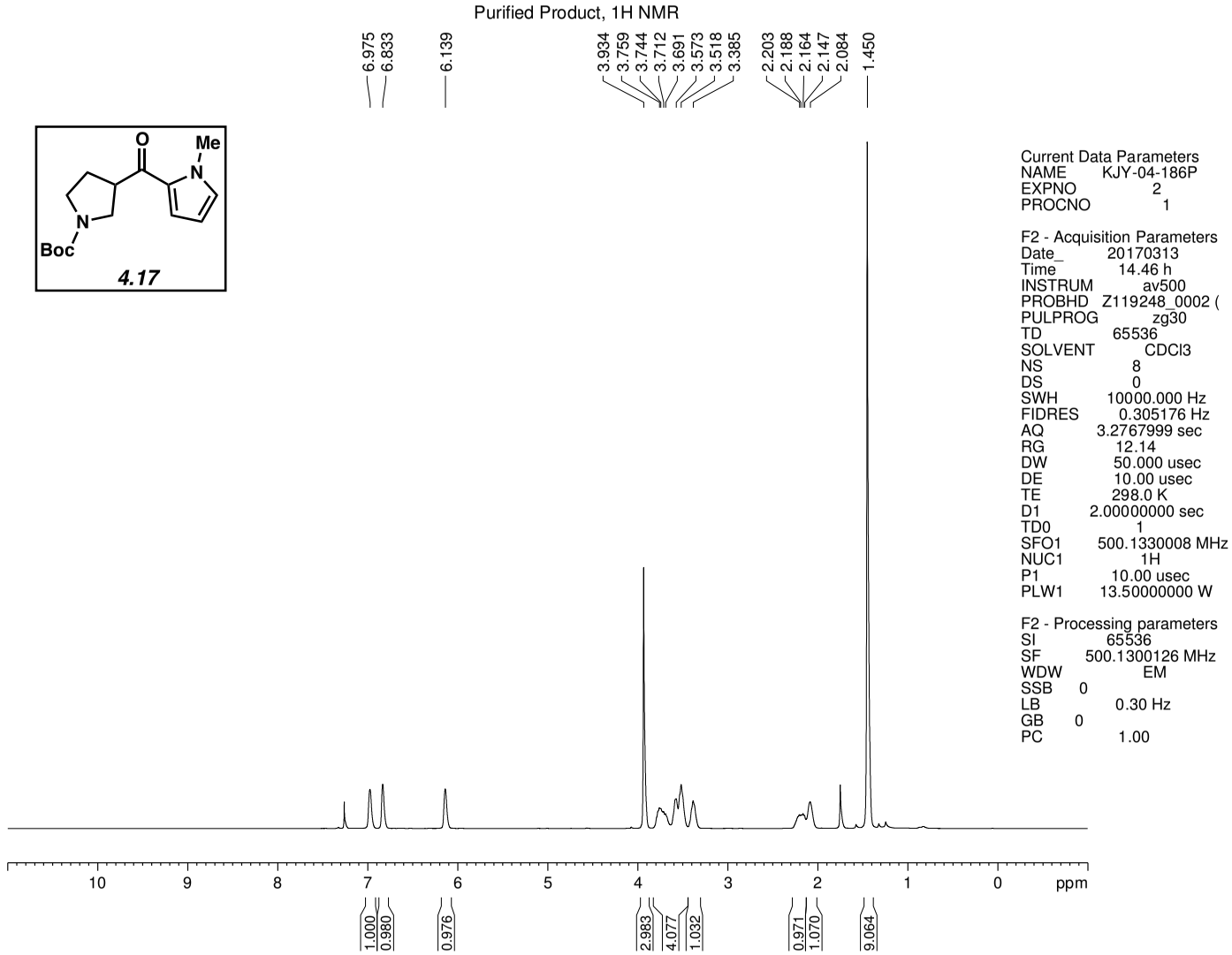

Figure 4.50 ^{1}H NMR (500 MHz, $CDCl_3$) of compound **4.17**.

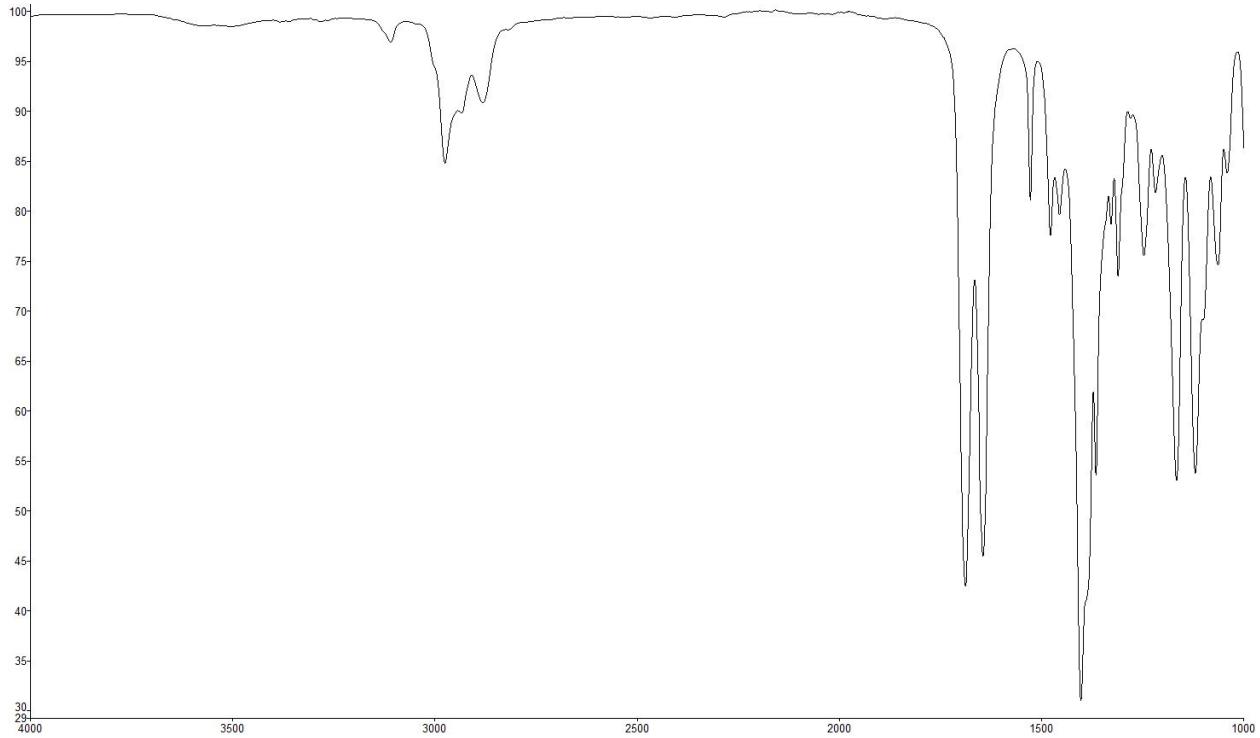

Figure 4.51 Infrared spectrum of compound **4.17**.

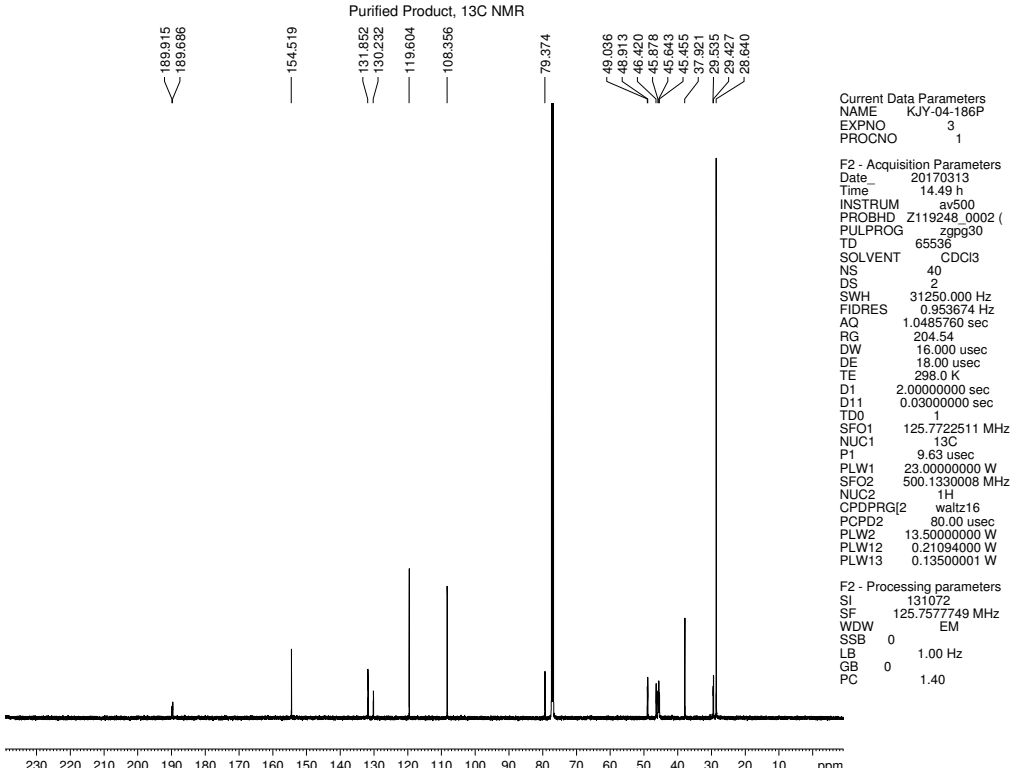

Figure 4.52 ^{13}C NMR (125 MHz, $CDCl_3$) of compound **4.17**.

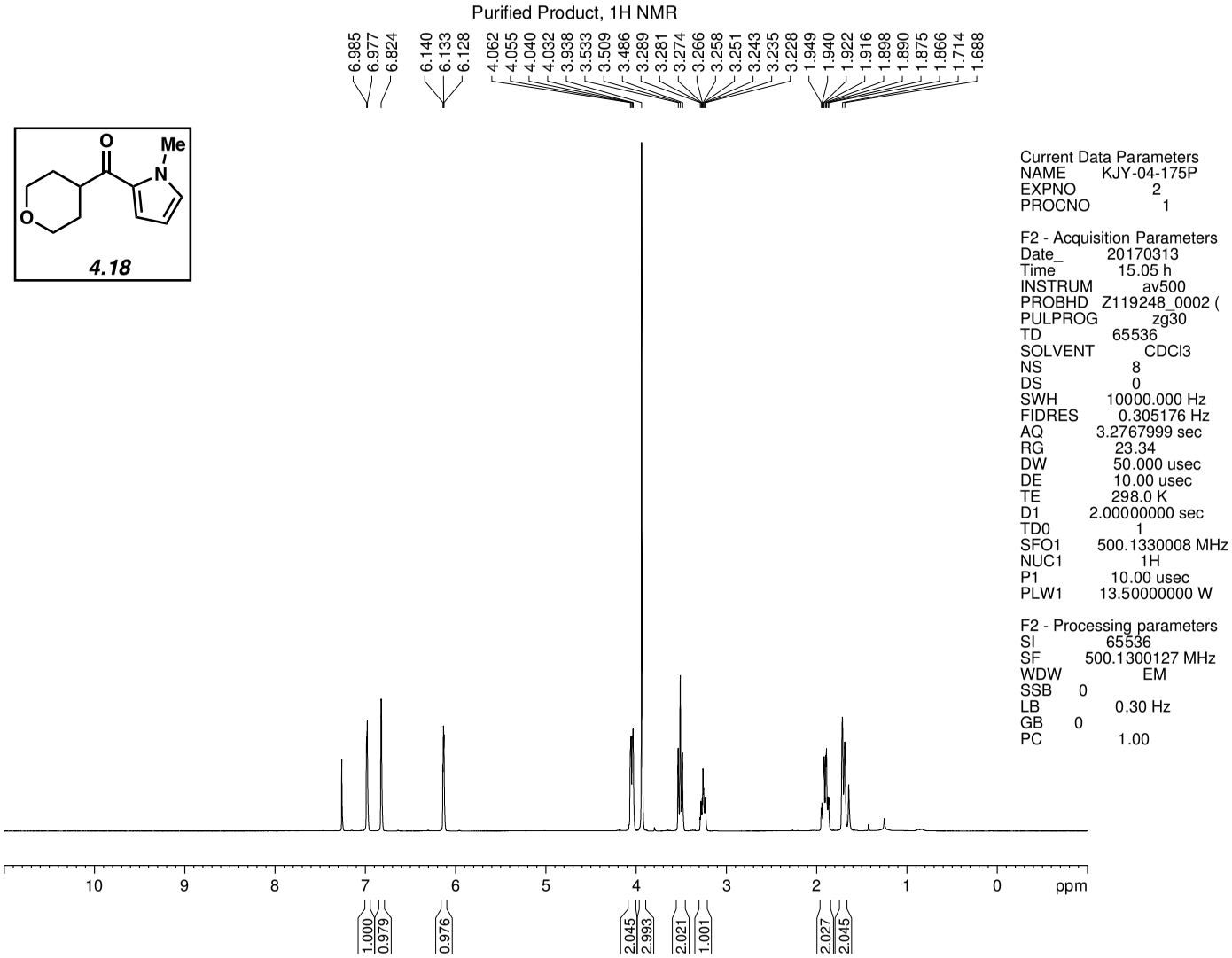

Figure 4.53 ^{1}H NMR (500 MHz, $CDCl_3$) of compound **4.18**.

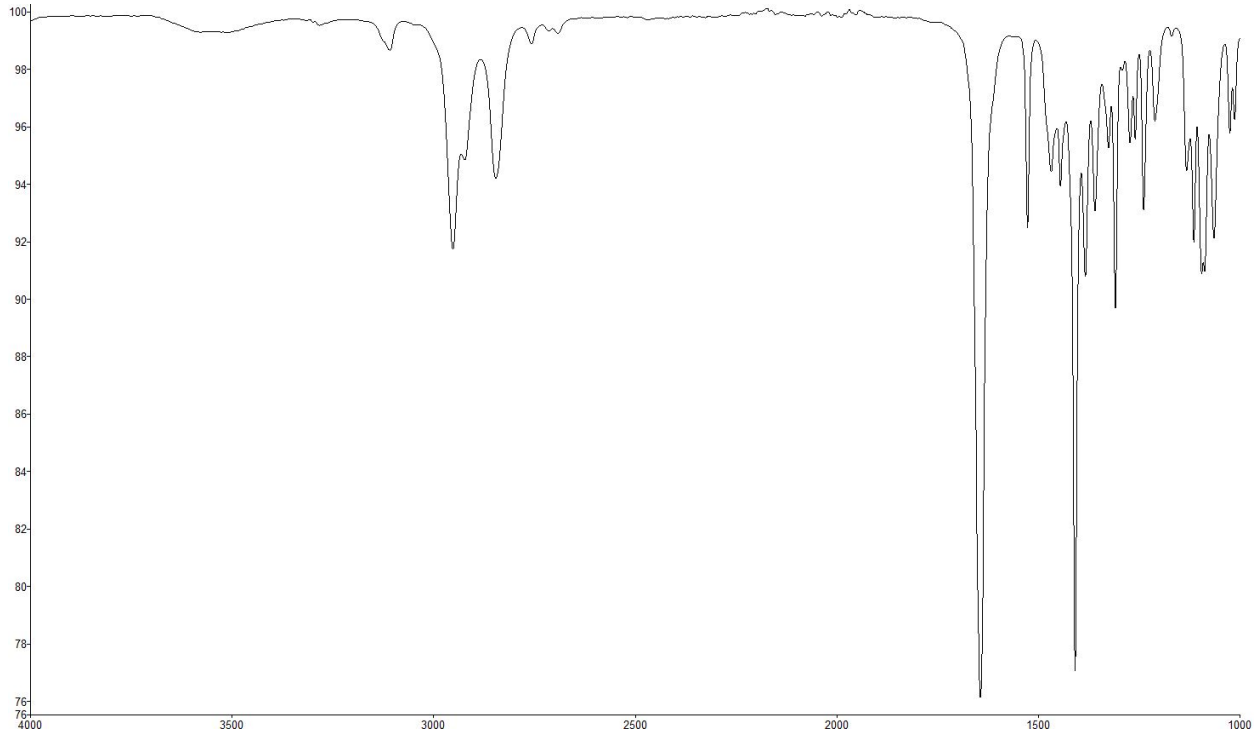

Figure 4.54 Infrared spectrum of compound **4.18**.

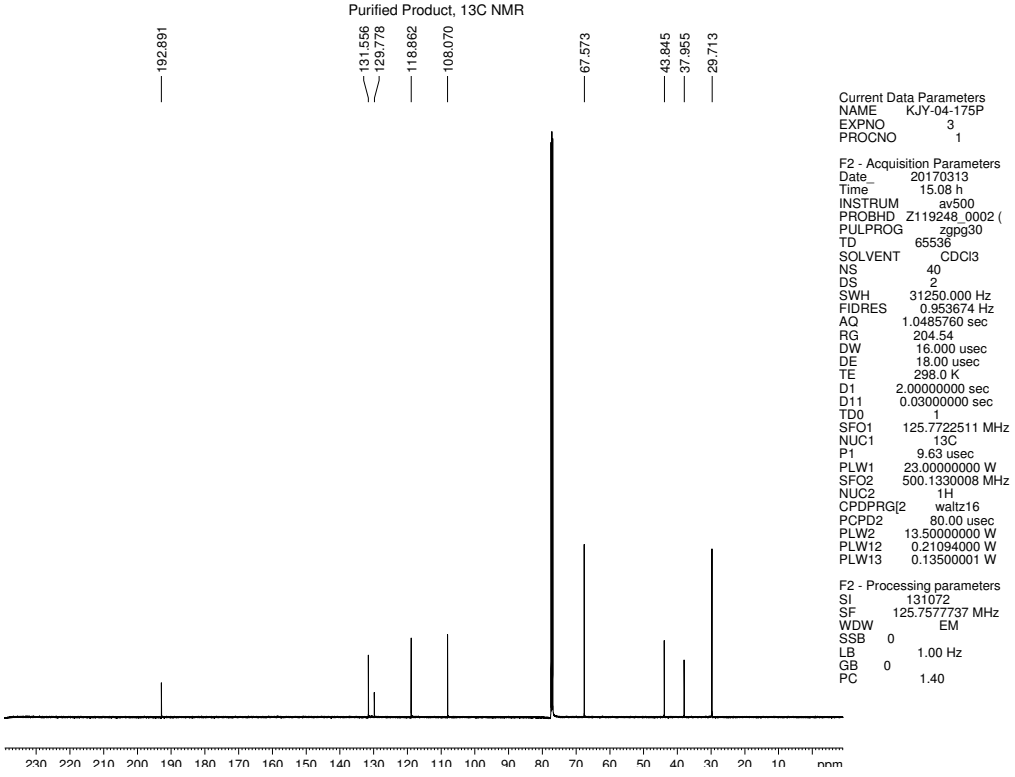

Figure 4.55 ^{13}C NMR (125 MHz, $CDCl_3$) of compound **4.18**.

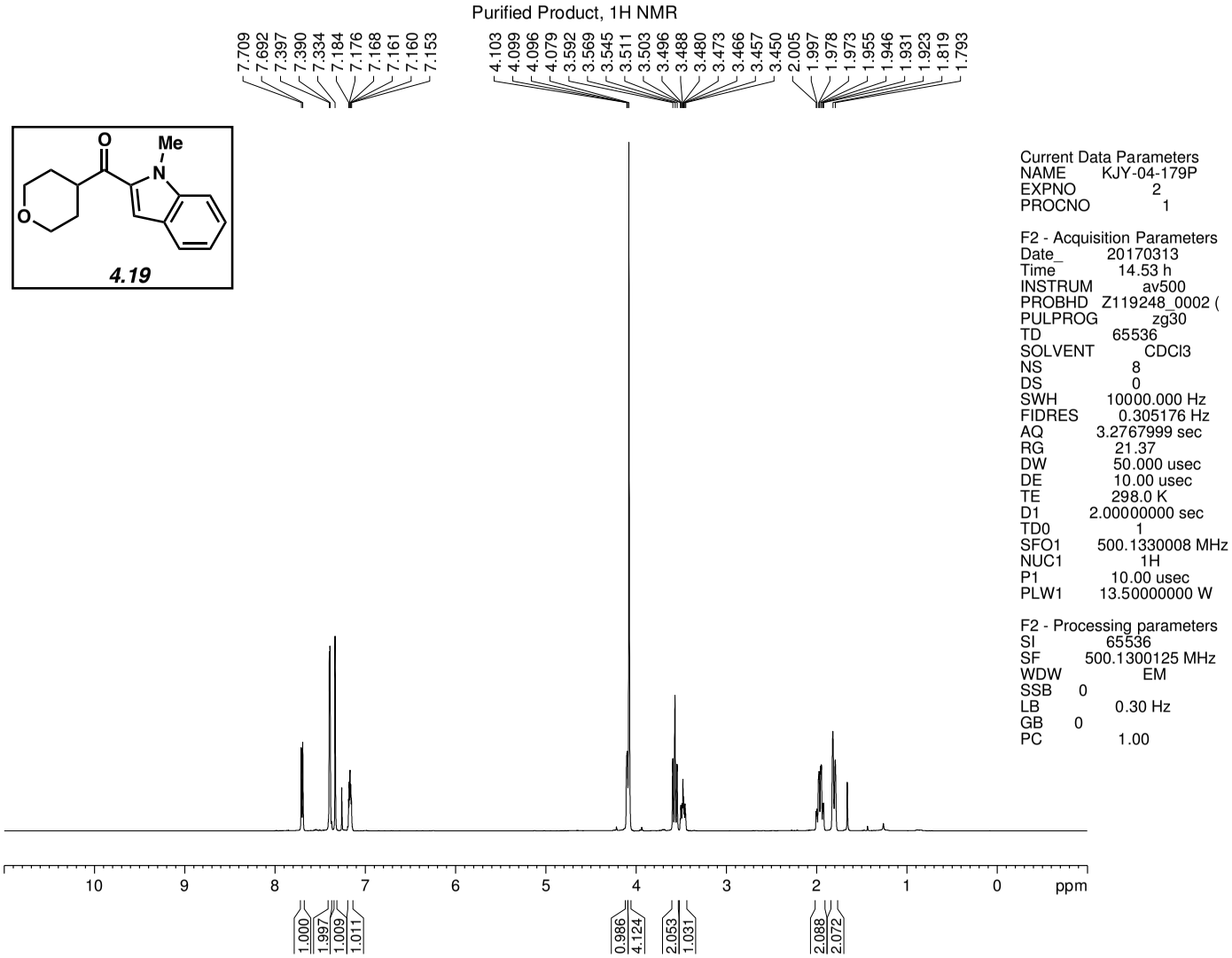

Figure 4.56 ^{1}H NMR (500 MHz, $CDCl_3$) of compound **4.19**.

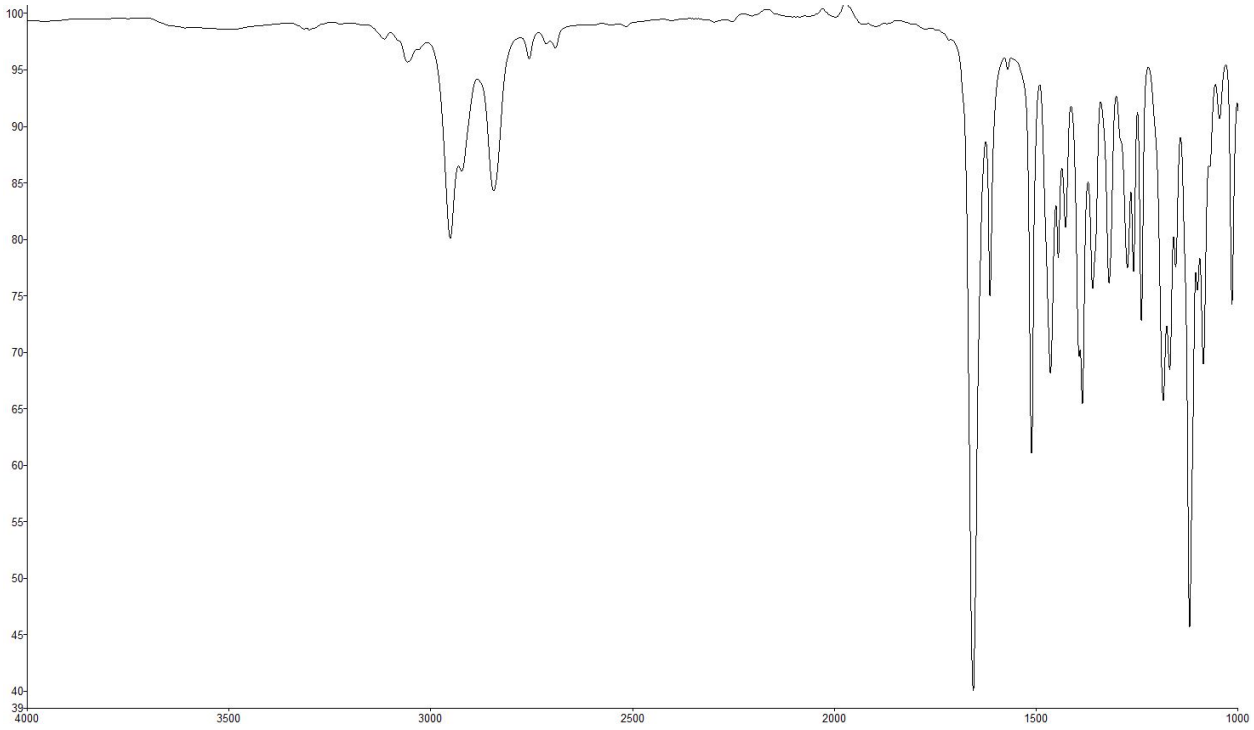

Figure 4.57 Infrared spectrum of compound **4.19**.

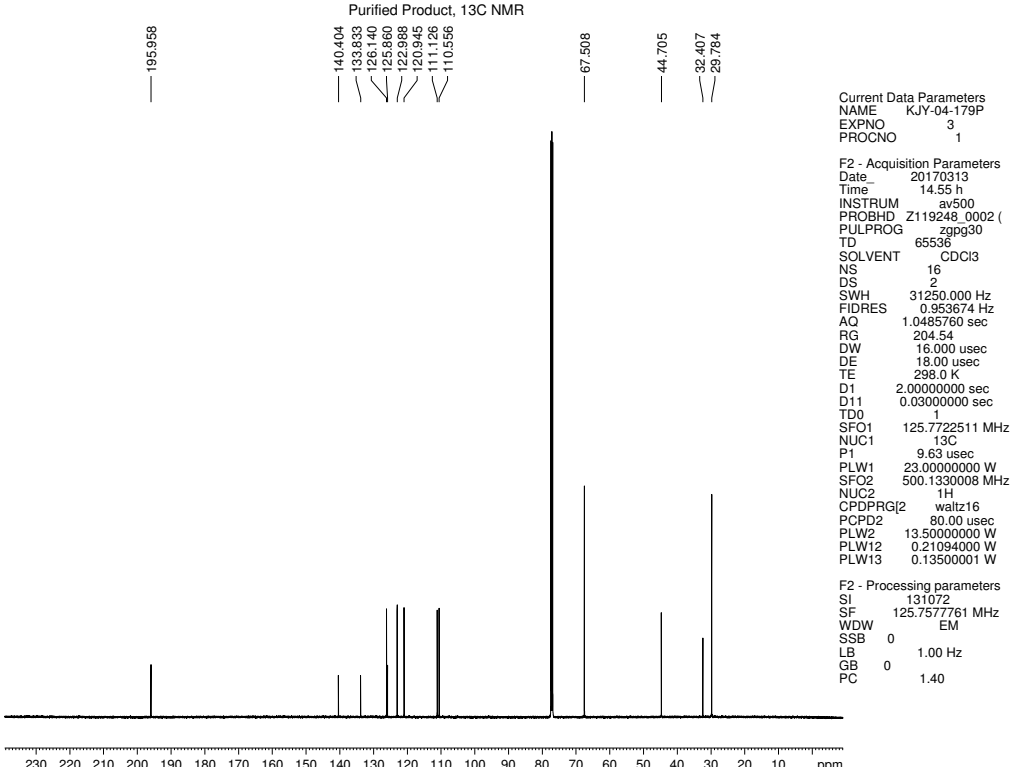

Figure 4.58 ^{13}C NMR (125 MHz, $CDCl_3$) of compound **4.19**.

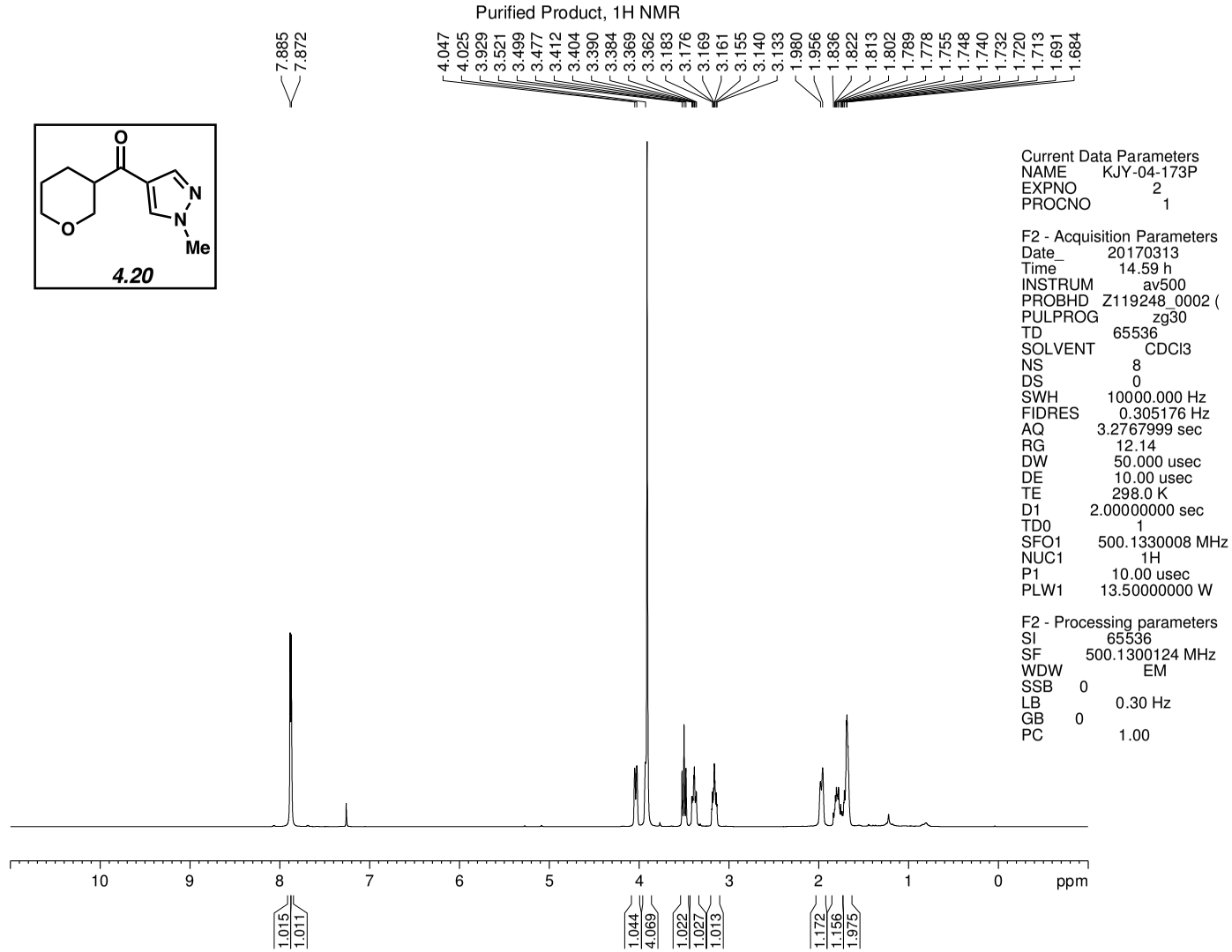

Figure 4.59 ^{1}H NMR (500 MHz, $CDCl_3$) of compound **4.20**.

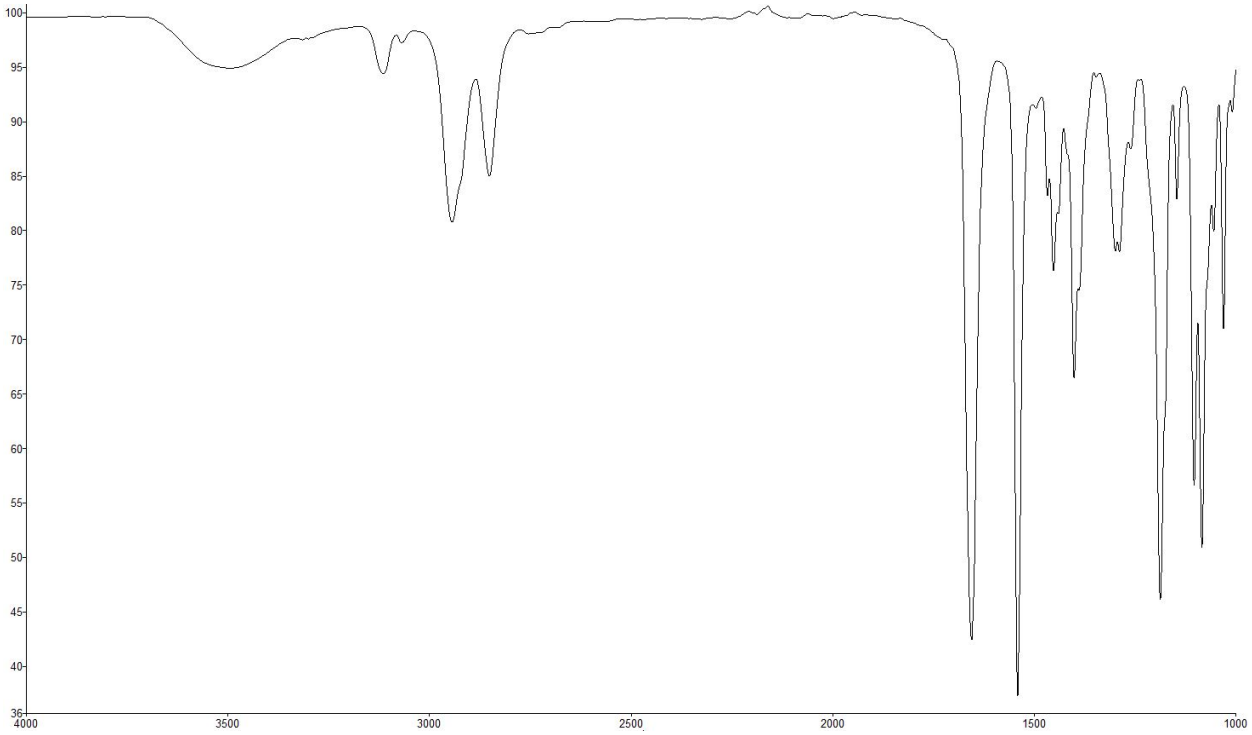

Figure 4.60 Infrared spectrum of compound **4.20**.

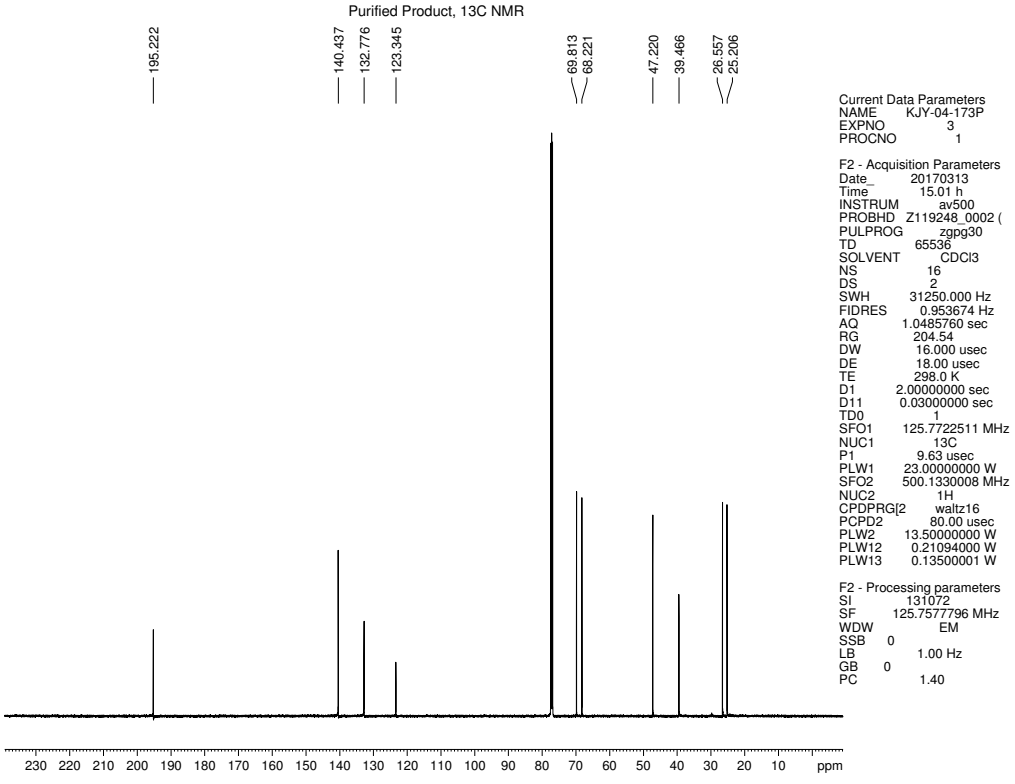

Figure 4.61 ^{13}C NMR (125 MHz, $CDCl_3$) of compound **4.20**.

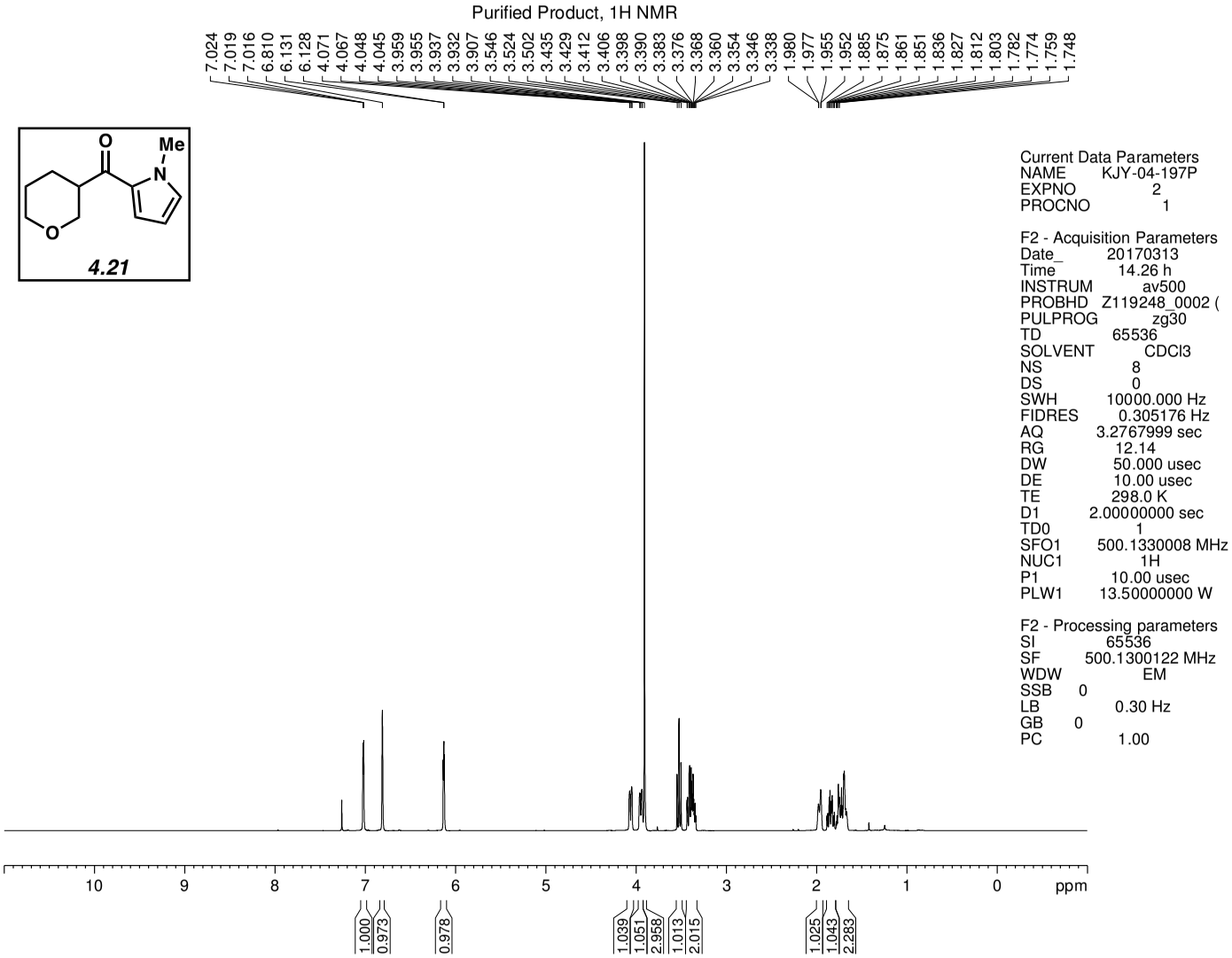

Figure 4.62 ^{1}H NMR (500 MHz, $CDCl_3$) of compound **4.21**.

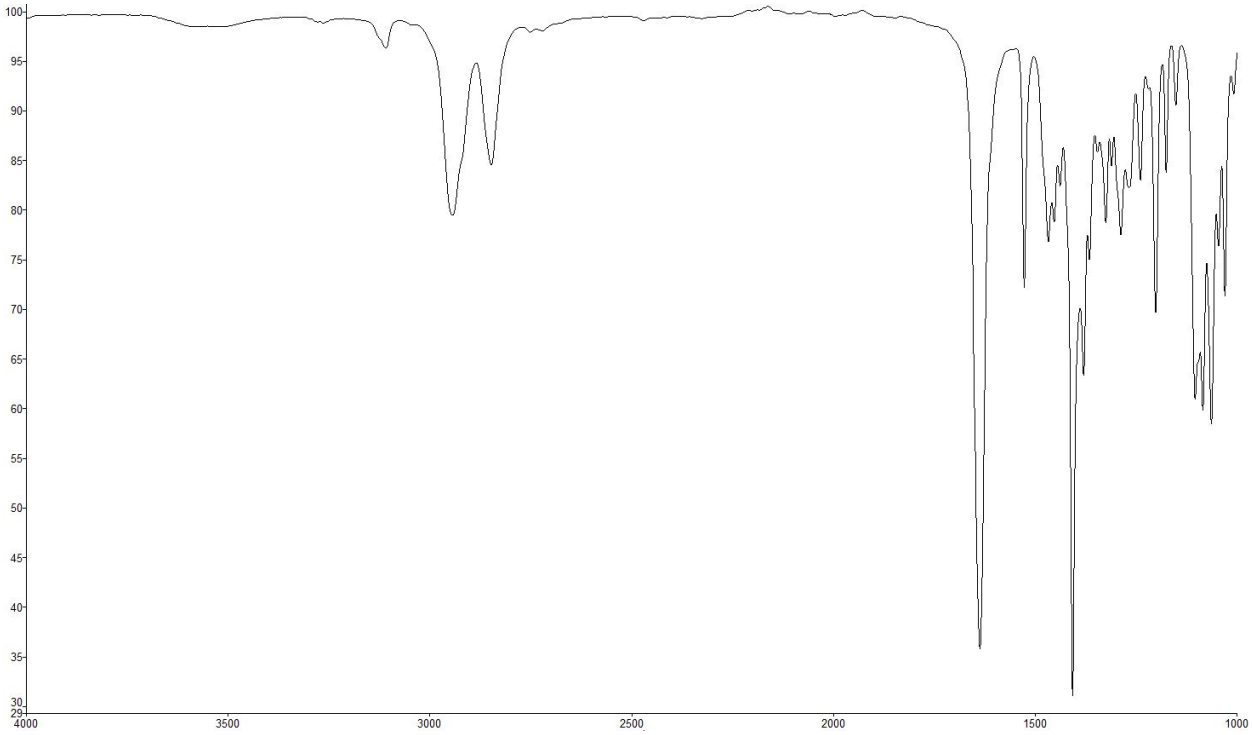

Figure 4.63 Infrared spectrum of compound **4.21**.

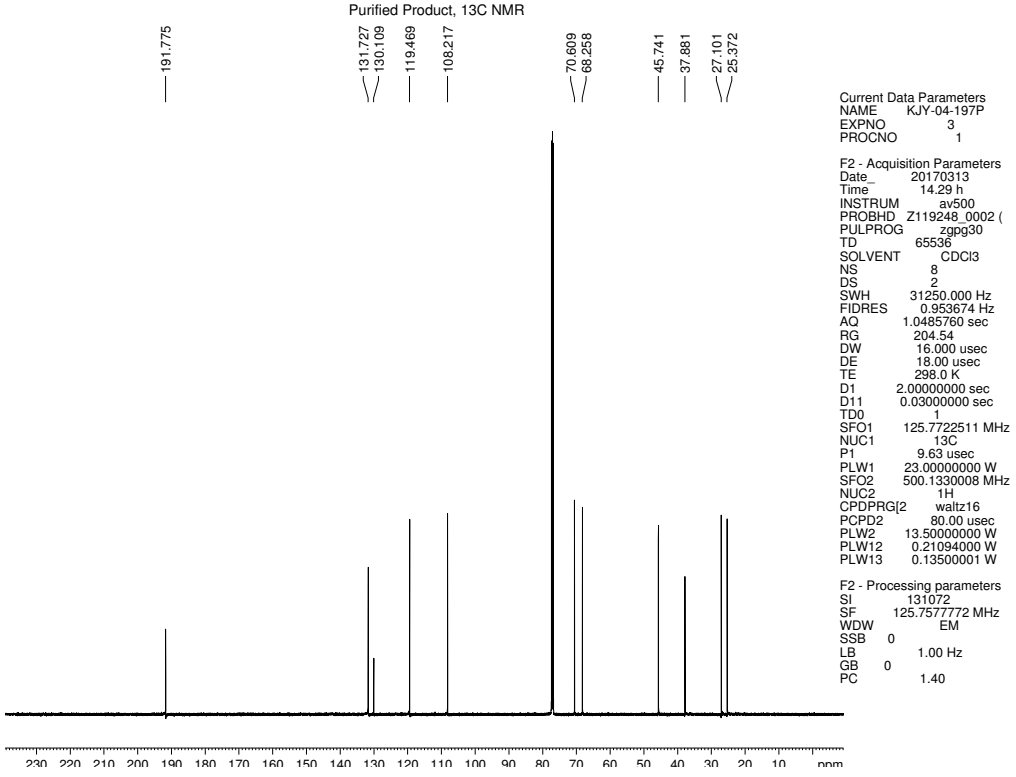

Figure 4.64 ^{13}C NMR (125 MHz, $CDCl_3$) of compound **4.21**.

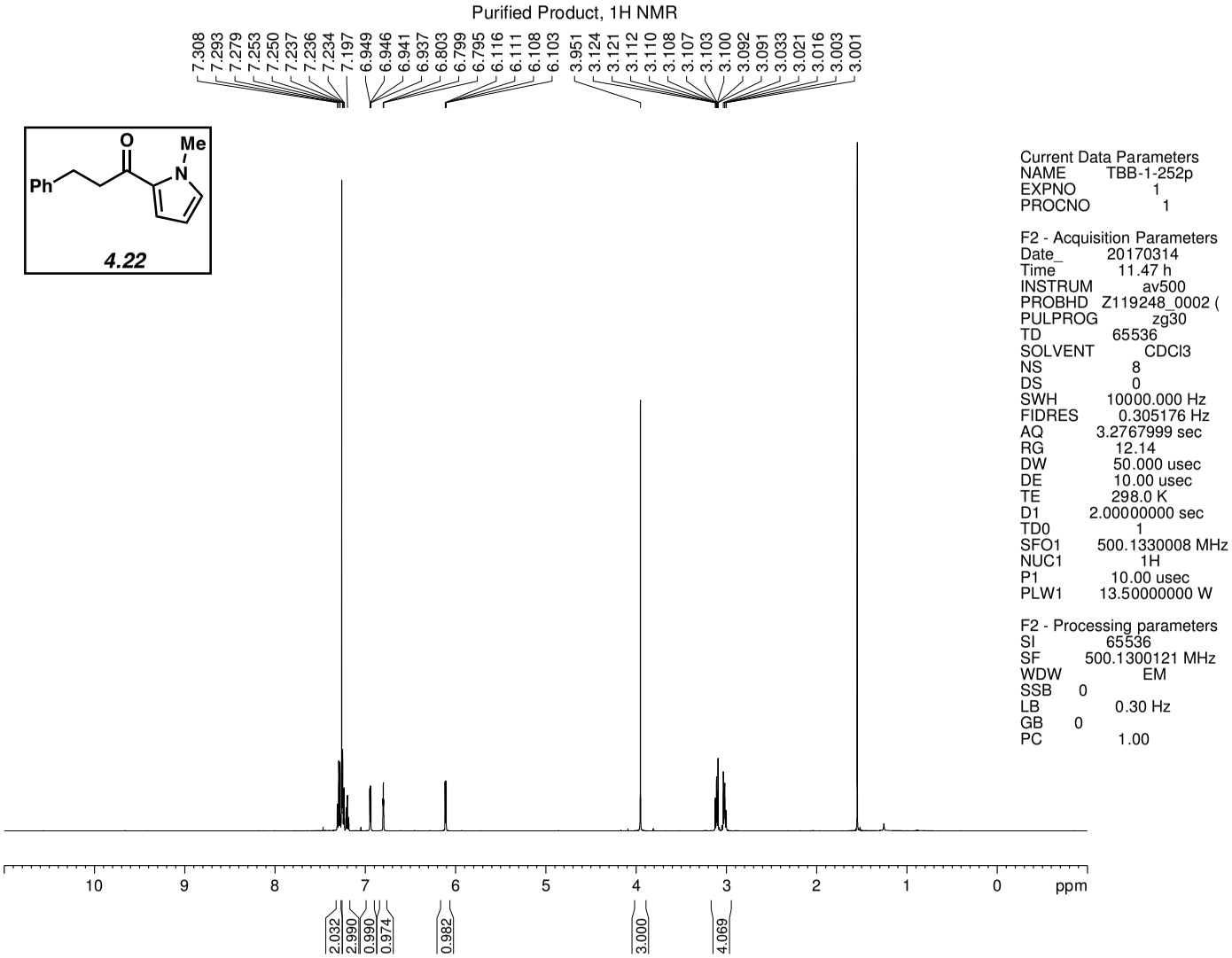

Figure 4.65 ^{1}H NMR (500 MHz, $CDCl_3$) of compound **4.22**.

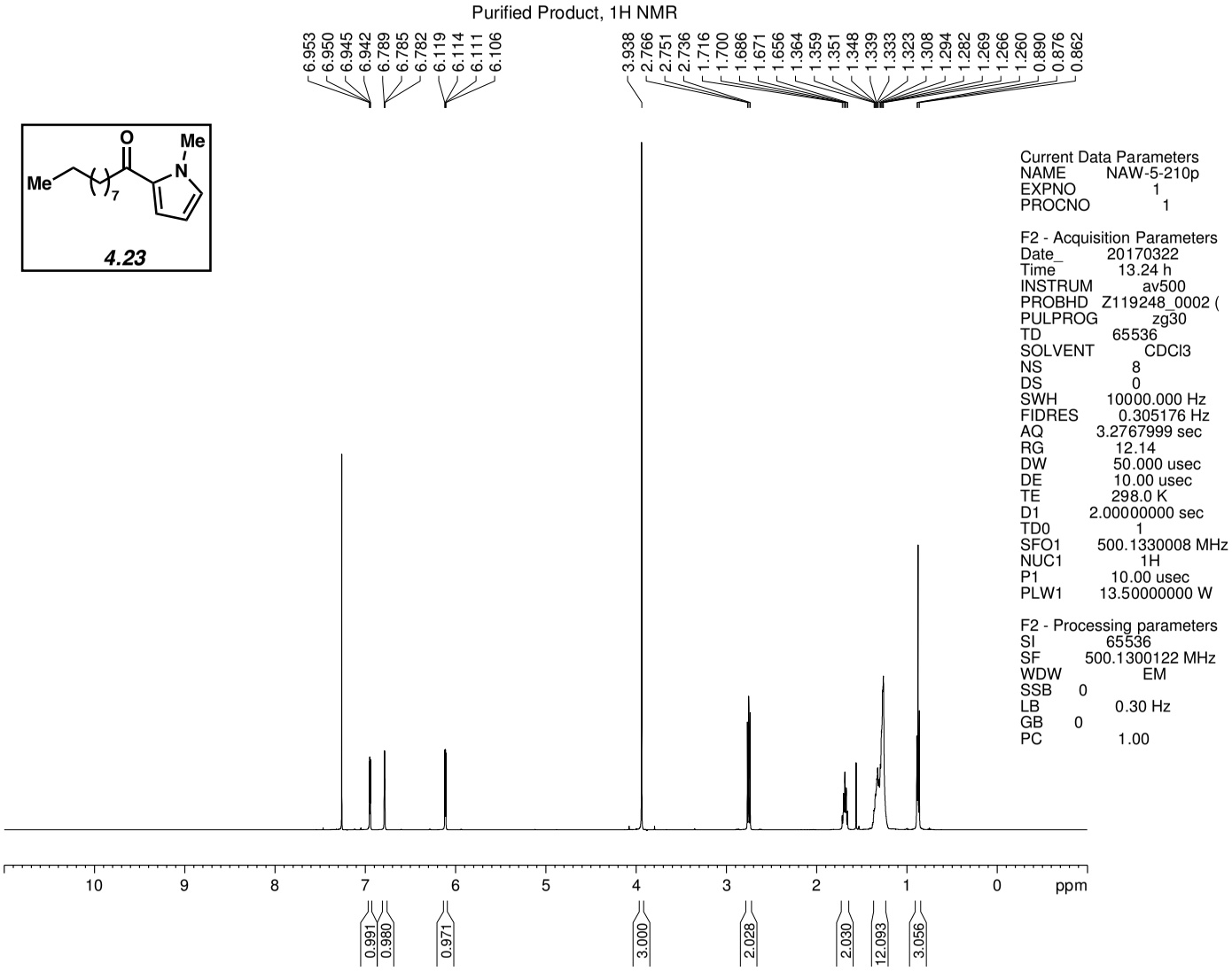

Figure 4.66 ^{1}H NMR (500 MHz, $CDCl_3$) of compound **4.23**.

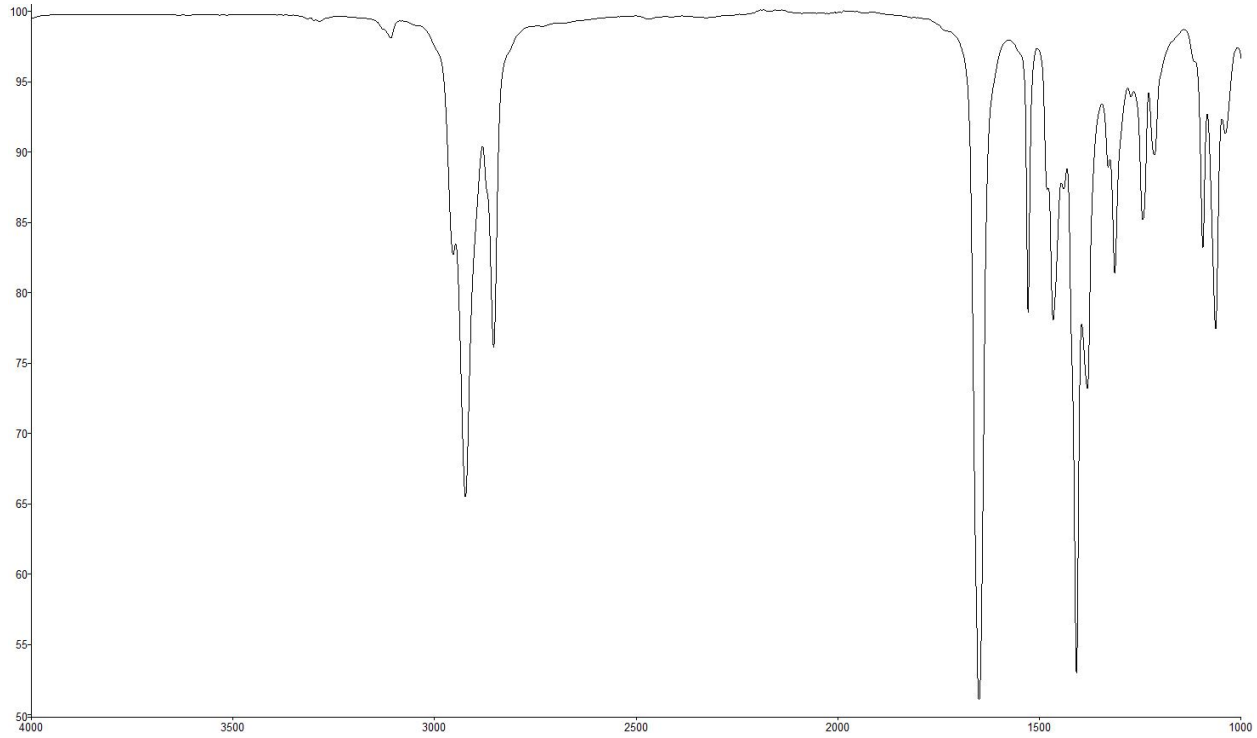

Figure 4.67 Infrared spectrum of compound **4.23**.

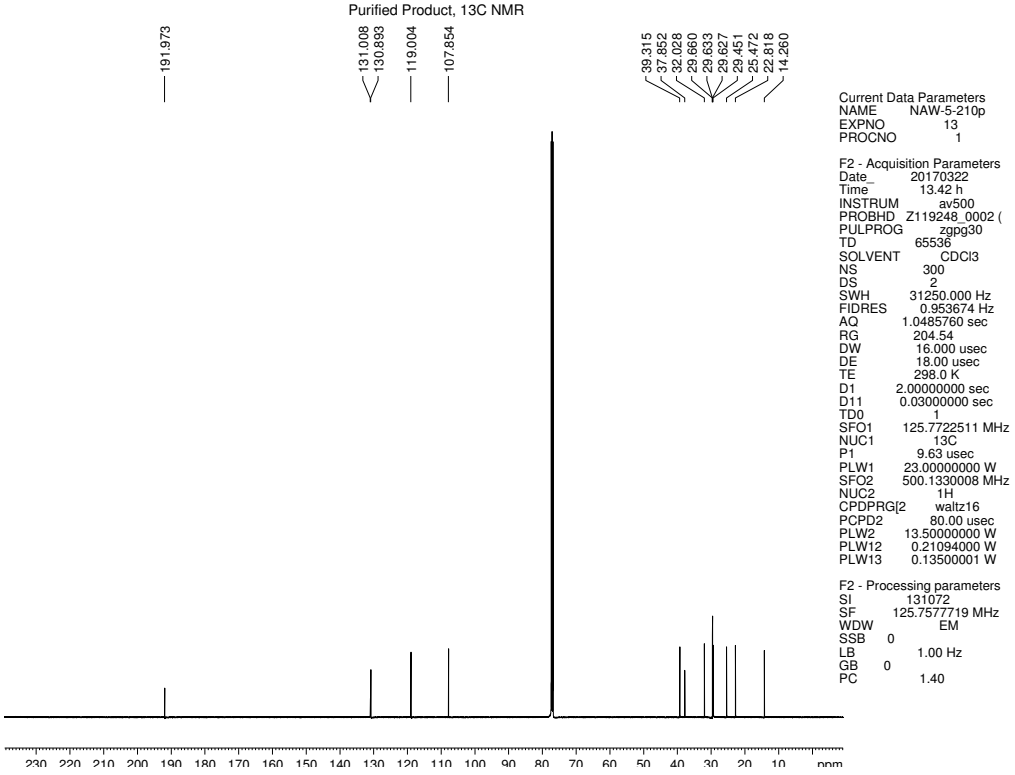

Figure 4.68 ^{13}C NMR (125 MHz, $CDCl_3$) of compound **4.23**.

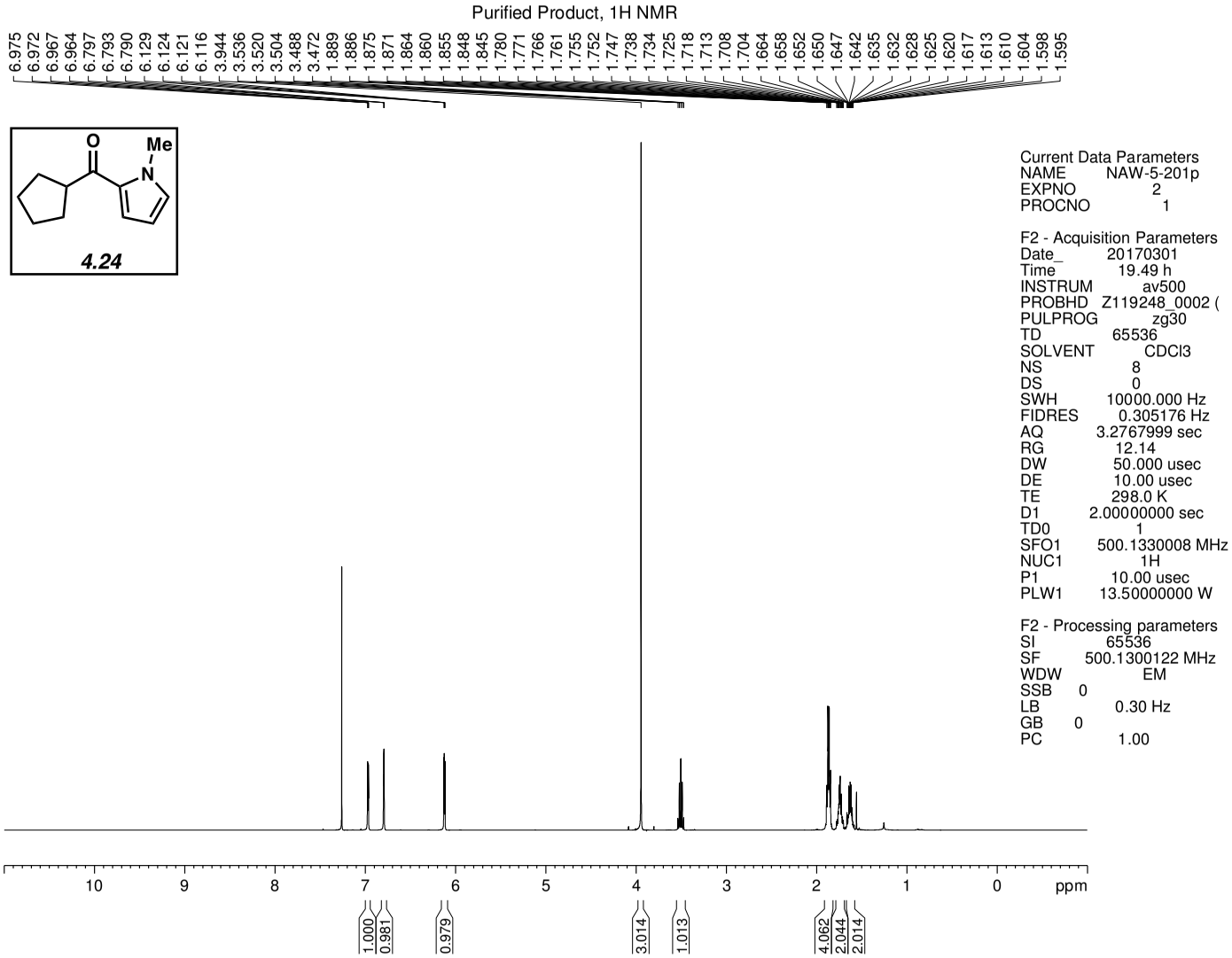

Figure 4.69 ^{1}H NMR (500 MHz, $CDCl_3$) of compound **4.24**.

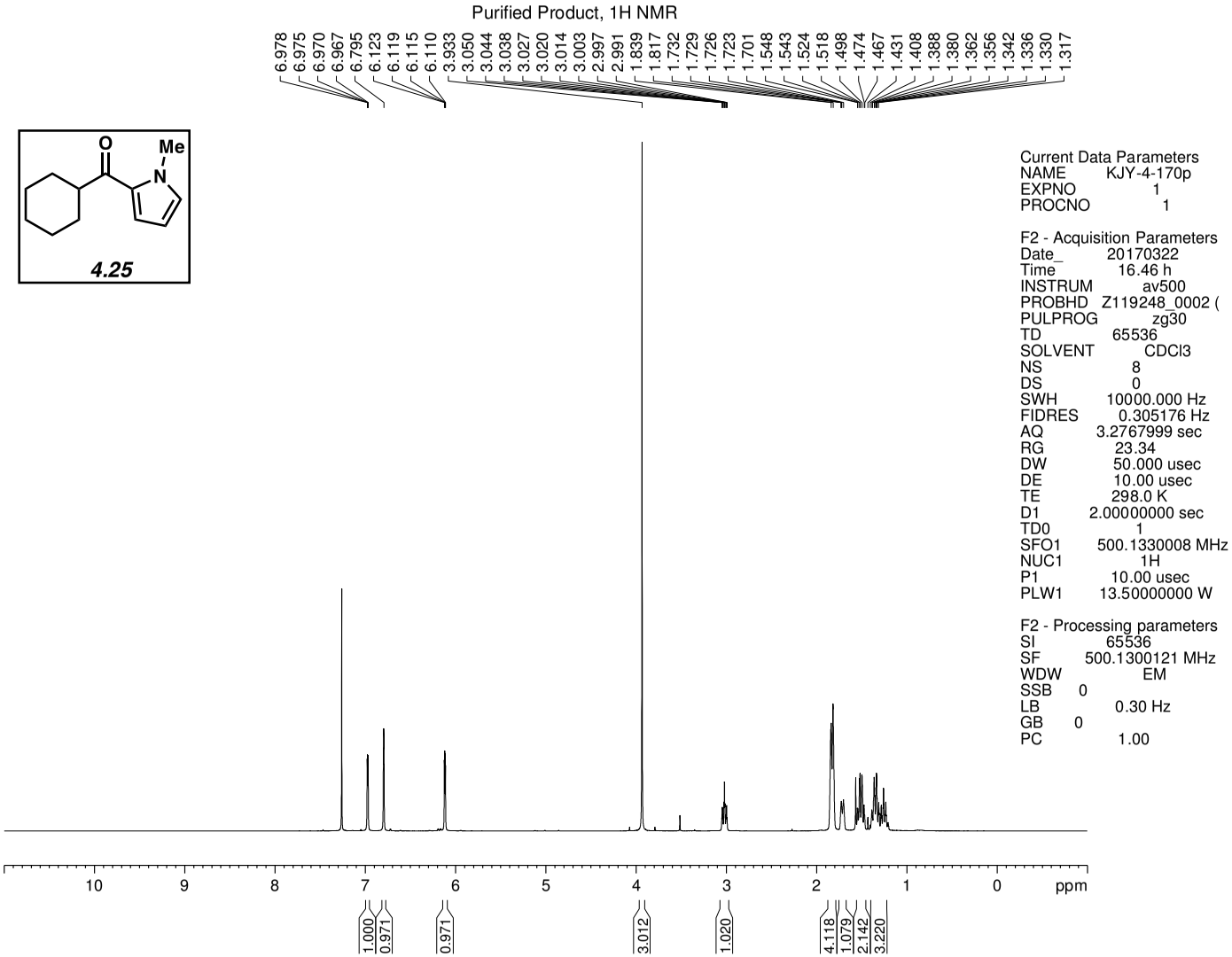

Figure 4.70 ^{1}H NMR (500 MHz, $CDCl_3$) of compound **4.25**.

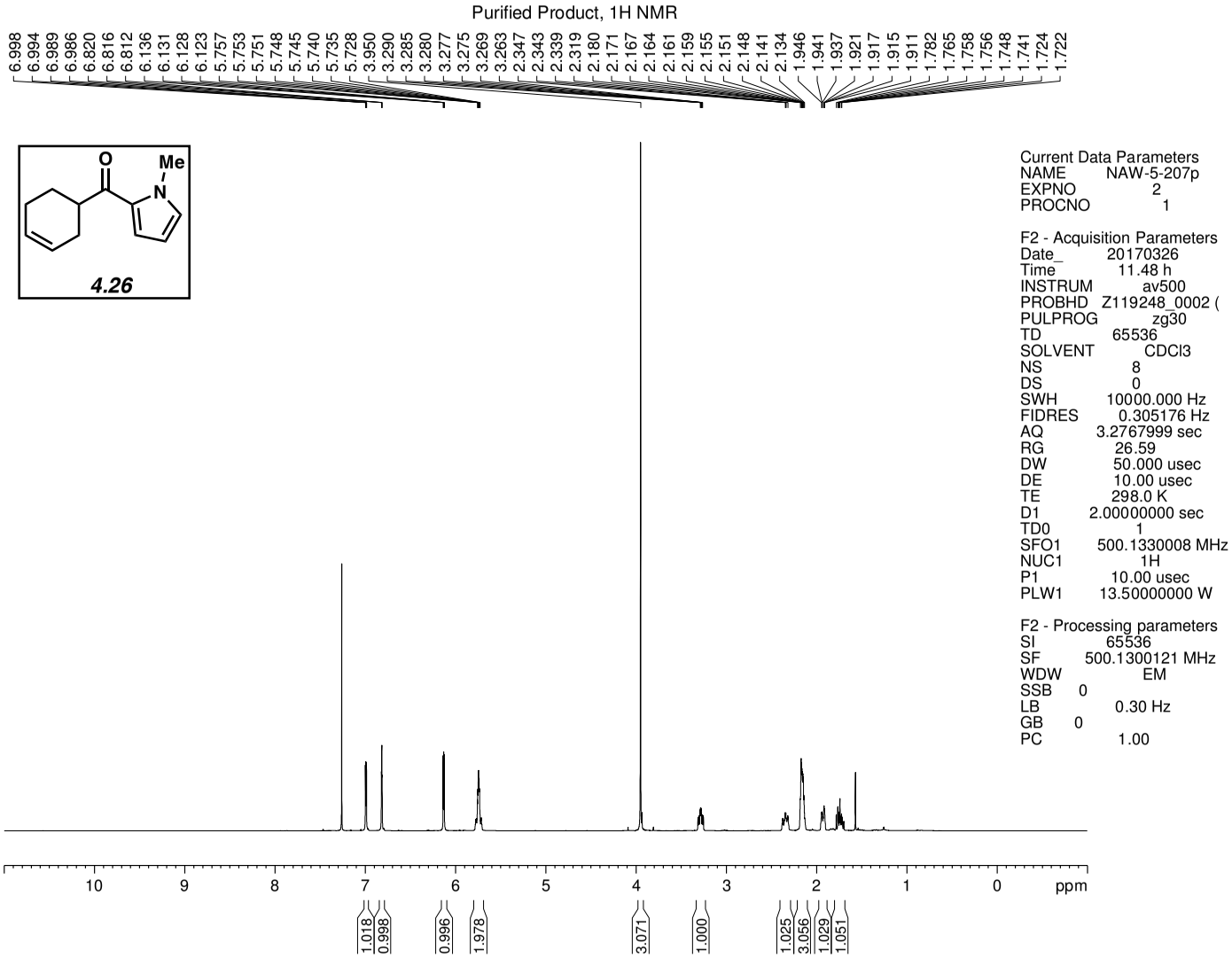

Figure 4.71 ^{1}H NMR (500 MHz, $CDCl_3$) of compound **4.26**.

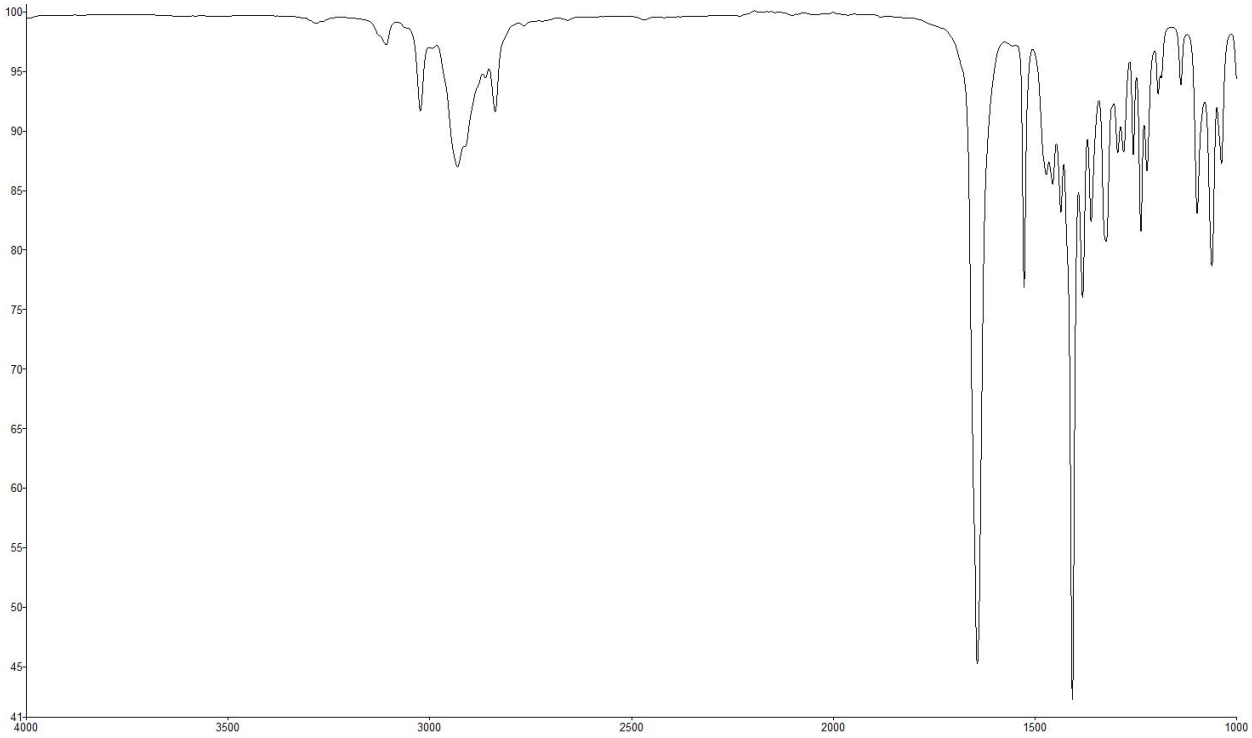

Figure 4.72 Infrared spectrum of compound **4.26**.

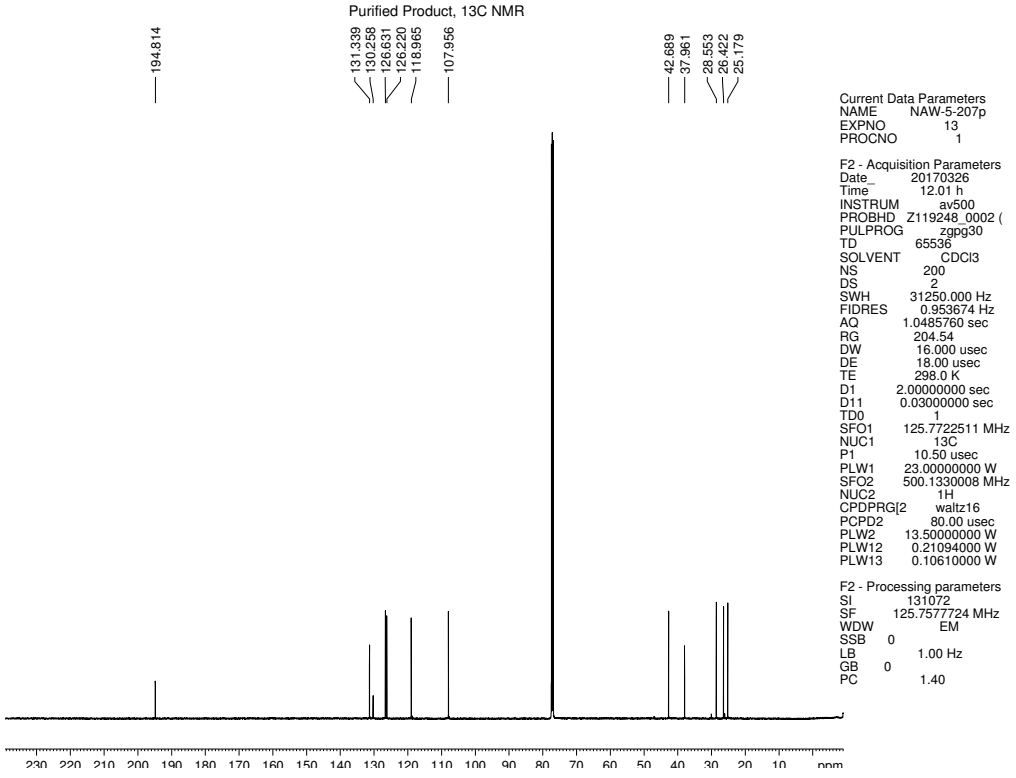

Figure 4.73 ^{13}C NMR (125 MHz, $CDCl_3$) of compound **4.26**.

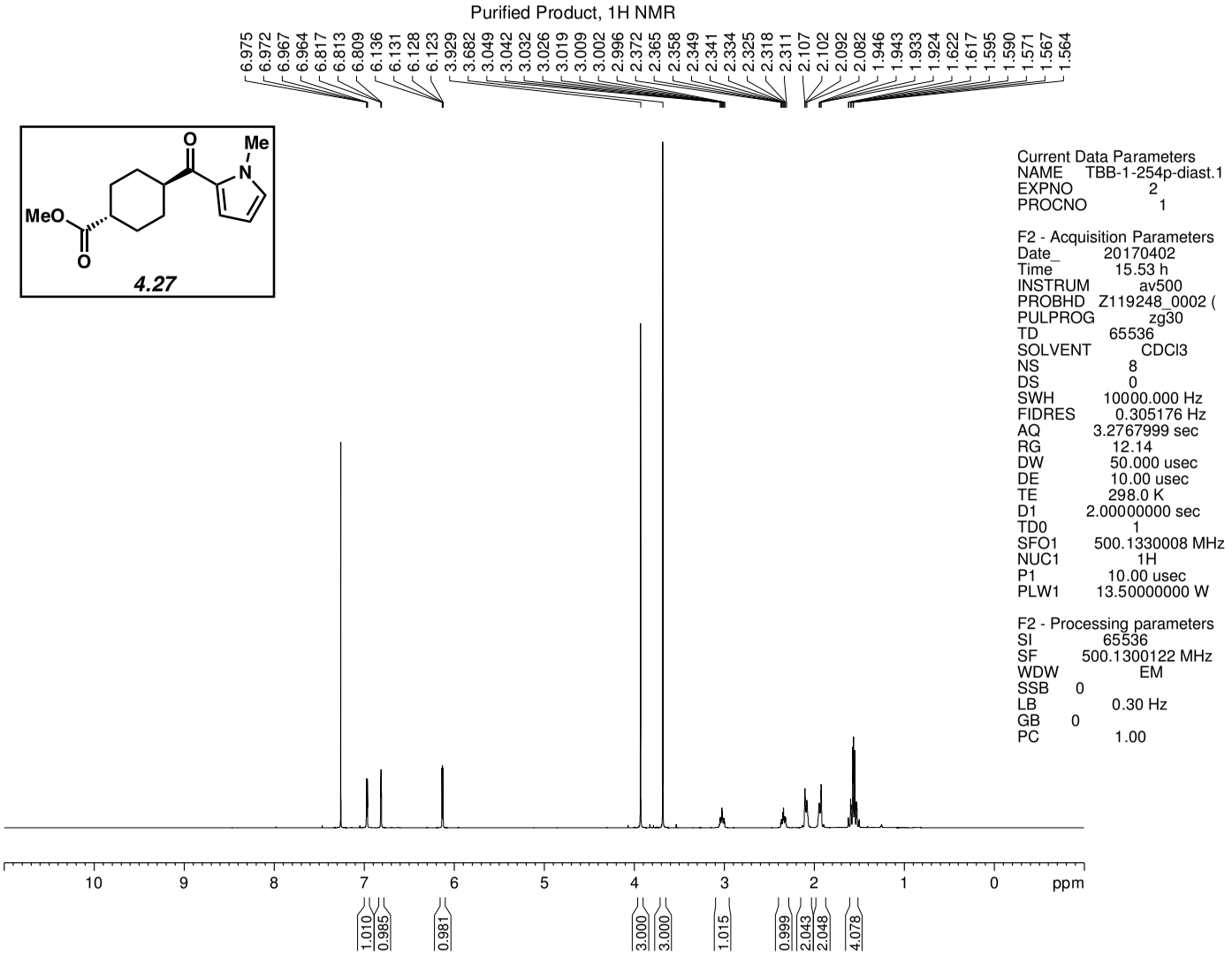

Figure 4.74 ^{1}H NMR (500 MHz, $CDCl_3$) of compound **4.27**.

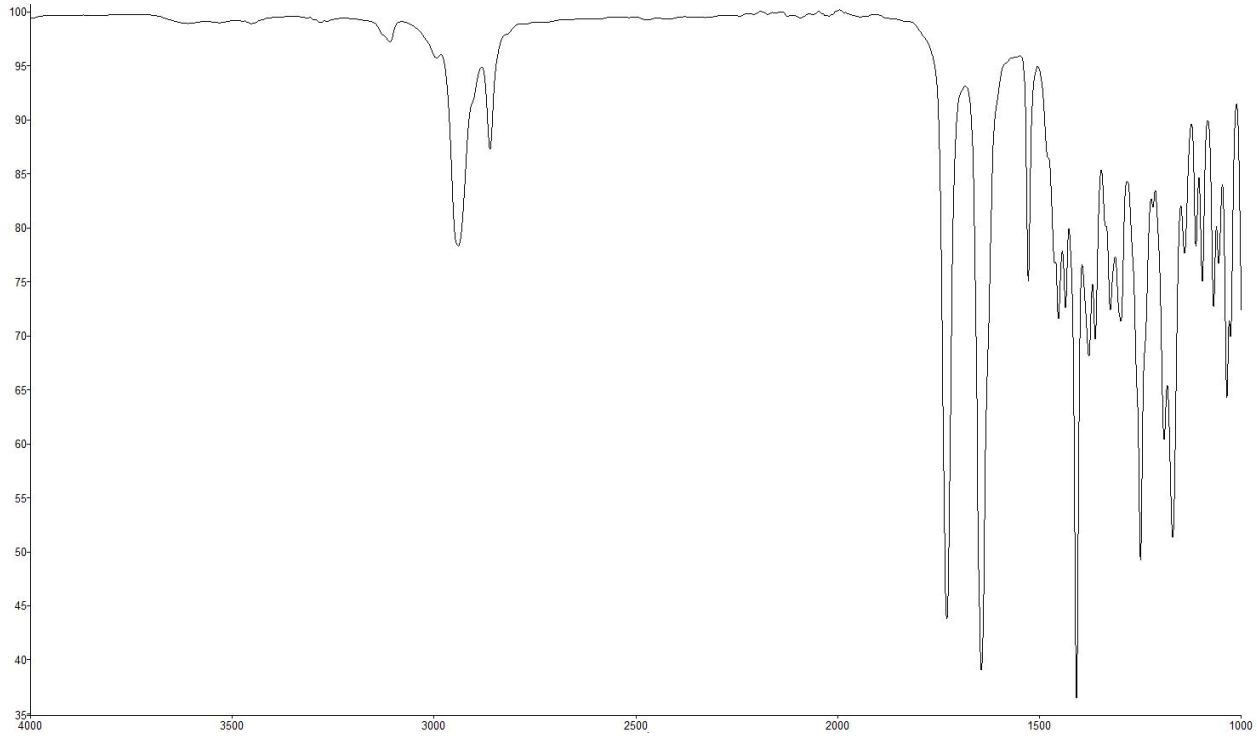

Figure 4.75 Infrared spectrum of compound **4.27**.

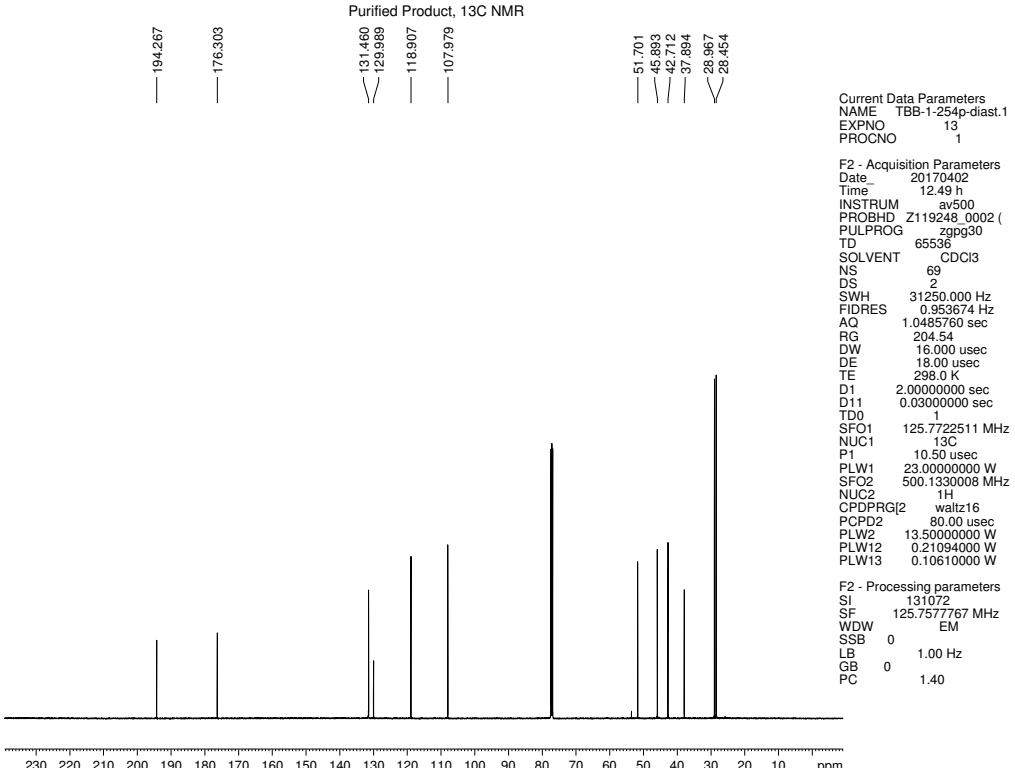

Figure 4.76 ^{13}C NMR (125 MHz, $CDCl_3$) of compound **4.27**.

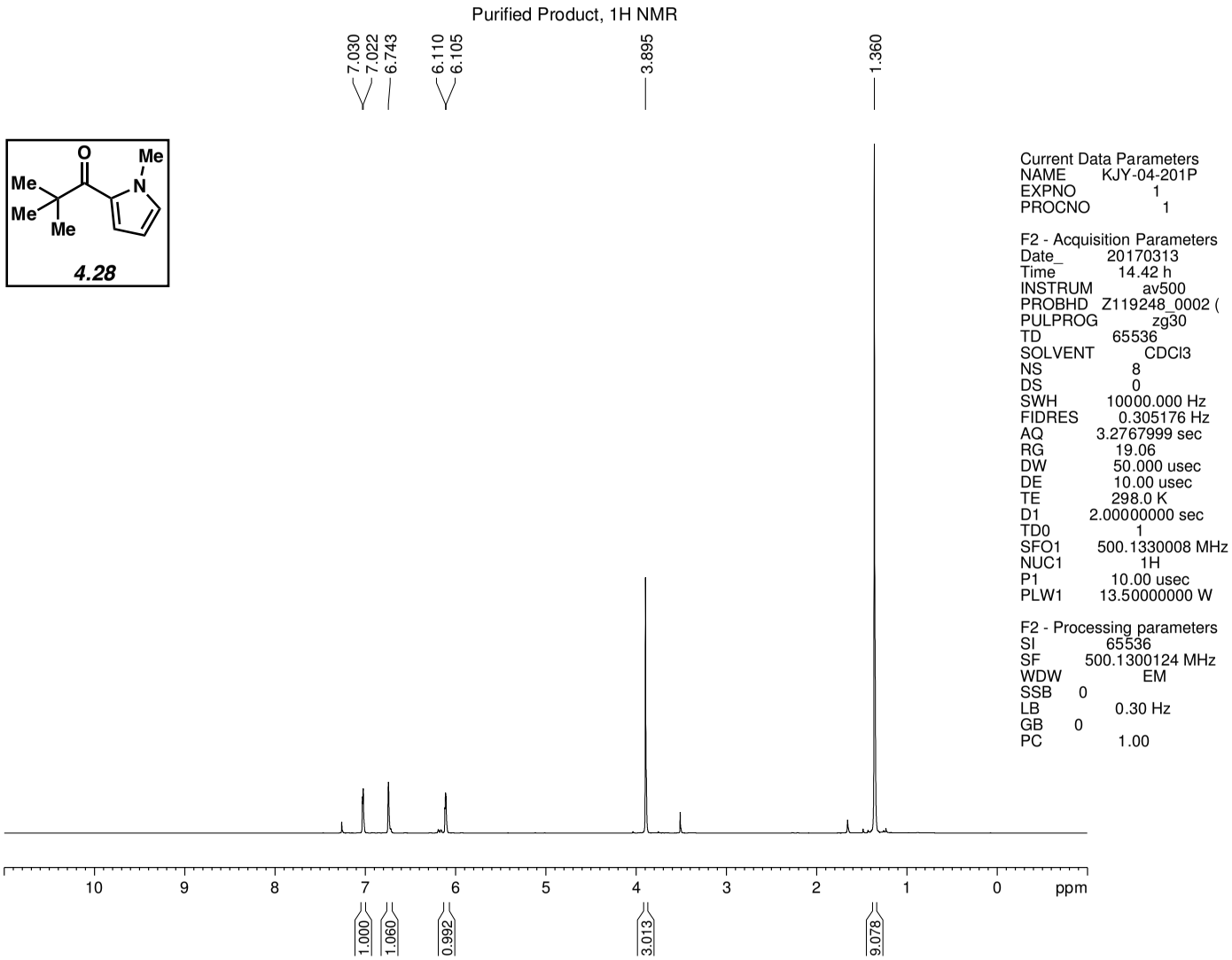

Figure 4.77 ^{1}H NMR (500 MHz, $CDCl_3$) of compound **4.28**.

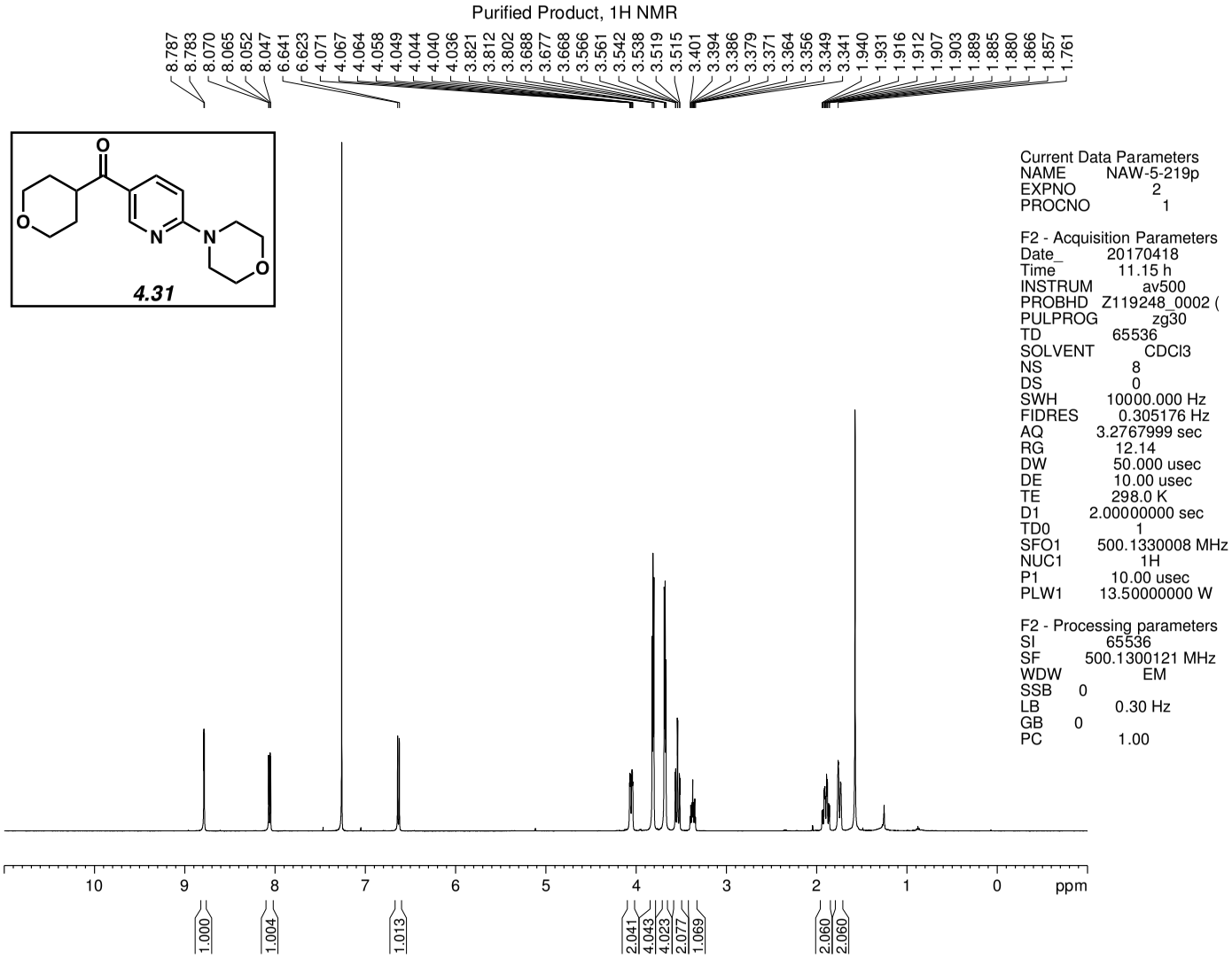

Figure 4.78 ^{1}H NMR (500 MHz, $CDCl_3$) of compound **4.31**.

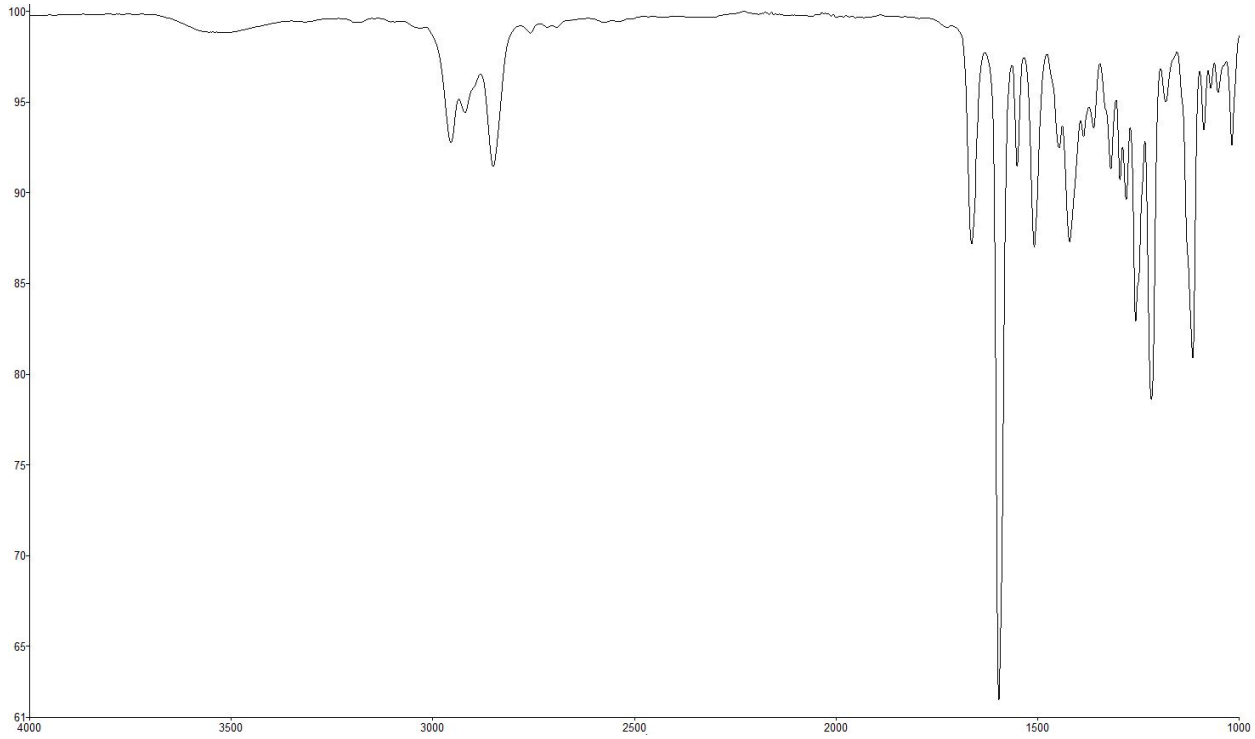

Figure 4.79 Infrared spectrum of compound **4.31**.

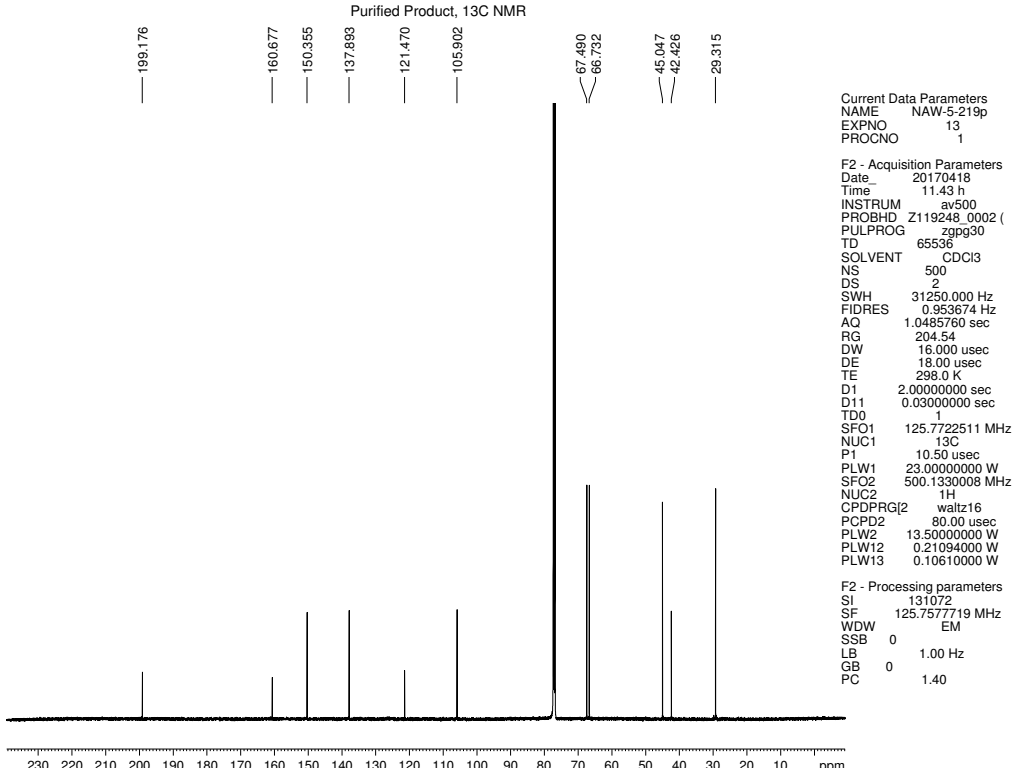

Figure 4.80 ^{13}C NMR (125 MHz, $CDCl_3$) of compound **4.31**.

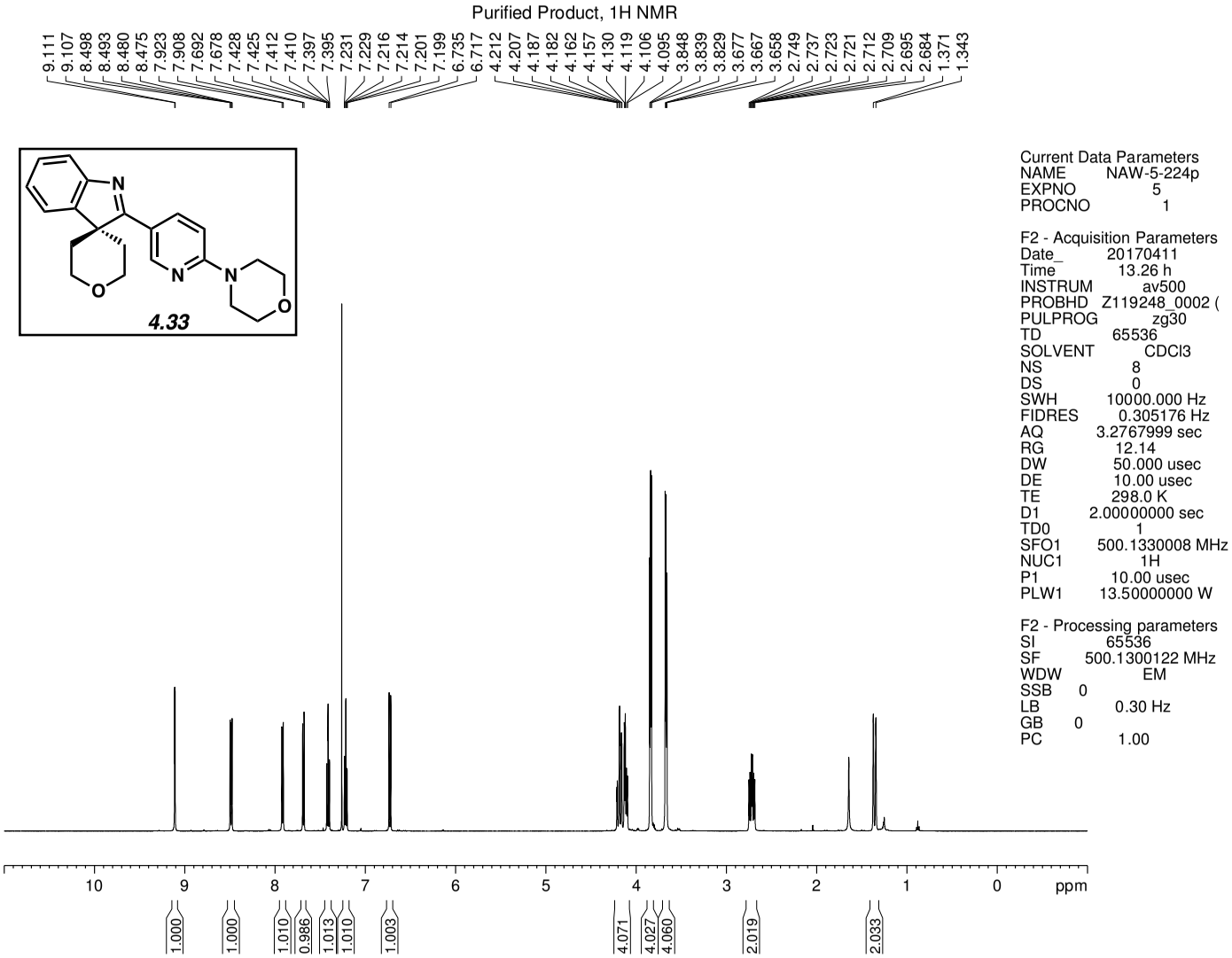

Figure 4.81 ^{1}H NMR (500 MHz, $CDCl_3$) of compound **4.33**.

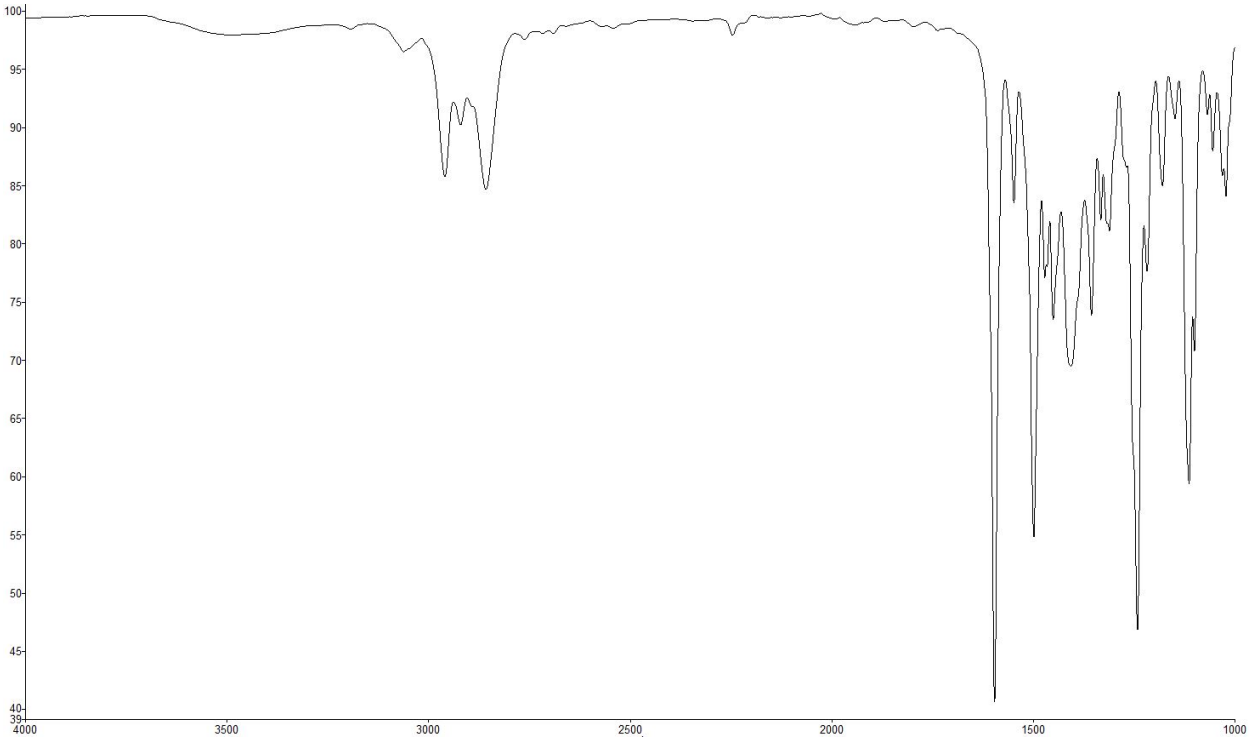

Figure 4.82 Infrared spectrum of compound **4.33**.

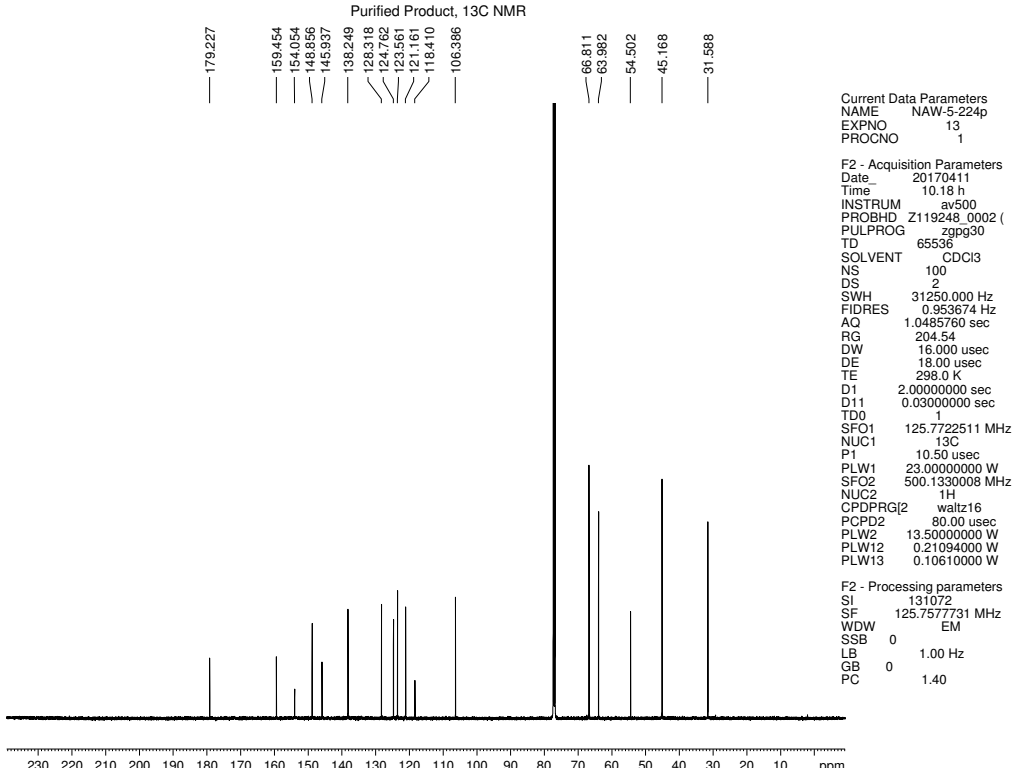

Figure 4.83 ^{13}C NMR (125 MHz, $CDCl_3$) of compound **4.33**.

4.10 Notes and References

(1) (a) Kotschy, A.; Timári, T. *Heterocycles from Transition Metal Catalysis: Formation and Functionalization*; Springer: Dordrecht, 2005. (b) *Metal-Catalyzed Cross-Coupling Reactions*; 2nd ed.; de Meijere, A., Diederich, F., Eds.; Wiley-VCH: Weinheim, 2004. (c) *Modern Arylation Methods*; Ackermann, L.; Ed.; Wiley-VCH: Weinheim, 2009. (d) Schröter, S.; Stock, C.; Bach, T. *Tetrahedron* **2005**, *61*, 2245–2267.

(2) Roughley, S. D.; Jordan, A. M. *J. Med. Chem.* **2011**, *54*, 3451–3479.

(3) Vitaku, E.; Smith, D. T.; Njardarson, J. T. *J. Med. Chem.* **2014**, *57*, 10257–10274.

(4) For selected examples, see: (a) Faul, M. M.; Winneroski, L. L. *Tetrahedron Lett.* **1997**, *38*, 4749–4752. (b) Bercot, E. A.; Rovis, T. *J. Am. Chem. Soc.* **2005**, *127*, 247–254. (c) Rieke, R. D.; Kim, S.-H. *Tetrahedron Lett.* **2011**, *52*, 1128–1131. (d) Jung, H.-S.; Cho, H.-H.; Kim, S.-H. *Tetrahedron Lett.* **2013**, *54*, 960–964. (e) Kobatake, T.; Yoshida, S.; Yorimitsu, H.; Oshima, K. *Angew. Chem. Int. Ed.* **2010**, *49*, 2340–2343. (f) Kim, S.-H.; Rieke, R. D. *Tetrahedron* **2010**, *66*, 3135–3146.

(5) For selected examples, see: (a) Tretyakov, E. V.; Romanenko, G. V.; Veber, S. L.; Redin, M. V.; Polushkin, A. V.; Tkacheva, A. O.; Ovcharenko, V. I. *Aust. J. Chem.* **2015**, *68*, 970–980. (b) Eicher, T.; Massonne, K.; Herrmann, M. *Synthesis* **1991**, 1173–1176. (c) Cherry, K.; Lebegue, N.; Leclerc, V.; Carato, P.; Yous, S.; Berthelot, P. *Tetrahedron Lett.* **2007**, *48*, 5751–5753. (d) Yamamoto, Y.; Yanagi, A. *Chem. Pharm. Bull.* **1982**, *30*, 2003–2010. (e) Golubev, A. S.; Sewald, N.; Burger, K. *Tetrahedron* **1996**, *52*, 14757–14776.

(6) (a) Gooßen, L. J.; Ghosh, K. *Angew. Chem. Int. Ed.* **2001**, *40*, 3458–3460. (b) Gooßen, L. J.; Ghosh, K. *Eur. J. Org. Chem.* **2002**, 3254–3257. (c) Yang, H.; Li, H.; Wittenberg, R.; Egi,

M.; Huang, W.; Liebeskind, L. S. *J. Am. Chem. Soc.* **2007**, *129*, 1132–1140. (d) Lovell, K. M.; Vasiljevik, T.; Araya, J. J.; Lozama, A.; Prevatt-Smith, K. M.; Day, V. W.; Dersch, C. M.; Rothman, R. B.; Butelman, E. R.; Kreek, M. J.; Prisinzano, T. E. *Bioorg. Med. Chem.* **2012**, *20*, 3100–3110. (e) Haddach, M.; McCarthy, J. R. *Tetrahedron Lett.* **1999**, *40*, 3109–3112. (f) Nique, F.; Hebbe, S.; Triballeau, N.; Peixoto, C.; Lefrancois, J.-M.; Jary, H.; Alvey, L.; Manioc, M.; Housseman, C.; Klaassen, H.; Van Beeck, K.; Guedin, D.; Namour, F.; Minet, D.; Van Der Aar, E.; Feyen, J.; Fletcher, S.; Blanque, R.; Robin-Jagerschmidt, C.; Deprez, P. *J. Med. Chem.* **2012**, *55*, 8236–8247.

(7) For nickel-catalyzed reactions involving cleavage of the amide C–N bond, see: (a) Hie, L.; Fine Nathel, N. F.; Shah, T.; Baker, E. L.; Hong, X.; Yang, Y.-F.; Liu, P.; Houk, K. N.; Garg, N. K. *Nature* **2015**, *524*, 79–83. (b) Weires, N. A.; Baker, E. L.; Garg, N. K. *Nat. Chem.* **2016**, *8*, 75–79. (c) Baker, E. L.; Yamano, M. M.; Zhou, Y.; Anthony, S. M.; Garg, N. K. *Nat. Commun.* **2016**, *7*, 11554. (d) Simmons, B. J.; Weires, N. A.; Dander, J. E.; Garg, N. K. *ACS Catal.* **2016**, *6*, 3176–3179. (e) Dander, J. E.; Weires, N. A.; Garg, N. K. *Org. Lett.* **2016**, *18*, 3934–3936. (f) Shi, S.; Szostak, M. *Org. Lett.* **2016**, *18*, 5872–5875. (g) Shi, S.; Szostak, M. *Chem. Eur. J.* **2016**, *22*, 10420–10424. (h) Dey, A.; Sasmal, S.; Seth, K.; Lahiri, G. K.; Maiti, D. *ACS Catal.* **2017**, *7*, 433–437. (i) Ni, S.; Zhang, W.; Mei, H.; Han, J.; Pan, Y. *Org. Lett.* **2017**, *19*, 2536–2539. (j) Medina, J. M.; Moreno, M.; Racine, S.; Du, S.; Garg, N. K. *Angew. Chem. Int. Ed.* **2017**, *56*, 6567–6571. (k) For a recent review, see: Dander, J. E.; Garg, N. K. *ACS Catal.* **2017**, *7*, 1413–1423.

(8) For the nickel-catalyzed decarbonylative coupling of amides with arylboronic esters, see: Shi, S.; Meng, G.; Szostak, M. *Angew. Chem. Int. Ed.* **2016**, *55*, 6959–6963.

(9) For the nickel-catalyzed decarbonylative borylation of amides, see: Hu, J.; Zhao, Y.; Liu, J.; Zhang, Y.; Shi, Z. *Angew. Chem. Int. Ed.* **2016**, *55*, 8718–8722.

(10) For palladium-catalyzed C–C bond forming reactions of amides, see: (a) Li, X.; Zou, G. *Chem. Commun.* **2015**, *51*, 5089–5092. (b) Li, X.; Zou, G. *J. Organomet. Chem.* **2015**, *794*, 136–145. (c) Meng, G.; Szostak, M. *Org. Biomol. Chem.* **2016**, *14*, 5690–5705. (d) Meng, G.; Szostak, M. *Org. Lett.* **2016**, *18*, 796–799. (e) Meng, G.; Szotak, M. *Angew. Chem. Int. Ed.* **2015**, *54*, 14518–14522. (f) Meng, G.; Szostak, M. *Org. Lett.* **2015**, *17*, 4364–4367. (g) Liu, C.; Meng, G.; Liu, Y.; Liu, R.; Lalancette, R.; Szostak, R.; Szostak, M. *Org. Lett.* **2016**, *18*, 4194–4197. (h) Lei, P.; Meng, G.; Szostak, M. *ACS Catal.* **2017**, *7*, 1960–1965. (i) Liu, C.; Liu, Y.; Liu, R.; Lalancette, R.; Szostak, R.; Szostak, M. *Org. Lett.* **2017**, *19*, 1434–1437. (j) Liu, C.; Meng, G.; Szostak, M. *J. Org. Chem.* **2016**, *81*, 12023–12030. (k) Meng, G.; Shi, S.; Szostak, M. *ACS Catal.* **2016**, *6*, 7335–7339. (l) Cui, M.; Wu, H.; Jian, J.; Wang, H.; Liu, C.; Stelck, D.; Zeng, Z. *Chem. Commun.* **2016**, *52*, 12076–12079. (j) Wu, H.; Li, Y.; Cui, M.; Jian, J.; Zeng, Z. *Adv. Synth. Catal.* **2016**, *358*, 3876–3880.

(11) For the nickel-catalyzed esterification of aliphatic amides, see: Hie, L.; Baker, E. L.; Anthony, S. M.; Desrosiers, J.-N.; Senanayake, C.; Garg, N. K. *Angew. Chem. Int. Ed.* **2016**, *55*, 15129–15132.

(12) For nickel / photoredox dual-catalyzed C–C bond formation from aliphatic amides, see: Amani, J.; Alam, R.; Badir, S.; Molander, G. A. *Org. Lett.* **2017**, *19*, 2426–2429.

(13) For pertinent reviews on nickel catalysis, see: (a) Rosen, B. M.; Quasdorf, K. W.; Wilson, D. A.; Zhang, N.; Resmerita, A.-M.; Garg, N. K.; Percec, V. *Chem. Rev.* **2011**, *111*, 1346–1416. (b) Tasker, S. Z.; Standley, E. A.; Jamison, T. F. *Nature* **2014**, *509*, 299–309. (c) Mesganaw,

T.; Garg, N. K. *Org. Process Res. Dev.* **2013**, *17*, 29–39. (d) Ananikov, V. P. *ACS Catal.* **2015**, *5*, 1964–1971.

(14) Nahm, S.; Weinreb, S. M. *Tetrahedron Lett.* **1981**, *22*, 3815–3818.

(15) For the classic Fischer indole synthesis, see: (a) Fischer, E.; Jourdan, F. *Ber. Dtsch. Chem. Ges.* **1883**, *16*, 2241–2245. (b) Fischer, E.; Hess, O. *Ber. Dtsch. Chem. Ges.* **1884**, *17*, 559–568.

(16) Allwood, D. M.; Blakemore, D. C.; Ley, S. V. *Org. Lett.* **2014**, *16*, 3064–3067.

(17) Wakeham, R. J.; Taylor, J. E.; Bull, S. D.; Morris, J. A.; Williams, J. M. J.; *Org. Lett.* **2013**, *15*, 702–705.

(18) Clerici, F.; Gelmi, M. L.; Rossi, L. M. *Synthesis* **1987**, 1025–1027.

(19) Barbero, M.; Cadamuro, S.; Degani, I.; Fochi, R.; Gatti, A.; Regondi, V. *J. Org. Chem.* **1988**, *53*, 2245–2250.

(20) Taylor, J. E.; Jones, M. D.; Williams, J. M. J.; Bull, S. D. *Org. Lett.* **2010**, *12*, 5740–5743.

CHAPTER FIVE

Nickel-Catalyzed Alkylation of Amide Derivatives

Bryan J. Simmons, Nicholas A. Weires, Jacob E. Dander, and Neil K. Garg.

ACS Catal. **2016**, *6*, 3176–3179.

5.1 Abstract

We report the first catalytic alkylation of amide derivatives, which relies on the use of non-precious metal catalysis. Amide derivatives are treated with organozinc reagents utilizing nickel catalysis to yield ketone products. The methodology is performed at ambient temperature and is tolerant of variation in both coupling partners. A precursor to a nanomolar glucagon receptor modulator was synthesized using the methodology, underscoring the mild nature of this chemistry and its potential utility in pharmaceutical synthesis. These studies are expected to further promote the use of amides as synthetic building blocks.

5.2 Introduction

The ability to activate traditionally unreactive functional groups as synthons continues to be a vital area of research. One particularly stable functionality is the amide.[1] The resonance stabilization of amides has been well understood for decades;[1,2] consequently, the use of amides in C–N bond cleavage reactions has remained limited. Recently, however, there has been much interest in breaking amide C–N bonds to forge new C–heteroatom and C–C bonds.[3,4,5,6,7] Such methodologies provide new tactics to prepare acyl derivatives, but with the key benefit of amide stability. The use of amides in multistep synthesis, followed by selective C–N bond activation and coupling, should ultimately prove advantageous in the synthesis of complex molecules.

The present study focuses on activating and coupling amides to build acyl C–C bonds in an intermolecular fashion (Figure 5.1). Such catalytic methodology would complement Weinreb amide chemistry, but without the use of highly basic and pyrophoric organometallic reagents.[8] Prior contributions in this area include Suzuki–Miyaura couplings (**5.1→5.2**) reported by Zou (Pd),[4] Szostak (Pd),[5] and our laboratory (Ni).[3b] In each of these cases, the nucleophilic coupling partner was restricted to *aryl* boronate species, thus limiting the application of this methodology. The corresponding *alkylative* coupling (**5.1→5.3**) would be highly desirable given the prevalence of alkyl ketones in molecules of biological importance and the versatility of alkyl ketones as synthetic building blocks. Herein, we report the first alkylative cross-coupling of amide derivatives.

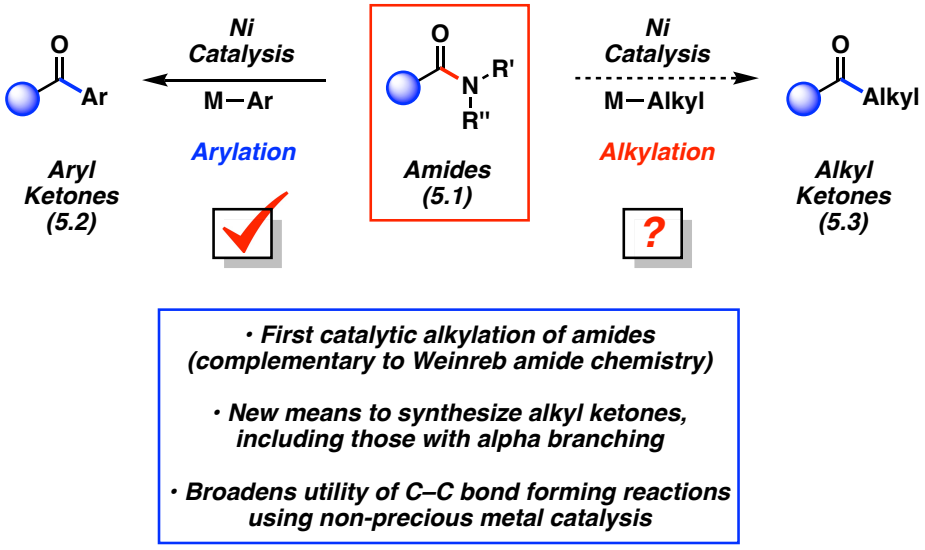

Figure 5.1. Nickel-catalyzed C–C bond forming reactions from amides.

Following unsuccessful attempts to couple amide derivatives with aliphatic boronic acids and esters, we opted to pursue the use of organozinc reagents as cross-coupling partners.[9] Our

earlier studies have relied on the use of nickel catalysis for amide C–N bond activation,[3] which is notable given that nickel is less expensive, more abundant, and displays a lower CO_2 footprint compared to its precious metal counterpart, palladium.[10] Catalytic acyl couplings[11] with organozinc reagents are well precedented using acid halides (Pd or Ni),[12] anhydrides (Pd, Ni, or Rh),[12a,13] and thioesters (Pd or Ni),[12a,b,14] but the corresponding coupling of amides has not been reported.

5.3 Development of the Coupling Using Amides with Various *N*-Substituents

To initiate our study, we examined the coupling of naphthamides **5.4** with benzylzinc bromide (**5.5**) in the presence of catalytic $Ni(cod)_2$ and the NHC ligand SIPr in THF (Scheme 5.1). Although several amide derivatives failed to undergo the coupling (entries 1–3), we were delighted to find that *N*-alkyl,Boc and *N*-alkyl,Ts derivatives could be utilized (entries 4–5, respectively).[15] *N*-Alkyl,Ts amides (e.g., **5.4e**) are well suited for use in multistep synthesis.[16] It should be noted that the successful reactions of **5.4d** and **5.4e** proceeded at room temperature, which compares favorably to the few existing examples of catalytic amide C–N bond activation (ca. 50–160 °C)[3,4,5,6,7] and highlights the mild nature of this coupling.

Scheme 5.1

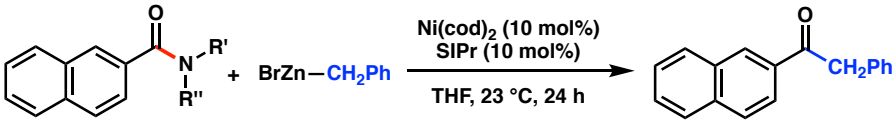

5.4 *5.5* *5.6*

Entry		*Recovered 5.4*	*Yield of Ketone 5.6*[b]
1	*5.4a*	*100%*	*0%*
2	*5.4b*	*51%*	*0%*
3	*5.4c*	*100%*	*0%*
4	*5.4d*	*40%*	*60%*
5	*5.4e*	*17%*	*81%*

[a] Conditions: $Ni(cod)_2$ (10 mol%), SIPr (10 mol%), substrate **5.4** (1.0 equiv), benzylzinc bromide (**5.5**, 1.5 equiv) and THF (1.0 M) at 23 °C for 24 h. [b] Yields determined by ^1H NMR analysis using hexamethylbenzene as an internal standard.

5.4 Scope of the Coupling with Respect to the Amide Substrate

Having found that the alkylative coupling of amide derivatives was indeed possible,[17] we evaluated the scope of the amide substrate (Figure 5.2). The use of the parent naphthyl substrate gave **5.6** in 80% isolated yield. Additionally, it was found that the methodology was not restricted to extended aromatics. For example, the substrate derived from benzoic acid coupled smoothly to furnish **5.7** in 74% yield. Substrates bearing electron-donating groups could also be employed, as demonstrated by the formation of **5.8**–**5.10**. From the latter two cases, it should be

emphasized that the presence of tertiary amines does not hinder catalysis. As shown by the formation of **5.11** and **5.12**, the electron-withdrawing –F and –CF_3 substituents were also tolerated.[18]

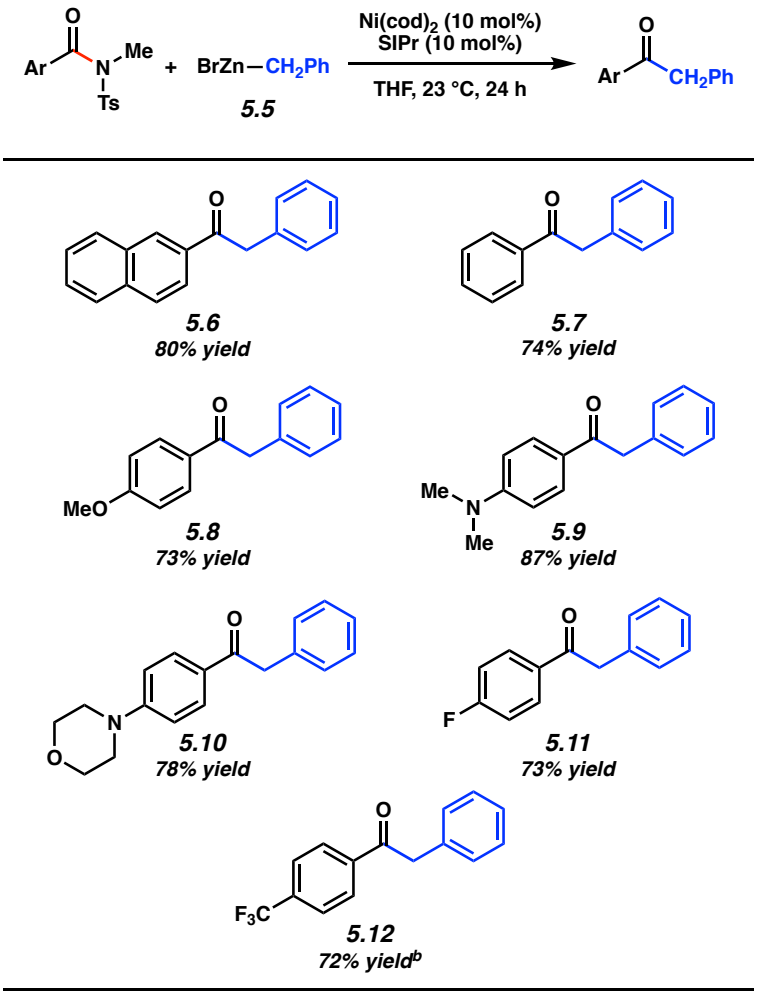

Figure 5.2. Scope of the amide substrate.[a]

[a] Conditions unless otherwise stated: $Ni(cod)_2$ (10 mol%), SIPr (10 mol%), substrate (1.0 equiv), benzylzinc bromide (**5.5**, 1.5 equiv) and THF (1.0 M) at 23 °C for 24 h. Yields shown reflect the average of two isolation experiments. [b] The corresponding *N*-Bn,Boc benzamide derivative was used.

5.5 Scope of the Coupling with Respect to the Organozinc Species

We also examined the scope of the organozinc reagent in this methodology (Figure 5.3).[19,20] *n*-Propylzinc bromide was successfully employed to furnish **5.13** in 80% yield. To assess the tolerance of the methodology toward b-branching, neopentylzinc iodide, a very hindered nucleophile was tested and found to undergo the desired coupling to furnish **5.14**. a-Branched nucleophiles could also be employed, as judged by the formation of **5.15** and **5.16**. Notably, couplings utilizing secondary organozinc reagents are known to be challenging.[21] Finally, cyclopentyl and cyclohexyl organozinc reagents underwent the desired coupling in good yield to deliver products **5.17** and **5.18**, respectively.

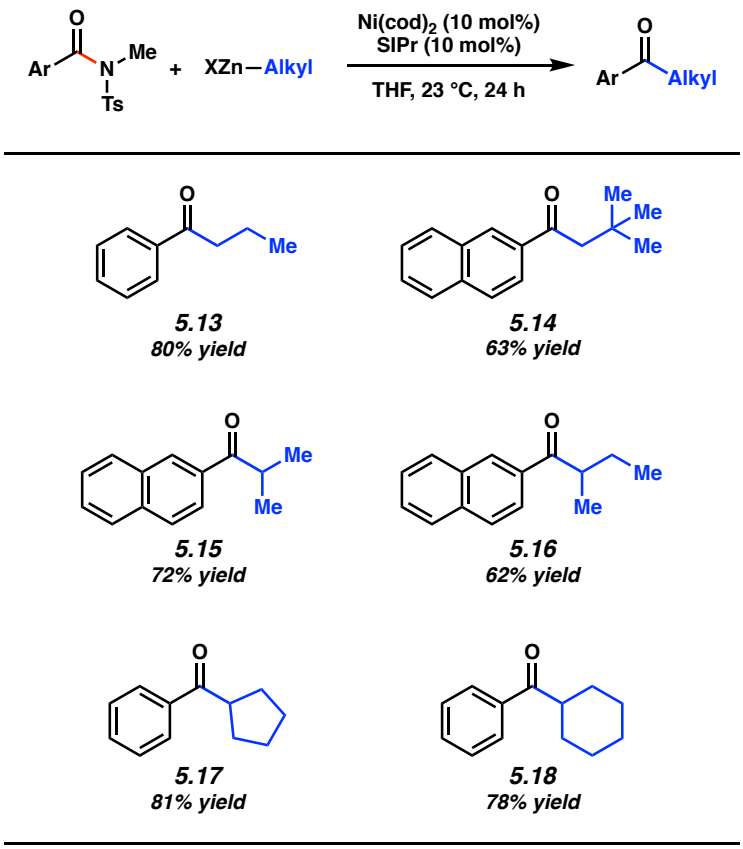

Figure 5.3. Scope of the organozinc coupling partner.[a]

[a] Conditions unless otherwise stated: $Ni(cod)_2$ (10 mol%), SIPr (10 mol%), substrate (1.0 equiv), organozinc reagent (1.5 equiv) and THF (1.0 M) at 23 °C for 24 h. Yields shown reflect the average of two isolation experiments.

5.6 Demonstration of Coupling on Gram Scale

The alkylative cross-coupling methodology was further probed in a synthetic application (Scheme 5.2). On gram-scale, amide derivative **5.19** was coupled with cyclohexylzinc iodide (**5.20**) using our optimal nickel-catalyzed reaction conditions. This transformation provided ketone **5.21** in 71% yield without disturbing the ester.[22] Ketone **5.21** is an intermediate in Pfizer's synthesis of the glucagon receptor modulator **5.22**.[23] The cross-coupling route to **5.21** provides a

favorable alternative to the known Weinreb amide displacement chemistry described in the literature, which proceeds in 34% yield.[23]

Scheme 5.2

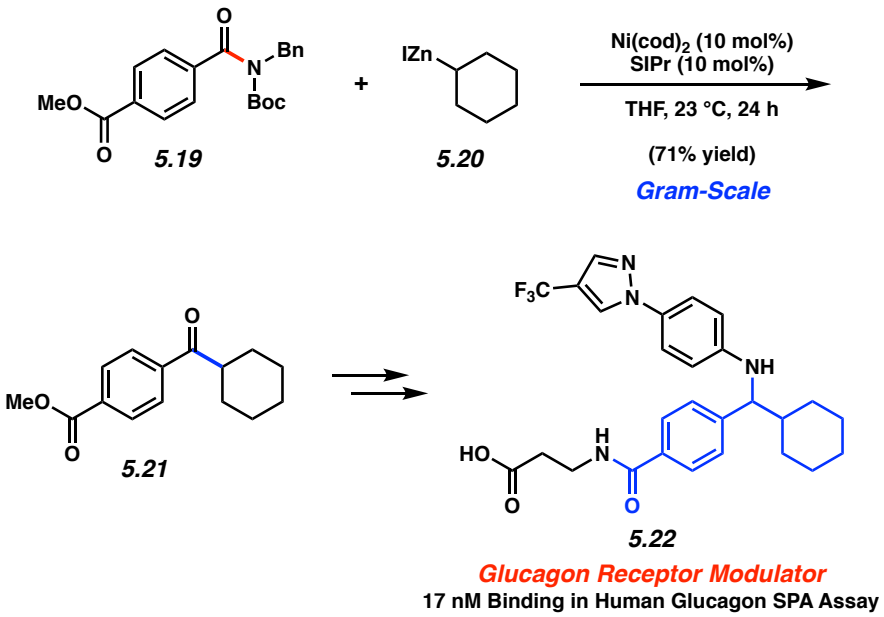

5.7 Conclusion

In summary, we have developed the first catalytic alkylation of amide derivatives. The transformation involves the coupling of *N*-alkyl,Ts or *N*-alkyl,Boc amides with organozinc reagents using nickel catalysis. The methodology proceeds at room temperature and is tolerant of variation in both the substrate and nucleophilic coupling partner. The synthesis of **5.21** underscores the mildness and scalability of this methodology, along with the applicability of this technology to pharmaceutical synthesis. As such, we expect these studies will further promote the use of amides as synthetic building blocks for use in drug and natural product synthesis.

5.8 Experimental Section

5.8.1 Materials and Methods

Unless stated otherwise, reactions were conducted in flame-dried glassware under an atmosphere of nitrogen and commercially obtained reagents were used as received. Non-commercially available substrates were synthesized following protocols specified in Section 5.8.2.1 in the Experimental Procedures. Prior to use, tetrahydrofuran was purified by distillation and taken through five freeze-pump-thaw cycles. Iodine was obtained from Spectrum Chemical. Benzyl bromide, 1-bromopropane, 1-iodo-2,2-dimethylpropane, 2-bromopropane, 2-bromobutane, iodocyclohexane, bromocyclopentane, acid chlorides **5.23**, **5.27**, and carboxylic acid **5.25** were obtained from Sigma–Aldrich and used as received. *N*,4-Dimethylbenzenesulfonamide (**5.24**) and carboxylic acid **5.29** were obtained from Combi-Blocks. $Ni(cod)_2$, SIPr, and Zn powder (325 mesh, 99.9%) were obtained from Strem Chemicals and stored in a glove box. Anhydrous lithium chloride (99%) was obtained from Alfa Aesar and stored in a glove box. Chlorotrimethylsilane and 1,2-dibromoethane were obtained from Alfa Aesar and Sigma–Aldrich, respectively, and distilled before use. Reaction temperatures were controlled using an IKAmag temperature modulator, and unless stated otherwise, reactions were performed at room temperature (approximately 23 °C). Thin-layer chromatography (TLC) was conducted with EMD gel 60 F254 pre-coated plates (0.25 mm for analytical chromatography and 0.50 mm for preparative chromatography) and visualized using a combination of UV, anisaldehyde, and potassium permanganate staining techniques. Silicycle Siliaflash P60 (particle size 0.040–0.063 mm) was used for flash column chromatography. ^{1}H NMR spectra were recorded on Bruker spectrometers (at 300, 400 and 500 MHz) and are reported relative to residual solvent signals. Data for ^{1}H NMR spectra are reported as follows: chemical shift (δ

ppm), multiplicity, coupling constant (Hz), integration. Data for ^{13}C NMR are reported in terms of chemical shift (at 75 and 125 MHz). ^{19}F NMR spectra were recorded on Bruker spectrometers (at 282 MHz) and reported in terms of chemical shift (δ ppm). IR spectra were recorded on a Perkin-Elmer UATR Two FT-IR spectrometer and are reported in terms of frequency absorption (cm^{-1}). High-resolution mass spectra were obtained on Thermo Scientific™ Exactive Mass Spectrometer with DART ID-CUBE.

5.8.2 Experimental Procedures

5.8.2.1 Syntheses of Amide Substrates

Representative Procedure A for the synthesis of amide substrates from Scheme 5.1, Figures 5.2 and 5.3 (synthesis of amide 5.4e is used as an example).

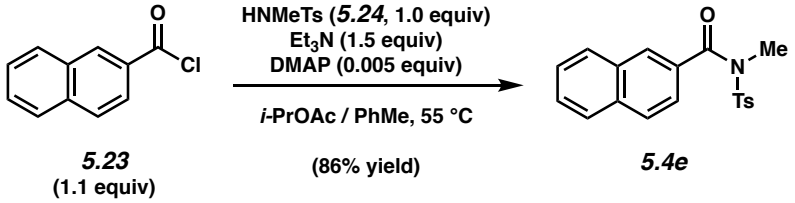

To a solution of sulfonamide **5.24** (3.00 g, 16.2 mmol, 1.0 equiv), DMAP (9.9 mg, 0.081 mmol, 0.005 equiv), triethylamine (3.40 mL, 24.3 mmol, 1.5 equiv), and *i*-PrOAc (35.2 mL) at 55 °C was added dropwise a solution of acid chloride **5.23** (3.41 g, 17.8 mmol, 1.1 equiv) in toluene (10.0 mL, 0.46 M in total) over 1 min. The reaction mixture was stirred at 55 °C for 1 h. After cooling the reaction mixture to room temperature, the reaction was quenched by the addition of 1.0 M aqueous HCl (10 mL). The resulting biphasic mixture was transferred to a separatory funnel with EtOAc (30 mL) and extracted with EtOAc (3 x 30 mL). The organic layers were combined, dried over Na_2SO_4, and the volatiles were removed under reduced pressure. The resulting crude residue was purified by flash chromatography (24:1

Hexanes:EtOAc → 14:1 Hexanes:EtOAc → 9:1 Hexanes:EtOAc) to yield amide **5.4e** (5.2 g, 86% yield) as a white solid. Amide **5.4e**: mp: 96–98 ºC; R_f 0.50 (7:3 Hexanes:EtOAc); ^{1}H NMR (500 MHz, $CDCl_3$): δ 8.07–8.06 (s, 1H), 7.87–7.84 (m, 5H), 7.62–7.53 (m, 3H), 7.34–7.32 (m, 2H), 3.34 (s, 3H), 2.44 (s, 3H); ^{13}C NMR (125 MHz, $CDCl_3$): δ 171.9, 145.2, 135.6, 135.1, 132.5, 132.0, 130.0, 129.9, 129.3, 128.8, 128.5, 128.5, 128.2, 127.3, 124.9, 36.0, 22.0; IR (film): 3060, 2954, 2922, 1682, 1356 cm^{-1}; HRMS-ESI (*m/z*) $[M + H]^+$ calcd for $C_{19}H_{18}NO_3S$, 340.10074; found 340.09984.

Representative Procedure B for the synthesis of amide substrates from Scheme 5.1, Figures 5.2 and 5.3 (synthesis of amide 5.26 is used as an example).

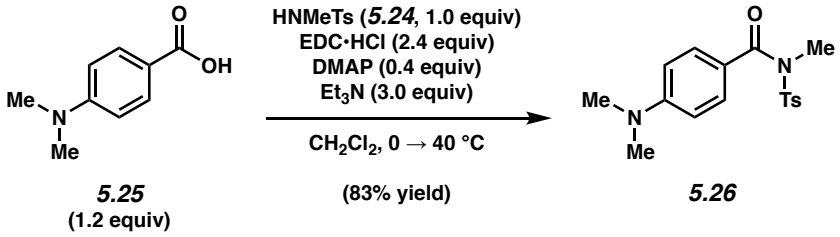

To a solution of sulfonamide **5.24** (1.00 g, 5.40 mmol, 1.0 equiv), EDC•HCl (2.48 g, 13.0 mmol, 2.4 equiv), DMAP (263 mg, 2.16 mmol, 0.4 equiv), triethylamine (2.30 mL, 16.2 mmol, 3.0 equiv), and CH_2Cl_2 (15.4 mL, 0.35 M) at 0 °C was added carboxylic acid **5.25** (1.07 g, 6.48 mmol, 1.2 equiv) as a solid in one portion. The reaction mixture was allowed to come to room temperature and then stirred at 40 °C for 16 h. After cooling to room temperature, the reaction mixture was transferred to a separatory funnel with EtOAc (30 mL) and washed with 1.0 M aqueous HCl (2 x 10 mL), followed by 1.0 M aqueous NaOH (2 x 10 mL), and deionized water (10 mL). The organic layer was dried over Na_2SO_4, and the volatiles were removed under reduced pressure. The resulting crude residue was purified by flash chromatography (20:1

Benzene:Et_2O) to yield amide **5.26** (1.48 g, 83% yield) as an off-white solid. Amide **5.26**: mp: 104–106 ºC; R_f 0.52 (3:2 Hexanes:EtOAc); ^{1}H NMR (500 MHz, $CDCl_3$): δ 7.85 (d, J = 8.2, 2H), 7.65 (d, J = 9.0, 2H), 7.31 (d, J = 8.2, 2H), 6.63 (d, J = 8.9, 2H), 3.20 (s, 3H), 3.05 (s, 6H), 2.43 (s, 3H); ^{13}C NMR (125 MHz, $CDCl_3$): δ 172.0, 153.7, 144.7, 135.5, 132.3, 129.8, 128.8, 120.5, 110.8, 40.4, 36.4, 21.9; IR (film): 3060, 2917, 2823, 1672, 1600 cm^{-1}; HRMS-ESI (*m/z*) [M + H]$^+$ calcd for $C_{17}H_{21}N_2O_3S$, 333.12729; found 333.12611.

Note: Supporting information for the syntheses of some amides shown in Scheme 5.1, Figures 5.2 and 5.3, and Scheme 5.2 have previously been reported: **5.4a**,[24a] **5.4b**,[24b] **5.4c**,[24c] **5.4d**,[24d] **5.36**,[24e] **5.37**,[24f] **5.38**,[24d] and **5.19**.[24d] Syntheses for the remaining substrates shown in Scheme 5.1, Figures 5.2 and 5.3 are as follows:

Any modifications of the conditions shown in the representative procedures above are specified in the following schemes.

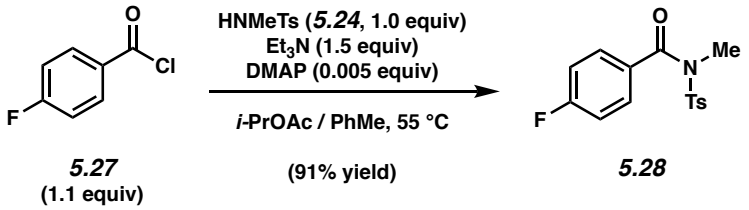

Amide 5.28. Followed representative procedure A. Purification by flash chromatography (9:1 Hexanes:EtOAc) generated amide **5.28** (91% yield) as a white solid. Amide **5.28**: mp: 80–83 °C; R_f 0.54 (7:3 Hexanes:EtOAc); ^{1}H NMR (500 MHz, $CDCl_3$): δ 7.77 (d, J = 8.3, 2H), 7.62–7.59 (m, 2H), 7.33 (d, J = 8.0, 2H), 7.12–7.08 (m, 2H), 3.24 (s, 3H), 2.45 (s, 3H); ^{13}C NMR (125 MHz, $CDCl_3$): δ 171.0, 165.3 (d, J_{C-F} = 253.9), 145.4, 135.3, 131.7 (d, J_{C-F} = 9.1) 131.1 (d, J_{C-F} = 3.3), 130.1, 128.6, 115.8 (d, J_{C-F} = 22.2), 35.8, 22.0; ^{19}F NMR (282 MHz, $CDCl_3$): δ 106.1; IR

(film): 3074, 2954, 2924, 1683, 1596 cm^{-1}; HRMS-ESI (*m/z*) $[M + H]^+$ calcd for $C_{15}H_{15}FNO_3S$, 308.07567; found 308.07463.

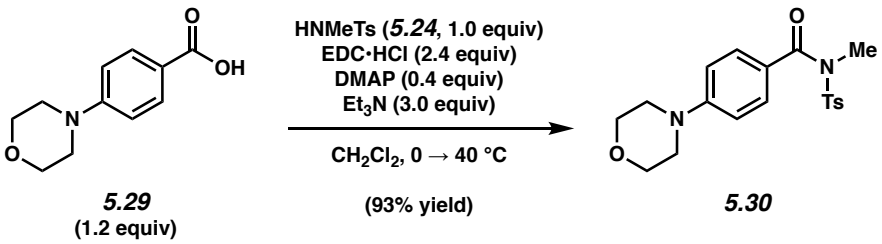

Amide 5.30. Followed representative procedure B. Purification by flash chromatography (1:1 Hexanes:EtOAc) generated amide **5.30** (93% yield) as a white solid. Amide **5.30**: mp: 141–143 ºC; R_f 0.60 (3:7 Hexanes:EtOAc); ^{1}H NMR (500 MHz, $CDCl_3$): δ 7.83 (d, *J* = 8.3, 2H), 7.63 (d, *J* = 8.8, 2H), 7.32 (d, *J* = 8.3, 2H), 6.84 (d, *J* = 8.8, 2H), 3.85 (t, *J* = 4.8, 4H), 3.29 (t, *J* = 4.8, 4H), 3.21 (s, 3H), 2.43 (s, 3H); ^{13}C NMR (125 MHz, $CDCl_3$): δ 171.7, 154.3, 144.9, 135.4, 131.8, 129.9, 128.8, 124.1, 113.5, 66.9, 47.9, 36.3, 22.0; IR (film): 3049, 2964, 2854, 1673, 1601 cm^{-1}; HRMS-ESI (*m/z*) $[M + H]^+$ calcd for $C_{19}H_{23}N_2O_4S$, 375.13785; found 375.13717.

5.8.2.2 Preparation of Organozinc Halides

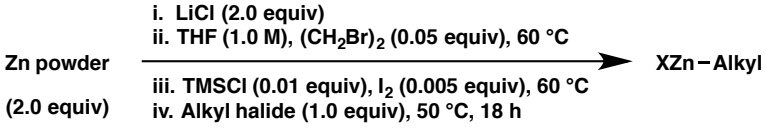

Following a modification of the procedure reported by Knochel,[25] a flame-dried 25 mL round bottom flask equipped with a magnetic stir bar and rubber septum was brought into a glove box where Zn powder (650 mg, 10.0 mmol, 2.0 equiv, Strem 325 mesh) and anhydrous LiCl (420 mg, 10.0 mmol, 2.0 equiv) were added. The flask was then removed from the glove box and heated with a heat gun for 10 min under high vacuum, cooled to room temperature, and then

backfilled with N_2. Freshly distilled THF (5.0 mL) and 1,2-dibromoethane (22 μL, 0.25 mmol, 0.05 equiv) were added via syringe and the reaction mixture was heated at 60 °C for 20 min. After cooling to room temperature, freshly distilled TMSCl (6 μL, 0.05 mmol, 0.01 equiv) followed by a solution of I_2 (6.4 mg, 0.025 mmol, 0.005 equiv) in THF (25 μL, 1.0 M) were added via syringe and the reaction mixture was heated again at 60 °C for 20 min. After cooling to room temperature, the alkyl halide (5.0 mmol, 1.0 equiv) was added dropwise via syringe over 1 min. A flame-dried air condenser was attached to the flask under N_2 and the reaction vessel was heated at 50 °C for 18 h. The reaction mixture was cooled to room temperature and allowed to stand for 1 h before the supernatant fluid was transferred to a flame-dried schlenk flask via syringe. The concentration of the organozinc halide was determined by iodometric titration using Knochel's procedure.[26]

Note: The use of organozinc reagents with lower titers led to lower yields in the subsequent coupling reactions.

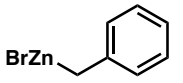

(***5.5***, 0.90–0.94 M)

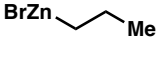

(***5.31***, 0.94 M)

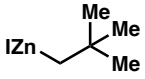

(***5.32***, 0.52 M)

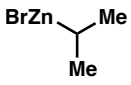

(***5.33***, 0.89 M)

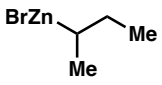

(***5.34***, 0.86 M)

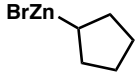

(***5.35***, 0.95 M)

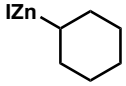

(***5.20***, 0.94 M)

5.8.2.3 Initial Survey of Naphthamide Substrates with Benzylzinc Bromide (5.5)

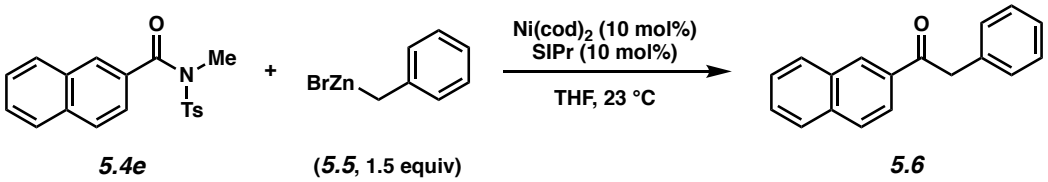

5.4e (*5.5*, 1.5 equiv) *5.6*

Representative Procedure for alkylation reactions of naphthamides from Tables 5.1 and 5.2 (coupling of amide 5.4e and benzylzinc bromide (5.5) is used as an example). A 1-dram vial was charged with a magnetic stir bar and flame-dried under reduced pressure, and then allowed to cool under N_2. Amide substrate **5.4e** (67.8 mg, 0.200 mmol, 1.0 equiv) and hexamethylbenzene (3.2 mg, 0.020 mmol, 0.1 equiv) were added, and the vial was flushed with N_2. The vial was taken into a glove box and charged with $Ni(cod)_2$ (5.5 mg, 0.020 mmol, 10 mol%) and SIPr (7.8 mg, 0.020 mmol, 10 mol%). Subsequently, THF (0.20 mL, 1.0 M) was added, and the vial was removed from the glove box and the reaction was allowed to stir at 23 °C for 1 h. Concurrently, the benzylzinc bromide solution (**5.5**) was heated in a water bath at 50 °C for 1 h. A portion of the preheated solution of **5.5** (333 μL, 0.300 mmol, 1.5 equiv, 0.90 M in THF) was then added to the reaction mixture dropwise via syringe over 3 sec. The vial was then capped with a Teflon-lined screw cap under a flow of N_2. The reaction mixture was allowed to stir at 23 °C for 24 h. The reaction was quenched by the addition of a saturated aqueous solution of NH_4Cl (0.5 mL), and the resulting aqueous layer was extracted with EtOAc (3 x 2 mL). The combined organics were filtered over a plug of silica gel (10 mL of EtOAc eluent). The volatiles were removed under reduced pressure, and the yield was determined by ^1H NMR analysis with hexamethylbenzene as an internal standard.

Any modifications of the conditions shown in the representative procedure above are specified below in Tables 5.1 and 5.2.

Table 5.1. Initial Survey of Naphthamide Substrates with Benzylzinc Bromide (**5.5**).[a]

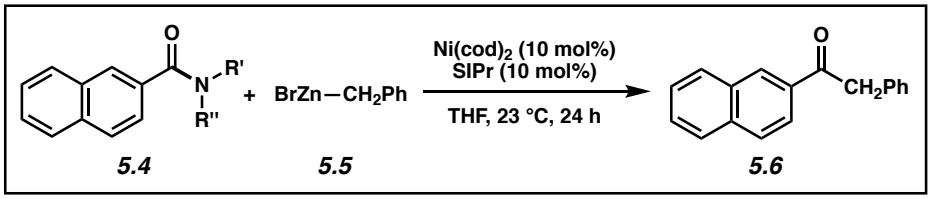

5.4 *5.5* *5.6*

Entry			*Recovered 5.4*	*Yield of Ketone 5.6*
1		*5.4a*	*100%*	*0%*
2	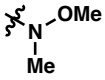	*5.4b*	*51%*	*0%*
3		*5.4c*	*100%*	*0%*
4		*5.4d*	*40%*	*60%*
5		*5.4e*	*17%*	*81%*

[a] Yields were determined by ^{1}H NMR analysis using hexamethylbenzene as an internal standard.

5.8.2.4 Relevant Control Experiments in the Alkylation of Amide 5.4e

Table 5.2. Relevant Control Experiments in the Alkylation of Amide **5.4e**.[a]

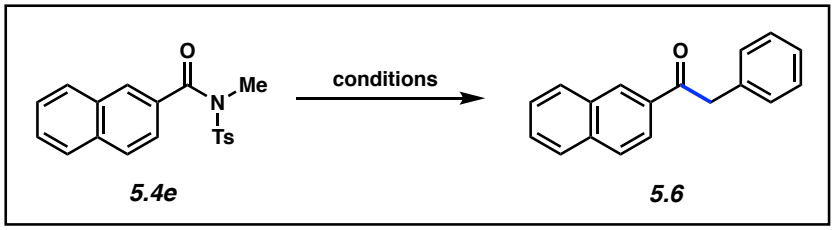

Reaction Conditions	*Experimental Results* 5.4e	5.6
BnZnBr (1.5 equiv), $Ni(cod)_2$ (10 mol%), SIPr (10 mol%) THF (1.0 M), 23 °C, 24 h	17%	81%
Control Experiments:		
BnZnBr (1.5 equiv) THF (1.0 M), 23 °C, 24 h	100%	0%
BnZnBr (1.5 equiv), SIPr (10 mol%) THF (1.0 M), 23 °C, 24 h	100%	0%
BnZnBr (1.5 equiv), $Ni(cod)_2$ (10 mol%) THF (1.0 M), 23 °C, 24 h	33%	35%[b]

[a] Yields were determined by ^1H NMR analysis using hexamethylbenzene as an internal standard.
[b] Some conversion to the ketone was observed in the absence of SIPr, but in greatly diminished yield relative to the experiment run with both $Ni(cod)_2$ and SIPr. Additionally, use of these conditions with other substrates was even less successful.

5.8.2.5 Scope of Methodology

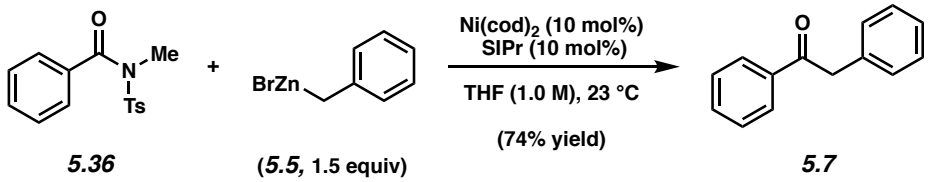

5.36 (*5.5,* 1.5 equiv) *5.7*

Representative Procedure (coupling of amide 5.36 and benzylzinc bromide (5.5) is used as an example). Ketone 5.7. A 1-dram vial was charged with a magnetic stir bar and flame-dried under reduced pressure, and then allowed to cool under N_2. Amide substrate **5.36** (57.8 mg, 0.200 mmol, 1.0 equiv) was added, and the vial was flushed with N_2. The vial was taken into a glove box and charged with $Ni(cod)_2$ (5.5 mg, 0.020 mmol, 10 mol%) and SIPr (7.8 mg, 0.020 mmol, 10 mol%). Subsequently, THF (0.20 mL, 1.0 M) was added, and the vial was removed from the glove box and the reaction was allowed to stir at 23 °C for 1 h. Concurrently, the benzylzinc bromide solution (**5.5**) was heated in a water bath at 50 °C for 1 h. A portion of the preheated solution of **5.5** (319 μL, 0.300 mmol, 1.5 equiv, 0.94 M in THF) was then added to the reaction mixture dropwise via syringe over 3 sec. The vial was then capped with a Teflon-lined screw cap under a flow of N_2. The reaction mixture was allowed to stir at 23 °C for 24 h. The reaction was quenched by the addition of a saturated aqueous solution of NH_4Cl (0.5 mL), and the resulting aqueous layer was extracted with EtOAc (3 x 2 mL). The combined organics were filtered over a plug of silica gel (10 mL of EtOAc eluent). The volatiles were removed under reduced pressure, and the crude residue was purified by preparative thin-layer chromatography (5:1 Hexanes:EtOAc) to yield ketone product **5.7** (74% yield, average of two experiments) as a white solid. Ketone **5.7**: R_f 0.54 (5:1 Hexanes:EtOAc). Spectral data match those previously reported.[27]

Any modifications of the conditions shown in the representative procedure above are specified in the following schemes, which depict all of the results shown in Figures 5.2 and 5.3.

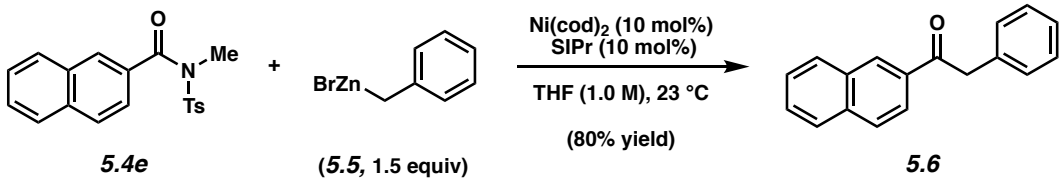

Ketone 5.6. Purification by preparative thin-layer chromatography (5:1 Hexanes:EtOAc) generated ketone **5.6** (80% yield, average of two experiments) as a white solid. Ketone **5.6**: R_f 0.53 (5:1 Hexanes:EtOAc). Spectral data match those previously reported.[27]

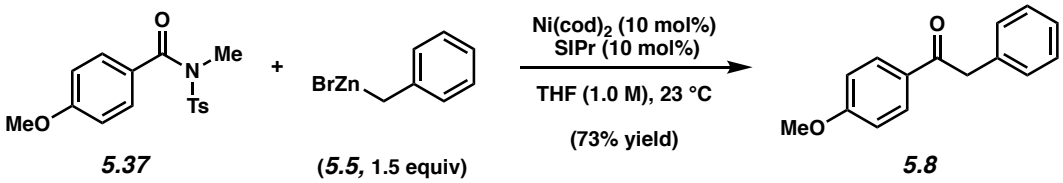

Ketone 5.8. Purification by preparative thin-layer chromatography (4:1 Hexanes:EtOAc) generated ketone **5.8** (73% yield, average of two experiments) as a white solid. Ketone **5.8**: R_f 0.46 (4:1 Hexanes:EtOAc). Spectral data match those previously reported.[28]

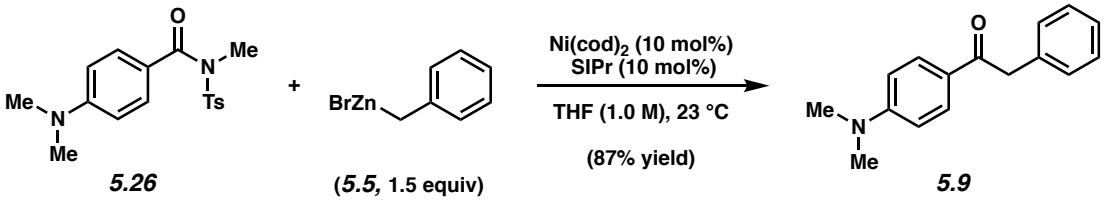

Ketone 5.9. Purification by flash chromatography (8:1:1 PhH:Et_2O:CH_2Cl_2) generated ketone **5.9** (87% yield, average of two experiments) as a white solid. Ketone **5.9**: R_f 0.46 (8:1:1 PhH:Et_2O:CH_2Cl_2). Spectral data match those previously reported.[29]

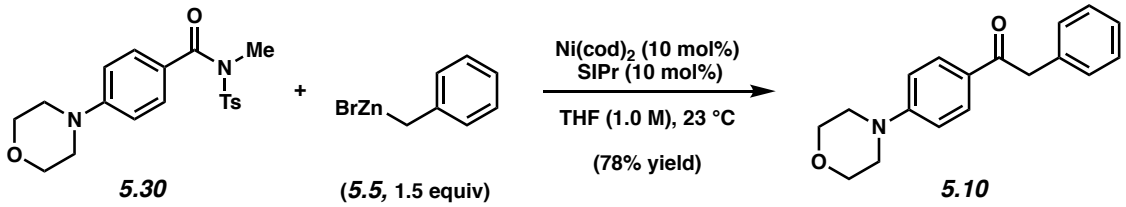

Ketone 5.10. Purification by flash chromatography (10:5:1 $CHCl_3$:Hexanes:CH_3CN) followed by preparative thin-layer chromatography (10:2:1 $CHCl_3$:Hexanes:CH_3CN) generated ketone **5.10** (78% yield, average of two experiments) as a white solid. Ketone **5.10**: mp: 138–139 °C; R_f 0.64 (3:2 Hexanes:EtOAc); ^{1}H NMR (500 MHz, CD_3CN): δ 7.94–7.88 (m, 2H), 7.33–7.19 (m, 5H), 6.95–6.89 (m, 2H), 4.21 (s, 2H), 3.77–3.73 (m, 4H), 3.29–3.24 (m, 4H); ^{13}C NMR (125 MHz, CD_3CN): δ 196.8, 155.5, 137.1, 131.4, 130.6, 129.4, 127.9, 127.4, 114.1, 67.1, 48.1, 45.5; IR (film): 3042, 2957, 2857, 2840, 1675, 1595 cm^{-1}; HRMS-ESI (*m/z*) $[M + H]^+$ calcd for $C_{11}H_8O_2$, 282.14940; found 282.14800.

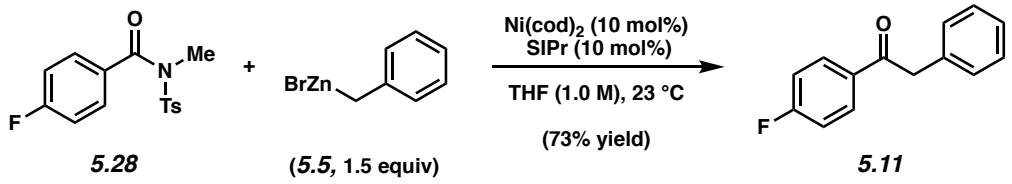

Ketone 5.11. Purification by preparative thin-layer chromatography (5:1 Hexanes:EtOAc) generated ketone **5.11** (73% yield, average of two experiments) as a white solid. Ketone **5.11**: R_f 0.50 (5:1 Hexanes:EtOAc). Spectral data match those previously reported.[27]

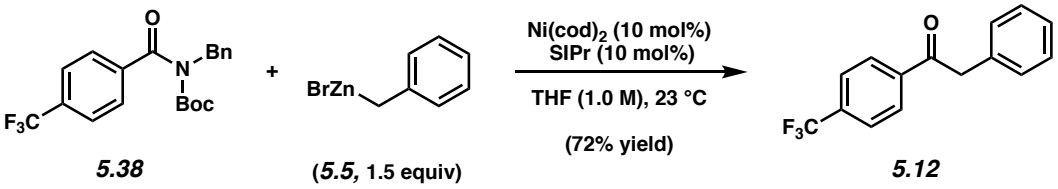

Ketone 5.12. Purification by flash chromatography (100% PhH) generated ketone **5.12** (72% yield, average of two experiments) as a white solid. Ketone **5.12**: R_f 0.68 (100% PhH). Spectral data match those previously reported.[30]

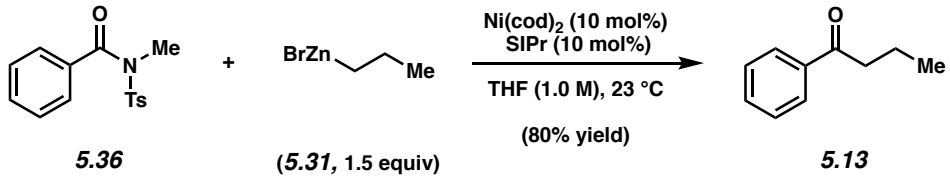

Ketone 5.13. Purification by preparative thin-layer chromatography (5:1 Hexanes:EtOAc) generated ketone **5.13** (80% yield, average of two experiments) as a colorless oil. Ketone **5.13**: R_f 0.57 (5:1 Hexanes:EtOAc). Spectral data match those previously reported.[27]

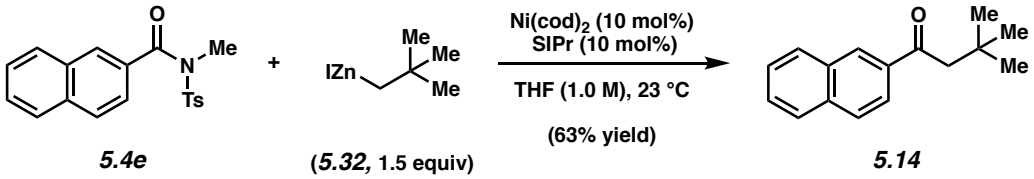

Ketone 5.14. Purification by preparative thin-layer chromatography (5:1 Hexanes:EtOAc) generated ketone **5.14** (63% yield, average of two experiments) as a colorless oil. Ketone **5.14**: R_f 0.63 (5:1 Hexanes:EtOAc). Spectral data match those previously reported.[31]

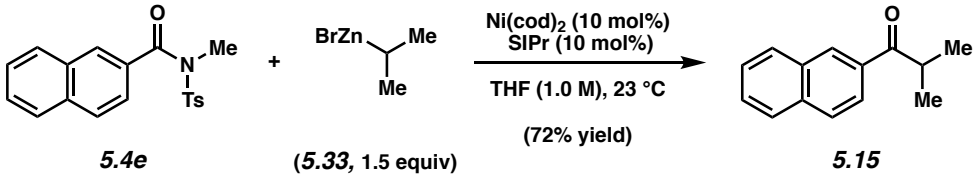

5.4e (*5.33,* 1.5 equiv) *5.15*

Ketone 5.15. Purification by preparative thin-layer chromatography (5:1 Hexanes:EtOAc) generated ketone **5.15** (72% yield, average of two experiments) as a colorless oil. Ketone **5.15**: R_f 0.64 (5:1 Hexanes:EtOAc). Spectral data match those previously reported.[32]

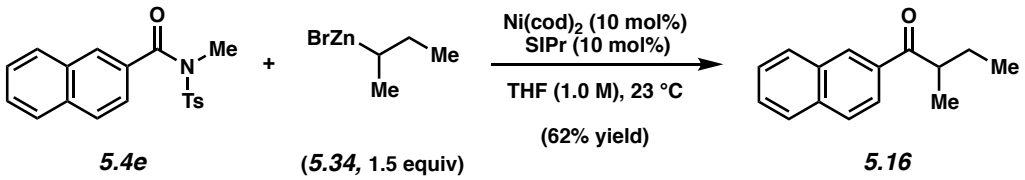

5.4e (*5.34,* 1.5 equiv) *5.16*

Ketone 5.16. Purification by preparative thin-layer chromatography (5:1 Hexanes:EtOAc) generated ketone **5.16** (62% yield, average of two experiments) as a colorless oil. Ketone **5.16**: R_f 0.44 (10:1 Hexanes:EtOAc); ^{1}H NMR (500 MHz, C_6D_6): δ 8.35 (br s, 1H), 8.13 (dd, *J* = 8.6, 1.6, 1H), 7.63 (d, *J* = 7.9, 1H), 7.56 (d, *J* = 8.6, 1H), 7.53 (d, *J* = 7.9, 1H) 7.27–7.19 (m, 1H), 3.26–3.18 (m, 1H), 1.93–1.83 (m, 1H), 1.48–1.38 (m, 1H), 1.14 (d, *J* = 6.9, 3H), 0.83 (t, *J* = 7.5, 3H);^{13}C NMR (125 MHz, CD_3CN): δ 205.3, 136.4, 135.2, 133.7, 130.7, 130.5, 129.5, 129.4, 128.6, 127.8, 125.0, 42.7, 27.6, 17.2, 12.0; IR (film): 3060, 2965, 2932, 2875, 1677, 1625 cm^{-1}; HRMS-ESI (*m/z*) $[M + H]^+$ calcd for $C_{11}H_8O_2$, 213.12794; found 213.12691.

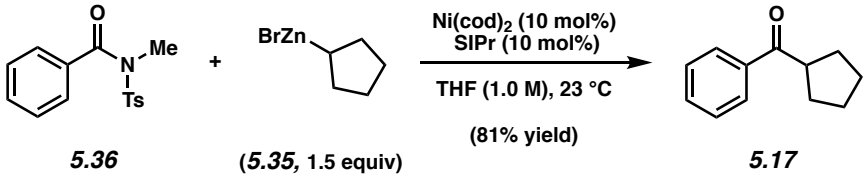

Ketone 5.17. Purification by preparative thin-layer chromatography (5:1 Hexanes:EtOAc) generated ketone **5.17** (81% yield, average of two experiments) as a colorless oil. Ketone **5.17**: R_f 0.64 (5:1 Hexanes:EtOAc). Spectral data match those previously reported.[33]

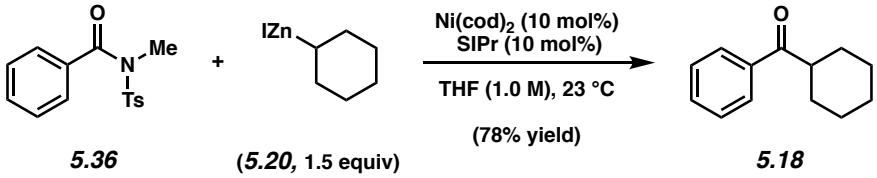

Ketone 5.18. Purification by preparative thin-layer chromatography (5:1 Hexanes:EtOAc) generated ketone **5.18** (78% yield, average of two experiments) as a colorless oil. Ketone **5.18**: R_f 0.54 (5:1 Hexanes:EtOAc). Spectral data match those previously reported.[34]

5.8.2.6 Gram-Scale Alkylation to Form Ketone 5.21

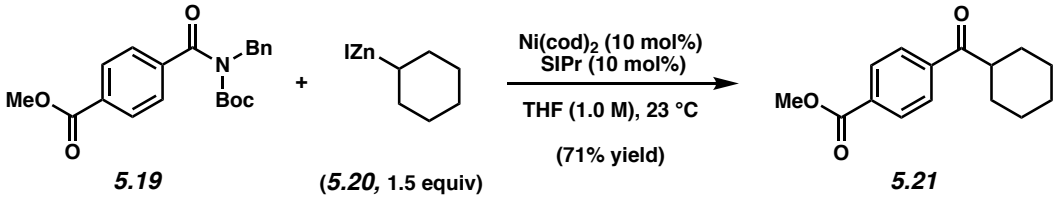

Ketone 5.21. A 20 mL scintillation vial was charged with a magnetic stir bar and flame-dried under reduced pressure, and then allowed to cool under N_2. Amide substrate **5.19** (1.00 g, 2.71 mmol, 1.0 equiv) was added, and the vial was flushed with N_2. The vial was taken into a glove box and charged with $Ni(cod)_2$ (74.5 mg, 0.270 mmol, 10 mol%) and SIPr (106 mg, 0.270 mmol, 10 mol%). Subsequently, THF (2.7 mL, 1.0 M) was added, and the vial was removed

from the glove box and the reaction was allowed to stir at 23 °C for 1 h. Concurrently, the cyclohexylzinc iodide solution (**5.20**) was heated in a water bath at 50 °C for 1 h. A portion of the preheated solution of **5.20** (4.32 mL, 4.07 mmol, 1.5 equiv, 0.94 M in THF) was then added to the reaction mixture dropwise via syringe over 5 sec. The vial was then capped with a Teflon-lined screw cap under a flow of N_2. The reaction mixture was allowed to stir at 23 °C for 24 h. The reaction was quenched by the addition of a saturated aqueous solution of NH_4Cl (3 mL), and the resulting aqueous layer was extracted with EtOAc (3 x 5 mL). The combined organics were filtered over a plug of silica gel (50 mL of EtOAc eluent). The volatiles were removed under reduced pressure, and the crude residue was purified by flash chromatography (24:1 Hexanes:EtOAc) to yield ketone product **5.21** (472 mg, 71% yield) as a pale yellow solid. Ketone **5.21**: R_f 0.50 (5:1 Hexanes:EtOAc). Spectral data match those previously reported.

5.9 Spectra Relevant to Chapter Five:

Nickel-Catalyzed Alkylation of Amide Derivatives

Bryan J. Simmons, Nicholas A. Weires, Jacob E. Dander, and Neil K. Garg.

ACS Catal. **2016**, *6*, 3176–3179.

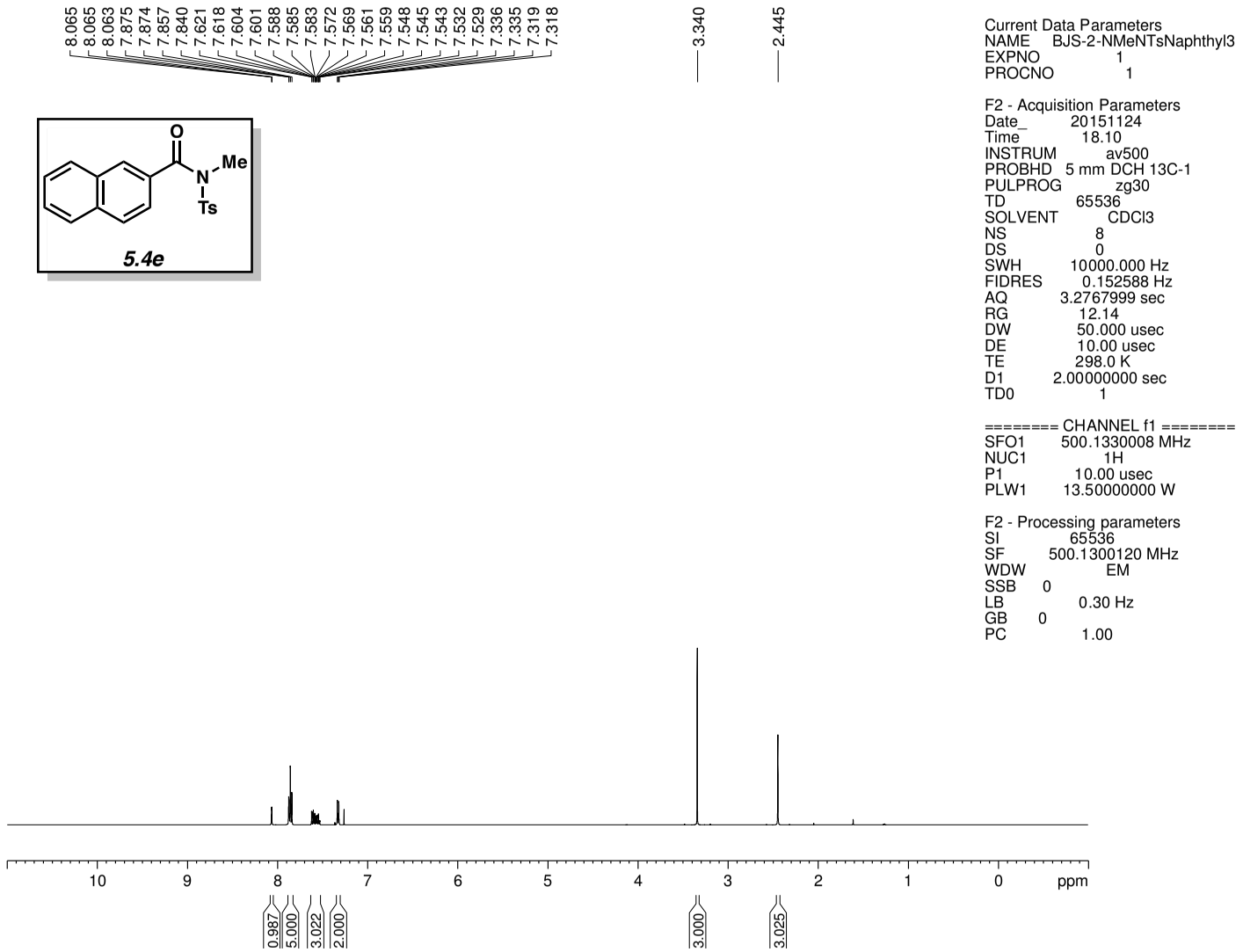

Figure 5.4 ^{1}H NMR (500 MHz, $CDCl_3$) of compound **5.4e**.

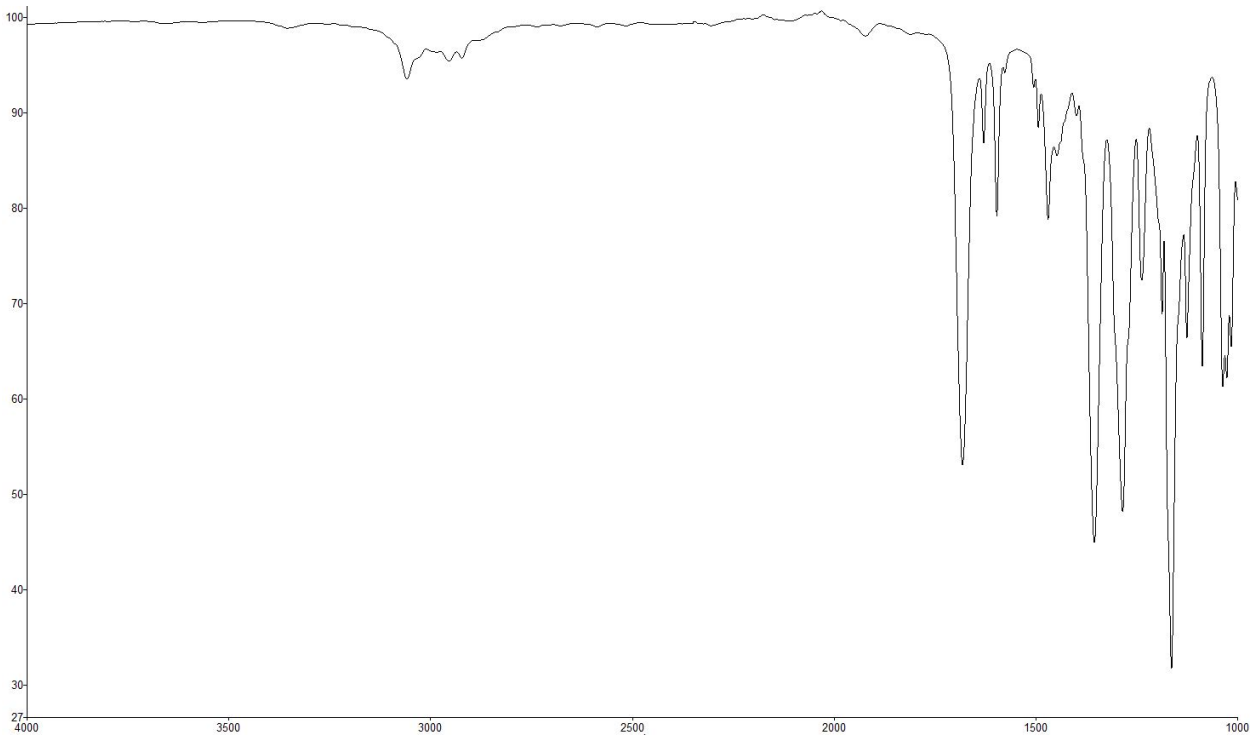

Figure 5.5 Infrared spectrum of compound **5.4e**.

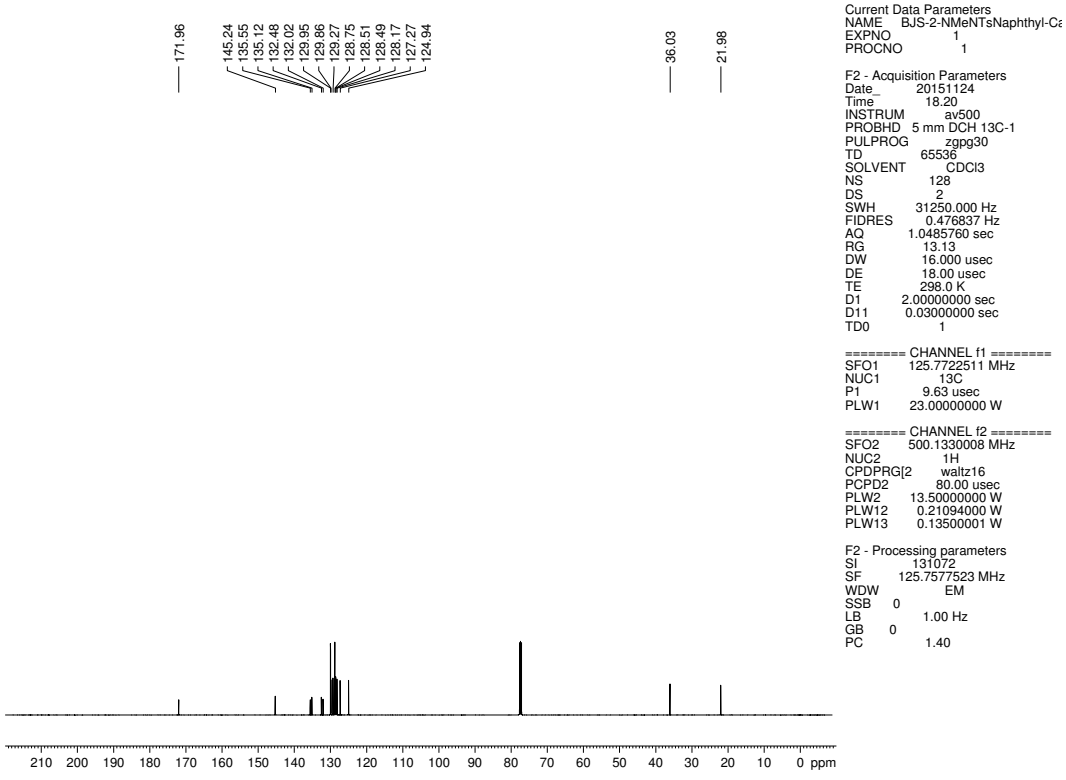

Figure 5.6 ^{13}C NMR (125 MHz, $CDCl_3$) of compound **5.4e**.

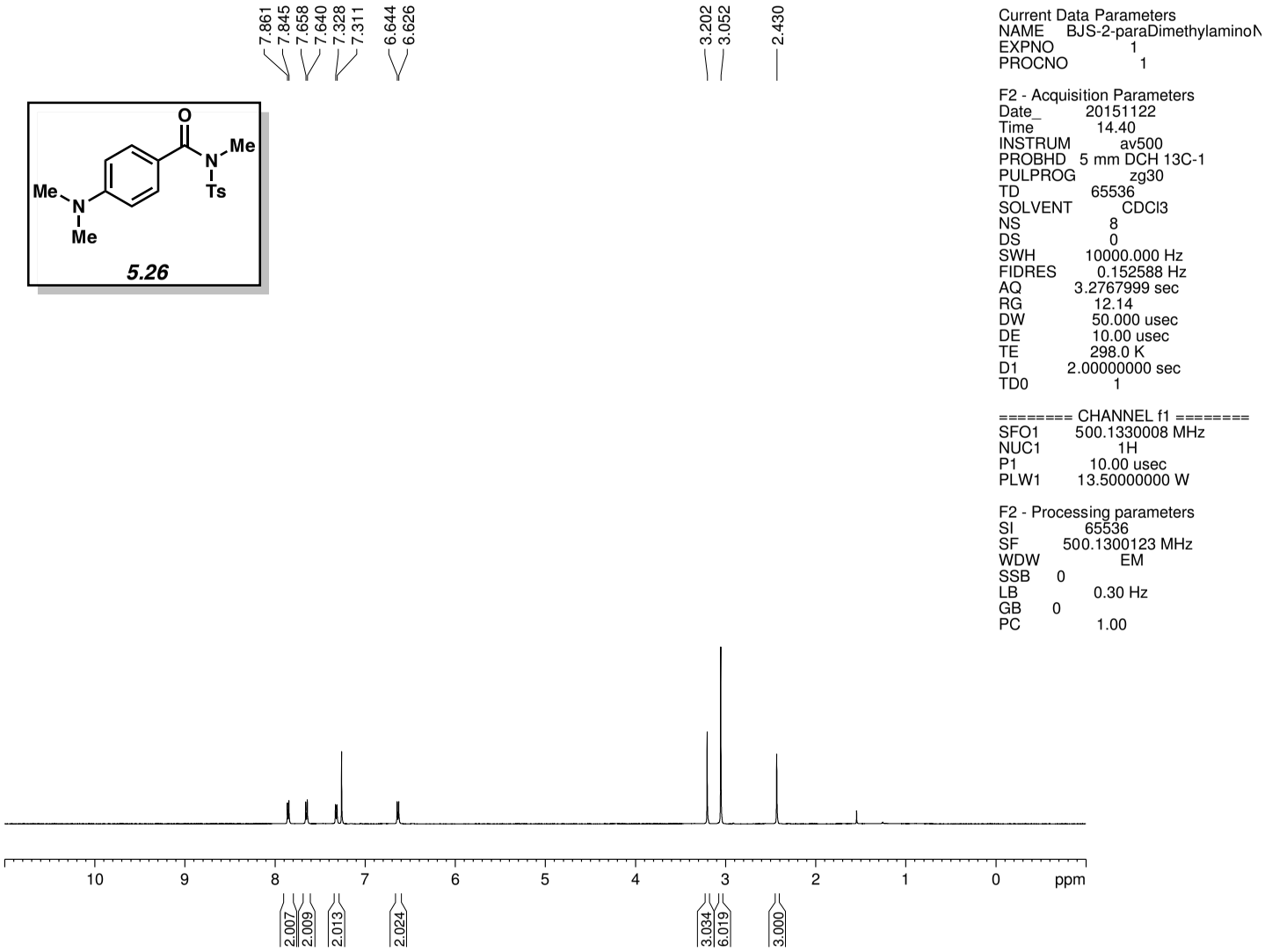

Figure 5.7 ^{1}H NMR (500 MHz, $CDCl_3$) of compound **5.26**.

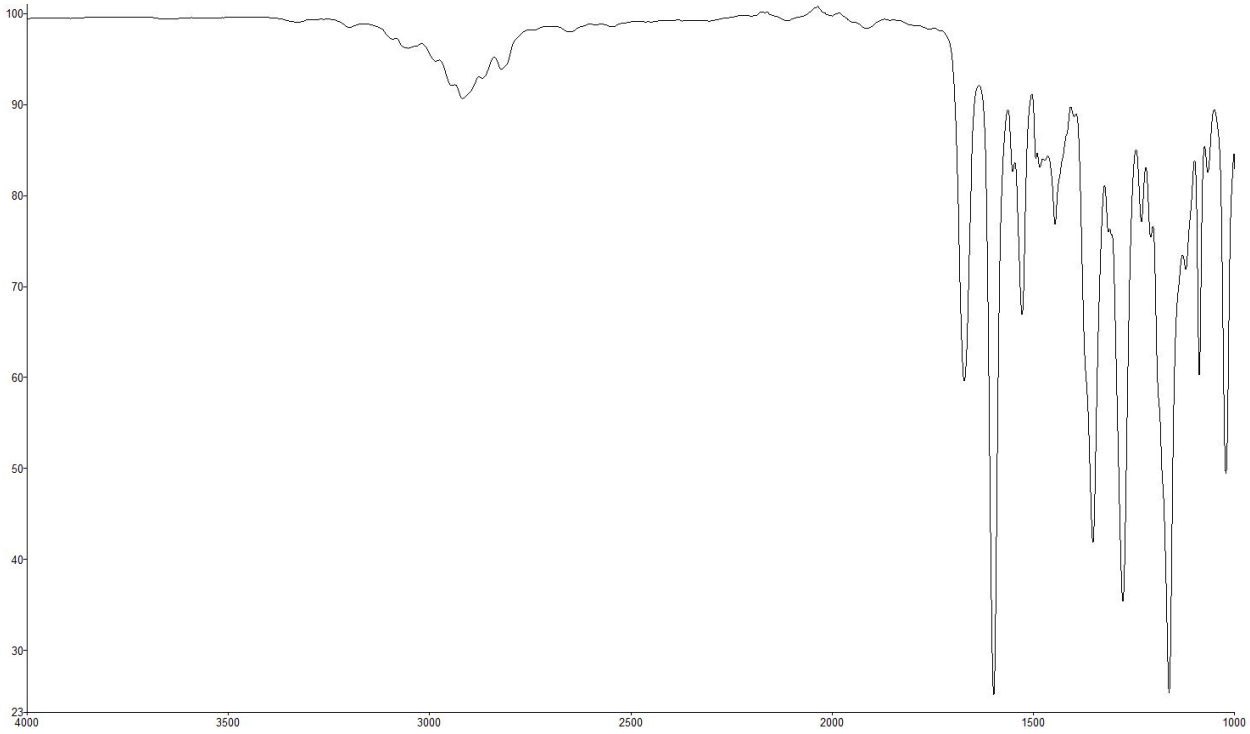

Figure 5.8 Infrared spectrum of compound **5.26**.

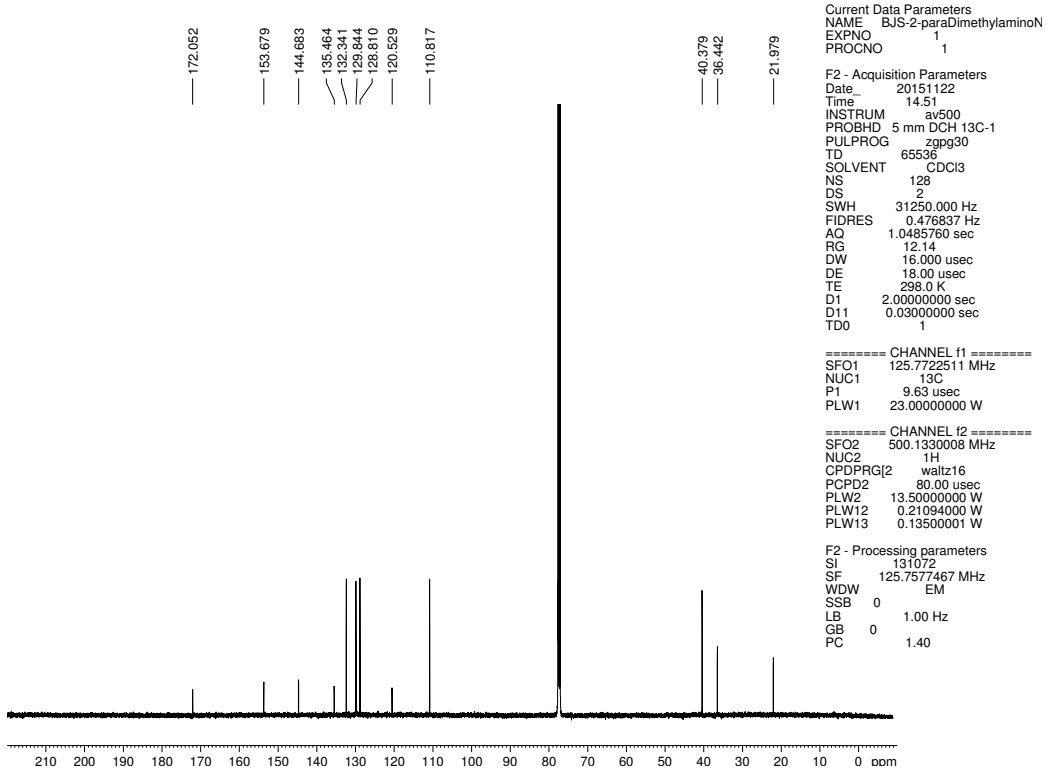

Figure 5.9 ^{13}C NMR (125 MHz, $CDCl_3$) of compound **5.26**.

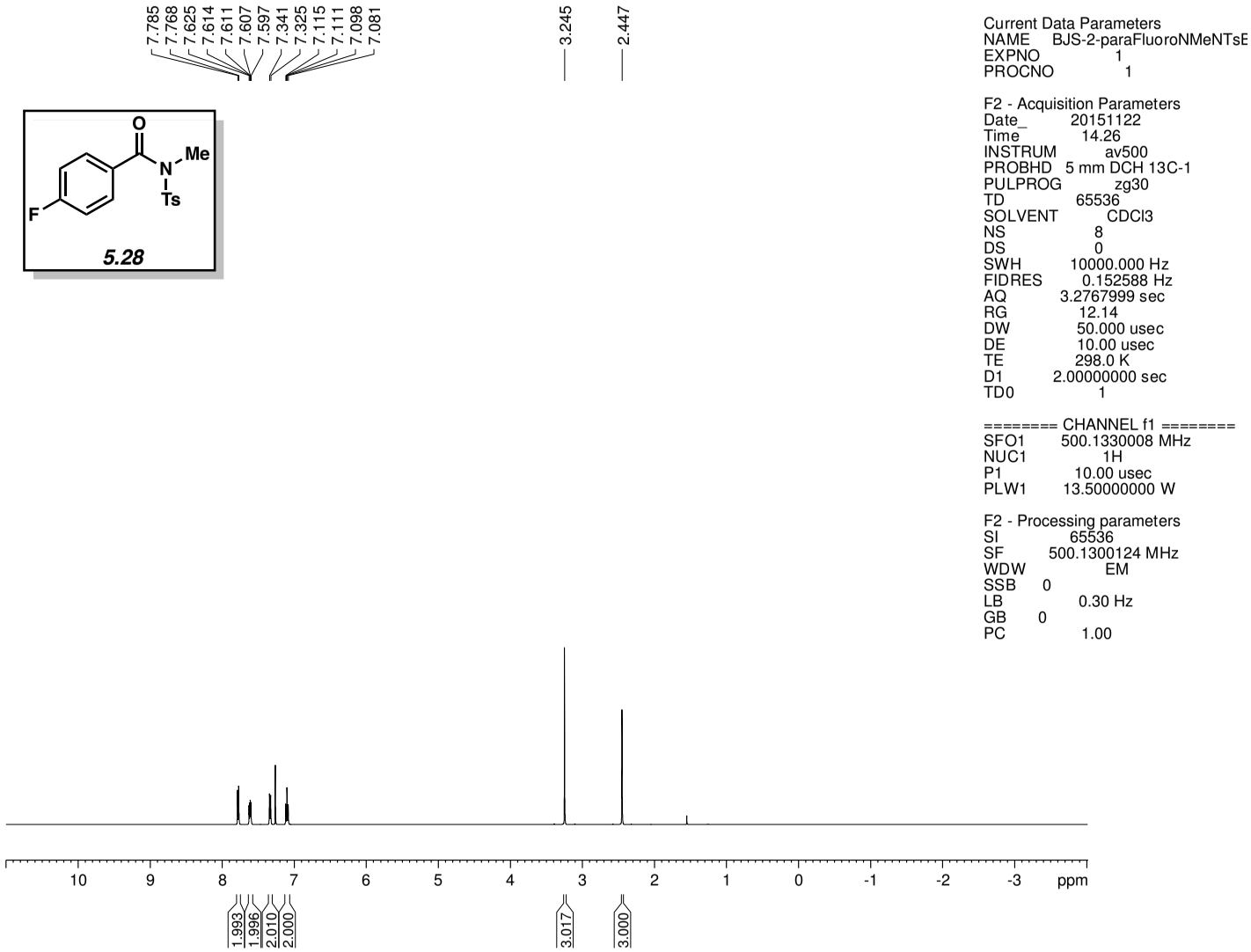

Figure 5.10 ^{1}H NMR (500 MHz, $CDCl_3$) of compound **5.28**.

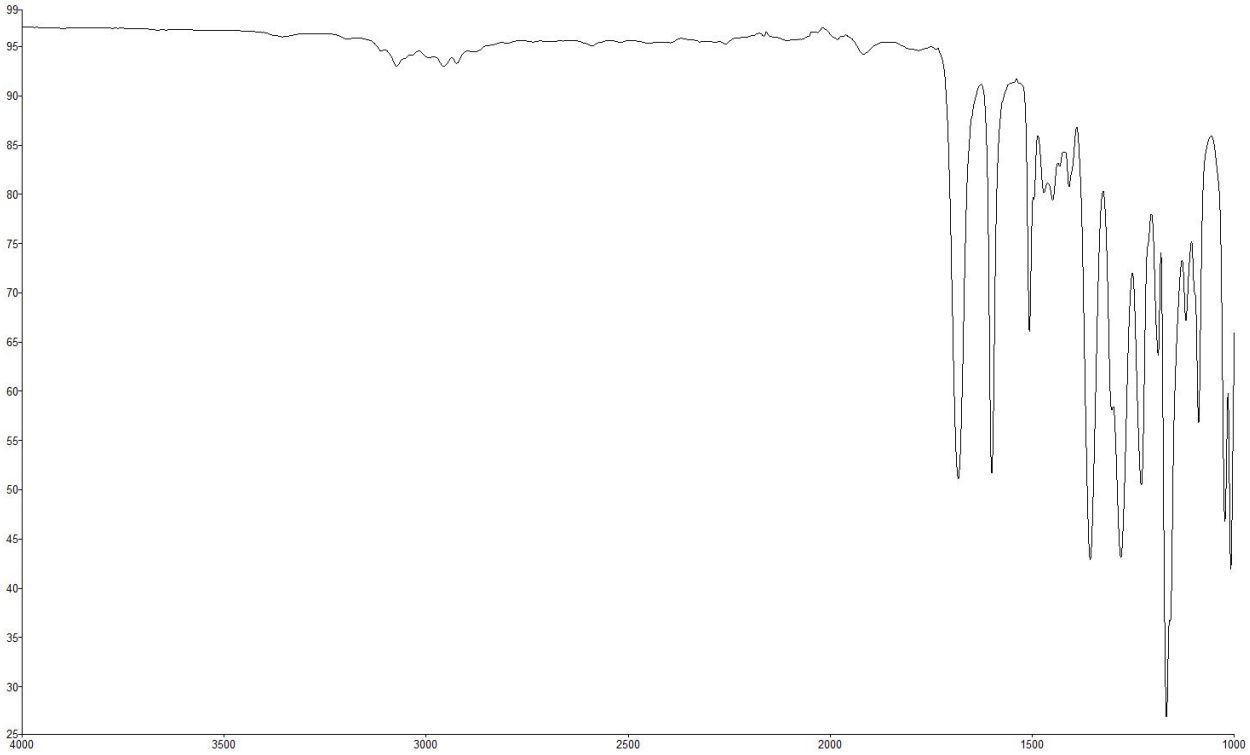

Figure 5.11 Infrared spectrum of compound **5.28**.

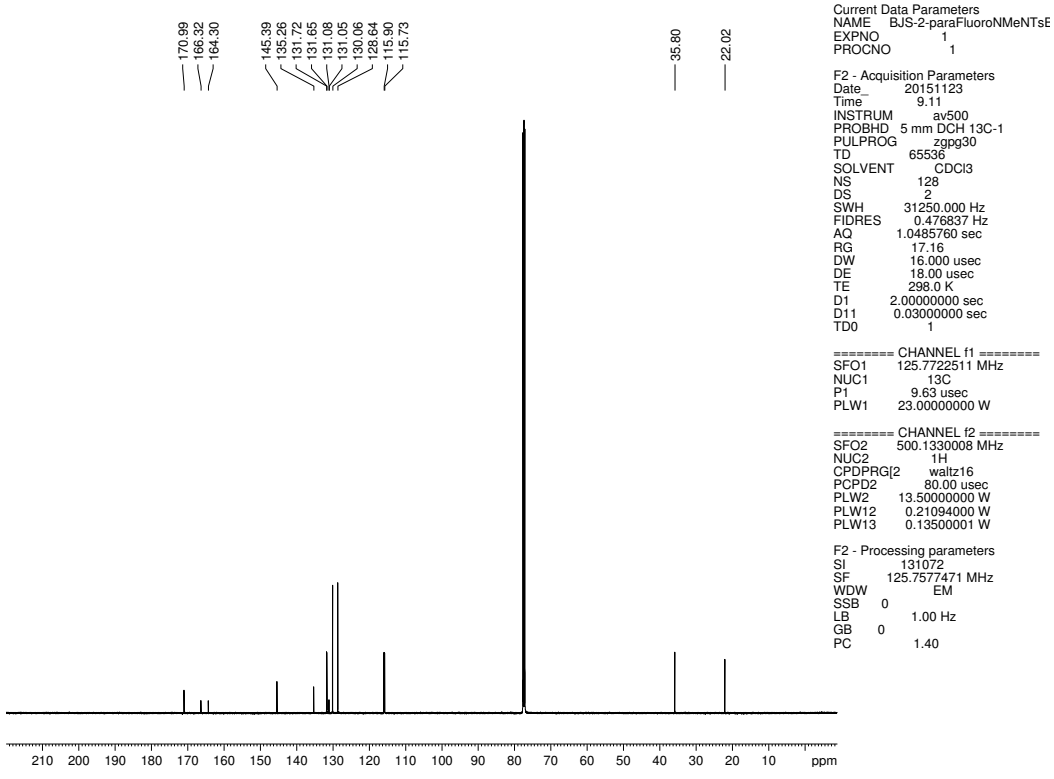

Figure 5.12 ^{13}C NMR (125 MHz, $CDCl_3$) of compound **5.28**.

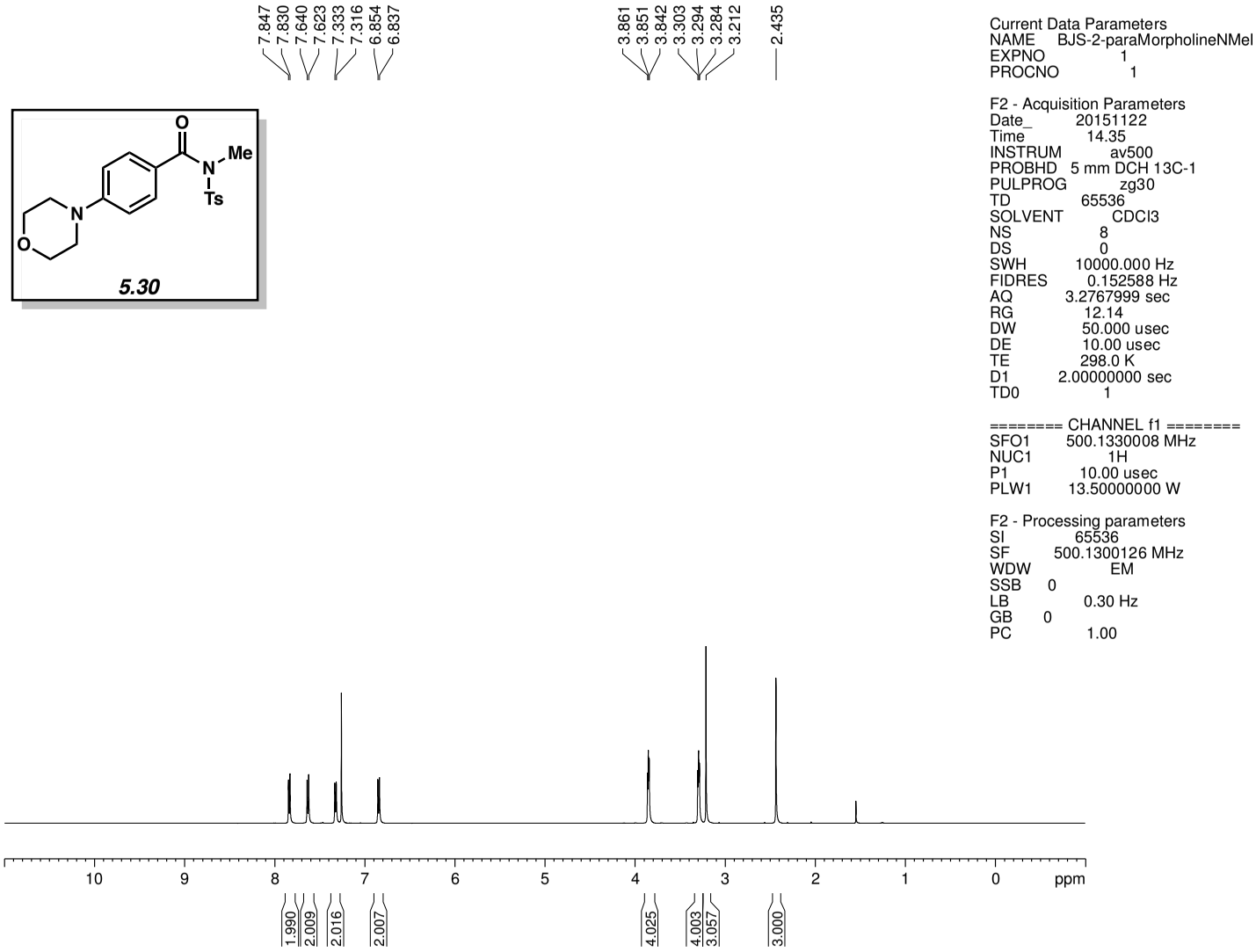

Figure 5.13 ^{1}H NMR (500 MHz, $CDCl_3$) of compound **5.30**.

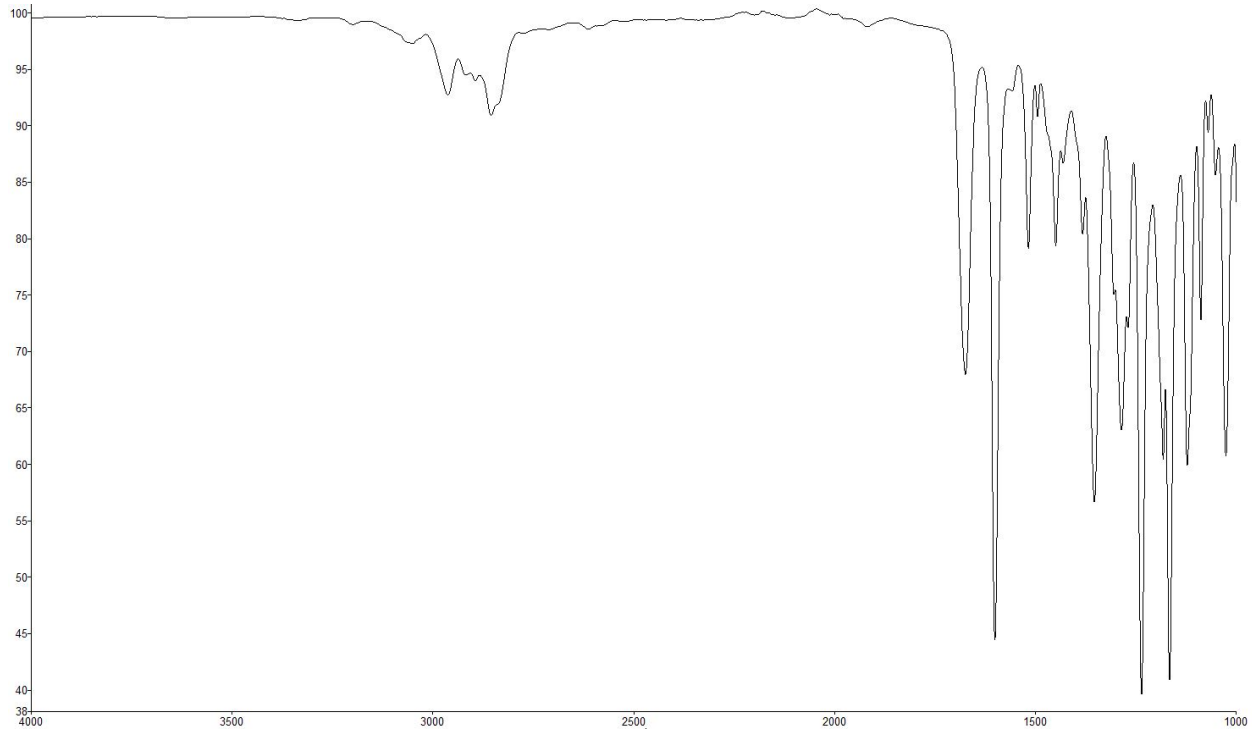

Figure 5.14 Infrared spectrum of compound **5.30**.

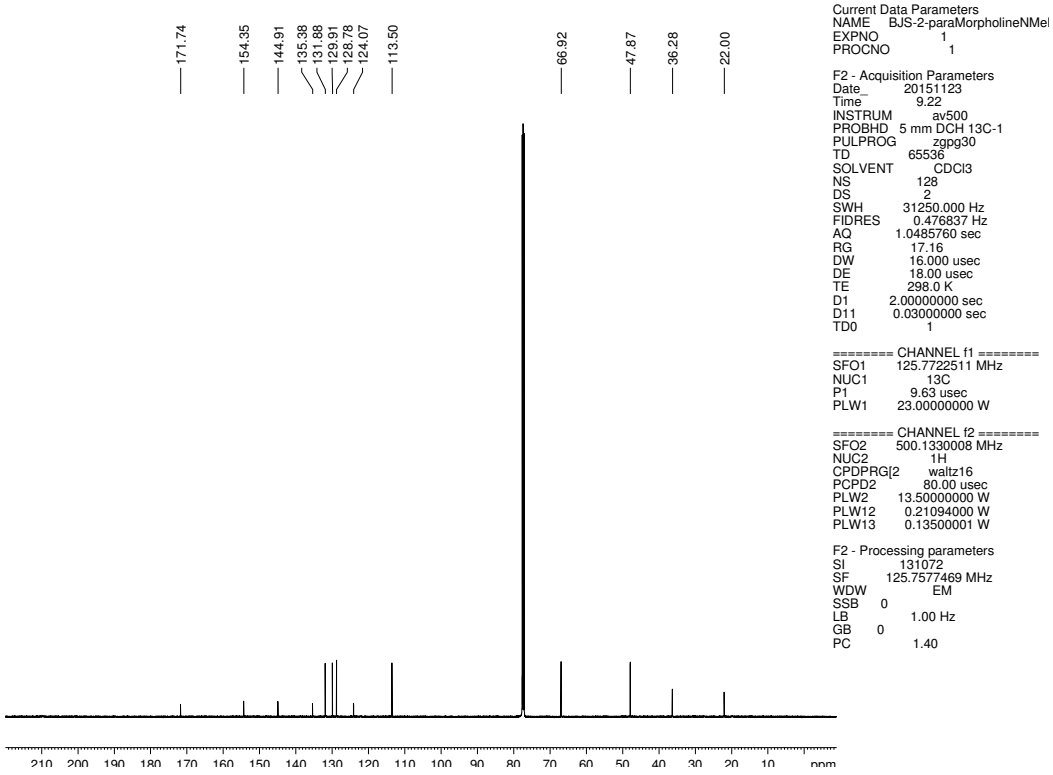

Figure 5.15 ^{13}C NMR (125 MHz, $CDCl_3$) of compound **5.30**.

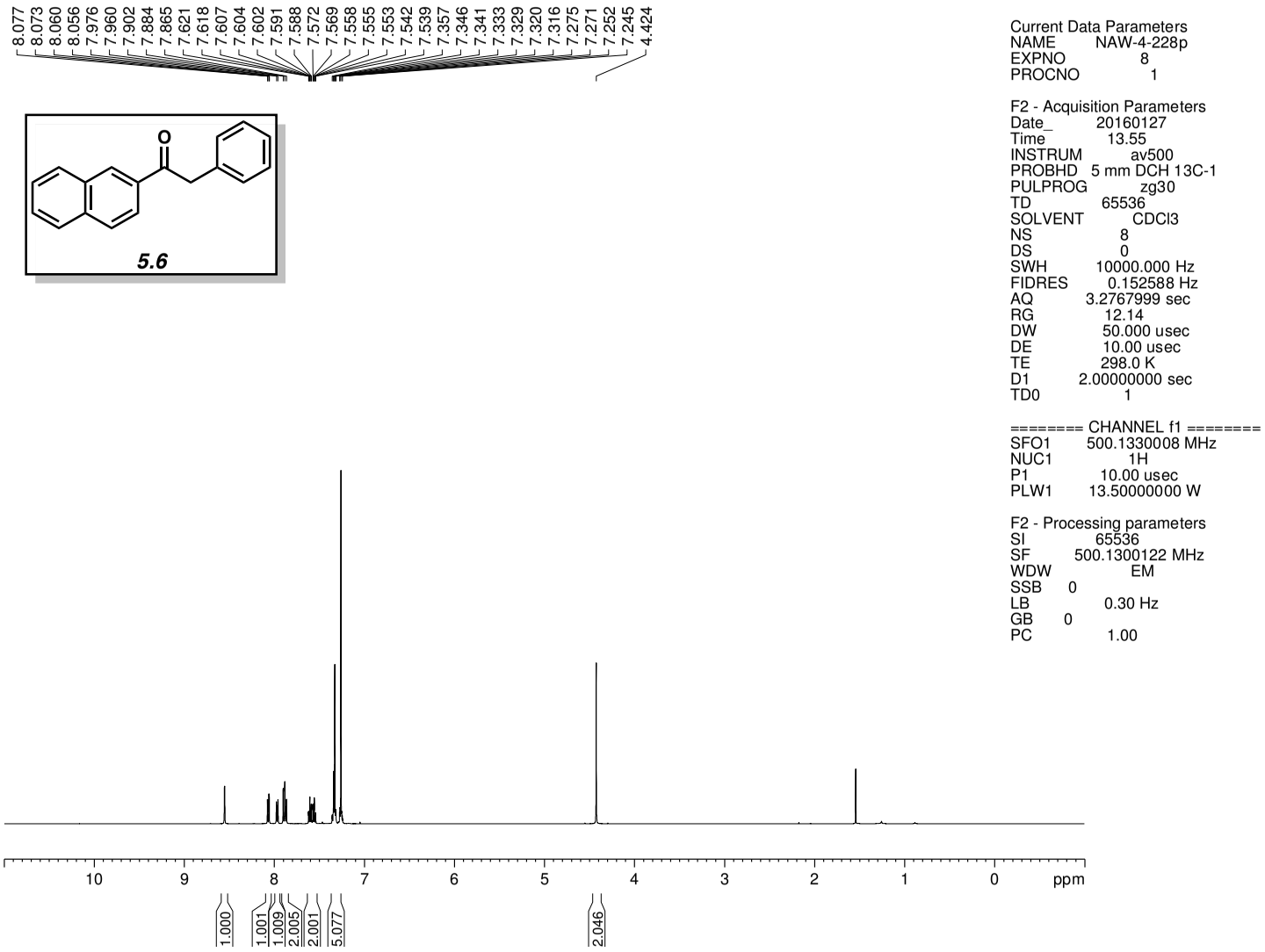

Figure 5.16 ^{1}H NMR (500 MHz, $CDCl_3$) of compound **5.6**.

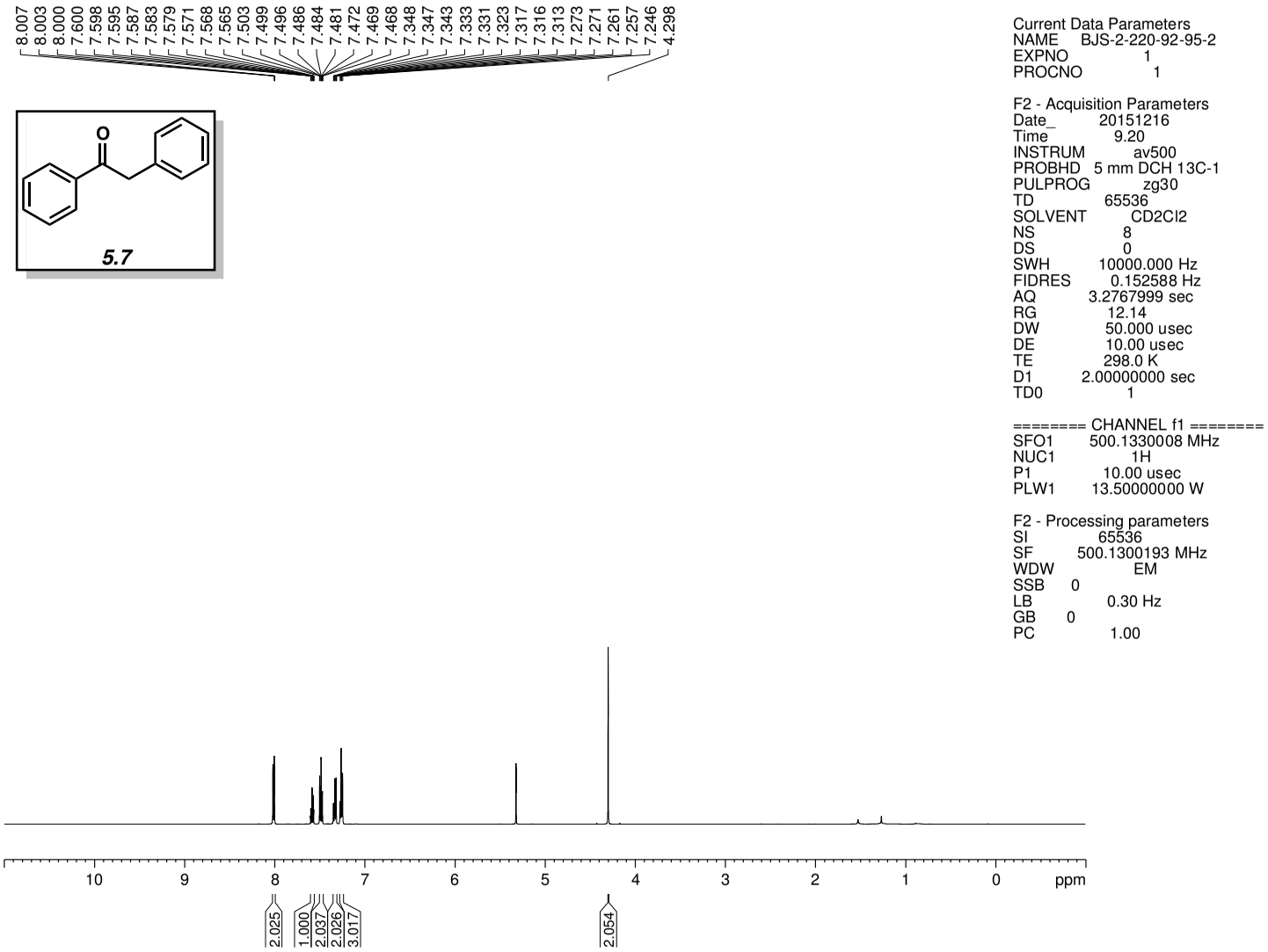

Figure 5.17 ^{1}H NMR (500 MHz, $CDCl_3$) of compound **5.7**.

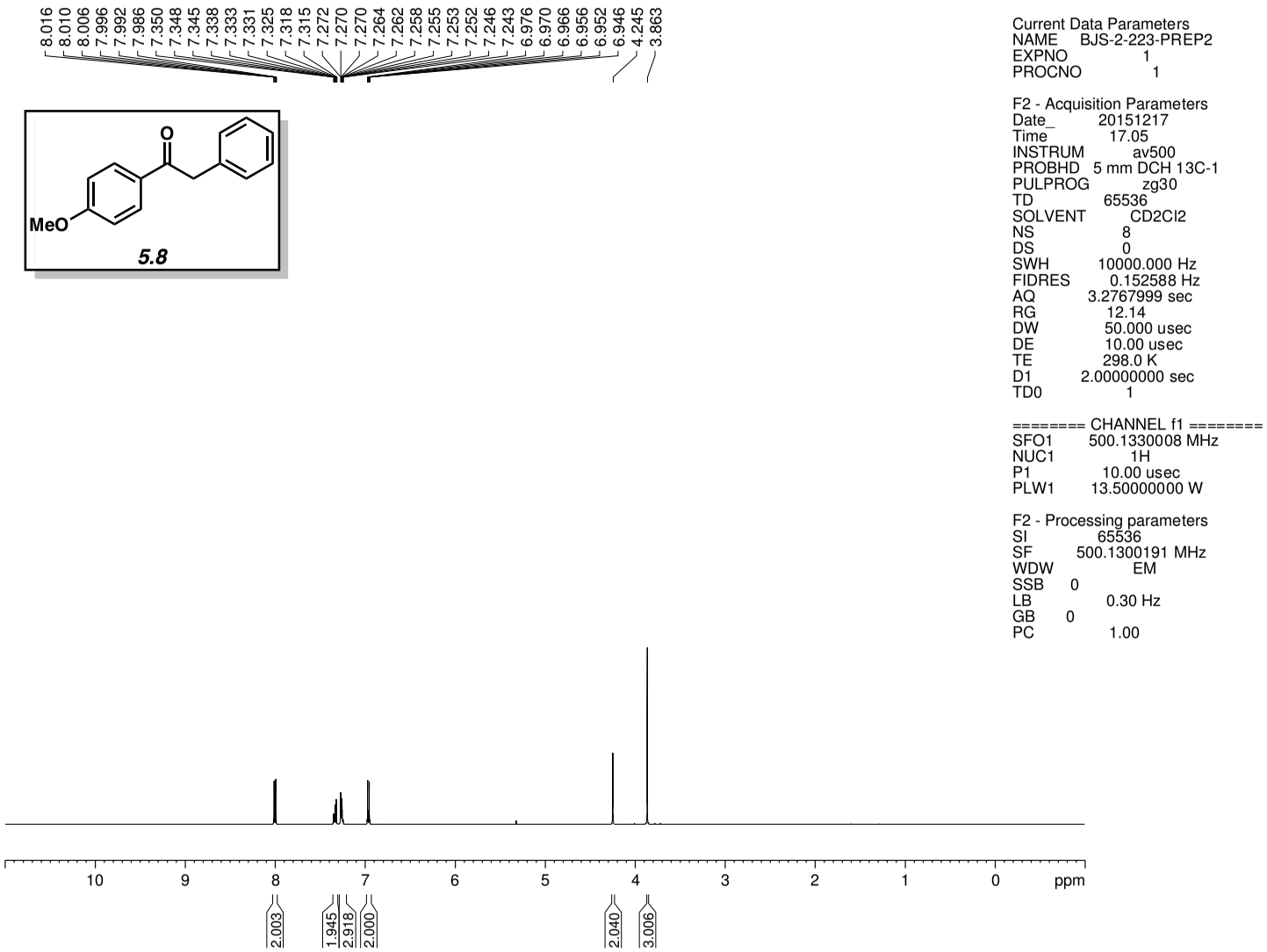

Figure 5.18 ^{1}H NMR (500 MHz, $CDCl_3$) of compound **5.8**.

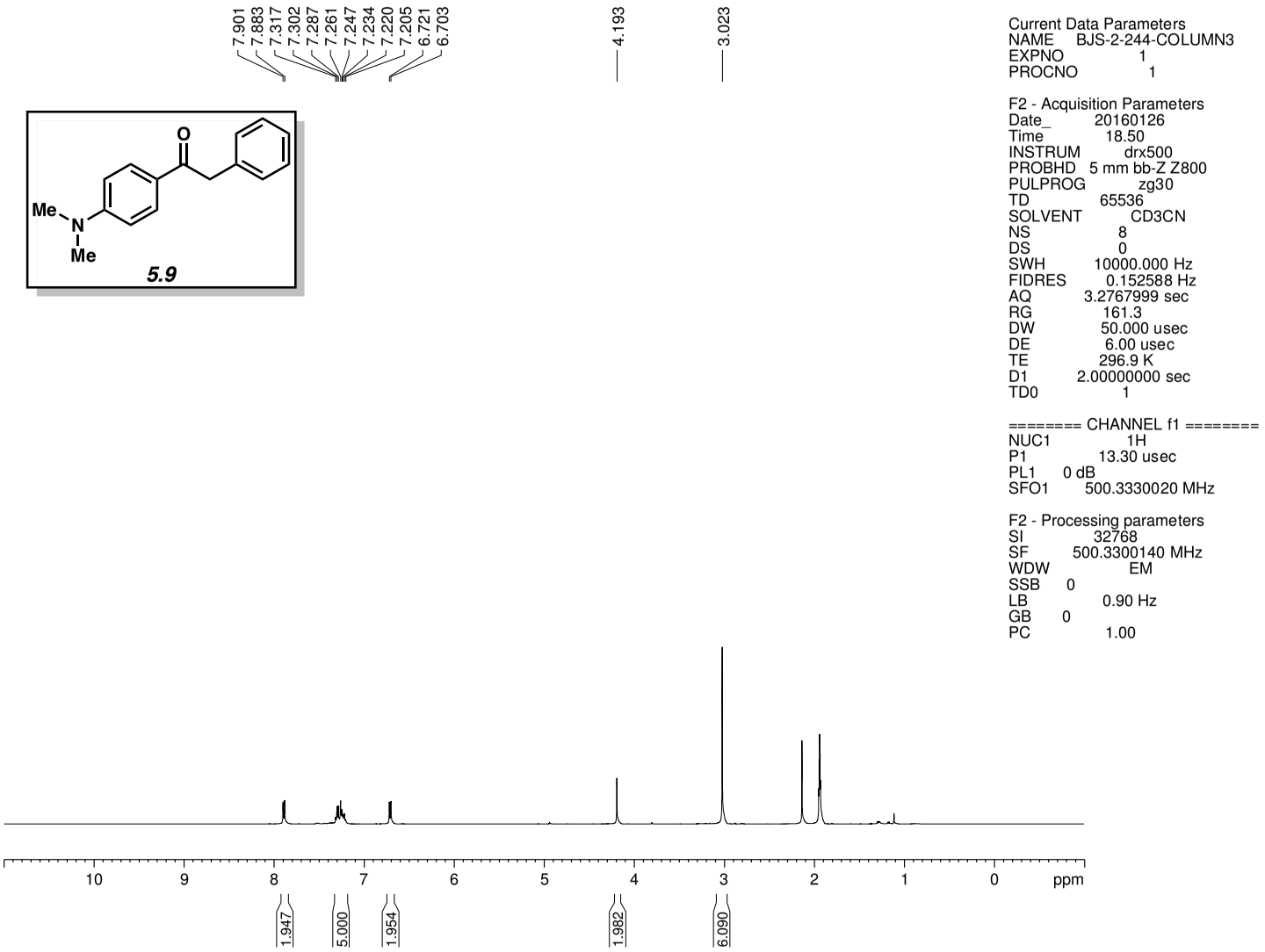

Figure 5.19 ^{1}H NMR (500 MHz, $CDCl_3$) of compound **5.9**.

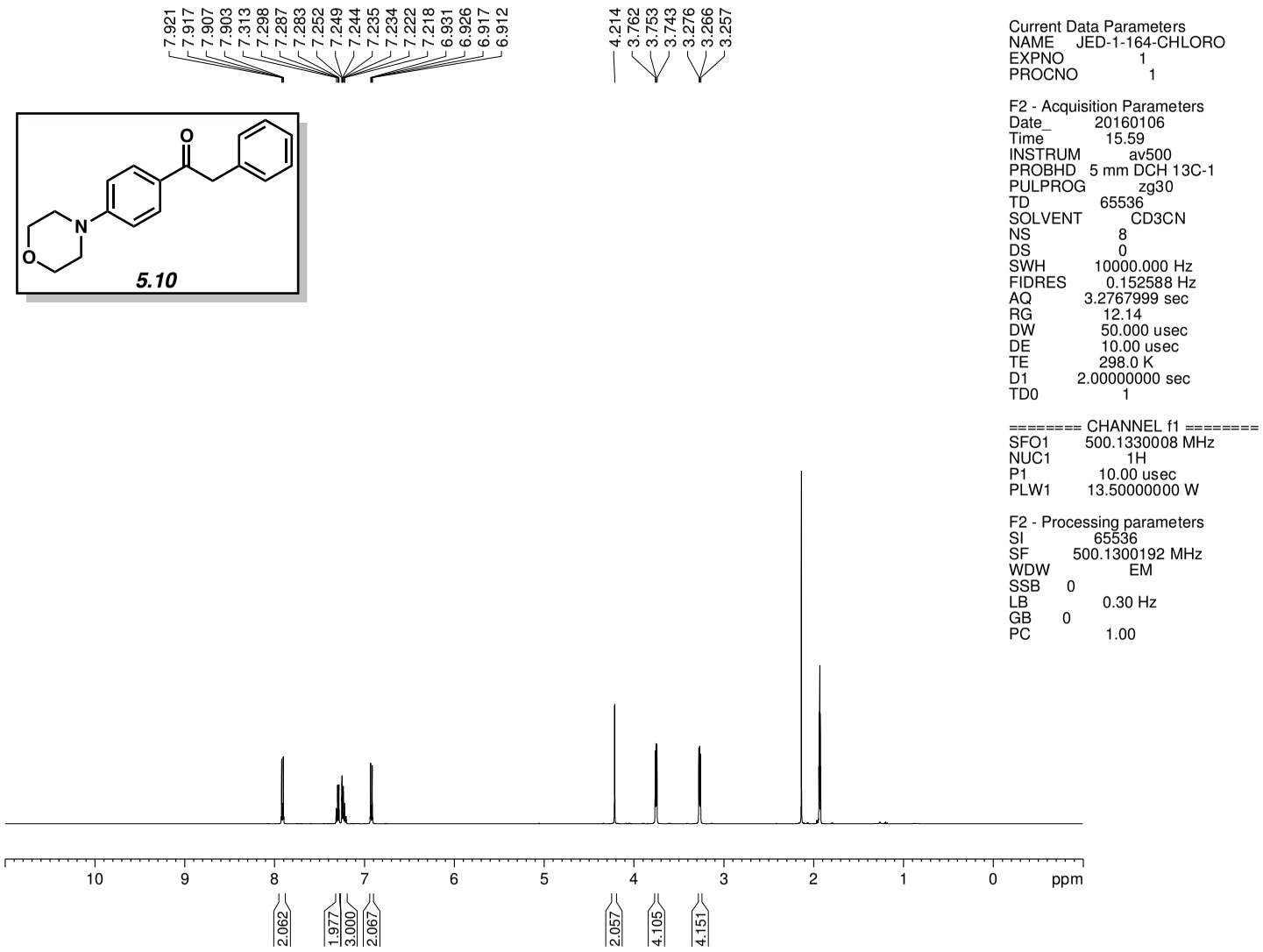

Figure 5.20 ^{1}H NMR (500 MHz, $CDCl_3$) of compound **5.10**.

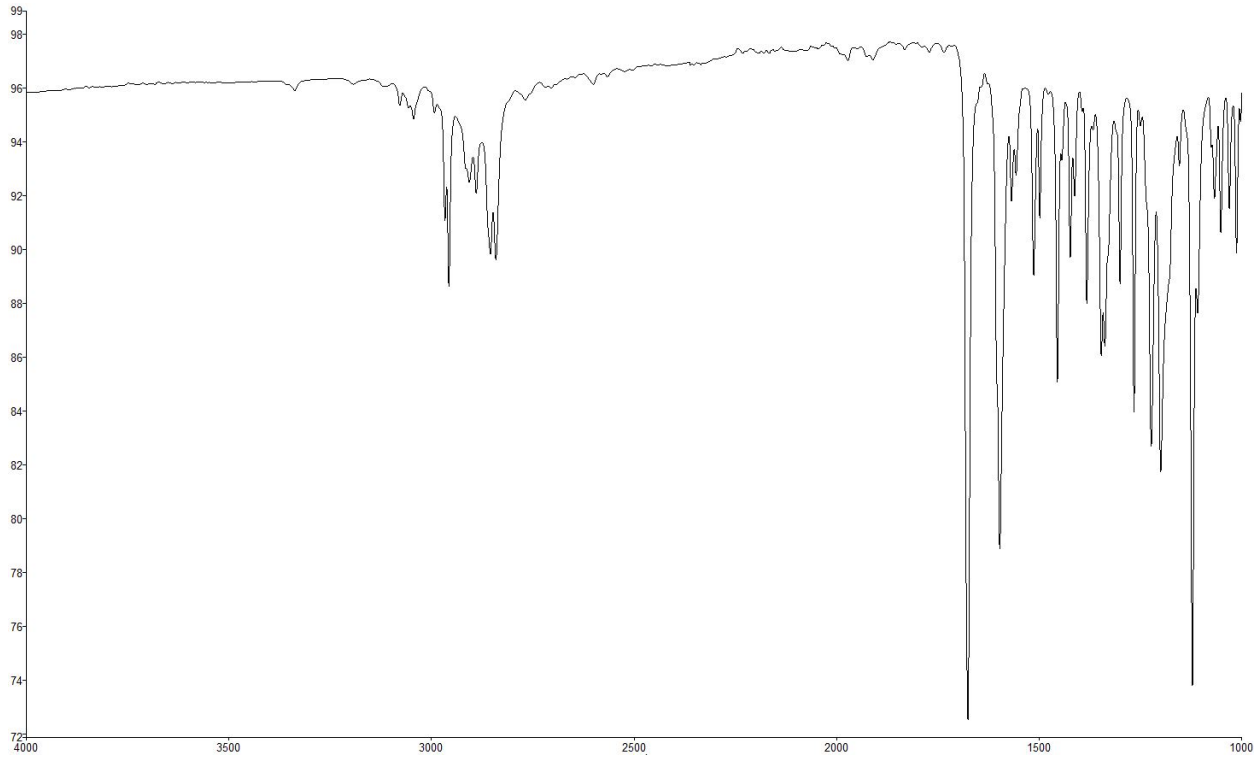

Figure 5.21 Infrared spectrum of compound **5.10**.

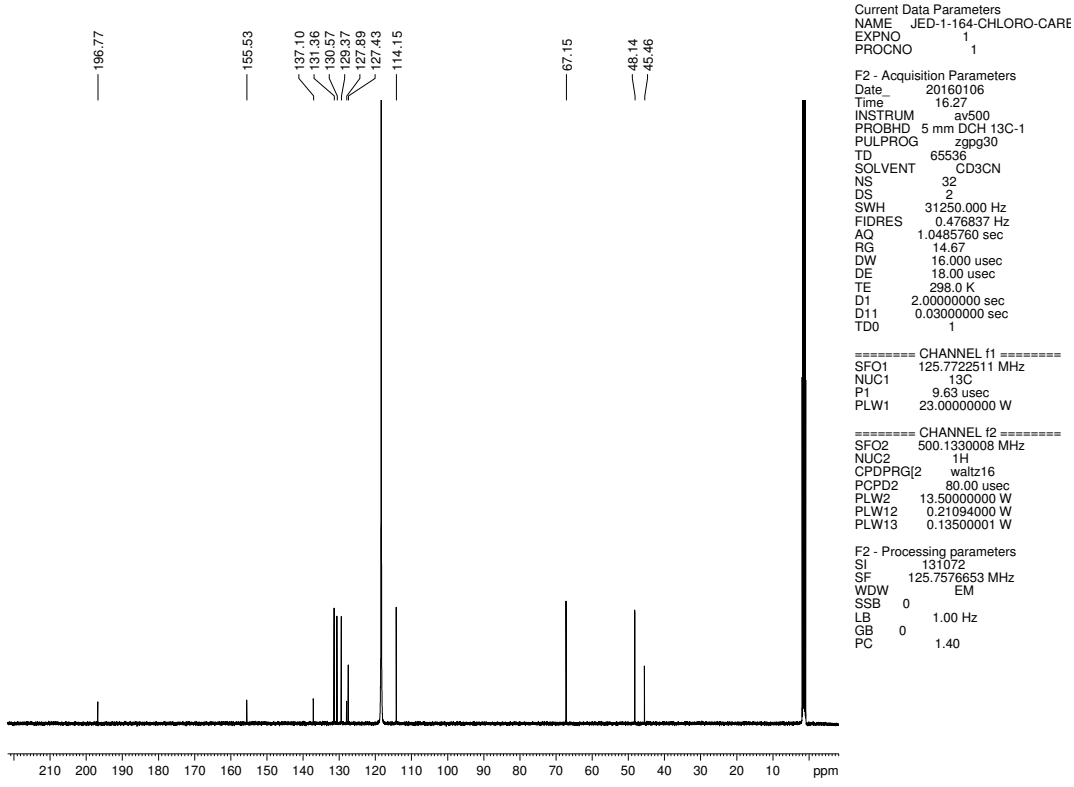

Figure 5.22 ^{13}C NMR (125 MHz, $CDCl_3$) of compound **5.10**.

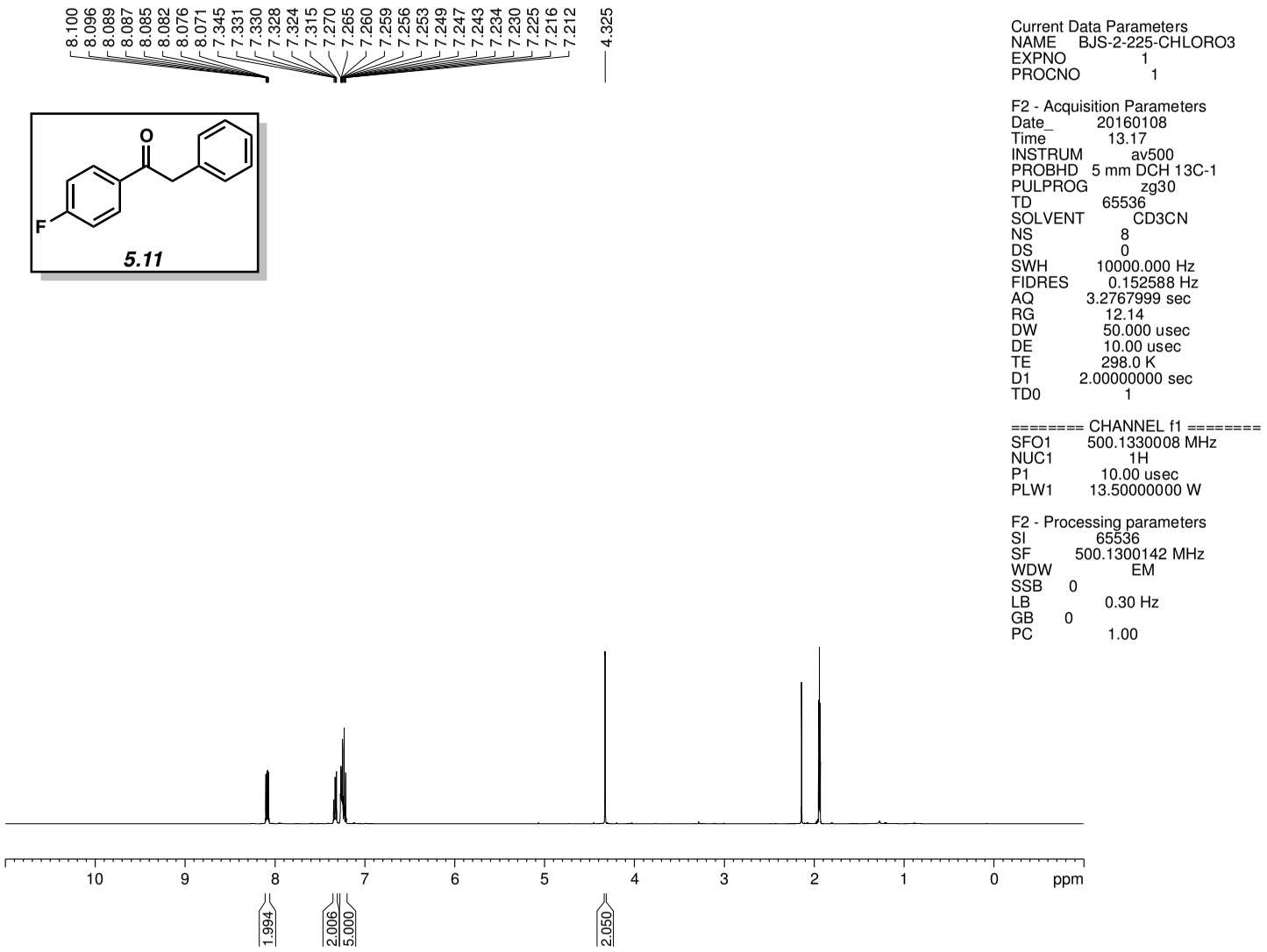

Figure 5.23 ^{1}H NMR (500 MHz, $CDCl_3$) of compound **5.11**.

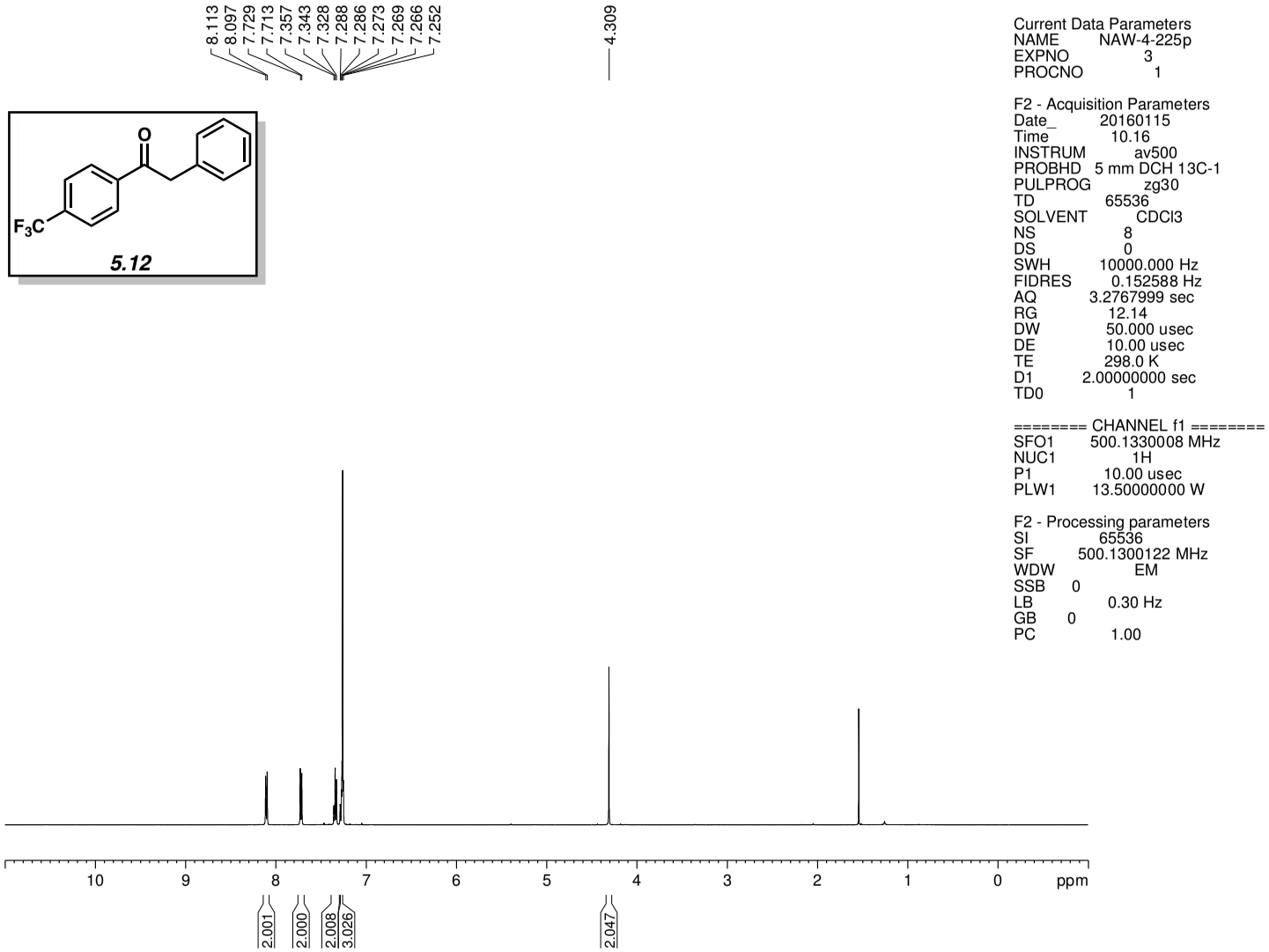

Figure 5.24 ^{1}H NMR (500 MHz, $CDCl_3$) of compound **5.12**.

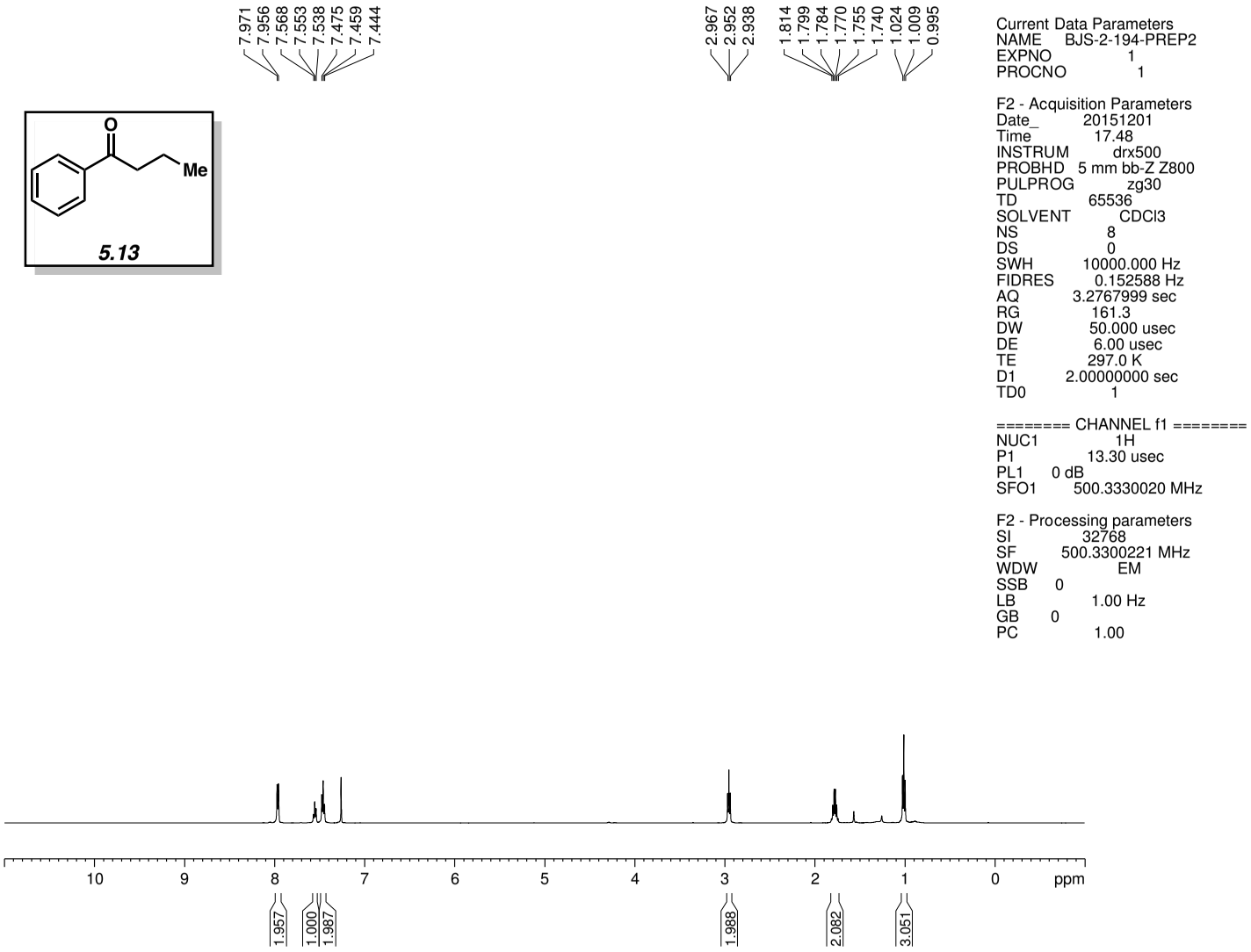

Figure 5.25 ^{1}H NMR (500 MHz, $CDCl_3$) of compound **5.13**.

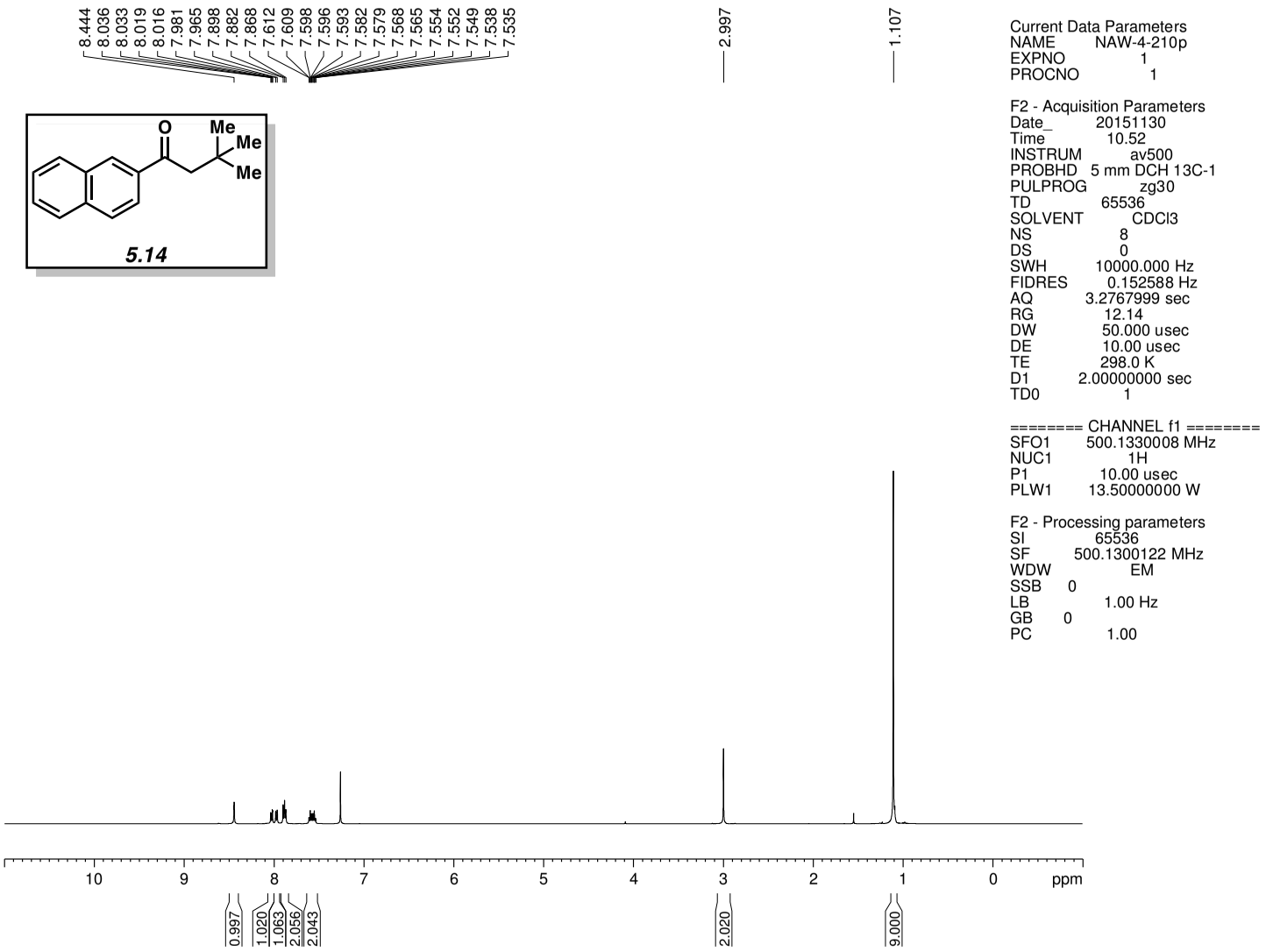

Figure 5.26 ^{1}H NMR (500 MHz, $CDCl_3$) of compound **5.14**.

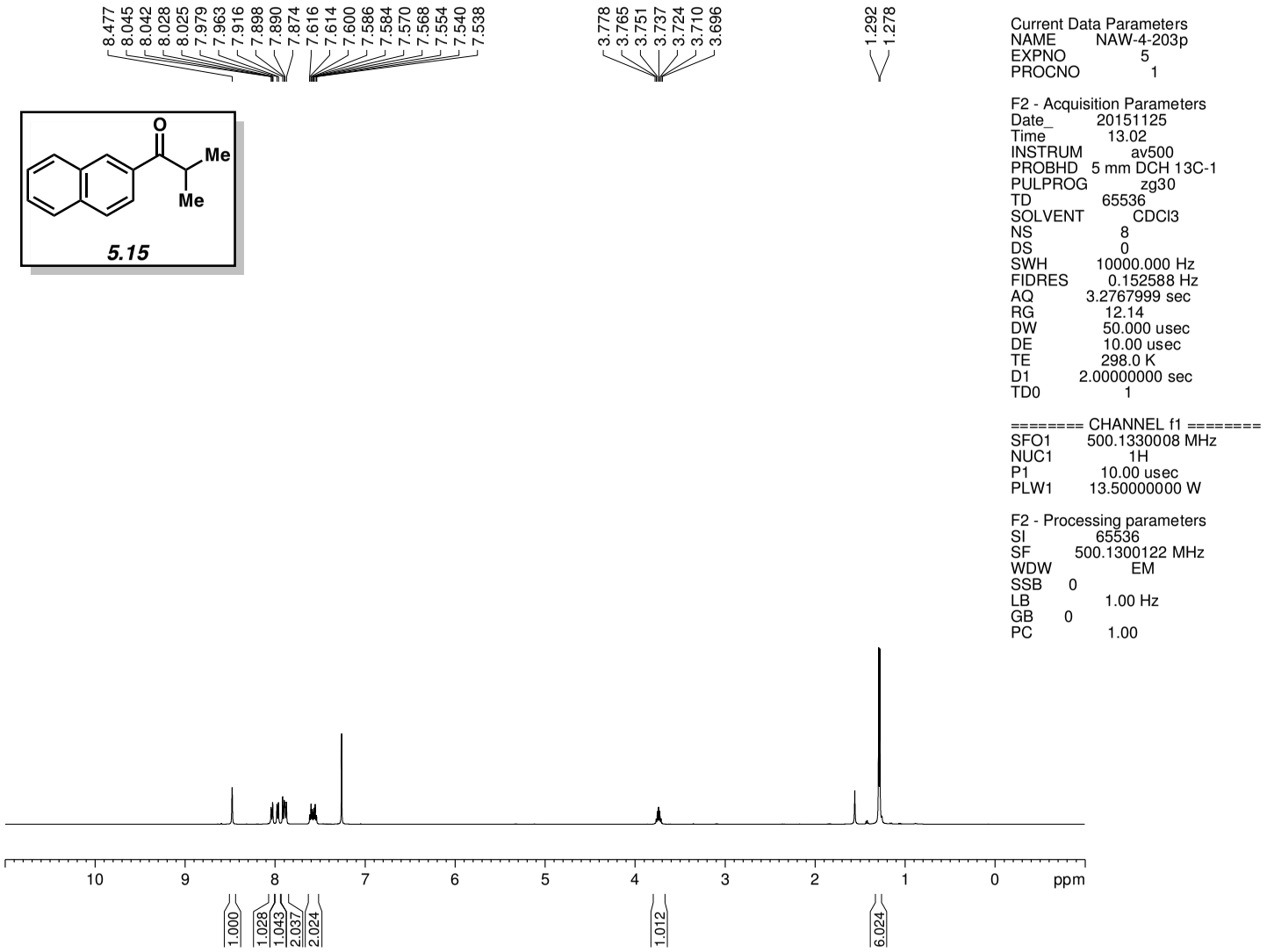

Figure 5.27 ^{1}H NMR (500 MHz, $CDCl_3$) of compound **5.15**.

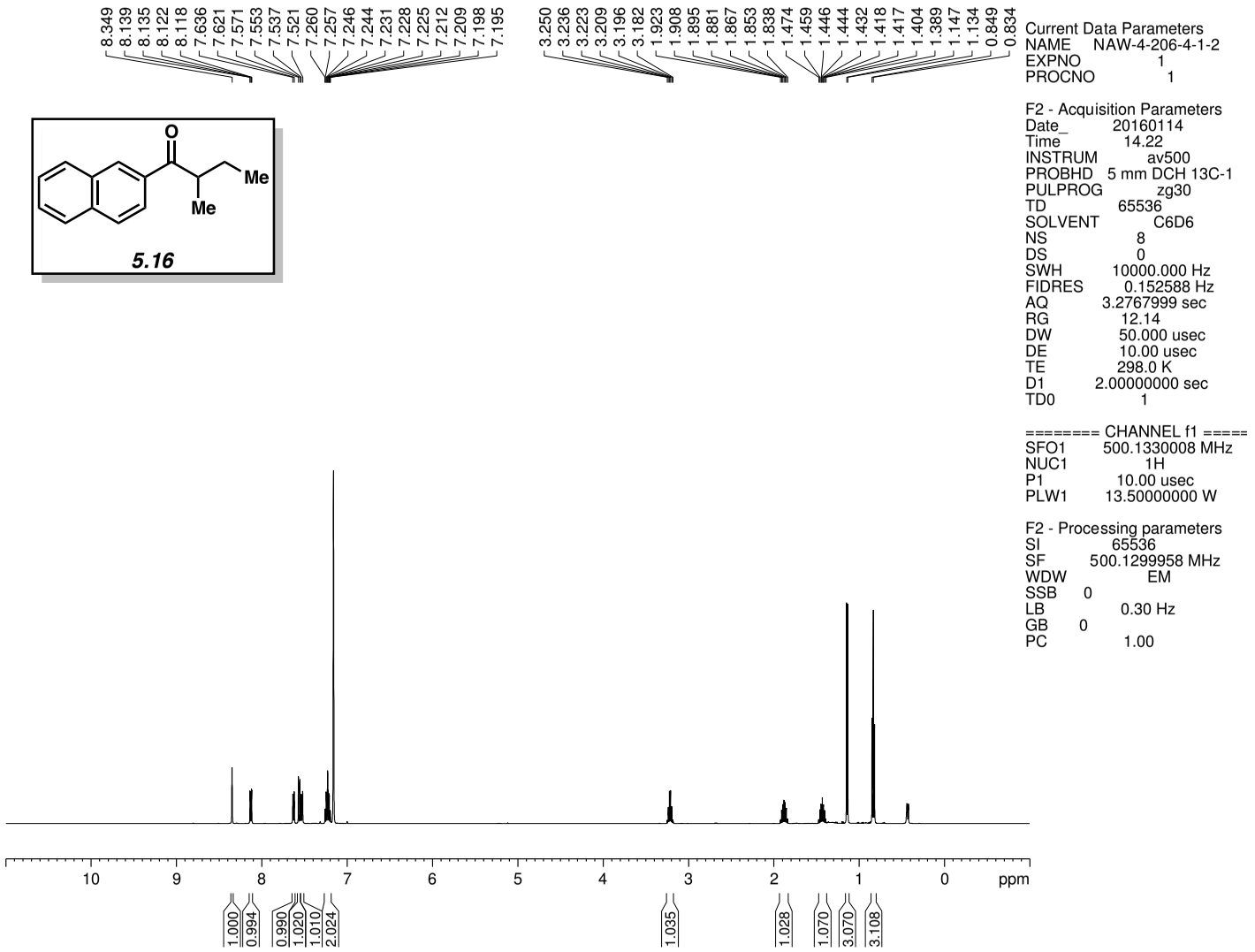

Figure 5.28 ^{1}H NMR (500 MHz, $CDCl_3$) of compound **5.16**.

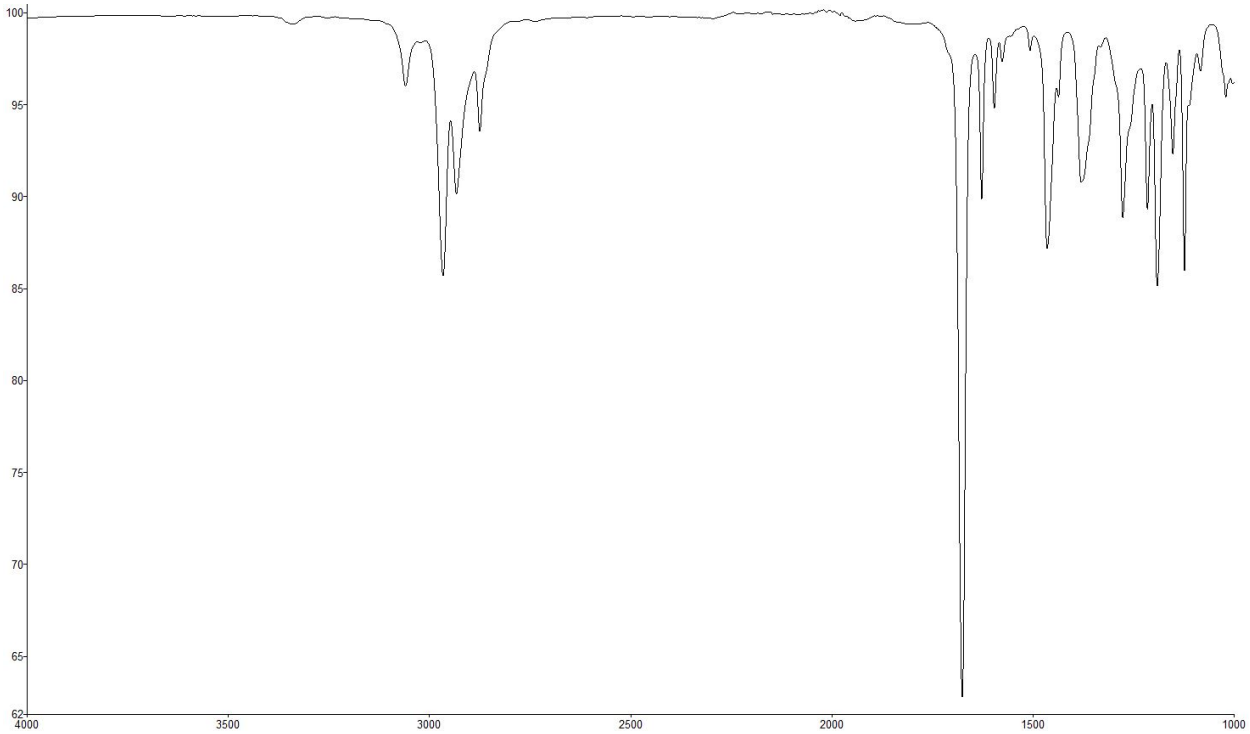

Figure 5.29 Infrared spectrum of compound **5.16**.

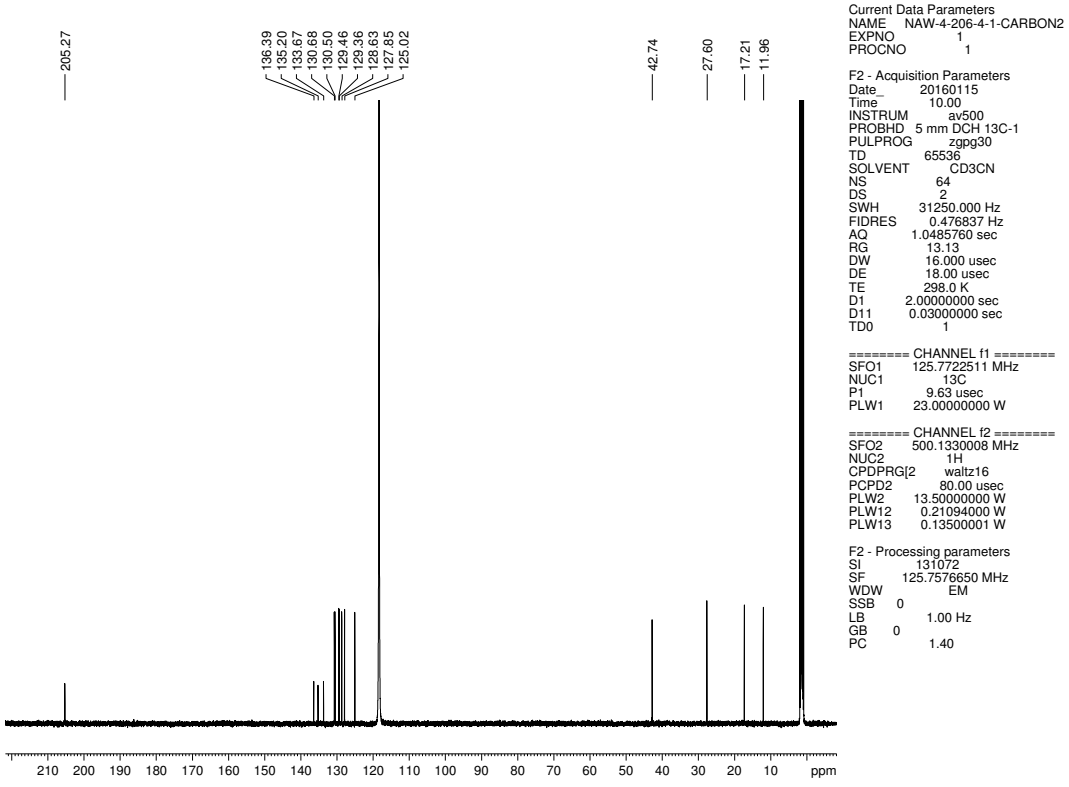

Figure 5.30 ^{13}C NMR (125 MHz, $CDCl_3$) of compound **5.16**.

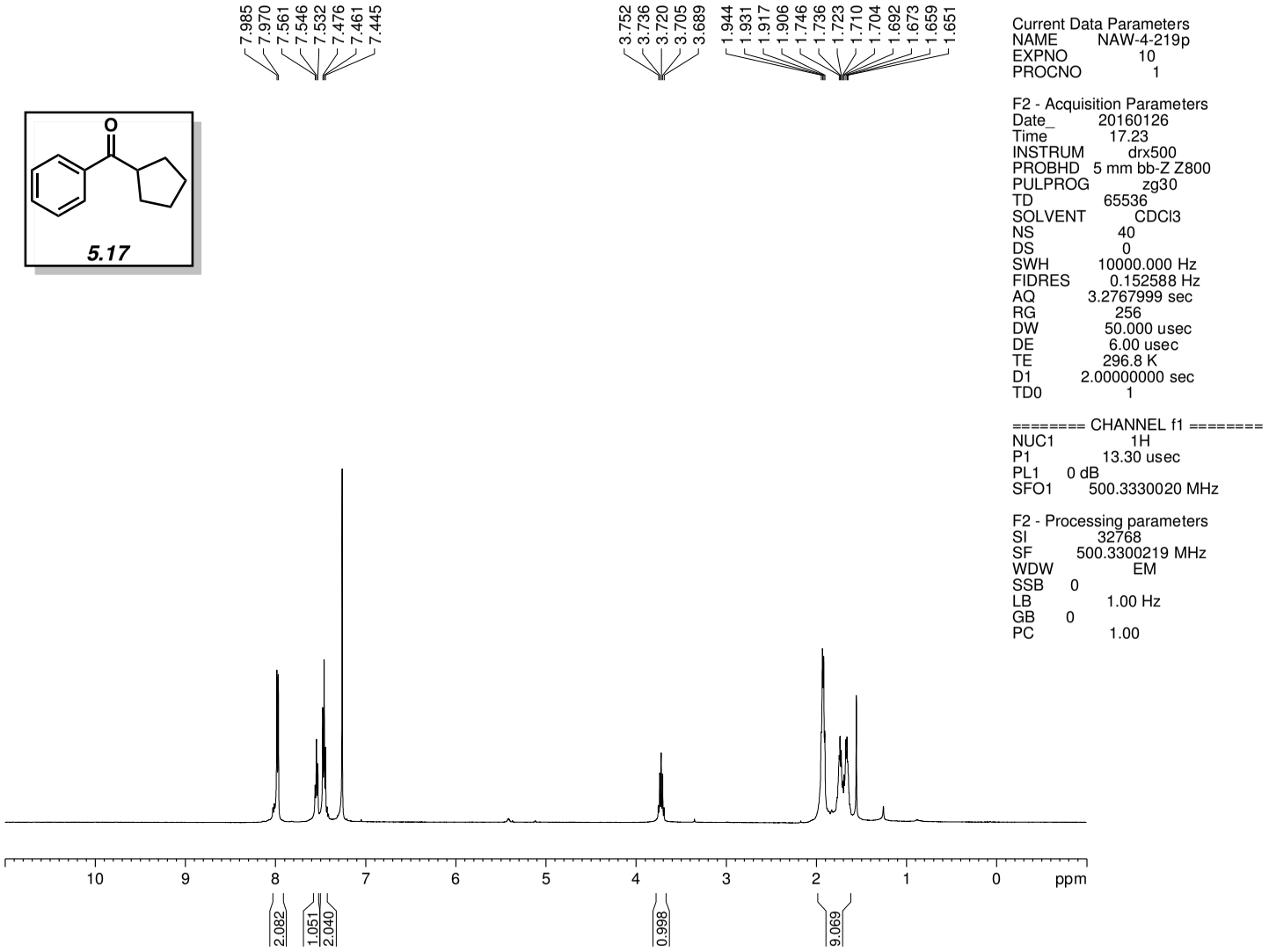

Figure 5.31 ^{1}H NMR (500 MHz, $CDCl_3$) of compound **5.17**.

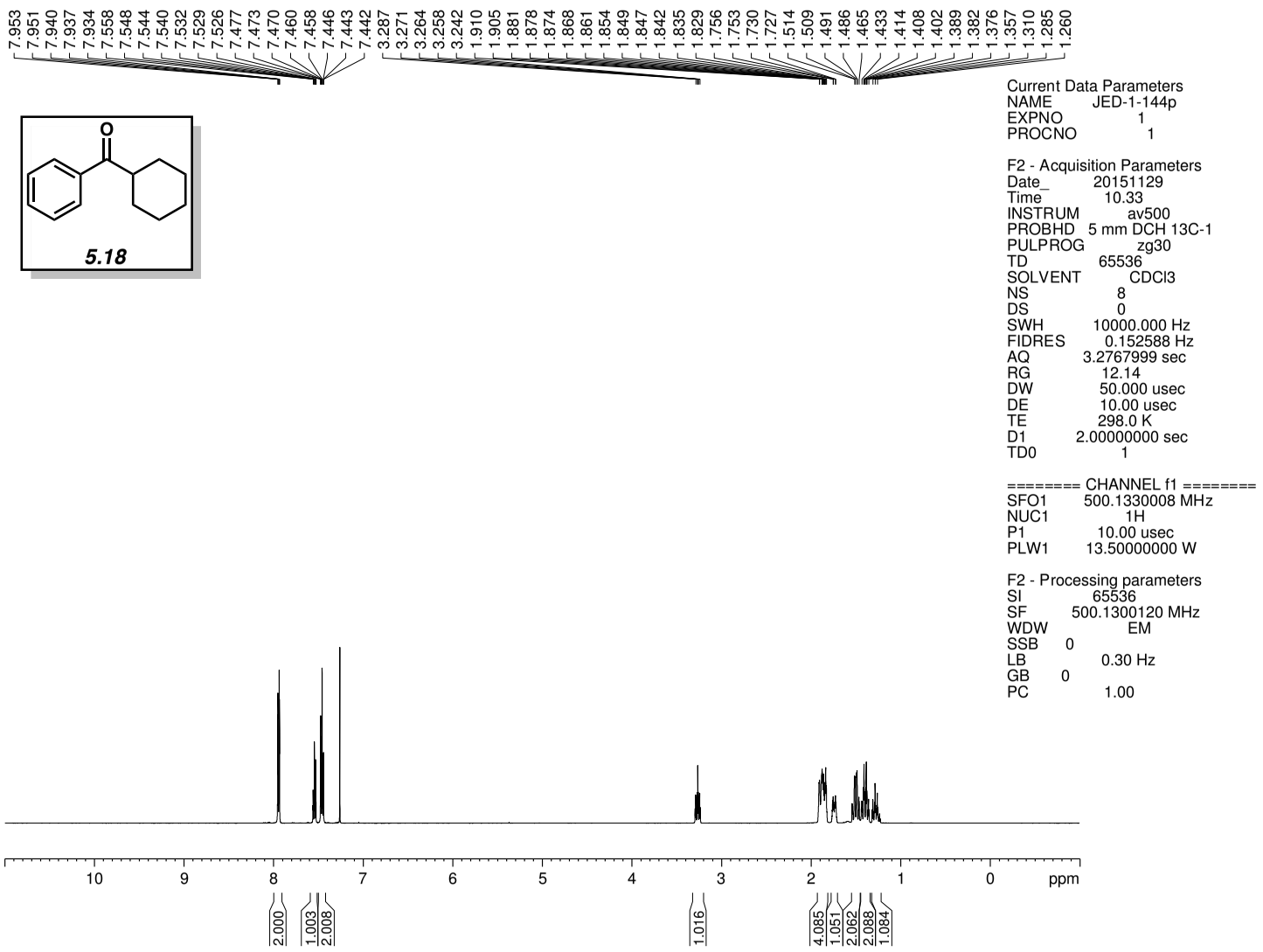

Figure 5.32 ^{1}H NMR (500 MHz, $CDCl_3$) of compound **5.18**.

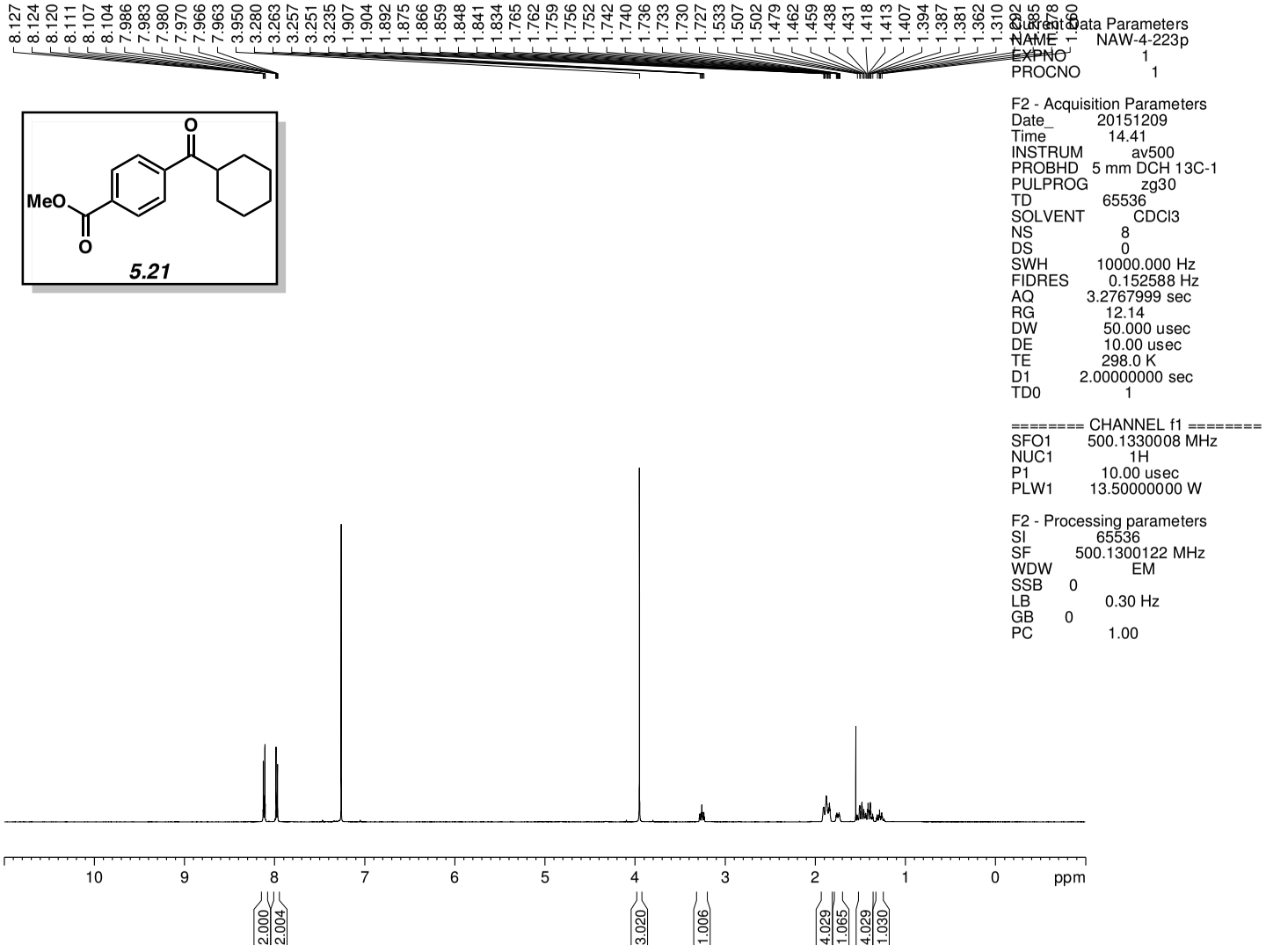

Figure 5.33 ^{1}H NMR (500 MHz, $CDCl_3$) of compound **5.21**.

5.10 Notes and References

(1) Greenberg, A., Breneman, C. M., Liebman, J. F., Eds. *The Amide Linkage: Structural Significance in Chemistry, Biochemistry, and Materials Science*; Wiley: New York, 2003; 1–672.

(2) Pauling, L.; Corey, R. B. *Proc. Natl. Acad. Sci. USA* **1951**, *37*, 729–740.

(3) (a) Hie, L.; Fine Nathel, N. F.; Shah, T. K.; Baker, E. L.; Hong, X.; Yang, Y.-F.; Liu, P.; Houk, K. N.; Garg, N. K. *Nature* **2015**, *524*, 79–83. (b) Weires, N. A.; Baker, E. L.; Garg, N. K. *Nat. Chem.* **2016**, *8*, 75–79.

(4) Li, X.; Zou, G. *Chem. Commun.* **2015**, *51*, 5089–5092.

(5) (a) Meng, G.; Szostak, M. *Org. Lett.* **2015**, *17*, 4364–4367. (b) Meng, G.; Szostak, M. *Org. Biomol. Chem.* **2016**, *14*, 5690–5707.

(6) For the activation of strained b-lactams using Pd, see: Yada, A.; Okajima, S.; Murakami, M. *J. Am. Chem. Soc.* **2015**, *137*, 8708–8711.

(7) For amide activation, accompanied by decarbonylation, see: (a) Meng, G.; Szostak, M. *Angew. Chem. Int. Ed.* **2015**, *54*, 14518–14522. (b) Meng, G.; Szostak, M. *Org. Lett.* **2016**, *18*, 796–799.

(8) Nahm, S.; Weinreb, S. M. *Tetrahedron Lett.* **1981**, *22*, 3815–3818.

(9) Organozinc halides are functional group tolerant and are not known to undergo nucleophilic attack on ketones, esters, or amides (including Weinreb amides). For pertinent discussions, see: (a) Cárdenas, D. J. *Angew. Chem. Int. Ed.* **2003**, *42*, 384–387. (b) Knochel, P.; Singer, R. D. *Chem. Rev.* **1993**, *93*, 2117–2188.

(10) (a) Rosen, B. M.; Quasdorf, K. W.; Wilson, D. A.; Zhang, N.; Resmerita, A.-M.; Garg, N. K.; Percec, V. *Chem. Rev.* **2011**, *111*, 1346–1416. (b) Tasker, S. Z.; Standley, E. A.; Jamison, T. F. *Nature* **2014**, *509*, 299–309. (c) Mesganaw, T.; Garg, N. K. *Org. Process Res. Dev.* **2013**, *17*, 29–39. (d) Ananikov, V. P. *ACS Catal.* **2015**, *5*, 1964–1971.

(11) For the coupling of acid chlorides with alkyl Grignard reagents, see: Scheiper, B.; Bonnekessel, M.; Krause, H.; Fürstner, A. *J. Org. Chem.* **2004**, *69*, 3943–3949.

(12) (a) Zhang, Y.; Rovis, T. *J. Am. Chem. Soc.* **2004**, *126*, 15964–15965. (b) Cherney, A. H.; Reisman, S. E. *Tetrahedron* **2014**, *70*, 3259–3265. (c) Harada, T.; Kotani, Y.; Katsuhira, T.; Oku, A. *Tetrahedron Lett.* **1991**, *32*, 1573–1576. (d) Negishi, E.-i.; Bagheri, V.; Chatterjee, S.; Luo, F.-T.; Miller, J. A.; Stoll, A. T. *Tetrahedron Lett.* **1983**, *24*, 5181–5184. (e) Iwai, T.; Nakai, T.; Mihara, M.; Ito, T.; Mizuno, T.; Ohno, T. *Synlett* **2009**, 1091–1094. (f) Grey, R. A. *J. Org. Chem.* **1984**, *49*, 2288–2289. (g) Sato, T.; Naruse, K.; Enokiya, M.; Fujisawa, T. *Chem. Lett.* **1981**, *10*, 1135–1138.

(13) (a) Wang, D.; Zhang, Z. *Org. Lett.* **2003**, *5*, 4645–4648. (b) Cook, M. J.; Rovis, T. *Synthesis* **2009**, 335–338. (c) Bercot, E. A.; Rovis, T. *J. Am. Chem. Soc.* **2002**, *124*, 174–175. (d) Bercot, E. A.; Rovis, T. *J. Am. Chem. Soc.* **2005**, *127*, 247–254. (e) Johnson, J. B.; Cook, M. J.; Rovis, T. *Tetrahedron* **2009**, *65*, 3202–3210. (f) Rogers, R. L.; Moore, J. L.; Rovis, T. *Angew. Chem. Int. Ed.* **2007**, *46*, 9301–9304. (g) Bercot, E. A.; Rovis, T. *J. Am. Chem. Soc.* **2004**, *126*, 10248–10249. (h) Johnson, J. B.; Yu, R. T.; Fink, P.; Bercot, E. A.; Rovis, T. *Org. Lett.* **2006**, *8*, 4307–4310. (i) Johnson, J. B.; Bercot, E. A.; Rowley, J. M.; Coates, G. W.; Rovis, T. *J. Am. Chem. Soc.* **2007**, *129*, 2718–2725. (j) Cook, M. J.; Rovis, T. *J. Am. Chem. Soc.* **2007**, *129*, 9302–9303.

(14) (a) Tokuyama, H.; Yokoshima, S.; Yamashita, T.; Fukuyama, T. *Tetrahedron Lett*. **1998**, *39*, 3189–3192. (b) Mori, Y.; Seki, M. *Tetrahedron Lett*. **2004**, *45*, 7343–7345. (c) Shimizu, T.; Seki, M. *Tetrahedron Lett*. **2002**, *43*, 1039–1042. (d) Miyazaki, T.; Han-ya, Y.; Tokuyama, H.; Fukuyama, T. *Synlett* **2004**, 477–480. (e) Shimizu, T.; Seki, M. *Tetrahedron Lett*. **2001**, *42*, 429–432. (f) Mori, Y.; Seki, M. *Adv*. *Synth*. *Catal*. **2007**, *349*, 2027–2038.

(15) The role of the *N*-substituents in amide C–N bond cleavage reactions is currently under investigation and will be described elsewhere in due course.

(16) *N*-Alkyl,Ts amides can be readily prepared by sulfonamide coupling of the corresponding carboxylic acid or acid halide (see the SI). For a discussion of the robustness of sulfonamides and their stability, see: Searles, S.; Nukina, S. *Chem*. *Rev*. **1959**, *59*, 1077–1103.

(17) Substrates derived from aliphatic carboxylic acids do not couple under the reported reaction conditions; studies to overcome this limitation are currently underway.

(18) Lower yields of **5.12** were obtained using the corresponding *N*-Me,Ts benzamide substrate. Generally, amides derived from electron-poor arenes were found to couple in higher yields when the *N*-Bn,Boc derivatives were employed.

(19) The organozinc bromide or iodide was used in accord with literature precedent for the formation of each organozinc species. Generally, alkyl bromides and iodides are known to undergo organozinc formation more readily than alkyl chlorides; see ref. 9b.

(20) Although primary and secondary organozinc species were well tolerated in the coupling, it was found that couplings with tertiary organozinc halides and organozinc reagents bearing heterocycles, acetals, and esters gave only trace amounts of product.

(21) Han, C.; Buchwald, S. L. *J*. *Am*. *Chem*. *Soc*. **2009**, *131*, 7532–7533.

(22) For the Ni-catalyzed activation of methyl esters, see: Hie, L.; Fine Nathel, N. F.; Hong, X.; Yang, Y.-F.; Houk, K. N.; Garg, N. K. *Angew. Chem. Int. Ed.* **2016**, *55*, 2810–2814. See ref. 10 for alternative examples of ester activation using nickel catalysis.

(23) Apnes, G. E.; Didluk, M. T.; Filipski, K. J.; Guzman-Perez, A.; Lee, E. C. Y.; Pfefferkorn, J. A.; Stevens, B. D.; Tu, M. M. Glucagon Receptor Modulators. U. S. Patent 20120202834, August 9th, 2012.

(24) (a) Allen, C. L.; Davulcu, S.; Williams, J. M. J. *Org. Lett.* **2010**, *12*, 5096–5099. (b) Krishnamoorthy, R.; Lam, S. Q.; Manley, C. M.; Herr, R. J. *J. Org. Chem.* **2010**, *75*, 1251–1258. (c) Baroudi, A.; Alicea, J.; Flack, P.; Kirincich, J.; Alabugin, I. V. *J. Org. Chem.* **2011**, *76*, 1521–1537. (d) Weires, N. A.; Baker, E. L.; Garg, N. K. *Nat. Chem.* **2016**, *8*, 75–79. (e) Yates, M. H.; Kallman, N. J.; Ley, C. P.; Wei, J. N. *Org. Process Res. Dev.* **2009**, *13*, 255–262. (f) Inamoto, Y.; Kaga, Y.; Nishimoto, Y.; Yasuda, M.; Baba, A. *Org. Lett.* **2013**, *15*, 3452–3455.

(25) Krasovskiy, A.; Malakhov, V.; Gavryushin, A.; Knochel, P. *Angew. Chem. Int. Ed.* **2006**, *45*, 6040–6044.

(26) Krasovskiy, A.; Knochel, P. *Synthesis* **2006**, 890–891.

(27) Zhao, B.; Lu, X. *Tetrahedron Lett.* **2006**, *47*, 6765–6768.

(28) Ahmad, I.; Pathak, V.; Vasudev, P. G.; Maurya, H. K.; Gupta, A. *RSC Adv.* **2014**, *4*, 24619–24634.

(29) Dolhem, E.; Barhdadi, R.; Folest, J. C.; Nédelec, J. Y.; Troupel, M. *Tetrahedron* **2001**, *57*, 525–529.

(30) Takemiya, A.; Hartwig, J. F. *J. Am. Chem. Soc.* **2006**, *128*, 14800–14801.

(31) Klemm, L. H.; Solomon, W. C.; Tamiz, A. P. *J. Org. Chem.* **1998**, *63*, 6503–6510.

(32) Jean, M.; Renault, J.; Uriac, P.; Capet, M.; van de Weghe, P. *Org. Lett.* **2007**, *9*, 3623–3625.

(33) Wu, J.; Yang, X.; He, Z.; Mao, X.; Hatton, T. A.; Jamison, T. F. *Angew. Chem. Int. Ed.* **2014**, *53*, 8416–8420.

(34) Gonzalez-de-Castro, A.; Xiao, J. *J. Am. Chem. Soc.* **2015**, *137*, 8206–8218.

CHAPTER SIX

Benchtop Delivery of $Ni(cod)_2$ Using Paraffin Capsules

Jacob E. Dander, Nicholas A. Weires, and Neil K. Garg.

Org. Lett. **2016**, *18*, 3934–3936.

6.1 Abstract

A facile method is reported that allows for $Ni(cod)_2$ to be used on the benchtop. The procedure involves the preparation of paraffin–$Ni(cod)_2$ capsules, which are stable to air and moisture. It is demonstrated that these readily available capsules can be used to promote a range of $Ni(cod)_2$-catalyzed transformations. These studies are expected to greatly facilitate the widespread use of $Ni(cod)_2$ in organic synthesis.

6.2 Introduction

In recent years, there has been an outpouring of new methodologies that involve the use of non-precious metal catalysts.[1] Nickel-catalyzed reactions, in particular, have grown increasingly popular because of nickel's high natural abundance, low cost, and low CO_2 footprint.[1] Moreover, the unique reactivity of nickel has opened new doors with regard to fundamental transformations.

A key challenge in the realm of nickel catalysis is the limited availability of Ni(0) precatalysts.[2] The most commonly used Ni(0) precatalyst is bis(1,5-cyclooctadiene)nickel(0) or $Ni(cod)_2$ (**6.1**, Figure 6.1), which has been employed in greater than 800 synthetic studies over the past three decades.[1,3] The cyclooctadiene ligands can be readily displaced by other ligands in situ, providing a means to examine and utilize various Ni/ligand combinations to enable a given

reaction. However, $Ni(cod)_2$ is not air-stable and requires handling in an inert atmosphere. Accordingly, the widespread use of $Ni(cod)_2$-promoted methodologies in chemical synthesis has remained limited.

One clever strategy for handling air sensitive catalysts is to prepare paraffin-based formulations. Inspired by the success of this approach in recent palladium-catalyzed cross-coupling reactions by Buchwald,[4] we sought to prepare paraffin–$Ni(cod)_2$ capsules.[5] Herein, we report a robust method to prepare these capsules and demonstrate that they can be used to perform a host of $Ni(cod)_2$-catalyzed reactions on the benchtop.

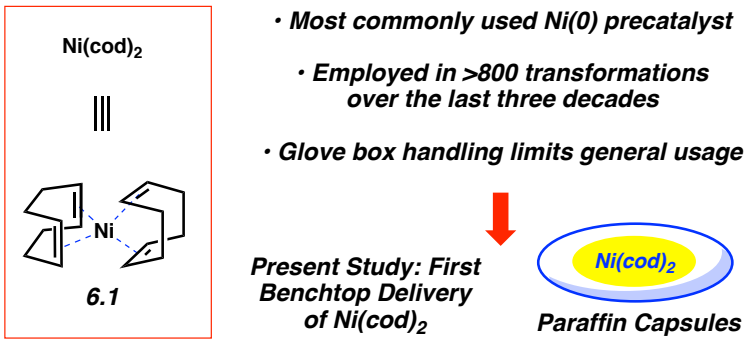

Figure 6.1. $Ni(cod)_2$ (**6.1**) and benchtop delivery using paraffin capsules (present study).

6.3 Preparation of Paraffin–Ni(cod)$_2$ Capsules

Our method for preparing the capsules is summarized in Figure 6.2. Melted paraffin wax (mp 53–57 °C) was placed into a standard brass mold. After cooling, the resulting wax cylinder was removed from the mold and trimmed to the desired size. Next, a cavity was bored in the wax cylinder using a standard drill bit. The resulting hollow and open capsule was brought into a glove box and charged with Ni(cod)$_2$. For some capsules, the air-sensitive NHC ligands SIPr or IPr were also added. After charging the capsules, a warm metal spatula was used to melt the top of the capsule closed. Removal from the glove box and re-dipping in molten wax (to ensure a proper seal) gave the desired capsules that were ready for use on the benchtop.[6]

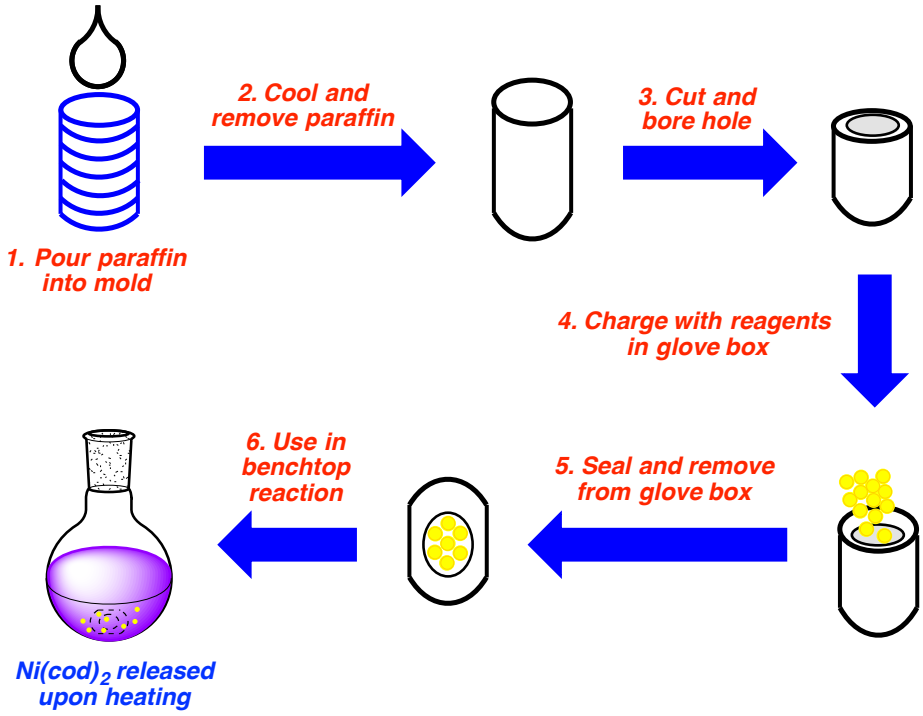

Figure 6.2. Preparation of paraffin–Ni(cod)$_2$ capsules.

6.4 Employment of Paraffin–Ni(cod)$_2$ Capsules in Amide C–N Bond Cleavage Reactions

As our laboratory has recently developed several new Ni(cod)$_2$-mediated reactions involving amide derivatives,[7] we were eager to test the paraffin–Ni(cod)$_2$ capsules in these processes. Figure 6.3 shows the success of these efforts. Initially, we sought to perform the esterification of amides.[7a] We were delighted to find that our procedure for benchtop delivery of Ni(cod)$_2$ facilitated the reaction of anilide **6.2** with (–)-menthol (**6.3**) to provide ester **6.4** in 95% yield. Having validated the feasibility of this approach, we examined several other reactions of amides. Transamidation of Boc-activated secondary amide **6.5** with morpholine (**6.6**) provided amide **6.7** in 87% yield.[7d] C–C bond formation from amides could also be achieved. For example, Suzuki–Miyaura cross-coupling of Boc-activated amide **6.8** with boronate **6.9** generated benzophenone **6.10** in 82% yield.[7b] Finally, Negishi coupling of amide **6.11** with organozinc halide **6.12** produced ketone **6.13**, albeit in slightly diminished yield.[7c]

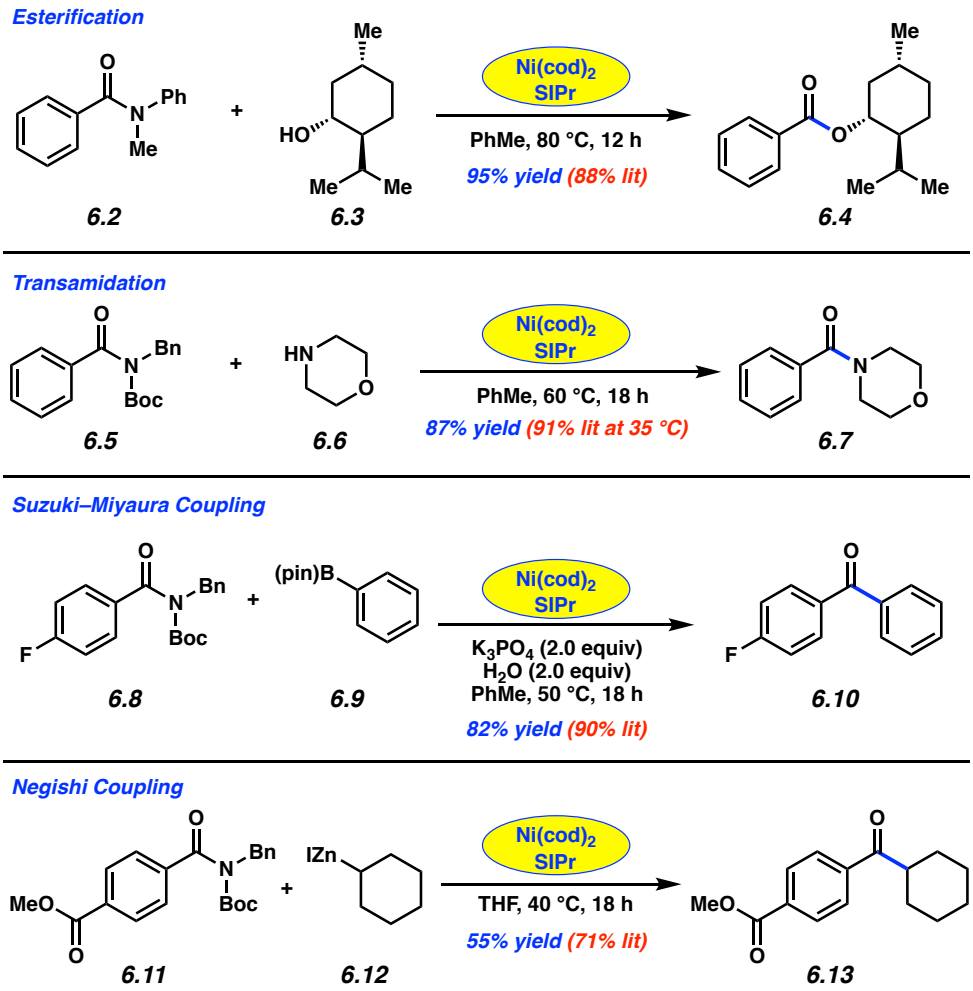

Figure 6.3. Ni-catalyzed reactions of amides using paraffin–Ni(cod)$_2$ capsules. 5–10% Ni(cod)$_2$ and 5–10% SIPr were employed. The yields shown reflect the average of two isolation experiments.

6.5 Exploration of Other Nickel-Catalyzed Reactions Using Paraffin–Ni(cod)$_2$ Capsules

Having validated the utility of the paraffin–Ni(cod)$_2$ capsules in the context of amide activation reactions, we tested the capsules in several other nickel-catalyzed processes (Figure 6.4). Buchwald–Hartwig coupling of sulfamate **6.14** with morpholine (**6.6**) furnished aniline derivative **6.15** using the benchtop variant of previously reported conditions.[8] Additionally, we tested the air-stable variant of Ni(cod)$_2$ in the context of the sp^2–sp^3 Suzuki–Miyaura cross-coupling.[9] Thus, alkyl bromide **6.16** was coupled with phenylboronic acid (**6.17**) to afford

arylated piperidine **6.18**.[2b] Another attractive use of $Ni(cod)_2$ lies in oxidative C–H functionalization reactions,[10,11] so we were keen to test the utility of our paraffin capsules in these methods as well. Under conditions developed by Chatani,[10] amide **6.19** underwent *N*-directed oxidative annulation with diphenylacetylene (**6.20**) to furnish isoquinolinone **6.21** in 88% yield. Finally, two oxidative conversions of aldehydes were tested. Oxidative esterification of aldehyde **6.22** with isopropanol (**6.23**) using Dong's recent methodology gave rise to ester **6.24** in excellent yield.[11] Moreover, oxidative amidation of benzaldehyde (**6.25**) with aniline (**6.26**) using paraffin-encapsulated $Ni(cod)_2$/IPr delivered amide **6.27**.[11] Of note, the paraffin–$Ni(cod)_2$ capsules can be employed in a variety of solvents (e.g., 1,4-dioxane, THF, 2-butanol, toluene), as long as the reaction mixture is heated to 40 °C or higher.

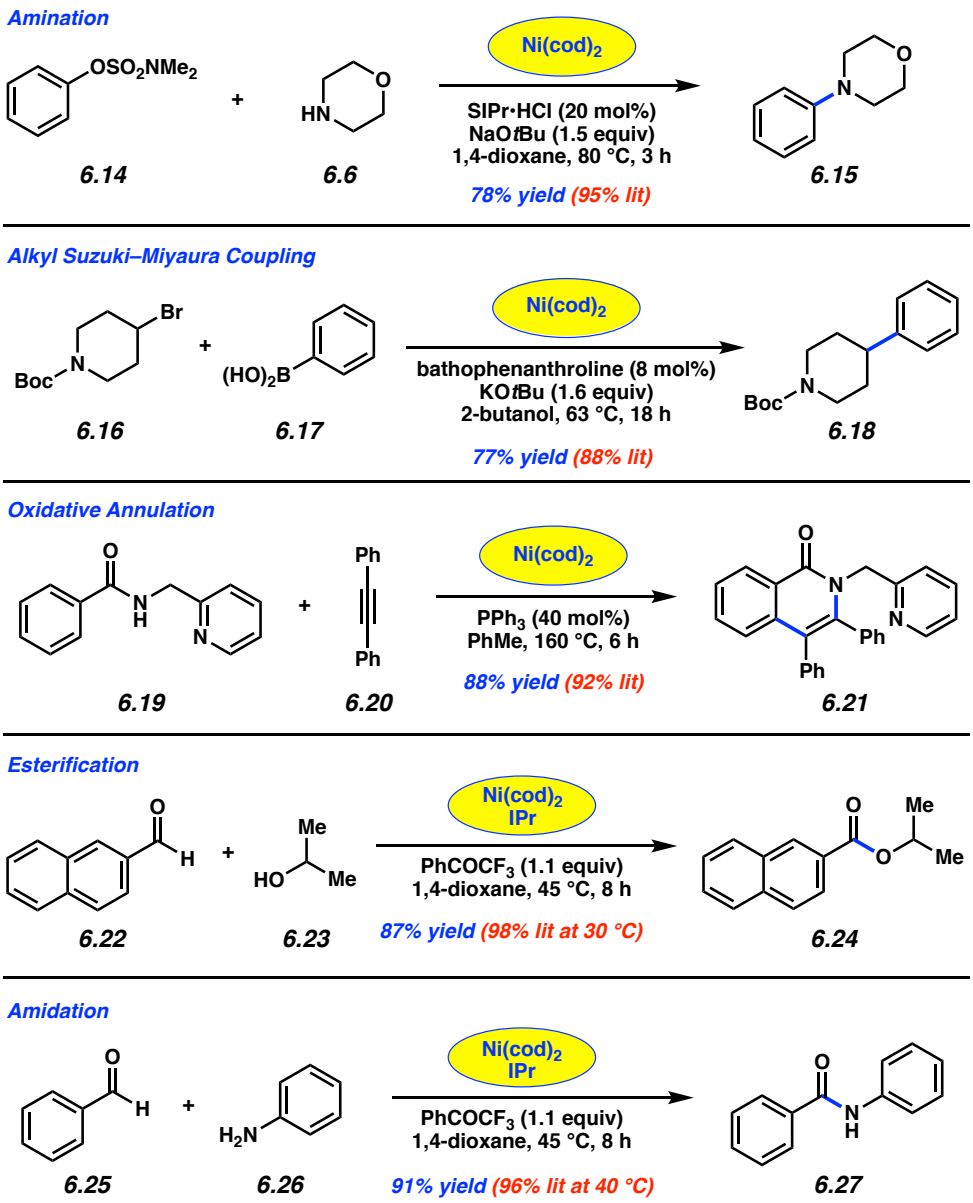

Figure 6.4. Ni-catalyzed amination, alkyl Suzuki–Miyaura coupling, oxidative annulation, esterification, and amidation using paraffin–Ni(cod)$_2$ capsules. 4–10% Ni(cod)$_2$ and 5–5.5% IPr was employed. The yields shown reflect the average of two isolation experiments.

6.6 Paraffin–Ni(cod)$_2$ Capsule Stability Tests and Gram-Scale Coupling

The paraffin–Ni(cod)$_2$ capsules were further evaluated via the experiments shown in Figure 6.5. In order to gauge the air stability of our paraffin–Ni(cod)$_2$ capsules, the esterification of amide **6.2** with (–)-menthol (**6.3**) was carried out with capsules that had been stored on the

benchtop for two weeks, one month, and two months. In all cases, the desired ester product **6.4** was obtained in >95% yield, indicating that prolonged exposure to atmospheric oxygen and water does not reduce the efficacy of the encapsulated Ni precatalyst.[12,13] We also performed a gram-scale coupling. To our delight, the benchtop esterification using one gram of substrate **6.2** delivered menthol ester **6.4** in 97% yield.

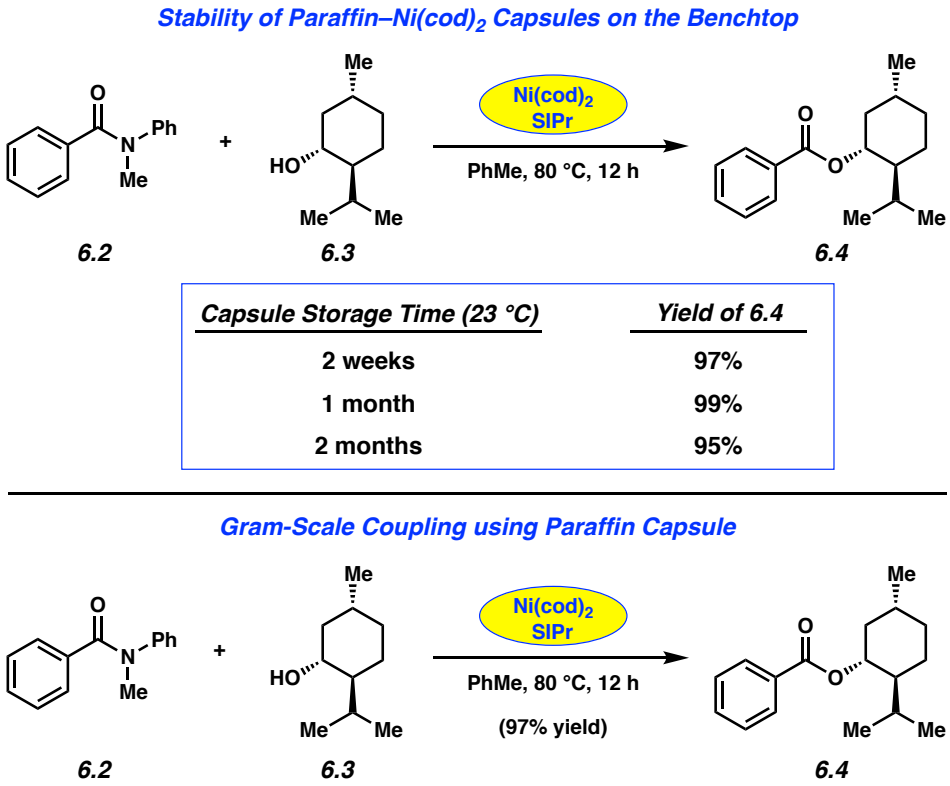

Figure 6.5. Stability tests of paraffin–Ni(cod)$_2$ capsules and gram-scale coupling. The yields for the stability test experiments were determined by ^{1}H NMR analysis using 1,3,5-trimethoxybenzene as an external standard. The yield for the gram-scale coupling reflects the yield of isolated product.

6.7 Conclusion

We have developed a facile approach that allows for $Ni(cod)_2$ to be used on the benchtop for the first time. Our strategy involves the preparation of paraffin–$Ni(cod)_2$ capsules, which are stable to air and moisture. The capsules, which will soon be commercially available,[14] promote a range of $Ni(cod)_2$-catalyzed transformations, including reactions of amides, aminations, alkyl Suzuki–Miyaura couplings, oxidative annulations, esterifications, and amidations. We hope that the method disclosed herein will help nurture the burgeoning field of nickel catalysis in academia and industry.

6.8 Experimental Section

6.8.1 Materials and Methods

Unless stated otherwise, reactions were conducted in flame-dried glassware under an atmosphere of nitrogen and commercially obtained reagents were used as received. Non-commercially available substrates were synthesized following protocols specified in Section 6.8.2.1 in the Experimental Procedures. Prior to use, toluene and tetrahydrofuran were purified by distillation and taken through five freeze-pump-thaw cycles, and 1,4-dioxane was purified by distillation and sparged with nitrogen for 20 min. Iodine and morpholine (**6.6**) were obtained from Spectrum Chemical, and morpholine (**6.6**) was distilled before use. Paraffin wax (mp 53–57 °C ASTM D 87), iodocyclohexane, 2-naphthaldehyde (**6.22**), aniline (**6.26**), benzylamine, acid chloride **6.28**, 2,2,2-trifluoroacetophenone, SIPr•HCl, and anhydrous 2-butanol were obtained from Sigma–Aldrich and used as received. Benzaldehyde (**6.25**) and 1,2-dibromoethane were obtained from Sigma–Aldrich and distilled before use. Phenylboronic acid pinacol ester (**6.9**) and 1-*N*-Boc-4-bromopiperidine (**6.16**) were obtained from Combi-Blocks. $Ni(cod)_2$, SIPr, IPr, and Zn powder (325 mesh, 99.9%) were obtained from Strem Chemicals and stored in a glove box. Triphenylphosphine was obtained from Strem Chemicals. Anhydrous lithium chloride (99%) was obtained from Alfa Aesar and stored in a glove box. Chlorotrimethylsilane, sodium *tert*-butoxide, and bathophenanthroline were obtained from Alfa Aesar, and chlorotrimethylsilane was distilled before use. Diphenylacetylene (**6.20**) and (–)-menthol (**6.3**) were obtained from Eastman Chemical Co., and (–)-menthol (**6.3**) was recrystallized before use. Phenylboronic acid (**6.17**) was obtained from Oakwood Products, Inc. K_3PO_4 was obtained from Acros. Isopropyl alcohol (**6.23**) was obtained from EMD and used as received. Reaction temperatures were controlled using an IKAmag temperature modulator, and unless stated otherwise, reactions were

performed at room temperature (approximately 23 °C). Thin-layer chromatography (TLC) was conducted with EMD gel 60 F254 pre-coated plates (0.25 mm for analytical chromatography and 0.50 mm for preparative chromatography) and visualized using a combination of UV, iodine, anisaldehyde, and potassium permanganate staining techniques. Silicycle Siliaflash P60 (particle size 0.040–0.063 mm) was used for flash column chromatography. ^{1}H NMR spectra were recorded on Bruker spectrometers (at 500 MHz) and are reported relative to residual solvent signals.

6.8.2 Experimental Procedures

6.8.2.1 Substrate Synthesis

Representative Procedure for the syntheses of amide substrates from Figure 6.3 (synthesis of amide 6.8 is used as an example).

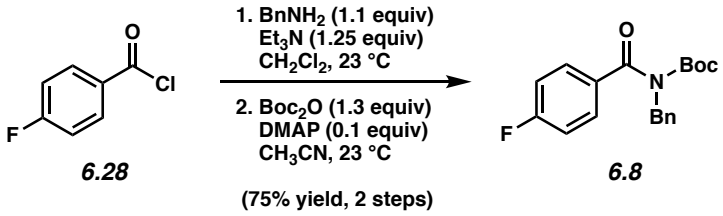

To a solution of acid chloride **6.28** (1.14 g, 7.18 mmol, 1.0 equiv), triethylamine (1.24 mL, 8.97 mmol, 1.25 equiv), and dichloromethane (10.0 mL), was added dropwise a solution of benzylamine (0.861 mL, 7.89 mmol, 1.1 equiv) in dichloromethane (4.4 mL, 0.5 M in total) over 3 min. The reaction mixture was stirred at 23 °C for 4 h, diluted with EtOAc (10 mL), and then washed successively with 1.0 M HCl (10 mL) and brine (10 mL). The organic layer was dried over Na_2SO_4 and concentrated under reduced pressure. The resulting crude solid material was used in the subsequent step without further purification.

To a flask containing the crude material from the previous step was added DMAP (76.9 mg, 0.630 mmol, 0.1 equiv), followed by acetonitrile (31.7 mL, 0.2 M). Boc_2O (1.80 g, 8.23 mmol, 1.3 equiv) was added in one portion and the reaction vessel was flushed with N_2. After stirring the reaction mixture at 23 °C for 25 h, the reaction was quenched by the addition of saturated aqueous $NaHCO_3$ (10 mL), transferred to a separatory funnel with EtOAc (10 mL) and H_2O (10 mL), and extracted with EtOAc (3 x 20 mL). The organic layers were combined, dried over Na_2SO_4, and evaporated under reduced pressure. The resulting crude residue was purified by flash chromatography (19:1 Hexanes:EtOAc) to yield amide **6.8** (1.74 g, 75% yield, over two steps) as a white solid. Spectral data match those previously reported.[7b]

Note: Supporting information for the syntheses of substrates shown in Figures 6.3, 6.4, and 6.5 have previously been reported: **6.2**,[15a] **6.5**,[15b] **6.8**,[7b] **6.11**,[7b] **6.14**,[15c] and **6.19**.[10]

6.8.2.2 Preparation of Cyclohexylzinc Iodide (6.12)

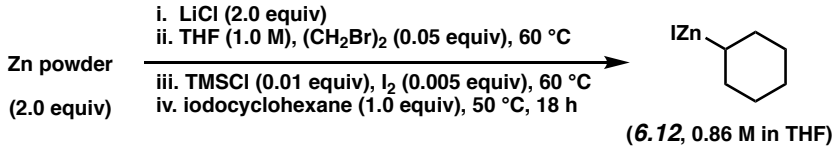

Following a modification of the procedure reported by Knochel,[16] a flame-dried 25 mL round bottom flask equipped with a magnetic stir bar and rubber septum was brought into a glove box where Zn powder (1.30 g, 20.0 mmol, 2.0 equiv, Strem 325 mesh) and anhydrous LiCl (840 mg, 20.0 mmol, 2.0 equiv) were added. The flask was then removed from the glove box and heated with a heat gun for 10 min under high vacuum, cooled to room temperature, and then backfilled with N_2. Freshly distilled THF (10.0 mL) and 1,2-dibromoethane (43 μL, 0.50 mmol, 0.05 equiv) were added via syringe and the reaction mixture was heated at 60 °C for 20 min. After cooling to room temperature, freshly distilled TMSCl (12 μL, 0.10 mmol, 0.01 equiv) followed by a

solution of I_2 (12.8 mg, 0.05 mmol, 0.005 equiv) in THF (50 μL, 1.0 M) were added via syringe and the reaction mixture was heated again at 60 °C for 20 min. After cooling to room temperature, iodocyclohexane (1.30 mL, 10.0 mmol, 1.0 equiv) was added dropwise via syringe over 1 min. A flame-dried air condenser was attached to the flask under N_2 and the reaction vessel was heated at 50 °C for 18 h. The reaction mixture was cooled to room temperature and allowed to stand for 1 h before the supernatant fluid was transferred to a flame-dried schlenk flask via syringe. The concentration of the organozinc halide was determined to be 0.86 M by iodometric titration using Knochel's procedure.[17]

6.8.2.3 Preparation of Paraffin–Ni(cod)$_2$ Capsules

Representative Procedure for the preparation of paraffin–Ni(cod)$_2$ capsules for Sections 6.8.2.5–6.8.2.14 in the Experimental Procedures (preparation of paraffin–Ni(cod)$_2$ capsules for use in section 6.8.2.5 in the Experimental Procedures is used as an example). Paraffin wax (mp 53–57 °C ASTM D 87) was melted in a 250 mL beaker suspended in an oil bath set to 80 °C.

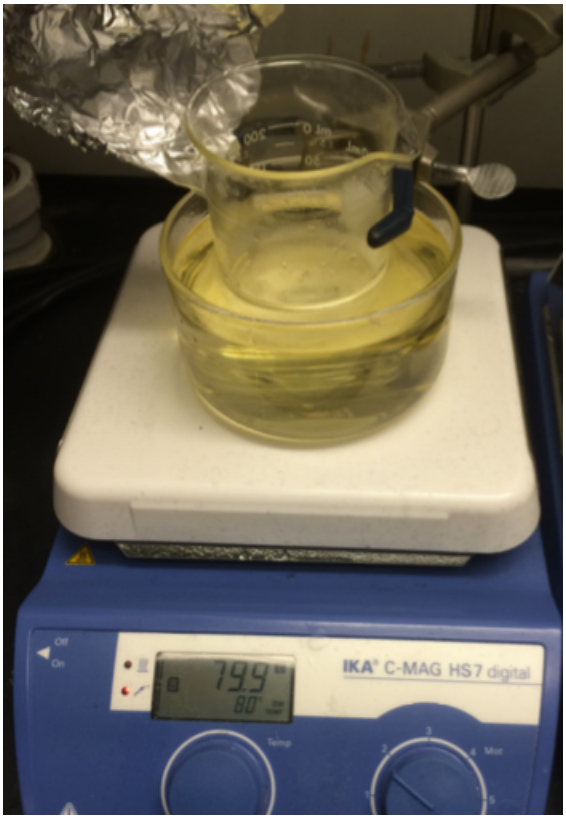

Approximately 1 mL of molten paraffin was then pipetted into a standard brass mold (Nipple Brass, 1/8 in x close) using a 5 3/4 in glass pipette and pipette bulb.

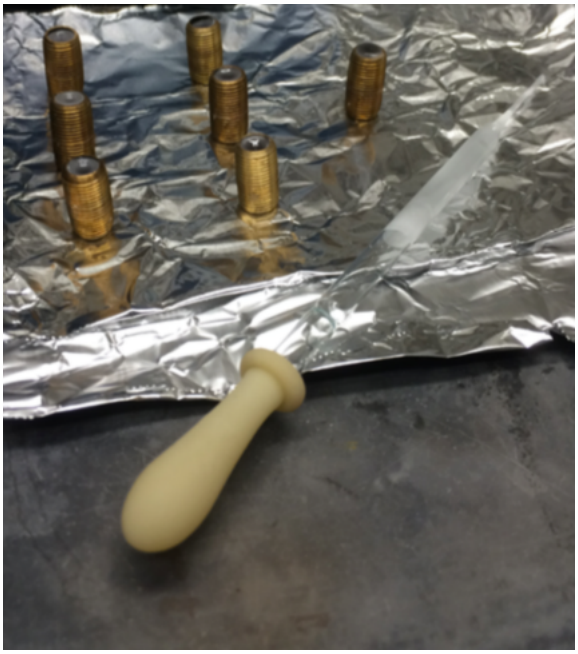

After cooling, the resulting wax cylinder was removed from the brass mold and trimmed to approximately 1 cm in length using a razor blade.

Next, a cavity was bored in the wax cylinder using a standard drill bit (5/32 in, black oxide), taking care not to bore through the entire cylinder.

The resulting hollow and open capsule was brought into a glove box, inserted into a 14/20 septum for ease of handling, and charged with $Ni(cod)_2$ (5.5 mg, 0.020 mmol, 10 mol%) and SIPr (7.8 mg 0.020 mmol, 10 mol%).

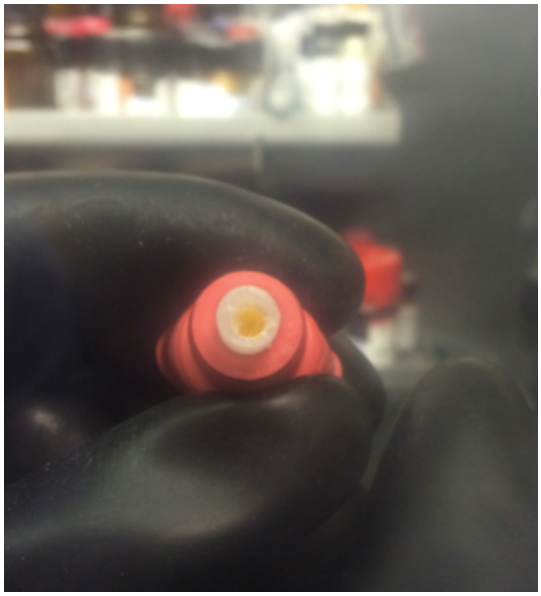

After charging the capsule, a warm metal spatula (maintained at approximately 80 °C using a hot plate in the glove box) was used to melt the top of the capsule closed. Removal from the glove box and re-dipping in molten wax (to ensure a proper seal) gave the desired capsules that were ready for use on the benchtop (Sections 6.8.2.5–6.8.2.14 in the Experimental Procedures).

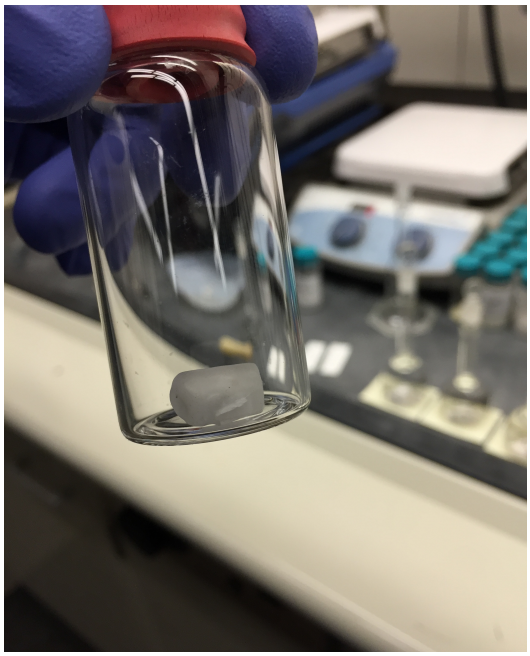

Note: Typically, paraffin–Ni(cod)$_2$ capsules generated in this way were used within 24 h of being prepared. For a detailed study of paraffin–Ni(cod)$_2$ capsule stability to air and moisture over prolonged periods of time, see Section 6.8.2.14 in the Experimental Procedures. For a detailed study of non-encapsulated Ni(cod)$_2$ and SIPr stability to air and moisture over prolonged periods of time, see Section 6.8.2.15 in the Experimental Procedures.

6.8.2.4 Preparation of Paraffin–Ni(cod)$_2$ Capsules for Gram-Scale Esterification

Representative Procedure for preparation of paraffin–Ni(cod)$_2$ capsules for Section 6.8.2.16 in the Experimental Procedures. Paraffin wax (mp 53–57 °C ASTM D 87) was melted in a 250 mL beaker suspended in an oil bath set to 80 °C. Approximately 9 mL of molten paraffin was then pipetted into a standard glass VWR culture tube (16 x 125 mm) using a 5 3/4 in glass pipette and pipette bulb. After cooling, the resulting wax cylinder was removed from the culture

tube (by scoring and carefully breaking the glass away from the paraffin) and trimmed to approximately 2.5 cm in length using a razor blade.

Next, a cavity was bored in the wax cylinder using a standard drill bit (3/8 in, black oxide), taking care not to bore through the entire cylinder.

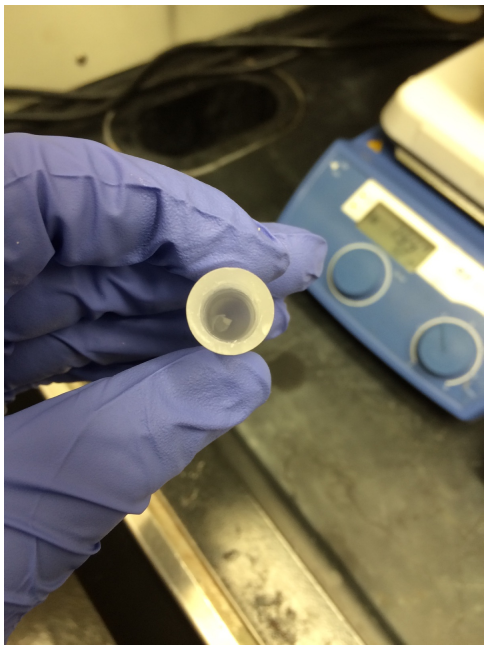

The resulting hollow and open capsule was brought into a glove box and charged with $Ni(cod)_2$ (130 mg, 0.474 mmol, 10 mol%) and SIPr (185 mg, 0.474 mmol, 10 mol%). After charging the capsule, a warm metal spatula (maintained at approximately 80 °C using a hot plate in the glove box) was used to melt the top of the capsule closed. Removal from the glove box and re-dipping in molten wax (to ensure a proper seal) gave the desired capsules that were ready for use on the benchtop (Section 6.8.2.16 in the Experimental Procedures).

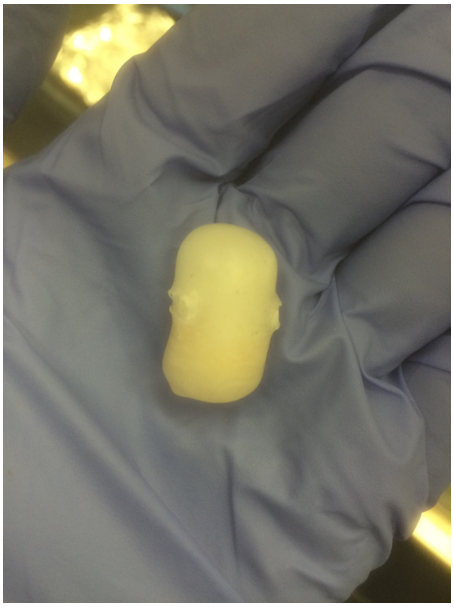

6.8.2.5 Esterification of Amide 6.2

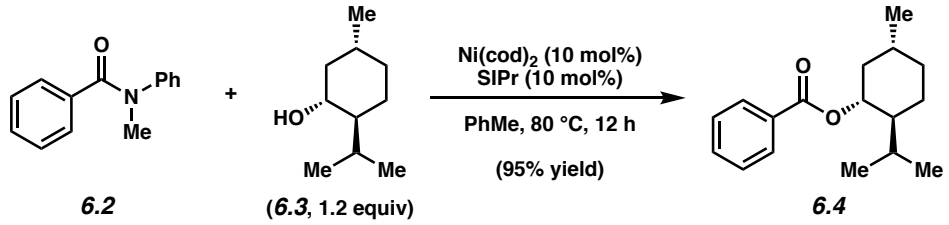

Ester 6.4. A 1-dram vial containing a magnetic stir bar was flame-dried under reduced pressure, and then allowed to cool under N_2. The vial was charged with amide substrate **6.2** (42.2 mg, 0.200 mmol, 1.0 equiv), (–)-menthol (**6.3**, 37.5 mg, 0.240 mmol, 1.2 equiv) and a paraffin capsule containing $Ni(cod)_2$ (5.5 mg, 0.020 mmol, 10 mol%) and SIPr (7.8 mg, 0.020 mmol, 10 mol%) prepared as described in Section 6.8.2.3 in the Experimental Procedures. The vial was flushed with N_2, and subsequently toluene (0.20 mL, 1.0 M) was added. The vial was capped with a Teflon-lined screw cap under a flow of N_2 and the reaction mixture was stirred at 80 °C for 12 h. After removing the vial from heat, the reaction mixture was transferred to a 100 mL round bottom flask containing 2.0 g of silica gel with hexanes (6.0 mL) and CH_2Cl_2 (6.0 mL).

The mixture was adsorbed onto the silica gel under reduced pressure and filtered over a plug of silica gel (100 mL of hexanes eluent to remove paraffin, then 100 mL of 4:1 Hexanes:EtOAc eluent). The volatiles were removed under reduced pressure, and the crude residue was purified by preparative thin-layer chromatography (5:1 Hexanes:EtOAc) to yield ester **6.4** (95% yield, average of two experiments) as a white solid. Ester **6.4**: R_f 0.58 (5:1 Hexanes:EtOAc). The reported literature yield is 88%.[7a] Spectral data match those previously reported.[18]

6.8.2.6 Transamidation of Amide 6.5

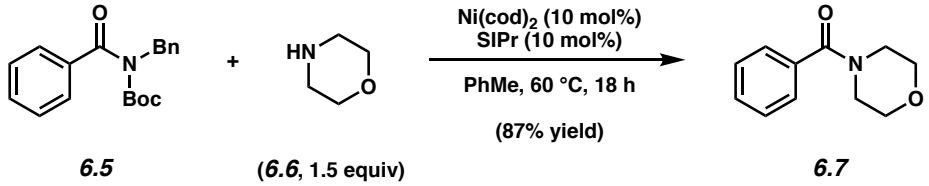

6.5 (*6.6*, 1.5 equiv) *6.7*

Amide 6.7. A 1-dram vial containing a magnetic stir bar was flame-dried under reduced pressure, and then allowed to cool under N_2. The vial was charged with amide substrate **6.5** (62.2 mg, 0.200 mmol, 1.0 equiv), morpholine (**6.6**, 37.0 mL, 0.300 mmol, 1.5 equiv), and a paraffin capsule containing $Ni(cod)_2$ (5.5 mg, 0.020 mmol, 10 mol%) and SIPr (7.8 mg, 0.020 mmol, 10 mol%) prepared as described in Section 6.8.2.3 in the Experimental Procedures. The vial was flushed with N_2, and subsequently toluene (0.20 mL, 1.0 M) was added. The vial was capped with a Teflon-lined screw cap under a flow of N_2 and the reaction mixture was stirred at 60 °C for 18 h. After removing the vial from heat, the reaction mixture was transferred to a 100 mL round bottom flask containing 2.0 g of silica gel with hexanes (6.0 mL) and CH_2Cl_2 (6.0 mL). The mixture was adsorbed onto the silica gel under reduced pressure and filtered over a plug of silica gel (100 mL of hexanes eluent to remove paraffin, then 100 mL of 2:1 Hexanes:EtOAc eluent). The volatiles were removed under reduced pressure, and the crude residue was purified

by preparative thin-layer chromatography (3:1 Hexanes:EtOAc) to yield amide **6.7** (87% yield, average of two experiments) as a colorless oil. Amide **6.7**: R_f 0.24 (1:1 Hexanes:EtOAc). The reported literature yield is 91% when the reaction is run at 35 °C.[7d] Spectral data match those previously reported.[19]

6.8.2.7 Suzuki–Miyaura Coupling of Amide 6.8

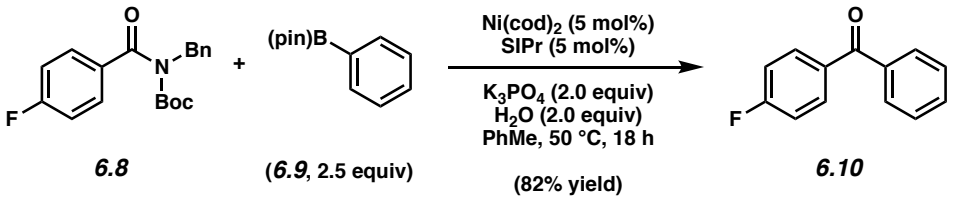

Ketone 6.10. A 1-dram vial was charged with anhydrous powdered K_3PO_4 (84.8 mg, 0.400 mmol, 2.0 equiv) and a magnetic stir bar. The vial and contents were flame-dried under reduced pressure, and then allowed to cool under N_2. The vial was charged with amide substrate **6.8** (65.8 mg, 0.200 mmol, 1.0 equiv), phenylboronic acid pinacol ester (**6.9**, 102.0 mg, 0.500 mmol, 2.5 equiv), and a paraffin capsule containing $Ni(cod)_2$ (2.8 mg, 0.010 mmol, 5 mol%) and SIPr (3.9 mg, 0.010 mmol, 5 mol%) prepared as described in Section 6.8.2.3 in the Experimental Procedures. The vial was flushed with N_2, and subsequently water (7.2 mL, 0.400 mmol, 2.0 equiv) and toluene (0.20 mL, 1.0 M) were added. The vial was capped with a Teflon-lined screw cap under a flow of N_2 and the reaction mixture was stirred vigorously (1,000 rpm) at 50 °C for 18 h. After removing the vial from heat, the reaction mixture was transferred to a 100 mL round bottom flask containing 2.0 g of silica gel with hexanes (6.0 mL) and CH_2Cl_2 (6.0 mL). The mixture was adsorbed onto the silica gel under reduced pressure and filtered over a plug of silica gel (50 mL of hexanes eluent to remove paraffin, then 50 mL of EtOAc eluent). The volatiles were removed under reduced pressure, and the crude residue was purified by preparative thin-

layer chromatography (8:1:1 Hexanes:Et_2O:CH_2Cl_2) to yield ketone **6.10** (82% yield, average of two experiments) as a white solid. Ketone **6.10**: R_f 0.58 (5:1 Hexanes:EtOAc). The reported literature yield is 90% when the reaction is run using 1.2 equiv boronate **6.9**.[7b] Spectral data match those previously reported.[20]

6.8.2.8 Negishi Coupling of Amide 6.11

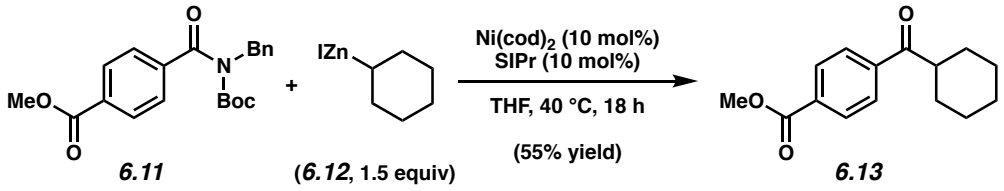

Ketone 6.13. A 1-dram vial was charged with a magnetic stir bar and flame-dried under reduced pressure, and then allowed to cool under N_2. The vial was charged with amide substrate **6.11** (73.8 mg, 0.200 mmol, 1.0 equiv) and a paraffin capsule containing $Ni(cod)_2$ (5.5 mg, 0.020 mmol, 10 mol%) and SIPr (7.8 mg, 0.020 mmol, 10 mol%) prepared as described in Section 6.8.2.3 in the Experimental Procedures. The vial was flushed with N_2, and subsequently THF (0.50 mL, 0.40 M) was added. The reaction mixture was allowed to stir at 40 °C for 1 h, over which time a red-orange color developed. Concurrently, the cyclohexylzinc iodide solution (**6.12**) was heated in a water bath at 50 °C for 1 h. A portion of the preheated solution of **6.12** (349 μL, 0.300 mmol, 1.5 equiv, 0.86 M in THF) was then added to the reaction mixture at 40 °C dropwise via syringe over 3 sec. The vial was capped with a Teflon-lined screw cap under a flow of N_2, and the reaction mixture was allowed to stir at 40 °C for 18 h. After removing the vial from heat, the reaction mixture was transferred to a 100 mL round bottom flask containing 2.0 g of silica gel with hexanes (6.0 mL) and CH_2Cl_2 (6.0 mL). The mixture was adsorbed onto the silica gel under reduced pressure and filtered over a plug of silica gel (50 mL of hexanes eluent

to remove paraffin, then 50 mL of EtOAc eluent). The volatiles were removed under reduced pressure, and the crude residue was purified by flash chromatography (24:1 Hexanes:EtOAc) to yield ketone **6.13** (55% yield, average of two experiments) as an off-white solid. Ketone **6.13**: R_f 0.50 (5:1 Hexanes:EtOAc). The reported literature yield is 71% when the reaction is run at 23 °C and 1.0 M.[7c] Spectral data match those previously reported.[21]

6.8.2.9 Amination of Sulfamate 6.14

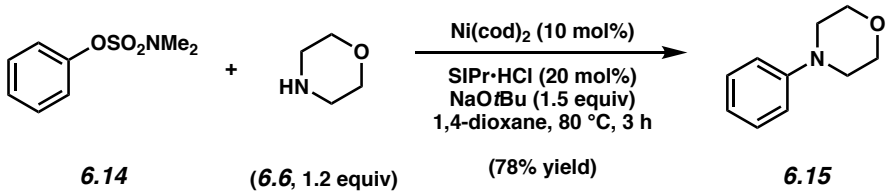

Amine 6.15. A 20 mL vial containing a magnetic stir bar was flame-dried under reduced pressure, and then allowed to cool under N_2. The vial was charged with morpholine (**6.6**, 52.4 mL, 0.600 mmol, 1.2 equiv), sulfamate **6.14** (100.5 mg, 0.500 mmol, 1.0 equiv), anhydrous powdered NaO*t*Bu (72.0 mg, 0.750 mmol, 1.5 equiv), SIPr•HCl (42.7 mg, 0.100 mmol, 20 mol%), and a paraffin capsule containing $Ni(cod)_2$ (13.8 mg, 0.050 mmol, 10 mol%) prepared as described in Section 6.8.2.3 in the Experimental Procedures. The vial was flushed with N_2, and subsequently 1,4-dioxane (2.5 mL, 0.20 M) was added. The vial was capped with a Teflon-lined screw cap under a flow of N_2 and the reaction mixture was stirred at 80 °C for 3 h. After removing the vial from heat, the reaction mixture was transferred to a 100 mL round bottom flask containing 3.0 g of silica gel with hexanes (6.0 mL) and CH_2Cl_2 (6.0 mL). The mixture was adsorbed onto the silica gel under reduced pressure and filtered over a plug of silica gel (100 mL of hexanes eluent to remove paraffin, then 100 mL of 1:1 Hexanes:EtOAc eluent). The volatiles were removed under reduced pressure, and the crude residue was purified by preparative thin-

layer chromatography (19:1 PhH:EtOAc) to yield amine **6.15** (78% yield, average of two experiments) as a white solid. Amine **6.15**: R_f 0.30 (9:1 Hexanes:EtOAc). The reported literature yield is 95% when the reaction is run using 5 mol% $Ni(cod)_2$ and 10 mol% SIPr•HCl.[8] Spectral data match those previously reported.[22]

6.8.2.10 Suzuki–Miyaura Coupling of Alkyl Halide 6.16

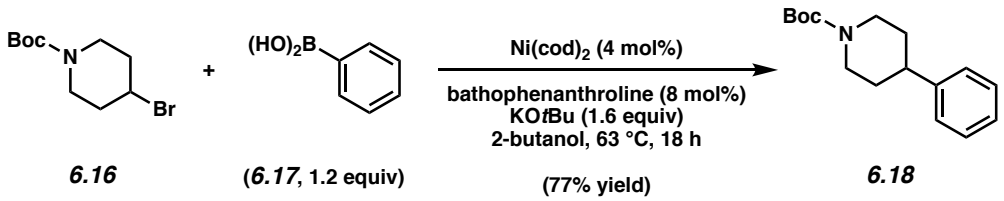

Carbamate 6.18. A 1-dram vial was charged with a magnetic stir bar and flame-dried under reduced pressure, and then allowed to cool under N_2. The vial was charged with anhydrous powdered KO*t*Bu (89.6 mg, 0.800 mmol, 1.6 equiv), phenylboronic acid (**6.17**, 73.2 mg, 0.600 mmol, 1.2 equiv), bathophenanthroline (13.2 mg, 0.040 mmol, 8 mol%), and a paraffin capsule containing $Ni(cod)_2$ (5.5 mg, 0.020 mmol, 4 mol%) prepared as described in Section 6.8.2.3 in the Experimental Procedures. The vial was flushed with N_2, and subsequently anhydrous 2-butanol (2.8 mL, 0.20 M) was added. The reaction mixture was allowed to stir at 63 °C for 10 min, over which time a deep purple color developed. A solution of alkyl halide **6.16** (132.0 mg, 0.500 mmol, 1.0 equiv, 2.5 M in anhydrous 2-butanol) was then added to the reaction mixture at 63 °C rapidly via syringe. The vial was capped with a Teflon-lined screw cap under a flow of N_2, and the reaction mixture was allowed to stir at 63 °C for 18 h. After removing the vial from heat, the reaction mixture was transferred to a 100 mL round bottom flask containing 2.0 g of silica gel with hexanes (6.0 mL) and CH_2Cl_2 (6.0 mL). The mixture was adsorbed onto the silica gel under reduced pressure and filtered over a plug of silica gel (50 mL of hexanes eluent to remove

paraffin, then 50 mL of EtOAc eluent). The volatiles were removed under reduced pressure, and the crude residue was purified by flash chromatography (24:1 Hexanes:EtOAc → 14:1 Hexanes:EtOAc) to yield carbamate **6.18** (77% yield, average of two experiments) as a colorless oil. Carbamate **6.18**: R_f 0.42 (5:1 Hexanes:EtOAc). The reported literature yield is 88%.[2b] Spectral data match those previously reported.[23]

6.8.2.11 Oxidative Annulation of Amide 6.19

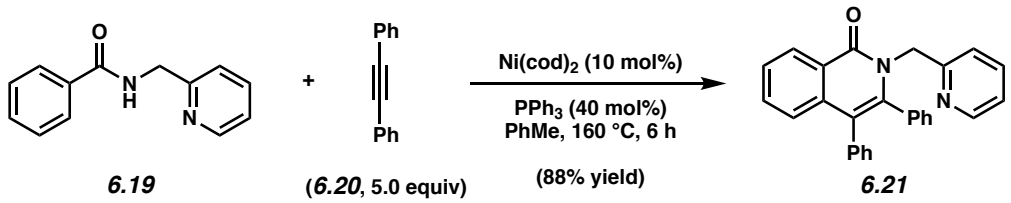

6.19 (*6.20*, 5.0 equiv) *6.21*

Isoquinolinone 6.21. A 1-dram vial was charged with a magnetic stir bar and flame-dried under reduced pressure, and then allowed to cool under N_2. The vial was charged with amide substrate **6.19** (106.0 mg, 0.500 mmol, 1.0 equiv), diphenylacetylene (**6.20**, 445.0 mg, 2.500 mmol, 5.0 equiv), triphenylphosphine (52.4 mg, 0.200, 40 mol%), and a paraffin capsule containing $Ni(cod)_2$ (13.8 mg, 0.050 mmol, 10 mol%) prepared as described in Section 6.8.2.3 in the Experimental Procedures. The vial was flushed with N_2, and subsequently toluene (2.0 mL, 0.25 M) was added. The vial was capped with a Teflon-lined screw cap under a flow of N_2 and the reaction mixture was stirred at 160 °C for 6 h. After removing the vial from heat, the reaction mixture was transferred to a 100 mL round bottom flask containing 2.0 g of silica gel with hexanes (6.0 mL) and CH_2Cl_2 (6.0 mL). The mixture was adsorbed onto the silica gel under reduced pressure and filtered over a plug of silica gel (50 mL of hexanes eluent to remove paraffin, then 50 mL of EtOAc eluent). The volatiles were removed under reduced pressure, and the crude residue was purified by flash chromatography (2:1 Hexanes:EtOAc → 1:1

Hexanes:EtOAc) to yield isoquinolinone **6.21** (88% yield, average of two experiments) as a tan solid. Isoquinolinone **6.21**: R_f 0.64 (100% EtOAc). The reported literature yield is 92%.[10] Spectral data match those previously reported.[10]

6.8.2.12 Esterification of Aldehyde 6.22

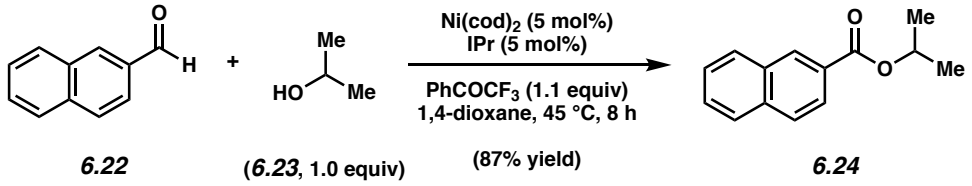

Ester 6.24. A 1-dram vial was charged with a magnetic stir bar and flame-dried under reduced pressure, and then allowed to cool under N_2. The vial was charged with a paraffin capsule containing $Ni(cod)_2$ (6.9 mg, 0.025 mmol, 5 mol%) and IPr (9.7 mg, 0.025 mmol, 5 mol%) prepared as described in Section 6.8.2.3 in the Experimental Procedures. The vial was flushed with N_2, and subsequently 1,4-dioxane (1.0 mL) was added. The reaction mixture was allowed to stir at 45 °C for 20 min, over which time a black color developed. A solution of isopropyl alcohol (**6.23**, 38.2 mL, 0.500 mmol, 1.0 equiv) in 1,4-dioxane (0.5 mL) was then added to the reaction mixture at 45 °C rapidly via syringe, followed by a solution of aldehyde **6.22** (78.0 mg, 0.500 mmol, 1.0 equiv) and 2,2,2-trifluoroacetophenone (76.6 mL, 0.550 mmol, 1.1 equiv) in 1,4-dioxane (1.0 mL, 0.20 M in total) in the same manner. The vial was capped with a Teflon-lined screw cap under a flow of N_2, and the reaction mixture was allowed to stir at 45 °C for 8 h. After removing the vial from heat, the reaction mixture was transferred to a 100 mL round bottom flask containing 3.0 g of silica gel with hexanes (6.0 mL) and CH_2Cl_2 (6.0 mL). The mixture was adsorbed onto the silica gel under reduced pressure and filtered over a plug of silica gel (100 mL of hexanes eluent to remove paraffin, then 100 mL of 2:1 Hexanes:EtOAc eluent).

The volatiles were removed under reduced pressure, and the crude residue was purified by preparative thin-layer chromatography (5:1 Hexanes:EtOAc) to yield ester **6.24** (87% yield, average of two experiments) as a colorless oil. Ester **6.24**: R_f 0.64 (5:1 Hexanes:EtOAc). The reported literature yield is 98% when the reaction is run at 30 °C.[11] Spectral data match those previously reported.[11]

6.8.2.13 Amidation of Aldehyde 6.25

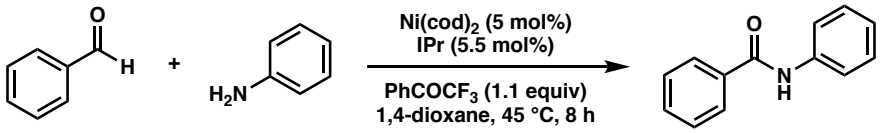

6.25 (*6.26*, 1.0 equiv) (91% yield) *6.27*

Amide 6.27. A 1-dram vial was charged with a magnetic stir bar and flame-dried under reduced pressure, and then allowed to cool under N_2. The vial was charged with a paraffin capsule containing $Ni(cod)_2$ (6.9 mg, 0.025 mmol, 5 mol%) and IPr (10.7 mg, 0.028 mmol, 5.5 mol%) prepared as described in Section 6.8.2.3 in the Experimental Procedures. The vial was flushed with N_2, and subsequently 1,4-dioxane (1.0 mL) was added. The reaction mixture was allowed to stir at 45 °C for 20 min, over which time a black color developed. A solution of aniline (**6.26**, 45.5 mL, 0.500 mmol, 1.0 equiv) in 1,4-dioxane (0.5 mL) was then added to the reaction mixture at 45 °C rapidly via syringe, followed by a solution of benzaldehyde (**6.25**, 50.7 mL, 0.500 mmol, 1.0 equiv) and 2,2,2-trifluoroacetophenone (76.6 mL, 0.550 mmol, 1.1 equiv) in 1,4-dioxane (1.0 mL, 0.20 M in total) in the same manner. The vial was capped with a Teflon-lined screw cap under a flow of N_2, and the reaction mixture was allowed to stir at 45 °C for 8 h. After removing the vial from heat, the reaction mixture was transferred to a 100 mL round bottom flask containing 3.0 g of silica gel with hexanes (6.0 mL) and CH_2Cl_2 (6.0 mL). The mixture was

adsorbed onto the silica gel under reduced pressure and filtered over a plug of silica gel (100 mL of hexanes eluent to remove paraffin, then 100 mL of EtOAc eluent). The volatiles were removed under reduced pressure, and the crude residue was purified by flash chromatography (9:1 Hexanes:EtOAc → 7:3 Hexanes:EtOAc → 1:1 Hexanes:EtOAc) to yield amide **6.27** (91% yield, average of two experiments) as an off-white solid. Amide **6.27**: R_f 0.19 (5:1 Hexanes:EtOAc). The reported literature yield is 96% when the reaction is run at 40 °C.[11] Spectral data match those previously reported.[11]

6.8.2.14 Air and Moisture Stability Tests of Paraffin–Ni(cod)$_2$ Capsules

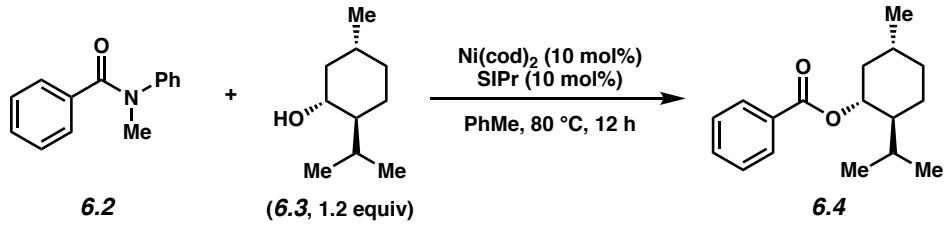

6.2 (*6.3*, 1.2 equiv) *6.4*

Representative Procedure for air and moisture stability tests of paraffin–Ni(cod)$_2$ capsules from Table 6.1 (coupling of amide 6.2 and (–)-menthol (6.3) is used as an example). A 1-dram vial containing a magnetic stir bar was flame-dried under reduced pressure, and then allowed to cool under N_2. The vial was charged with amide substrate **6.2** (42.2 mg, 0.200 mmol, 1.0 equiv), (–)-menthol (**6.3**, 37.5 mg, 0.240 mmol, 1.2 equiv) and a paraffin capsule containing Ni(cod)$_2$ (5.5 mg, 0.020 mmol, 10 mol%) and SIPr (7.8 mg, 0.020 mmol, 10 mol%) prepared as described in Section 6.8.2.3 in the Experimental Procedures that had been stored on the benchtop under the indicated conditions. The vial was flushed with N_2, and subsequently toluene (0.20 mL, 1.0 M) was added. The vial was capped with a Teflon-lined screw cap under a flow of N_2 and the reaction mixture was stirred at 80 °C for 12 h. After removing the vial from heat, the reaction mixture was transferred to a 100 mL round bottom flask containing 2.0 g of silica gel

with hexanes (6.0 mL) and CH_2Cl_2 (6.0 mL). The mixture was adsorbed onto the silica gel under reduced pressure and filtered over a plug of silica gel (100 mL of hexanes eluent to remove paraffin, then 100 mL of 4:1 Hexanes:EtOAc eluent). 1,3,5-trimethoxybenzene (10.1 mg, 0.060 mmol, 30 mol%) was then added to the crude mixture, the volatiles were removed under reduced pressure, and the yield was determined by ^{1}H NMR analysis with 1,3,5-trimethoxybenzene as an external standard.

Any modifications of the conditions shown in the representative procedure above are specified below in Table 6.1.

Table 6.1. Air and Moisture Stability Tests of Paraffin–$Ni(cod)_2$ Capsules.[a]

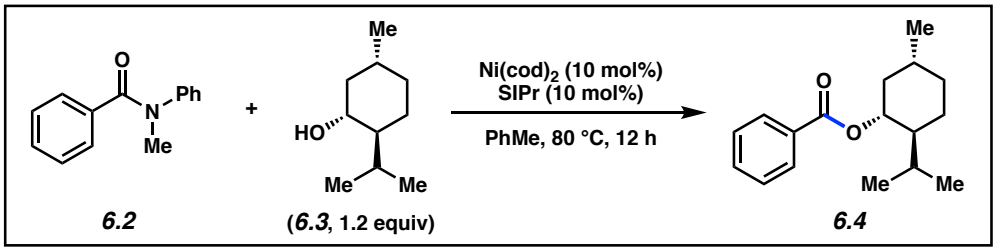

6.2 (***6.3***, 1.2 equiv) ***6.4***

Reaction Conditions	***Experimental Results*** ***6.2***	***6.4***
Paraffin capsule containing $Ni(cod)_2$ (10 mol%) and SIPr (10 mol%) stored on the benchtop under ambient temperature, oxygen, and moisture for 24 hours before use	0%	96%
Paraffin capsule containing $Ni(cod)_2$ (10 mol%) and SIPr (10 mol%) stored on the benchtop under ambient temperature, oxygen, and moisture for 2 weeks before use	0%	97%
Paraffin capsule containing $Ni(cod)_2$ (10 mol%) and SIPr (10 mol%) stored on the benchtop under ambient temperature, oxygen, and moisture for 1 month before use	0%	99%
Paraffin capsule containing $Ni(cod)_2$ (10 mol%) and SIPr (10 mol%) stored on the benchtop under ambient temperature, oxygen, and moisture for 2 months before use	0%	95%
Paraffin capsule containing $Ni(cod)_2$ (10 mol%) and SIPr (10 mol%) submerged under water for 1 hour before drying and use	0%	97%

[a] Yields were determined by ^1H NMR analysis using 1,3,5-trimethoxybenzene as an external standard.

6.8.2.15 Air Stability Tests of Non-encapsulated $Ni(cod)_2$ and SIPr

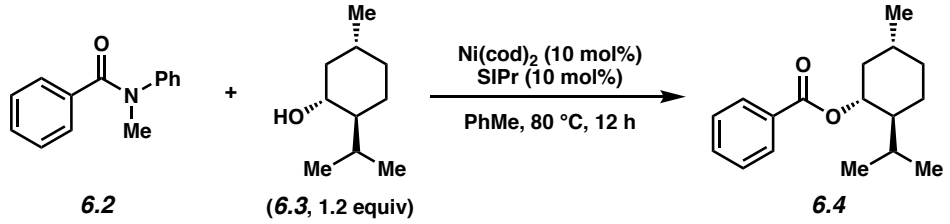

6.2 (*6.3*, 1.2 equiv) *6.4*

Representative Procedure for air and moisture stability tests of non-encapsulated $Ni(cod)_2$ and SIPr from Table 6.2 (coupling of amide 6.2 and (–)-menthol (6.3) is used as an example). A 1-dram vial containing a magnetic stir bar was flame-dried under reduced pressure, and then allowed to cool under N_2. The vial was charged with amide substrate **6.2** (42.2 mg, 0.200 mmol, 1.0 equiv), (–)-menthol (**6.3**, 37.5 mg, 0.240 mmol, 1.2 equiv) and $Ni(cod)_2$ (5.5 mg, 0.020 mmol, 10 mol%) that had been stored on the benchtop under ambient conditions for the indicated amount of time. The vial was flushed with N_2, taken into a glove box, and charged with SIPr (7.8 mg, 0.020 mmol, 10 mol%). The vial was then removed from the glove box, and subsequently toluene (0.20 mL, 1.0 M) was added. The vial was capped with a Teflon-lined screw cap under a flow of N_2 and the reaction mixture was stirred at 80 °C for 12 h. After cooling to 23 °C, the mixture was diluted with hexanes (0.5 mL) and filtered over a plug of silica gel (10 mL of EtOAc eluent). 1,3,5-trimethoxybenzene (10.1 mg, 0.060 mmol, 30 mol%) was then added to the crude mixture, the volatiles were removed under reduced pressure, and the yield was determined by ^1H NMR analysis with 1,3,5-trimethoxybenzene as an external standard.

Any modifications of the conditions shown in the representative procedure above are specified below in Table 6.2.

Table 6.2. Air Stability Tests of Non-encapsulated $Ni(cod)_2$ and SIPr.[a]

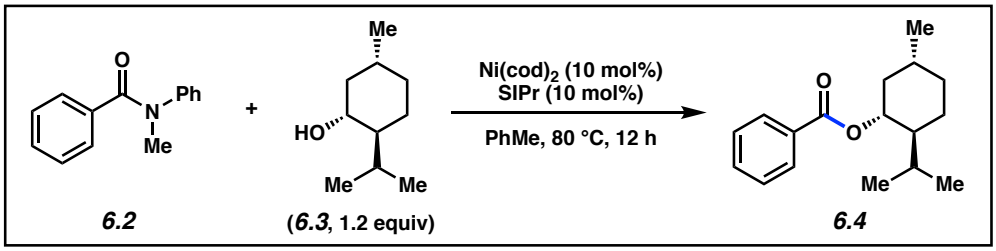

6.2 (***6.3***, 1.2 equiv) ***6.4***

Reaction Conditions	***Experimental Results*** ***6.2***	***6.4***
$Ni(cod)_2$ (10 mol%) stored on the benchtop under ambient temperature, oxygen, and moisture for 1 hour before use	13%	87%
$Ni(cod)_2$ (10 mol%) stored on the benchtop under ambient temperature, oxygen, and moisture for 24 hours before use	8%	92%
$Ni(cod)_2$ (10 mol%) stored on the benchtop under ambient temperature, oxygen, and moisture for 1 week before use	99%	0%
$Ni(cod)_2$ (10 mol%) and SIPr (10 mol%) stored on the benchtop under ambient temperature, oxygen, and moisture for 1 hour before use	96%	0%

[a] Yields were determined by ^1H NMR analysis using 1,3,5-trimethoxybenzene as an external standard.

6.8.2.16 Gram-Scale Esterification of Amide 6.2 Using a Paraffin–Ni(cod)$_2$ Capsule

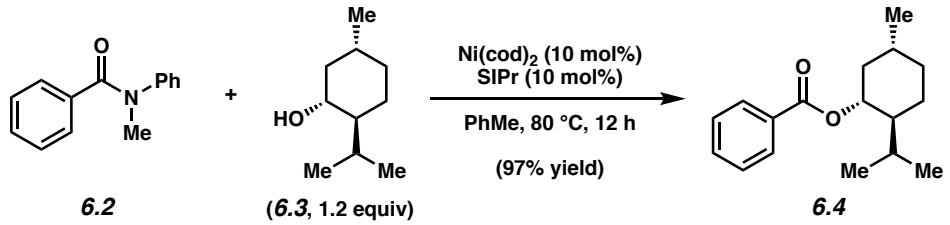

6.2 (*6.3*, 1.2 equiv) *6.4*

Ester 6.4. A 20 mL vial containing a magnetic stir bar was flame-dried under reduced pressure, and then allowed to cool under N_2. The vial was charged with amide substrate **6.2** (1.00 g, 4.74 mmol, 1.0 equiv), (–)-menthol (**6.3**, 887 mg, 5.69 mmol, 1.2 equiv), and a paraffin capsule containing Ni(cod)$_2$ (130 mg, 0.474 mmol, 10 mol%) and SIPr (185 mg, 0.474 mmol, 10 mol%) prepared as described in Section 6.8.2.4 in the Experimental Procedures. The vial was flushed with N_2, and subsequently toluene (4.74 mL, 1.0 M) was added. The vial was capped with a Teflon-lined screw cap under a flow of N_2 and the reaction mixture was stirred at 80 °C for 12 h. After removing the vial from heat, the reaction mixture was transferred to a 100 mL round bottom flask containing 8.0 g of silica gel with hexanes (12.0 mL) and CH_2Cl_2 (12.0 mL). The mixture was adsorbed onto the silica gel under reduced pressure and filtered over a plug of silica gel (500 mL of hexanes eluent to remove paraffin, then 1,000 mL of 100:1 Hexanes:EtOAc eluent). The volatiles were removed under reduced pressure, and the crude residue was purified by flash chromatography (100:1 Hexanes:EtOAc) to yield ester **6.4** (1.20 g, 97% yield) as a white solid. Spectral data match those previously reported.[18]

6.9 Spectra Relevant to Chapter Six:

Benchtop Delivery of $Ni(cod)_2$ Using Paraffin Capsules

Jacob E. Dander, Nicholas A. Weires, and Neil K. Garg.

Org. Lett. **2016**, *18*, 3934–3936.

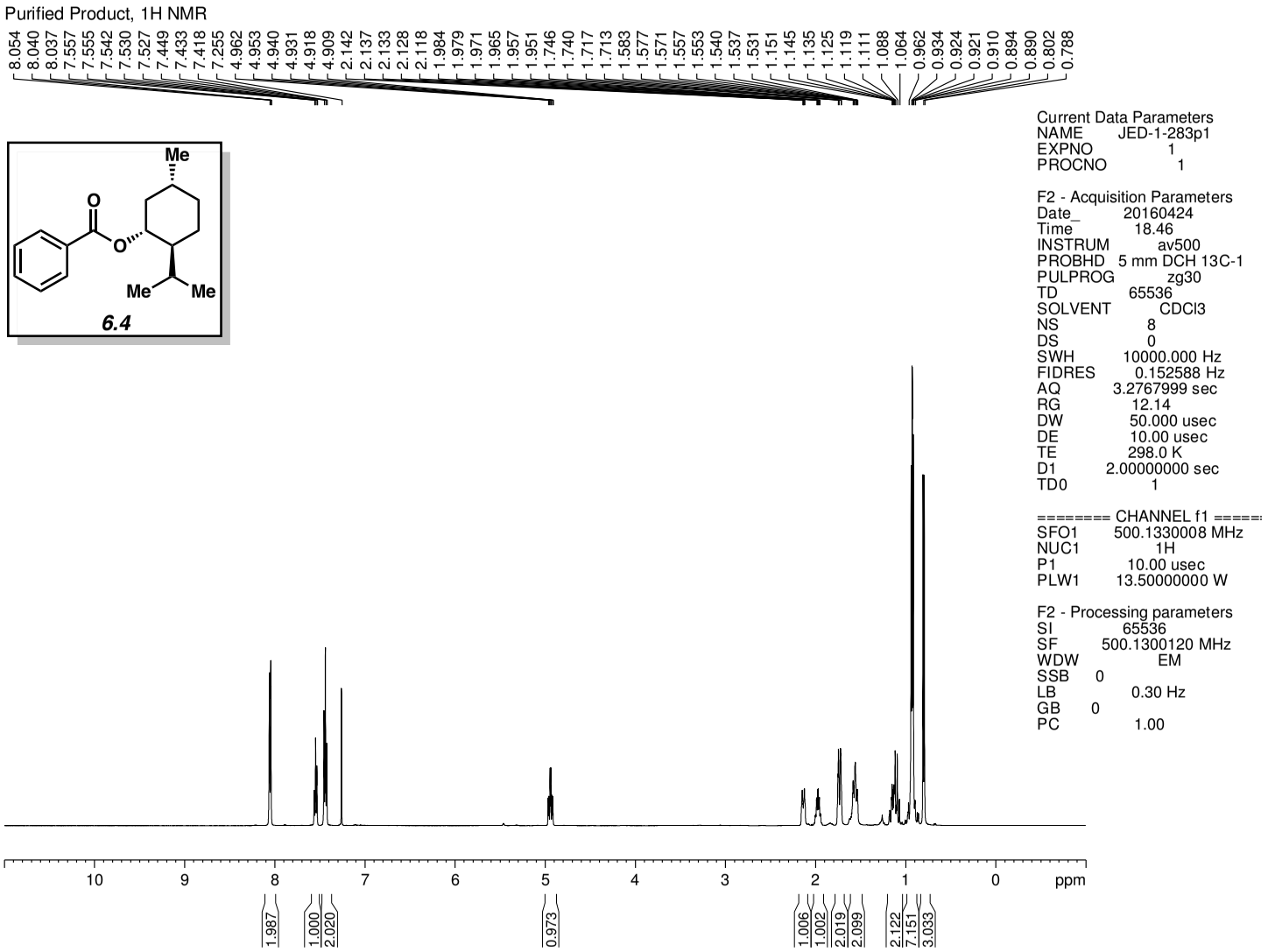

Figure 6.6 ^{1}H NMR (500 MHz, $CDCl_3$) of compound **6.4**.

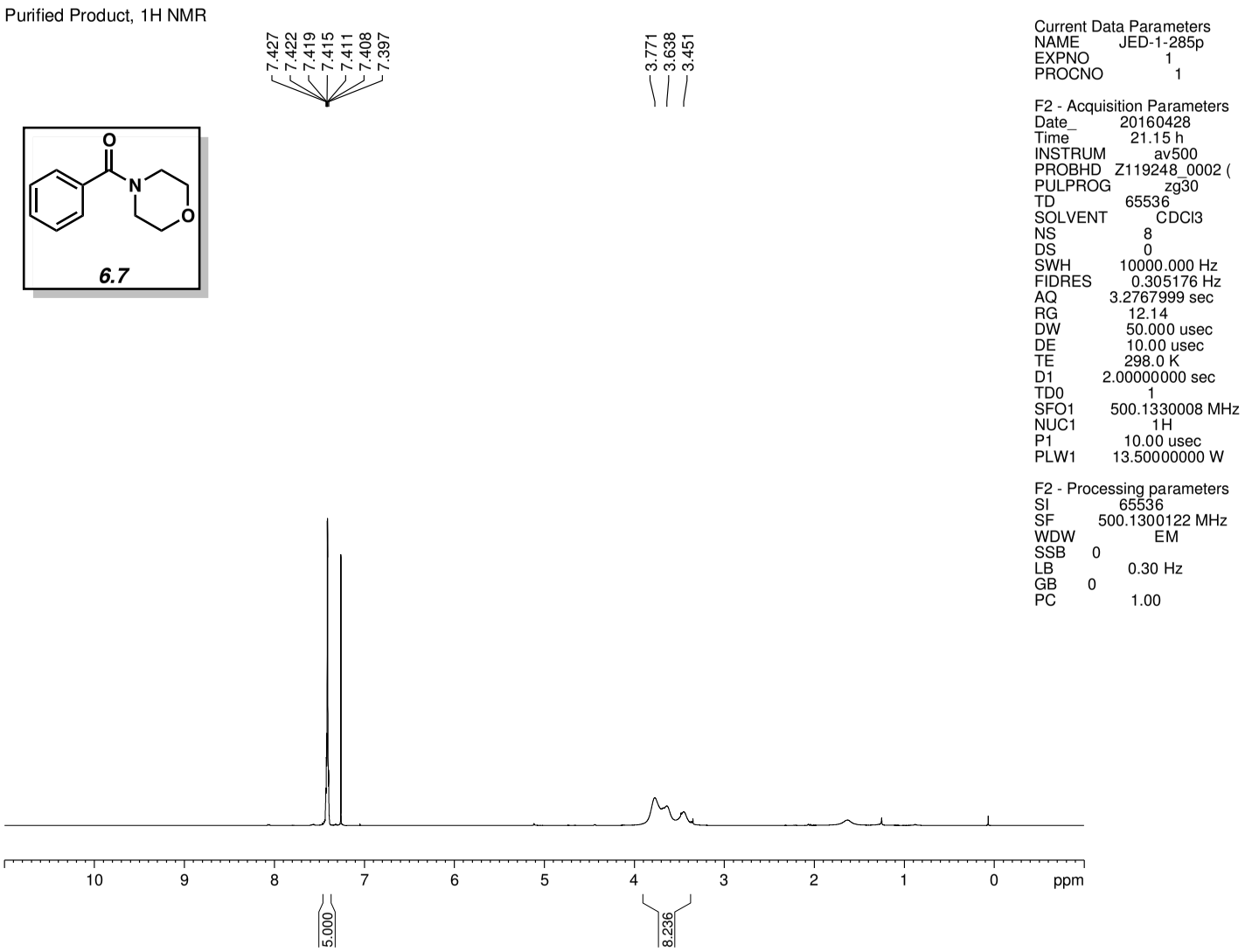

Figure 6.7 ^{1}H NMR (500 MHz, $CDCl_3$) of compound **6.7**.

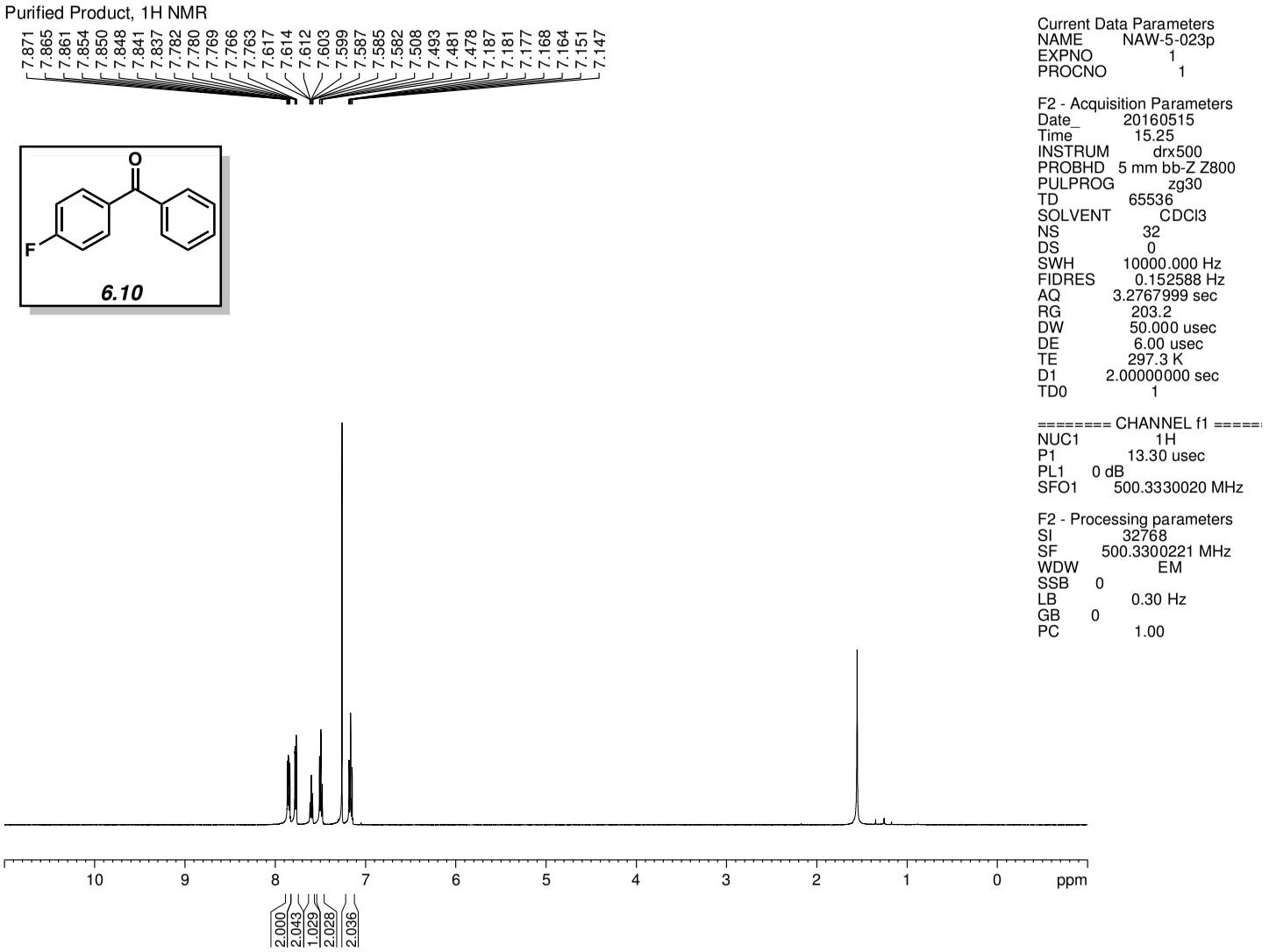

Figure 6.8 ^{1}H NMR (500 MHz, $CDCl_3$) of compound **6.10**.

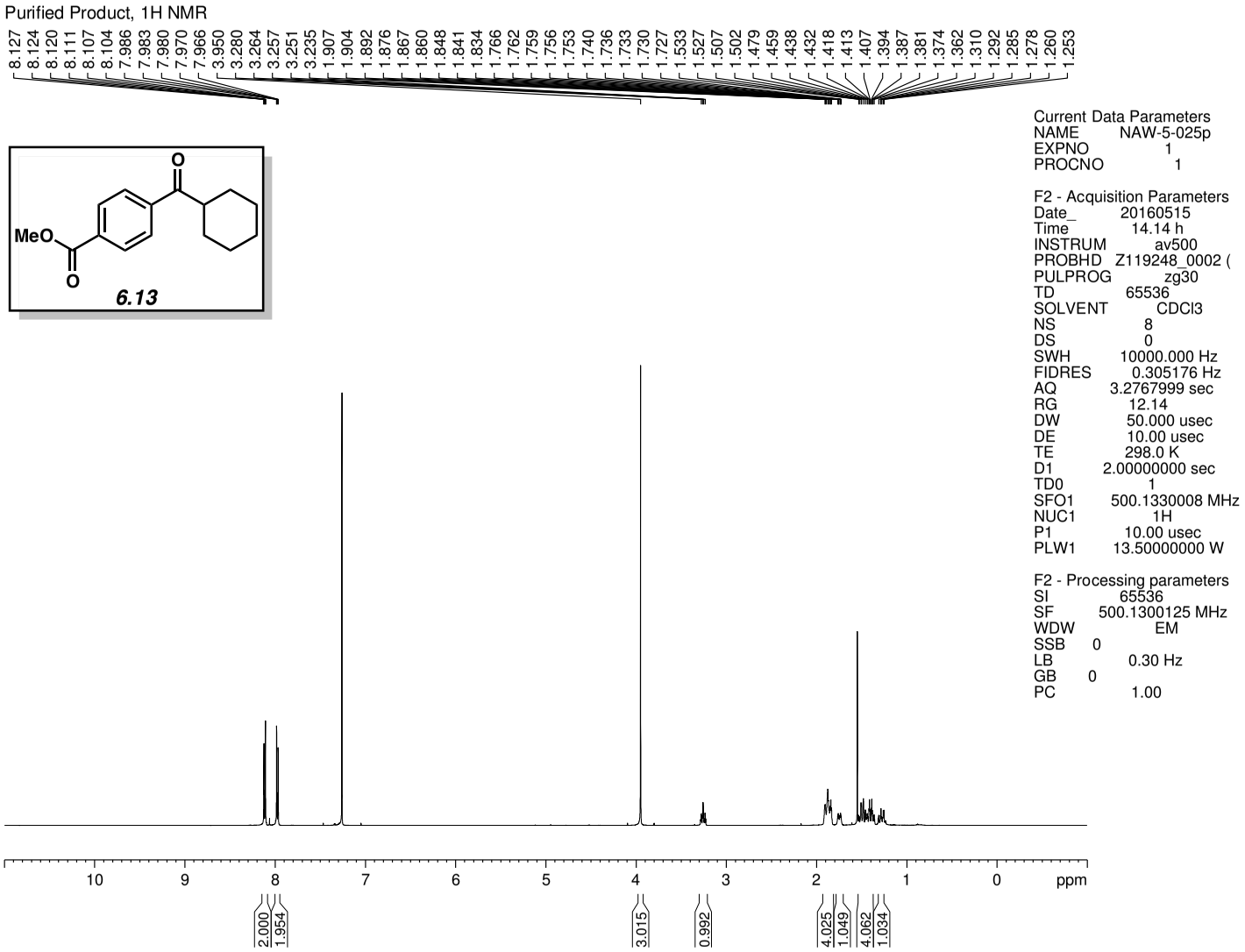

Figure 6.9 ^{1}H NMR (500 MHz, $CDCl_3$) of compound **6.13**.

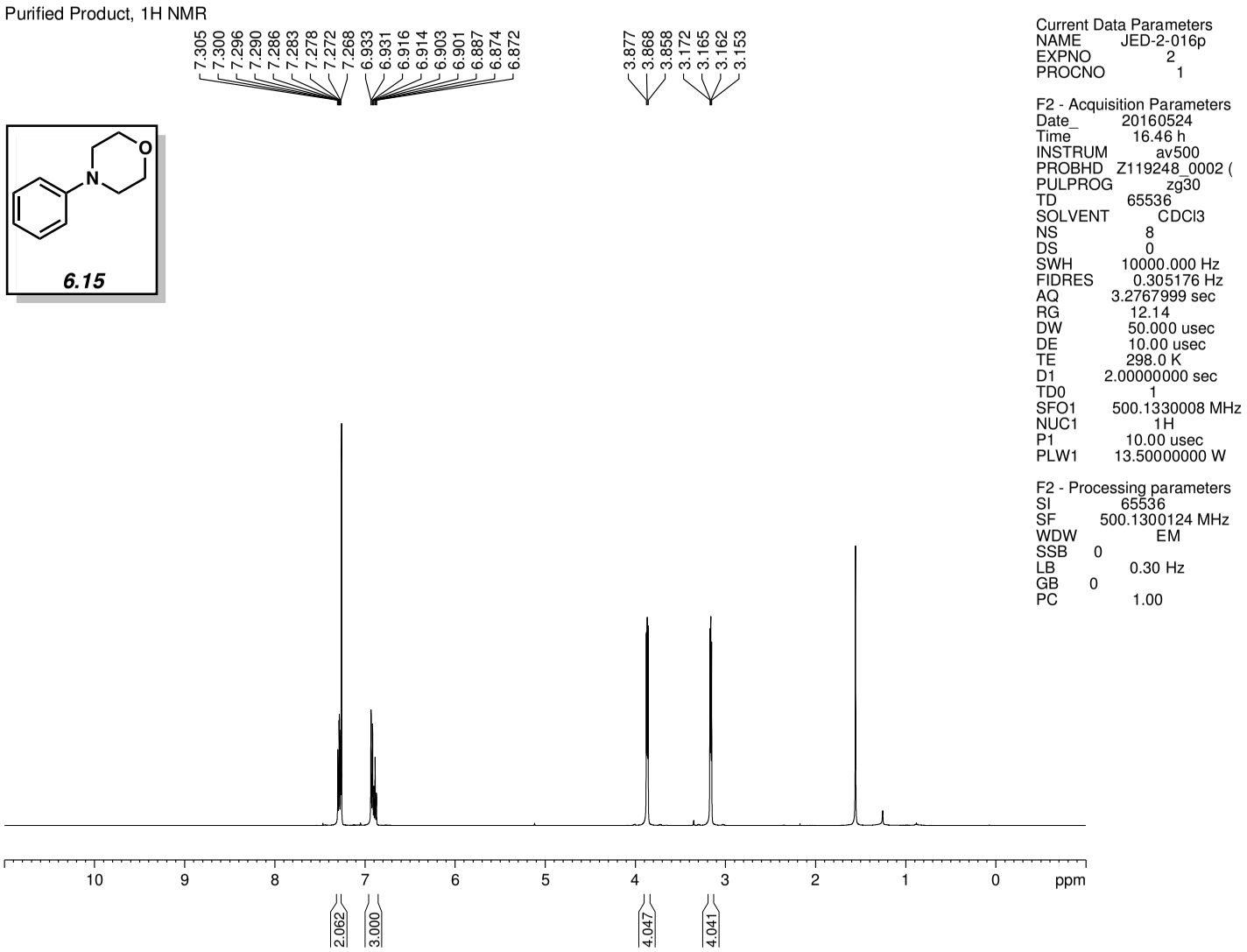

Figure 6.10 ^{1}H NMR (500 MHz, $CDCl_3$) of compound **6.15**.

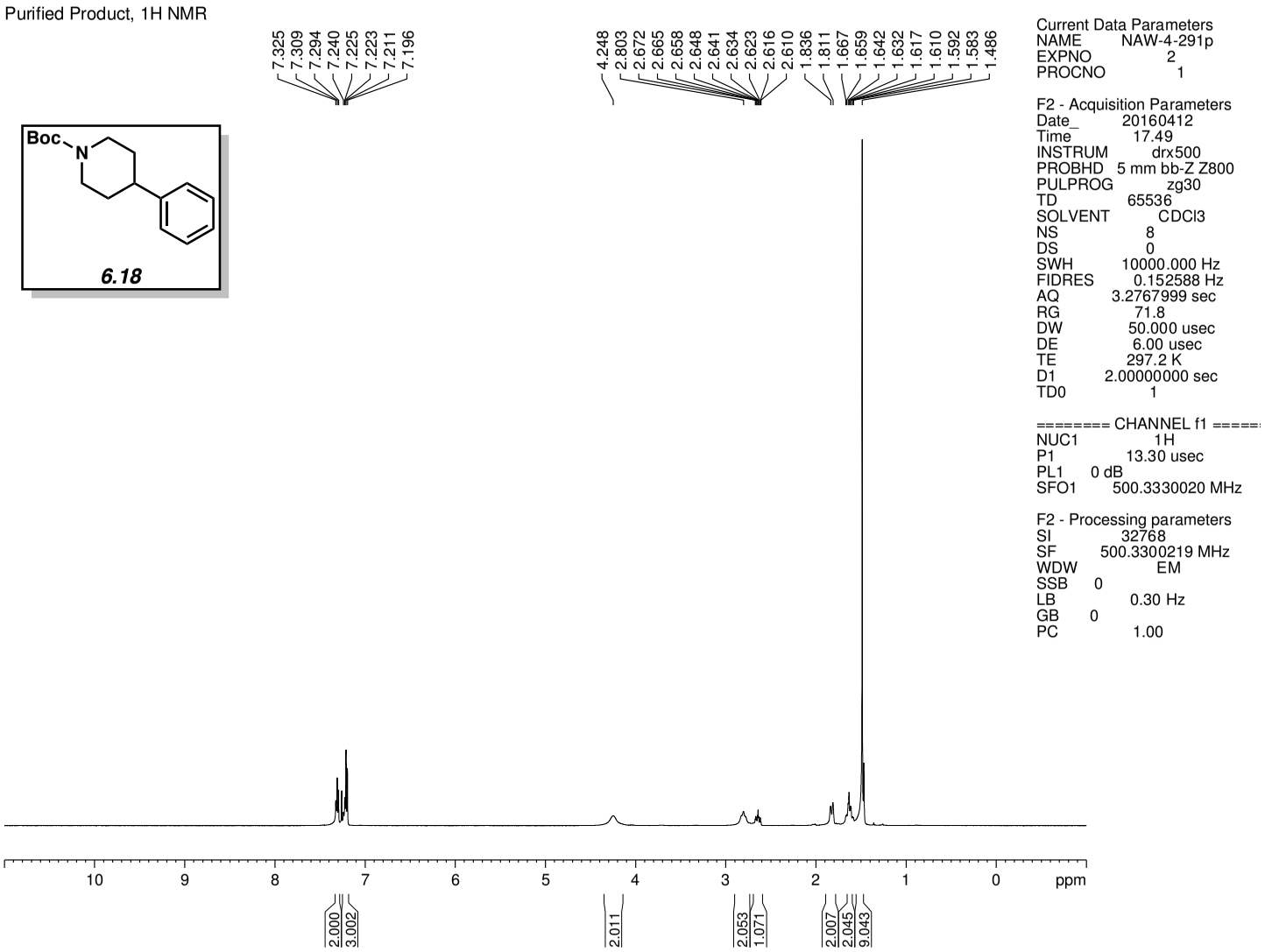

Figure 6.11 ^{1}H NMR (500 MHz, $CDCl_3$) of compound **6.18**.

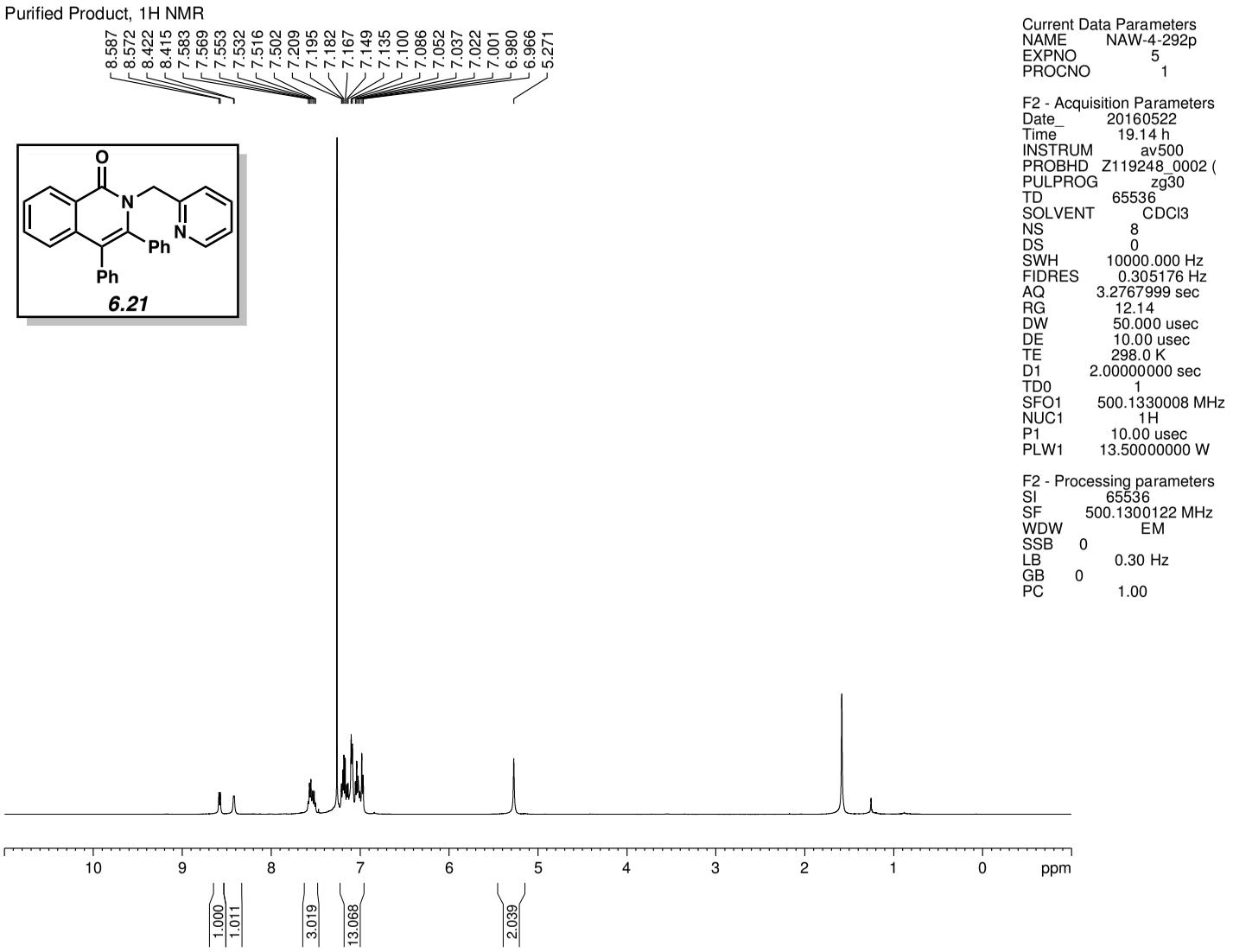

Figure 6.12 ^{1}H NMR (500 MHz, $CDCl_3$) of compound **6.21**.

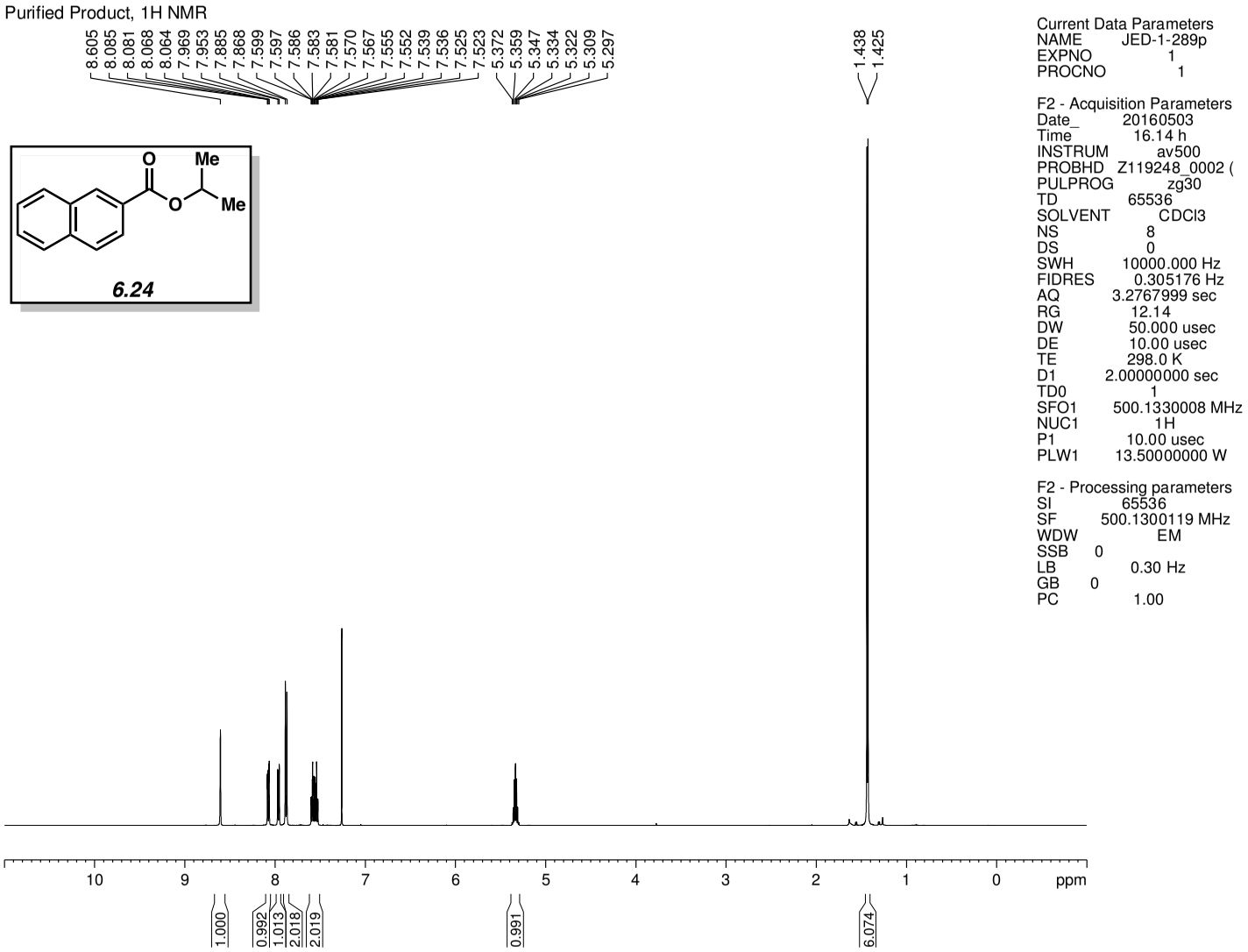

Figure 6.13 ^{1}H NMR (500 MHz, $CDCl_3$) of compound **6.24**.

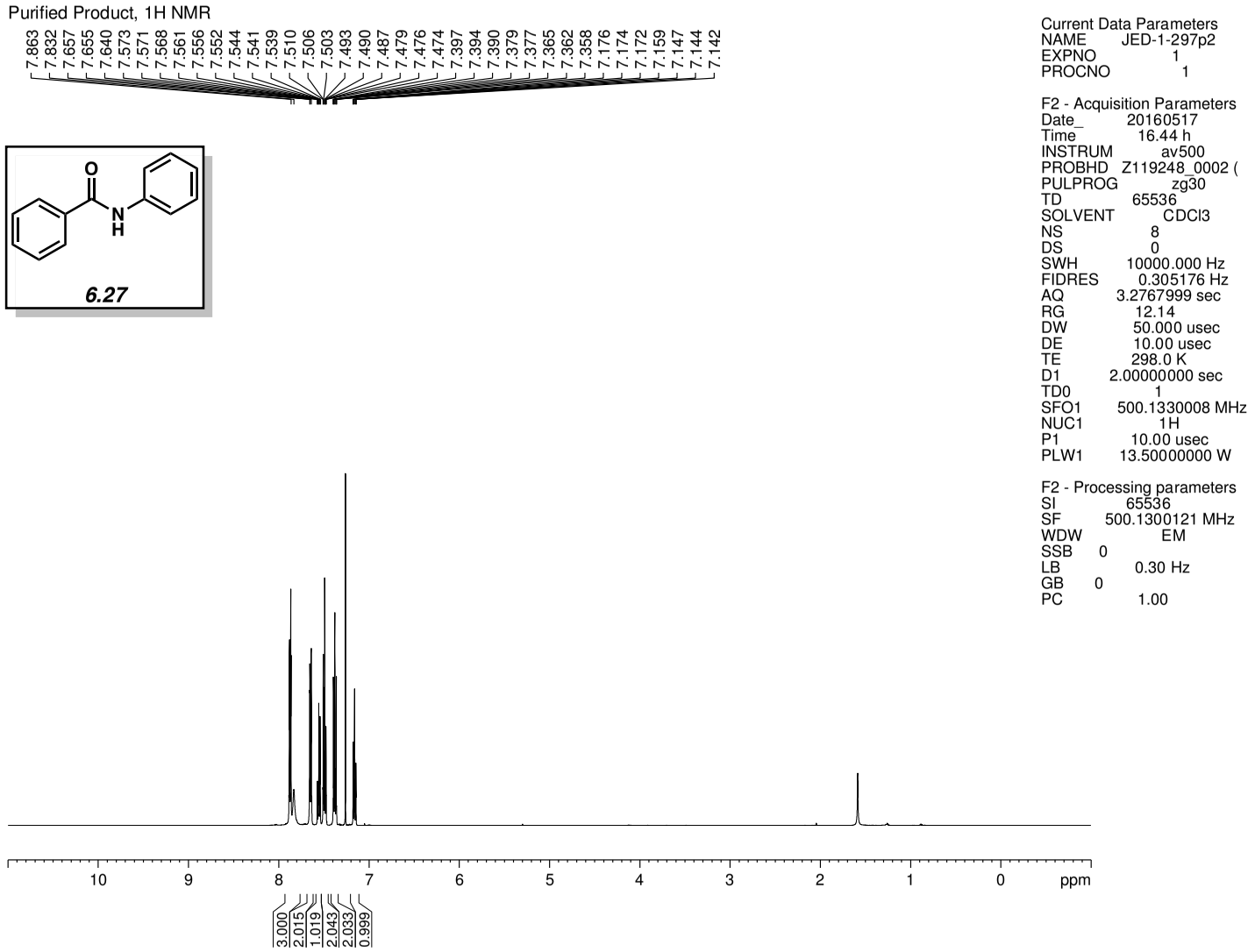

Figure 6.14 ^{1}H NMR (500 MHz, $CDCl_3$) of compound **6.27**.

6.10 Notes and References

(1) (a) Rosen, B. M.; Quasdorf, K. W.; Wilson, D. A.; Zhang, N.; Resmerita, A.-M.; Garg, N. K.; Percec, V. *Chem. Rev.* **2011**, *111*, 1346–1416. (b) Tasker, S. Z.; Standley, E. A.; Jamison, T. F. *Nature* **2014**, *509*, 299–309. (c) Mesganaw, T.; Garg, N. K. *Org. Process Res. Dev.* **2013**, *17*, 29–39. (d) Ananikov, V. P. *ACS Catal.* **2015**, *5*, 1964–1971.

(2) An attractive workaround involves the use of air-stable Ni(II) precatalysts with in situ reduction. For recent examples, see: (a) Shields, J. D.; Gray, E. E.; Doyle, A. G.; *Org. Lett.* **2015**, 17, 2166–2169. (b) Magano, J.; Monfette, S.; *ACS Catal.* **2015**, *5*, 3120–3123 (c) Standley, E. A.; Jamison, T. F. *J. Am. Chem. Soc.* **2013**, 135, 1585–1592. (d) Park, N. H.; Teverovskiy, G.; Buchwald, S. L. *Org. Lett.* **2014**, *16*, 220–223. (e) Ge, S.; Hartwig, J. F. *Angew. Chem. Int. Ed.* **2012**, *51*, 12837–12841. (f) Leowanawat, P.; Zhang, N.; Safi, M.; Hoffman, D.J.; Fryberger, M.C.; George, A.; Percec, V. *J. Org. Chem.* **2012**, *77*, 2885–2892 (g) Zhang, N.; Hoffman, D. J.; Gutsche, N.; Gupta, J.; Percec, V. *J. Org. Chem.* **2012**, *77*, 5956–5864. (h) Jezorek, R. L.; Zhang, N.; Leowanawat, P.; Bunner, M. H.; Gutsche, N.; Pesti, A. K. R.; Olsen, J. T.; Percec, V. *Org. Lett.* **2014**. *16*, 6326. (i) Malineni, J.; Jezorek, R. L.; Zhang, N.; Percec, V. *Synthesis*, **2016**, *48*, on line; DOI: 10.1055/s-0035-1562342. (j): Malineni, J.; Jezorek, R. L.; Zhang, N.; Percec, V. *Synthesis*, **2016**, *48*, 2795–2807. (k) Leowanawat, P.; Zhang, N.; Resmerita, A.-M.; Rosen, B. M.; Percec, V. *J. Org. Chem.* **2011**, *76*, 9946–9955; (l) Leowanawat, P.; Zhang, N.; Percec, V. *J. Org. Chem.* **2012**, **77**, 1018–1025.

(3) Scifinder search for bis(1,5-cyclooctadiene)nickel(0) being used as a reagent yielded hits corresponding to 848 original manuscripts since 1985. (accessed 28 April, 2016).

(4) In a recent seminal study, Buchwald demonstrated that Pd/ligand combinations could be dosed into paraffin capsules with applications in C–N bond formation; see: Sather, A. C.; Lee, H. G.; Colombe, J. R.; Zhang, A.; Buchwald, S. L. *Nature* **2015**, *524*, 208–211.

(5) Paraffin has been used to impart stability to air and moisture sensitive reagents in a variety of contexts. For examples of paraffin-reagent dispersions, see: (a) Taber, D. F.; Li, H.-Y. *Novel stable compositions of water and oxygen sensitive compounds and their method of preparation*. U.S. Patent 20050288257, Dec. 29, 2005. (b) Fang, Y.; Liu, Y.; Ke, Y.; Guo, C.; Zhu, N.; Mi, X.; Ma, Z.; Hu, Y. *Appl. Catal. A* **2002**, *235*, 33–38. (c) Taber, D. F.; Frankowski, K. J. *J. Org. Chem.* **2003**, *68*, 6047–6048. (d) Taber, D. F.; Nelson, C. G. *J. Org. Chem.* **2006**, *71*, 8973–8974. For examples of reagents encapsulated in paraffin, see: (e) Kosak, K. M.; Kosak, M. K. *Preparation of wax beads containing a reagent for release by heating*. U.S. Patent 5413924, May 9, 1995. (f) Shen, C.; Spannenberg, A.; Wu, X.-F. *Angew. Chem. Int. Ed.* **2016**, *55*, 5067–5070.

(6) Normally, the capsules used in Figures 6.3 and 6.4 contained 2–14 mg of $Ni(cod)_2$, although it is estimated that these capsules could safely hold up to 35 mg of $Ni(cod)_2$. Additionally, larger capsules can be prepared to hold greater amounts of $Ni(cod)_2$. At the conclusion of a reaction, the paraffin wax can be removed by dry-loading the reaction mixture on SiO_2 and purifying using hexanes and CH_2Cl_2.

(7) a) Hie, L.; Fine Nathel, N. F.; Shah, T. K.; Baker, E. L.; Hong, X.; Yang, Y.-F.; Liu, P.; Houk, K. N.; Garg, N. K. *Nature* **2015**, *524*, 79–83. (b) Weires, N. A.; Baker, E. L.; Garg, N. K. *Nat. Chem.* **2016**, *8*, 75–79. (c) Simmons, B. J.; Weires, N. A.; Dander, J. E.; Garg, N. K.

ACS Catal. **2016**, *6*, 3176–3179. (d) Baker, E. L.; Yamano, M. M.; Zhou, Y.; Anthony, S. M.; Garg, N. K. *Nat*. *Commun*. **2016**, 7, 11554.

(8) Ramgren, S. D.; Silberstein, A. L.; Yang, Y.; Garg, N. K. *Angew*. *Chem*. *Int*. *Ed*. **2011**, *50*, 2171–2173.

(9) Zhou, J.; Fu, G. C. *J*. *Am*. *Chem*. *Soc*. **2004**, *126*, 1340–1341.

(10) Shiota, H.; Ano, Y.; Aihara, Y.; Fukumoto, Y.; Chatani, N. *J*. *Am*. *Chem*. *Soc*. **2011**, *133*, 14952–14955.

(11) Whittaker, A. M.; Dong, V. M. *Angew*. *Chem*. *Int*. *Ed*. **2015**, *54*, 1312–1315.

(12) The robustness of the paraffin–Ni(cod)$_2$ capsules with regard to exposure to water was also tested. A capsule that had been submerged in water for 1 h and subsequently dried with a paper towel was found to promote the esterification of amide **6.2** with (–)-menthol (**6.3**) to give **6.4** in 94% yield.

(13) The esterification of amide **6.2** with (–)-menthol (**6.3**) was also carried out using non-encapsulated Ni(cod)$_2$ and SIPr that had been exposed to air. After only 1 h of air exposure, the attempted esterifcation led to the full recovery of starting material.

(14) Paraffin capsules containing Ni(cod)$_2$ and Ni(cod)$_2$/SIPr will soon be available commercially from TCI (TCIchemicals.com) and Sigma-Aldrich. The capsules and their TCI product numbers are as follows (Sigma-Aldrich product numbers are pending): Bis(1,5-cyclooctadiene)nickel(0) (Wax encapsulated): B5417; Bis(1,5-cyclooctadiene)nickel(0) - 1,3-Bis(2,6-diisopropylphenyl)imidazolidin-2-ylidene (Wax encapsulated): B5418.

(15) (a) Li, Y.; Jia, F.; Li, Z. *Chem. Eur. J.* **2013**, *19*, 82–86. (b) Johnson II, D. C.; Widlanski, T. S. *Tetrahedron Lett.* **2004**, *45*, 8483–8487. (c) King, J. F.; Lee, T. M.-L. *Can. J. Chem.* **1981**, *59*, 356–361.

(16) Krasovskiy, A.; Malakhov, V.; Gavryushin, A.; Knochel, P. *Angew. Chem. Int. Ed.* **2006**, *45*, 6040–6044.

(17) Krasovskiy, A.; Knochel, P. *Synthesis* **2006**, 890–891.

(18) Ueda, T.; Konishi, H.; Manabe, K. *Org. Lett.* **2013**, *15*, 5370–5373.

(19) Verma, S. K.; Ghorpade, R.; Pratap, A.; Kaushik, M. P. *Tetrahedron Lett.* **2012**, *53*, 2373–2376.

(20) Li, M.; Wang, C.; Ge, H. *Org. Lett.* **2011**, *13*, 2062–2064.

(21) Bechara, W. S.; Pelletier, G.; Charette, A. B. *Nat. Chem.* **2012**, *4*, 228–234.

(22) Barker, T. J.; Jarvo, E. R. *J. Am. Chem. Soc.* **2009**, *131*, 15598–15599.

(23) Vechorkin, O.; Proust, V.; Hu, X. *J. Am. Chem. Soc.* **2009**, *131*, 9756–9766.

CHAPTER SEVEN

Kinetic Modeling of the Nickel-Catalyzed Esterification of Amides

Nicholas A. Weires, Daniel D. Caspi, and Neil K. Garg.

ACS Catal. [Just accepted manuscript] DOI: 10.1021/acscatal.7b01444.

7.1 Abstract

Nickel-catalyzed coupling reactions provide exciting tools in chemical synthesis. However, most methodologies in this area require high catalyst loadings, which commonly range from 10–20 mol% nickel. Through an academic-industrial collaboration, we demonstrate that kinetic modeling can be used strategically to overcome this problem, specifically within the context of the Ni-catalyzed conversion of amides to esters. The successful application of this methodology to a multigram-scale coupling, using only 0.4 mol% Ni, highlights the impact of this endeavor.

7.2 Introduction

New synthetic methodologies have the potential to greatly impact pharmaceutical manufacturing, which in turn can have a positive effect on human health. Although there is no shortage of new chemical transformations being reported each year, the likelihood of any of these being adopted in a pharmaceutical manufacturing process remains quite low. Indeed, process chemists often rely on a handful of common transformations that proceed reliably and efficiently, and as such the barrier for adopting a new methodology in a large-scale pharmaceutical manufacturing process can be substantial.[1] A key hurdle lies in practical gaps between the typical academic methodology and an economical manufacturing process. For

instance, the pressures of manufacturing deadlines may prohibit industrial optimization of published academic methodologies. As such, the earlier a methodology can be rendered scalable and efficient, the more likely it is to be implemented in drug synthesis.

One burgeoning area of academic research that is in principle well-suited for large-scale manufacturing is the field of nickel-catalyzed cross-couplings. This is not only because of the high natural abundance, low cost, and low CO_2 footprint of nickel, but also because of its unique ability to effect novel or challenging transformations (Figure 7.1).[2] However, nickel-catalyzed cross-couplings reported by academic labs often employ high catalyst loadings. For example, as shown in Figure 7.1, upon surveying >80 manuscripts published in top journals since 2015 involving nickel-catalyzed cross-couplings, we found that the vast majority of methodologies use ≥5 mol% nickel, with greater than half of those methodologies employing 10–20 mol% nickel.[3] Indeed, examples that require less than 5 mol% nickel are uncommon. In our own experience, the high catalyst loadings in part stem from the desire to identify broadly applicable reaction conditions and pressures to publish before potential competitors. Although these burdens are not likely to subside, the greater attention to developing process-friendly variants of nickel-catalyzed couplings by academic labs could only lead to better chances of such methodologies being adopted industrially.

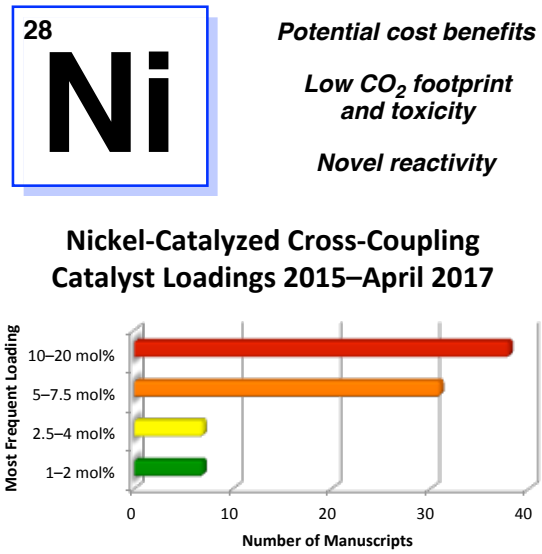

Figure 7.1. Features of nickel catalysis and the most frequently employed catalyst loadings in nickel-catalyzed cross-coupling reactions published January 2015–April 2017.

Prompted by discussions with industrial colleagues, we established a collaboration targeted at rendering a recently developed nickel-mediated coupling more catalytically efficient. The reaction we chose to pursue is the nickel-catalyzed conversion of amides to esters, which represents a unique and challenging transformation.[4,5,6,7,8,9] An example of this reaction is depicted in Figure 7.2, wherein benzamide **7.1** is coupled with (–)-menthol (**7.2**) to furnish ester **7.3** in 88% yield. Notably, this reaction proceeds at 80 °C using both 10 mol% $Ni(cod)_2$ and 10 mol% SIPr in toluene (0.66 M).[4,10] At the time this reaction was developed, initial reaction optimization efforts to lower the catalyst loading were unsuccessful. We sought to revisit this challenge through an academic / industrial collaboration that relied on a combination of experiments and kinetic modeling, the latter of which is a tool commonly employed industrially, but less often in academic pursuits.[11,12,13] In this manuscript, we describe the success of these efforts, which allow for amide esterification to take place using catalyst loadings as low as 0.4 mol% Ni.

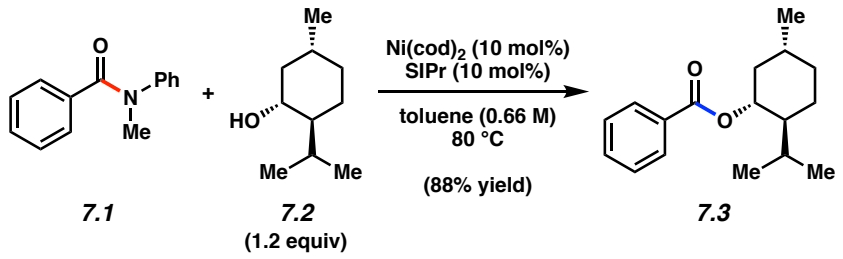

Figure 7.2. Previously reported nickel-catalyzed coupling of benzamide **7.1** with (–)-menthol (**7.2**) to furnish ester **7.3** using 10 mol% Ni.

7.3 Development of the Kinetic Model

To initiate our studies, we identified the coupling of benzamide **7.1** with (–)-menthol (**7.2**) as a practical reaction choice for several reasons, including: (a) the high purity to which (–)-menthol (**7.2**) can be obtained by recrystallization, (b) the robustness of the reaction, and (c) the low volatility of all reagents under the reaction conditions. Initial attempts to reduce the reaction temperature from the reported 80 °C revealed that the coupling had reached >90% conversion after approximately 8 h at 40 °C (Table 7.1, entry 1). *DynoChem* software[14] was used to derive rate information from this coupling, and roughly one dozen further exploratory experiments were then designed to probe the sensitivity of the observed reaction rate to changes in a number of reaction variables. Parameters that were examined included: (a) ligand to metal ratio, (b) equivalents of (–)-menthol (**7.2**), (c) presence of product / byproduct spikes, (d) length of time holding the catalyst at a given temperature prior to substrate addition, (e) catalyst loading, and (f) reaction concentration.[15] With the guidance of the software used, it was determined that only a small number of these experiments involved changes to kinetically relevant reaction variables (Table 7.1). It was demonstrated that changes in temperature, concentration, and catalyst loading had a marked impact on the reaction rate (entries 2–5).[16] However, the stoichiometry of the alcohol, in addition to numerous other variables, did not influence the reaction rate.

Table 7.1. Experiments used to train the kinetic model.[a]

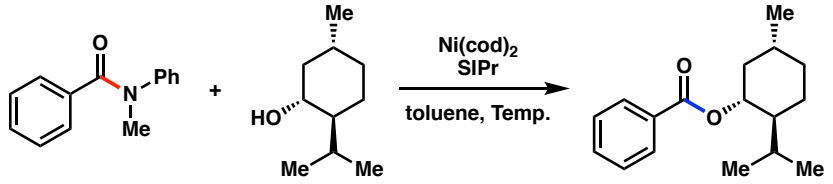

7.1 *7.2* (1.2 equiv) *7.3*

Entry	$Ni(cod)_2$	Temp.	Concentration	Max Conversion[b]	Time
1	10.0 mol%	40 °C	0.66 M	92%	8 h
2	10.0 mol%	33 °C	0.66 M	70%	6 h
3	10.0 mol%	50 °C	0.66 M	91%	4 h
4	0.5 mol%	65 °C	1.16 M	77%	8 h
5	0.1 mol%	80 °C	1.16 M	13%	1 h

[a] All reactions were performed on 0.50–1.00 mmol scale with respect to amide **7.1** using 1.2 equiv (–)-menthol (**7.2**) and a 1:1 ratio of $Ni(cod)_2$:SIPr in toluene.[10] [b] Conversion was determined by SFC analysis using biphenyl as an internal standard.

The data in Table 7.1 were utilized to build a kinetic model, and a simplified reaction pathway was constructed based on prior computational studies from the Houk laboratory, as well as extensive literature precedent (Figure 7.3).[4,17] The fitted model supports three fundamental steps, which are in agreement with the literature[4]: oxidative addition (k_1), ligand exchange (k_2), and reductive elimination (k_3). The model fitting implicates oxidative addition as the rate-determining step (k_1), which is consistent with previously reported computational predictions (23.0 kcal/mol *DynoChem* vs 26.0 kcal/mol DFT calculations).[4] In addition, the presence of a catalyst degradation pathway (k_4) was also found. These degradation kinetics (k_4) were represented by a simplified first-order pathway from the catalyst resting state (NiL). Although details of the catalyst degradation pathway are unknown, NiL was selected as the most abundant catalyst species in the reaction, as oxidative addition is rate-limiting. The regressed rate constants

and associated activation energies are depicted in Figure 7.3. Since the rate of ligand exchange (k_2) and reductive elimination (k_3) were not found to be rate-limiting, an arbitrary fast rate was used for fitting. Further independent experiments were then conducted under atypical reaction conditions in order to verify the model prediction capabilities, and such experiments were found to be successful in validating the model.[18]

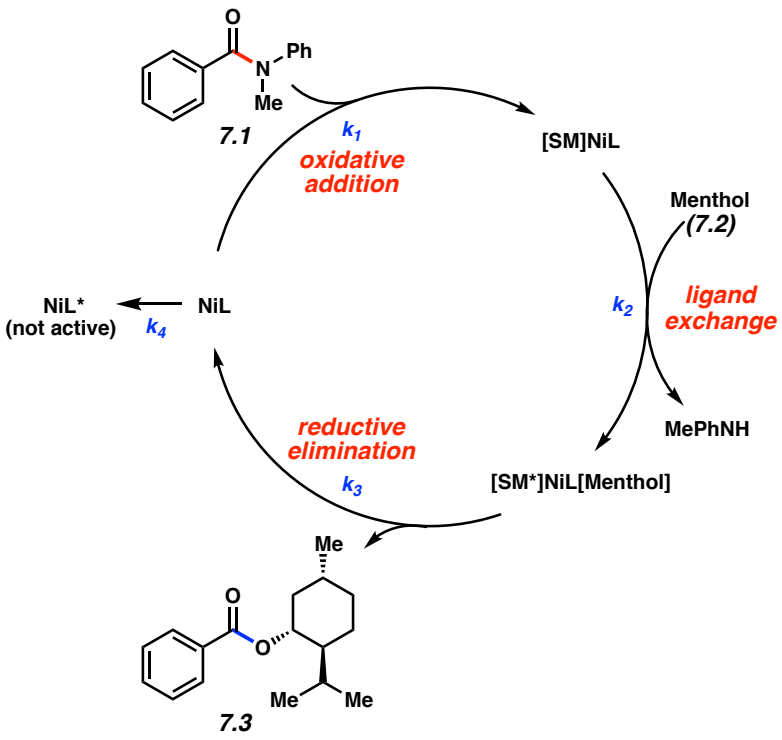

Refined Forward Rate Constants (k)[a]	Activation Energy (E_a) (kJ/mol)[b]
$k_1 = (2.00 \pm 0.06) \times 10^{-3}$ L/mol·s	$E_{a1} = 97 \pm 2$
$k_2 = 10$ L/mol·s[c]	$E_{a2} = 0$[d]
$k_3 = 10$ s^{-1}[c]	$E_{a3} = 0$[d]
$k_4 = (1.42 \pm 0.38) \times 10^{-6}$ s^{-1}	$E_{a4} = 151 \pm 5$

Figure 7.3. Simplistic reaction pathway, calculated rate constants, and energies of activation for the esterification reaction.

[a] Rate constants are reported at 40 °C. The ± values represent the 95% confidence interval obtained from the *DynoChem* fitting of the data to the kinetic model. [b] For comparison, the corresponding values in kcal/mol are as follows: $E_{a1} = 23.0 \pm 0.5$ kcal/mol; $E_{a4} = 36.1 \pm 1.0$ kcal/mol. [c] This reaction is fast and not rate limiting, therefore an arbitrary fast rate of 10 was selected for subsequent fitting. [d] Reaction rate was a weak function of temperature within the explored temperature range.

7.4 Prediction of Suitable Reaction Conditions

With a working kinetic model in hand, thousands of *in silico* simulations were performed in a matter of minutes in order to visualize the multidimensional relationships between

concentration, temperature, and catalyst loading (Figure 7.4). On the basis of these calculations, 2.0 mol% Ni catalyst at 60 °C in toluene (approximately 1.04 M)[10] was chosen as an optimal set of conditions that would provide a balance between reaction conversion and catalyst degradation. These conditions were then used to further probe the generality of the coupling.[19]

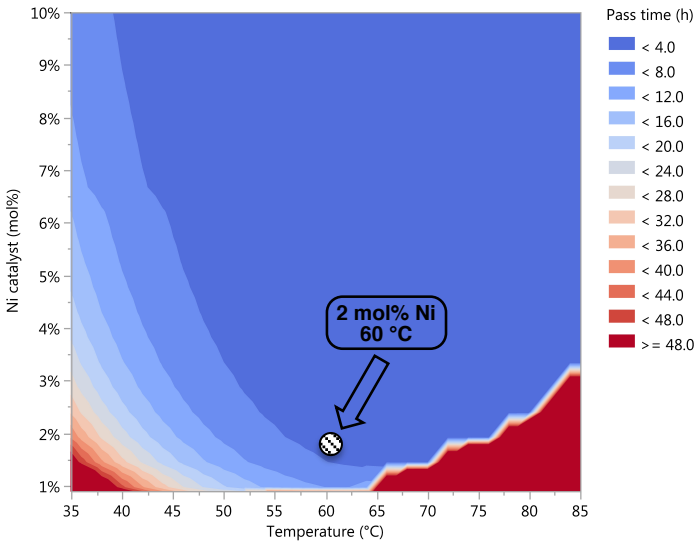

Figure 7.4. *In silico* simulations of reaction pass time (95% conversion) as a function of Ni catalyst (mol%) and temperature (°C) for overall reaction concentrations of 1.00–1.30 M.[10] Contour plot depicts the result of several thousand simulations.

7.5 Scope of the Esterification Using 2.0 mol% Nickel

Having projected suitable conditions that would require only 2.0 mol% Ni, efforts turned to verifying this prediction (Figure 7.5). These conditions were found to be broadly applicable to a number of amide substrates **7.4** and alcohol coupling partners **7.5** to furnish ester products **7.6** with high efficiencies. For example, methyl benzoate (**7.7**) could be obtained in good yields from benzamide derivatives possessing either *N*-Me,Ph or *N*-Bn,Boc nitrogen substitutions. Additionally, extended aromatic systems were tolerated, as demonstrated by the formation of **7.8**

in 92% yield. Notably, the conditions were found to be tolerant of heterocycles, as suggested by the preparation of isoquinoline derivative **7.9** in 66% yield. The alcohol coupling partner was also varied, permitting the generation of interesting ester products such as cyclopropane **7.10** in 75% yield. Moreover, secondary alcohol nucleophiles were found to be competent in the coupling, allowing for the formation of **7.11** and **7.3** in quantitative yields. Finally, an ester derived from a tertiary alcohol could also be accessed, as demonstrated by the production of adamantyl ester **7.12**. As shown, yields were generally comparable to those reported in the literature using 10 mol% Ni.[4]

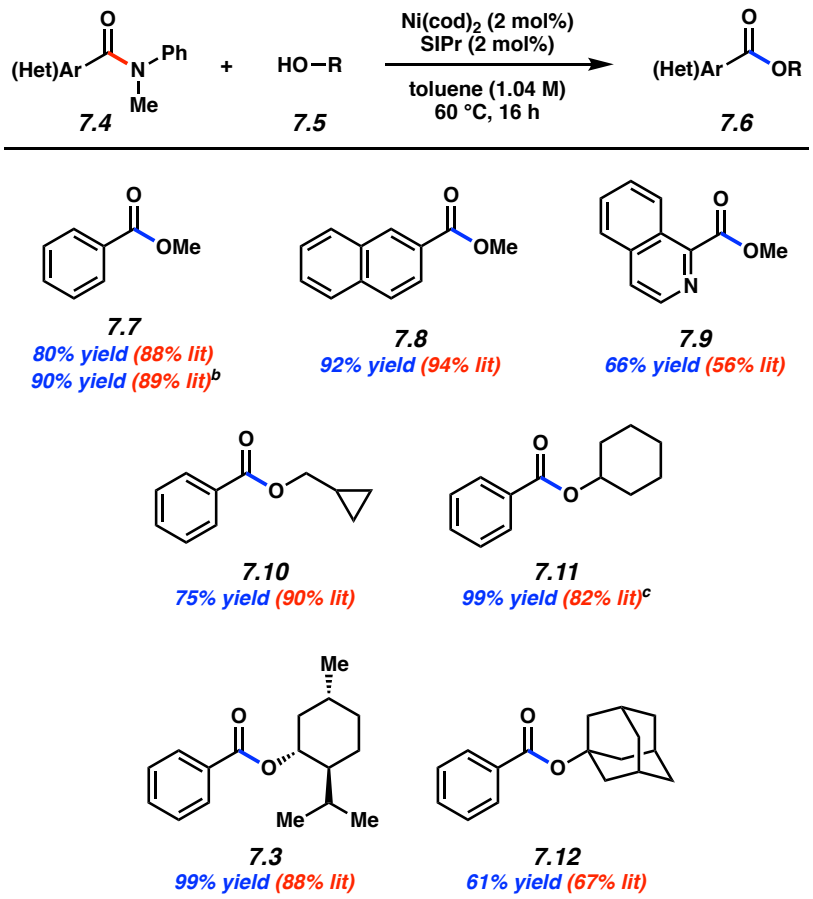

Figure 7.5. Exploration of scope in the esterification.[a]

[a] All reactions were performed on 0.50 mmol scale using 1.2 equiv alcohol, 2.0 mol% $Ni(cod)_2$, and 2.0 mol% SIPr in toluene (1.04 M) at 60 °C for 16 h. Yields determined by ^1H NMR analysis using hexamethylbenzene as an external standard. [b] Coupling performed with the corresponding *N*-Bn,Boc benzamide. [c] 97% isolated yield obtained after silica gel chromatography.

7.6 Identification of Conditions Using 0.4 mol% Nickel and Multigram Scale Coupling

With the aim of minimizing the catalyst loading further, additional simulations were performed using less than 1.0 mol % Ni.[18] The simulation results predicted that the esterification of benzamide **7.1** with (–)-menthol (**7.2**) could reach nearly full conversion in less than 56 h if performed at 45 °C with 0.4 mol% Ni in toluene at high concentrations (1.52 M)[10] (Figure 7.6).[20] These predicted reaction conditions using only 0.4 mol% Ni were thus attempted on 5 gram scale

to test the scalability of the coupling. To our delight, this effort afforded ester **7.3** in nearly quantitative yield.[21] Compared to our original disclosure, this reaction uses 25-fold less $Ni(cod)_2$ and >10-fold less of the SIPr ligand. If each reaction variable had been tested independently, this result would have likely been discovered in a much less concise manner, if at all. However, by employing a kinetic model, a catalyst degradation pathway was identified that informed the careful tuning of the reaction conditions, in turn permitting an efficient coupling to take place. This example, which showcases a rare use of less than 0.5 mol% Ni in a catalytic coupling, underscores the value of kinetic modeling and bodes well for the increasingly widespread adoption of nickel catalysis in industry.

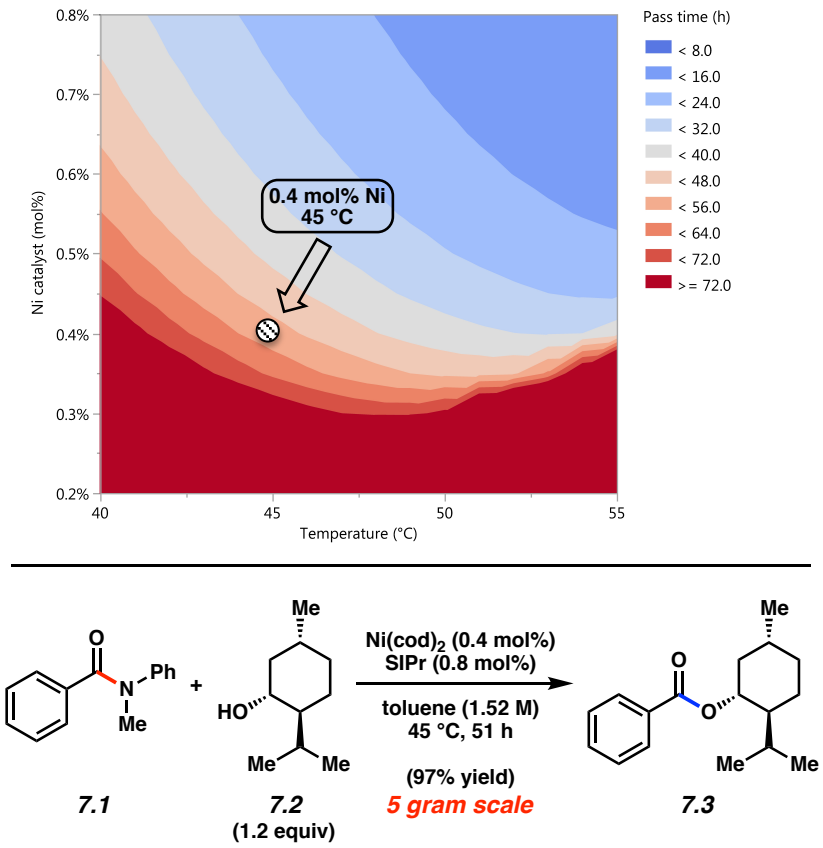

Figure 7.6. *In silico* simulations of reaction pass time (95% conversion) as a function of Ni catalyst (mol%) and temperature (°C) for overall reaction concentrations of 1.44–1.74 M[10] and 5 gram scale coupling of benzamide **7.1** with (–)-menthol (**7.2**) using 0.4 mol% Ni.[a]

[a] Contour plot depicts the result of several thousand simulations. Conditions: 5.00 g amide **7.1**, 1.2 equiv (–)-menthol (**7.2**), 0.4 mol% $Ni(cod)_2$, and 0.8 mol% SIPr in toluene (1.52 M) at 45 °C for 51 h. Yield refers to isolated yield after column chromatography.

7.7 Conclusion

In summary, we have developed a kinetic model that allowed for the optimization of the nickel-catalyzed esterification of amides. The model-predicted reaction conditions, involving a five-fold reduction in catalyst loading to 2.0 mol% Ni, were tested and deemed suitable for a variety of coupling partners. Further simulations using the kinetic model predicted the coupling of benzamide **7.1** and (–)-menthol (**7.2**) could then take place using as little as 0.4 mol% Ni. This

forecast was validated, as demonstrated by a multigram scale coupling that proceeded in nearly quantitative yield. Thus, guided by reaction kinetics, the esterification of amides was optimized in a concise manner and was rendered substantially more efficient. These studies are expected to facilitate the adoption of kinetic modeling as a powerful tool in academic methodology design for the expedited translation of those methodologies into industry.

7.8 Experimental Section

7.8.1 Materials and Methods

Unless stated otherwise, reactions were conducted in flame-dried glassware under an atmosphere of nitrogen or argon and commercially obtained reagents were used as received. Non-commercially available substrates were synthesized following known protocols: **7.1**,[22a] **7.13**,[22b] **7.14**,[22c] **7.15**.[4] Prior to use, toluene was purified by distillation and taken through five freeze-pump-thaw cycles and alcohols were either purified by distillation or recrystallization. $Ni(cod)_2$ and SIPr (CAS No. 258278-28-3) were obtained from Strem Chemicals and stored in a glove box. Reaction temperatures were controlled using an IKAmag temperature modulator, and unless stated otherwise, reactions were performed at room temperature (approximately 23 °C). Thin-layer chromatography (TLC) was conducted with EMD gel 60 F254 pre-coated plates (0.25 mm for analytical chromatography and 0.50 mm for preparative chromatography) and visualized using a combination of UV, iodine, anisaldehyde, and potassium permanganate staining techniques. Silicycle Siliaflash P60 (particle size 0.040–0.063 mm) was used for flash column chromatography. ^1H NMR spectra were recorded on Bruker spectrometers (at 500 MHz) and are reported relative to residual solvent signals. Analysis of reaction mixtures in Section 7.8.2.1 in the Experimental Procedures was carried out on a Mettler Toledo SFC (supercritical fluid chromatography) with a Daicel ChiralPak OD-H column using 10% CH_3CN as the polar cosolvent and 226 nm as the wavelength of observation.

7.8.2 Experimental Procedures

7.8.2.1. Development and Verification of the Kinetic Model

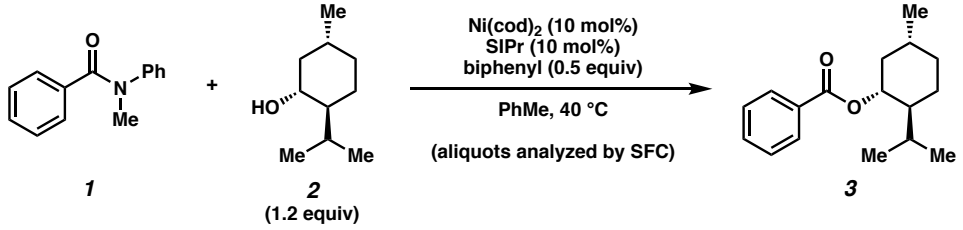

Representative Procedure (coupling of amide 7.1 and (–)-menthol (7.2) is used as an example). Ester 7.3. A 1-dram vial containing a magnetic stir bar was flame-dried under reduced pressure, and then allowed to cool under N_2. Amide substrate **7.1** (211 mg, 1.00 mmol, 1.0 equiv), (–)-menthol (**7.2**, 187 mg, 1.20 mmol, 1.2 equiv), and biphenyl[23] (77.0, 0.500 mmol, 0.5 equiv) were added, and the vial was flushed with N_2. The vial was taken into a glove box and charged with $Ni(cod)_2$ (27.5 mg, 0.100 mmol, 10 mol%) and SIPr (39.1 mg, 0.100 mmol, 10 mol%). Subsequently, toluene (1.0 mL, 0.66 M)[10] was added. The vial was sealed with a Teflon-lined septum cap and stirred at 40 °C in the glove box. Periodically, aliquots of the homogeneous reaction mixture (approximately 50 mL each) were removed via syringe, placed into a 25 mL volumetric flask, and diluted to the mark with HPLC grade CH_3CN. Reaction conversion was then determined by SFC analysis with biphenyl as an internal standard. Typically, 4–6 aliquots were analyzed per reaction. The data was then plotted graphically and rate information was derived using *DynoChem*.[14]

Any modifications of the conditions shown in the representative procedure above are specified below in Tables 7.2, 7.3, and 7.4.

A number of exploratory experiments were designed to scope the sensitivity of the observed reaction rate to the following parameters: (a) ligand to metal ratio, (b) equivalents of (–)-menthol (**7.2**), (c) presence of product / byproduct spikes, and (d) length of time holding the catalyst at a given temperature prior to substrate addition (Table 7.2). No significant impact on the reaction rate was observed from changes to any of these variables.

Table 7.2. Summary of Exploratory Reaction Conditions.

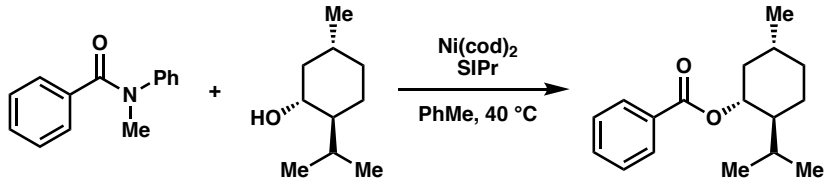

7.1 *7.2* *7.3*

Entry	Data Source	$Ni(cod)_2$	SIPr:$Ni(cod)_2$ ratio	(–)-Menthol (equiv)	MePhNH spike (equiv)	Product spike (equiv)
1	NAW-5-043	10 mol%	1:1	1.2	0.50	–
2	NAW-5-044	10 mol%	1:1	1.2	–	0.50
3[a]	NAW-5-045	10 mol%	1:1	1.2	–	–
4[b]	NAW-5-046	10 mol%	1:1	1.2	–	–
5	NAW-5-047	5 mol%	2:1	1.2	–	–
6	NAW-5-052	10 mol%	1:2	1.2	–	–
7	NAW-5-058	10 mol%	1:1	1.8	–	–

[a] Catalyst, ligand, alcohol, and toluene were held at 40 °C for 36 min before addition of substrate. [b] Catalyst, ligand, alcohol, and toluene were held at 40 °C for 654 min before addition of substrate.

The following reaction parameters were then selected for further evaluation: (a) temperature, (b) catalyst loading, and (c) reaction concentration. A handful of experiments were then used to train the model, varying temperatures as well as the amount of catalyst (Table 7.3). As expected, changes to these variables had a marked impact on the reaction kinetics.

Table 7.3. Summary of Experiments Used to Train the Model.

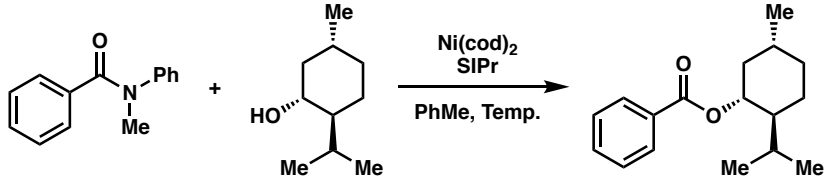

7.1 *7.2* (1.2 equiv) *7.3*

Entry	Data Source	$Ni(cod)_2$ / SIPr	Temp.	Concentration[a]	Max Conversion	Time
1	NAW-5-042	10 mol%	40 °C	0.66 M	92%	8 h
2	NAW-5-061	10 mol%	33 °C	0.66 M	70%	6 h
3	NAW-5-060	10 mol%	50 °C	0.66 M	91%	4 h
4	NAW-5-073	0.5 mol%	65 °C	1.16 M	77%	8 h
5	NAW-5-069	0.1 mol%	80 °C	1.16 M	13%	1 h

[a] Volume was approximated by summing the masses of all reactants, reagents, and solvent with an assumed overall density of 0.87 g/mL (toluene).

A simplistic reaction pathway was constructed using literature precedent as well as modeling work performed by the Houk laboratory on this transformation (Figure 7.7).[4] Moreover, the obtained data was utilized to develop a kinetic model using *DynoChem* software. A review of the data in Table 7.3 also indicated the presence of a catalyst degradation pathway, as many reactions (in particular, entry 5) did not reach full conversion. The degradation kinetics (k_4) were represented by a simplified first-order pathway from the catalyst resting state (NiL). The regressed values and associated standard error of k_1 and k_4 are shown in Figure 7.7 below. The rate of ligand exchange (k_2) and reductive elimination (k_3) were not found to be rate-determining, and therefore an arbitrary fast rate was selected for fitting.

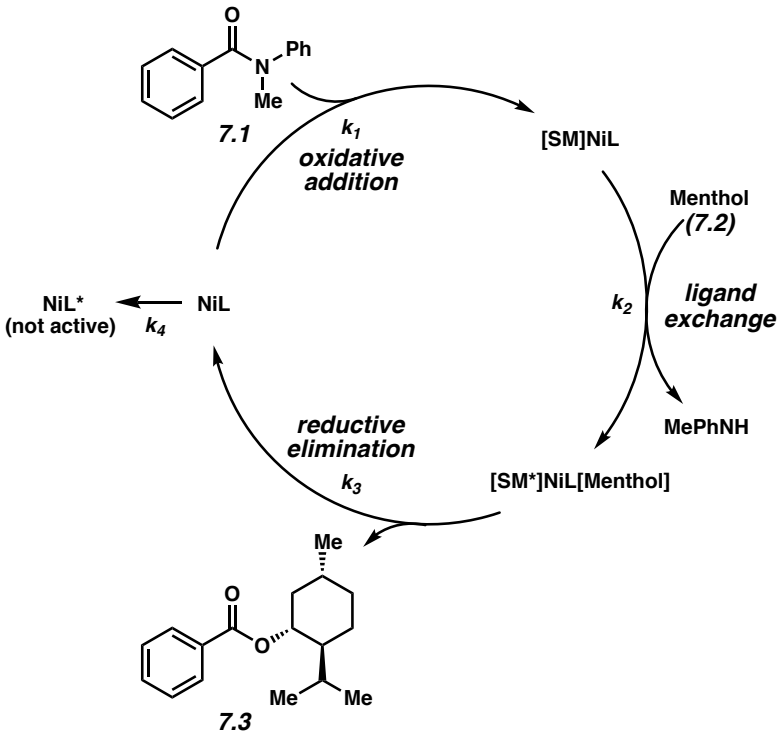

Refined Forward Rate Constants (k)[a]	Activation Energy (E_a) (kJ/mol)[b]
k_1 = (2.00 ± 0.06) x 10^{-3} L/mol·s	E_{a1} = 97 ± 2
k_2 = 10 L/mol·s[c]	E_{a2} = 0[d]
k_3 = 10 s^{-1}[c]	E_{a3} = 0[d]
k_4 = (1.42 ± 0.38) x 10^{-6} s^{-1}	E_{a4} = 151 ± 5

[a] Rate constants are reported at 40 °C. The ± values represent the 95% confidence interval obtained from the *DynoChem* fitting of the data to the kinetic model. [b] For comparison, the corresponding values in kcal/mol are as follows: E_{a1} = 23.0 ± 0.5 kcal/mol; E_{a4} = 36.1 ± 1.0 kcal/mol. [c] This reaction is fast and not rate limiting, therefore an arbitrary fast rate of 10 was selected for subsequent fitting. [d] Reaction rate was a weak function of temperature within the explored temperature range.

Figure 7.7. Simplistic Reaction Pathway and Calculated Rate Constants

The experimentally observed time course data for each experiment in Table 7.3 was described accurately by the developed kinetic model described above (Figure 7.8).

NW-5-042

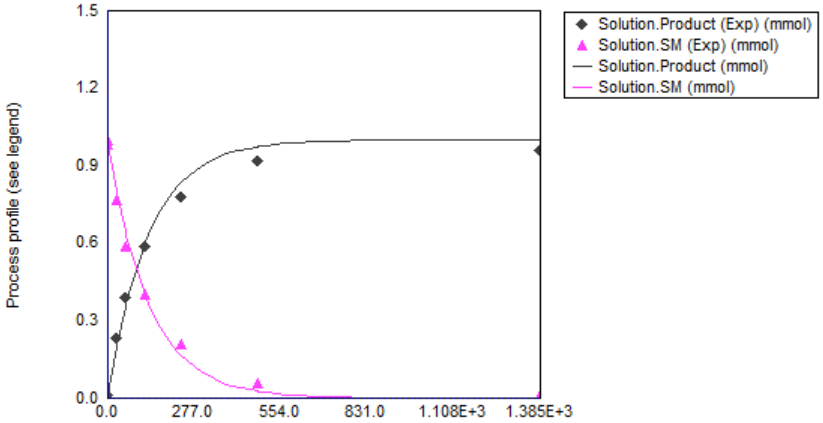

NW-5-061

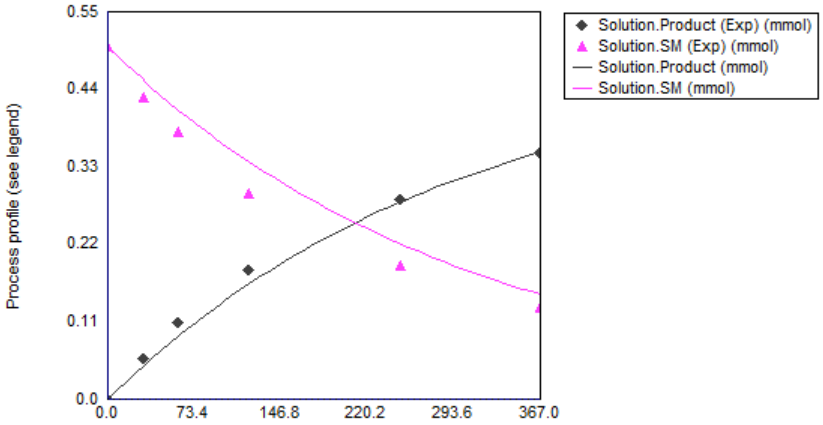

NW-5-060

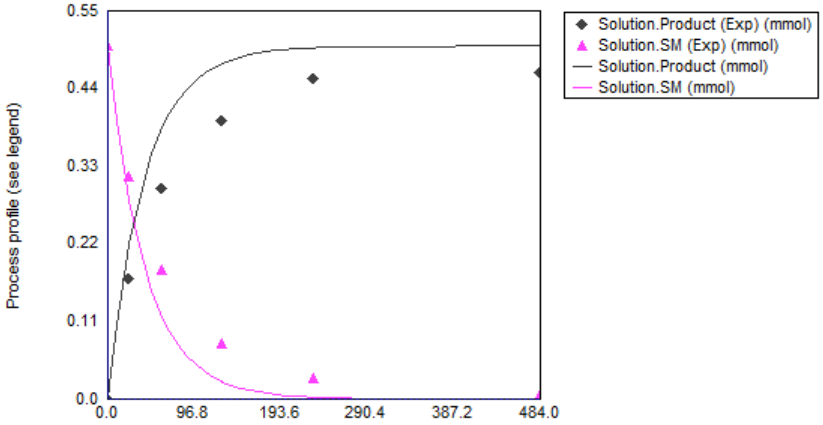

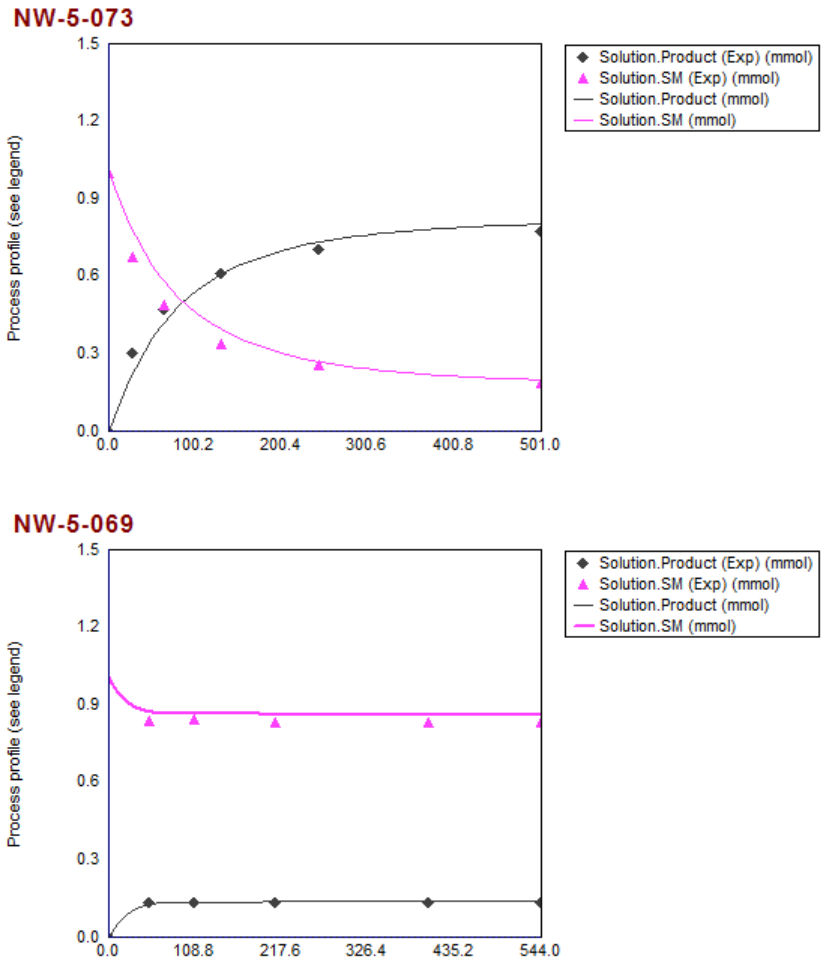

Figure 7.8. Concentration Profiles of Observed Values (Points) vs. Calculated Values (Curves); x-axes: time (min); y-axes: mmol

Further independent experiments, which were not part of the training data set to estimate rate constants, were performed under atypical reaction conditions (Table 7.4). These experiments were used to verify the model prediction capabilities, with the model observed to have done a good job of predicting atypical reaction behavior (Figure 7.9).

Table 7.4. Summary of Experiments Used to Verify the Model.

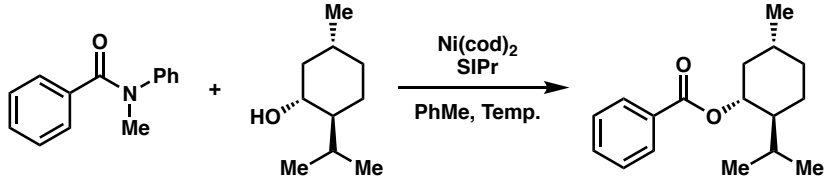

7.1 *7.2* (1.2 equiv) *7.3*

Entry	Data Source	$Ni(cod)_2$	SIPr:$Ni(cod)_2$ ratio	Temp.	Concentration[a]	Max Conversion
1	NAW-5-111	0.2 mol%	1:1	45 °C	1.78 M	77%
2	NAW-5-105	0.4 mol%	1:1	45 °C	1.51 M	91%
3	NAW-5-114	0.4 mol%	1:1	45 °C	1.51 M	76%
4	NAW-5-119	0.4 mol%	2:1	45 °C	1.51 M	85%
5	NAW-5-124	0.4 mol%	3:2	45 °C	1.51 M	77%
6	NAW-5-083	0.5 mol%	1:1	45 °C	1.16 M	81%
7	NAW-5-102	0.6 mol%	1:1	45 °C	1.31 M	94%
8	NAW-5-090[b]	10 mol%	1:1	50 °C	0.66 M	92%
9	NAW-5-080	1 mol%	1:1	55 °C	1.16 M	94%
10	NAW-5-067	1 mol%	1:1	60 °C	1.04 M	89%
11	NAW-5-072	0.1 mol%	1:1	80 °C	1.16 M	14%

[a] Volume was approximated by summing the masses of all reactants, reagents, and solvent with an assumed overall density of 0.87 g/mL (toluene). [b] Catalyst, ligand, alcohol, and toluene were held at 50 °C for 12.6 h before addition of substrate.

NW-5-111

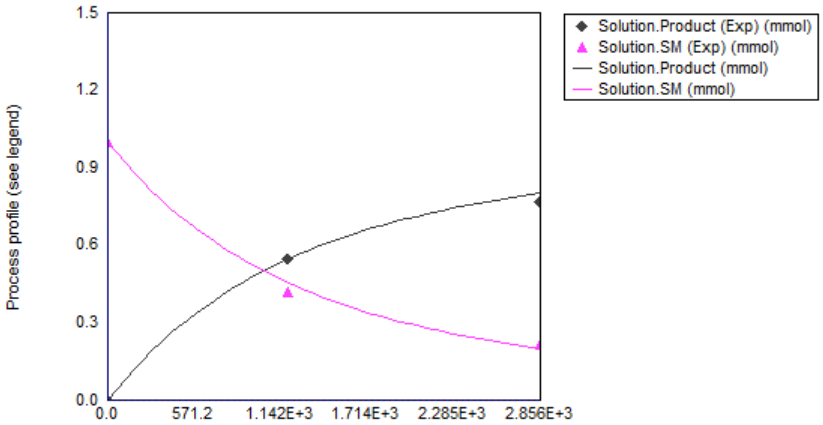

NW-5-105

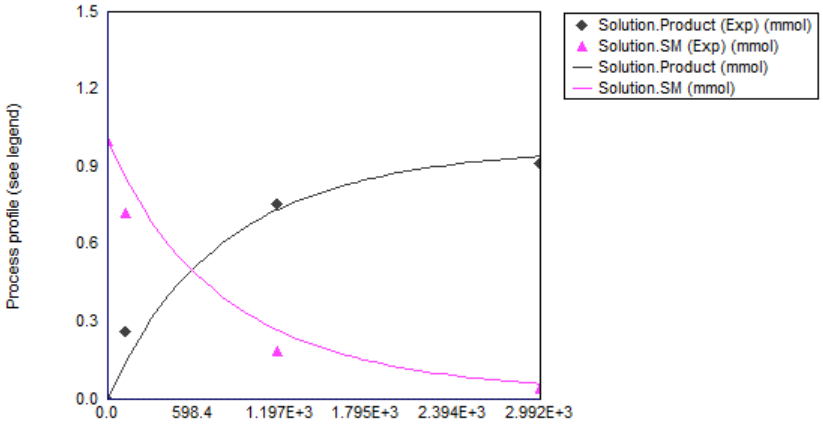

NW-5-114

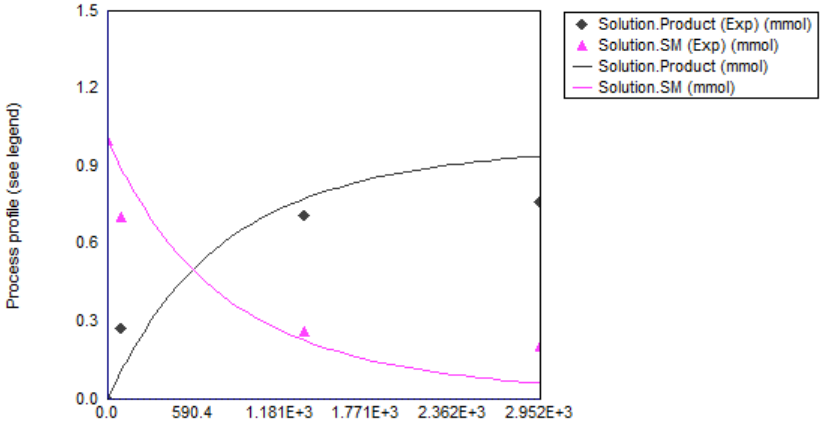

NW-5-119

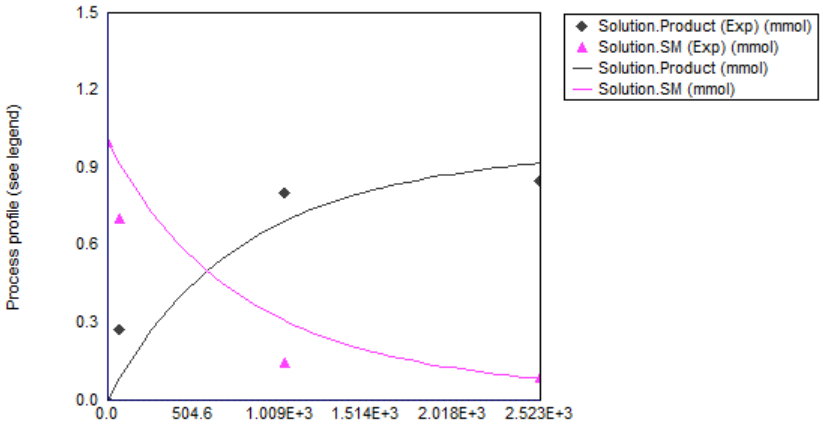

NW-5-124

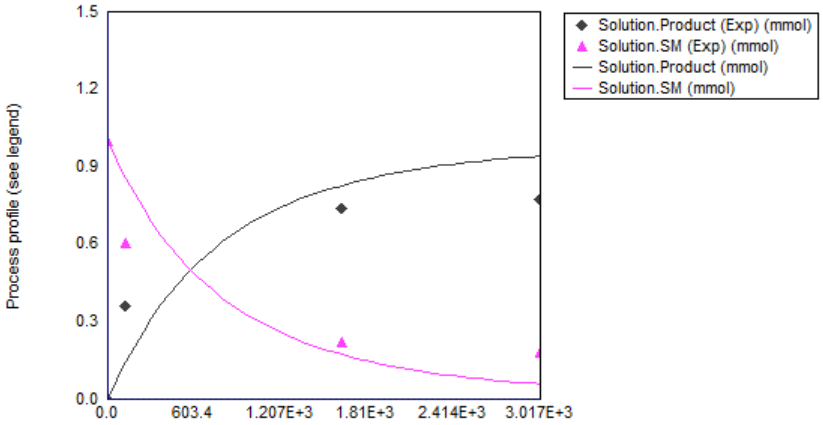

NW-5-083

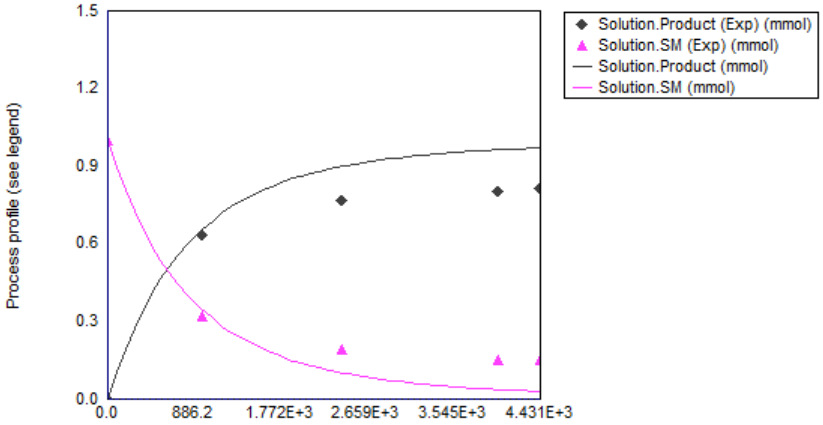

NW-5-102

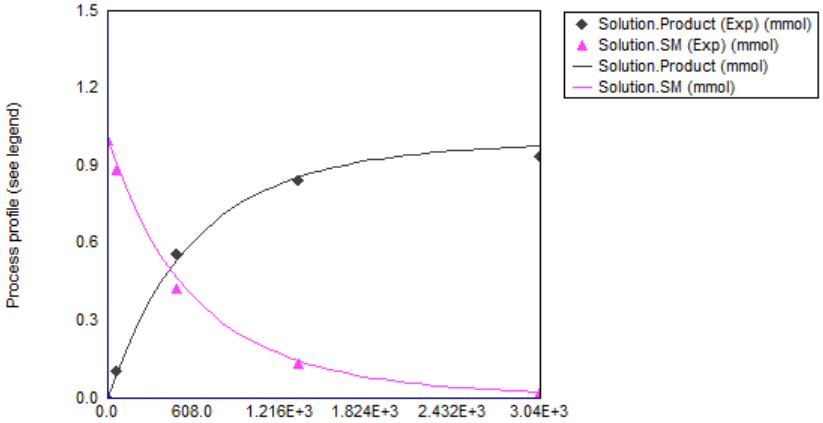

NW-5-090

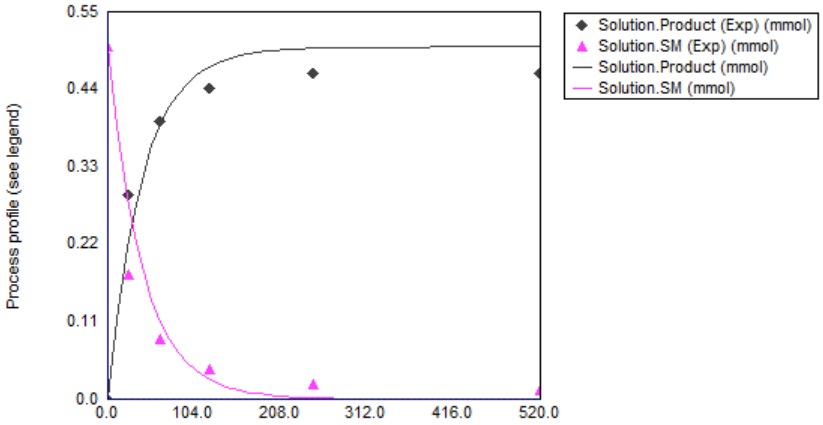

NW-5-080

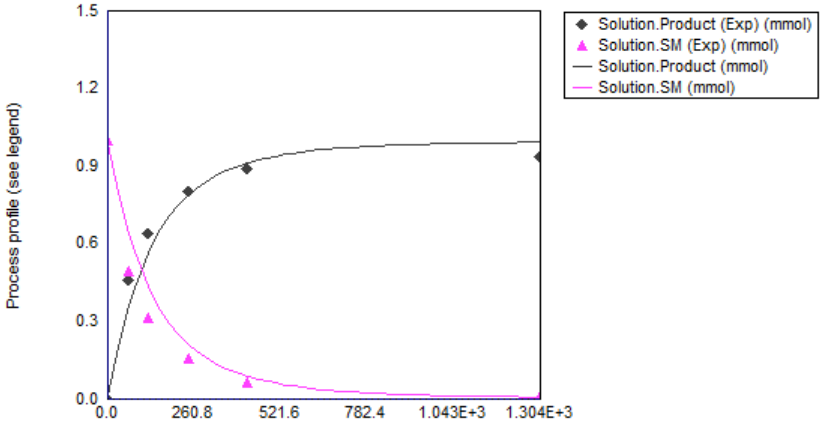

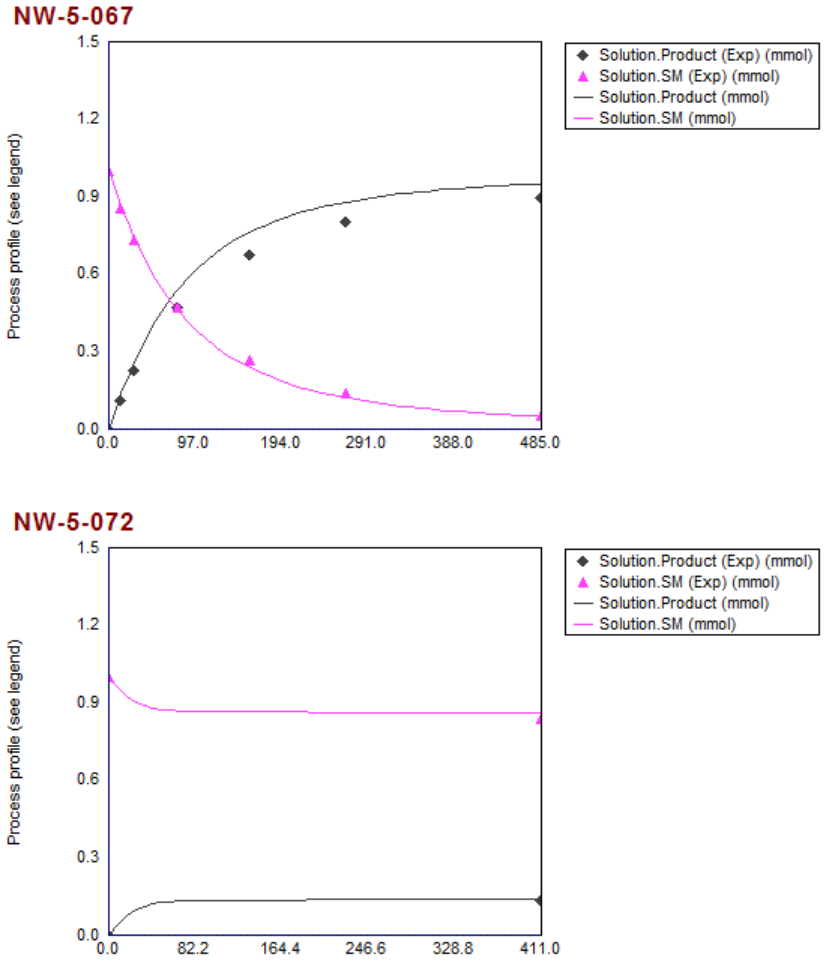

Figure 7.9. Concentration Profiles of Observed Values (Points) vs. Calculated Values (Curves); x-axes: time (min); y-axes: mmol

With a working kinetic model in hand, thousands of *in silico* simulations were performed in minutes in order to visualize the multidimensional relationships between (a) reaction concentration, (b) reaction temperature, and (c) catalyst loading. These calculations were carried out with both catalyst loadings above and below 1.0 mol% (Figures 7.10 and 7.11).

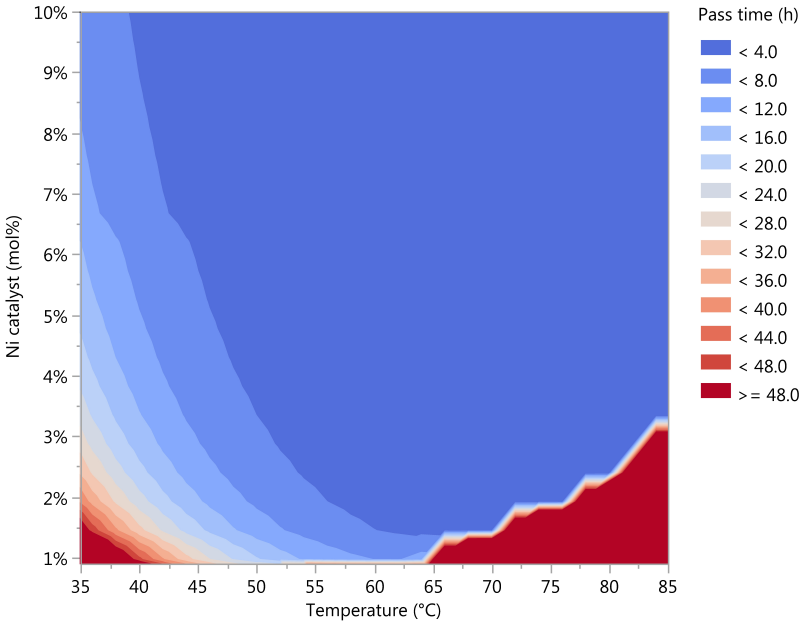

Figure 7.10. *In Silico* Simulations of Reaction Pass Time (95% Conversion) as a Function of Ni Catalyst (mol%) and Temperature for Overall Reaction Concentrations of 1.00–1.30 M.[10]

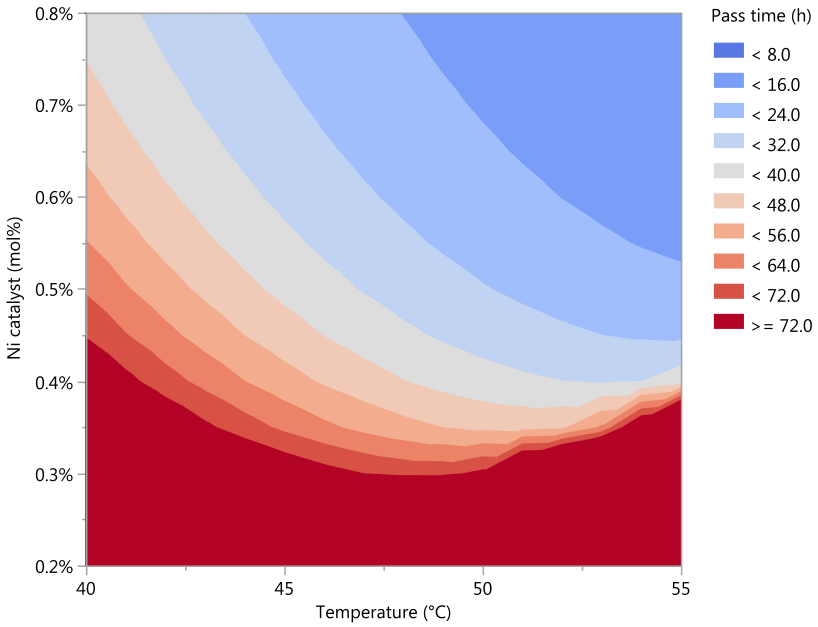

Figure 7.11. *In Silico* Simulations of Reaction Pass Time (95% Conversion) as a Function of Ni Catalyst (mol%) and Temperature for Overall Reaction Concentrations of 1.44–1.74 M.[10]

7.8.2.2. Scope of Coupling Using 2 mol% Nickel

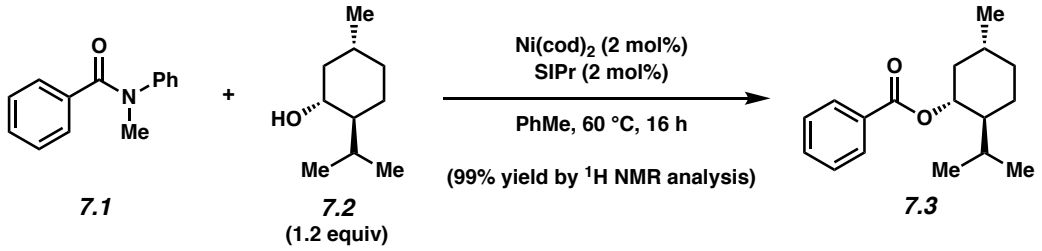

Representative Procedure (coupling of amide 7.1 and (–)-menthol (7.2) is used as an example). Ester 7.3. A 1-dram vial containing a magnetic stir bar was flame-dried under reduced pressure, and then allowed to cool under N_2. Amide substrate **7.1** (106 mg, 0.500 mmol, 1.0 equiv) and (–)-menthol (**7.2**, 93.6 mg, 0.600 mmol, 1.2 equiv) were added, and the vial was flushed with N_2. The vial was taken into a glove box and charged with $Ni(cod)_2$ (2.8 mg, 0.010 mmol, 2 mol%) and SIPr (3.9 mg, 0.010 mmol, 2 mol%). Subsequently, toluene (0.25 mL, 1.04 M)[10] was added. The vial was sealed with a Teflon-lined screw cap, removed from the glove box, and stirred at 60 °C for 16 h. After cooling to 23 °C, the mixture was diluted with hexanes (0.5 mL) and filtered over a plug of silica gel (10 mL EtOAc eluent). The volatiles were removed under reduced pressure, and the yield was determined by ^1H NMR analysis with hexamethylbenzene as an external standard. Purification by preparative thin-layer chromatography (5:1 Hexanes:EtOAc) generated ester **7.3** as a white solid. Ester **7.3**: R_f 0.68 (5:1 Hexanes:EtOAc). The reported literature yield is 88%.[4] Spectral data match those previously reported.[24]

Any modifications of the conditions shown in the representative procedure above are specified in the following schemes, which depict all of the results shown in Figure 7.5.

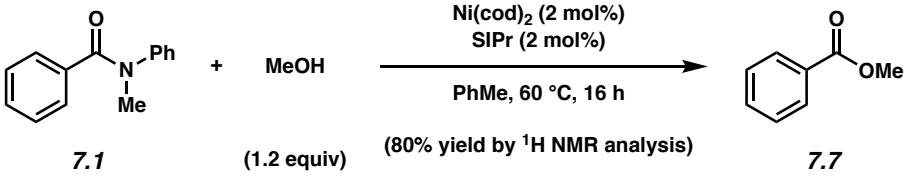

Ester 7.7. ^{1}H NMR analysis of the crude reaction mixture indicated an 80% yield of ester **7.7** relative to hexamethylbenzene external standard. Purification by preparative thin-layer chromatography (5:1 Hexanes:EtOAc) generated ester **7.7** as a clear oil. Ester **7.7**: R_f 0.52 (5:1 Hexanes:EtOAc). The reported literature yield is 88%.[4] Spectral data match those previously reported.[25]

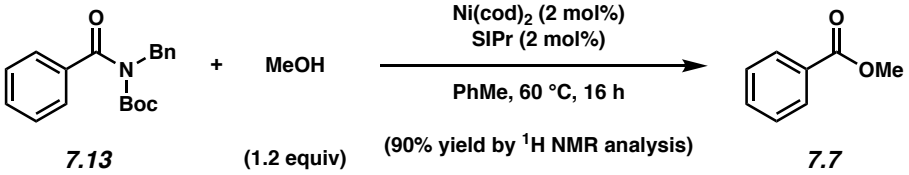

Ester 7.7. ^{1}H NMR analysis of the crude reaction mixture indicated a 90% yield of ester **7.7** relative to hexamethylbenzene external standard. Purification by preparative thin-layer chromatography (5:1 Hexanes:EtOAc) generated ester **7.7** as a clear oil. Ester **7.7**: R_f 0.52 (5:1 Hexanes:EtOAc). The reported literature yield is 89%.[4] Spectral data match those previously reported.[25]

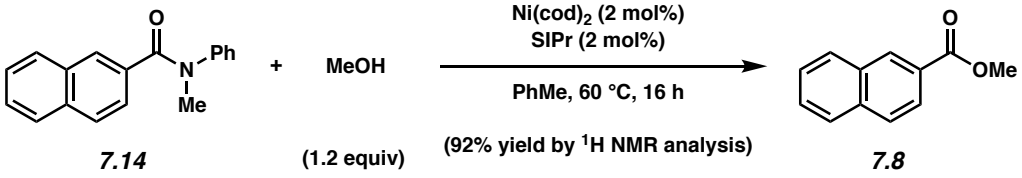

Ester 7.8. ^{1}H NMR analysis of the crude reaction mixture indicated a 92% yield of ester **7.8** relative to hexamethylbenzene external standard. Purification by preparative thin-layer chromatography (100% PhH) generated ester **7.8** as a white solid. Ester **7.8**: R_f 0.50 (5:1

Hexanes:EtOAc). The reported literature yield is 94%.[4] Spectral data match those previously reported.[26]

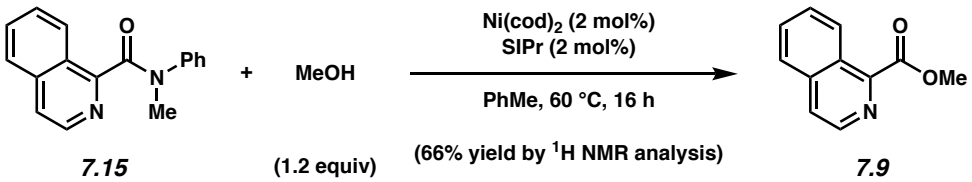

7.15 (1.2 equiv) *7.9*

Ester 7.9. ^{1}H NMR analysis of the crude reaction mixture indicated a 66% yield of ester **7.9** relative to hexamethylbenzene external standard. Purification by preparative thin-layer chromatography (1:1 Hexanes:EtOAc) generated ester **7.9** as a clear oil. Ester **7.9**: R_f 0.30 (2:1 Hexanes:EtOAc). The reported literature yield is 56%.[4] Spectral data match those previously reported.[27]

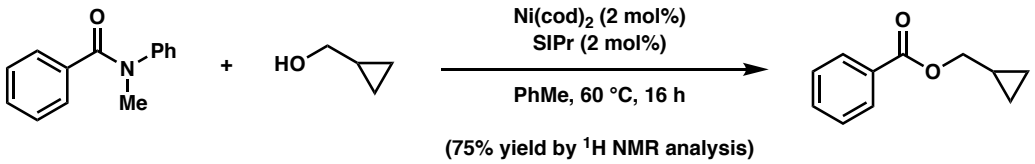

7.1 *7.16* (1.2 equiv) *7.10*

Ester 7.10. ^{1}H NMR analysis of the crude reaction mixture indicated a 75% yield of ester **7.10** relative to hexamethylbenzene external standard. Purification by flash chromatography (49:1 Hexanes:EtOAc) generated ester **7.10** as a clear oil. Ester **7.10**: R_f 0.65 (5:1 Hexanes:EtOAc). The reported literature yield is 90%.[4] Spectral data match those previously reported.[4]

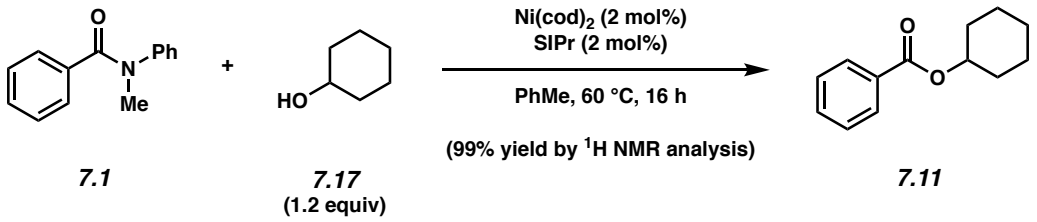

Ester 7.11. ^{1}H NMR analysis of the crude reaction mixture indicated a 99% yield of ester **7.11** relative to hexamethylbenzene external standard. Purification by preparative thin-layer chromatography (5:1 Hexanes:EtOAc) generated ester **7.11** as a clear oil. Ester **7.11**: R_f 0.56 (5:1 Hexanes:EtOAc). The reported literature yield is 82%.[4] Spectral data match those previously reported.[28]

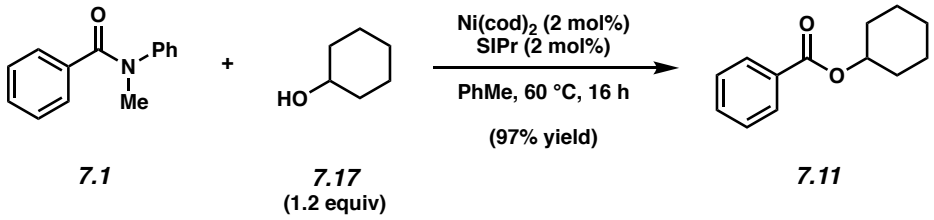

Ester 7.11. Purification by flash chromatography (49:1 Hexanes:EtOAc) generated ester **7.11** (99.3 mg, 97% yield) as a clear oil. Ester **7.11**: R_f 0.56 (5:1 Hexanes:EtOAc). The reported literature yield is 82%.[4] Spectral data match those previously reported.[28]

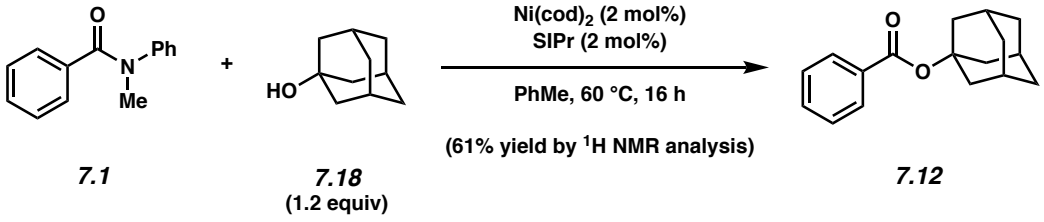

Ester 7.12. ^{1}H NMR analysis of the crude reaction mixture indicated a 61% yield of ester **7.12** relative to hexamethylbenzene external standard. Purification by preparative thin-layer chromatography (5:1 Hexanes:EtOAc) generated ester **7.12** as a white solid. Ester **7.12**: R_f 0.64

(5:1 Hexanes:EtOAc). The reported literature yield is 67%.[4] Spectral data match those previously reported.[29]

7.8.2.3. Multigram Scale Coupling Using 0.4 mol% Nickel

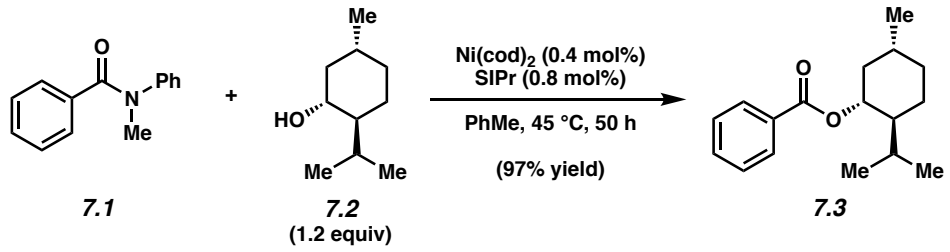

Ester 7.3. A 20 mL scintillation vial containing a magnetic stir bar was flame-dried under reduced pressure, and then allowed to cool under N_2. Amide substrate **7.1** (5.00 g, 23.7 mmol, 1.0 equiv) and (–)-menthol (**7.2**, 4.44 g, 28.4 mmol, 1.2 equiv) were added, and the vial was flushed with N_2. The vial was taken into a glove box and charged with $Ni(cod)_2$ (26.0 mg, 0.0947 mmol, 0.4 mol%) and SIPr (74.1 mg, 0.190 mmol, 0.8 mol%). Subsequently, toluene (4.74 mL, 1.52 M)[10] was added. The vial was sealed with a Teflon-lined screw cap, removed from the glove box, and stirred at 45 °C for 50 h. After cooling to 23 °C, the mixture was diluted with hexanes (7 mL) and filtered over a plug of silica gel (500 mL EtOAc eluent). The volatiles were removed under reduced pressure, and the crude residue was purified by flash chromatography (99:1 Hexanes:EtOAc → 49:1 Hexanes:EtOAc → 24:1 Hexanes:EtOAc) to yield ester **7.3** (5.99 g, 97% yield) as a white solid. Ester **7.3**: R_f 0.68 (5:1 Hexanes:EtOAc). The reported literature yield is 88%.[4] Spectral data match those previously reported.[24]

7.8.2.4. Complete List of Digital Object Identifiers (DOIs) Used to Compile Figure 7.1

SciFinder search for the research topic "nickel, cross-coupling" yielded hits corresponding to 83 original manuscripts in the journals *J. Am. Chem. Soc.*, *Angew. Chem. Int. Ed.*, *Science*, *Nature*, *Nat. Chem.*, and *Nat. Commun.* since 2015 (accessed 20 April, 2017). The manuscripts were then analyzed on an individual basis to determine the most frequently employed catalyst loading in each case. The following is a complete list of Digital Object Identifiers (DOIs) corresponding to sampled manuscripts used to compile Figure 7.1:

10.1002/anie.201409739

10.1002/anie.201410322

10.1002/anie.201410875

10.1002/anie.201500404

10.1002/anie.201502502

10.1002/anie.201502882

10.1002/anie.201503204

10.1002/anie.201503297

10.1002/anie.201503936

10.1002/anie.201504963

10.1002/anie.201505136

10.1002/anie.201505699

10.1002/anie.201506147

10.1002/anie.201507494

10.1002/anie.201509444

10.1002/anie.201510497

10.1002/anie.201511438

10.1002/anie.201601206

10.1002/anie.201601351

10.1002/anie.201601914

10.1002/anie.201601991

10.1002/anie.201604406

10.1002/anie.201604429

10.1002/anie.201604696

10.1002/anie.201605162

10.1002/anie.201605463

10.1002/anie.201605593

10.1002/anie.201606458

10.1002/anie.201606529

10.1002/anie.201607856

10.1002/anie.201607959

10.1002/anie.201611720

10.1002/anie.201611819

10.1002/anie.201700097

10.1002/anie.201702402

10.1021/ja511913h

10.1021/ja512498u

10.1021/ja512946e

10.1021/ja513079r

10.1021/ja513166w

10.1021/jacs.5b00473

10.1021/jacs.5b01909

10.1021/jacs.5b02503

10.1021/jacs.5b02945

10.1021/jacs.5b03870

10.1021/jacs.5b04725

10.1021/jacs.5b06466

10.1021/jacs.5b10963

10.1021/jacs.5b11244

10.1021/jacs.5b13211

10.1021/jacs.6b00250

10.1021/jacs.6b01533

10.1021/jacs.6b03253

10.1021/jacs.6b03384

10.1021/jacs.6b03465

10.1021/jacs.6b06862

10.1021/jacs.6b07567

10.1021/jacs.6b08075

10.1021/jacs.6b08397

10.1021/jacs.6b08507

10.1021/jacs.6b11412

10.1021/jacs.6b11962

10.1021/jacs.7b00049

10.1021/jacs.7b01705

10.1021/jacs.7b02389

10.1021/jacs.7b02742

10.1021/jacs.7b03448

10.1038/nature14676

10.1038/nature14875

10.1038/nature19056

10.1038/nature22307

10.1038/nchem.2388

10.1038/nchem.2587

10.1038/nchem.2741

10.1038/ncomms11073

10.1038/ncomms11129

10.1038/ncomms11676

10.1038/ncomms12937

10.1038/ncomms8508

10.1038/ncomms9404

10.1126/science.aaf6123

10.1126/science.aaf6635

10.1126/science.aam7355

7.9 Spectra Relevant to Chapter Seven:

Kinetic Modeling of the Nickel-Catalyzed Esterification of Amides

Nicholas A. Weires, Daniel D. Caspi, and Neil K. Garg.

ACS Catal. [Just accepted manuscript] DOI: 10.1021/acscatal.7b01444.

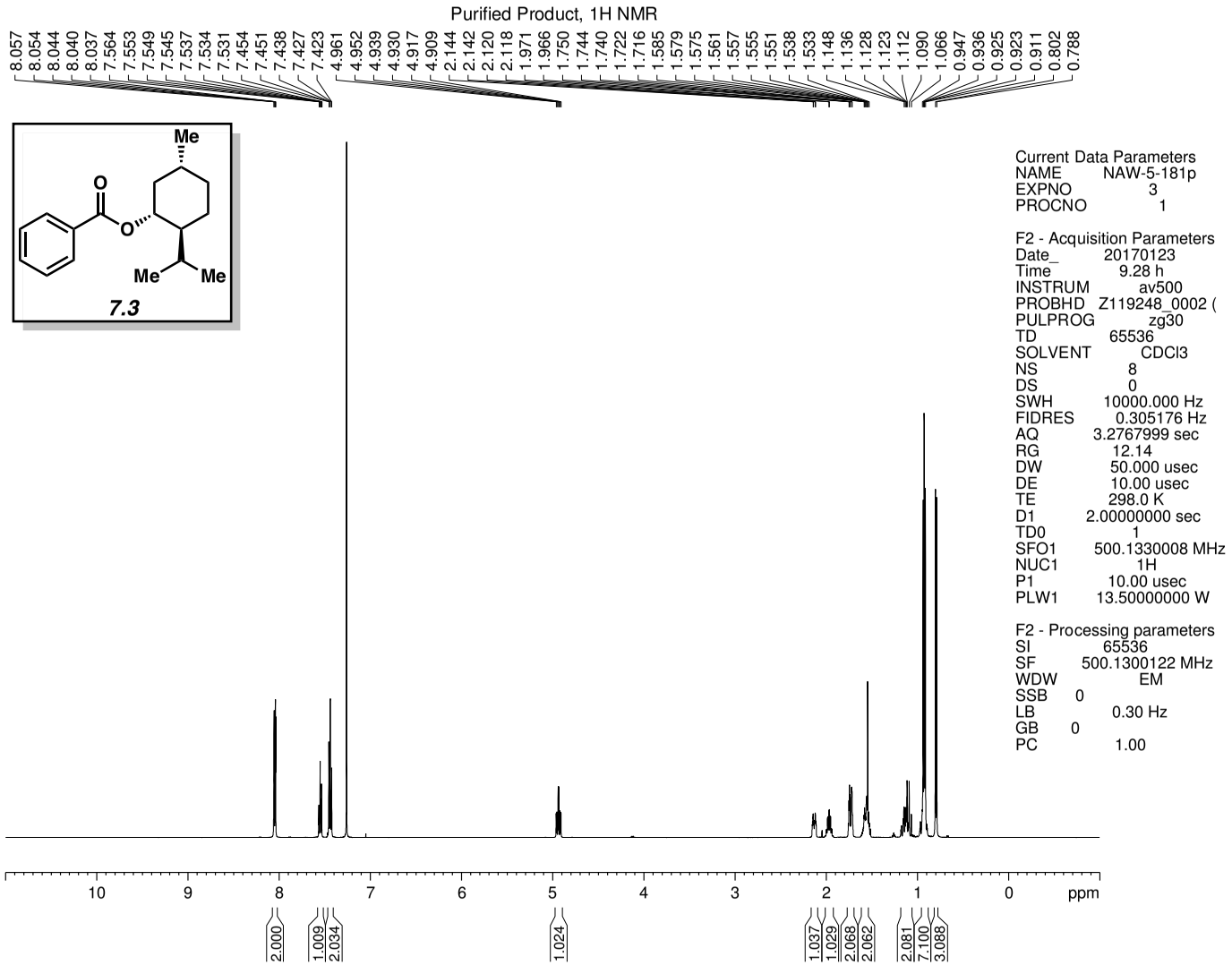

Figure 7.12 ^{1}H NMR (500 MHz, $CDCl_3$) of compound **7.3**.

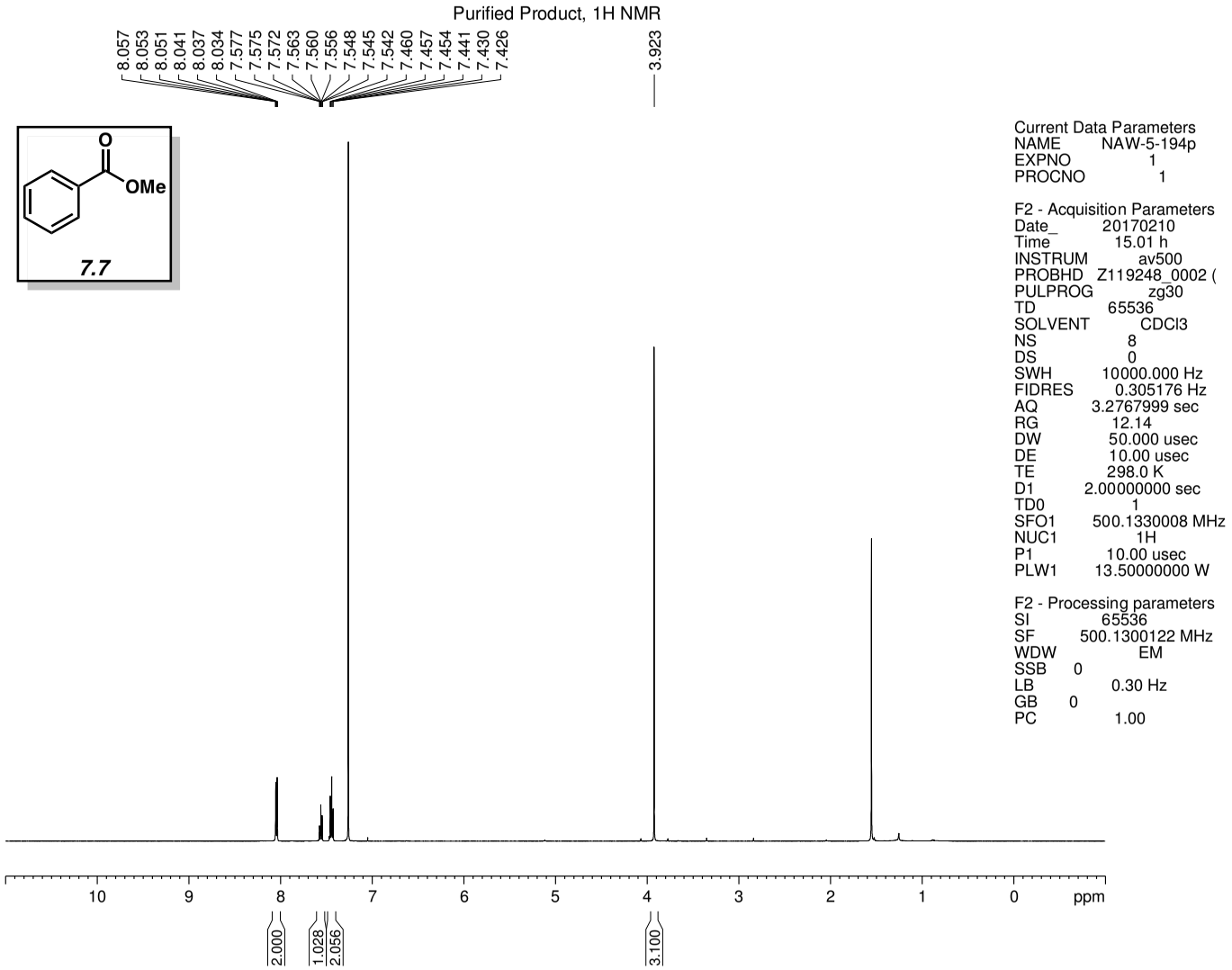

Figure 7.13 ^{1}H NMR (500 MHz, $CDCl_3$) of compound **7.7**.

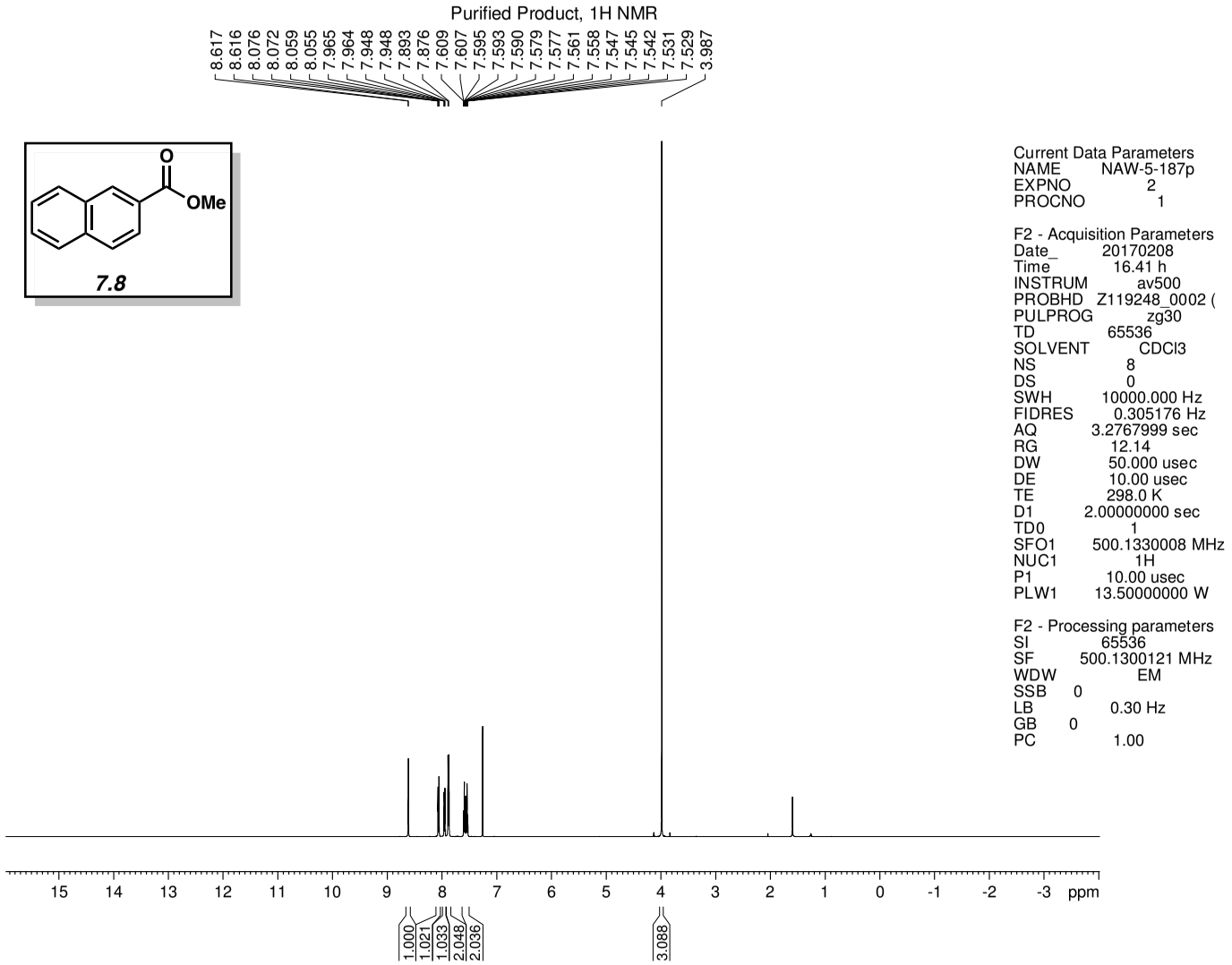

Figure 7.14 ^{1}H NMR (500 MHz, $CDCl_3$) of compound **7.8**.

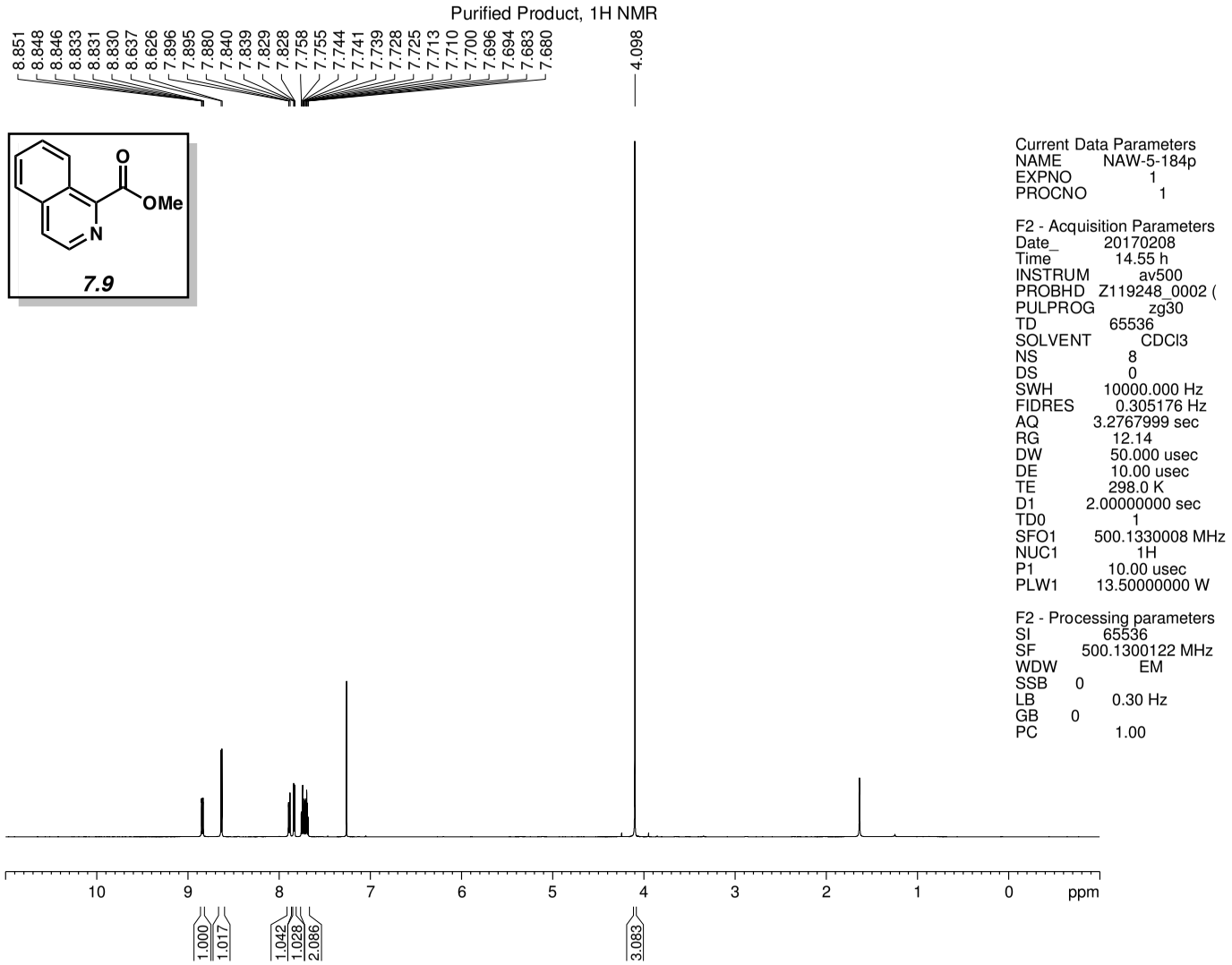

Figure 7.15 ^{1}H NMR (500 MHz, $CDCl_3$) of compound **7.9**.

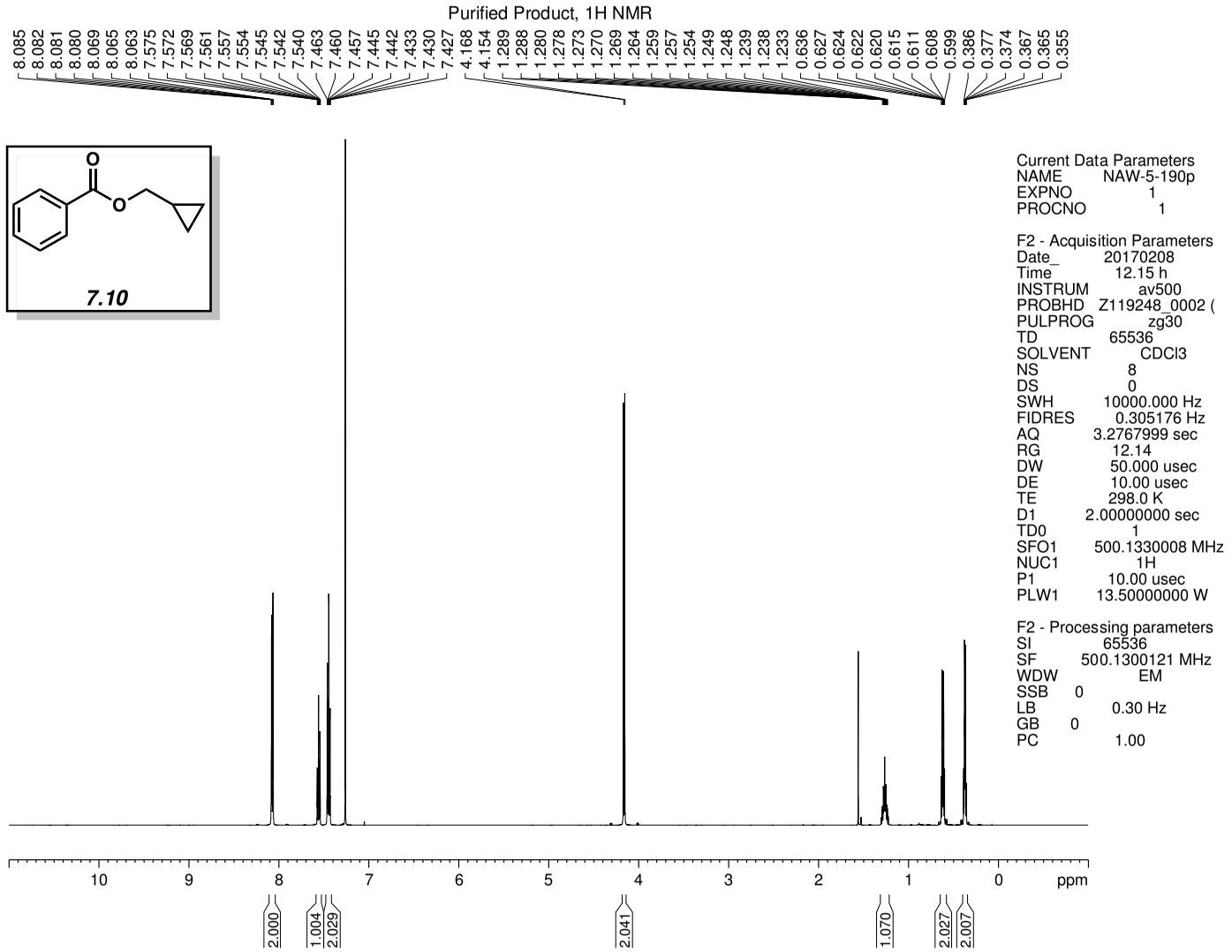

Figure 7.16 ^{1}H NMR (500 MHz, $CDCl_3$) of compound **7.10**.

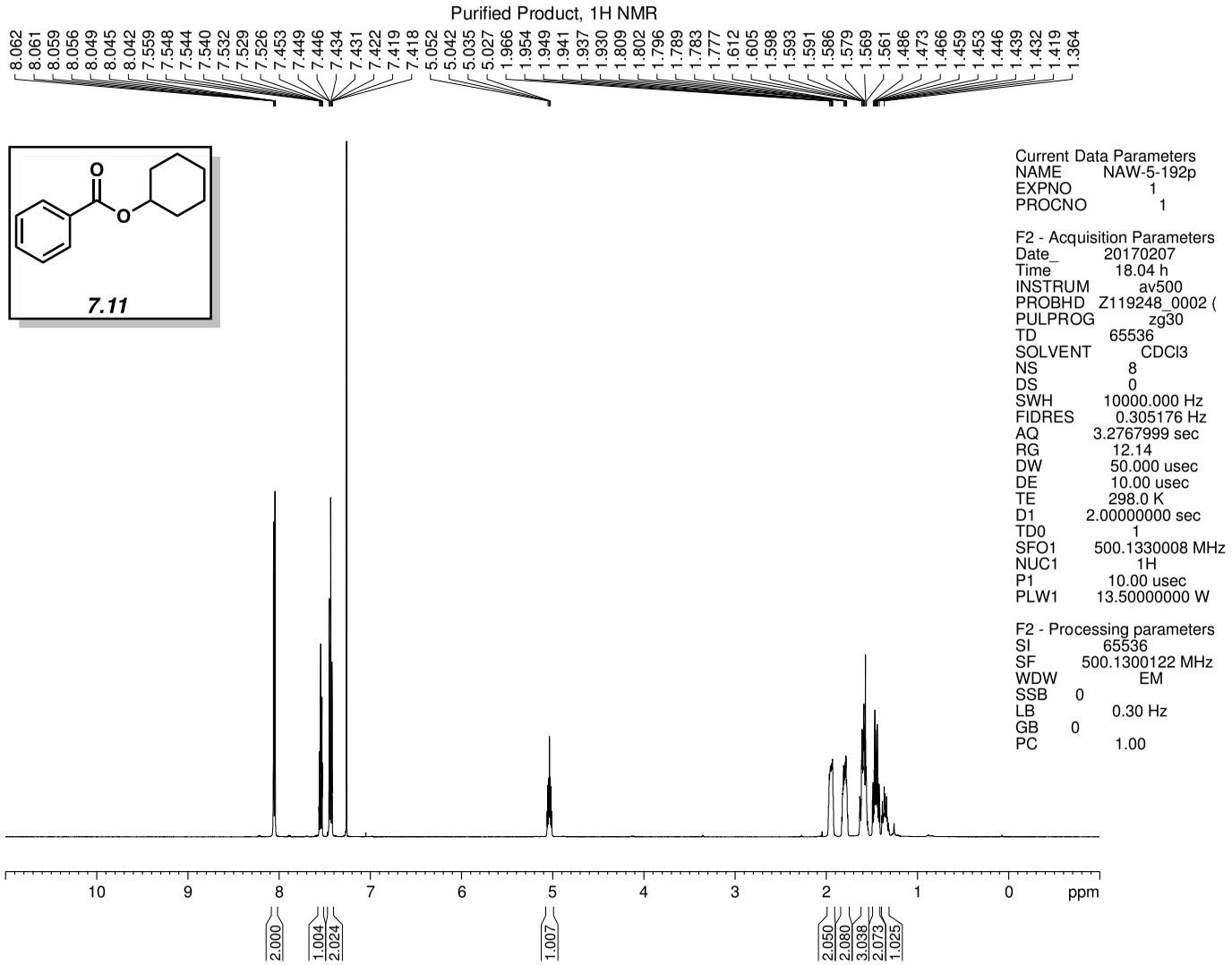

Figure 7.17 ^{1}H NMR (500 MHz, $CDCl_3$) of compound **7.11**.

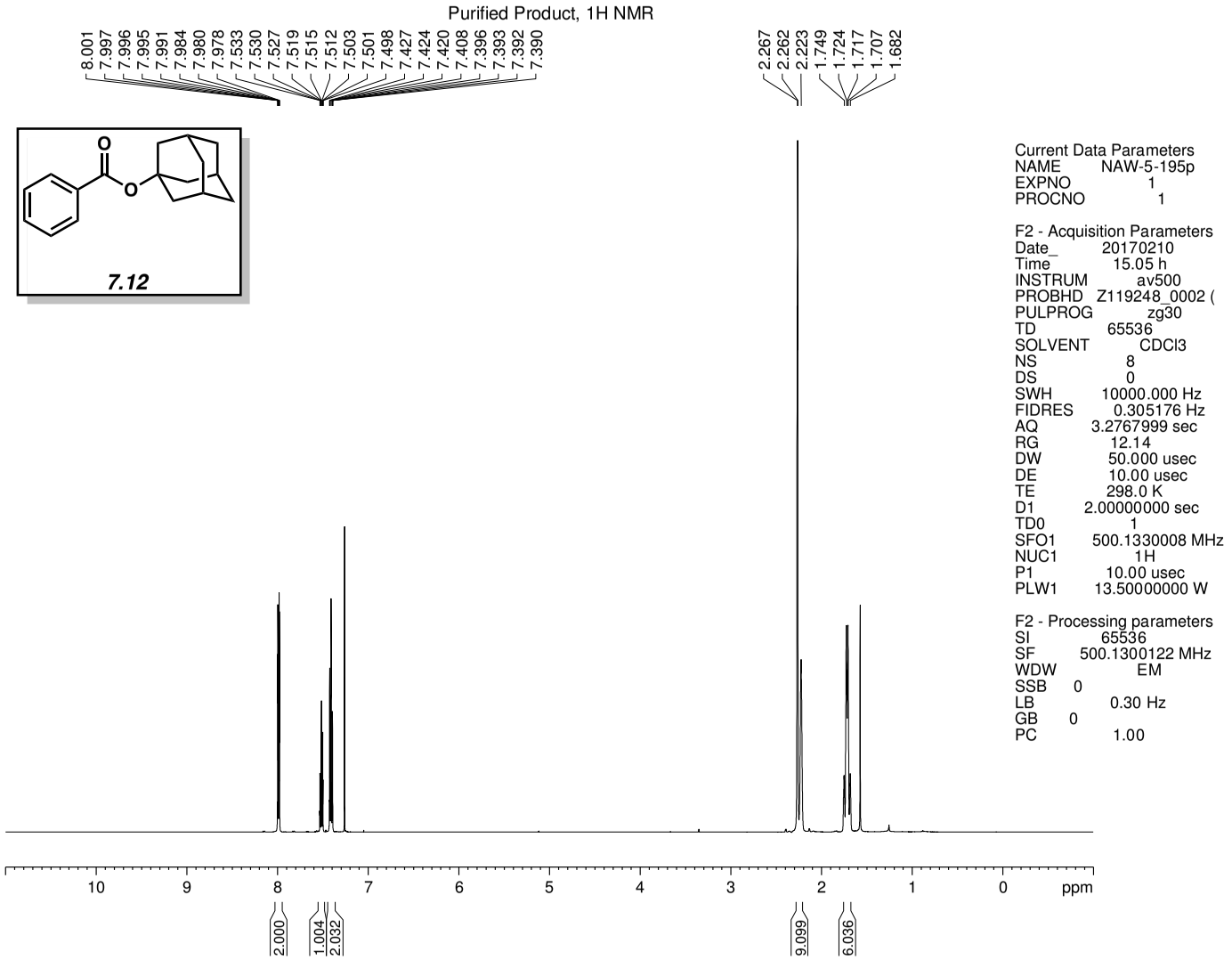

Figure 7.18 ^{1}H NMR (500 MHz, $CDCl_3$) of compound **7.12**.

7.10 Notes and References

(1) (a) *Pharmaceutical Process Chemistry*. Shioiri, T., Izawa, K., Konoike, T., Eds.; Wiley-VCH: Weinheim, 2010; 1–526. (b) *New Horizons of Process Chemistry*. Tomioka, K., Shioiri, T., Sajiki, H., Eds.; Springer: Gateway East, 2017; 1–285.

(2) For pertinent reviews on nickel catalysis, see: (a) Rosen, B. M.; Quasdorf, K. W.; Wilson, D. A.; Zhang, N.; Resmerita, A.-M.; Garg, N. K.; Percec, V. *Chem. Rev*. **2011**, *111*, 1346–1416. (b) Tasker, S. Z.; Standley, E. A.; Jamison, T. F. *Nature* **2014**, *509*, 299–309. (c) Mesganaw, T.; Garg, N. K. *Org. Process Res. Dev*. **2013**, *17*, 29–39. (d) Ananikov, V. P. *ACS Catal*. **2015**, *5*, 1964–1971.

(3) SciFinder search for the research topic ”nickel, cross-coupling” yielded hits corresponding to 83 original manuscripts in the journals *J. Am. Chem. Soc*., *Angew. Chem. Int. Ed*., *Science*, *Nature*, *Nat. Chem*., and *Nat. Commun*. since 2015. (accessed 20 April, 2017).

(4) Hie, L.; Fine Nathel, N. F.; Shah, T.; Baker, E. L.; Hong, X.; Yang, Y.-F.; Liu, P.; Houk, K. N.; Garg, N. K. *Nature* **2015**, *524*, 79–83.

(5) For the nickel-catalyzed esterification of aliphatic amides, see: Hie, L.; Baker, E. L.; Anthony, S. M.; Desrosiers, J.-N.; Senanayake, C.; Garg, N. K. *Angew. Chem. Int. Ed*. **2016**, *55*, 15129–15132.

(6) For other nickel-catalyzed reactions involving cleavage of the amide C–N bond, see: (a) Weires, N. A.; Baker, E. L.; Garg, N. K. *Nat. Chem*. **2016**, *8*, 75–79. (b) Baker, E. L.; Yamano, M. M.; Zhou, Y.; Anthony, S. M.; Garg, N. K. *Nat. Commun*. **2016**, *7*, 11554. (c) Simmons, B. J.; Weires, N. A.; Dander, J. E.; Garg, N. K. *ACS Catal*. **2016**, *6*, 3176–3179. (d) Dander, J. E.; Weires, N. A.; Garg, N. K. *Org. Lett*. **2016**, *18*, 3934–3936. (e) Shi, S.;

Szostak, M. *Org. Lett.* **2016**, *18*, 5872–5875. (f) Shi, S.; Szostak, M. *Chem. Eur. J.* **2016**, *22*, 10420–10424. (g) Dey, A.; Sasmal, S.; Seth, K.; Lahiri, G. K.; Maiti, D. *ACS Catal.* **2017**, *7*, 433–437. (h) For a recent review, see: Dander, J. E.; Garg, N. K. *ACS Catal.* **2017**, *7*, 1413–1423.

(7) For palladium-catalyzed C–C bond forming reactions of amides, see: (a) Li, X.; Zou, G. *Chem. Commun.* **2015**, *51*, 5089–5092. (b) Li, X.; Zou, G. *J. Organomet. Chem.* **2015**, *794*, 136–145. (c) Meng, G.; Szostak, M. *Org. Biomol. Chem.* **2016**, *14*, 5690–5705. (d) Meng, G.; Szostak, M. *Org. Lett.* **2016**, *18*, 796–799. (e) Meng, G.; Szotak, M. *Angew. Chem. Int. Ed.* **2015**, *54*, 14518–14522. (f) Meng, G.; Szostak, M. *Org. Lett.* **2015**, *17*, 4364–4367. (g) Liu, C.; Meng, G.; Liu, Y.; Liu, R.; Lalancette, R.; Szostak, R.; Szostak, M. *Org. Lett.* **2016**, *18*, 4194–4197. (h) Lei, P.; Meng, G.; Szostak, M. *ACS Catal.* **2017**, *7*, 1960–1965. (i) Liu, C.; Liu, Y.; Liu, R.; Lalancette, R.; Szostak, R.; Szostak, M. *Org. Lett.* **2017**, *19*, 1434–1437. (j) Liu, C.; Meng, G.; Szostak, M. *J. Org. Chem.* **2016**, *81*, 12023–12030. (k) Meng, G.; Shi, S.; Szostak, M. *ACS Catal.* **2016**, *6*, 7335–7339. (l) Cui, M.; Wu, H.; Jian, J.; Wang, H.; Liu, C.; Stelck, D.; Zeng, Z. *Chem. Commun.* **2016**, *52*, 12076–12079. (m) Wu, H.; Li, Y.; Cui, M.; Jian, J.; Zeng, Z. *Adv. Synth. Catal.* **2016**, *358*, 3876–3880.

(8) For the nickel-catalyzed decarbonylative coupling of amides with arylboronic esters, see: Shi, S.; Meng, G.; Szostak, M. *Angew. Chem. Int. Ed.* **2016**, *55*, 6959–6963.

(9) For the nickel-catalyzed decarbonylative borylation of amides, see: Hu, J.; Zhao, Y.; Liu, J.; Zhang, Y.; Shi, Z. *Angew. Chem. Int. Ed.* **2016**, *55*, 8718–8722.

(10) Concentration was calculated by approximating volume as the sum of the masses of all reactants, reagents, and solvent with an assumed overall density of 0.87 g/mL (toluene). Experimentally measured densities for reaction mixtures ranged from 0.85–0.91 g/mL.

(11) For reviews of kinetic modeling in homogeneous catalytic processes, see: (a) Chaudhari, R. V.; Seayad, A.; Jayasree, S. *Catal. Today* **2001**, *66*, 371–380. (b) Blackmond, D. G. *J. Am. Chem. Soc.* **2015**, *137*, 10852–10866.

(12) For selected examples of kinetic modeling in industry, see: (a) Changi, S. M.; Wong, S.-W. *Org. Process Res. Dev.* **2016**, *20*, 525–539. (b) Susanne, F.; Smith, D. S.; Codina, A. *Org. Process Res. Dev.* **2012**, *16*, 61–64. (c) Burt, J. L.; Braem, A. D.; Ramirez, A.; Mudryk, B.; Rossano, L.; Tummala, S. *J. Pharm. Innov.* **2011**, *6*, 181–192. (d) Hallow, D. M.; Mudryk, B. M.; Braem, A. D.; Tabora, J. E.; Lyngberg, O. K.; Bergum, J. S.; Rossano, L. T.; Tummala, S. *J. Pharm. Innov.* **2010**, *5*, 193–203. (e) Massari, L.; Panelli, L.; Hughes, M.; Stazi, F.; Maton, W.; Westerduin, P.; Scaravelli, F.; Bacchi, S. *Org. Process Res. Dev.* **2010**, *14*, 1364–1372.

(13) For selected examples of kinetic modeling in academia, see: (a) Rosner, T.; Le Bars, J.; Pfaltz, A.; Blackmond, D. G. *J. Am. Chem. Soc.* **2001**, *123*, 1848–1855. (b) Ji, Y.; Plata, R. E.; Regens, C. S.; Hay, M.; Schmidt, M.; Razler, T.; Qiu, Y.; Geng, P.; Hsiao, Y.; Rosner, T.; Eastgate, M. D.; Blackmond, D. G. *J. Am. Chem. Soc.* **2015**, *137*, 13272–13281. (c) Ruiz-Castillo, P.; Blackmond, D. G.; Buchwald, S. L. *J. Am. Chem. Soc.* **2015**, *137*, 3085–3092.

(14) DynoChem®, by Scale-up Systems, is a leading process development and scale-up software for scientists and engineers working in the pharmaceutical industry and interfaces directly with Microsoft Excel.

(15) Reactions were performed in an inert atmosphere glove box; aliquots were taken periodically and analyzed by SFC using biphenyl as an internal standard in order to monitor reaction progress. In general, five aliquots were taken per experiment to chart the reaction profile.

(16) Lower catalyst loadings (i.e., entries 4 and 5) were run at higher temperatures and concentrations solely to achieve conversion in a reasonable timeframe.

(17) Although the kinetic model can itself provide insight into possible mechanistic steps, it is helpful to have some understanding of the mechanism of the reaction in question prior to optimization.

(18) See Table 7.4 for details.

(19) Although the esterification of benzamide **7.1** with (–)-menthol (**7.2**) could be optimized further, conditions using 2.0 mol% Ni at 60 °C with the extended reaction time of 16 h were selected for additional explorations of scope.

(20) It was observed empirically that a 2:1 ligand:metal ratio facilitated this coupling at catalyst loadings below 1.0 mol% Ni, likely helping to stabilize the catalyst and impede degradation. The mechanism of the catalyst degradation is not yet well understood.

(21) This outcome is the result of direct optimization of the esterification of benzamide **7.1** with (-–)-menthol (**7.2**). To achieve similar efficiencies with other coupling partners, independent optimizations would likely have to be carried out based on individual reaction kinetics.

(22) (a) Li, Y.; Jia, F.; Li, Z. *Chem. Eur. J.* **2013**, *19*, 82–86. (b) Johnson II, D. C.; Widlanski, T. S. *Tetrahedron Lett.* **2004**, *45*, 8483–8487. (c) Baroudi, A.; Alicea, J.; Flack, P.; Kirincich, J.; Alabugin, I. V. *J. Org. Chem.* **2011**, *76*, 1521–1537.

(23) Biphenyl is not required for the coupling to take place and does not affect the reaction rate.

(24) Ueda, T.; Konishi, H.; Manabe, K. *Org. Lett.* **2013**, *15*, 5370–5373.

(25) Zhang, C.; Feng, P.; Jiao, N. *J. Am. Chem. Soc.* **2013**, *135*, 15257–15262.

(26) Correa, A.; Leon, T.; Martin, R. *J. Am. Chem. Soc.* **2014**, *136*, 1062–1069.

(27) Dong, J.; Shi, X.-X.; Yan, J.-J.; Xing, J.; Xhang, Q.; Xiao, S. *Eur. J. Org. Chem.* **2010**, *36*, 6987–6992.

(28) Hanato, M.; Furuya, Y.; Shimmura, T.; Moriyama, K.; Kamiya, S.; Maki, T.; Ishihara, K. *Org. Lett.* **2011**, *13*, 426–429.

(29) Liu, Z.; Ma, Q.; Liu, Y.; Wang, Q. *Org. Lett.* **2014**, *16*, 236–239.